

## Electronic Acknowledgement Receipt

<b>EFS ID:</b>	42151237
<b>Application Number:</b>	15809815
<b>International Application Number:</b>	
<b>Confirmation Number:</b>	5137
<b>Title of Invention:</b>	Methods for Treating Metastatic Pancreatic Cancer Using Combination Therapies Comprising Liposomal Irinotecan and Oxaliplatin
<b>First Named Inventor/Applicant Name:</b>	Eliel Bayever
<b>Customer Number:</b>	153749
<b>Filer:</b>	Mary Rucker Henninger/Richard King
<b>Filer Authorized By:</b>	Mary Rucker Henninger
<b>Attorney Docket Number:</b>	263266-421428
<b>Receipt Date:</b>	12-MAR-2021
<b>Filing Date:</b>	10-NOV-2017
<b>Time Stamp:</b>	16:22:27
<b>Application Type:</b>	Utility under 35 USC 111(a)

### Payment information:

Submitted with Payment	no
------------------------	----

### File Listing:

Document Number	Document Description	File Name	File Size(Bytes)/ Message Digest	Multi Part /.zip	Pages (if appl.)
1	Non Patent Literature	Chen_2012_abst.pdf	1014725  <small>08303e7855ee21626a95a8dbec253bcc41b71cb9</small>	no	6

### Warnings:

CSPC Exhibit 1114

<b>Information:</b>					
2	Non Patent Literature	Chiang_2016.pdf	706559	no	8
			4987a2fa4c35dc01ab793b48500e58ef659eb415		
<b>Warnings:</b>					
<b>Information:</b>					
3	Non Patent Literature	Chibaudel_2016.pdf	120430	no	8
			54666eeef1ed58c9a5dfe71db739089cefbbc90		
<b>Warnings:</b>					
<b>Information:</b>					
4	Non Patent Literature	Chiesa_2010.pdf	156314	no	8
			79787e89497871db80805bc1d9a4020ce5332990		
<b>Warnings:</b>					
<b>Information:</b>					
5	Non Patent Literature	Chu_1990.pdf	2554554	no	11
			4014a1f9ce916c77267a70a0dc0337b40ff1ca9		
<b>Warnings:</b>					
<b>Information:</b>					
6	Non Patent Literature	Clarke_ASCO_2015_poster.pdf	1986097	no	7
			ecc5439facde7a734283f5ed7126545ed3f8a860		
<b>Warnings:</b>					
<b>Information:</b>					
7	Non Patent Literature	Clarke_ASCO_2015_abstract.pdf	66742	no	2
			974ec465db12a3526002f7aed8662192f7c08c88		
<b>Warnings:</b>					
<b>Information:</b>					
8	Non Patent Literature	Colbern_1998.pdf	495236	no	6
			a5370da402df4a37912b1201dd291e93ec81dc1a		
<b>Warnings:</b>					
<b>Information:</b>					

9	Non Patent Literature	Comella_2003.pdf	83435	no	5
			14811c091d1f9757c85796f02680568324dc28dd		

**Warnings:**

**Information:**

10	Non Patent Literature	Cortes_2018_abstract.pdf	172262	no	3
			d1bc270cd3a34f7a9febef624aa7287360b6e3f7		

**Warnings:**

**Information:**

11	Non Patent Literature	Daleke_1990.pdf	1426806	no	15
			f626d1f328411e080752d45a9a3e68f9b5b0086d		

**Warnings:**

**Information:**

<b>Total Files Size (in bytes):</b>			8783160		
-------------------------------------	--	--	---------	--	--

**This Acknowledgement Receipt evidences receipt on the noted date by the USPTO of the indicated documents, characterized by the applicant, and including page counts, where applicable. It serves as evidence of receipt similar to a Post Card, as described in MPEP 503.**

**New Applications Under 35 U.S.C. 111**

**If a new application is being filed and the application includes the necessary components for a filing date (see 37 CFR 1.53(b)-(d) and MPEP 506), a Filing Receipt (37 CFR 1.54) will be issued in due course and the date shown on this Acknowledgement Receipt will establish the filing date of the application.**

**National Stage of an International Application under 35 U.S.C. 371**

**If a timely submission to enter the national stage of an international application is compliant with the conditions of 35 U.S.C. 371 and other applicable requirements a Form PCT/DO/EO/903 indicating acceptance of the application as a national stage submission under 35 U.S.C. 371 will be issued in addition to the Filing Receipt, in due course.**

**New International Application Filed with the USPTO as a Receiving Office**

**If a new international application is being filed and the international application includes the necessary components for an international filing date (see PCT Article 11 and MPEP 1810), a Notification of the International Application Number and of the International Filing Date (Form PCT/RO/105) will be issued in due course, subject to prescriptions concerning national security, and the date shown on this Acknowledgement Receipt will establish the international filing date of the application.**

<b>INFORMATION DISCLOSURE STATEMENT BY APPLICANT</b> ( Not for submission under 37 CFR 1.99)	Application Number		15809815	
	Filing Date		2017-11-10	
	First Named Inventor		Eliel Bayever	
	Art Unit		1612	
	Examiner Name		Celeste A. RONEY	
	Attorney Docket Number		01208-0007-01US	

**U.S.PATENTS**

Examiner Initial*	Cite No	Patent Number	Kind Code <sup>1</sup>	Issue Date	Name of Patentee or Applicant of cited Document	Pages,Columns,Lines where Relevant Passages or Relevant Figures Appear
	1					

If you wish to add additional U.S. Patent citation information please click the Add button.

**U.S.PATENT APPLICATION PUBLICATIONS**

Examiner Initial*	Cite No	Publication Number	Kind Code <sup>1</sup>	Publication Date	Name of Patentee or Applicant of cited Document	Pages,Columns,Lines where Relevant Passages or Relevant Figures Appear
	1					

If you wish to add additional U.S. Published Application citation information please click the Add button.

**FOREIGN PATENT DOCUMENTS**

Examiner Initial*	Cite No	Foreign Document Number <sup>3</sup>	Country Code <sup>2</sup> i	Kind Code <sup>4</sup>	Publication Date	Name of Patentee or Applicant of cited Document	Pages,Columns,Lines where Relevant Passages or Relevant Figures Appear	T <sup>5</sup>
	1							

If you wish to add additional Foreign Patent Document citation information please click the Add button

**NON-PATENT LITERATURE DOCUMENTS**

Examiner Initials*	Cite No	Include name of the author (in CAPITAL LETTERS), title of the article (when appropriate), title of the item (book, magazine, journal, serial, symposium, catalog, etc), date, pages(s), volume-issue number(s), publisher, city and/or country where published.	T <sup>5</sup>



**INFORMATION DISCLOSURE  
STATEMENT BY APPLICANT**  
( Not for submission under 37 CFR 1.99)

Application Number	15809815
Filing Date	2017-11-10
First Named Inventor	Eliel Bayever
Art Unit	1612
Examiner Name	Celeste A. RONEY
Attorney Docket Number	01208-0007-01US

1	DaunoXome (daunorubicin citrate liposome injection) package insert, rev. December 2011, 11 pages.
2	DAYYANI F, et al., Abstract B14. "CA 19-9 levels in patients with metastatic pancreatic adenocarcinoma receiving first-line therapy with liposomal irinotecan plus 5-fluorouracil/leucovorin and oxaliplatin (NAPOX)," In Proceedings of the AACR Special Conference on Pancreatic Cancer: Advances in Science and Clinical Care; September 6-9, 2019; Boston, MA; Cancer Res. 2019; 79(24 Suppl): Abstract nr B14, 3 printed pages.
3	DELORD J, et. al., "A Phase I Clinical and Pharmacokinetic Study of Capecitabine (Xeloda®) and Irinotecan Combination Therapy (XELIRI) in Patients With Metastatic Gastrointestinal Tumours," Br J Cancer. 92(5):820-6 (2005).
4	DERKSEN J, et. al., "Interaction of Immunoglobulin-Coupled Liposomes with Rat Liver Macrophages In Vitro," Exp Cell Res. 168(1):105-15 (1987).
5	DEWHIRST M, et al., "Microvascular Studies on the Origins of Perfusion-Limited Hypoxia," Br J Cancer Suppl. 27: S247-51 (1996).
6	DICKO A, et al., "Intra and Inter-Molecular Interactions Dictate the Aggregation State of Irinotecan Co-Encapsulated with Floxuridine Inside Liposomes," Pharm Res. 25(7):1702-13 (2008).
7	DOS SANTOS N, et al., "Improved Retention of Idarubicin After Intravenous Injection Obtained for Cholesterol-Free Liposomes," Biochim Biophys Acta. 1561(2):188-201 (2002).
8	DRUMMOND D, et al., "Clinical Development of Histone Deacetylase Inhibitors as Anticancer Agents," Annu Rev Pharmacol Toxicol. 45:495-528 and C1-C2 (2005).
9	DRUMMOND D, et al., "Development of a Highly Stable and Targetable Nanoliposomal Formulation of Topotecan," J Control Release. 141(1):13-21 (2010). Epub 2009.
10	DRUMMOND D, et al., "Improved Pharmacokinetics and Efficacy of a Highly Stable Nanoliposomal Vinorelbine," J Pharmacol Exp Ther. 328(1):321-30 (2009). Epub 2008.
11	DRUMMOND D, et al., "Liposome Targeting to Tumors using Vitamin and Growth Factor Receptors," Vitam Horm. 60:285-332 (2000).

**INFORMATION DISCLOSURE  
STATEMENT BY APPLICANT**  
( Not for submission under 37 CFR 1.99)

Application Number	15809815
Filing Date	2017-11-10
First Named Inventor	Eliel Bayever
Art Unit	1612
Examiner Name	Celeste A. RONEY
Attorney Docket Number	01208-0007-01US

12	DRUMMOND D, et al., "Pharmacokinetics and In Vivo Drug Release Rates in Liposomal Nanocarrier Development," J Pharm Sci. 97(11):4696-740 (2008).
13	DRUMMOND D, et al., Chapter 8, "Intraliposomal Trapping Agents for Improving In Vivo Liposomal Drug Formulation Stability," In Liposome Technology, Third Edition, Volume 2, Ed. G. Gregoriadis, pp. 149-168 (2006).
14	DRUMMOND D, et al., Chapter 9, "Liposomal Drug Delivery Systems for Cancer Therapy," In Drug Discovery Systems in Cancer Therapy, Ed. D Brown, Humana Press, Totowa, NJ, pp. 191-213 (2004).
15	DUFFOUR J, et al., "Efficacy of Prophylactic Anti-Diarrhoeal Treatment in Patients Receiving Campto for Advanced Colorectal Cancer," Anticancer Res. 22(6B): 3727-31 (2002).
16	ELINZANO H, et al., "Nanoliposomal Irinotecan and Metronomic Temozolomide for Patients With Recurrent Glioblastoma BrUOG329, A Phase I Brown University Oncology Research Group Trial," Am J Clin Oncol. 44(2):49-52 (2021). Epub 2020 version, pages 1-4.
17	ELINZANO H, et al., Abstract e14548. "Nanoliposomal Irinotecan and Metronomic Temozolomide for Patients With Recurrent Glioblastoma: BrUOG329, A Phase IB/IIA Brown University Oncology Research Group (BrUOG) Trial," J Clin Oncol. 38(15_Suppl):e14548 DOI: 10.1200/JCO.2020.38.15_suppl.e14548 (2020), 2 printed pages.
18	EMERSON D, et al., "Antitumor Efficacy, Pharmacokinetics, and Biodistribution of NX 211: A Low-Clearance Liposomal Formulation of Lurtotecan," Clin Cancer Res. 6(7):2903-12 (2000).
19	English translation of title and abstract for HASEGAWA, Y, "Biomarker as Predictive Safety Testing in Oncology", IGAKU NO AYUMI (Journal of Clinical and Experimental Medicine), 224(13):1171-4 (2008) (original in Japanese).
20	EP Patent Application No. 05745505.7: European Search Report mailed on September 1, 2010, 6 pages.
21	EP2861210: Proprietor's statement of grounds of appeal to opposition decision dated December 30, 2019, 35 pages.
22	EP2861210: Proprietor's Main and Auxiliary Requests MR, AR1, AR2, and AR3 with Proprietor's Statement of Grounds of Appeal in Opposition Proceedings filed December 30, 2019, 4 pages.

**INFORMATION DISCLOSURE  
STATEMENT BY APPLICANT**  
( Not for submission under 37 CFR 1.99)

Application Number	15809815
Filing Date	2017-11-10
First Named Inventor	Eliel Bayever
Art Unit	1612
Examiner Name	Celeste A. RONEY
Attorney Docket Number	01208-0007-01US

23	EP2861210: Proprietor's statement of grounds of appeal to opposition decision dated December 30, 2019, D23 (Declaration of Amy McKee M.D.) including D23A (Hoos W, et al., "Pancreatic Cancer Clinical Trials and Accrual in the United States." J Clin Oncol. 31(27):3432-8 (2013) and accompanying Appendix Table A1, Table A2, and Figure A1) and D23B (BIO Industry Analysis: Clinical Development Success Rates 2006-2015, July 2016), 44 total pages.
24	EP2861210: Proprietor's statement of grounds of appeal to opposition decision dated December 30, 2019, D24 (Declaration of Bruce Belanger, Ph.D.), 2 pages.
25	EP2861210: Reply to proprietor's grounds of appeal following opposition and cover letter, dated July 27, 2020, 35 pages.
26	EP2861210: Reply to proprietor's grounds of appeal to opposition decision dated July 27, 2020, D15c (EU clinical trial database for NAPOLI-1 study from October 12, 2012, corresponds to D15b), 10 pages.
27	EP2861210: Reply to proprietor's grounds of appeal to opposition decision dated July 27, 2020, D25 (CHEN P, et al., "Comparing Routes of Delivery for Nanoliposomal Irinotecan Shows Superior Anti-Tumor Activity of Local Administration in Treating Intracranial Glioblastoma Xenografts," Neuro Oncol. 15(2):189-97 (2013), Epub 21 Dec 2012).
28	EP2861210: Reply to proprietor's grounds of appeal to opposition decision dated July 27, 2020, D26 (DRUMMOND D, et al., "Development of a Highly Active Nanoliposomal Irinotecan Using a Novel Intraliposomal Stabilization Strategy," Cancer Res. 66(6):3271-77 (2006)).
29	EP2861210: Reply to proprietor's grounds of appeal to opposition decision dated July 27, 2020, D27 (ROY A, et al., "A Randomized Phase II Study of PEP02 (MM-398), Irinotecan or Docetaxel as a Second-Line Therapy in Patients With Locally Advanced or Metastatic Gastric or Gastro-Oesophageal Junction Adenocarcinoma," Ann Oncol. 24(6):1567-73 (2013)).
30	EP2861210: Reply to proprietor's grounds of appeal to opposition decision dated July 27, 2020, D28 (SVENSON S, "Clinical Translation of Nanomedicines," Current Opinion in Solid State and Materials Science. 16(6):287-294 (2012), article in press version, 7 pages).
31	EP2861210: Reply to proprietor's grounds of appeal to opposition decision dated July 27, 2020, D29 (MAKRILIA N, et al., "Treatment for Refractory Pancreatic Cancer. Highlights from the '2011 ASCO Gastrointestinal Cancers Symposium'. San Francisco, CA, USA, January 20-22, 2011," J Pancreas. 12(2):110-3 (2011)).
32	EP2861210: Reply to proprietor's grounds of appeal to opposition decision dated July 27, 2020, D30 (CHEN L, et al., "Phase I Study of Biweekly Liposome Irinotecan (PEP02, MM-398) in Metastatic Colorectal Cancer Failed on First-line Oxaliplatin-based Chemotherapy," J Clin Oncol. 30(4_suppl):Abstract 613 (2012), 5 printed pages.).
33	EP2861210: Reply to proprietor's grounds of appeal to opposition decision dated July 27, 2020, D31 (CUNNINGHAM D, et al., "Randomized Phase II Study of PEP02, Irinotecan, or Docetaxel as a Second-Line Therapy in Gastric or Gastroesophageal Junction Adenocarcinoma," J Clin Oncol. 29(4_suppl):Abstract 6 (2011), 5 printed pages).

**INFORMATION DISCLOSURE  
STATEMENT BY APPLICANT**  
( Not for submission under 37 CFR 1.99)

Application Number		15809815
Filing Date		2017-11-10
First Named Inventor	Eliel Bayever	
Art Unit		1612
Examiner Name	Celeste A. RONEY	
Attorney Docket Number		01208-0007-01US

34	EP2861210: Reply to proprietor's grounds of appeal to opposition decision dated July 27, 2020, D32 (GERBER D, "Miscellaneous Agents--Cytotoxics and Hormonal Agents," J Thorac Oncol. 7(12 Suppl 5):S387-9 (2012)).
35	EP2861210: Reply to proprietor's grounds of appeal to opposition decision dated July 27, 2020, D33 (NOBLE C, et al., "Novel Nanoliposomal CPT-11 Infused by Convection-Enhanced Delivery in Intracranial Tumors: Pharmacology and Efficacy," Cancer Res. 66(5):2801-6 (2006)).
36	EP2861210: Reply to proprietor's grounds of appeal to opposition decision dated July 27, 2020, D34 (KRAUZE M, et al., "Convection-Enhanced Delivery of Nanoliposomal CPT-11 (Irinotecan) and PEGylated Liposomal Doxorubicin (Doxil) in Rodent Intracranial Brain Tumor Xenografts," Neuro Oncol. 9(4):393-403 (2007)).
37	EP2861210: Reply to proprietor's grounds of appeal to opposition decision dated July 27, 2020, D35 (MULLARD A, "How Much Do Phase III Trials Cost?" Nat Rev Drug Discov. 17(11):777 (2018)).
38	EP2861210: Reply to proprietor's grounds of appeal to opposition decision dated July 27, 2020, D36 (The Medicines for Human Use (Clinical Trials) Regulations, 2004, 86 pages).
39	ETTRICH T, et al., "Liposomal Irinotecan (nal-IRI) Plus 5-Fluorouracil (5-FU) and Leucovorin (LV) or Gemcitabine Plus Cisplatin in Advanced Cholangiocarcinoma: The AIO-NIFE-Trial, an Open Label, Randomized, Multicenter Phase II Trial," Poster presented at the American Society of Clinical Oncology (ASCO) Annual Meeting, Chicago, Illinois, June 1-5, 2018, 5 pages.
40	ETTRICH T, et al., Abstract TPS4145. "Liposomal Irinotecan (nal-IRI) Plus 5-Fluorouracil (5-FU) and Leucovorin (LV) or Gemcitabine Plus Cisplatin in Advanced Cholangiocarcinoma: The AIO-NIFE-Trial, an Open Label, Randomized, Multicenter Phase II Trial," J Clin Oncol. 36(15_Suppl):TPS4145 DOI: 10.1200/JCO.2018.36.15_suppl.TPS4145 (2018), 2 printed pages.
41	European Medicines Agency Assessment Report for Onivyde, Committee for Medicinal Products for Human Use (CHMP), 21 July 2016, 107 pages.
42	FALCONE A, et al., "Sequence Effect of Irinotecan and Fluorouracil Treatment on Pharmacokinetics and Toxicity in Chemotherapy-Naive Metastatic Colorectal Cancer Patients," J Clin Oncol. 19(15):3456-62 (2001).
43	FANNON M, et al., "Sucrose Octasulfate Regulates Fibroblast Growth Factor-2 Binding, Transport, and Activity: Potential for Regulation of Tumor Growth," J Cell Physiol. 215(2):434-41 (2008), NIH public access author manuscript version, 19 pages.
44	FARNCOMBE M, "Management of Bleeding in a Patient with Colorectal Cancer: A Case Study," Support Care Cancer. 1(3):159-160 (1993).

**INFORMATION DISCLOSURE  
STATEMENT BY APPLICANT**  
( Not for submission under 37 CFR 1.99)

Application Number	15809815
Filing Date	2017-11-10
First Named Inventor	Eliel Bayever
Art Unit	1612
Examiner Name	Celeste A. RONEY
Attorney Docket Number	01208-0007-01US

45	FDA, "Draft Guidance on Daunorubicin Citrate," Jul 2014, 6 pages.
46	FDA, "Draft Guidance on Doxorubicin Hydrochloride," Recommended Feb 2010, Revised Nov 2013, Dec 2014, 6 pages.
47	FIORAVANTI A, et. al., "Metronomic 5-Fluorouracil, Oxaliplatin and Irinotecan in Colorectal Cancer," Eur J Pharmacol. 619(1-3): 8-14 (2009).
48	FLEMING G, et. al., "Phase I and Pharmacokinetic Study of 24-Hour Infusion 5-Fluorouracil and Leucovorin in Patients With Organ Dysfunction," Ann Oncol. 14(7):1142-7 (2003).
49	FREISE C, et al., "Characterization of a Cyclosporine-Containing Liposome," Transplant Proc. 23(1 Pt 1):473-4 (1991).
50	FREISE C, et al., "Increased Efficacy of Cyclosporin Liposomes in a Rat Orthotopic Liver Transplant Model," Surgical Forum. 43:395-7 (1992).

If you wish to add additional non-patent literature document citation information please click the Add button

**EXAMINER SIGNATURE**

Examiner Signature	<input type="text"/>	Date Considered	<input type="text"/>
--------------------	----------------------	-----------------	----------------------

\*EXAMINER: Initial if reference considered, whether or not citation is in conformance with MPEP 609. Draw line through a citation if not in conformance and not considered. Include copy of this form with next communication to applicant.

<sup>1</sup> See Kind Codes of USPTO Patent Documents at [www.USPTO.GOV](http://www.USPTO.GOV) or MPEP 901.04. <sup>2</sup> Enter office that issued the document, by the two-letter code (WIPO Standard ST.3). <sup>3</sup> For Japanese patent documents, the indication of the year of the reign of the Emperor must precede the serial number of the patent document. <sup>4</sup> Kind of document by the appropriate symbols as indicated on the document under WIPO Standard ST.16 if possible. <sup>5</sup> Applicant is to place a check mark here if English language translation is attached.

<b>INFORMATION DISCLOSURE STATEMENT BY APPLICANT</b> ( Not for submission under 37 CFR 1.99)	Application Number	15809815
	Filing Date	2017-11-10
	First Named Inventor	Eliel Bayever
	Art Unit	1612
	Examiner Name	Celeste A. RONEY
	Attorney Docket Number	01208-0007-01US

**CERTIFICATION STATEMENT**

Please see 37 CFR 1.97 and 1.98 to make the appropriate selection(s):

That each item of information contained in the information disclosure statement was first cited in any communication from a foreign patent office in a counterpart foreign application not more than three months prior to the filing of the information disclosure statement. See 37 CFR 1.97(e)(1).

**OR**

That no item of information contained in the information disclosure statement was cited in a communication from a foreign patent office in a counterpart foreign application, and, to the knowledge of the person signing the certification after making reasonable inquiry, no item of information contained in the information disclosure statement was known to any individual designated in 37 CFR 1.56(c) more than three months prior to the filing of the information disclosure statement. See 37 CFR 1.97(e)(2).

See attached certification statement.

The fee set forth in 37 CFR 1.17 (p) has been submitted herewith.

A certification statement is not submitted herewith.

**SIGNATURE**

A signature of the applicant or representative is required in accordance with CFR 1.33, 10.18. Please see CFR 1.4(d) for the form of the signature.

Signature	/Mary R. Henninger/	Date (YYYY-MM-DD)	2021-03-12
Name/Print	Mary R. Henninger	Registration Number	56992

This collection of information is required by 37 CFR 1.97 and 1.98. The information is required to obtain or retain a benefit by the public which is to file (and by the USPTO to process) an application. Confidentiality is governed by 35 U.S.C. 122 and 37 CFR 1.14. This collection is estimated to take 1 hour to complete, including gathering, preparing and submitting the completed application form to the USPTO. Time will vary depending upon the individual case. Any comments on the amount of time you require to complete this form and/or suggestions for reducing this burden, should be sent to the Chief Information Officer, U.S. Patent and Trademark Office, U.S. Department of Commerce, P.O. Box 1450, Alexandria, VA 22313-1450. **DO NOT SEND FEES OR COMPLETED FORMS TO THIS ADDRESS. SEND TO: Commissioner for Patents, P.O. Box 1450, Alexandria, VA 22313-1450.**

## Privacy Act Statement

The Privacy Act of 1974 (P.L. 93-579) requires that you be given certain information in connection with your submission of the attached form related to a patent application or patent. Accordingly, pursuant to the requirements of the Act, please be advised that: (1) the general authority for the collection of this information is 35 U.S.C. 2(b)(2); (2) furnishing of the information solicited is voluntary; and (3) the principal purpose for which the information is used by the U.S. Patent and Trademark Office is to process and/or examine your submission related to a patent application or patent. If you do not furnish the requested information, the U.S. Patent and Trademark Office may not be able to process and/or examine your submission, which may result in termination of proceedings or abandonment of the application or expiration of the patent.

The information provided by you in this form will be subject to the following routine uses:

1. The information on this form will be treated confidentially to the extent allowed under the Freedom of Information Act (5 U.S.C. 552) and the Privacy Act (5 U.S.C. 552a). Records from this system of records may be disclosed to the Department of Justice to determine whether the Freedom of Information Act requires disclosure of these records.
2. A record from this system of records may be disclosed, as a routine use, in the course of presenting evidence to a court, magistrate, or administrative tribunal, including disclosures to opposing counsel in the course of settlement negotiations.
3. A record in this system of records may be disclosed, as a routine use, to a Member of Congress submitting a request involving an individual, to whom the record pertains, when the individual has requested assistance from the Member with respect to the subject matter of the record.
4. A record in this system of records may be disclosed, as a routine use, to a contractor of the Agency having need for the information in order to perform a contract. Recipients of information shall be required to comply with the requirements of the Privacy Act of 1974, as amended, pursuant to 5 U.S.C. 552a(m).
5. A record related to an International Application filed under the Patent Cooperation Treaty in this system of records may be disclosed, as a routine use, to the International Bureau of the World Intellectual Property Organization, pursuant to the Patent Cooperation Treaty.
6. A record in this system of records may be disclosed, as a routine use, to another federal agency for purposes of National Security review (35 U.S.C. 181) and for review pursuant to the Atomic Energy Act (42 U.S.C. 218(c)).
7. A record from this system of records may be disclosed, as a routine use, to the Administrator, General Services, or his/her designee, during an inspection of records conducted by GSA as part of that agency's responsibility to recommend improvements in records management practices and programs, under authority of 44 U.S.C. 2904 and 2906. Such disclosure shall be made in accordance with the GSA regulations governing inspection of records for this purpose, and any other relevant (i.e., GSA or Commerce) directive. Such disclosure shall not be used to make determinations about individuals.
8. A record from this system of records may be disclosed, as a routine use, to the public after either publication of the application pursuant to 35 U.S.C. 122(b) or issuance of a patent pursuant to 35 U.S.C. 151. Further, a record may be disclosed, subject to the limitations of 37 CFR 1.14, as a routine use, to the public if the record was filed in an application which became abandoned or in which the proceedings were terminated and which application is referenced by either a published application, an application open to public inspections or an issued patent.
9. A record from this system of records may be disclosed, as a routine use, to a Federal, State, or local law enforcement agency, if the USPTO becomes aware of a violation or potential violation of law or regulation.

**DaunoXome®**  
(daunorubicin citrate liposome injection)

Rx only

**WARNINGS**

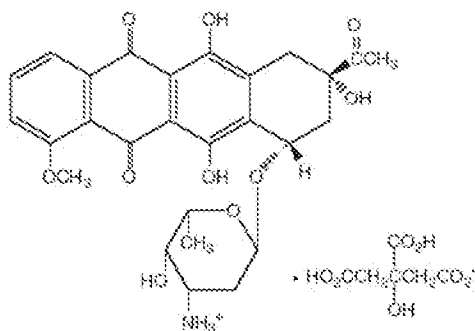
1. Cardiac function should be monitored regularly in patients receiving DaunoXome (daunorubicin citrate liposome injection) because of the potential risk for cardiac toxicity and congestive heart failure. Cardiac monitoring is advised especially in those patients who have received prior anthracyclines or who have pre-existing cardiac disease or who have had prior radiotherapy encompassing the heart.
2. Severe myelosuppression may occur.
3. DaunoXome should be administered only under the supervision of a physician who is experienced in the use of cancer chemotherapeutic agents.
4. Dosage should be reduced in patients with impaired hepatic function. (See **DOSAGE AND ADMINISTRATION**)
5. A triad of back pain, flushing, and chest tightness has been reported in 13.8% of the patients (16/116) treated with DaunoXome in the Phase III clinical trial, and in 2.7% of treatment cycles (27/994). This triad generally occurs during the first five minutes of the infusion, subsides with interruption of the infusion, and generally does not recur if the infusion is then resumed at a slower rate.

**DESCRIPTION**

DaunoXome (daunorubicin citrate liposome injection) is a sterile, pyrogen-free, preservative-free product in a single use vial for intravenous infusion.

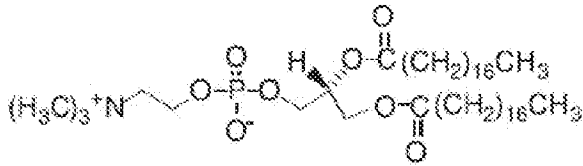
DaunoXome contains an aqueous solution of the citrate salt of daunorubicin encapsulated within lipid vesicles (liposomes) composed of a lipid bilayer of distearoylphosphatidylcholine and cholesterol (2:1 molar ratio), with a mean diameter of about 45 nm. The lipid to drug weight ratio is 18.7:1 (total lipid:daunorubicin base), equivalent to a 10:5:1 molar ratio of distearoylphosphatidylcholine:cholesterol:daunorubicin. Daunorubicin is an anthracycline antibiotic with antineoplastic activity, originally obtained from *Streptomyces peucetius*. Daunorubicin has a 4-ring anthracycline moiety linked by a glycosidic bond to daunosamine, an amino sugar. Daunorubicin may also be isolated from *Streptomyces coeruleorubidus* and has the following chemical name: (8*S-cis*)-8-acetyl-10-[3-amino-2,3,6-trideoxy- $\alpha$ -L-lyxo-hexopyranosyl]oxy]-7,8,9,10-tetrahydro-6,8,11-trihydroxy-1-methoxy-5,12-naphthacenedione hydrochloride.

Daunorubicin citrate has the following chemical structure:



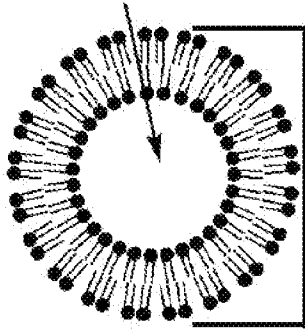


DSPC (distearoylphosphatidylcholine) has the following chemical structure:




The following represents the idealized, spherical morphology of a liposome:

This represents the aqueous core that contains daunorubicin citrate.



The diameter of the liposomes in DaunoXome is between 35 and 65 nm.

 represents a molecule of DSPC.

**Note:** Liposomal encapsulation can substantially affect a drug's functional properties relative to those of the unencapsulated drug.

**In addition, different liposomal drug products may vary from one another in the chemical composition and physical form of the liposomes. Such differences can substantially affect the functional properties of liposomal drug products.**

Each vial contains daunorubicin citrate equivalent to 50 mg of daunorubicin base, encapsulated in liposomes consisting of 704 mg distearoylphosphatidylcholine and 168 mg cholesterol. The liposomes encapsulating daunorubicin are dispersed in an aqueous medium containing 2,125 mg sucrose, 94 mg glycine, and 7 mg calcium chloride dihydrate in a total volume of 25 mL/vial. The pH of the dispersion is between 4.9 and 6.0. The liposome dispersion should appear red and translucent.

## CLINICAL PHARMACOLOGY

### Mechanism of Action

DaunoXome is a liposomal preparation of daunorubicin formulated to maximize the selectivity of daunorubicin for solid tumors *in situ*. While in the circulation, the DaunoXome formulation helps to protect the entrapped daunorubicin from chemical and enzymatic degradation, minimizes protein binding, and generally decreases uptake by normal (non-reticuloendothelial system) tissues. The specific mechanism by which DaunoXome is able to deliver daunorubicin to solid tumors *in situ* is not known. However, it is believed to be a function of increased permeability of the tumor neovasculature to some particles in the size range of DaunoXome. In animal studies, daunorubicin has been shown to accumulate in tumors to a greater extent when administered as DaunoXome than when administered as daunorubicin. Once within the tumor environment, daunorubicin is released over time enabling it to exert its antineoplastic activity.

### Pharmacokinetics

Following intravenous injection of DaunoXome, plasma clearance of daunorubicin shows monoexponential decline. The pharmacokinetic parameter values for total daunorubicin following a single 40 mg/m<sup>2</sup> dose of DaunoXome administered over a 30 – 60 minute period to patients with AIDS-related Kaposi's sarcoma and following a single rapid intravenous, 80 mg/m<sup>2</sup> dose of conventional daunorubicin to patients with disseminated solid malignancies are shown in Table I.

**TABLE I**  
**PHARMACOKINETIC PARAMETERS OF DAUNOXOME IN AIDS PATIENTS WITH KAPOSI'S SARCOMA AND REPORTED PARAMETERS FOR CONVENTIONAL DAUNORUBICIN**

Parameter (units)	<sup>a</sup> DaunoXome	<sup>b</sup> Conventional Daunorubicin
Plasma Clearance (mL/min)	17.3 ± 6.1	<sup>c</sup> 236 ± 181
Volume of Distribution (L)	6.4 ± 1.5	1006 ± 622
Distribution Half-Life (h)	4.41 ± 2.33	0.77 ± 0.3
Elimination Half-Life (h)	————	55.4 ± 13.7

<sup>a</sup> N=30; <sup>b</sup> N=4; <sup>c</sup> Calculated

The plasma pharmacokinetics of DaunoXome differ significantly from the results reported for conventional daunorubicin hydrochloride. DaunoXome has a small steady-state volume of distribution of 6.4 L, (probably because it is confined to vascular fluid volume), and clearance of 17 mL/min. These differences in the volume of distribution and clearance result in a higher daunorubicin exposure (in terms of plasma AUC) from DaunoXome than with conventional daunorubicin hydrochloride. The apparent elimination half-life of DaunoXome (daunorubicin citrate liposome injection) is 4.4 hours, far shorter than that of daunorubicin, and probably represents a distribution half-life. Although preclinical biodistribution data in animals suggest that DaunoXome crosses the normal blood-brain barrier, it is unknown whether DaunoXome crosses the blood-brain barrier in humans.

**Metabolism:** Daunorubicinol, the major active metabolite of daunorubicin, was detected at low levels in the plasma following intravenous administration of DaunoXome.

No formal assessments of pharmacokinetic drug–drug interactions between DaunoXome and other agents have been conducted.

**Special Populations:** The pharmacokinetics of DaunoXome have not been evaluated in women, in different ethnic groups, or in subjects with renal and hepatic insufficiency.

### Clinical Study

In an open-label, randomized, controlled clinical study conducted at 13 centers in the U.S.A. and Canada in advanced (25 or more mucocutaneous lesions; the development of 10 or more lesions in a one month period of time; symptomatic visceral involvement; or tumor-associated edema) HIV-related Kaposi's sarcoma, two treatment regimens were compared as first line cytotoxic therapy: DaunoXome 40 mg/m<sup>2</sup> and ABV (doxorubicin (Adriamycin®<sup>1</sup>) 10 mg/m<sup>2</sup>, bleomycin 15 U, and vincristine 1.0 mg). All drugs were administered intravenously every 2 weeks. Responses were assessed using the AIDS Clinical Trials Group Oncology Committee of the National Institute of Allergy and Infectious Diseases (ACTG) criteria (a response required at least one of any of the following for at least 28 days: a. ≥ 50% reduction in the number; b. ≥ 50% reduction in the sums of the products of the largest perpendicular diameters of bidimensionally measurable marker lesions; or c. complete flattening of ≥ 50% of all previously raised lesions). Table II summarizes the efficacy results.

1. Adriamycin is a registered trademark of Pharmacia & Upjohn Co., Kalamazoo, MI.

**TABLE II**  
**EFFICACY DATA**  
**FIRST LINE CYTOTOXIC THERAPY FOR ADVANCED KAPOSI'S SARCOMA**

	<b>DaunoXome n=116</b>	<b>ABV n=111</b>
Response Rate	23%*	30%
Duration of Response, Median	110 days**	113 days
Time to Progression, Median	92 days ***	105 days
Survival	342 days ****	291 days

\* The 95% confidence interval for difference in the response rates (ABV – DaunoXome) was (-5%, 18%).

\*\* The hazard ratio (ABV/DaunoXome) for duration of response was 0.80, and the 95% confidence intervals were (0.44, 1.46).

\*\*\* The hazard ratio (ABV/DaunoXome) for time to progression was 0.78, and the 95% confidence intervals were (0.57, 1.07).

\*\*\*\* The hazard ratio for mortality (ABV/DaunoXome) was 1.29, and 95% confidence intervals were (0.92, 1.79).

Twenty of the 33 ABV responders responded to therapy by criteria more stringent than flattening of lesions (i.e., shrinkage of lesions and/or reduction in the number of lesions). Eleven of the 27 DaunoXome responders responded to therapy by criteria other than flattening of lesions. Photographic evidence of tumor response to DaunoXome and ABV was comparable across all anatomic sites (e.g., face, oral cavity, trunk, legs, and feet).

#### **INDICATIONS AND USAGE**

DaunoXome is indicated as a first line cytotoxic therapy for advanced HIV-associated Kaposi's sarcoma. DaunoXome is not recommended in patients with less than advanced HIV-related Kaposi's sarcoma.

#### **CONTRAINDICATIONS**

Therapy with DaunoXome is contraindicated in patients who have experienced a serious hypersensitivity reaction to previous doses of DaunoXome or to any of its constituents.

#### **WARNINGS**

DaunoXome is intended for administration under the supervision of a physician who is experienced in the use of cancer chemotherapeutic agents.

The primary toxicity of DaunoXome is myelosuppression, especially of the granulocytic series, which may be severe, and associated with fever and may result in infection. Effects on the platelets and erythroid series are much less marked. Careful hematologic monitoring is required and since patients with HIV infection are immunocompromised, patients must be observed carefully for evidence of intercurrent or opportunistic infections.

Special attention must be given to the potential cardiac toxicity of DaunoXome. Although there is no reliable means of predicting congestive heart failure, cardiomyopathy induced by anthracyclines is usually associated with a decrease of the left ventricular ejection fraction (LVEF). Cardiac function should be evaluated in each patient by means of a history and physical examination before each course of DaunoXome and determination of LVEF should be performed at total cumulative doses of DaunoXome of 320 mg/m<sup>2</sup>, and every 160 mg/m<sup>2</sup> thereafter.

Patients who have received prior therapy with anthracyclines (doxorubicin > 300 mg/m<sup>2</sup> or equivalent), have pre-existing cardiac disease, or have received previous radiotherapy encompassing the heart may be less "cardiac" tolerant to

treatment with DaunoXome. Therefore, monitoring of LVEF at cumulative DaunoXome doses should occur prior to therapy and every 160 mg/m<sup>2</sup> of DaunoXome.

In patients with Kaposi's sarcoma, congestive heart failure has been reported in one patient at a cumulative dose of 340 mg/m<sup>2</sup> of DaunoXome. In eight Kaposi's sarcoma patients, LVEF decreases were reported at cumulative doses ranging from 200 mg/m<sup>2</sup> to 2100 mg/m<sup>2</sup> (median dose 320 mg/m<sup>2</sup>) of DaunoXome. In clinical studies in malignancies other than Kaposi's sarcoma and treated with doses of DaunoXome greater than the recommended dose of 40 mg/m<sup>2</sup>, congestive heart failure has been reported at a cumulative dose as low as 200 mg/m<sup>2</sup> of DaunoXome; seven patients have been reported with LVEF decreases. The proportion of patients at risk for cardiotoxicity is unknown because the denominator is uncertain since there were several instances of missing repeat cardiac evaluations.

A triad of back pain, flushing, and chest tightness has been reported in 13.8% of the patients (16/116) treated with DaunoXome in the randomized clinical trial and in 2.7% of treatment cycles (27/994). This triad generally occurs during the first five minutes of the infusion, subsides with interruption of the infusion, and generally does not recur if the infusion is then resumed at a slower rate. This combination of symptoms appears to be related to the lipid component of DaunoXome, as a similar set of signs and symptoms has been observed with other liposomal products not containing daunorubicin.

Daunorubicin has been associated with local tissue necrosis at the site of drug extravasation. Although no such local tissue necrosis has been observed with DaunoXome, care should be taken to ensure that there is no extravasation of drug when DaunoXome is administered.

Dosage should be reduced in patients with impaired hepatic function. (See **DOSAGE AND ADMINISTRATION**)

#### **Pregnancy Category D**

DaunoXome can cause fetal harm when administered to a pregnant woman. DaunoXome was administered to rats on gestation days 6 through 15 at 0.3, 1.0 or 2.0 mg/kg/day, (about 1/20th, 1/6th, or 1/3rd the recommended human dose on a mg/m<sup>2</sup> basis). DaunoXome produced severe maternal toxicity and embryoletality at 2.0 mg/kg/day and was embryotoxic and caused fetal malformations (anophthalmia, microphthalmia, incomplete ossification) at 0.3 mg/kg/day. Embryotoxicity was characterized by increased embryo-fetal deaths, reduced numbers of litters, and reduced litter sizes.

There are no studies of DaunoXome in pregnant women. If DaunoXome is used during pregnancy, or if the patient becomes pregnant while taking DaunoXome, the patient must be warned of the potential hazard to the fetus. Patients should be advised to avoid becoming pregnant while taking DaunoXome.

## **PRECAUTIONS**

### **Drug Interactions**

In the patient population studied, DaunoXome has been administered to patients receiving a variety of concomitant medications (e.g., antiretroviral agents, antiviral agents, anti-infective agents). Although interactions of DaunoXome (daunorubicin citrate liposome injection) with other drugs have not been observed, no systematic studies of interactions have been conducted.

### **Carcinogenesis, Mutagenesis, and Impairment of Fertility**

No carcinogenesis, mutagenesis, or impairment of fertility studies were conducted with DaunoXome.

**Carcinogenesis:** Carcinogenicity and mutagenicity studies have been conducted with daunorubicin, the active component of DaunoXome. A high incidence of mammary tumors was observed about 120 days after a single intravenous dose of 12.5 mg/kg daunorubicin in rats (about 2 times the human dose on a mg/m<sup>2</sup> basis). **Mutagenesis:** Daunorubicin was mutagenic in *in vitro* tests (Ames assay, V79 hamster cell assay), and clastogenic in *in vitro* (CCRF-CEM human lymphoblasts) and in *in vivo* (SCE assay in mouse bone marrow) tests. **Impairment of Fertility:** Daunorubicin intravenous doses of 0.25 mg/kg/day (about 8 times the human dose on a mg/m<sup>2</sup> basis) in male dogs caused testicular atrophy and total aplasia of spermatocytes in the seminiferous tubules.

**Pregnancy**

Pregnancy "Category D". See WARNINGS Section.

**Pediatric Use**

Safety and effectiveness in pediatric patients have not been established.

**Use in the Elderly**

Safety and effectiveness in the elderly have not been established.

**Special Populations**

Safety has not been established in patients with pre-existing hepatic or renal dysfunction.

**ADVERSE REACTIONS**

DaunoXome contains daunorubicin, encapsulated within a liposome. Conventional daunorubicin has acute myelosuppression as its dose limiting side effect, with the greatest effect on the granulocytic series. In addition, daunorubicin causes alopecia, and nausea and vomiting in a significant number of patients treated. Extravasation of conventional daunorubicin can cause severe local tissue necrosis. Chronic therapy at total doses above 300 mg/m<sup>2</sup> causes a cumulative-dose-related cardiomyopathy with congestive heart failure.

Administered as DaunoXome, daunorubicin has substantially altered pharmacokinetics and some differences in toxicity. The most important acute toxicity of DaunoXome remains myelosuppression, principally of the granulocytic series, with much less marked effects on the platelets and erythroid series.

In an open-label, randomized, controlled clinical trial conducted in 13 centers in the U.S.A. and Canada in advanced HIV-related Kaposi's sarcoma, two treatment regimens were compared as first line cytotoxic therapy: DaunoXome and ABV (doxorubicin (Adriamycin®), bleomycin, and vincristine). All drugs were administered intravenously every 2 weeks. The safety data presented below include all reported or observed adverse experiences, including those not considered to be drug related. Patients with advanced HIV-associated Kaposi's sarcoma are seriously ill due to their underlying infection and are receiving several concomitant medications including potentially toxic antiviral and antiretroviral agents. The contribution of the study drugs to the adverse experience profile is therefore difficult to establish.

Table III summarizes the important safety data.

**TABLE III  
SUMMARY OF IMPORTANT SAFETY DATA**

	<b>DaunoXome (N=116) % of patients</b>	<b>ABV (N=111) % of patients</b>
Neutropenia (< 1000 cells/mm <sup>3</sup> )	36%	35%
Neutropenia (< 500 cells/mm <sup>3</sup> )	15%	5%
Opportunistic Infections/Illnesses, % of patients	40%	27%
Median time to first Opportunistic Infections/Illnesses	214 days	412 days**
Number of cases with absolute reduction in ejection fraction of 20 - 25%*	3	1
Number of cases removed from therapy due to cardiac causes*	2	0
Alopecia All grades % of patients	8%	36%***
Neuropathy All grades % of patients	13%	41%***

\* The denominator is uncertain since there were several instances of missing repeat cardiac evaluations.

\*\* p = 0.21

\*\*\* p = < 0.001

A triad of back pain, flushing and chest tightness was reported in 13.8% of the patients (16/116) treated with DaunoXome in the Phase III clinical trial and in 2.7% of treatment cycles (27/994). Most of the episodes were mild to moderate in severity (12% of patients and 2.5% of treatment cycles).

Mild alopecia was reported in 6% of patients treated with DaunoXome and moderate alopecia in 2% of patients. Mild nausea was reported in 35% of DaunoXome patients, moderate nausea in 16% of patients and severe nausea in 3% of patients. For patients treated with DaunoXome, mild vomiting was reported in 10%, moderate in 10%, and severe in 3% of patients. Although grade 3 – 4 injection site inflammation was reported in 2 patients treated with DaunoXome, no instances of local tissue necrosis were observed with extravasation.

Table IV is a listing of all the mild-moderate and severe adverse events reported on both treatment arms in Protocol 103-09 in  $\geq 5\%$  of DaunoXome patients.

**TABLE IV  
ADVERSE EXPERIENCES: PROTOCOL 103-09**

	DaunoXome (N = 116)		ABV (N = 111)	
	Mild Moderate	Severe	Mild Moderate	Severe
Nausea	51%	3%	45%	5%
Fatigue	43%	6%	44%	7%
Fever	42%	5%	49%	5%
Diarrhea	34%	4%	29%	6%
Cough	26%	2%	19%	0%
Dyspnea	23%	3%	17%	3%
Headache	22%	3%	23%	2%
Allergic Reactions	21%	3%	19%	2%
Abdominal Pain	20%	3%	23%	4%
Anorexia	21%	2%	26%	2%
Vomiting	20%	3%	26%	2%
Rigors	19%	0%	23%	0%
Back Pain	16%	0%	8%	0%
Increased Sweating	12%	2%	12%	0%
Neuropathy	12%	1%	38%	3%
Rhinitis	12%	0%	6%	0%
Edema	9%	2%	8%	1%
Chest Pain	9%	1%	7%	0%
Depression	7%	3%	6%	0%
Malaise	9%	1%	11%	1%
Stomatitis	9%	1%	8%	0%
Alopecia	8%	0%	36%	0%
Dizziness	8%	0%	9%	0%
Sinusitis	8%	0%	5%	1%
Arthralgia	7%	0%	6%	0%
Constipation	7%	0%	18%	0%
Myalgia	7%	0%	12%	0%
Pruritus	7%	0%	14%	0%
Insomnia	6%	0%	14%	0%
Influenza-like symptoms	5%	0%	5%	0%
Tenesmus	4%	1%	1%	0%
Abnormal vision	3%	2%	3%	0%

The following adverse events were reported in  $\leq 5\%$  of patients treated with DaunoXome, tabulated by body system.

**Body As A Whole:** Injection site inflammation

**Cardiovascular:** Hot flushes, hypertension, palpitation, syncope, tachycardia. In other follow-up clinical trials of DaunoXome (daunorubicin citrate liposome injection) use in treatment of Kaposi's sarcoma or other malignancies, the following serious cardiac events were reported: Pericardial effusion, pericardial tamponade, ventricular extrasystoles, cardiac arrest, sinus tachycardia, atrial fibrillation, pulmonary hypertension, myocardial infarction, supraventricular tachycardia, angina pectoris (see WARNINGS section).

**Digestive:** Increased appetite, dysphagia, GI hemorrhage, gastritis, gingival bleeding, hemorrhoids, hepatomegaly, melena, dry mouth, tooth caries

**Hemic and Lymphatic:** Lymphadenopathy, splenomegaly

**Metabolic and Nutritional:** Dehydration, thirst

**Nervous:** Amnesia, anxiety, ataxia, confusion, convulsions, emotional lability, abnormal gait, hallucination, hyperkinesia, hypertonia, meningitis, somnolence, abnormal thinking, tremor

**Respiratory:** Hemoptysis, hiccups, pulmonary infiltration, increased sputum

**Skin:** Folliculitis, seborrhea, dry skin

**Special Senses:** Conjunctivitis, deafness, earache, eye pain, taste perversion, tinnitus

**Urogenital:** Dysuria, nocturia, polyuria

## **OVERDOSAGE**

The symptoms of acute overdosage are increased severities of the observed dose-limiting toxicities of therapeutic doses of DaunoXome, myelosuppression (especially granulocytopenia), fatigue, and nausea and vomiting.

## **DOSAGE AND ADMINISTRATION**

DaunoXome should be administered intravenously over a 60 minute period at a dose of  $40 \text{ mg/m}^2$ , with doses repeated every two weeks. Blood counts should be repeated prior to each dose, and therapy withheld if the absolute granulocyte count is less than  $750 \text{ cells/mm}^3$ . Treatment should be continued until there is evidence of progressive disease (e.g., based on best response achieved: new visceral sites of involvement, or progression of visceral disease; development of 10 or more new, cutaneous lesions or a 25% increase in the number of lesions compared to baseline; a change in the character of 25% or more of all previously counted flat lesions to raised; increase in surface area of the indicator lesions), or until other intercurrent complications of HIV disease preclude continuation of therapy.

### **Patients with Impaired Hepatic and Renal Function**

Limited clinical experience exists in treating hepatically and renally impaired patients with DaunoXome.

Therefore, based on experience with daunorubicin HCl, it is recommended that the dosage of DaunoXome be reduced if the bilirubin or creatinine is elevated as follows: Serum bilirubin 1.2 to 3 mg/dL, give  $\frac{3}{4}$  the normal dose; serum bilirubin or creatinine  $> 3 \text{ mg/dL}$ , give  $\frac{1}{2}$  the normal dose.



Do not mix DaunoXome with other drugs.

### **Preparation Of Solution**

DaunoXome should be diluted 1:1 with 5% Dextrose Injection (D5W) before administration. Each vial of DaunoXome contains daunorubicin citrate equivalent to 50 mg daunorubicin base, at a concentration of 2 mg/mL. The recommended concentration after dilution is 1 mg daunorubicin/mL of solution.

### **Use aseptic technique.**

Aseptic technique must be strictly observed in all handling, since no preservative or bacteriostatic agent is present in DaunoXome or in the materials recommended for dilution.

Withdraw the calculated volume of DaunoXome from the vial into a sterile syringe, and transfer it into a sterile infusion bag containing an equivalent amount of D5W. Administer diluted DaunoXome immediately. If not used immediately, diluted DaunoXome should be refrigerated at 2°– 8 °C (36°– 46°F) for a maximum of 6 hours.

**Caution: The only fluid which may be mixed with DaunoXome is D5W; DaunoXome must not be mixed with saline, bacteriostatic agents such as benzyl alcohol, or any other solution.**

Do not use an in-line filter for the intravenous infusion of DaunoXome.

**All parenteral drug products should be inspected visually for particulate matter and discoloration prior to administration, whenever solution and container permit. DaunoXome is a translucent dispersion of liposomes that scatters light to some degree. Do not use DaunoXome if it appears opaque, or has precipitate or foreign matter present.**

Procedures for proper handling and disposal of anticancer drugs should be followed.<sup>1-8</sup>

### **HOW SUPPLIED**

DaunoXome is a translucent, red, liposomal dispersion supplied in single use vials, each sealed with a synthetic rubber stopper and aluminum sealing ring with a plastic cap. DaunoXome provides daunorubicin citrate equivalent to 50 mg of daunorubicin base, at a concentration of 2 mg/mL.

DaunoXome is supplied under NDC 10885-001-01 for a single unit pack.

### **Storage**

Store DaunoXome in a refrigerator, 2°–8°C (36°–46°F). Do not freeze. Protect from light.

### **REFERENCES**

1. ONS Clinical Practice Committee. Cancer Chemotherapy Guidelines and Recommendations for Practice. Pittsburg, Pa: Oncology Nursing Society; 1999:32–41.
2. Recommendations for the Safe Handling of Parenteral Antineoplastic Drugs. Washington, DC: Division of Safety, Clinical Center Pharmacy Department and Cancer Nursing Services, National Institutes of Health; 1992. US Dept of Health and Human Services, Public Health Service Publication NIH 92-2621.
3. AMA Council on Scientific Affairs. Guidelines for Handling Parenteral Antineoplastics. *JAMA*. 1985;253:1590–1591.

4. National Study Commission on Cytotoxic Exposure - Recommendations for Handling Cytotoxic Agents. 1987. Available from Louis P. Jeffrey, Sc.D., Chairman, National Study Commission on Cytotoxic Exposure. Massachusetts College of Pharmacy and Allied Health Sciences, 179 Longwood Avenue, Boston, MA 02115.
5. Clinical Oncological Society of Australia. Guidelines and Recommendations for Safe Handling of Antineoplastic Agents. *Med J Australia*. 1983;1:426-428.
6. Jones RB, Frank R, Mass T. Safe Handling of Chemotherapeutic Agents: A Report from the Mount Sinai Medical Center. *CA-A Cancer J for Clin*. 1983;33:258-263.
7. American Society of Hospital Pharmacists. ASHP Technical Assistance Bulletin on Handling Cytotoxic and Hazardous Drugs. *Am J Hosp Pharm*. 1990;47:1033-1049.
8. Controlling Occupational Exposure to Hazardous Drugs. (OSHA Work-Practice Guidelines). *Am J Health-Syst Pharm*. 1996;53:1669-1685.

GALEN LOGO

Manufactured for  
Galen US Inc.  
25 Fretz Road  
Souderton  
PA 18964

**For medical information about DaunoXome (daw-nuh-zome), call 1-800-280-5708**

DaunoXome is a registered trademark of Galen Limited.  
Copyright 2011, Galen Limited.

All rights reserved.

Rev. December 2011

# CANCER RESEARCH

Clinical Trials

## Abstract B14: CA 19-9 levels in patients with metastatic pancreatic adenocarcinoma receiving first-line therapy with liposomal irinotecan plus 5-fluorouracil/leucovorin and oxaliplatin (NAPOX)

Farshid Dayyani, Patrick M. Boland, Andrew Dean, Christopher H. Lieu, Teresa Macarulla, Bin Zhang, Bruce Belanger, Yan Moore, Fiona Maxwell, Tiffany Wang, and Zev A. Weinberg

DOI: 10.1159/1538-7445.PANCA19-B14 Published December 2019

Article

Info & Metrics

Abstracts: AACR Special Conference on Pancreatic Cancer: Advances in Science and Clinical Care; September 6-9, 2019; Boston, MA

### Abstract

**Introduction:** Liposomal irinotecan (nal-IRI) plus 5-fluorouracil/leucovorin (5-FU/LV) is approved for patients with metastatic pancreatic adenocarcinoma (mPAC) after disease progression following gemcitabine-based therapy. The combination of nal-IRI+5-FU/LV plus oxaliplatin (NAPOX) is being investigated as first-line treatment for patients with mPAC in a phase 1/2, open-label, dose exploration and dose expansion study (NCT02551991). This exploratory analysis investigated changes in carbohydrate antigen (CA) 19-9 levels, and their association with response rates, in patients with mPAC receiving NAPOX.

**Methods:** After establishing a recommended dose in the exploration phase of study NCT02551991 (nal-IRI 50 mg/m<sup>2</sup> [free-base equivalent], oxaliplatin 60 mg/m<sup>2</sup>, LV 400 mg/m<sup>2</sup>, 5-FU 2400 mg/m<sup>2</sup> on days 1 and 15 of each 28-day cycle), 25 patients were enrolled into the dose expansion phase, resulting in a total of 32 patients treated at the selected dose level (pooled population; PP). The data cut-off for this interim analysis was when all treated patients had completed at least 16 weeks of follow-up. CA 19-9 levels were assessed at baseline and up to week 16.

**Results:** Overall, 30 of the 32 treated patients in the PP had available CA 19-9 data at baseline. The median CA 19-9 level at baseline was 316 U/mL, with 23 (77%) patients having baseline CA 19-9 levels above the normal level (>37 U/mL). Among patients with baseline CA 19-9 levels >37 U/mL and measurements up to week 16 (n = 17), the median best reduction from baseline in CA 19-9 was 35.9%; a best CA 19-9 reduction of ≥20%, ≥50%, and ≥70% was achieved by 59% (10/17), 41% (7/17), and 24% (4/17) of patients, respectively. A total of 72% (23/32) treated patients achieved disease control by week 16 (DCR16), and the overall response rate (ORR; complete response or partial response over entire follow-up period) was 34% (11/32). In treated patients with any reduction in CA 19-9 by week 16, the DCR16 rate was 88% (14/16) and the ORR was 83% (10/16). Among patients with above-normal baseline CA 19-9 levels and any CA 19-9 reduction by week 16, the DCR16 rate was 83% (10/12) and the ORR was 67% (8/12). Rates of DCR16 and ORR increased with greater CA 19-9 reductions, reaching 100% and 75-83%, respectively, in patients with a CA 19-9 decrease of ≥70%.

**Conclusion:** In patients with mPAC, first-line NAPOX therapy (with a dosing schedule of nal-IRI 50 mg/m<sup>2</sup>, oxaliplatin 60 mg/m<sup>2</sup>, LV 400 mg/m<sup>2</sup>, and 5-FU 2400 mg/m<sup>2</sup> on days 1 and 15 of each 28-day cycle) resulted in substantial reductions in CA 19-9 levels from baseline, indicative of antitumor activity. Response rates were higher in patients with greater CA 19-9 reductions. Further assessment of CA19-9 levels and response rates over a longer follow-up period is ongoing.

**Citation Format:** Farshid Dayyani, Patrick M. Boland, Andrew Dean, Christopher H. Lieu, Teresa Macarulla, Bin Zhang, Bruce Belanger, Yan Moore, Fiona Maxwell, Tiffany Wang, Zev A. Weinberg. CA 19-9 levels in patients with metastatic pancreatic adenocarcinoma receiving first-line therapy with liposomal irinotecan plus 5-fluorouracil/leucovorin and oxaliplatin (NAPOX) [abstract]. In: Proceedings of the AACR Special Conference on Pancreatic Cancer: Advances in Science and Clinical Care; 2019 Sept 6-9; Boston, MA. Philadelphia (PA): AACR; Cancer Res 2019;79(24 Suppl):Abstract nr B14.



December 2019  
Volume 79, Issue 24 Supplement  
Table of Contents

- 1111-1111
- 1111-1111
- 1111-1111
- 1111-1111
- 1111-1111
- 1111-1111
- 1111-1111
- 1111-1111

Search this issue



Sign up for alerts

Request Permissions

Share

Article Alerts

Print

Email Article

Cite

Citation Tools

Related Articles

No related articles found.

Google Scholar

Cited By...

More in this TOC Section

Home

Alerts

Feedback

Privacy Policy



Articles

Online First

Current Issue

Past Issues

Meeting Abstracts

Info for

Authors

Subscribers

Advertisers

Librarians

[Reviews](#)

[About Cancer Research](#)

[About the Journal](#)

[Editorial Board](#)

[Permissions](#)

[Submit a Manuscript](#)

Copyright © 2020 by the American Association for Cancer Research.

*Cancer Research Online* ISSN: 1538-7440

*Cancer Research Print* ISSN: 0008-5472

*Journal of Cancer Research* ISSN: 0008-7015

*American Journal of Cancer* ISSN: 0732-183x



# A phase I clinical and pharmacokinetic study of capecitabine (Xeloda<sup>®</sup>) and irinotecan combination therapy (XELIRI) in patients with metastatic gastrointestinal tumours

J.P. Delord<sup>1</sup>, J.Y. Pierga<sup>2</sup>, V. Dieras<sup>2</sup>, F. Bertheault-Cvitkovic<sup>3</sup>, F.L. Turpin<sup>3</sup>, F. Lokiec<sup>3</sup>, I. Lochon<sup>1</sup>, E. Chatelut<sup>1</sup>, P. Canat<sup>1</sup>, R. Guimbaud<sup>1</sup>, D. Mery-Mignard<sup>4</sup>, X. Cornen<sup>5</sup>, Z. Mouri<sup>5</sup> and R. Bugat<sup>1</sup>

<sup>1</sup>Institut Claudius Regaud, 20-24, rue du Port Saint Pierre, Toulouse 31052, France; <sup>2</sup>Institut Curie, Paris, France; <sup>3</sup>Centre René Huguenin, Saint-Cloud, France; <sup>4</sup>Aventis Pharmaceuticals, Paris, France; <sup>5</sup>Roche, Paris, France

Capecitabine is a highly active oral fluoropyrimidine that is an attractive alternative to 5-fluorouracil in colorectal cancer treatment. The current study, undertaken in 27 patients with gastrointestinal tumours, aimed to assess the toxicity and potential for significant pharmacokinetic interactions of a combination regimen incorporating capecitabine with 3-weekly irinotecan (XELIRI). Irinotecan (200 and 250 mg m<sup>-2</sup>) was administered as a 90-min infusion on day 1 in combination with escalating capecitabine doses (700–1250 mg m<sup>-2</sup> twice daily) administered on days 2–15 of a 3-week treatment cycle. Pharmacokinetics were characterised on days 1 and 2 of the first two cycles. A total of 103 treatment cycles were administered. The principal dose-limiting toxicities were diarrhoea and neutropenia. Capecitabine 1150 mg m<sup>-2</sup> twice daily with irinotecan 250 mg m<sup>-2</sup> was identified as the maximum-tolerated dose and capecitabine 1000 mg m<sup>-2</sup> with irinotecan 250 mg m<sup>-2</sup> was identified as the recommended dose for further study. Analyses confirmed that there were no significant pharmacokinetic interactions between the two agents. The combination was clinically active, with complete and partial responses achieved in heavily pretreated patients. This study indicates that XELIRI is a potentially feasible and clinically active regimen in patients with advanced gastrointestinal cancer.

British Journal of Cancer (2005) 92, 820–826. doi:10.1038/sj.bjc.6602354 www.bjccancer.com

Published online 1 March 2005

© 2005 Cancer Research UK

**Keywords:** capecitabine; irinotecan; phase I; pharmacokinetic

5-Fluorouracil (5-FU) has been the backbone of treatment for colorectal cancer (CRC) for more than 40 years. During this time, a number of schedules and regimens have been investigated. Irinotecan, a topoisomerase I inhibitor, is an effective treatment in patients with advanced/metastatic CRC unresponsive or resistant to 5-FU-based chemotherapy. Two pivotal, phase III studies in metastatic CRC, which demonstrated superior survival for irinotecan compared with best supportive care and infused 5-FU-based therapy, established irinotecan as a new agent for the second-line treatment of 5-FU-pretreated CRC (Cunningham *et al*, 1998; Rougier *et al*, 1998). In addition, combination of irinotecan with intravenous 5-FU/leucovorin (LV) was shown to significantly improve response rate, time to disease progression (TTP) and overall survival compared with 5-FU/LV alone in patients with previously untreated metastatic CRC (Douillard *et al*, 2000; Saltz *et al*, 2000). Recently, however, a high incidence of early treatment-related deaths was noted with the administration of the weekly irinotecan plus bolus intravenous 5-FU/LV schedule in this setting, and it has been suggested that continuous infusion 5-FU may be a

safer option than bolus 5-FU for combination with irinotecan (Rothenberg *et al*, 2001).

Capecitabine (Xeloda; F Hoffmann-La Roche, Nutley, NJ, USA) is an oral fluoropyrimidine carbamate, which was rationally designed to mimic continuous infusion 5-FU. With capecitabine, 5-FU is generated preferentially in tumour tissue through high intratumoral concentrations of thymidine phosphorylase (TP) (Miwa *et al* 1998; Schüller *et al* 2000). Human pharmacokinetic studies, using validated methods for estimation of capecitabine and its metabolites, have shown that capecitabine is rapidly and almost completely absorbed through the gastrointestinal wall (Reigner *et al*, 2001). Capecitabine is metabolised to 5-FU via a three-step enzymatic cascade (Miwa *et al* 1998). In the first step, capecitabine is hydrolysed by hepatic carboxylesterase to 5'-deoxy-5-fluorocytidine (5'-DFCR), which is in turn converted by cytidine deaminase to 5'-deoxy-5-fluorouridine (5'-DFUR), the immediate precursor of 5-FU. The final step in the activation to 5-FU is mediated by TP, an enzyme that is highly active in tumour tissue compared with healthy tissue (Miwa *et al*, 1998).

Capecitabine is replacing 5-FU in CRC treatment. Two large, phase III trials including more than 1200 patients have demonstrated that, as first-line therapy for metastatic CRC, capecitabine achieves significantly superior response rates, with at least equivalent TTP and overall survival compared with 5-FU/LV (Hoff *et al*, 2001; Van Cutsem *et al*, 2001, 2004). Notably, the superior

\*Correspondence: Dr J.P. Delord; E-mail: delord\_j@icr.fndccc.fr

Received 9 August 2004; revised 19 November 2004; accepted 23 November 2004; published online 1 March 2005

tumour response rate for capecitabine was particularly pronounced among the subpopulation of patients who had received prior adjuvant treatment with 5-FU. Capecitabine demonstrated an improved safety profile compared with 5-FU/LV and is associated with a very low incidence of alopecia and myelosuppression (Cassidy *et al*, 2002). The only adverse event occurring more frequently with capecitabine than with 5-FU/LV is hand-foot syndrome, which is easily managed by treatment interruption and dose reduction, and is never life threatening. Phase II studies of capecitabine in gastric and pancreatic cancer have also shown promising activity and a favourable safety profile (Cartwright *et al*, 2002; Hong *et al*, 2002; Koizumi *et al*, 2003).

In addition, capecitabine is a highly active component of combination treatment for metastatic CRC. A large international study has shown that capecitabine is highly active in combination with oxaliplatin, achieving a response rate of 55%, median TTP of 7.7 months and overall survival of 19.5 months as first-line therapy (Cassidy *et al*, 2004). The combination of capecitabine and irinotecan is supported by their different mechanisms of action. In preclinical evaluation, the combination of capecitabine and irinotecan demonstrated at least additive activity and was highly curative in tumour xenograft models (Cao *et al* 2001; Hapke *et al*, 2001). Additionally, capecitabine and irinotecan show only partial overlap of key toxicities. The predominant adverse events associated with irinotecan are neutropenia and diarrhoea. In a phase II study of 3-weekly irinotecan in patients with metastatic CRC, Grade 3/4 neutropenia and diarrhoea were observed in 40 and 26% of patients, respectively (Van Cutsem *et al*, 1999). Capecitabine is also associated with diarrhoea, but only minimal myelosuppression. In an integrated analysis of two large phase III trials of capecitabine in patients with metastatic CRC, Grade 3/4 diarrhoea was reported in 13% of patients, but Grade 3/4 neutropenia was observed in only 2% of patients (Cassidy *et al*, 2002). The significantly lower rates of diarrhoea and neutropenia occurring with capecitabine compared with 5-FU/LV (Mayo Clinic regimen) observed in these trials suggest that capecitabine may also be a better-tolerated combination partner for irinotecan.

The metabolic activation of both irinotecan and capecitabine is dependent on hepatic carboxylesterase activity. Irinotecan is cleaved by hepatic carboxylesterases to form the active metabolite SN-38, which is a potent inhibitor of topoisomerase I (Kuhn, 1998). As discussed above, the first step of the tumour-specific activation of capecitabine is conversion to the intermediate 5'-DFCR by hepatic carboxylesterase (Miwa *et al*, 1998). Consequently, there is potential for pharmacokinetic interaction between irinotecan and capecitabine.

There is therefore a clear rationale for investigating capecitabine in combination with irinotecan in patients with advanced gastrointestinal cancer. The current phase I clinical and pharmacokinetic study assessed the feasibility of combination therapy with capecitabine and irinotecan (XELIRI) in patients with advanced/metastatic gastrointestinal tumours. The primary objective of the study was to determine the maximum-tolerated dose (MTD) and dose-limiting toxicities (DLTs) of capecitabine, administered twice daily, on days 2–15 in combination with irinotecan, administered as a 90-min infusion, on day 1 of a 21-day treatment cycle. In addition, the study investigated whether significant pharmacokinetic interactions occur between the component agents, and evaluated the safety profile and antitumour activity of the XELIRI regimen.

## PATIENTS AND METHODS

This phase I, open-label, dose-escalation study of capecitabine and irinotecan combination therapy in patients with solid tumours of the gastrointestinal tract was conducted in three French Cancer

Centres, in accordance with the International Good Practice principles and local ethical and regulatory requirements.

## Eligibility

The study included patients aged 18–75 years with histologically proven gastrointestinal tract cancer and no satisfactory options for further treatment. Patients were required to have a life expectancy  $\geq 3$  months, Eastern Cooperative Oncology Group (ECOG) performance status 0–2, absolute neutrophil count  $\geq 2000 \mu\text{l}^{-1}$ , platelet count  $\geq 100\,000 \mu\text{l}^{-1}$ , haemoglobin  $\geq 10 \text{ g dl}^{-1}$ , serum creatinine  $\leq 1.25 \mu\text{mol l}^{-1}$ , total bilirubin  $\leq 1.25$  times the upper normal limit (UNL), transaminases  $\leq 3$  times UNL, as well as prothrombin time and international normalised ratio within normal limits, and no evidence of severe infection, intestinal occlusion or subocclusion, or central nervous system metastasis. All patients provided written informed consent prior to study-specific screening procedures.

Patients were excluded from the study if they had received previous treatment with a topoisomerase inhibitor (irinotecan or other) or capecitabine, or had previously experienced allergic reactions to 5-FU. Additionally, patients were excluded if they had previously received total body irradiation or abdominopelvic radiation. Patients undergoing major abdominal surgery within 4 weeks of study entry or those with a history of serious cardiovascular disorder or renal, hepatic or metabolic disease that could potentially compromise the metabolism of the study drug were also excluded. Additional exclusion criteria included treatment with 5-FU within 4 weeks of study entry or with mitomycin C, nitrosourea compounds or extended radiation therapy within 6 weeks of study entry.

## Drug administration and dose escalation

Escalating doses of irinotecan ( $200$ – $350 \text{ mg m}^{-2}$ ) were administered in an intravenous infusion over 90 min on day 1 of a 3-weekly treatment cycle. Oral capecitabine ( $700$ – $1250 \text{ mg m}^{-2}$ ) was administered twice daily (approximately 12 h apart), within 30 min after a meal, on days 2–15. Antiemetic and anti-diarrhoeal treatments and preventative therapy for irinotecan-induced early-onset anticholinergic syndrome were administered according to the policies at each centre.

At least three patients were recruited at each dose level and the dose was escalated when three patients had completed two treatment cycles without DLTs. If one or more of the three patients developed a DLT, the dose level was expanded to a total of at least six patients. If fewer than three of the six patients experienced a DLT, dose escalation was permitted, but if three or more of six patients experienced a DLT at a single dose level, that dose level was identified as the MTD. The dose level preceding the MTD was identified as the recommended dose and three additional patients were treated at this dose. No inpatient dose escalation was permitted.

The maximum duration of treatment was six cycles. After this time, further treatment could be administered at the discretion of the investigator.

## Dose-limiting toxicities

Adverse events were classified according to the National Cancer Institute (NCI) Common Toxicity Criteria (CTC) Version 2.0. (1999). Any of the following toxicities occurring during the first two cycles of chemotherapy were considered dose limiting: any Grade 3 or 4 nonhaematologic toxicity (excluding alopecia and nausea); Grade 4 neutropenia or Grade 4 thrombocytopenia lasting for more than 7 days or accompanied by concomitant infection or bleeding, respectively; febrile neutropenia; nausea or vomiting preventing intake of capecitabine for at least 3 consecutive days;

and any treatment-related adverse event causing a delay in the administration of the second treatment cycle.

### Patient and tumour evaluation

Patients were evaluated at baseline, on a weekly basis during the first two treatment cycles and at 3-weekly intervals thereafter. Evaluations included a complete clinical examination and recording of all adverse events, including severity and outcome. Complete blood counts (CBC) were performed at least twice weekly and blood chemistry analysis was performed weekly. A clinical tumour evaluation was performed during these visits, with the objective of detecting disease progression. A final evaluation, including a complete clinical examination, assessment of adverse events, CBC and blood chemistry analysis was conducted at the end of treatment.

In patients with measurable disease, tumour evaluation, based on World Health Organization (WHO) criteria, was performed at baseline, every 3 weeks for 6 weeks and at 9-weekly intervals thereafter. The best overall response was defined as the best response recorded from the start of treatment to disease progression. Complete responses (CR) and partial responses (PR) were confirmed by a second tumour assessment after 4 weeks. TTP was defined as the time from the start of treatment until disease progression.

### Pharmacokinetic evaluation

Pharmacokinetic evaluation was conducted during cycles 1 and 2. To determine the pharmacokinetics of irinotecan, blood was sampled for analysis of irinotecan and its metabolites 7-ethyl-10-hydroxycamptothecin (SN-38), SN-38 glucuronide and 7-ethyl-10-[4-*N*-(5-aminoheptanoic acid)-1-piperidino]-carbonyloxycamptothecin (APC) on day 1. Sampling times for irinotecan analysis included pretreatment and 3.0, 3.5, 9.5, 11.5, and 24.0 h after the start of the 90-min intravenous infusion. Plasma was recovered immediately after blood collection and the concentrations of irinotecan and its metabolites were measured by high-performance liquid chromatography (HPLC) as described previously (Rivory and Robert, 1995). Estimates of pharmacokinetic parameters of irinotecan and SN-38 were obtained by Bayesian analysis and POSTHOC option using the NONMEM program (version V, level 1.1, GloboMax Inc., Hanover, MD, USA) and a database of 67 previously evaluated samples (Chabot *et al*, 1995). The plasma area under the concentration-time curves (AUCs) of SN-38 glucuronide were determined using a limited-sampling method with stepwise linear regression, as recommended by Mick *et al* (1996). Plasma AUC of APC was determined by trapezoidal rule up to 24 h after the beginning of the irinotecan infusion (without extrapolation to infinity). The AUC values of irinotecan and its metabolites were compared between cycle 1 (before capecitabine administration) and cycle 2 (after a 2-week period of capecitabine treatment and 1-week wash-out) by using a paired Student's *t*-test.

For analysis of capecitabine and its metabolites, blood samples were collected on day 2 before capecitabine administration and at 0.5, 1.0, 2.0, 3.0, 4.0, 6.0, 8.0 and 12.0 h after administration. Plasma was recovered immediately after blood collection and concentrations of capecitabine and its metabolites 5'-DFCR, 5'-DFUR and 5-FU were measured using a validated reversed-phase HPLC technique with ultraviolet detection, slightly modified from the one described previously (Reigner *et al*, 1998). The AUC values were calculated using the linear trapezoidal rule. For capecitabine and its metabolites, the pharmacokinetic analysis was performed using the MicroPharm software (S Urien, Inserm-CR18, Saint-Cloud, France) and the Statview program (Abacus Concept Inc., USA) was used for the statistical analysis of the pharmacokinetic parameters.

## RESULTS

### Patient characteristics and disposition

A total of 27 patients were recruited to the study, from November 1999 to December 2001, of whom all were evaluable for safety, with 23 evaluable for tumour response. Patient characteristics are summarised in Table 1. The median age was 58 years (range 33–72 years) and the majority of patients (93%) had ECOG performance status 0 or 1. Most patients (78%) had CRC, four patients (15%) had gastric cancer and two patients (7%) had pancreatic cancer. With the exception of one tumour with epidermal histology, all tumours were adenocarcinomas and all patients had stage IV disease at study entry. Most patients had undergone prior surgery (85%) and had received previous chemotherapy, including 5-FU (81%).

### DLTs and recommended dose level

No DLTs occurred in patients treated at dose levels 1–3 (Table 2). At dose level 4 (capecitabine 1000 mg m<sup>-2</sup> twice daily and irinotecan 250 mg m<sup>-2</sup>), one patient developed Grade 3 diarrhoea and Grade 4 neutropenia with septicaemia on day 6 of the first cycle. No further DLTs were experienced by the six patients treated at this dose level. Three of six patients treated at dose level 5 (capecitabine 1150 mg m<sup>-2</sup> twice daily and irinotecan 250 mg m<sup>-2</sup>) developed DLTs: one patient experienced Grade 3 diarrhoea and abdominal pain by day 11 of the first cycle; one patient experienced Grade 3 diarrhoea and Grade 4 neutropenia on day 8 of the second cycle; and a further patient developed Grade 4 diarrhoea and Grade 3 vomiting by day 15 of the second cycle. To confirm the recommended dose, three additional patients were treated at dose level 4. As one patient

**Table 1** Baseline patient demographics (*n* = 27)

Parameter	No. (%)
Median age, years (range)	58 (33–72)
Gender	
Male	18 (67)
Female	9 (33)
ECOG performance status	
0	13 (48)
1	12 (45)
2	2 (7)
Primary tumour site	
Colorectal	21 (78)
Gastric	4 (15)
Pancreas	2 (7)
Histology	
Adenocarcinoma	26 (96)
Squamous cell carcinoma	1 (4)
Median number of metastatic lesions (range)	3 (1–5)
Prior treatment	
Surgery	23 (85)
Radiotherapy	6 (22)
No. of prior chemotherapy regimens <sup>a</sup>	
0	5 (19)
1	13 (48)
2	3 (11)
> 2	6 (22)

ECOG = Eastern Cooperative Oncology Group; 5-FU = 5-fluorouracil. <sup>a</sup>All regimens, including 5-FU.



**Table 2** Incidence of DLTs during dose escalation

Dose level	Capecitabine (mg m <sup>-2</sup> twice daily)	Irinotecan (mg m <sup>-2</sup> )	No. of patients		
			Treated	With DLT	DLTs
1	700	200	4	0	
2	850	200	3	0	
3	1000	200	4	0	
4	1000	250	10	1	Grade 3 diarrhoea, Grade 4 neutropenia/septicaemia
5	1150	250	6	3	Grade 3 diarrhoea/abdominal pain Grade 3 diarrhoea/Grade 4 neutropenia Grade 4 diarrhoea/Grade 3 vomiting

DLTs = dose-limiting toxicities.

was not evaluable for safety, a total of 10 patients were treated at this dose level. No further DLTs were observed. Therefore, the MTD was dose level 5 (capecitabine 1150 mg m<sup>-2</sup> twice daily and irinotecan 250 mg m<sup>-2</sup>) and dose level 4 (capecitabine 1000 mg m<sup>-2</sup> twice daily and irinotecan 250 mg m<sup>-2</sup>) was identified as the recommended dose for further phase II study. Overall, among the 10 patients treated at dose level 4, only one patient experienced a DLT.

### Safety profile

A total of 103 treatment cycles were administered to 27 patients and 16 patients received at least four cycles. The median duration of treatment was 2.8 months (range 0.07–16.1 months). Of the 10 patients treated at dose level 4, six patients received four or more treatment cycles. No cumulative toxicities were observed in patients completing more than four cycles.

The most frequent treatment-related adverse events were gastrointestinal disturbances, and the majority of cases were mild or moderate in intensity. Table 3 shows the incidence of Grade 3/4 adverse events by dose level. The only Grade 4 adverse events were diarrhoea in two patients (treated at dose level 5), nausea and vomiting, each in one patient (treated at dose level 4), and neutropenia in two patients (one treated at dose level 4, the other at dose level 5). Notably, only one patient (treated at dose level 3) experienced Grade 3 hand-foot syndrome.

### Pharmacokinetics

During cycle 1, plasma samples for pharmacokinetic studies were obtained from 23 patients on days 1 and 2. Pharmacokinetic data were evaluated in 23 patients during cycle 2. The mean AUC values for irinotecan and its metabolites are shown in Table 4. There were no significant differences between cycles 1 and 2 in AUC values for both irinotecan and SN-38. The AUC values of SN-38 glucuronide and APC were significantly different ( $P < 0.05$ ) between cycles 2 and 1 (% change from cycles 1 to 2: +15.3 and -19.3%, respectively). The mean AUC values for capecitabine, 5'-DFCR, 5'-DFUR and 5-FU are shown in Table 5. No significant differences were observed between cycles 1 and 2 at dose levels 1–5.

### Antitumour activity

Among 23 evaluable patients, an objective response to treatment was observed in two pretreated patients with CRC: a CR in one patient treated at dose level 4 and a PR in one patient treated at dose level 5 (Table 6). In addition, four patients achieved disease stabilisation. Among the eight evaluable patients treated at dose level 4 (the recommended dose for phase II evaluation), median TTP was 3.5 months (range 1.4–10.2 months).

**Table 3** Grade 3/4 treatment-related adverse events

Dose level	Adverse events: Grade 3/Grade 4				
	1 (n = 4)	2 (n = 3)	3 (n = 4)	4 (n = 10)	5 (n = 6)
Capecitabine (mg m <sup>-2</sup> twice daily)	700	850	1000	1000	1150
Irinotecan (mg m <sup>-2</sup> )	200	200	200	250	250
Nausea	1/0	0/0	1/0	0/1	2/0
Diarrhoea	1/0	0/0	1/0	2/0	1/2
Vomiting	1/0	0/0	0/0	0/1	2/0
Stomatitis	0/0	0/0	0/0	0/0	1/0
Anaemia	1/0	0/0	1/0	0/0	0/0
Abdominal pain	0/0	0/0	0/0	0/0	1/0
Hand-foot syndrome	0/0	0/0	1/0	0/0	0/0
Leucopenia	1/0	0/0	0/0	1/0	1/0
Lymphopenia	0/0	0/0	0/0	0/0	2/0
Neutropenia	2/0	0/0	0/0	1/1	0/1

### DISCUSSION

This study demonstrates that XELIRI (capecitabine plus irinotecan) is a feasible and promising new treatment for patients with metastatic gastrointestinal tumours. The recommended dosing schedule was identified as capecitabine 1000 mg m<sup>-2</sup> twice daily on days 2–15 in combination with irinotecan 250 mg m<sup>-2</sup>, administered as a 90-min infusion, on day 1 of every 21-day cycle.

The benefits of combination therapy with irinotecan and 5-FU are well established, with phase III studies showing that the addition of irinotecan to intravenous 5-FU/LV significantly improves efficacy, including overall survival, compared with 5-FU/LV alone in patients with previously untreated metastatic CRC (Douillard *et al*, 2000; Saltz *et al*, 2000). It has been suggested that continuous infusion 5-FU may be a safer option in combination with irinotecan than bolus 5-FU (Rothenberg *et al*, 2001). Capecitabine is an oral agent providing chronic dosing that mimics continuous infusion 5-FU with a favourable safety profile compared with bolus intravenous 5-FU/LV (Hoff *et al*, 2001; Van Cutsem *et al*, 2001; Cassidy *et al*, 2002). Twice daily dosing with oral capecitabine offers numerous opportunities for dose adjustment during the treatment cycle, allowing safety to be readily optimised in patients receiving XELIRI. In addition, tumour-activated capecitabine may offer an enhanced therapeutic index via the generation of 5-FU preferentially in tumour. Replacement of infused 5-FU/LV with oral capecitabine is expected to simplify and improve the convenience of irinotecan/fluoropyrimidine combination therapy, because the XELIRI regimen requires only one clinic visit per 3-week cycle and avoids the inconvenience and potential complications associated with the protracted intravenous access required with infusional regimens.

The current phase I/pharmacokinetic study has demonstrated the feasibility of XELIRI. The MTD was identified as irinotecan

**Table 4** Mean AUC values for irinotecan and its metabolites

	AUC $\mu\text{g ml}^{-1} \text{h}$ (CV, %)							
	Irinotecan		SN-38		SN-38 glucuronide		APC	
	Cycle 1	Cycle 2	Cycle 1	Cycle 2	Cycle 1	Cycle 2	Cycle 1	Cycle 2
Dose levels 1–3 (n = 10)	11.6 (25)	11.9 (28)	0.518 (62)	0.539 (57)	0.838 (33)	0.909 (43) <sup>a</sup>	2.24 (59) <sup>a</sup>	2.25 (44)
Dose levels 4 and 5 (n = 13)	14.9 (41)	16.0 (51)	0.587 (113)	0.640 (87)	0.876 (66)	1.043 (77)	1.61 (37) <sup>b</sup>	1.34 (40) <sup>a</sup>
Cycle 2 vs cycle 1 (% change $\pm$ 95% CI)	+6.2 ( $\pm$ 10.1)		+16.4 ( $\pm$ 20.2)		+15.3 ( $\pm$ 13.0)		–19.3% ( $\pm$ 15.3)	
P-value	NS		NS		<0.05		<0.05	

AUC = area under the curve; SN-38 = 7-ethyl-10-hydroxycamptothecin; APC = 7-ethyl-10-[4-N-(5-aminopeptanoic acid)-1-piperidino]-carbonyloxycamptothecin; NS = not significant. <sup>a</sup>Not available for one patient. <sup>b</sup>Not available for two patients.

**Table 5** Mean AUC values for capecitabine, 5-FU and its metabolites

Capecitabine twice daily dose ( $\text{mg m}^{-2}$ )	AUC <sub>(0–12h)</sub> (s.d.) ( $\text{mg ml}^{-1} \text{h}$ )							
	Capecitabine		5-FU		5'-DFCR		5'-DFUR	
	Cycle 1	Cycle 2	Cycle 1	Cycle 2	Cycle 1	Cycle 2	Cycle 1	Cycle 2
700	3652 (1234)	3208 (820)	555 (157)	322 (130)	1929 N/A	2087 (910)	13495 (4335)	11179 (1300)
850	4343 (793)	4248 (1156)	407 (70)	465 (210)	1286 (586)	1890 (1164)	11916 (1518)	10887 (1914)
1000	7700 (3046)	7322 (3620)	478 (172)	598 (326)	6149 (3818)	7285 (3610)	14341 (6769)	15836 (3048)
1150	11553 (5814)	11188 (7377)	621 (156)	516 (189)	9967 (3526)	11110 (2520)	18001 (2572)	16289 (5383)

AUC = area under the curve; s.d. = standard deviation; 5-FU = 5-fluorouracil; DFCR = 5'-deoxy-5-fluorocytidine; DFUR = 5'-deoxy-5-fluorouridine; N/A = not available.

**Table 6** Antitumour activity of XELIRI – best response

Dose level	Irinotecan ( $\text{mg m}^{-2}$ )	Capecitabine ( $\text{mg m}^{-2}$ twice daily)	CR	PR	Stable disease	Progressive disease
1 (n = 3)	200	700				3
2 (n = 3)	200	850				3
3 (n = 4)	200	1000			1	3
4 (n = 8)	250	1000	1 <sup>a</sup>		2	5
5 (n = 5)	250	1150		1 <sup>b</sup>	1	3
Total (n = 23)			1	1	4	17

CR = complete response; PR = partial response. <sup>a</sup>Patient with colorectal cancer (CRC) who had previously demonstrated a partial response to 5-FU/oxaliplatin. <sup>b</sup>Patient with CRC who had previously demonstrated PR and CR, as well as disease stabilisation, after treatment with three previous 5-FU-based regimens.

250  $\text{mg m}^{-2}$  as a 90-min infusion on day 1 plus oral capecitabine 1150  $\text{mg m}^{-2}$  twice daily on days 2–15, every 21 days. DLTs were assessed during the first two cycles of treatment in order to evaluate the potential for cumulative toxicity. The principal DLTs were diarrhoea and neutropenia, which are typical of fluoropyrimidine/irinotecan combinations (Saltz *et al*, 1996; Vanhoefler *et al*, 1999). The recommended dose is capecitabine 1000  $\text{mg m}^{-2}$  twice daily on days 2–15 combined with irinotecan 250  $\text{mg m}^{-2}$  administered as a 90-min infusion, on day 1 of every 21-day cycle. Among the 10 patients treated at this dose level, only one patient experienced a DLT.

Overall, the combination demonstrated a predictable safety profile, which was consistent with the known toxicity profiles of the single agents. The most commonly occurring adverse events were gastrointestinal disturbances, asthenia and neutropenia. However, Grade 1/2 diarrhoea occurred in the majority (75%) of patients experiencing this side effect, indicating that it was effectively managed in most patients by supportive measures and antidiarrhoeal medication. Similarly, Grade 1/2 neutropenia occurred in 75% of patients experiencing this side effect. Grade 3 and 4 neutropenia occurred in only four and two patients, respectively. Notably, Grade 3 hand-foot syndrome, a cutaneous

side effect that is typical of infused fluoropyrimidines, was observed in only one patient.

Hepatic carboxylesterase is involved in the metabolism of capecitabine and irinotecan (Kuhn, 1998; Miwa *et al*, 1998). A pharmacokinetic evaluation was therefore performed to confirm the feasibility of administering capecitabine and irinotecan in combination and to determine the potential for interactions between these two agents. The similar AUC values for irinotecan and its metabolites during cycles 1 and 2 indicate that the administration of capecitabine does not impact significantly on either the AUC of irinotecan or SN-38 in this administration schedule. However, it should be noted that the drug-free period between treatment cycles precludes any definitive conclusions about the potential direct pharmacokinetic impact of capecitabine on irinotecan metabolism. Moreover, statistical differences were observed for the AUCs of nonactive metabolites (i.e. SN-38 glucuronide and APC), but the absolute change was less than 20%. Taken together, the changes in AUCs observed between cycles 1 and 2 (i.e. +16.4% for SN-38, +15.3% for SN-38 glucuronide and –19.3% for APC) indicate that the metabolism of irinotecan was modified between cycles without any change in the overall clearance of irinotecan. So far, no systemic changes in the

pharmacokinetics of irinotecan and its metabolites have been described from cycles 1 to 2 when the agents are administered alone. Intraindividual variability of 14, 35 and 38% between cycles have been observed for plasma AUC of irinotecan, SN-38 and SN-38 glucuronide, respectively, but the number of cycles delivered did not significantly influence any of the pharmacokinetic parameters (Canal *et al*, 1996). Therefore, the changes in AUC observed in the current study are most likely attributable to the interaction of irinotecan with capecitabine. The trend we observed is consistent with the observation by Falcone *et al* (2001) that the AUC of SN-38 is increased when irinotecan infusion is preceded by 5-FU. In this study, the SN-38 AUC was 40% lower when irinotecan preceded 5-FU administration compared with the reverse sequence. However, whereas in the Falcone study 5-FU was administered immediately before irinotecan, in the current study, there was a 1-week wash-out period between administration of capecitabine and irinotecan. This schedule difference may explain the greater influence of 5-FU on irinotecan metabolism in the study by Falcone *et al* (2001), compared with the modest changes in the current study.

As expected, the AUC of capecitabine appears to increase linearly with dose escalation during both cycles 1 and 2. However, no significant differences in the AUC of capecitabine were observed between cycles 1 and 2; therefore, confirming that irinotecan does not have a major impact on the metabolism of capecitabine. This observation is consistent with the fact that no cumulative toxicity was observed at dose levels 4 and 5 in patients receiving more than two cycles.

Preliminary data from other pilot studies evaluating XELIRI (irinotecan 240–360 mg m<sup>-2</sup> on day 1, or 100 mg m<sup>-2</sup> on days 1 and 8, with intermittent oral capecitabine 1000 mg m<sup>-2</sup> administered twice daily on days 1–14, every 3 weeks) in the first-line treatment of metastatic CRC have demonstrated promising activity with an acceptable safety profile (Bajetta *et al*, 2001; Kerr *et al*, 2002; Borner *et al*, 2003; Grothey *et al*, 2003). The current schedule affords convenience benefits compared with XELIRI regimens requiring weekly administration of irinotecan.

In a recent phase I study evaluating weekly intravenous irinotecan and capecitabine administered twice daily on days 1–14 of a 21-day cycle, the dose recommended for further evaluation was irinotecan 70 mg m<sup>-2</sup> and capecitabine 1000 mg m<sup>-2</sup> (Tewes *et al*, 2003). The study, which evaluated first-line XELIRI in patients with metastatic CRC, demonstrated good activity, with an

overall response rate of 38%. It is worth noting that a UK/Dutch phase I study has identified a recommended regimen identical to that of the current study (Kerr *et al*, 2002). Preliminary data reported from a phase II trial show that this regimen (irinotecan 250 mg m<sup>-2</sup> on day 1, followed by intermittent oral capecitabine 1000 mg m<sup>-2</sup> twice daily for 14 days, every 3 weeks) is highly active as first-line therapy for metastatic CRC, achieving an objective response rate of 42% and median TTP of 7.1 months (Patt *et al*, 2003).

The response rate and median TTP achieved with XELIRI compare favourably with the results from randomised trials evaluating either infused or bolus 5-FU in combination with irinotecan as first-line therapy (Douillard *et al*, 2000; Saltz *et al*, 2000; Goldberg *et al*, 2003). In the current study, the vast majority of patients had received prior chemotherapy for treatment of advanced disease and more than one-third of patients had received multiple chemotherapy regimens. All chemotherapy-pretreated patients had received at least one 5-FU-based regimen. One patient treated at the recommended dose achieved a CR and a further patient treated at the MTD demonstrated a PR. Notably, both patients demonstrating a response to XELIRI had received prior treatment with 5-FU. Furthermore, in the patient demonstrating a PR, the current regimen was administered in the fourth-line setting. A further two patients experienced disease stabilisation at the recommended dose.

In conclusion, the XELIRI regimen is shown to be a feasible and clinically active chemotherapy regimen in patients with advanced gastrointestinal cancer. XELIRI offers a simplified regimen that is less cumbersome for patients and avoids the discomfort and complications associated with the central venous access required with continuous infusion 5-FU. The lack of pharmacokinetic interaction between capecitabine and irinotecan lends further support for evaluation of this XELIRI regimen in the phase II setting. Accordingly, the European Organization for the Research and Treatment of Cancer is currently evaluating XELIRI vs irinotecan plus infusional 5-FU/LV as first-line treatment for advanced CRC.

## ACKNOWLEDGEMENTS

We would like to thank Muriel Poublanc, Valerie Laurence and Vincent Leon for their clinical assistance.

## REFERENCES

- Bajetta E, Cortinovis D, Cassata A, Siena S, Cartei G, Pinotti G, Carreca L, Lambiase A (2001) Activity and safety of capecitabine and irinotecan (CPT-11) in association as first-line chemotherapy in advanced colorectal cancer (ACRC). *Eur J Cancer* 37(supplement 6): S293 (Abstract 1082)
- Borner MM, Dietrich D, Popescu R, Wernli M, Saletti P, Rauch D, Herrmann R, Koerberle D, Honegger H, Roth A (2003) A randomised phase II study of capecitabine (CAP) and two different schedules of irinotecan (IRI) in first-line treatment of metastatic colorectal cancer (MCC). *Proc Am Soc Clin Oncol* 22: 266 (Abstract 1068)
- Canal F, Gay C, Dezeuze A, Douillard JY, Bugat R, Brunet R, Adenis A, Heraut P, Lokiec F, Mathieu-Boue A (1996) Pharmacokinetics and pharmacodynamics of irinotecan during a phase II clinical trial in colorectal cancer. Pharmacology and Molecular Mechanisms Group of the European Organization for Research and Treatment of Cancer. *J Clin Oncol* 14: 2688–2695
- Cao S, Hapke G, Rustum YM (2001) Enhanced antitumor activity of Xeloda by irinotecan in nude mice bearing human A253 and FaDu head and neck xenografts. *Proc Am Assoc Clin Res* 20: 86
- Cartwright TH, Cohn A, Varkey JA, Chen YM, Sztatowski TP, Cox JV, Schulz JJ (2002) Phase II study of oral capecitabine in patients with advanced or metastatic pancreatic cancer. *J Clin Oncol* 20: 160–164
- Cassidy J, Tabernero J, Twelves C, Brunet R, Butts C, Conroy T, Debraud F, Figier A, Grossmann J, Sawada N, Schoffski P, Sobrero A, Van Cutsem E, Diaz-Rubio E (2004) XELOX (Capecitabine plus oxaliplatin): active first-line therapy for patients with metastatic colorectal cancer. *J Clin Oncol* 22: 2084–2091
- Cassidy J, Twelves C, Van Cutsem E, Hoff P, Bajetta E, Boyer M, Bugat R, Burger U, Garin A, Graeven U, McKendric J, Maroun J, Marshall J, Osterwalder B, Perez-Manga G, Rosso R, Rougier P, Schilsky RL (2002) First-line oral capecitabine therapy in metastatic colorectal cancer: a favorable safety profile compared with i.v. 5-fluorouracil/leucovorin. Capecitabine CRC Study Group. *Ann Oncol* 13: 566–575
- Chabot GG, Abigeres D, Catimel G, Culine S, de Forni M, Extra JM, Mahjoubi M, Heraut P, Armand JP, Bugat R (1995) Population pharmacokinetics and pharmacodynamics of irinotecan (CPT-11) and active metabolite SN-38 during phase I trials. *Ann Oncol* 6: 141–151
- Cunningham D, Pyrhonen S, James RD, Punt CJ, Hickish TF, Heikkila R, Johannesen TB, Starkhammar H, Topham CA, Awad L, Jacques C, Heraut P (1998) Randomised trial of irinotecan plus supportive care versus supportive care alone after fluorouracil failure for patients with metastatic colorectal cancer. *Lancet* 352: 1413–1418
- Douillard JY, Cunningham D, Roth AD, Navarro M, James RD, Karasek P, Jandik P, Iveson T, Carmichael J, Alabi M, Grifa G, Awad L, Rougier P

- (2000) Irinotecan combined with fluorouracil compared with fluorouracil alone as first-line treatment for metastatic colorectal cancer: a multicentre randomised trial. *Lancet* 355: 1041-1047
- Falcone A, Di Paolo A, Masi G, Allegrini G, Danesi R, Lencioni M, Pfanner E, Comis S, Del Tacca M, Conte P (2001) Sequence effect of irinotecan and fluorouracil treatment on pharmacokinetics and toxicity in chemotherapy-naïve metastatic colorectal cancer patients. *J Clin Oncol* 19: 3456-3462
- Goldberg RM, Morton RF, Sargent DJ, Fuchs C, Ramanathan RK, Williamson SK, Findlay BP (2003) N9741: oxaliplatin (Oxal) or CPT-11+5-fluorouracil (5FU)/leucovorin (LV) or oxal+CPT-11 in advanced colorectal cancer (CRC). Updated efficacy and quality of life (QOL) data from an intergroup study. *Proc Am Soc Clin Oncol* 22: 252 (Abstract 1009)
- Grothey A, Jordan K, Kellner O, Constantin C, Dietrich G, Kroening H, Mantovani L, Schlichting C, Forstbauer H, Schmoll HJ (2003) Capecitabine plus irinotecan (CAPIRI) vs capecitabine plus oxaliplatin (CAPOX) as first-line therapy of advanced colorectal cancer (ACRC): updated results of a randomized phase II trial. *Eur J Cancer* 1(supplement 5): S90 (Abstract 295)
- Hapke G, Cao S, Rustum YM (2001) Enhanced antitumor activity of Xeloda by irinotecan in nude mice bearing A253 and FaDu head and neck xenografts. *Proc Am Assoc Cancer Res* 42: 86 (Abstract 464)
- Hoff PM, Ansari R, Batist G, Cox J, Kocha W, Kuperminc M, Maroun J, Walde D, Weaver C, Harrison E, Burger HU, Osterwalder B, Wong AO, Wong R (2001) Comparison of oral capecitabine versus intravenous fluorouracil plus leucovorin as first-line treatment in 605 patients with metastatic colorectal cancer: results of a randomized phase III study. *J Clin Oncol* 19: 2282-2292
- Hong YS, Song SY, Cho JY, Lee SI, Chung HC, Choi SH, Noh SH, Park JN, Han JY, Kang JH, Lee KS (2002) A phase II trial of capecitabine (Xeloda) in chemotherapy naive patients with advanced and/or metastatic gastric cancer. *Proc Am Soc Clin Oncol* 21: 156a (Abstract 623)
- Kerr DJ, Ten Bokkel Huinink WW, Ferry DR, Rea DW, Boussard BM, Oullid-Aissa D, Frings S, Nordier JW (2002) A phase I/II study of CPT-11 in combination with capecitabine as first-line chemotherapy for metastatic colorectal cancer (MCR). *Proc Am Soc Clin Oncol* 21: 161a (Abstract 643)
- Koizumi W, Saigenji K, Ujite S, Terashima M, Sakata Y, Taguchi T, Clinical Study Group of Capecitabine (2003) A phase II study of capecitabine (Xeloda™) in patients with advanced/metastatic gastric carcinoma. *Oncology* 64: 232-236
- Kuhn JG (1998) Pharmacology of irinotecan. *Oncology (Huntingt)* 12: 39-42
- Mick R, Gupta E, Vokes EE, Ratain MJ (1996) Limited-sampling models for irinotecan pharmacokinetics-pharmacodynamics: prediction of biliary index and intestinal toxicity. *J Clin Oncol* 14: 2012-2019
- Miwa M, Ura M, Nishida M, Sawada N, Ishikawa T, Mori K, Shimma N, Umeda I, Ishitsuka H (1998) Design of a novel oral fluoropyrimidine carbamate, capecitabine, which generates 5-fluorouracil selectively in tumours by enzymes concentrated in human liver and cancer tissue. *Eur J Cancer* 34: 1274-1281
- Patt YZ, Leibmann J, Diamandidis D, Eckhardt SG, Javle M, Justice GR, Keiser W, Lee F-C, Miller W, Lin E (2003) Capecitabine plus irinotecan (XELIRI) in first-line metastatic colorectal cancer (MCR): update on a phase II trial. *Eur J Cancer* 1(supplement 5): S93 (Abstract 304)
- Reigner B, Blesch K, Weidekamm E (2001) Clinical pharmacokinetics of capecitabine. *Clin Pharmacokinet* 40: 85-104
- Reigner B, Verweij J, Dirix L, Cassidy J, Twelves C, Allman D, Weidekamm E, Roos B, Banken L, Utoh M, Osterwalder B (1998) Effect of food on the pharmacokinetics of capecitabine and its metabolites following oral administration in cancer patients. *Clin Cancer Res* 4: 941-948
- Rivory LP, Robert J (1993) Identification and kinetics of a beta-glucuronide metabolite of SN-38 in human plasma after administration of the camptothecin derivative irinotecan. *Cancer Chemother Pharmacol* 36: 176-179
- Rothenberg ML, Meropol NJ, Poplin EA, Van Cutsem E, Wadler S (2001) Mortality associated with irinotecan plus bolus fluorouracil/leucovorin: summary findings of an independent panel. *J Clin Oncol* 19: 3801-3807
- Rougier P, Van Cutsem E, Bajetta E, Niederle N, Possinger K, Labianca R, Navarro M, Morant R, Bleiberg H, Wils J, Awad L, Heraut P, Jacques C (1998) Randomised trial of irinotecan versus fluorouracil by continuous infusion after fluorouracil failure in patients with metastatic colorectal cancer. *Lancet* 352: 1407-1412
- Saltz LB, Cox JV, Blanke C, Rosen LS, Fehrenbacher L, Moore MJ, Maroun JA, Adjeeland SP, Locker PK, Pirotta N, Elfring GL, Miller LL (2000) Irinotecan plus fluorouracil and leucovorin for metastatic colorectal cancer. *N Engl J Med* 343: 905-914
- Saltz LB, Kanowitz J, Kemeny NE, Schaaf L, Spriggs D, Staton BA, Berkery R, Steger C, Eng M, Dietz A, Locker P, Kelsen DP (1996) Phase I clinical and pharmacokinetic study of irinotecan, fluorouracil, and leucovorin in patients with advanced solid tumors. *J Clin Oncol* 14: 2959-2967
- Schüller J, Cassidy J, Dumont E, Roos B, Durston S, Banken L, Utoh M, Mori K, Weidekamm E, Reigner B (2000) Preferential activation of capecitabine in tumor following oral administration to colorectal cancer patients. *Cancer Chemother Pharmacol* 45: 291-297
- Tewes M, Schleucher N, Achterrath W, Wilke HJ, Frings S, Seeber S, Harstrick A, Rustum YM, Vanhoefer U (2003) Capecitabine and irinotecan as first-line chemotherapy in patients with metastatic colorectal cancer: results of an extended phase I study. *Ann Oncol* 14: 1442-1448
- Van Cutsem E, Cunningham D, Ten Bokkel Huinink WW, Punt CI, Alexopoulos CG, Dirix L, Symann M, Blijham GH, Cholet P, Fillet G, Van Groeningen C, Vannetzel JM, Levi F, Panagos G, Unger C, Wils J, Cote C, Blanc C, Heraut P, Bleiberg H (1999) Clinical activity and benefit of irinotecan (CPT-11) in patients with colorectal cancer truly resistant to 5-fluorouracil (5-FU). *Eur J Cancer* 35: 54-59
- Van Cutsem E, Hoff PM, Harper P, Bukowski RM, Cunningham D, Dufour P, Graeven U, Lokich J, Madajewicz S, Maroun JA, Marshall JL, Mitchell EP, Perez-Manga G, Rougier P, Schmiegel W, Schoelmerich J, Sobrero A, Schilsky RL (2004) Oral capecitabine versus intravenous 5-fluorouracil and leucovorin: integrated efficacy data and novel analyses from two large, randomised, phase III trials. *Br J Cancer* 90: 1190-1197
- Van Cutsem E, Twelves C, Cassidy J, Allman D, Bajetta E, Boyer M, Bugat R, Findlay M, Frings S, Jahn M, McKendrick J, Osterwalder B, Perez-Manga G, Rosso R, Rougier P, Schmiegel WH, Seitz JF, Thompson P, Vieitez JM, Weitzel C, Harper P (2001) Xeloda Colorectal Cancer Study Group *et al*. Oral capecitabine compared with intravenous 5-fluorouracil plus leucovorin (Mayo Clinic regimen) in patients with metastatic colorectal cancer: results of a large phase III study. *J Clin Oncol* 19: 4697-4706
- Vanhoefer U, Harstrick A, Köhne GH, Achterrath W, Rustum YM, Seeber S, Wilke H (1999) Phase I study of a weekly schedule of irinotecan, high-dose leucovorin, and infusional 5-fluorouracil as first-line chemotherapy in patients with advanced colorectal cancer. *J Clin Oncol* 17: 907-913

## Interaction of Immunoglobulin-Coupled Liposomes with Rat Liver Macrophages In Vitro

J. T. P. DERKSEN,<sup>1,\*</sup> H. W. M. MORSELT,<sup>1</sup> D. KALICHARAN,<sup>2</sup>  
C. E. HULSTAERT<sup>2</sup> and G. L. SCHERPHOF<sup>1</sup>

<sup>1</sup>Laboratory of Physiological Chemistry, University of Groningen, 9712 KZ Groningen,  
and <sup>2</sup>Centre for Medical Electron Microscopy, University of Groningen,  
9713 EZ Groningen, The Netherlands

The interaction between liposomes coated with covalently linked rabbit immunoglobulin (RbIg-liposomes), and rat liver macrophages (Kupffer cells) in monolayer culture was studied biochemically with radioactive tracers and morphologically by electron microscopy. The attachment of immunoglobulin (Ig) to liposomes caused a five-fold increase in liposome uptake by the Kupffer cells at 37°C, in comparison with uncoated liposomes. The uptake was linear with time for at least 4 h and linear with liposome concentration up to a lipid concentration of 0.2 mM. At 4°C uptake, probably representing cell surface-bound liposomes, was reduced to a level of approx. 20% of the 37°C values. Involvement of the Fc receptor in the uptake process was indicated by the reduction of RbIg-liposome uptake by more than 75% as a result of preincubating the cells with heat-aggregated human or rabbit Ig at concentrations (less than 2 mg/ml) at which bovine serum albumin (BSA) had virtually no effect on uptake. At high concentrations (10–35 mg/ml), however, albumin also reduced liposome uptake significantly (20–30%), which suggests an interaction of the RbIg-liposomes with the Kupffer cells that is partially non-specific. RbIg-liposome uptake was dependent on the amount of RbIg coupled to the liposomes. Maximal uptake values were reached at about 200 µg RbIg/µmol liposomal lipid. Electron microscopic observations on cells incubated with horseradish peroxidase-containing RbIg-liposomes demonstrated massive accumulation of peroxidase reaction product in intracellular vacuoles, showing that the uptake observed by label association represents true internalization. ©

1987 Academic Press, Inc.

It is now widely accepted that liposomes injected intravenously in the rat are taken up to a large extent by liver macrophages (Kupffer cells) [1–3] with the exception of certain small unilamellar vesicles, which may reach the hepatocytes in large quantities. In vitro experiments have confirmed that isolated Kupffer cells are able to bind and subsequently ingest liposomes by an endocytotic route [4]. Although this inherent affinity of Kupffer cells for liposomes may, on the one hand, frustrate the targeting to other liver cells such as hepatocytes [5], it may, on the other hand, also be exploited to study the endocytotic process per se.

As a model particle in the study of endocytosis, liposomes offer a number of advantages over other model particles such as latex beads, erythrocytes, and colloidal gold. Liposomes are easy to prepare from biodegradable compounds and they can be made to encapsulate either markers for morphological studies

---

\* To whom offprint requests should be sent. Address: Laboratory of Physiological Chemistry, University of Groningen, Bloemsingel 10, 9712 KZ Groningen, The Netherlands.

such as horseradish peroxidase and fluorescent dyes or lipid- or water-soluble radioactive markers for biochemical studies, enabling us to monitor the metabolic fate of these substances. In addition, to allow specific interaction with cell surface receptors, the surface of liposomes can be modified conveniently by including glycolipids in the liposomal membrane [5] or by covalent attachment of proteins to the liposomal surface [6].

To compare the uptake and processing characteristics of liposomes interacting non-specifically with the Kupffer cells as described in detail by Dijkstra et al. [4, 7, 8] with those of liposomes interacting in a more specific way with these cells, we prepared liposomes to which rabbit immunoglobulin was covalently coupled (RbIg-liposomes). Since these liposomes expose immunoglobulin Fc moieties, they should be able to bind to the Fc receptors present on the Kupffer cell membrane [9, 10], and subsequently be ingested by the Fc receptor-mediated endocytosis pathway [11].

In this study we describe some aspects of the interaction of such RbIg-liposomes with Kupffer cells in monolayer culture.

## MATERIALS AND METHODS

### *Materials*

Egg-yolk phosphatidylcholine (type V-E), cholesterol (type CH-S), dicetylphosphate, cytochalasin B (CB), colchicine, bovine serum albumin (BSA) (Cohn fraction V) bovine-, rabbit- and human gammaglobulin (Cohn fraction II) and 4-(2-hydroxyethyl)-1-piperazine ethanesulfonic acid (HEPES) were from Sigma.  $^3\text{H}$ [Inulin was purchased from the Radiochemical Centre, Amersham, Bucks, England and  $^3\text{H}$ cholesterylolate from New England Nuclear, Boston, Mass., USA. Dextran T-40 was from Pharmacia, Uppsala, Sweden.

### *Liposomes*

Large unilamellar vesicles were prepared in 10 mM HEPES/135 mM NaCl buffer (pH 7.4), containing  $^3\text{H}$ inulin (1 mM) when required, according to Szoka & Papahadjopoulos [12] and sized by extrusion through 200 nm polycarbonate membranes, pore size 0.2  $\mu\text{m}$  (Nuclepore). The liposomes were composed of egg-phosphatidylcholine, cholesterol, dicetylphosphate and maleimido-4-(*p*-phenylbutyryl) phosphatidylethanolamine (MPB-PE) (synthesized as described by Martin & Papahadjopoulos [13]) in a molar ratio of 19:16:4:1. To the lipid mixture, trace amounts of  $^3\text{H}$ cholesterylolate were added when required. RbIg was covalently attached to these liposomes as described previously [6]. Briefly, MPB-PE-containing liposomes (10  $\mu\text{mol}$  total lipid) in 0.5 ml HEPES/NaCl buffer were incubated with 0.5 ml of a solution of 7 mg/ml RbIg, thiolated to 3–4 mol sulfhydryl groups per mol RbIg with the heterobifunctional reagent N-succinimidyl-S-acetylthioacetate [14]. After isolation of the RbIg-coupled liposomes with a flotation method on a dextran gradient [15] the resulting liposomes were assayed for phosphate and protein content. RbIg-liposomes thus prepared were found to contain between 180 and 220 g RbIg/mol of liposomal lipid. After resuspending the liposomes in HEPES/NaCl buffer aggregates that might have been formed during the coupling and isolation procedure were removed by forced filtration of the liposomes through a polycarbonate membrane, pore size 0.4  $\mu\text{m}$ . This filtration step caused about 10% release of encapsulated solute.

### *Kupffer Cells*

Kupffer cells were isolated from female Wistar rats (170–210 g) by pronase digestion of the liver and purified by centrifugal elutriation, basically according to Knook & Sleyster [16] with some modifications as described by Dijkstra et al. [4].  $5 \times 10^5$  cells were plated out in 0.5 ml Dulbecco's modification of Eagle's Medium (DMEM, Flow), containing 10 mM  $\text{NaHCO}_3$ , 20 mM HEPES, 20% fetal calf serum (FCS) (Gibco), 100 IU/ml penicillin G and 100  $\mu\text{g}/\text{ml}$  streptomycin (Gist-Brocades, Delft, The

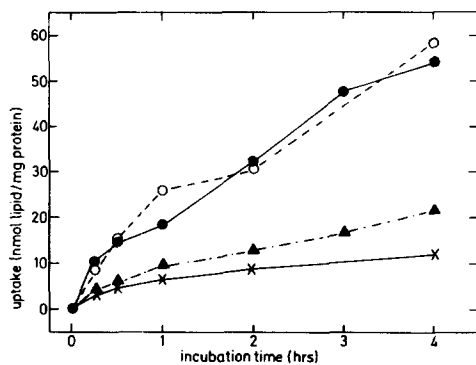


Fig. 1. Uptake of RbIg-liposomes by Kupffer cells and inhibition by BSA and aggregated human immunoglobulin. [ $^3\text{H}$ ]Cholesteryloleate-labelled RbIg-liposomes were added to Kupffer cells to a concentration of 50 nmol total lipid/ml in the absence (●) or presence of 1 mg/ml BSA (○) or 1 mg/ml aggregated human immunoglobulin (▲) and incubated at 37°C. As a control, non-opsonized liposomes of the same lipid composition were used (×). At the indicated times, cell-associated radioactivity was measured and liposome uptake was calculated.

Netherlands) per well on 24-well culture plates (Linbro, Flow). Twenty-four hours after seeding, the medium containing 20% FCS was replaced by medium containing 10% FCS. Forty-eight hours after seeding, cells were used for experiments.

### Incubations

Unless indicated otherwise incubations were performed in quadruplicate in 0.5 ml medium without antibiotics or serum. Inhibitors were added to the incubation medium 30 min before addition of the liposomes as 50-fold concentrated stock solutions, except for CB which was dissolved in dimethylsulfoxide (DMSO) and added to medium in advance, resulting in a final DMSO concentration of 0.2%. Liposomes were added to the medium as concentrated suspensions, usually 2 mM total lipid concentration. At the end of the incubation period, the incubation medium was pipetted off and the cells were washed six times with cold phosphate-buffered saline (PBS, pH 7.4). Cells were digested in 0.7 ml NaOH (0.5 N) and assayed for protein and radioactivity.  $^3\text{H}$  radioactivity was counted in plasmasol (Packard) in a LKB Wallac liquid scintillation counter.

### Electron Microscopy

After incubating the Kupffer cells with liposomes, containing 20 mg/ml horseradish peroxidase in their aqueous volume, the monolayers were washed with PBS and fixed for 5 min at 20°C in 2% glutaraldehyde in 0.1 M cacodylate buffer (pH 7.4). After washing in cacodylate buffer to remove the fixative, the cells were incubated for the ultrastructural demonstration of peroxidase activity in 0.05% diaminobenzidine and 0.01%  $\text{H}_2\text{O}_2$  in PBS for 30 min in the dark at 37°C. Subsequently the cells were washed with PBS and 6.8% saccharose in 0.1 M cacodylate buffer (pH 7.4) and postfixed in 1%  $\text{OsO}_4$ , 1.5%  $\text{K}_4\text{Fe}(\text{CN})_6$  in 0.1 M cacodylate buffer pH 7.4. After rinsing in 0.1 M cacodylate buffer, pH 7.4, the cells were dehydrated in an alcohol series and embedded in Epon 812. Ultrathin sections were examined without staining as adequate contrast was obtained by the postfixation.

### Other Methods

Protein was determined by Peterson's [17] microassay modification of the procedure described by Lowry et al. [18]. Bovine gammaglobulin was used as a standard. Phospholipid phosphorus was determined after perchloric acid (PCA) destruction according to Böttcher [19].

## RESULTS

The uptake of RbIg-liposomes by Kupffer cells proceeds linearly with time up to at least 4 h of incubation, at which time more than 50 nmol of liposomal lipid is associated with the cells per mg of cell protein (fig. 1). The coupling of the immunoglobulin to liposomes increases the uptake more than five-fold, compared with control liposomes. This increase in uptake can be inhibited to a large extent

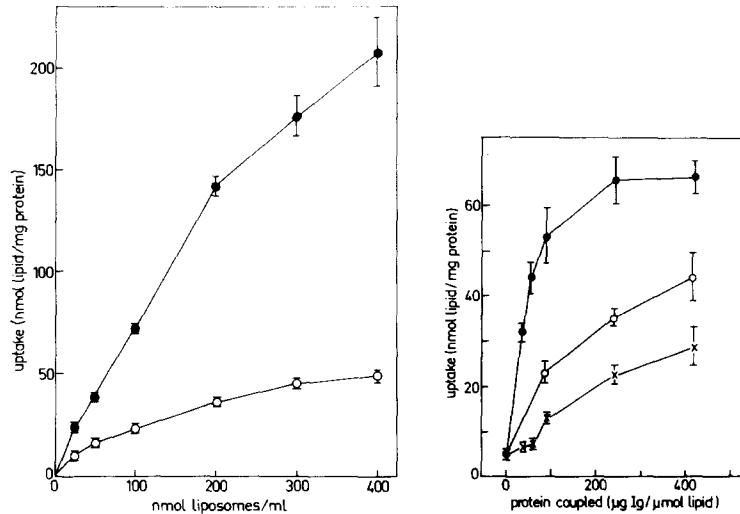


**Fig. 2.** Kupffer cell uptake of RbIg-liposomes at 37°C and 4°C. Varying amounts of [<sup>3</sup>H]cholesteryloleate-labelled RbIg-liposomes were added to Kupffer cells, resulting in liposome concentrations as indicated. After 4 h of incubation at 4°C (○) or 37°C (●) cell-associated radioactivity was measured and liposome uptake was calculated (mean ± SD, *n*=4).

**Fig. 3.** Uptake of RbIg-liposomes by Kupffer cells; dependency on RbIg-liposome coupling ratio. To [<sup>3</sup>H]cholesteryloleate-labelled liposomes, varying amounts of RbIg were coupled. These RbIg-liposome preparations were added to Kupffer cells to a concentration of 50 nmol total lipid per ml in the absence (●) or presence of 1 mg/ml of either aggregated human (×) or rabbit (○) immunoglobulin. After 4 h of incubation at 37°C, cell-associated radioactivity was measured and liposome uptake was calculated (mean ± SD of four incubations).

by pre-incubating the cells with 1 mg/ml heat-aggregated human immunoglobulin but not with BSA. The amount of RbIg-liposomes taken up by the Kupffer cells increases linearly with increasing liposome concentration up to a concentration of 200 nmol of liposomal lipid per ml (fig. 2). At this concentration, nearly 150 nmol of lipid is taken up per mg of cell protein in a period of 4 h. Beyond 200 nmol/ml the uptake curve levels off but does not reach a maximum up to 400 nmol/ml. At 4°C the amount of liposomes bound reaches plateau values at about 400 nmol total liposomal lipid/ml, at which point about 50 nmol liposomes is bound per mg of cellular protein. Assuming a protein content of 0.1 ng per Kupffer cell and an average liposome diameter of 300 nm, this means that, per cell, about 1 500 liposomes become bound [20]. At an incubation temperature of 37°C a substantially larger number of liposomes associate with the Kupffer cells, indicating internalization of the liposomes and perhaps also an increased binding to the cells (fig. 2).

Fig. 3 shows that the uptake of RbIg-liposomes by the Kupffer cells is dependent on the amount of RbIg coupled to the liposomes. When more than 200 µg of RbIg is coupled per µmol of liposomal lipid, i.e. more than 2 500 molecules of RbIg per vesicle [20], there is no further increase in liposome uptake. When the



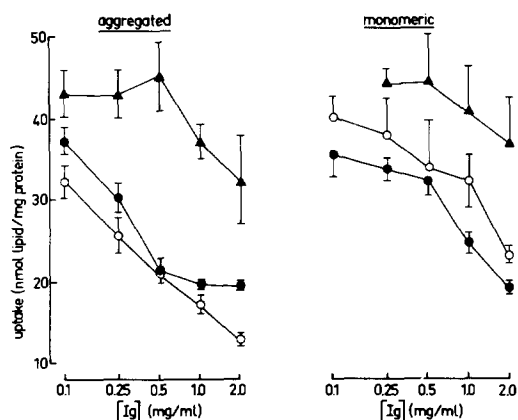


Fig. 4. Kupffer cell uptake of RbIg-liposomes. Inhibition by bovine, rabbit and human immunoglobulin. [ $^3\text{H}$ ]Cholesteryloleate-labelled RbIg-liposomes were added to Kupffer cells to a concentration of 50 nmol total lipid per ml in presence of increasing amounts of (left) heat-aggregated; or (right) monomeric bovine ( $\blacktriangle$ ), rabbit ( $\bullet$ ) or human ( $\circ$ ) immunoglobulin. After 4 h of incubation at  $37^\circ\text{C}$  cells were harvested. Liposome uptake was calculated from cell-associated radioactivity; in absence of immunoglobulins it was  $38.9 \pm 3.5$  nmol lipid/mg protein (mean  $\pm$  SD,  $n=8$ ).

coupling ratio of RbIg to liposomes reaches about  $500 \mu\text{g RbIg}/\mu\text{mol lipid}$ , the liposome suspension becomes turbid and the liposomes start to precipitate, indicating extensive aggregation, as was also observed by Martin & Kung [21].

At a coupling ratio of  $500 \mu\text{g RbIg}/\mu\text{mol lipid}$  about 5 100 molecules of immunoglobulin are coupled [20], assuming a liposome diameter of 400 nm, a molecular weight of 150 kD for IgG and neglecting the small amount of IgM in the RbIg preparation. The surface area of liposomes with a diameter of 400 nm is approx.  $\times 10^5 \text{ nm}^2$ . If we envisage IgG molecules as spheres with a diameter of 11 nm [22], we can calculate that a monolayer of closely packed IgG molecules around these liposomes contains, maximally, 5 300 molecules, i.e. roughly equivalent to  $500 \mu\text{g}/\mu\text{mol}$  of lipid. Apparently, the RbIg-liposomes start to aggregate when this value is reached, possibly by free sulphhydryl interaction of RbIg molecules on apposing liposomes. At these coupling ratios we observed a sharp increase in the quantity of liposomes associating with the Kupffer cells (not shown), probably as a result of attachment of large liposome aggregates to the cells.

The uptake of RbIg-liposomes can be inhibited by preincubation of the cells with heat-aggregated immunoglobulins. Aggregated human immunoglobulin appears to be a more effective inhibitor in this system than aggregated rabbit immunoglobulin (fig. 3). The strongest inhibitory effect was observed in the low protein-lipid coupling range, i.e. below  $100 \mu\text{g RbIg}/\mu\text{mol liposomal lipid}$ . When more than  $500 \mu\text{g RbIg}/\mu\text{mol lipid}$  is coupled, inhibition of the uptake of RbIg-liposomes by aggregated human and rabbit immunoglobulin is reduced even further (not shown), also suggesting the involvement of non-specific binding of RbIg-liposome aggregates to the cells at this high coupling ratio.

The ability of aggregated immunoglobulin to inhibit RbIg-liposome uptake depends on the animal species from which the immunoglobulin was derived (fig. 4). For instance, aggregated bovine immunoglobulin has little inhibitory effect on RbIg-liposome uptake at concentrations below 1 mg/ml. Aggregated rabbit and human immunoglobulin start to inhibit RbIg-liposome uptake already at concen-

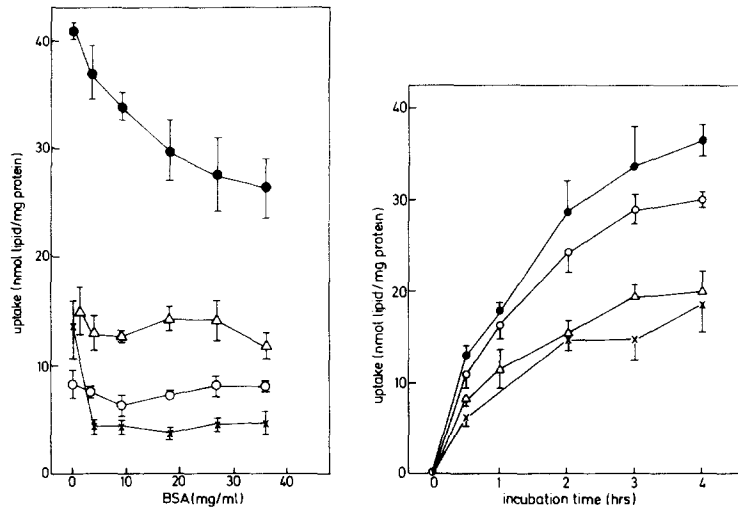


Fig. 5. Effect of BSA on Kupffer cell liposome uptake. [ $^3\text{H}$ ]Cholesteryloleate-labelled control (●) or RbIg-liposomes were added to Kupffer cells to a concentration of 50 nmol total lipid/ml in presence of 0–36 mg/ml BSA. In one series of incubations, 1 mg/ml heat-aggregated human immunoglobulin was present additionally ( $\Delta$ ). The Kupffer cells were incubated at 4°C ( $\times$ ) or 37°C (●,  $\blacktriangle$ ,  $\circ$ ) for 4 h; liposome uptake was calculated from cell-associated radioactivity.

Fig. 6. Inhibition of Kupffer cell uptake of RbIg-liposomes by colchicine and CB. [ $^3\text{H}$ ]Inulin-labelled RbIg-liposomes were added to Kupffer cells to a concentration of 50 nmol total lipid/ml in absence (●) or presence of colchicine (50  $\mu\text{M}$ ) ( $\circ$ ), CB (40  $\mu\text{M}$ ) ( $\Delta$ ) or both ( $\times$ ) and incubated at 37°C. At indicated times, cell-associated radioactivity was measured and liposome uptake was calculated (mean  $\pm$  SD,  $n=4$ ).

trations as low as 0.1 mg/ml, the human material being slightly more effective than that from rabbit. In monomeric form, immunoglobulin is less effective than in aggregated form. To obtain equivalent inhibition a 4–5-fold higher concentration of monomeric immunoglobulin is required. Moreover, bovine immunoglobulin in monomeric form is the least effective inhibitor of the three immunoglobulins tested.

Fig. 5 shows the effect of a non-immunoglobulin protein on Kupffer cell-liposome uptake. Increasing BSA concentrations reduce the RbIg-liposome uptake by as much as about 30% of its control value at a concentration of 36 mg/ml. The uptake of control liposomes is not affected by BSA at any concentration whatsoever. When 1 mg/ml aggregated human immunoglobulin is added to the culture medium the liposome uptake falls from 41 to 15 nmol lipid/mg cellular protein. In that case BSA does not cause any additional inhibition of uptake, irrespective of the BSA concentration. Cells were also incubated with RbIg-liposomes at 4°C in the presence of increasing BSA concentrations. Under those conditions the quantity of liposomes bound to the cells drops by more than 60% in presence of 4 mg/ml BSA, to a level which remains constant upon further increase in BSA concentration up to 40 mg/ml.

The uptake of RbIg-liposomes by Kupffer cells can be inhibited substantially by the phagocytosis inhibitor CB (fig. 6). Colchicine, on the other hand, does not significantly inhibit the uptake of RbIg-liposomes; also the combination of colchicine and CB does not produce an increase of the effect of CB alone.

The RbIg-liposomes bind very tightly to the cell surface. As is shown in table 1 it is practically impossible to detach bound liposomes from the cells. Neither a chase with aggregated immunoglobulin nor more rigorous methods like EGTA or trypsin treatment can remove the liposomes from the cell surface, even though at the concentration used, trypsin and EGTA do detach cells from the culture dishes.

Electronmicrographs of Kupffer cells incubated with RbIg-liposomes containing horseradish peroxidase as a marker show the liposomes to be present inside the cells (fig. 7). While Kupffer cells incubated in medium without liposomes are virtually devoid of peroxidase reaction product (fig. 7a), peroxidase activity can be demonstrated in secondary lysosomes as early as after 10 min of incubation with RbIg-liposomes (fig. 7b). After 60 min of incubation of the Kupffer cells with RbIg-liposomes the cells are filled with extremely large vacuoles containing peroxidase activity (fig. 7c). We observed the same sequence when non-Rb Ig-coupled liposomes were employed [4].

## DISCUSSION

Opsonized erythrocytes [9, 23, 24], opsonized bacteria [25] and especially immunoglobulin-coated colloidal-gold particles [26, 27] have been very useful in elucidating morphological aspects of Fc-receptor-mediated interaction between cells and particles. Such model particles are less suitable to obtain quantitative data on their uptake and on their metabolic fate following ingestion than are opsonized liposomes; the latter can be prepared in various sizes and compositions with a large variety of radioactive tracers, adapted to the specific require-

Table 1. Release of pre-bound RbIg-liposomes

Treatment	nmol liposomes bound/mg cellular protein
DMEM	15.9±0.8
agg-Hum-Ig (0.4%)	13.0±1.1
EGTA (10 mM)	14.6±0.7
Trypsin (0.1%)	13.6±0.5
EGTA (10 mM) + trypsin (0.1%)	12.9±1.2
EGTA (20 mM) + trypsin (0.4%)	12.0±1.1

Kupffer cells were incubated with [<sup>3</sup>H]cholesteryloleate-labelled RbIg-liposomes (50 nmol/ml) at 4°C for 4 h. Non-bound RbIg-liposomes were removed by washing with cold PBS. After a second incubation with aggregated human immunoglobulin (agg-Hum-Ig), EGTA or trypsin in PBS or with DMEM at 4°C for 30 min, adherent cells were harvested and the residual amount of liposomes bound to Kupffer cells was determined (mean±SD, n=4).

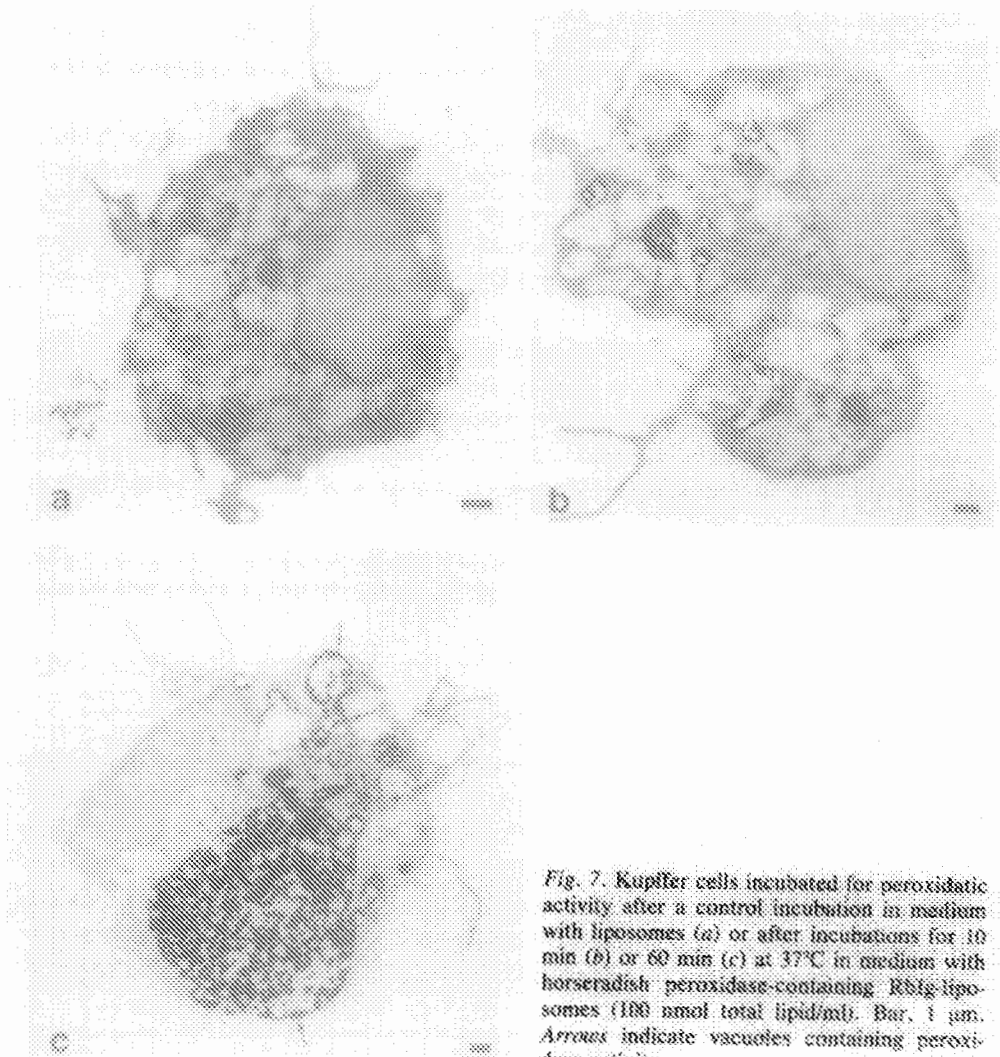


*Fig. 7.* Kupffer cells incubated for peroxidatic activity after a control incubation in medium with liposomes (a) or after incubations for 10 min (b) or 60 min (c) at 37°C in medium with horseradish peroxidase-containing Rb1g-liposomes (100 nmol total lipid/ml). Bar, 1  $\mu$ m. Arrows indicate vacuoles containing peroxidase activity.

ments of the experiment. In most of these studies, liposomes were used containing a phospholipid hapten, such as dinitrophenylcaproyl-phosphatidyl ethanolamine [28–31] or nitroxide spin-labelled phosphatidylcholine [28, 32, 33]. These haptentated liposomes were opsonized with anti-hapten antibodies and after purification the liposomes were allowed to interact with cells.

A disadvantage of this approach is that extensive aggregation of the liposomes may occur, especially if liposome purification involves centrifugation and resuspension steps [31]. This may lead to a high degree of particle heterogeneity, resulting in liposome uptake values which depend on the size of the aggregates rather than on the opsonization proper. An additional problem in this procedure

is that the interaction of antibody with liposomes is non-covalent, which may lead to release of antibody from the liposomes upon dilution of the suspension in the blood-stream or in the incubation medium.

We prepare homogeneous opsonized liposome suspensions by covalent coupling of thiolated rabbit immunoglobulin to liposomes containing reactive maleimide groups. This procedure results in RbIg-liposome suspensions with highly reproducible encapsulated volume and amount of RbIg coupled. Using these RbIg-liposomes we found a 5–10-fold stimulation of the uptake by the opsonization, which is an order of magnitude lower than reported by Hsu & Juliano [13]. This difference may be explained by the absence of large liposome-antibody aggregates in our experiments.

Not all species of immunoglobulins inhibit RbIg-liposome uptake equally well (figs 3, 4). Bovine immunoglobulin is clearly the least effective inhibitor, while rabbit immunoglobulin and human immunoglobulin do not differ much in inhibitory potency. This may be a reflection of the specificity of the Kupffer cell Fc receptor. The affinity of macrophage Fc receptors can vary for different IgG subclasses [34] as well as for immunoglobulins derived from different animal species [35–37]. Also the observation that immunoglobulins inhibit RbIg-liposome uptake by Kupffer cells more potently in aggregated than in monomeric form can be traced back to a difference in Fc-receptor affinity. The equilibrium constant for binding of aggregated human IgG to mouse Kupffer cells is about 6-fold higher than that of monomeric human IgG [38]. The large number of Fc moieties exposed in aggregated immunoglobulin and in multivalent immune complexes results in a virtually irreversible attachment to the cell surface [39, 40]. This probably also explains why the RbIg-liposomes, once bound, cannot be detached by an immunoglobulin chase,  $\text{Ca}^{2+}$ -chelator or protease treatment, conditions under which monomeric IgG [39], asialoglycoproteins [41, 42] and mannose–protein conjugates [43] readily detach from their receptors.

The uptake of RbIg-liposomes by Kupffer cells is clearly dependent upon the amount of RbIg coupled to the liposomes (fig. 3). The extent of inhibition by aggregated immunoglobulin, however, decreases with increasing RbIg/liposome coupling ratio. This would suggest that with increasing coupling ratios the uptake of RbIg-liposomes becomes less Fc receptor-specific and gradually attains the character of non-specific particle uptake. Also the partial suppression of the uptake of RbIg-liposomes by BSA concentrations that do not affect uptake of non-RbIg-coupled liposomes (fig. 5) suggests that the uptake of RbIg-liposomes can be ascribed at least in part to interaction of the liposomes with Kupffer cells by a mechanism other than Fc-receptor binding. Since non-RbIg-coupled control liposomes are also endocytosed by Kupffer cells (figs 1, 5), we conclude that the uptake of RbIg-liposomes by Kupffer cells is the net result of at least two mechanisms operating simultaneously. Firstly, the most substantial part of the uptake of RbIg-liposomes by Kupffer cells is inhibitable with (aggregated)-immunoglobulin indicating involvement of Fc receptors. Secondly, Kupffer cells

phagocytose non-coated liposomes because of their particulate nature; this uptake can be increased by providing the particles with a net negative charge [8, 44]. Control experiments with BSA-coupled liposomes did not indicate any stimulatory effect of BSA on the uptake of these liposomes [3]. Moreover, Torchilin et al. showed that coating liposomes with BSA rather inhibited the uptake of these liposomes by macrophages [45].

Our observation that RbIg-liposome uptake by Kupffer cells is inhibited more effectively by CB than by colchicine, is consistent with the finding of Pratten et al. that, in contrast to CB, the inhibitory effect of colchicine on phagocytosis decreases with increasing particle size [46].

It is virtually impossible to measure accurately in our system inhibition of phagocytosis by metabolic inhibitors, since the concentrations required of such agents cause the cells to detach from the culture plates. Calculation of liposome uptake on the basis of a selection of relatively few not fully inhibited cells that remain attached to the plates leads to an overestimation of the uptake and thus to an underestimation of the inhibitory effect. This phenomenon, which also occurs when cells are depleted of divalent cations with EDTA, is also evident from data obtained by Munthe-Kaas [9]. EGTA, on the other hand, does not cause severe detachment of cells from the culture plates at a concentration of 5 mM. Thus we could show that no significant inhibition of RbIg-liposome uptake by Kupffer cells occurs in the presence of EGTA, whereas uptake of control liposomes is inhibited to a large extent, in agreement with previously published work of our group [8]. Apparently, external  $\text{Ca}^{2+}$  is not required for binding and, perhaps, also uptake of IgG-coated liposomes. Hällgren et al. [47] also showed that binding of IgG-opsonized sheep erythrocytes to Kupffer cells does not require  $\text{Ca}^{2+}$ , in contrast to the binding of IgM-opsonized sheep erythrocytes. Although the initiation of ingestion of RbIg-liposomes may require the presence of a high intracellular  $\text{Ca}^{2+}$  concentration, it has been shown that a substantial portion of this can be derived from the release of  $\text{Ca}^{2+}$  from intracellular stores [48].

The authors wish to thank Jan Wijbenga and Bert Dontje for expert help with the cell isolations and Rinske Kuperus for preparing the manuscript. These investigations were carried out under the auspices of the Netherlands Foundation for Medical Research (FUNGO), with financial support from the Organisation for the Advancement of Pure Research (ZWO) (grant project no. 135360).

## REFERENCES

1. Roerdink, F, Dijkstra, J, Hartman, G, Bolscher, B & Scherphof, G, *Biochim biophys acta* 677 (1981) 79.
2. Scherphof, G, Roerdink, F, Dijkstra, J, Ellens, H, De Zanger, R & Wisse, E, *Biol cell* 47 (1983) 47.
3. Scherphof, G L, Dijkstra, J, Spanjer, H H, Derksen, J T P & Roerdink, F, *Ann NY acad sci* 446 (1985) 368.
4. Dijkstra, J, Van Galen, W J M, Hulstaert, C E, Kalicharan, D, Roerdink, F & Scherphof, G L, *Exp cell res* 150 (1984) 161.
5. Spanjer, H H, Morselt, H & Scherphof, G L, *Biochim biophys acta* 774 (1984) 49.

*Exp Cell Res* 168 (1987)

6. Derksen, J T P & Scherphof, G L, *Biochim biophys acta* 814 (1985) 151.
7. Dijkstra, J, Van Galen, M, Regts, D & Scherphof, G, *Eur j biochem* 148 (1985) 161.
8. Dijkstra, J, Van Galen, M & Scherphof, G, *Biochim biophys acta* 813 (1985) 287.
9. Munthe-Kaas, A C, *Exp cell res* 99 (1976) 319.
10. Zahlten, R N, Rogoff, T M & Steer, C J, *Fed proc* 40 (1981) 2460.
11. Steinman, R M, Mellman, I S, Muller, W A & Cohn, Z A, *J cell biol* 96 (1983) 1.
12. Szoka, F & Papahadjopoulos, D, *Proc natl acad sci US* 75 (1978) 4194.
13. Martin, F J & Papahadjopoulos, D, *J biol chem* 257 (1982) 286.
14. Duncan, R J S, Weston, P D & Wrigglesworth, R, *Anal biochem* 132 (1983) 68.
15. Heath, T D, Macher, B A & Papahadjopoulos, D, *Biochim biophys acta* 640 (1981) 66.
16. Knook, D L & Sleyster, E, *Exp cell res* 99 (1976) 444.
17. Peterson, G L, *Anal biochem* 83 (1977) 346.
18. Lowry, O H, Rosebrough, N J, Farr A L & Randall, R J, *J biol chem* 193 (1951) 265.
19. Böttcher, C J F, Van Gent, C M & Pries, C, *Anal chim acta* 24 (1961) 203.
20. Wilschut, J, *Liposome methodology in pharmacology and biology* (ed L D Leserman & J Barbet) p. 9. INSERM, Marseille (1982).
21. Martin, F J & Kung, V T, *Ann NY acad sci* 446 (1985) 447.
22. Amzel, L M & Poljak, R, *Ann rev biochem* 48 (1979) 961.
23. Munthe-Kaas, A C, Kaplan, G & Seljelid, R, *Exp cell res* 103 (1976) 201.
24. Lehnert, B E & Morrow, P E, *Immunol comm* 13 (1984) 313.
25. Griffin, Jr F M, *Proc natl acad sci US* 78 (1981) 3853.
26. Kiss, A L & Rohlich, P, *Eur j cell biol* 34 (1984) 88.
27. Hedin, U, Stenseth, K & Thyberg, J, *Eur j cell biol* 35 (1984) 41.
28. Petty, H R, Hafeman, D G & McConnell, H, *J immunol* 125 (1980) 2391.
29. Leserman, L D, Weinstein, J N, Blumenthal, R & Terry, W D, *Proc natl acad sci US* 77 (1980) 4089.
30. Petty, H R, Hafeman, D G & McConnell, H M, *J cell biol* 89 (1981) 223.
31. Hsu, M J & Juliano, R L, *Biochim biophys acta* 720 (1982) 411.
32. Lewis, J T, Hafeman, D G & McConnell, H M, *Biochemistry* 19 (1980) 5376.
33. Munn, M W & Parce, J W, *Biochim biophys acta* 692 (1982) 101.
34. Unkeless, J C, Fleit, H & Mellman, I S, *Adv in immunol* 31 (1981) 247.
35. Gaafar, H A & Doyle, J, *Proc soc exp biol med* 136 (1971) 121.
36. Leslie, R G Q & Niemets, A H, *Immunology* 37 (1979) 835.
37. Burton, D R, *Mol immunol* 22 (1985) 161.
38. Sancho, J, Gonzalez, E, Escanero, J F & Egido, J, *Immunology* 53 (1985) 283.
39. Dower, S K, Titus, J A, DeLisi, L & Segal, D M, *Biochemistry* 20 (1981) 6335.
40. Leslie, R G Q, *Mol immunol* 22 (1985) 513.
41. Harford, J, Klausner, R R & Ashwell, G, *Biol cell* 51 (1984) 173.
42. Townsend, R R, Wall, D A, Hubbard, A L & Lee, Y C, *Proc natl acad sci US* 81 (1984) 466.
43. Stahl, P, Schlesinger, P H, Sigardson, E, Rodman, J S & Lee, Y C, *Cell* 19 (1980) 207.
44. Ono, T & Awai, M, *Acta histochem cytochem* 17 (1984) 547.
45. Torchilin, V P, Berdichevsky, V R, Barsukov, A A & Smirnov, V N, *FEBS lett* 111 (1980) 184.
46. Pratten, M K & Lloyd, J B, *Biochim biophys acta* 881 (1986) 307.
47. Hällgren, R, Sjöström, P & Bill, A, *Immunology* 34 (1978) 347.
48. Young, J D-E, Ko, S S & Cohn, Z A, *Proc natl acad sci US* 81 (1984) 5430.

Received April 7, 1986

Revised version received July 21, 1986



## Microvascular studies on the origins of perfusion-limited hypoxia

MW Dewhirst<sup>1</sup>, H Kimura<sup>1</sup>, SWE Rehmus<sup>1</sup>, RD Braun<sup>2</sup>, D Papahadjopoulos<sup>3</sup>, K Hong<sup>3</sup> and TW Secomb<sup>4</sup>

Departments of <sup>1</sup>Radiation Oncology and <sup>2</sup>Ophthalmology Duke University Medical Center, Durham, NC 27710, USA; <sup>3</sup>Department of Cellular and Molecular Pharmacology University of California, San Francisco, CA 94143, USA; <sup>4</sup>Department of Physiology, Arizona Health Sciences Center, University of Arizona, Tucson, AZ 85724, USA.

**Summary** Two forms of hypoxia are thought to exist in tumours: (1) hypoxia caused by limitations of its diffusion (chronic hypoxia); and (2) hypoxia caused by changes in perfusion (acute hypoxia). Indirect information suggests the existence of perfusion-limited hypoxia, but there is no direct proof that fluctuations in blood flow can lead to hypoxia, nor is there any information regarding potential causes of fluctuant flow. In this study, we have begun to explore these questions using R3230AC tumours transplanted into rat dorsal-flap window chambers. Two types of fluctuant flow have been observed. The first type, usually confined to single vessels, is typified by instability of flow magnitude and direction, and total vascular stasis occurs, but only for a few seconds at a time (4% incidence). The second type of fluctuation occurs in groups of vessels and is cyclic, with cycle times ranging from 20–60 min. Total vascular stasis does not necessarily occur, but the fluctuations in red cell flux are accompanied by changes in vascular oxygen content, as measured by microelectrodes. Another source of chronic hypoxia has also been identified in these experiments. Nine per cent (9%) of vessels examined had plasma flow, but very low or absent red cell flux over periods of many minutes.

**Keywords:** vascular homeostasis; red cell flux; radiation sensitivity

Observations of fluctuant flow in tumour microvessels have been recognised since the invention of the window chamber model by Algire (Algire, 1943; Algire and Chalkley, 1945; Algire and Legallis, 1949; Endrich *et al.*, 1979; Endrich *et al.*, 1982; Intaglietta *et al.*, 1977; Yamaura and Matsuzawa, 1979). Speculations about the consequences of such behaviour on tumour oxygenation and radiation response have been made, but proof has been indirect. Yamaura and Matsuzawa (1979) found that window chamber tumours were most likely to recur near the tumour margin after irradiation, where intermittent blood flow was observed. Brown (1979) found radiobiologically viable hypoxic cells in the periphery of EMT6 tumours after treatment with a hypoxic cell cytotoxin. Such cells could have arisen from intermittent blood flow and consequential acute hypoxia between administration of the hypoxic cytotoxin and radiation exposure.

Evidence that intermittent blood flow leads to radiobiological hypoxia comes from studies of the radioresponse of tumour cells residing near or far from vessels, as determined from Hoechst 33342 dye staining (Chaplin *et al.*, 1987). Using matched pairs of fluorescent DNA-binding dyes, Trotter *et al.* (1991) found evidence for coordinated fluctuations in the staining intensity of contiguous vessels, suggesting that acute hypoxia may not require total cessation of tumour blood flow.

To date, however, there have been no studies that have provided direct quantitative data on the incidence and effects of fluctuant blood flow on tumour oxygenation, nor have there been any direct investigations into the underlying mechanisms. In this report we show that fluctuant blood flow occurs in two forms: (1) isolated vessels; and (2) groups of contiguous vessels. The latter behaviour we believe is due to arteriolar vasomotion. We also show that fluctuations in red cell flux – short of total vascular stasis – may be responsible for acute periods of hypoxia. Finally, we have identified

vessels that have plasma flow, but are largely devoid of red cells. These vessels may represent a previously unidentified source of chronic hypoxia.

### Materials and methods

#### Animal model

Fischer-344 rats (Charles River Laboratories, Raleigh, NC, USA), were surgically implanted with cutaneous window chambers, using methods previously described (Papenfuss *et al.*, 1979). R3230AC mammary tumours were transplanted into the window chambers at the time of surgery. The animals were housed in an environmental chamber, with normal light–dark cycles and access to food and water *ad libitum* for 9–11 days before experimentation. All protocols were approved by the Duke Animal Care and Use Committee.

#### Anaesthesia

Animals were anaesthetised using i.p. sodium pentobarbital (40–50 mg kg<sup>-1</sup>) for all surgical and experimental procedures. Rectal temperature was maintained at 37°C using thermostatically controlled blankets (Model 50-7503 homeothermic blanket, Harvard Bioscience, N. Natick, MA, USA). Blood pressures and heart rates were monitored (AT-codas, Dataq Instruments, Akron, OH, USA) from femoral arterial waveforms (Gould P23XL, Gould Instrument Systems, Cleveland, OH, USA).

#### Videomicroscopy

Videomicroscopy of window chamber microvasculature was used (Zeiss Photomicroscope III, Carl Zeiss, New York, USA), with either transillumination (40 W tungsten source) or epifluorescence (xenon arc source and rhodamine filter sets). Data were acquired using a CCD camera for transillumination (MTI CCD-72, Dage-MTI, Michigan City, MI, USA) or a silicon intensified tube camera for fluorescence microscopy (Model C2400-08, Hammamatsu Photonics, Hammamatsu City, Japan) and recorded to videotape (SVO-9500MD, Sony Corporation of America,

Correspondence: MW Dewhirst, Department of Radiation Oncology, DUMC-3455, Duke University Medical Center, Durham, NC 27710, USA. Presented at the 9th International Conference on Chemical Modifiers of Cancer Treatment, Christ Church, Oxford, UK, 22–26 August, 1995.



San Jose, CA, USA). A videotimer image was superimposed on all videotapes for record keeping (CTG-55 Video Timer, For.A. Co., Los Angeles, CA, USA).

### Liposomes

Liposomes were prepared according to a repeated freezing–thawing and extrusion method (Szoka and Papahadjopoulos, 1980). Liposome composition consisted of hydrogenated soya-phosphatidylcholine/cholesterol/polyethyleneglycol (*M*<sub>w</sub> 2000)-derivatised phosphatidylethanolamine/rhodamine-labelled phosphatidylethanolamine with molar ratio 60:40:2.4:0.48. Phospholipids were purchased from Avanti Polar Lipids, (Alabaster, AL, USA). Lipids were mixed in chloroform solution and the solvent was removed under reduced pressure at 50°C. Preheated buffer (20 mM Hepes, 145 mM sodium chloride, pH 7.2) at 55°C was added to dry lipids to yield a final phospholipid concentration of 10 mM. Multilamellar vesicles were formed by vortexing. After the lipids were fully hydrated, the sample was repeatedly frozen (–80°C) and thawed (55°C) to reduce the number of bilayers. The sample was then extruded three times through polycarbonate filter membranes with 0.2 µm pore diameters.

### Experimental protocols

**Red cell flux** Red cell flux was measured using a technique similar to that described previously (Brizel *et al.*, 1993), except that donor red cells were labelled with carbocyanine instead of fluorescein (Unthank *et al.*, 1993). The labelled red cells were administered *i.v.* to yield a fluorocrit of approximately 1%. Peripheral blood samples were analysed by flow cytometry before and after each experiment to determine the fluorocrit. In some experiments plasma was visualised by addition of liposomes. These liposomes (mean diameter of 0.2 µm) do not leak out of tumour vessels to an appreciable extent (Gaber *et al.*, 1996). Thus, they can be used to identify the path of plasma in the microvessels and to define vessel dimensions. Liposomes and red cells could be simultaneously visualised. Red cells were very bright compared with the liposomes, so the fluorescence from the liposomes did not mask the presence of labelled red cells (Figure 1). Red cell flux was then determined by counting the number of labelled red cells passing a defined point in a

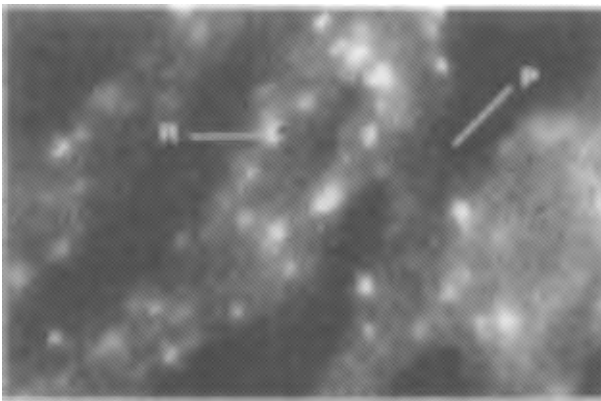


**Figure 1** Demonstration of video method for identification of red cells and liposome plasma marker. The fluorescence of carbocyanine-labelled red cells is superimposed on a background plasma marker of rhodamine-labelled liposomes. Red cells are clearly visible over the light background staining of the liposomes. Some red cells are seen in this grabbed frame as streaks of light. Under video playback, however, they are readily distinguished from the plasma liposomes. R, appearance of labelled red cells. P, plasma channel.

vessel over 1 min periods. The red cell flux was determined by dividing the counted labelled cells by the fluorocrit.

**Perivascular oxygenation** Oxygen concentration of vessels was measured using recessed tip microelectrodes, with tip diameters of 3–6 µm (Dewhirst *et al.*, 1992). Briefly, access to vessels was accomplished by removing one window and suffusing the surface of the window tissue with media bubbled with nitrogen to remove dissolved oxygen. Microelectrodes were positioned next to vessel walls using a micromanipulator (Model MO102E, Narishige Inc., Narishige, Japan). Polarographic current was measured (Chemical Microsensor, Model 1201, Diamond General Development Corporation, Ann Arbor, MI, USA), digitised and recorded continuously on computer using the CODAS software described above.

**Arteriolar diameter measurements** As the tumour grows in the window chamber, it recruits arteriolar feeders from the underlying fascial plane. Tumour arterioles are identified by looking for three characteristics: (1) divergent flow; (2) straight wall, with birefringence that is associated with the intimal layer; and (3) direct connection to microvessels that enter the tumour mass. Arteriolar diameters were measured using an image shearing monitor (Model 907, IPM, La Jolla, CA, USA).

## Results

### Red cell flux

The total period of observation ranged from 60 to 120 min. Two types of fluctuant flow were observed: (1) isolated fluctuation in single vessels; and (2) coordinated changes in red cell flux in contiguous vessels.

Fluctuant flow in isolated vessels was easy to identify, because such vessels showed dramatic changes in red cell flux, with a rapid time constant, frequent periods of stasis and no changes in diameter. In a total of 173 vessel segments evaluated in five experiments, eight vessels of this type were seen, giving an overall incidence of 4.4%; however, no vessels of this type were seen in two of the five experiments. In one example, a vessel showed flow stoppage or flow reversal a total of 110 times over a 120 min interval. The longest period of total stasis was 19 s. Usually, vessels maintained this behaviour throughout the experiment; thus, the behaviour did not move from one vessel segment to another.

We examined videotapes to see if any new vessels appeared during experiments that were not evident from the beginning, since such behaviour could also be indicative of vascular collapse followed by reopening or reperfusion. We did not find any examples of this type of behaviour, suggesting that total vascular collapse does not occur in unperturbed conditions in this model.

The second type of variation in red cell flux occurred coordinately in groups of vessels. The cycle time ranged from 15–60 min. Representative examples are shown in Figure 2.

An unexpected finding was that some vascular segments seemed to carry plasma flow (seen because of the presence of the fluorescent liposome plasma marker), but few red cells. We quantified this behaviour by analysing a 5 min period of videotape from each experiment. Any vessel that had less than two labelled red cells pass through it during that period was considered to be devoid of red cell flux. Since the labelled fraction was about 1% in these experiments, we can assume that the total red cell flux over the 5 min interval was probably less than 100 cells per minute. Vessels with plasma flow were seen in all three experiments in which this type of analysis was done. Out of a total of 310 vessel segments examined, 28 demonstrated plasma flow, giving an overall incidence of 9%. It appeared that low-flux vessels tended to be of smaller diameter, relative to the overall distribution of diameters, but further analysis is needed.

*Perivascular oxygenation vs red cell flux*

The changes in red cell flux are coordinated with changes in vascular oxygenation. One example is shown where a 3-fold drop in red cell flux was correlated with a concomitant drop in intravascular  $pO_2$  from 24 to 15 mmHg (Figure 3).

*Arteriolar vasomotion*

We examined temporal changes in arteriolar diameter in two experiments (Figure 4a and b). In both cases a complex vasomotor pattern of high frequency-low amplitude oscillation was superimposed on a lower frequency-higher amplitude oscillation. In one case, the oscillatory pattern was coordinated between a 100  $\mu\text{m}$  arteriole and several of its daughter vessels. In the other example, where no direct connection between two arterioles was observed in the preparation, the vasomotor activity did not seem to be coordinated. The temporal characteristics of slower frequency oscillations were similar to the oscillations in red cell flux that we reported above, suggesting a cause and effect relationship between the two.

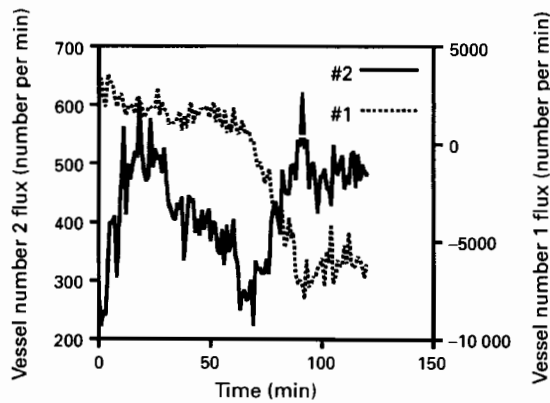


**Figure 2** Temporal changes in red cell flux of individual microvessels. In this example, coordinated changes in flux occurred in all vessels in the field of view. Two examples are shown. One vessel showed obvious sinusoidal fluctuations. Red cell flux in the second vessel gradually slowed over the first 60 min before reaching total stasis. Shortly thereafter, flow direction reversed and the red cell flux regained momentum, in the opposite direction, to actually surpass the baseline magnitude.

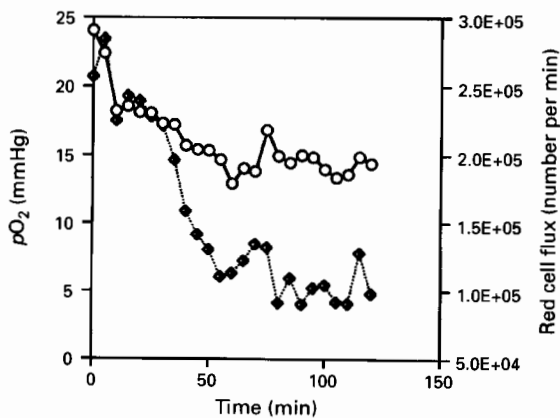


**Figure 3** Concomitant changes in red cell flux (. . .  $\diamond$  . . .) and vessel oxygen content ( $-\circ-$ ).

**Discussion**

In these experiments we present the first direct data in tumours to link temporal changes in microvessel red cell flux with changes in the oxygen content of the same vessel. These data clearly indicate that there is potential for perfusion-limited hypoxia in this tumour model, and that total vascular stasis is not required. The temporal patterns in red cell flux in groups of vessels are similar to patterns of arteriolar vasomotion, and suggest a cause and effect relationship. Theoretical analyses which include the competing effects of supply vs demand for oxygen, will delineate more clearly the extent of tissue volume that might be affected by such fluctuations in red cell flux and oxygen content (Secomb *et al.*, 1989). The most convincing published data to link

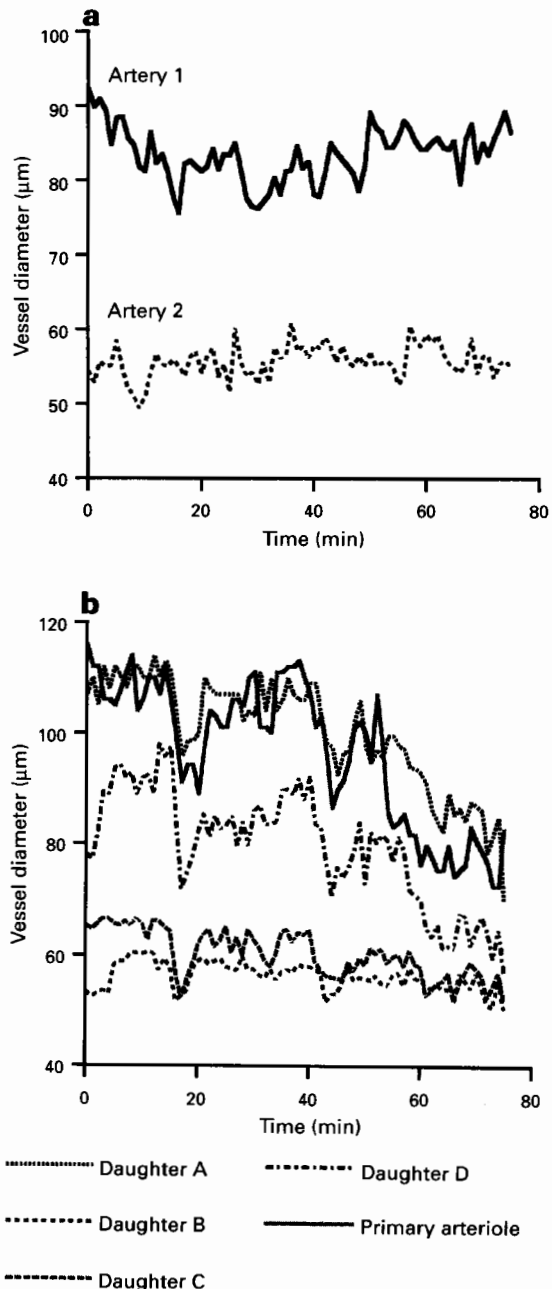


**Figure 4** Arteriolar vasomotor activity in two preparations. (a) vasomotor activity in two vessels does not seem to be coordinated. (b) Coordinated changes are seen between a large arteriole and several daughter arterioles.

fluctuant blood flow to hypoxia-induced radiation resistance comes from the classic work by Chaplin *et al.* (1986). When a freely diffusible dye, Hoechst 33342, was injected into mice 20 min before irradiation, there was no relation between staining intensity of tumour cells and radiation resistance. In contrast, when the dye was given simultaneously with treatment, there was a direct correlation between stain intensity and radiosensitivity, suggesting that cells nearest the vasculature were more aerobic and thus more radio-sensitive. The presence of intermittent blood flow was thought to be responsible for the loss of correlation between stain intensity and radioresistance when 20 min was allowed to elapse between dye administration and irradiation.

The same investigators combined the Hoechst dye technique with fluorescent cadmium disulphide microparticles (Chaplin *et al.*, 1987). When the two agents were administered simultaneously, SCCVII tumour vessels containing microparticles were always stained with the Hoechst dye as well. In contrast, when there was a 20 min time interval between administration of the two agents, there was a substantial level of mismatch. Similar results have been reported in other murine tumour lines, suggesting that this phenomenon is fairly ubiquitous (Jirtle, 1988; Minchinton *et al.*, 1990).

Previous reports have also suggested that total cessation of vessel flow may not be necessary for induction of hypoxia. This notion comes from studies using the SCCVII tumour and the administration of two fluorescent dyes, either coincidentally or sequentially (Trotter *et al.*, 1991). Using image analysis, regions of decreased staining intensity were identified as well as complete lack of staining for one dye vs the other. The overall incidence of a complete lack of staining of one dye vs the other was 8%, which is similar to the incidence of vessels with complete vascular stasis or intermittent blood flow reported in this study (4%), and previously (Dewhirst *et al.*, 1992). Thus, we believe that the pattern of total dye mismatch which is reported in the literature is caused by temporary vascular stasis (intermittent flow).

Trotter *et al.* (1991) also observed regions of contiguous vessel segments, called 'patches', which showed reduced staining intensity. They speculated that such vessels never reached total vascular stasis, but did experience periods of reduced flow between the time of administration of the first

and second dye. This result is consistent with our observation of coordinated cyclic variations in red cell flux. Our data on temporal kinetics of red cell flux and arteriolar diameter suggest cycle times from nadir to nadir ranging from 15 to 60 min. Thus, we agree that this phenomenon is most likely to be caused by arteriolar vasomotion.

Vasomotor activity is a well-known phenomenon which has been observed in normal arterioles. Recent studies of isolated tumour arteries indicate that the phenomenon is likely to be due to local regulatory changes in vessel function, rather than systemic vasomotor stimuli, since vasomotor activity was observed when these vessels were perfused *ex vivo*. Less vasomotor activity was seen in control normal arteries (Kennovin *et al.*, 1994).

Theoretical simulations suggest that the extent to which vasomotion affects oxygenation of adjacent cells in normal tissues is dependent upon the frequency (Secomb *et al.*, 1989). Higher frequency oscillations in red cell flux (e.g., 1 Hz) are likely to affect only cells immediately next to the vessel and the effect is relatively independent of oxygen consumption rate. Lower frequency oscillations, however, are likely to affect more tissue volume and, in this case, oxygen consumption rate will play a role in determining the extent of the effect. Studies of the effects of arteriolar vasomotion on oxygen transport in tumour tissues are needed.

The presence of some vessel segments with detectable plasma flow but low or absent red cell flux, indicates an additional source of chronic hypoxia. It has been speculated that such vessels might occur in tumours (Teicher *et al.*, 1991), but to our knowledge this is the first direct evidence for their existence. The overall incidence was 9%. If this translates to an average of 9% of the tumour volume, then this could be a significant source of hypoxia. Fortunately, this form of chronic hypoxia could be more readily corrected than true diffusion-limited hypoxia, since vascular channels pre-exist that could allow for passage of oxygen-containing solutions to such vessels.

#### Acknowledgements

This work was supported by grants from the NIH NCI CA40355 and The Howard Hughes Medical Institute.

#### References

- ALGIRE GH. (1943). Adaptation of transparent-chamber technique to mouse. *J. Natl Cancer Inst.*, **4**, 1–11.
- ALGIRE GH AND CHALKLEY HW. (1945). Vascular reactions of normal and malignant tissues, *in vivo* I. Vascular reactions of mice to wounds and to normal and neoplastic transplants. *J. Natl Cancer Inst.*, **6**, 73–85.
- ALGIRE GH AND LEGALLIS FY. (1949). Recent developments in transparent-chamber technique as adapted to mouse. *J. Natl Cancer Inst.*, **10**, 225–253.
- BRIZEL DM, KLITZMAN B, COOK JM, EDWARDS J, ROSNER G AND DEWHIRST MW. (1993). A comparison of tumor and normal tissue microvascular hematocrits and red cell fluxes in a rat window chamber model. *Int. J. Radiat. Oncol. Biol. Phys.*, **25**, 269–276.
- BROWN JM. (1979). Evidence for acutely hypoxic cells in mouse tumors, and a possible mechanism for reoxygenation. *Br. J. Radiol.*, **52**, 650–656.
- CHAPLIN DJ, DURAND RE AND OLIVE PL. (1986). Acute hypoxia in tumors: implications for modifiers of radiation effects. *Int. J. Radiat. Oncol. Biol. Phys.*, **12**, 1279–1282.
- CHAPLIN DJ, OLIVE PL AND DURAND RE. (1987). Intermittent blood flow in a murine tumor: radiobiological effects. *Cancer Res.*, **47**, 597–603.
- DEWHIRST MW, ONG ET, KLITZMAN B, SECOMB TW, VINUYA RZ, DODGE R, BRIZEL D AND GROSS JF. (1992). Perivascular oxygen tensions in a transplantable mammary tumor growing in a dorsal flap window chamber. *Radiat. Res.*, **130**, 171–182.
- ENDRICH B, INTAGLIETTA M, REINHOLD HS AND GROSS JF. (1979). Hemodynamic characteristics in microcirculatory blood channels during early tumor growth. *Cancer Res.*, **39**, 17–23.
- ENDRICH B, HAMMERSEN F, GOTZ A AND MESSMER K. (1982). Microcirculatory blood flow, capillary morphology, and local oxygen pressure of the hamster amelanotic melanoma A-Mel-3. *J. Natl Cancer Inst.*, **68**, 475–485.
- GABER MH, WU NZ, HONG K, HUANG SK, DEWHIRST MW AND PAPAHDJOPOULOS D. (1996). Thermosensitive liposomes: Extravasation and release of contents in tumor microvascular networks. *Int. J. Radiat. Oncol. Biol. Phys.* (in press).
- INTAGLIETTA M, MYERS RR, GROSS JF AND REINHOLD HS. (1977). Dynamics of microvascular flow in implanted mouse mammary tumors. *Bibliotheca Anatomica*, **15**, 273–276.
- JIRTLE RL. (1988). Chemical modification of tumor blood flow. *Int. J. Hyperthermia*, **4**, 355–372.
- KENNOVIN GD, FLITNEY FW AND HIRST DG. (1994). Upstream modification of vasoconstrictor responses in rat epigastric artery supplying an implanted tumour. *Adv. Exp. Med. Biol.*, **345**, 411–416.
- MINCHINTON AJ, DURAND RE AND CHAPLIN DJ. (1990). Intermittent blood flow in the KHT sarcoma—flow cytometry studies using Hoechst 33342. *Br. J. Cancer*, **62**, 195–200.
- PAPENFUSS D, GROSS JF, INTAGLIETTA M AND TREESE FA. (1979). A transparent access chamber for the rat dorsal skin fold. *Microvasc. Res.*, **18**, 311–318.



- SECOMB TW, INTAGLIETTA M AND GROSS JF. (1989). Effects of vasomotion on microcirculatory mass transport. *Prog. Appl. Microcirc.*, **15**, 49–61.
- SZOKA FC AND PAPAHDJOPOULOS D. (1980). Comparative properties and methods of preparation of lipid vesicles (liposomes). *Am. Rev. Biophys. Bioeng.*, **9**, 467–508.
- TEICHER BA, HERMAN TS, HOPKINS RE AND MENON K. (1991). Effect of oxygen level on the enhancement of tumor response to radiation by perfluorochemical emulsions or a bovine hemoglobin preparation. *Int. J. Radiat. Oncol. Biol. Phys.*, **21**, 969–974.
- TROTTER MJ, CHAPLIN DJ AND OLIVE PL. (1991). Possible mechanisms for intermittent blood flow in the murine SCCVII carcinoma. *Int. J. Radiat. Biol.*, **60**, 139–146.
- UNTHANK JL, LASH JM, NIXON JC, SIDNER RA AND BOHLEN HG. (1993). Evaluation of carbocyanine-labeled erythrocytes for microvascular measurements. *Microvasc. Res.*, **45**, 193–210.
- YAMAURA H AND MATSUZAWA T. (1979). Tumor regrowth after irradiation. An experimental approach. *Int. J. Radiat. Biol.*, **35**, 201–219.

## Research Paper

# Intra and Inter-Molecular Interactions Dictate the Aggregation State of Irinotecan Co-Encapsulated with Floxuridine Inside Liposomes

Awa Dicko,<sup>1</sup> April A. Frazier,<sup>1</sup> Barry D. Liboiron,<sup>1</sup> Anne Hinderliter,<sup>2</sup> Jeff F. Ellena,<sup>3</sup> Xiaowei Xie,<sup>1</sup> Connie Cho,<sup>1</sup> Tom Weber,<sup>1</sup> Paul G. Tardi,<sup>1</sup> Donna Cabral-Lilly,<sup>4</sup> David S. Cafiso,<sup>3</sup> and Lawrence D. Mayer<sup>1,5</sup>

Received December 14, 2007; accepted February 19, 2008; published online March 5, 2008

**Purpose.** The inter/intramolecular interactions between drugs (floxuridine, irinotecan) and excipients (copper gluconate, triethanolamine) in the dual-drug liposomal formulation CPX-1 were elucidated in order to identify the physicochemical properties that allow coordinated release of irinotecan and floxuridine and maintenance of the two agents at a fixed, synergistic 1:1 molar ratio.

**Methods.** Release of irinotecan and floxuridine from the liposomes was assessed using an *in vitro*-release assay. Fluorescence, Nuclear Magnetic Resonance spectroscopy (NMR) and UV-Vis were used to characterize the aggregation state of the drugs within the liposomes.

**Results.** Coordinated release of the drugs from liposomes was disrupted by removing copper gluconate. Approximately 45% of the total irinotecan was detectable in the copper-containing CPX-1 formulation by NMR, which decreased to 19% without copper present in the liposomal interior. Formation of higher order, NMR-silent aggregates was associated with slower and uncoordinated irinotecan release relative to floxuridine and loss of the synergistic drug/drug ratio. Solution spectroscopy and calorimetry revealed that while all formulation components were required to achieve the highest solubility of irinotecan, direct drug-excipient binding interactions were absent.

**Conclusions.** Long-range interactions between irinotecan, floxuridine and excipients modulate the aggregation state of irinotecan, allowing for simultaneous release of both drugs from the liposomes.

**KEY WORDS:** copper gluconate; CPX-1; rotational diffusion; spectroscopy; triethanolamine.

## INTRODUCTION

The use of nanoscale carriers has expanded beyond applications with single therapeutic agents to systems designed for delivery of drug combinations in a coordinated fashion. Examples include nanoscale delivery systems that first expose solid tumors to an anti-angiogenesis agent to cause vascular collapse followed by the slow release of a cytotoxic agent to kill the tumor cells directly (1), as well as combinations co-formulated to maintain fixed drug ratios after administration *in vivo* (2). The latter approach relates to recent evidence that the therapeutic activity of many anticancer drug combinations

is dependent on the molecular ratio of the combined drugs, where certain ratios can interact synergistically while other ratios of the same agents can be antagonistic (2,3). Liposomal carriers have been applied to combination therapy to develop formulations that efficiently co-encapsulate two antineoplastic agents in a single liposome and maintain their ratio in the plasma after *i.v.* administration, overcoming disparate *in vivo* clearance mechanisms that typically disrupt the ratio of injected drugs when administered as a free drug cocktail. A similar concept was more recently used to co-encapsulate fludarabine and mitoxantrone in liposomes for the potential treatment of leukemia and lymphoma (4).

CPX-1 is a liposomal formulation of irinotecan and floxuridine that maintains the synergistic 1:1 molar ratio of the two drugs for up to 24 h in the plasma of mice and humans while at the same time makes the drugs bioavailable (2,3,5–9). CPX-1 has demonstrated dramatically increased therapeutic activity in preclinical tumor models compared to free drug cocktail and has provided encouraging signs of therapeutic activity in clinical trials (6,7). The importance of maintaining the 1:1 molar ratio of irinotecan/floxuridine is highlighted in Table I. Liposome formulations were prepared containing irinotecan/floxuridine molar ratios of 10:1, 1:1 and 0.1:1. Previous studies (2) demonstrated that *in vitro*, the 10:1 drug ratio is antagonistic in the HT-29 human colorectal cancer cell line and the 0.1:1 drug ratio is antagonistic in the Capan-1 human pancreatic cancer cell line. In both tumor

**Electronic supplementary material** The online version of this article (doi:10.1007/s11095-008-9561-z) contains supplementary material, which is available to authorized users.

<sup>1</sup> Celator Pharmaceuticals Corp., 1779 W 75th Avenue, Vancouver, British Columbia V6P 6P2, Canada.

<sup>2</sup> Department of Chemistry and Biochemistry, College of Science and Engineering, University of Minnesota-Duluth, 1039 University Drive, Duluth, Minnesota 55812-3020, USA.

<sup>3</sup> Department of Chemistry, University of Virginia, McCormick Road, P.O. Box 400319, Charlottesville, Virginia 22904-4319, USA.

<sup>4</sup> Celator Pharmaceuticals Inc., 303B College Road East, Princeton, New Jersey 08540, USA.

<sup>5</sup> To whom correspondence should be addressed. (e-mail: lmayer@celatorpharma.com)

**Table 1.** Drug Ratio Dependent *In Vivo* Efficacy of Irinotecan/Floxuridine Combinations Co-Encapsulated Inside 100 nm DSPC/DSPG/Chol (7:2:1) Liposomes

Irinotecan/Floxuridine Molar Ratio Inside Liposomes	Plasma Irinotecan/Floxuridine Molar Ratio Range over 24 h <sup>a</sup>	Log Cell Kill at MTD <sup>b</sup>	
		HT-29	Capan-1
10:1	7.2–15.3	1.48	ND
1:1	0.93–1.43	1.71	1.81
0.1:1	0.07–0.13	ND	0.56

Adapted from (2)

MTD maximum tolerable dose, ND not determined

<sup>a</sup>Drug levels determined by HPLC in plasma samples collected from mice after intravenous injection of CPX-1 [2]<sup>b</sup>Log cell kill =  $[T - C]/(3.32 \times T_d)$  where  $T - C$  is the treatment induced delay for tumors to reach a specified size and  $T_d$  is the tumor doubling time (7 days for both tumor models)

lines, the 1:1 molar ratio was strongly synergistic. When these liposome formulations were administered intravenously to mice, the plasma irinotecan/floxuridine ratio was maintained very near the formulated drug ratio over 24 h (Table 1). This allowed us to test whether the efficacy of this drug combination was drug ratio dependent *in vivo*. The degree of antitumor activity can be quantified by determining the log cell kill (LCK) provided by treatments based on the delay in tumor growth to a pre-specified size (2). In the HT-29 solid tumor model, the synergistic 1:1 molar ratio was more efficacious than the 10:1 molar ratio and in fact, the 10:1 molar ratio was less efficacious than liposomal irinotecan alone. Similarly, the synergistic 1:1 molar ratio was markedly more efficacious than the antagonistic 0.1:1 molar ratio in the Capan-1 solid tumor model and the antagonist combination was approximately fivefold less active than liposomal irinotecan alone. Consequently, it is clear that optimal therapeutic activity *in vivo* is dependent on maintaining the molar ratio of irinotecan/floxuridine near 1:1 as significant divergence in either direction could lead to loss of efficacy.

The importance of characterizing co-formulated drug combination delivery systems stems from the fact that the physicochemical interactions between drugs and excipients likely modulate the drug disposition and physical state inside liposomes which ultimately will dictate drug release and *in vivo* performance. We have demonstrated that liposomes containing copper gluconate/triethanolamine (TEA) at pH 7.0 are able to actively sequester irinotecan (5) without employing acidic pH gradients that could lead to lipid and/or drug instability during storage due to acid-mediated hydrolysis (10–14). Although unbuffered copper sulfate can be used to encapsulate irinotecan, high copper concentrations are required and the pH inside the liposomes is very low (pH 3.5). To reduce the amount of copper required and maintain the pH near neutrality, copper gluconate was chosen and was found to be superior in percentage encapsulation and drug retention compared to copper sulfate (5). Subsequent investigations revealed that the loading of irinotecan into liposomes was mediated by a charge-neutral stoichiometric exchange of TEA out of the liposome with concurrent irinotecan exchange into the liposome resulting in irinotecan self-association upon accumulation (15).

We have previously shown that coordinated release of irinotecan and floxuridine could be achieved by altering the concentration of cholesterol (Chol) of distearoylphosphatidylcholine/ distearoylphosphatidylglycerol (DSPC/DSPG) based formulations containing copper gluconate/TEA (5). The retention of floxuridine in plasma was optimal in formulations with less than 20 mol% cholesterol while increasing cholesterol concentration enhanced irinotecan retention. CPX-1 liposomes composed of DSPC/DSPG/Chol, 7:2:1 exhibited matched release rates for both drugs that were maintained for prolonged time after *in vivo* administration (5). Additional characterization of CPX-1 revealed that the release of irinotecan could also be dependent on its aggregation state inside liposomes (15). Floxuridine and numerous excipients present inside CPX-1 liposomes may interact with irinotecan, individually or in combination, and this could dictate the self-association of irinotecan. Therefore, in the present study, an in-depth characterization of the interactions of irinotecan with floxuridine, copper gluconate and TEA was undertaken in order to establish the physicochemical features that control irinotecan release from liposomes.

## MATERIAL AND METHODS

### Materials

Distearoylphosphatidylglycerol (DSPG) and distearoylphosphatidylcholine (DSPC) were purchased from Lipoid (Newark, NJ, USA). Cholesterol (Chol) was obtained from Solvay (Houston, TX, USA). Irinotecan hydrochloride trihydrate was obtained as a dry powder from ScinoPharm Taiwan, Ltd. (Tainan, Taiwan). Floxuridine was obtained from the Zhejiang Hisun Pharmaceutical Company (Taizhou City, China). Copper gluconate was purchased from Purac (Lincolnshire, IL, USA). All other chemicals were obtained from Sigma Chemical Company (St. Louis, MO, USA).

### Preparation of the Formulations

The formulations were prepared by a process where irinotecan and floxuridine are encapsulated in pre-formed liposomes generated by a solvent emulsion and size reduction procedure as previously described (5,15). Briefly, the lipids (DSPC/DSPG/Chol, 7:2:1, mol%) were dispersed in solutions of 100 mM copper gluconate/180 mM TEA (pH 7.0, referred to as CPX-1) or 10 mM sodium gluconate/180 mM TEA (pH 7.0, referred to as copper-free formulation). The liposomes were extruded at 70°C through two stacked 100 nm polycarbonate filters using a water jacketed extrusion apparatus. The external buffer was exchanged for sucrose phosphate EDTA buffer at pH 7.0 (SPE) using tangential flow chromatography. The coencapsulation of irinotecan and floxuridine was carried out by mixing the drug solution and the liposomes for 1 h at 50°C. The unencapsulated drugs were removed by exchanging the external liposomal buffer into sucrose phosphate buffer at pH 7.0 (SP) using tangential flow chromatography.

### *In Vitro* Release (IVR) Assay

CPX-1 or the copper-free formulations were added to the phosphate incubation buffer (Octyl  $\beta$ -D-glucopyranoside

(OGP)/EDTA, pH 5.25) preheated at 37°C in a shaking water bath. Aliquots collected at selected timepoints over 24 h were centrifuged at 10,000×g for 20 min using Microcon YM-100 centrifugal filters units (Millipore, Billerica, MA) to separate the encapsulated material from the released drugs. Irinotecan and floxuridine were assayed by high performance liquid chromatography (HPLC) using Waters C<sub>18</sub> reverse phase columns. The percentage of drug release was calculated as the molar ratio of free drug to total drug.

### Cryogenic Transmission Electron Microscopy

The cryogenic transmission electron microscopy (cryo-EM) investigations were performed with a Zeiss EM 902A Transmission Electron Microscope (Carl Zeiss NTS, Oberkochen, Germany). The procedure used for sample preparation and image recording is described in Almgren *et al.* (16). Briefly, a small drop (~1 µl) of sample was deposited on a copper grid covered with a perforated polymer film covered with a thin carbon layer on both sides. Excess liquid was removed by means of blotting with a filter paper, leaving a thin film of the solution on the grid. Immediately after blotting, the sample was vitrified in liquid ethane, held just above its freezing point. Samples were kept below -165°C and protected against atmospheric conditions during both transfer to the microscope and examination. Images were recorded under low dose conditions at 105,000× magnification with a defocus of 3 µm.

### Nuclear Magnetic Resonance (NMR) Spectroscopy

#### Sample Preparation

The peaks of the external SP buffer solution of CPX-1 interfere with those of the internal liposomal components. To resolve this problem, the external SP buffer was replaced with an approximate iso-osmotic buffer of 150 mM sodium chloride (NaCl) or 150 mM NaCl/40 mM sodium phosphate, pH 7.0 in deuterium oxide (D<sub>2</sub>O). Four aliquots of 75 µl of liposomes were applied to a Sephadex G-50, 1 ml spin column. The liposome fraction was collected in the void volume by centrifuging at 515×g for 2 min. The samples were diluted to 3 mM irinotecan and/or 3 mM floxuridine. 3-(trimethylsilyl)-1-propanesulfonic acid (DSS; Sigma-Aldrich Canada, Oakville, ON) was used as an internal chemical shift and intensity standard.

#### <sup>1</sup>H NMR Measurements

One dimensional proton NMR (1D <sup>1</sup>H NMR) spectra were acquired on a Bruker Avance 400 MHz spectrometer (Bruker Biospin, Milton, ON). Advanced Chemistry Development's (ACD) 1D/2D NMR Processor was used to analyze the NMR data (Advanced Chemistry Development, v. 10.01, Toronto, ON). Linewidth measurements were made as the full width at half maximum (FWHM) of calculated Lorentzian-Gaussian (1:1) peaks, iteratively fitted to the experimental spectrum through a least squares routine in the ACD software.

Integration of irinotecan and floxuridine proton resonant peak intensities (in the region 6–8 ppm) was used as a means

to determine the concentration of the freely soluble portion of each drug in the liposomal formulations, using the common assumption that precipitated and/or highly aggregated drug portions (if present) are NMR-silent. Resonant peak full width at half maximum (FWHM) was used as an indicator of the tumbling rate (and hence size) of the molecule under study, using the well-characterized globular protein ubiquitin amide as a linewidth standard of known molecular morphology (i.e. spherical) and weight (8.6 kDa). A full description of the relationships between molecule size, tumbling rate and NMR linewidth is given in the Discussion section.

### Ultraviolet-Visible (UV-Vis) Spectroscopy

Samples of increasing concentrations of irinotecan were made by dissolving the drug powder in water at 50°C. UV-Vis spectroscopy was carried out on a Shimadzu UV-2401PC (Shimadzu Scientific Instruments, Columbia, MD) and a Varian Cary 4000 equipped with a 6×6 Peltier sample holder (Varian, Palo Alto, CA). A wavelength range of 280–500 nm was collected and a slit width of 1.0 nm was used. Measurements were made at ambient temperature using quartz cells with a 10 or 1 mm path length.

### Fluorescence Spectroscopy

Samples were prepared with increasing concentrations of irinotecan in water to approximately 1 mM. Duplicates of these titration samples were prepared in the presence of 1 mM floxuridine or 1 mM copper gluconate/TEA. The measurements were made using a Varian Cary Eclipse fluorescence spectrophotometer (Varian, Palo Alto, CA). Data were collected at room temperature using a small cuvette. The excitation wavelength was 425 nm.

### Isothermal Titration Calorimetry

Isothermal titration calorimetry (ITC) experiments were carried out on a Microcal VP-ITC (Microcal, Northampton, MA). Each experiment was carried out at 25°C in high feedback mode/gain, and a reference power of 10 µCal/s. The spacing between each injection varied between experiments over a range of 300 to 480 s required to reestablish a stable baseline. Data analysis was carried out using Origin 7.0 (Originlab, Northampton, MA).

### Irinotecan Solubility Assay

Irinotecan absorbs light readily and has an extinction coefficient at 370 nm of 22,500±200 M<sup>-1</sup> cm<sup>-1</sup> whether in double distilled water or SP buffer. Irinotecan was added to the following solutions at a theoretical concentration of 85 mM:

1. Water
2. 90 mM floxuridine
3. 100 mM copper gluconate/180 mM TEA, pH 7.0
4. 100 mM copper gluconate/180 mM TEA, pH 7.0+ 90 mM floxuridine
5. 10 mM sodium gluconate/180 mM TEA, pH 7.0

Samples were heated at 50°C, vortexed, pH adjusted to 7.0 using NaCl or HCl, then centrifuged at 2,500×g for 10 min

to pellet any undissolved irinotecan. One milliliter aliquots from the supernatant were taken and placed in 1.5 ml Eppendorf tubes. These tubes were spun for an additional 10 min at 15,000×g to pellet any remaining undissolved irinotecan. By visual inspection, the solutions were clear when samples were taken for absorbance measurements. UV-Vis absorbance readings were taken on a Shimadzu UV-2401PC (Shimadzu Scientific Instruments, Columbia, MD). Due to the concentrated nature of the solutions, the aliquots were diluted to an appropriate concentration with water, such that the absorbance reading was below 1.5.

## RESULTS

### Effect of Entrapped Copper Gluconate on the Physical State of Irinotecan and Floxuridine Inside Liposomes

In a previous study, we demonstrated that TEA mediated irinotecan encapsulation into copper gluconate/TEA containing liposomes (15). We speculated that irinotecan interacted with neighboring drug molecules resulting in larger supramolecular complexes that were retained inside the liposomes. To elucidate the impact of copper gluconate on the drug's aggregation state, we designed a copper-free formulation containing the same amount of TEA as in CPX-1 that was capable of encapsulating both irinotecan and floxuridine in a similar TEA-dependent manner. The internal buffer of the copper-free formulation consisted of 10 mM sodium gluconate/180 mM TEA, pH 7.0.

An *in vitro* drug release (IVR) assay was performed to compare the release rate of irinotecan from copper-free and CPX-1 liposomes. The performance of CPX-1 relies on maintaining the 1:1 ratio for both floxuridine and irinotecan and avoiding significant deviation from this synergistic ratio is critical for optimal therapeutic activity. The IVR assay was designed as a simple, reproducible, sensitive and validateable tool to detect changes in drug release from different formulations that may affect performance. It also provides a valuable quality control measure to assure batch-to-batch uniformity. In this assay, the liposomes were incubated at 37°C in the presence of a membrane perturbing surfactant

(OGP) that induced increased membrane permeability to mimic conditions *in vivo*. Drug released from the liposomes was determined by quantifying the concentration of drug in the filtrate after ultrafiltration of the test solution whereas the liposomes and entrapped contents were retained in the retentate reservoir. Figure 1 shows similar floxuridine release rates from both CPX-1 and copper-free liposomes when incubated over 24 h at 37°C. Approximately 50% of the entrapped irinotecan was released from CPX-1 within 6 h at 37°C, but irinotecan release from copper-free liposomes was only 25% at 6 h and less than 45% after 24 h at 37°C, compared to greater than 60% for CPX-1.

Interestingly, cryo-EM analysis of CPX-1 did not reveal any morphological features that were distinct from the copper-free formulation. As shown in Fig. 2, there was no evidence of drug crystallization or precipitation inside the liposomes and also no apparent changes in the membrane structure were observed. Both liposomes presented a regular, faceted polyhedral surface morphology. Occasionally, an additional internal lamellae or an electron dense line was observed in the liposomes interior. This feature was attributed to invaginated planes of gel phase lipid arising from the polyhedral shape of the liposomes since such structures were also present in the liposomes prior to drug loading (data not shown).

To delineate the physicochemical basis for the differences in irinotecan IVR results for CPX-1 and copper-free liposomes, proton NMR spectra were acquired on both formulations and the free drugs in solution. The solution state NMR spectrum in the aromatic region of an equimolar mixture of irinotecan and floxuridine is shown in Fig. 3a. Peaks in the aromatic region were assigned to either floxuridine or irinotecan through measurement of the individual drugs in solution (data not shown). The aromatic protons of irinotecan appear at approximately 7.2, 7.7 and 7.8 ppm while floxuridine has two doublets centered at 7.4 and 8.0 ppm. Figure 3b shows the <sup>1</sup>H NMR spectrum of CPX-1 (1) and the copper-free formulation (2) in the 5–9 ppm region. Peak identities were assigned using individual liposomal drugs spectra (data not shown) and were shifted compared to the solution state spectrum. Casual inspection

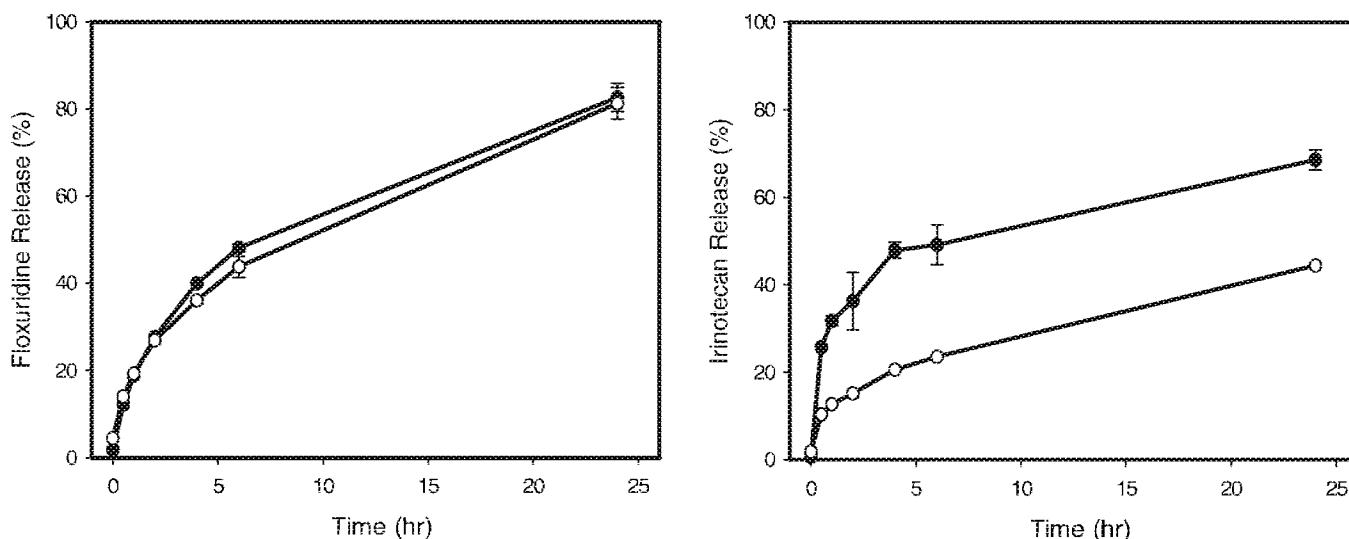


Fig. 1. *In vitro* release of floxuridine and irinotecan from CPX-1 (filled circle) and copper-free liposomes (open circle).



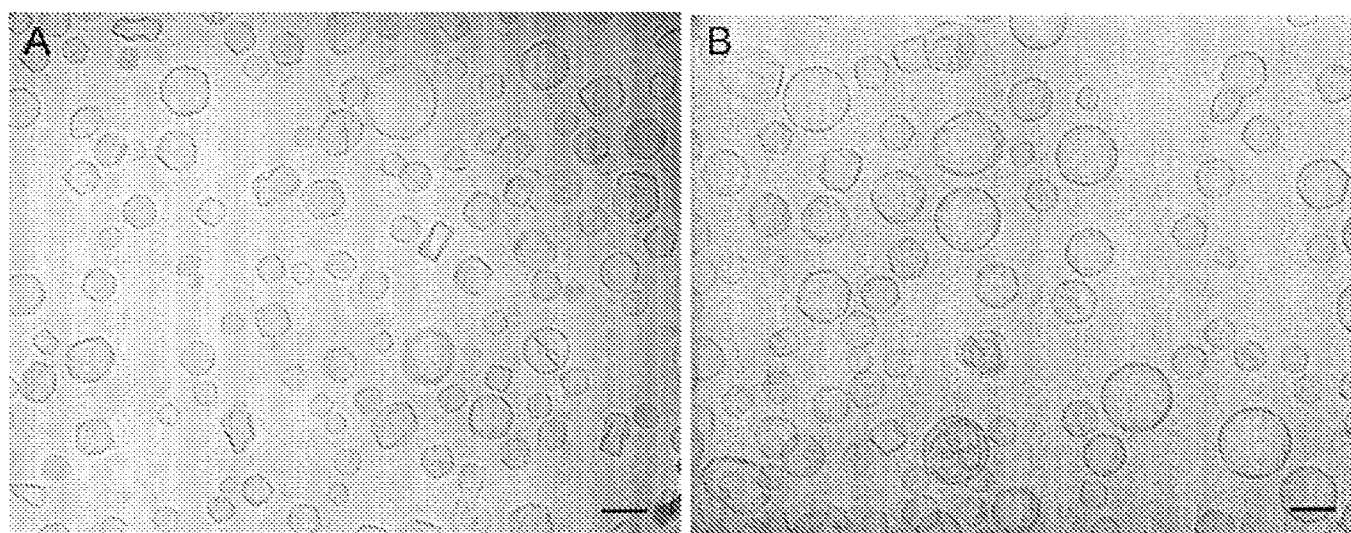


Fig. 2. Cryo-electron micrographs of (A) CPX-1 and (B) copper-free formulations. The scale bar represents 100 nm.

reveals a clear broadening of the aromatic proton signals (between 6 and 8 ppm) for both formulations relative to the free drugs and a reduction in irinotecan peak intensities relative to the floxuridine peaks. Additionally, irinotecan peak intensities are smaller in the copper-free formulation relative to CPX-1.

The integrated intensities of floxuridine and irinotecan downfield peaks between 6 and 8 ppm in the copper-free and CPX-1 formulations are presented in Table II. The intensity of the DSS peak at 0 ppm was used as an internal concentration standard such that its integral was set to a value equal to the DSS concentration in millimolar units. Thus, floxuridine concentration can be gauged directly from the integrated intensity reported in Table II as the high field (HF, at ~6.1 ppm) and low field (LF, at ~7.8 ppm) peaks each correspond to one proton. A large proportion of the available floxuridine (3 mM) is observed by  $^1\text{H}$  NMR in both samples; 94% of the drug is accounted for in the copper-free formu-

lation while approximately 75% of the total floxuridine is detected in CPX-1. The increased line broadening of floxuridine peaks in CPX-1 is likely due to paramagnetic broadening from the copper gluconate/TEA buffer system.

For irinotecan, the peaks between 6.5 and 7.5 ppm (Fig. 3b) correspond to four aromatic protons. If 100% of the irinotecan were observed, an integrated intensity of 12 ( $4 \times 3$  mM) would be measured. The data in Table II show that in the case of the copper-free formulation, only approximately 19% of the available irinotecan can be observed in the  $^1\text{H}$  NMR spectrum. For CPX-1, this value increases to approximately 45%.

In both formulations, the NMR peaks of the two drugs are very broad compared to the spectrum in solution (Table III). Irinotecan line broadening is similar in the copper-free *versus* the CPX-1 formulation: linewidths at 7.25 ppm are 56 and 52 Hz, respectively, compared to 2–3 Hz for the comparable signals in a solution of free irinotecan. At 7.1 ppm, the

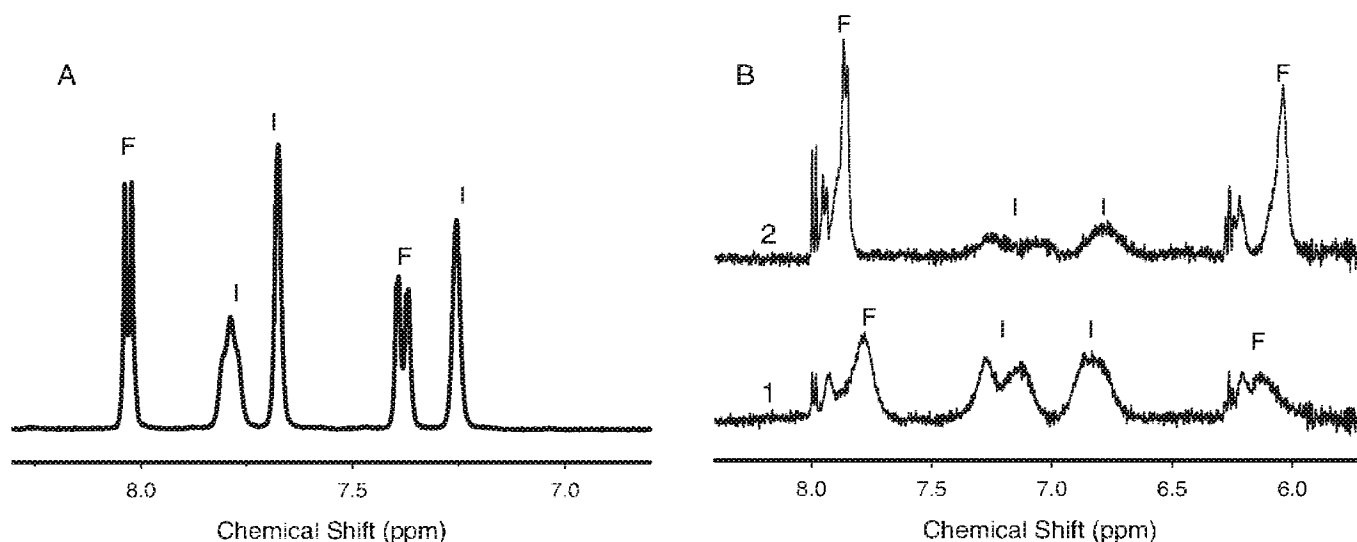


Fig. 3. Proton NMR spectra of (A) a mixture of 3 mM irinotecan (*I*) and 3 mM floxuridine (*F*) in water; (B) CPX-1 (*I*) and copper-free liposomes (*2*).

**Table II.** Integrated NMR Signal Intensities of Floxuridine and Irinotecan Relative to the Internal DSS Concentration Standard for the Copper-Free and CPX-1 Formulations (Drug Concentrations are 3 mM)

Sample	Low Field Floxuridine	Irinotecan	High Field Floxuridine	% Floxuridine Observed <sup>b</sup>	% Irinotecan Observed <sup>b</sup>
Protons	1	4	1	–	–
Copper-free	2.82	2.24	2.94	94.0	18.7
CPX-1	2.50	5.39	1.71 <sup>a</sup>	75.0	44.9

<sup>a</sup>The integrated intensity of this peak is reduced due to the presence of paramagnetic Cu(II) in the copper gluconate buffer. Analysis of  $T_1$  relaxation times (data not shown) indicate that only this peak is susceptible to augmented relaxation and decreased intensity due to transient Cu(II) coordination to a small portion of the available floxuridine. This feature has the effect of reducing the observable floxuridine for this peak only. The low field peak of the CPX-1 sample was used to determine the amount of observable floxuridine.

<sup>b</sup>Calculated as the integrated intensity divided by the number of protons, multiplied by the DSS concentration to yield the concentration of observable drug.

linewidth is less for CPX-1 (29 Hz) *versus* the copper-free formulation (49 Hz). The peaks of floxuridine appear sharper in the copper-free sample compared to CPX-1, suggesting that this broadening effect is due to the presence of paramagnetic copper ions. The full width at half maximum (FWHM) of two of the aromatic proton resonances for irinotecan in solution and the two liposomal formulations are reported in Table III. For comparison, the reported linewidth of the protons of ubiquitin amide (6 Hz), a 8.6 kDa globular protein, is also listed (17). At constant temperature, the resonant linewidth is directly proportional to the spin-spin ( $T_2$ ) relaxation time in NMR, which in turn is a product of the rotational correlation time of the molecule under study. Slow molecular tumbling leads to augmented  $T_2$  (transverse) spin-spin relaxation rates that can measurably broaden the resonant proton signals, and in extreme cases, thwart detection of the proton in the NMR experiment (18). As the molecular dynamics of ubiquitin amide are well studied, it is useful for comparison as a large macromolecule of roughly spherical shape against the tumbling behavior of NMR-detectable irinotecan aggregates in CPX-1.

### Solution State Characterization of Irinotecan

The above NMR data indicated that the state of irinotecan aggregation in CPX-1 was different from that in the copper-free formulation and this, in turn, correlated with altered irinotecan *in vitro* release kinetics. Thus, a systematic characterization study was undertaken to identify the nature of interactions between excipients and drugs in CPX-1 that could impact the self-association state of irinotecan. This study was performed in solution to avoid interferences from the liposomes.

**Table III.** Full Width at Half Maximum (FWHM, in Hertz) of Irinotecan Proton NMR Resonances for Irinotecan in Solution and in the CPX-1 and Copper-Free Liposomal Formulations (Drug Concentrations are 3 mM)

Sample	Peak 1		Peak 2	
	FWHM	$\delta$ (ppm)	FWHM	$\delta$ (ppm)
Solution	3.4	7.75	2.1	7.350
CPX-1	56	7.25	29	7.12
Copper-free	52	7.25	49	7.06
Ubiquitin amide	6 Hz			

### Influence of Floxuridine and CPX-1 Excipients on Irinotecan Solubility

We investigated the impact of floxuridine, copper gluconate/TEA buffer, both copper gluconate/TEA buffer plus floxuridine, and copper-free buffer (10 mM sodium gluconate/180 mM TEA) on the solubility of irinotecan (all solutions adjusted to pH 7.0 pre- and post-addition of irinotecan). For these comparisons, sufficient irinotecan was added to provide a concentration of 85 mM if all drug was dissolved. This concentration was selected based on the calculated effective drug concentration inside CPX-1. In the absence of any added solutes, irinotecan, heated to 50°C and then allowed to cool to ambient temperature, provided a soluble concentration of 29 mM (Table IV). Addition of either floxuridine or copper gluconate/TEA individually to irinotecan (at concentrations present inside CPX-1 liposomes) resulted in an increase in irinotecan solubility to 46 and 48 mM, respectively. Interestingly, combining floxuridine and copper gluconate/TEA resulted in the highest level of irinotecan solubility at 62 mM (Table IV). This is in contrast to results obtained when irinotecan is exposed to the copper-free buffer where irinotecan solubility drops to 3 mM. It should be noted that upon solubilization of irinotecan at high concentrations in the presence of floxuridine plus copper gluconate/TEA, a well-defined flocculation characterized by rapid settling and a clear supernatant was formed.

**Table IV.** Solubility Assay for Irinotecan Demonstrates that CPX-1 Excipients Have a Notable Effect on Irinotecan Solubility

Buffer Condition	Irinotecan Concentration in solution (mM)
H <sub>2</sub> O	29
90 mM floxuridine	46
100 mM copper gluconate/180 mM TEA	48
100 mM Copper gluconate/180 mM TEA+90 mM floxuridine	62
10 mM sodium gluconate/180 mM TEA	3

The theoretical maximum concentration of irinotecan is 85 mM based on the mass of drug weighed out and the volume of solvent. The concentration of floxuridine is 90 mM. See "MATERIALS AND METHODS" for a detailed description of buffer components.

### Irinotecan Does Not Directly Interact with Copper Gluconate/TEA and Floxuridine

To further examine the influence of CPX-1 excipients on irinotecan solubility, isothermal titration calorimetry (ITC) and fluorescence studies were performed. Depending on the design and nature of the components involved, ITC can be used to quantitatively characterize the direct binding or partitioning of one substance into another (19). The heats generated by injecting 15 mM irinotecan into a solution of 5 mM floxuridine were of a magnitude on the order of the heats evolved from the heat of dilution upon injection of irinotecan into 100 mM HEPES at pH 7.0 (see Electronic supplementary material). The lack of any heats of interaction indicates that irinotecan does not directly interact with floxuridine.

Fluorescence emission scans were obtained for the titration of irinotecan in water in the presence of various excipients. The amount of fluorescence at 446 nm was plotted as a function of irinotecan concentration for aqueous solutions in the absence of added solutes or in the presence of floxuridine or copper gluconate/TEA (all at pH 7.0, see Electronic supplementary material). In all samples, fluorescence intensity increases similarly, up to an irinotecan concentration of approximately 200  $\mu\text{M}$  after which successive quenching is observed with increasing irinotecan concentration. Peak intensity losses for 1 mM irinotecan in water, with 1 mM floxuridine or with 1 mM copper gluconate/TEA were calculated to be 42%, 36% and 34% respectively. The onset and degree of fluorescence quenching was comparable for all three irinotecan solutions.

### Self-association of Irinotecan in Solution

Based on the calculated high intraliposomal concentration of irinotecan (85 mM) and its strong tendency for self-association (20), the majority of the intraliposomal drug would be expected to be oligomerized. UV-Vis spectroscopy was used here to verify this hypothesis. Monomeric irinotecan is characterized by two absorption peaks of near equal

absorbance at approximately 358 and 370 nm (15,21,22). Upon dimerization/self-association, irinotecan exhibited a shifting and loss of absorbance from the higher wavelength peak (370 nm) in comparison to the lower wavelength peak (358 nm, see Electronic supplementary material). At concentrations of irinotecan in the millimolar range, its spectrum is characteristic of a dimer/oligomer as demonstrated by the sloping rather than biphasic shape of the spectra. By normalizing the spectra to the intensity at a single wavelength (358 nm), the change in shape becomes readily apparent (Fig. 4a). To examine spectral shifts at irinotecan concentrations which are relevant to defining the inner liposome environment of CPX-1, advantage was taken of a short pathlength quartz cuvette to gather data where irinotecan was in or near its dimer/aggregated state. The use of 1 mm pathlength cuvette allowed the self-association of irinotecan to be examined over relevant drug concentrations without signal saturation. By normalizing the spectra of Fig. 4a to a single wavelength, a binding association constant may be calculated. The two wavelengths selected with which to normalize the absorbance data were 358 and 365 nm. The total change in absorbance was determined from 10 to 1200  $\mu\text{M}$ . The fractional change ( $\theta$ ) between these extremes was calculated and the data plotted as fractional change in absorbance versus total concentration of irinotecan ( $[I]_{\text{total}}$ ; Fig. 4b). The equilibrium relationship was fit by the following derived partition function (Eq. 1):

$$\theta = \frac{K[I]_{\text{total}}}{(1 + K[I]_{\text{total}})} \quad (1)$$

where  $K$  represents the association constant.

Which can be used to determine dissociation constants ( $K_D$ ) according to Eq. 2:

$$\theta = \frac{[I]_{\text{total}}}{(K_D + [I]_{\text{total}})} \quad (2)$$

The calculated dissociation constant was  $260 \pm 50 \mu\text{M}$  so at loading conditions of 85 mM, there was approximately

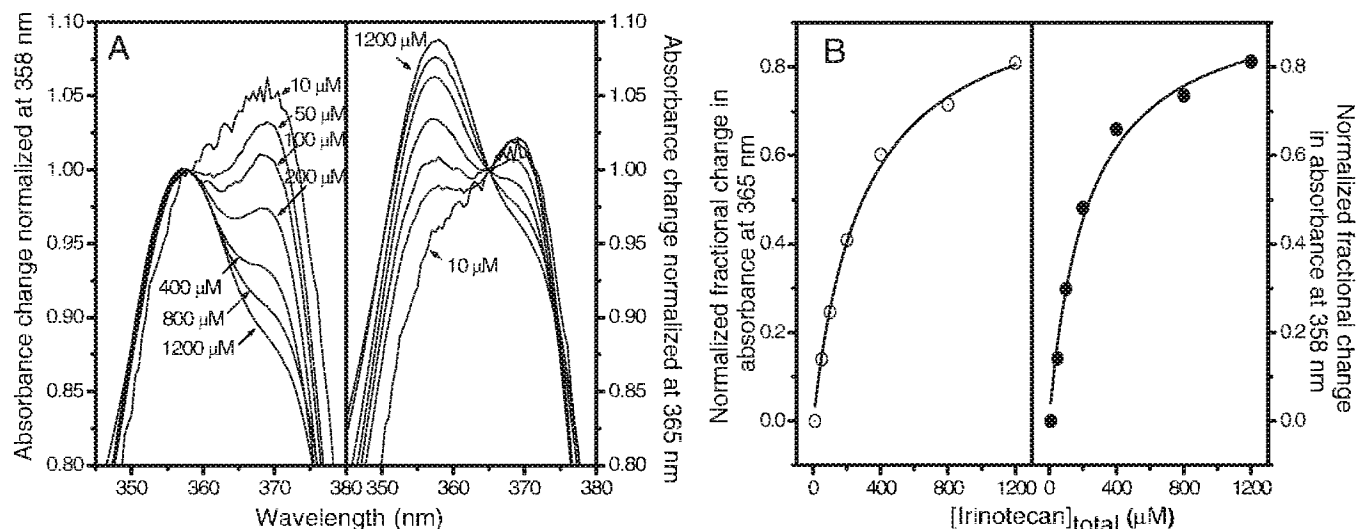


Fig. 4. **A** Change in absorbance of irinotecan, normalized at 358 nm (left) and 365 nm (right) for various concentrations. **B** Dissociation constant was generated by fitting the normalized change in absorbance versus total irinotecan concentration. Note that as it is not possible to generate an absorbance for 0  $\mu\text{M}$  irinotecan, some error is introduced into the fit which is reflected in the line not passing through the 10  $\mu\text{M}$  data point.

4.5 mM of monomeric irinotecan. This is consistent with irinotecan being predominantly in an oligomerized state in CPX-1. In addition, the spectral profile indicative of drug self-association was also observed at low pHs indicating that the aggregation of irinotecan was unaffected by its protonation state (data not shown).

## DISCUSSION

CPX-1 is a liposomal formulation designed to maintain the synergistic 1:1 molar ratio of irinotecan and floxuridine in the plasma after i.v. administration while at the same time make the drugs bioavailable. In a previous study, we showed that the encapsulation of irinotecan was mediated by TEA in association with copper gluconate, leading to a final drug complex that is retained inside liposomes (15). However, the factors that controlled drug retention were not fully understood. The goal of the present study was to characterize the physical state of the drugs inside the liposomes and the potential interactions between drugs and excipients of CPX-1 in order to establish the parameters that dictate drug retention and ultimately the biological performance of this liposomal formulation. Also, in view of the potential clinical utility of drug combinations co-formulated in liposomal delivery systems, these investigations provide an approach to characterizing the biophysical properties of co-formulated drugs that can be applied to a range of different combinations.

The comparison of the *in vitro* release profile of the drugs in CPX-1 and copper-free formulations at comparable drug/lipid ratios revealed that the absence of copper gluconate had negligible effects on floxuridine release but was associated with decreased release of irinotecan. The lack of an observable change in either liposome morphology or internal structure by cryo-EM led to the hypothesis that the addition of copper gluconate might have some chemical and/or physical effect within the liposome that was manifested in augmented release characteristics for irinotecan in CPX-1. It should be noted that formation of copper-irinotecan and copper-topotecan complexes have been shown to result in drug precipitation inside liposomes that is observable by cryo-EM (14,23). We have previously reported that irinotecan was capable of forming a complex with unbuffered copper sulfate solution but unlikely with copper gluconate due to the presence of the strongly chelating gluconate ligands ( $\log K=18.2;15,24$ ). The absence of a drug precipitate in CPX-1 is in line with the lack of direct copper gluconate-irinotecan interactions.

The biological activity of CPX-1 is dependent on the ability to reproducibly control drug retention within the liposomes such that the 1:1 molar ratio of irinotecan/floxuridine is maintained (2). Drummond *et al.* (13) and Ramsay *et al.* (23) have shown a correlation between increased drug retention and increased antitumor activity for irinotecan encapsulated liposomes. However, in the case of CPX-1, it is also necessary to coordinate the release of both drugs in order to prevent the formation of antagonistic ratios. In the case of irinotecan and floxuridine, the retention of the latter drug was first optimized by manipulating the lipid composition using low-cholesterol membranes (5). The irinotecan release was then manipulated to match the release of floxuridine. Consequently, this formulation represents conditions that

maximize the retention of both drugs while avoiding the generation of antagonistic drug ratios which would arise if irinotecan retention was further increased. Thus, a thorough chemical and spectroscopic characterization of the states of irinotecan and floxuridine within CPX-1 and copper-free formulations was conducted in order to understand the basis for this controlled drug retention.

The most direct probe of the intraliposomal drugs' physical states was  $^1\text{H}$  NMR. The aromatic protons of both irinotecan and floxuridine were easily detected and found to be sensitive to the presence of copper gluconate. In the case of floxuridine, this sensitivity was observed as paramagnetic line broadening; the two peaks at  $\sim 6.1$  and  $\sim 7.8$  ppm were relatively sharp and defined in the copper-free formulation but noticeably broadened in CPX-1 due to the presence of paramagnetic copper ions. Conversely, the four aromatic irinotecan molecules were more readily observed in CPX-1 compared to the copper-free formulation. Integration of peak intensities relative to an internal standard allowed for quantitation of observed floxuridine and irinotecan in both formulations (see Table II). For CPX-1, approximately 45% of the irinotecan could be observed; this value dropped to 19% in the copper-free formulation. Clearly, copper gluconate affects the physical state of irinotecan inside the liposomes. However, for the portion of irinotecan that could be observed in the CPX-1 and copper-free formulations, linewidth measurements suggest that the two species have similar properties.

Considering the known aggregation behaviour of irinotecan in solution (20), the NMR-silent portion of irinotecan is likely formed into a large aggregate that is rotationally immobile on the NMR timescale. Observation of protein  $^1\text{H}$  resonances is limited by an upper limit on molecular weight of approximately 35–50 kDa (25). For globular proteins, molecules of this size have a spherical diameter of 5–7 nm, within the detection limit of cryo-EM given the defocus setting and ice thickness (0.5  $\mu\text{m}$ ) used in this work (16). Cryo-EM images of the copper-free and CPX-1 formulations, however, showed no evidence of large globular irinotecan aggregates, even in the copper-free formulation in which up to 81% of the available irinotecan would be presumed to be highly aggregated. Such observations would appear to be inconsistent with each other.

## Predicted Morphology of Irinotecan Aggregates

Large molecular weight irinotecan aggregates are expected to form helical-like structures, based on the flat aromatic ring stacking of monomers with a slight twist of the overlapping aromatic planes predicted from UV-Vis, NMR and CD spectroscopy (20) and molecular modeling studies (data not shown). From simple computer imaging, irinotecan molecular dimensions are estimated as  $22 \times 7 \times 2.5$  Å with an intermolecular distance of 3.5 Å. Therefore, for an aggregate of  $N$  monomers, the aggregate length  $a$  is approximated by Eq. 3:

$$a = (2.5 \times N) + (3.5 \times (N - 1)) \quad (3)$$

The diameter is estimated as an average of the molecular planar axes lengths  $((22+7)/2=14.5$  Å) due to the helical twist between each monomer. Thus, the predicted shape of a large

irinotecan aggregate is most closely approximated by a prolate ellipsoid (Fig. 5).

### Theoretical Prediction of Maximal Aggregate Size for NMR-Observed Irinotecan Fraction

Analysis of the linewidth of irinotecan proton resonances in the CPX-1 and copper-free formulations relative to the average proton linewidth of ubiquitin amide yields some insight into the size limit of NMR-observable irinotecan aggregates. Under conditions of constant temperature, the slow tumbling of macromolecules is the main determinant of the linewidth, due to the reduction in spin-spin relaxation time ( $T_2$ ;38). For a spherical macromolecule, the rotational correlation time ( $\tau_c$ ) is related directly to molecular weight ( $M_r$ ) from Stokes' Law (Eq. 4):

$$\tau_c = \frac{4\pi\eta_w r_H^3}{3k_B T} \quad (4)$$

where  $r_H = \left(\frac{3VM_r}{4\pi N_A}\right)^{\frac{1}{3}}$

In the above equations,  $\eta_w$  is the solvent viscosity,  $k_B$  is the Boltzmann constant and  $T$  is temperature in Kelvin. The hydrodynamic radius ( $r_H$ ) is estimated from the specific volume of the protein (typically 0.73 ml/g). Ubiquitin amide therefore has a calculated rotational correlation time of 3.8 ns for a hydrodynamic radius of 14 Å. Waters of hydration are neglected from the calculated radius.

Cavanagh *et al.* (17) used the relationships between spin-spin relaxation time ( $T_2$ ) and rotational correlation time to construct a plot correlating the latter with observed linewidth. This relationship can be used to obtain an estimate of the rotational correlation time of an ubiquitin-like species that would have a proton resonant linewidth measured in the  $^1\text{H}$  NMR spectrum of CPX-1. Given the observed NMR linewidths for irinotecan aggregates in the CPX-1 formulation of 29 and 56 Hz (Table III), correlation of these linewidths to Cavanagh's plot gives estimated observed rotational correlation times of 12 and 20 ns, respectively, for the NMR-observable portion of irinotecan in CPX-1.

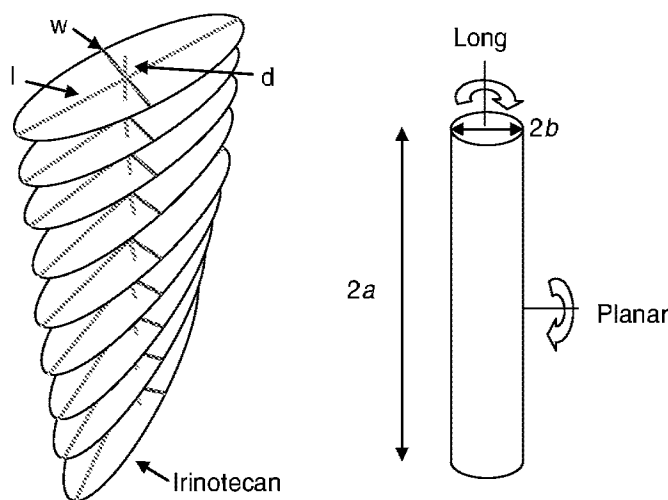


**Fig. 5.** *Left:* Schematic diagram of aggregated irinotecan showing individual molecular axes, length ( $l$ ), width ( $w$ ) and depth ( $d$ ). *Right:* Rotation axes and semiaxes definition for a rod-like aggregate.

### Rotational Diffusion of Ellipsoidal Versus Spherical Aggregates

The prediction above can be verified through calculation of rotational diffusion coefficients for both a spherical and ellipsoidal aggregate. Given the dimensions of the prolate ellipsoid with long and short axes  $a$  and  $b$ , Perrin reported the following equations for calculation of rotational diffusion coefficients of the major ( $D_{\parallel}$ , Eq. 5) and minor ( $D_{\perp}$ , Eq. 6) semiaxes of revolution (26–28):

$$D_{\parallel} = \frac{3k_B T}{32\pi\eta} \frac{2a - b^2 G(a, b)}{(a^2 - b^2)b^2} \quad (5)$$

$$D_{\perp} = \frac{3k_B T}{32\pi\eta} \frac{(2a^2 - b^2)G(a, b) - 2a}{a^4 - b^4} \quad (6)$$

where

$$G(a, b) = \frac{2}{(a^2 - b^2)^{\frac{3}{2}}} \ln \left( \frac{a + (a^2 - b^2)^{\frac{1}{2}}}{b} \right),$$

for  $a > b$  (prolate ellipsoid)

The rotational correlation times for an ellipsoid (three total) and sphere (isotropic, therefore one) are (29):

$$\tau_1 = (D_{\parallel} + 5D_{\perp})^{-1} \quad (7a)$$

$$\tau_2 = (4D_{\parallel} + 2D_{\perp})^{-1} \quad (7b)$$

$$\tau_3 = (6D_{\perp})^{-1} \quad (7c)$$

$$\tau_{\text{sphere}} = (6D_o)^{-1} \quad (7d)$$

In NMR spectroscopy, for slow tumbling species, the observed linewidth would be generally dependent on the fastest rotational correlation time of the aggregate. For an ellipsoidal particle, it is expected that  $D_{\parallel} > D_{\perp}$  due to the reduced displacement of solvent during rotation about the long axis. Therefore,  $\tau_2$  will yield the fastest rotational correlation time as it contains the largest contribution from  $D_{\parallel}$ . The rotational diffusion coefficients ( $D_{\parallel}$ ,  $D_{\perp}$ ) and  $\tau_2$  correlation times for ellipsoidal irinotecan aggregates of various sizes, along with spherical aggregates of an equivalent volume were calculated (see Electronic supplementary material). The highly impaired rotational diffusion about the planar axis is apparent in  $\tau_3$  which is solely dependent on  $D_{\perp}$ . For an aggregate of  $N=100$ ,  $\tau_3$  is calculated to be 2.17  $\mu\text{s}$ , compared to 15 ns for both  $\tau_2$  and a sphere of equivalent volume to the  $N=100$  ellipsoid. This calculation demonstrates the dramatic loss in long axis mobility for a prolate ellipsoid relative to a sphere of the same volume. For  $N=100$ , the aggregate is estimated to be 60 nm long and 1.45 nm in

average diameter due to the helical twist of irinotecan aggregates. This rod-like ellipsoid has an identical volume as a sphere with a diameter of 5 nm. As stated above, a spherical aggregate of this size would be observable in the cryogenic electron micrograph presented herein. The ellipsoid shape, however, presents a small cross-sectional dimension across the long axis such that it is most accurately described as a filament and likely only visible by electron microscopy under the conditions used here, if packaged in a higher order assembly of the filaments. The cryo-EM images presented here do not give any indication of such behaviour.

The estimated rotational correlation times for liposomal irinotecan are 12–20 ns, depending on which observed line-width is used (29 and 56 Hz, Table III). These times correlate to aggregates of 80–130 monomers, using the fastest rotational correlation time,  $\tau_2$  (see Electronic supplementary material). The aggregates would be expected to have dimensions of between 50 and 70 nm in length and identical diameters of 1.45 nm. This calculation gives an estimate on the NMR-observable irinotecan aggregate size and provides a mean by which irinotecan can form large macromolecular adducts yet remain undetected by conventional imaging methods. Presumably, the undetected irinotecan (55% in CPX-1 and 81% in the copper-free formulation) is aggregated such that the rotation is impaired and the augmented  $^1\text{H } T_2$  relaxation time is too fast for reliable NMR detection.

#### Intermolecular Limit to Aggregate Size for Observation of NMR Signals

An upper limit on the NMR-observable size is also predicted based on intermolecular interactions of discrete aggregate species. Above a certain number of polymer chains per unit volume, rod-like polymers or aggregates begin to influence the rotational tumbling of neighbouring chains, such

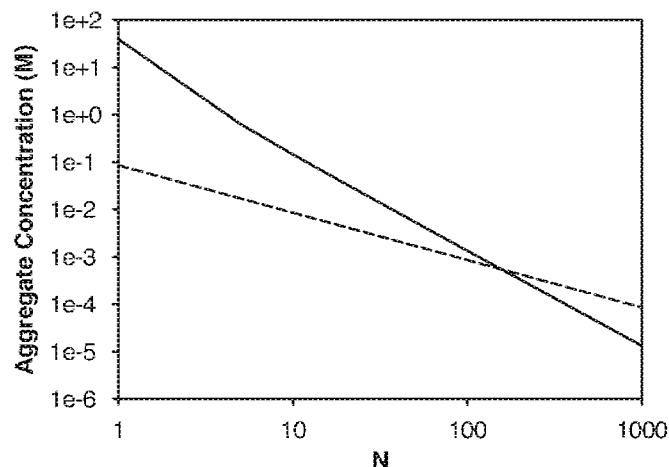


**Fig. 6.** Limit in rod-like aggregate concentration for isotropic rotational diffusion (solid line) as calculated from Eq. 8, with the actual irinotecan aggregate concentration for aggregates of size  $N$  (dashed line). Parameters used in the calculation were an encapsulated irinotecan concentration of 86 mM, and aggregate dimensions of  $L = [(3.5 \times N) + (2.5 \times (N - 1))] \text{ \AA}$  and  $d = 14.5 \text{ \AA}$ . Aggregate concentration was calculated by dividing the total irinotecan concentration by  $N$ .

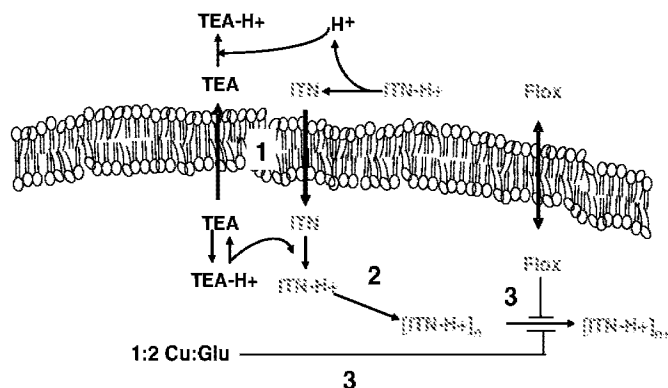


**Fig. 7.** Mechanism of drug loading of CPX-1, highlighting the neutral antiport active loading of irinotecan, the passive loading of floxuridine, and the roles of TEA and copper gluconate. 1 TEA is responsible for irinotecan loading via neutral antiport exchange mechanism. 2 Subsequent self-association of irinotecan enhances drug retention. 3 Copper gluconate/TEA and floxuridine together block large, higher order oligomerization of irinotecan via long-range interactions, thus allowing irinotecan to leak from the liposomes at the same rate as floxuridine.

that the rotational diffusion becomes anisotropic. This phenomenon is known as the log-jam effect for concentrated polymer solutions (30). Onsager (31) described the onset of this effect as a function of the rod dimensions in Eq. 8:

$$c_i = \frac{4.253}{dL^2} \quad (8)$$

Where  $d$  and  $L$  are the diameter and length of the polymer or aggregate rod, respectively, and  $c_i$  is the number of polymer units per unit volume. Division of the result by Avogadro's number yields the polymer concentration limit for isotropic tumbling behaviour. This calculation would assume a well behaved system of polymers/aggregates of narrow size distribution, with little to no flexibility in the rod.

For CPX-1, with an estimated internal irinotecan concentration of 85 mM, Eq. 8 can be used to calculate an upper limit on aggregate size ( $N$ ) before the isotropic limit is exceeded and molecular tumbling is further impaired. Using the same aggregate dimensions as in the previous analysis, the change in the isotropic limit as a function of aggregate size can be calculated concurrently with the aggregate concentration. The latter is calculated simply as the total irinotecan concentration divided by the number of monomers per aggregate. These calculated values (isotropic limit from Eq. 8 and the actual irinotecan aggregate concentration) are plotted as a function of aggregate size  $N$  in Fig. 6. Examination of the intersection point of the calculated concentration with the isotropic limit gives an aggregate size of  $N \leq 160$  monomers. This result suggests that for aggregates exceeding this size, isotropic rotation of the long rod-like aggregate will be steadily influenced by the presence of other neighbouring aggregate chains. Such interference will impair rotational diffusion, leading a reduction in  $T_2$  relaxation time and loss of signal in the NMR experiment. This calculated result correlates and supports earlier calculations considering the slow axial tumbling of elongated prolate ellipsoids in solution.

## Summary

The self-association of irinotecan in the presence of floxuridine and copper gluconate/TEA buffer was consistent with a long-range ordering and reduction of total charge in colloidal systems (32). At pH 7.0, the majority of irinotecan would be positively charged ( $pK_a=8.1$ ), balanced by the partial negative charge of floxuridine ( $pK_a=7.4$ ). This reduction in total charge modulates the aggregation of colloidal and positively-charged irinotecan by allowing for a closer approach of the suspended particles. Such long-range interactions are not typically detected by spectroscopic and calorimetric techniques, consistent with the ITC and fluorescence data presented here. Drugs-excipients interactions in CPX-1 serve to limit the size of irinotecan oligomers, greatly increasing the relative amount of irinotecan that exists in a rotationally mobile fraction that is NMR-detectable. The interplay between all excipients and drugs of CPX-1 is depicted in Fig. 7. The rate of irinotecan release is likely dependent on the oligomerization state of irinotecan inside the liposome, where larger, higher order oligomers are associated with decreased release rates. One role of copper gluconate in CPX-1 appears to be to inhibit large irinotecan aggregate formation. Taken together, the data presented here indicate that floxuridine and the excipients in CPX-1 maintain irinotecan in a physicochemical state that facilitates coordinated drug release and maintenance of the 1:1 molar drug ratio *in vivo*.

## ACKNOWLEDGMENT

The authors would like to thank Dr. Sharon Johnstone for helpful discussions and Brianne O'Callaghan for technical support. We would like to recognize the superior NMR service provided by Drs. Maria Ezhova and Nick Burlinson at the University of British Columbia NMR Facility. We are also grateful to Goran Karlsson and Dr. Katarina Edwards at Uppsala University in Sweden for the cryo-EM work.

## REFERENCES

1. S. Sengupta, D. Eavarone, I. Capiia, G. Zhao, N. Watson, T. Kiziltepe, and R. Sasisekharan. Temporal targeting of tumor cells and neovasculature with a nanoscale delivery system. *Nature*. **436**:568–572 (2005).
2. L. D. Mayer, T. O. Harasym, P. G. Tardi, N. L. Harasym, C. R. Shew, S. A. Johnstone, E. C. Ramsay, M. B. Bally, and A. S. Janoff. Ratiometric dosing of anticancer drug combinations: controlling drug ratios after systemic administration dictates therapeutic activity in tumor-bearing mice. *Mol. Cancer Ther.* **5**:1854–1863 (2006).
3. T. O. Harasym, P. G. Tardi, S. A. Johnstone, L. D. Mayer, M. B. Bally, and A. S. Janoff. Fixed drug ratio liposomes formulations of combination cancer therapeutics. In G. Gregoriadis (ed.), *Liposome Technology, 3rd ed.*, CRC, Boca Raton, FL, 2007, pp. 25–48.
4. X. Zhao, J. Wu, N. Muthusamy, J. C. Byrd, and R. J. Lee. Liposomal coencapsulated fludarabine and mitoxantrone for lymphoproliferative disorder treatment. *J. Pharm. Sci.* **97**:1508–1572 (2007).
5. P. G. Tardi, R. C. Gallagher, S. A. Johnstone, N. Harasym, M. Webb, M. B. Bally, and L. D. Mayer. Co-encapsulation of irinotecan and floxuridine into low cholesterol-containing liposomes that coordinate drug release *in vivo*. *Biochim. Biophys. Acta*. **1768**:678–687 (2007).
6. G. Batist, K. Chi, W. Miller, S. Chia, F. Hasanbasic, A. Fistic, L. M. Mayer, C. Swenson, A. S. Janoff, and K. Gelmon. Phase I study of CPX-1, a fixed ratio formulation of irinotecan (iri) and floxuridine (flox), in patients with advanced solid tumors. ASCO Annual Meeting, 2014 (2006).
7. G. Batist, W. Miller, L. Mayer, A. Janoff, C. Swenson, A. Louie, K. Chi, S. Chia, and K. Gelmon. Ratiometric dosing of irinotecan (IRI) and floxuridine (FLOX) in a phase I trial: A new approach for enhancing the activity of combination chemotherapy. *J. Clin. Oncol.* **25**:109s (2007).
8. T. O. Harasym, P. G. Tardi, N. L. Harasym, P. Harvie, S. Johnstone, and L. D. Mayer. Increased preclinical efficacy of irinotecan and floxuridine co-encapsulated inside liposomes is associated with tumor delivery of synergistic drug ratios. *Oncol. Res.* **16**:361–374 (2007).
9. L. D. Mayer, and A. S. Janoff. Optimizing combination chemotherapy by controlling drug ratios. *Mol. Interv.* **7**:216–223 (2007).
10. Y. Barenholz, S. Amselem, D. Goren, R. Cohen, D. Gelvan, A. Samuni, E. B. Golden, and A. Gabizon. Stability of liposomal doxorubicin formulations: problems and prospects. *Med. Res. Rev.* **13**:449–491 (1993).
11. M. Grit, and D. J. Crommelin. Chemical stability of liposomes: Implications for their physical stability. *Chem. Phys. Lipids*. **64**:3–18 (1993).
12. C. O. Noble, M. T. Krauze, D. C. Drummond, Y. Yamashita, R. Saito, M. S. Berger, D. B. Kirpotin, K. S. Bankiewicz, and J. W. Park. Novel nanoliposomal CPT-11 infused by convection-enhanced delivery in intracranial tumors: pharmacology and efficacy. *Cancer Res.* **66**:2801–2806 (2006).
13. D. C. Drummond, C. O. Noble, Z. Guo, K. Hong, J. W. Park, and D. B. Kirpotin. Development of a highly active nanoliposomal irinotecan using a novel intraliposomal stabilization strategy. *Cancer Res.* **66**:2171–2177 (2006).
14. A. S. Taggar, J. Alnajim, M. Anantha, A. Thomas, M. Webb, E. Ramsey, and M. B. Bally. Copper-topotecan complexation mediates drug accumulation into liposomes. *J. Control. Release*. **114**:78–88 (2006).
15. A. Dicko, P. G. Tardi, X. Xie, and L. D. Mayer. Role of copper gluconate/triethanolamine in irinotecan encapsulation inside the liposomes. *Int. J. Pharm.* **337**:219–228 (2007).
16. M. Almgren, K. Edwards, and G. Karlsson. Cryo transmission electron microscopy of liposomes and related structures. *Colloids Surf. A*. **174**:3–21 (2000).
17. J. Cavanagh, A. G. Palmer III, W. J. Fairbrother, N. J. Skelton, and M. Rance. *Protein NMR Spectroscopy: Principles and Practice*. Academic, San Diego, 1996.
18. G. S. Rule, and T. K. Hitchens. *Fundamentals of Protein NMR Spectroscopy*. Springer, Berlin, 2005.
19. T. Wiseman, S. Williston, J. F. Brandts, and L. N. Lin. Rapid measurement of binding constants and heats of binding using a new titration calorimeter. *Anal. Biochem.* **179**:131–137 (1989).
20. R. Aiyama, H. Nagai, S. Sawasa, T. Yokokura, H. Itokawa, and M. Nakanishi. Determination of self-association of irinotecan hydrochloride (CPT-11) in aqueous solution. *Chem. Pharm. Bull.* **40**:2810–2813 (1992).
21. I. Chourpa, J.-M. Millot, G. D. Sockalingum, J.-F. Riou, and M. Manfait. Kinetics of lactone hydrolysis in antitumor drugs of camptothecin series as studied by fluorescence spectroscopy. *Biochim. Biophys. Acta*. **1379**:353–366 (1998).
22. I. Nabeiev, F. Fleury, I. Kudelina, Y. Pommier, F. Charton, J.-F. Riou, A. J. Alix, and M. Manfait. Spectroscopic and biochemical characterization of self-aggregates formed by antitumor drugs of the camptothecin family. *Biochem. Pharmacol.* **55**:1163–1174 (1998).
23. E. Ramsay, J. Alnajim, M. Anantha, J. Zastre, H. Yan, M. Webb, D. Waterhouse, and M. Bally. A novel liposomal irinotecan formulation with significant anti-tumor activity: Use of the divalent cation ionophore A23187 and copper-containing liposomes to improve drug retention. *Eur. J. Pharm. Biopharm.* (2008) in press.
24. L. Pecsok, and R. S. Juvet Jr. The gluconate complexes. I. Copper gluconate in strongly basic media. *J. Am. Chem. Soc.* **77**:202–206 (1955).

25. H. Yu. Extending the size limit of protein nuclear magnetic resonance. *Proc. Natl. Acad. Sci. U. S. A.* **96**:332-334 (1999).
26. F. Perrin. The Brownian [sic] movement of an ellipsoïde [sic]—The dielectric dispersion of ellipsoidal molecules. *J. de Phys. et Rad.* **5**:497-511 (1934).
27. F. Perrin. Brownian movement of an ellipsoid (ii): free rotation and fluorescence depolarization. Translation and diffusion of ellipsoidal molecules. *J. de Phys. et Rad.* **7**:1-11 (1936).
28. G. A. Barrall, K. Schmidt-Rohr, Y. K. Lee, K. Landfester, H. Zimmermann, G. C. Chiang, and A. Pines. Rotational diffusion measurements of suspended colloidal particles using two-dimensional exchange nuclear magnetic resonance. *J. Chem. Phys.* **104**:509-520 (1996).
29. J. R. Lakowicz. *Principles of Fluorescence Spectroscopy* (3rd ed.). Springer Science + Business Media, Singapore, 2006.
30. E. C. Chung, and J. Chung. Rotational diffusion coefficient of rod-like polymer with a slight flexibility in semidilute and concentrated solutions. *Poly. Bull.* **21**:105-112 (1989).
31. L. Onsager. The effects of shape on the interaction of colloidal particles. *Ann. N.Y. Acad. Sci.* **51**:627-659 (1949).
32. A. R. Gennaro (Ed.). *Remington: The Science and Practice of Pharmacy*, 20th ed., Lippincott Williams & Wilkins, Philadelphia, 2000.



## Improved retention of idarubicin after intravenous injection obtained for cholesterol-free liposomes

Nancy Dos Santos<sup>a,b,\*</sup>, Lawrence D. Mayer<sup>a,c,d</sup>, Sheela A. Abraham<sup>a,b</sup>,  
Ryan C. Gallagher<sup>d</sup>, Kelly A.K. Cox<sup>a</sup>, Paul G. Tardi<sup>d</sup>, Marcel B. Bally<sup>a,b,d</sup>

<sup>a</sup> Department of Advanced Therapeutics, British Columbia Cancer Agency, 600 West 10th Avenue, Vancouver, BC, Canada V5Z 4E6

<sup>b</sup> Department of Pathology and Laboratory Medicine, University of British Columbia, Koerner Pav, 2211 Westbrook Mall, Vancouver, BC, Canada V6T 2B5

<sup>c</sup> Faculty of Pharmaceutical Sciences, University of British Columbia, 2146 East Mall, Vancouver, BC, Canada V6T 1Z3

<sup>d</sup> Celator Technologies, Inc., 202-604 West Broadway, Vancouver, BC, Canada V5Z 1G1

Received 26 September 2001; received in revised form 27 December 2001; accepted 3 January 2002

### Abstract

To date there has been a focus on the application of sterically stabilized liposomes, composed of saturated diacylphospholipid, polyethylene glycol (PEG) conjugated lipids (5–10 mole%) and cholesterol (CH) (> 30 mole%), for the systemic delivery of drugs. However, we are now exploring the utility of liposome formulations composed of diacylphospholipid conjugated PEG mixtures prepared in the absence of added cholesterol, with the primary objective of developing formulations that retain encapsulated drug better than comparable formulations prepared with cholesterol. In this report the stability of cholesterol-free distearoylphosphatidylcholine (DSPC):distearoylphosphatidylethanolamine (DSPE)-PEG<sub>2000</sub> (95:5 mol/mol) liposomes was characterized in comparison to cholesterol-containing formulations DSPC:CH (55:45 mol/mol) and DSPC:CH:DSPE-PEG<sub>2000</sub> (50:45:5 mol/mol/mol), *in vivo*. Circulation longevity of these formulations was determined in consideration of variables that included varying phospholipid acyl chain length, PEG content and molecular weight. The application of cholesterol-free liposomes as carriers for the hydrophobic anthracycline antibiotic, idarubicin (IDA), was assessed. IDA was encapsulated using a transmembrane pH gradient driven process. To determine stability *in vivo*, pharmacokinetic studies were performed using 'empty' and drug-loaded [<sup>3</sup>H]cholesteryl hexadecyl ether radiolabeled liposomes administered intravenously to Balb/c mice. Inclusion of 5 mole% of DSPE-PEG<sub>2000</sub> or 45 mole% cholesterol to DSPC liposomes increased the mean plasma area under the curve (AUC<sub>0–24h</sub>) 19-fold and 10-fold, respectively. Cryo-transmission electron micrographs of IDA loaded liposomes indicated that the drug formed a precipitate within liposomes. The mean AUC<sub>0–4h</sub> for free IDA was 0.030 μmole h/ml as compared to 1.38 μmole h/ml determined for the DSPC:DSPE-PEG<sub>2000</sub> formulation, a 45-fold increase, demonstrating that IDA was retained better in cholesterol-free compared to cholesterol-containing liposomes. © 2002 Elsevier Science B.V. All rights reserved.

**Keywords:** Polyethylene glycol; Liposome; Drug delivery; Idarubicin; Cholesterol

Abbreviations: AUC, area under the curve; CH, cholesterol; CHE, cholesteryl hexadecyl ether; cryo-TEM, cryo-transmission electron microscopy; DMPC, 1,2-dimyristoyl-*sn*-glycero-3-phosphatidylcholine; DPPC, 1,2-dipalmitoyl-*sn*-glycero-3-phosphatidylcholine; DSPC, 1,2-distearoyl-*sn*-glycero-3-phosphatidylcholine; DSPE, 1,2-distearoyl-*sn*-glycero-3-phosphatidylethanolamine; PEG, polyethylene glycol; MPS, mononuclear phagocytic system; HBS, HEPES buffered saline; PC, phosphatidylcholine; PE, phosphatidylethanolamine; *T<sub>c</sub>*, phase transition temperature

\* Corresponding author, at address a. Fax: 604-877-6011. E-mail address: ndossant@bccancer.bc.ca (N. Dos Santos).

## 1. Introduction

Many drugs have shown improved therapeutic properties when administered in a liposome encapsulated form. This is a consequence of liposome mediated changes in drug pharmacokinetics and biodistribution that can (i) decrease toxicity and drug metabolism and/or (ii) enhance cellular or tumor drug delivery which, in turn, engenders improved antitumor activity. The progressive success of lipid carrier technology is reflected by the approval of various liposomal formulations of doxorubicin (Myocet, Doxil) and daunorubicin (DaunoXome) for human use [1–3]. The development of liposomes as effective drug delivery systems was achieved, in part, as a consequence of improved properties obtained following incorporation of membrane rigidifying agents such as cholesterol. In fact, some of the early research on liposomes as delivery systems for i.v. applications demonstrated that the presence of cholesterol (i) enhanced retention of entrapped solutes [4–8], (ii) diminished interaction with serum proteins [9,10], (iii) reduced phospholipid loss by phospholipases and lipoproteins [11–13], (iv) reduced macrophage digestion [14] and (v) maintained membrane fluidity over a wide temperature range. It is believed that a combination of these factors collectively yielded lipid carriers that were resilient within the biological milieu in terms of both liposome structure stability and retention of entrapped solutes.

Although neutral liposomes prepared of phosphatidylcholine species and cholesterol were effective as drug carriers, there remained perceived drawbacks to the technology. In particular, the rapid elimination of the liposomes following i.v. injection, an observation associated with liposome accumulation in the mononuclear phagocytic system (MPS), was not fully optimized. Although appropriately designed formulations prepared of phospholipids and cholesterol did provide substantial improvements in drug delivery to diseased sites residing in non-MPS organs [15], it was proposed that additional benefits would be achieved if the rate of liposome elimination could be reduced. These conventional formulations, therefore, were superseded by second generation liposomes termed ‘sterically stabilized’ or Stealth, that incorporate a surface coating consisting of either a ganglioside  $GM_1$  or synthetic neutral polymer polyethylene glycol

(PEG) [16,17]. These novel formulations significantly advanced and broadened the application of cholesterol-containing liposome formulations. In addition to previously mentioned attributes of conventional cholesterol-containing liposomes, sterically stabilized liposomes exhibit significantly greater circulation half-lives [18–21] and the elimination behavior of these liposomes was no longer as sensitive to liposomal lipid dose [22,23]. Subsequent studies illustrated that a longer circulation half-life could facilitate higher drug accumulation within sites of tumor growth [24–26] and this was associated with greater antitumor activity [27–29]. Furthermore, incorporation of PEG modified lipids has provided flexibility in altering the liposome composition, while maintaining the pharmacokinetic behavior of lipid carriers and therefore we investigated the properties of liposomes prepared in the absence of cholesterol for the intended purpose of retaining entrapped drugs.

Given the progress in liposome technology as delivery systems for anticancer drugs, some may find it surprising that this simple methodology is not applied more generically to other cancer drugs. In principle, liposomes must be developed with desirable and controlled release properties that are selected on the basis of the drug being entrapped. More specifically, we argue that liposomal lipid composition cannot be viewed in generic terms, where one liposome formulation is suitable for all drugs. Rather it is critical for the liposome to be designed around the drug of interest. In our laboratory we determine the suitability of a liposome formulation by an iterative process which correlates pharmacodynamic behavior of the encapsulated drug with the plasma elimination and biodistribution behavior of the liposomal carrier. A critical measured parameter obtained in these studies is in vivo drug release rate which, in turn, is critically dependent on lipid composition. It is well understood that liposomal formulations prepared using zwitterionic lipids, such as diacylphosphatidylcholine, and cholesterol are effective as drug carriers, but the benefits for a given anticancer drug depend on their ability to retain drug following i.v. administration. Further, simple changes in phospholipid acyl chain length can have dramatic effects on in vivo drug release rates [30]. In general, as acyl chain length increases, drug retention increases [31]. There

are some drugs, however, which are simply not retained well in these phospholipid/cholesterol formulations, even when the acyl chain length increases to C22 and exhibit gel to liquid crystal transitions above 100°C. Another solution to improve drug retention is based on preparation of liposomes without cholesterol. This has not been explored thoroughly, but there are now compelling reasons to consider the potential of cholesterol-free liposomes as carriers. As a direct consequence of cholesterol's interactions with phospholipids, the permeability of a liposome increases at temperatures below the phase transition temperature ( $T_c$ ) of the bulk lipid component [32,33]. Thus, membranes (absent of cholesterol) consisting of gel phase lipids ( $T_c > 40^\circ\text{C}$ ) will form a more rigid membrane capable of retaining contents for *in vivo* administration. Additional incorporation of surface stabilizing PEGs will further prevent surface–surface interactions to facilitate prolonged circulation lifetimes. To date little is known about the application of cholesterol-free liposomes for retention of entrapped solutes and these reasons, alone, were sufficient to propose that cholesterol-free liposomes may be relevant carriers for agents that are not currently retained in conventional formulations.

## 2. Materials and methods

### 2.1. Lipids and chemicals

Dimyristoylphosphatidylcholine (DMPC), dipalmitoylphosphatidylcholine (DPPC) and distearoylphosphatidylcholine (DSPC) lipids were purchased from Northern Lipids (Vancouver, BC, Canada). Phosphatidylethanolamine (dimyristoylphosphatidylethanolamine (DMPE), dipalmitoylphosphatidylethanolamine (DPPE) and distearoylphosphatidylethanolamine (DSPE) conjugated polyethylene glycol lipids were obtained from Avanti Polar Lipids (Alabaster, AL, USA). HEPES, citric acid, Sephadex G-50, cholesterol (CH), [ $^{14}\text{C}$ ]lactose and [ $^3\text{H}$ ]-cholesterol hexadecyl ether (CHE) were obtained from NEN Life Science Products (Oakville, ON, Canada). Idamycin (idarubicin hydrochloride for injection) is manufactured by Pharmacia and Upjohn (Boston, MA, USA) and obtained from the British Columbia Cancer Agency.

### 2.2. Preparation of liposomes

Liposome samples were composed mainly of DSPC:DSPE-PEG<sub>2000</sub> (95:5 mol/mol), DSPC:CH (55:45 mol/mol) or DSPC:CH:DSPE-PEG<sub>2000</sub> (50:45:5 mol/mol/mol). In some studies variations of these compositions were prepared by altering the phosphatidylcholine acyl chain length (DPPC or DMPC), PEG molecular weight (750 and 5000) or content (2, 10, 15 molar percent). All liposome samples were prepared by the extrusion technique [34]. Briefly, lipids were initially dissolved in chloroform and mixed together in a test tube at the appropriate mole ratios. [ $^3\text{H}$ ]CHE was added as a non-exchangeable, non-metabolizable lipid marker [35,36]. The chloroform was evaporated under a stream of nitrogen gas and the sample was placed in a high vacuum overnight. The lipid films were rehydrated by gentle mixing and heating in HEPES buffered saline (HBS; 20 mM HEPES, 150 mM NaCl, pH 7.45). The newly formed multilamellar vesicles (MLVs) were passed 10 times through an extruding apparatus (Northern Lipids) containing two stacked 100 nm polycarbonate filters. The mean diameter and size distribution of each liposome preparation, analyzed by a NICOMP Model 270 Submicron particle sizer (Pacific Scientific, Santa Barbara, CA, USA) operating at 632.8 nm, was typically  $110 \pm 30$  nm.

### 2.3. Lactose trapping

To determine the trapped volume, liposomes were prepared as mentioned and hydrated in HBS (pH 7.4) containing [ $^{14}\text{C}$ ]lactose (NEN Life Science Products). Following extrusion and sizing, 100  $\mu\text{l}$  aliquots were passed down mini Sephadex G-50 spin columns. Trapped volume was determined by the following equation:

$$\text{Trapped volume} = \frac{(A/B)}{(C/D)} \times (\text{sample volume}) \quad (1)$$

$A$  = [ $^{14}\text{C}$ ]lactose dpm eluted from spin column;  
 $B$  = [ $^{14}\text{C}$ ]lactose dpm of initial suspension prior to gel filtration/100  $\mu\text{l}$ ;  
 $C$  = [ $^3\text{H}$ ]CHE dpm eluted;  
 $D$  = specific activity of lipid stock (dpm/ $\mu\text{mole}$  total lipid).

Analysis of [ $^{14}\text{C}$ ]lactose release was determined by aliquoting 10 mM extruded liposome sample in a

dialysis membrane (Spectrum Laboratories, Rancho Dominguez, CA, USA) placed in HBS buffer (pH 7.4) solution at 37°C for 48 h. Aliquots were removed at various time points and run down mini Sephadex G-50 spin columns.

#### 2.4. Remote loading of idarubicin

The remote loading procedure has been well characterized for weak bases such as anthracyclines, especially doxorubicin [37]. We have also employed this technique for the active entrapment of idarubicin. Liposomes were prepared following hydration of lipid films in citrate (300 mM citric acid; pH 4.0). Following extrusion and size determination, liposomes were passed down a Sephadex G-50 column equilibrated with HBS (pH 7.45) to exchange the external buffer. The resulting liposomes have a trans-membrane pH gradient, pH 4.0 inside and pH 7.45 outside, and were subsequently stored at 4°C. On the day of the experiment liposomes and drug were incubated at defined temperatures in separate test tubes and subsequently mixed together.

#### 2.5. Time dependent analysis of drug loading

To determine the optimal conditions for drug loading of IDA in cholesterol-free liposomes at a 0.2 drug to lipid ratio, IDA and liposomes (with an established pH gradient) were heated at various temperatures (37°C and 65°C) for 5 min, mixed together and placed at the same temperature. At 1, 2, 5, 10, 15, 30, and 60 min post mixing, 100 µl aliquots were added to G-50 spin columns (1 ml). Sephadex G-50 spin columns were prepared by adding glass wool to 1 ml syringe and Sephadex G-50 beads packed by centrifugation (720 × g, 1 min). Following addition of the sample to the column, the liposome fraction was collected in the void volume (centrifugation 720 × g, 1 min) and both lipid and drug content were analyzed. The lipid concentration was measured by [<sup>3</sup>H]CHE radioactive counts and IDA was determined by a spectrophotometric assay at 480 nm. The spectrophotometric assay consisted of an aliquot of the eluted sample made up to 100 µl with deionized water and 900 µl 1% Triton X-100. Samples were heated in boiling water to the cloud point of the detergent and cooled to room temperature, absor-

bance was measured (Du-64 spectrophotometer, Beckman) and compared to a standard curve.

#### 2.6. Cryo-transmission electron microscopy

Cholesterol-free liposomes were analyzed by cryo-transmission electron microscopy (cryo-TEM) and performed in the laboratory of Dr. Katarina Edwards in Uppsala, Sweden. The method employed and interpretation of liposome images have been previously described [38]. Briefly, in a climate chamber a drop of the liposome solution was placed on a copper grid containing a polymer film and blotted, forming a thin aqueous layer on the membrane. The sample was flash frozen in ethane allowing the film to vitrify, an essential step to prevent crystal formation. The copper grid containing the sample was transferred to an electron microscope at liquid nitrogen temperature where it was analyzed.

#### 2.7. Mice

Female Balb/c mice (6–8 weeks), 20–22 g, breeders were purchased from Charles River Laboratories (St. Constant, PC) and bred in house. Mice were housed in microisolator cages and given free access to water and food. The room environment was maintained according to standard operating procedures established at the BC Cancer Agency Joint Animal Facility. All animal studies were conducted according to procedures approved by the University of British Columbia's Animal Care Committee and these studies were performed in accordance with the current guidelines established by the Canadian Council of Animal Care.

#### 2.8. Plasma elimination of liposomes

To determine in vivo drug retention behavior and circulation longevity, pharmacokinetic studies were performed. 'Empty' or drug loaded [<sup>3</sup>H]CHE radiolabeled liposomes were administered intravenously to the lateral tail vein of Balb/c female mice. Studies comparing [<sup>3</sup>H]CHE with radiolabeled [<sup>3</sup>H]DPPC were also completed (data not shown) and the results for the two lipid labels were comparable for cholesterol-free formulations. The doses of liposomes and IDA were 165 µmoles/kg lipid and 33 µmoles/kg

IDA, respectively. At various time points post drug administration, blood was collected by tail nick or cardiac puncture. The plasma was prepared and a standard liquid scintillation counting and a standard extraction assay (see below) determined both lipid and IDA content, respectively.

The mean area under the curve (AUC) for a defined time interval was determined from the concentration–time curves and subsequent calculation by the standard trapezoidal rule. The plasma data were modeled using the WinNONLIN Version 1.5 pharmacokinetic software (Pharsight, CA, USA).

### 2.9. Idarubicin extraction assay

IDA was isolated from plasma in the following manner. An aliquot of plasma sample was added to the 16×100 mm test tube and made up to 800  $\mu$ l with distilled water. Subsequently 100  $\mu$ l of both 10% SDS and 10 mM H<sub>2</sub>SO<sub>4</sub> were added, vortexed, and followed by the addition of 2 ml of 1:1 isopropanol/chloroform. Samples were placed in –80°C for 1 h. All tubes were equilibrated to room temperature, vortexed and centrifuged at 1000×g for 10 min. The bottom organic phase was carefully pipetted into a clean test tube and samples were measured on an LS 50B luminescence spectrometer (Perkin-Elmer, UK) using an excitation wavelength of 485 (5 nm bandpass) and an emission wavelength of 535 (10 nm bandpass) within 30–45 min.

## 3. Results

### 3.1. Circulation longevity of cholesterol-free liposomes

Given that the pharmacokinetic behavior of an encapsulated drug will be dependent on the pharmacokinetic characteristics of the drug carrier, studies were completed to assess circulation longevity of various liposome formulations. The cholesterol-free liposome formulation composed of DSPC:DSPE-PEG<sub>2000</sub> (95:5 molar ratio) was compared with cholesterol-containing formulations consisting of DSPC:CH (55:45) and DSPC:CH:DSPE-PEG<sub>2000</sub> (50:45:5). Each liposome formulation was injected intravenously into the lateral tail vein of mice and at various time points aliquots of EDTA prepared

plasma were analyzed to determine total lipid/ml plasma. As shown in Fig. 1, DSPC liposomes were rapidly eliminated from the circulation with less than 6% of the injected dose (<0.2  $\mu$ moles/ml plasma) present at 1 h post administration and an estimated mean area under the curve (AUC<sub>0–24h</sub>) of 2.38  $\mu$ moles h/ml. Inclusion of cholesterol into the membrane resulted in a 10-fold increase in the mean AUC<sub>0–24h</sub>; however, at 24 h post administration less than 1% of the injected dose remained in the plasma compartment. Inclusion of 5 mole% DSPE-PEG<sub>2000</sub> into the DSPC:CH formulation resulted in a 2-fold increase in the mean AUC in comparison to DSPC:CH (55:45), a result which is consistent with many other reports demonstrating that incorporation of PEG modified lipids can enhance the circulation lifetime of liposomes [23]. Inclusion of 5 mole% DSPE-PEG<sub>2000</sub> into DSPC liposomes without cholesterol engendered significant increases in circulation lifetimes when compared to DSPC formulations without stabilizing lipids. There was a 19-fold increase in mean AUC<sub>0–24h</sub>, and 29% of the injected dose was present in the circulation after 24 h. This result demonstrated that polyethylene glycol conjugated lipids are an essential component of cholesterol-free lipo-

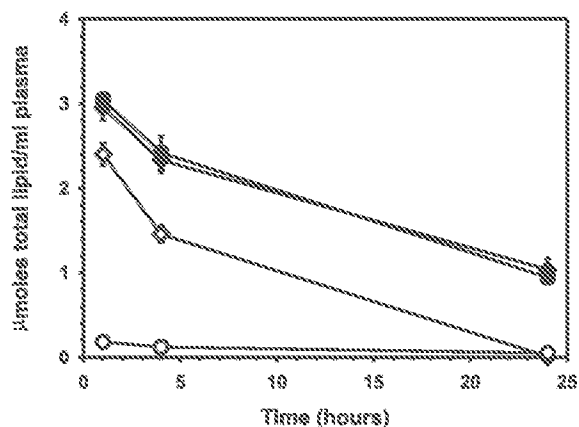


Fig. 1. Elimination of cholesterol-free liposomes from the circulation. Large unilamellar liposomes radiolabeled with [<sup>3</sup>H]CHE were administered intravenously via the dorsal tail vein of female Balb/c mice at an approximate dose of 150  $\mu$ moles/kg total lipid. Blood was collected at 1, 4 and 24 h by tail nick and cardiac puncture procedures, respectively. An aliquot of plasma was used to determine liposomal lipid content as described in Section 2. ◆, DSPC:CH:DSPE-PEG<sub>2000</sub> (50:45:5); ◇, DSPC:CH (55:45); ●, DSPC:DSPE-PEG<sub>2000</sub> (95:5); ○, DSPC (100). Each data point represents the average lipid plasma concentration  $\pm$ S.D. for four mice.

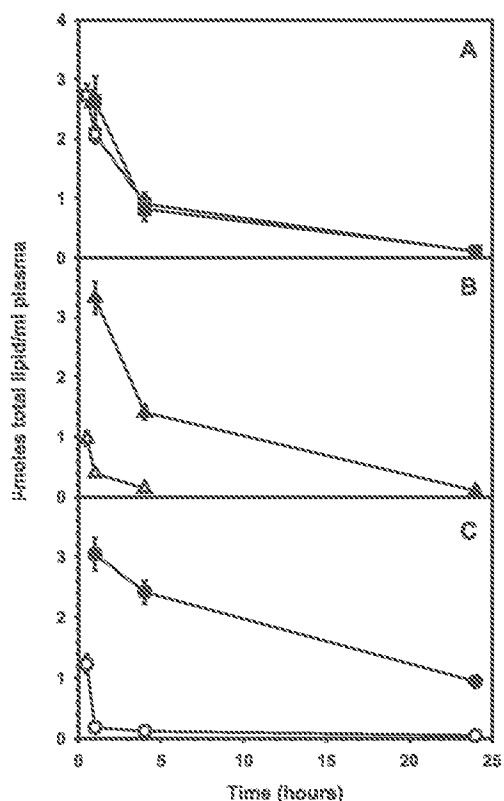


Fig. 2. Elimination of liposomes prepared using phosphatidylcholine species with varying acyl chain lengths in the absence and presence of PE-PEG<sub>2000</sub>. Mice were injected with liposomes as described in Fig. 1. Liposomes of varying acyl chain lengths DSPC (Panel C), DPPC (Panel B) and DMPC (Panel A) both in the absence (open symbols) and the presence (closed symbols) of 5 mole% of PE-PEG<sub>2000</sub> were evaluated. Each data point represents the average lipid plasma concentration  $\pm$ S.D. for four mice.

somes if they are to be used as systemically viable drug carriers.

While characterizing cholesterol-free liposome formulations it was of importance to decide which formulation would be optimal for application as a delivery system for a relatively hydrophobic anticancer agent, such as IDA. The influence of 5 mole% phosphatidylethanolamine (PE)-PEG on the plasma elimination of liposomes containing various acyl chain lengths of phosphatidylcholine, DSPC (C:18), DPPC (C:16) and DMPC (C:14), was evaluated in Fig. 2. In these studies the acyl chain length of the corresponding PE conjugated to PEG contained the same number of carbons to ensure optimal mixing conditions; however, it is now well established that the short chain (C:14 and less) PEG modified PEs

are rapidly exchanged out of liposomal membranes after i.v. administration [39,40]. As the acyl chain length of the phospholipid increased, a more significant difference in circulation longevity between phosphatidylcholine (PC) and PC:PE-PEG<sub>2000</sub> (95:5) liposomes was observed. As suggested above, differences in PEG-lipid induced effects on the liposomal systems may be attributed to the phase state of the liposomes whereby a more liquid-crystalline phase lipid may facilitate rapid exchange of lipid components out of and into the liposomal membrane following i.v. injection. Although DMPC liposomes appear to be eliminated at the same rate as DMPC:DMPE-PEG<sub>2000</sub> (95:5) liposomes, upon closer examination we have resolved that DMPC liposomes are not stable, a result that is consistent with previous observations [41]. Studies evaluating the retention of encapsulated [<sup>14</sup>C]lactose indicated that both DMPC and DPPC liposomes lost encapsulated contents rapidly following injection but DSPC retained entrapped lactose over 48 h (data not shown).

### 3.2. Influence of polyethylene glycol content and molecular weight on cholesterol-free liposome circulation longevity

Previous studies have demonstrated that the elimination rate of cholesterol-containing systems increases following PEG incorporation, a result that is dependent on both PEG content and molecular weight [42–44]. As shown in Figs. 3 and 4, variations in PEG-lipid content from 2 to 15 mole%, and PEG molecular weight, from PEG<sub>750</sub> to PEG<sub>5000</sub>, had no significant impact on altering the plasma elimination circulation longevity of DSPC liposomes. It should be noted that as PEG concentration was increased to levels in excess of 15 mole% in DSPC liposomes, the solution became clear indicative of non-liposomal micelles or bilayer disc formation [45], a result which is consistent with other reports [46,47]. Furthermore, in the studies reported here it was established that the DSPC:PEG<sub>2000</sub> formulations with PEG-lipid content up to 15 mole% existed as a single liposome population, but the 20 mole% PEG-lipid formulation existed as two distinct populations as judged by cryo-TEM analysis and fractionation on Sepharose CL-4B (data not shown). When using DPPC, incorporation of 15 mole% PEG resulted in a formulation of a

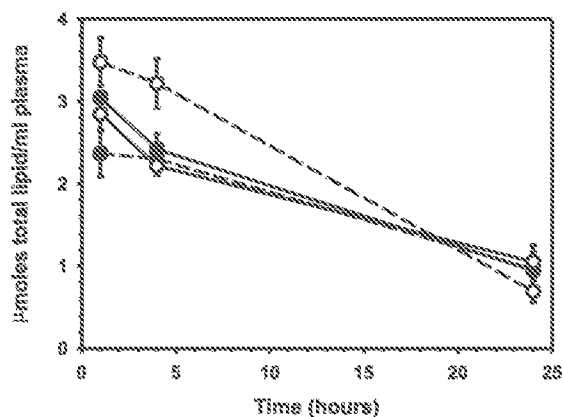


Fig. 3. Elimination of DSPC liposomes containing increasing mole% PE-PEG<sub>2000</sub>. Mice were injected with liposomes as described in Fig. 1. DSPC liposomes containing 2 (—●—), 5 (—●—), 10 (—○—), and 15 (—○—) mole% PEG were evaluated. Each data point represents the average total lipid plasma concentration  $\pm$  S.D. for four mice.

single population of bilayer disks. As suggested by the data in Fig. 3, even levels of PEG lipid as low as 2 mole% are adequate to maximize the circulation lifetime of these cholesterol-free formulations.

### 3.3. Optimal drug loading conditions for idarubicin

The primary purpose of evaluating the pharmacokinetic behavior of the cholesterol-free liposomes was to determine whether in the absence of cholesterol,

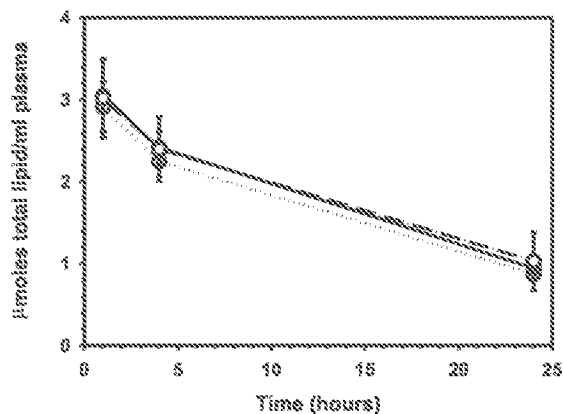


Fig. 4. Elimination of DSPC liposomes containing varying molecular weights of 5 mole% DSPE-PEG. Mice were injected with liposomes as described in Fig. 1. DSPC liposomes containing 5 mole% DSPE-PEG where the PEG molecular weight was 750 (—○—), 2000 (—●—) and 5000 (—○—). Each data point represents the average total lipid plasma concentration  $\pm$  S.D. for four mice.

the *in vivo* retention of drugs poorly retained by cholesterol-containing formulations could be improved. Since the drug retention attributes of anthracycline derivatives may be correlated to their hydrophobicity, we chose to assess the use of DSPC:PEG<sub>2000</sub> liposomes to enhance the drug retention of one of the most hydrophobic anthracyclines, idarubicin [48]. A liposomal formulation of IDA displaying enhanced drug circulation lifetimes has not been obtained to date, presumably because the IDA is rapidly released from cholesterol-containing systems. The first step required evaluating the influence of cholesterol on IDA release involved preparation of drug loaded formulations. The studies described here have used the well established pH gradient based loading technique for anthracyclines. In partic-

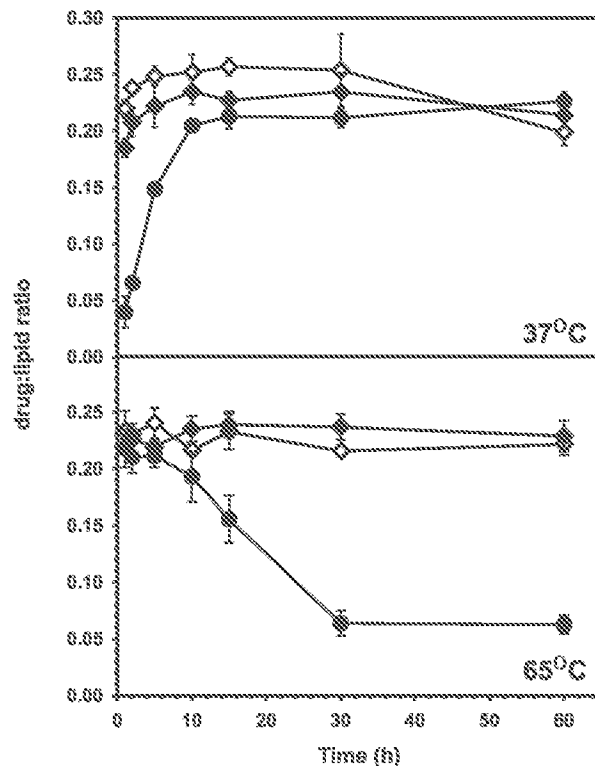


Fig. 5. Idarubicin loading into liposomes. Liposomes (5 mM) were incubated with 1 mM idarubicin (drug:lipid ratio 0.2) at 37°C and 65°C. At various time points, 100  $\mu$ l of the incubating mixture were run down mini Sephadex G-50 spin columns and subsequently analyzed for lipid and drug concentrations by liquid scintillation counting and a standard anthracycline absorbance assay as described in Section 2. Drug loading was compared between DSPC:DSPE-PEG<sub>2000</sub> (95:5 mol/mol) (●), DSPC:CH (55:45 mol/mol) (◇) and DSPC:CH:DSPE-PEG<sub>2000</sub> (50:45:5 mol/mol/mol) (◆) liposomes.

ular IDA was loaded at 37°C and 65°C into liposomes exhibiting an approx. 3.5 unit transmembrane pH gradient. As indicated in Fig. 5, IDA displayed optimal loading in cholesterol-free liposomes at 37°C. The accumulation of drug into the liposomes was rapid, with >95% encapsulation observed in 15 min, after drug addition. In comparison, no difference was observed in DSPC:CH liposomes loading at 37°C and 65°C.

#### 3.4. Evaluation of liposomal idarubicin by cryo-transmission electron microscopy

Previous studies have explored the structure of doxorubicin within liposomes, linking the formation of citrate doxorubicin precipitates to improved retention [49]. To assess the physical state of encapsulated IDA, cryo-electron microscopy was used. 'Empty' and drug loaded DSPC:DSPE-PEG<sub>2000</sub> (95:5 mol/mol) liposomes were analyzed and the resulting cryo-TEM images have been summarized in Fig. 6. As shown by the representative micrographs in Fig. 6 panels A and C, there was an observed difference in

structure between 'empty' cholesterol-free and cholesterol-containing liposomes. Several DSPC:DSPE-PEG<sub>2000</sub> (95:5 mol/mol) liposomes within the field of view have angular surface features whereas DSPC:CH:DSPE-PEG<sub>2000</sub> (50:45:5 mol/mol/mol) liposomes consisted primarily as smooth and rounded membranes. In both cholesterol-free (Fig. 6B) and cholesterol-containing liposomes (Fig. 6D) with encapsulated IDA, a precipitate was evident inside the liposomes, resulting in the 'coffee bean' structure observed by others for liposomal formulations of doxorubicin. Although these cryo-TEM images do not eliminate the possibility of IDA interaction with the lipid membrane, it can be concluded that both cholesterol-containing and cholesterol-free formulations have some of the entrapped IDA present as a precipitate in the aqueous core of the liposome.

#### 3.5. Pharmacokinetic analysis of liposomal idarubicin

Pharmacokinetic studies were performed to determine the IDA retention attributes of the cholesterol-

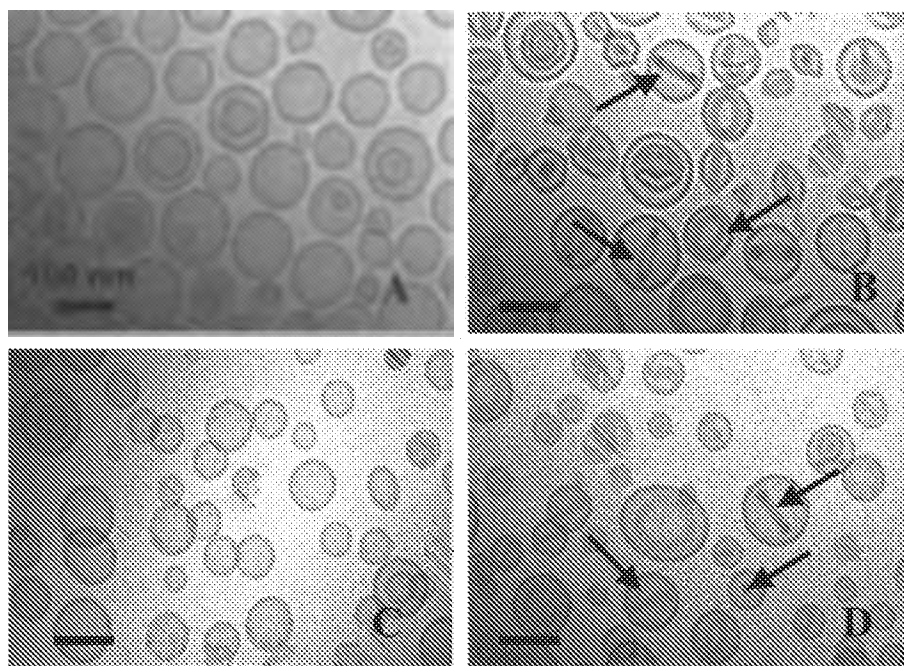


Fig. 6. Cryo-transmission electron micrographs of 'empty' and idarubicin-containing cholesterol-free and cholesterol-containing liposomes. DSPC:DSPE-PEG<sub>2000</sub> (95:5 mol/mol) (A) and DSPC:CH:DSPE-PEG<sub>2000</sub> (50:45:5 mol/mol/mol) (C) liposomes were prepared and cryo-TEM were obtained after establishment of a transmembrane pH gradient, but prior to drug loading. Cryo-electron micrographs of IDA loaded liposomes demonstrated precipitation (see arrows) of idarubicin in cholesterol-free (B) and cholesterol-containing liposomes (D). Bar represents 100 nm.



free formulation *in vivo*. Liposomes were prepared at a 0.2 drug to lipid ratio and subsequently injected *i.v.* into mice at a dose of 165  $\mu\text{moles/kg}$  lipid and 33  $\mu\text{moles/kg}$  IDA. The plasma elimination profile of IDA and lipid, as well as the calculated drug to lipid ratio in the plasma compartment are shown in Fig. 7. In the absence of a drug carrier, idarubicin is rapidly eliminated with <3% of the injected dose present after 15 min. This is in sharp contrast to the results obtained when IDA is administered encapsulated in DSPC:DSPE-PEG<sub>2000</sub> (95:5 mol/mol ratio). The  $\text{AUC}_{0-4\text{h}}$  for free IDA was 0.03  $\mu\text{mole h/ml}$  in com-

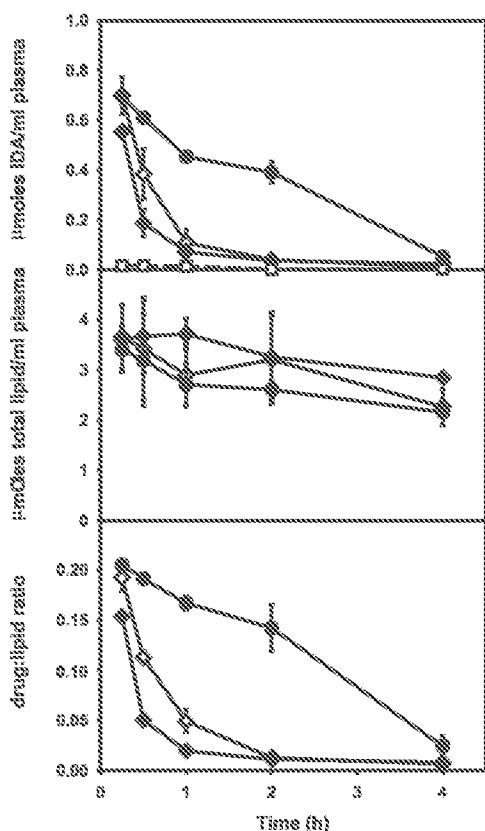


Fig. 7. Plasma elimination of liposomal idarubicin following *i.v.* injection of cholesterol-free and cholesterol-containing liposomes. Large unilamellar liposomes radiolabeled with [<sup>3</sup>H]CHE were administered intravenously via the dorsal tail vein of female Balb/c mice at an approximate dose of 165  $\mu\text{moles/kg}$  total lipid and 33  $\mu\text{moles/kg}$  IDA. Blood was collected at 0.25, 0.5, 1, 2 and 4 h. Plasma was prepared and aliquots were assayed for lipid and IDA concentration as described in Section 2. Prolonged circulation longevity of IDA was observed in DSPC:DSPE-PEG<sub>2000</sub> (95:5) (●) in comparison to DSPC:CH:DSPE-PEG<sub>2000</sub> (50:45:5) (◆), DSPC:CH (55:45) (◇), and free IDA (□). Each data point represents the average total lipid plasma concentration  $\pm$  S.D. for four mice.

parison to 1.38  $\mu\text{mole h/ml}$  for cholesterol-free liposomes. The greatest retention of IDA was achieved using cholesterol-free liposomes, resulting in an  $\text{AUC}_{0-4\text{h}}$  that was 45-fold higher than for free IDA. The lipid elimination profiles are consistent with the data shown in Figs. 1 and 2, suggesting that unlike vincristine and doxorubicin [49,50], IDA encapsulation does not cause a significant change in liposome elimination. The calculated changes in drug to lipid ratios indicate that the drug retention attributes of the cholesterol-free formulation are the best and the data support our contention that cholesterol-free liposomes provide a format to be used to deliver drugs not well retained in cholesterol-containing liposomes.

#### 4. Discussion

These studies have focused on cholesterol-free liposome delivery systems, with the aim of establishing their utility for delivery of hydrophobic drugs, such as idarubicin. Prior to establishment of liposome formulations designed for drug delivery applications [7,13,51,52], cholesterol-free vesicles were the standard model for biological membranes. Thus there is a great deal of existing literature on the *in vitro* physical and chemical properties of liposomes prepared without cholesterol. We do believe that this existing literature provides a solid foundation on which to support the development of cholesterol-free liposomes as intravenous delivery systems. Despite extensive studies of cholesterol-free formulations, there has been little emphasis on their application as drug carriers other than DPPC formulations being considered as thermosensitive formulations [53–55]. Others have focused on the physico-chemical and biological attributes of cholesterol-free liposomes including phase transition temperature determination by differential scanning calorimetry [47], X-ray diffraction [56], and protein binding [57,58], permeability [59] and pharmacokinetic studies [19,42]. Collectively these studies provide conclusive evidence that cholesterol-free liposomes have distinctive properties that may be beneficial for drug carriers. However, when this information has been applied to drugs, such as doxorubicin, the cholesterol-free formulation, even when stabilized by PEG-lipid incor-

poration, exhibit poor drug retention when compared to cholesterol-containing formulations [55]. We believe that this is due, in part, to the chemical attributes of the drug used and the phase transition temperature of DPPC ( $T_c \sim 39^\circ\text{C}$ ). For a temperature sensitive carrier, it may be advantageous to select lipids that have a characteristic  $T_c$  just above body temperature, considering that lipids become more permeable near their phase transition temperature. Therefore selection of lipids with a higher  $T_c$  than  $40^\circ\text{C}$  may facilitate greater retention of entrapped solutes. We believe that this report provides, for the first time, evidence that cholesterol-free liposomes can exhibit improved drug retention attributes, thus providing the opportunity to develop such formulations for drugs that are poorly retained in cholesterol-containing liposomes.

Within the context of this paper, a direct comparison of cholesterol-free DSPC:DSPE-PEG<sub>2000</sub> (95:5 mol/mol) liposomes with other successful drug carrier formulations including conventional DSPC:CH (55:45 mol/mol) and sterically stabilized DSPC:CH:DSPE-PEG<sub>2000</sub> (50:45:5 mol/mol/mol) liposomes is provided. There are two important observations pertaining to cholesterol-free liposomes that warrant further discussion. First and foremost, PEG is an essential component of cholesterol-free liposomes. Its presence engenders enhanced circulation longevity, apparently in a manner that is independent of PEG concentration and molecular weight. Secondly, idarubicin encapsulated in cholesterol-free liposomes demonstrated greater retention *in vivo*, independent of the formation of a precipitate structure within liposomes.

Our results indicate that DSPC:DSPE-PEG<sub>2000</sub> (95:5 mol/mol) liposomes exhibit circulation lifetimes comparable to sterically stabilized liposome formulations (DSPC:CH:DSPE-PEG<sub>2000</sub>; 50:45:5 mol/mol/mol). Woodle et al. have also demonstrated that PEG-PE:PC:CH (1:10:5 molar ratio) and PEG-PE:PC (0.15:0.85 molar ratio) liposomes exhibited similar circulation lifetimes, with circulation half-lives of 15.8 h and 14.9 h, respectively [23]. In the absence of surface grafted PEGs, cholesterol-free DSPC liposomes were rapidly eliminated, an observation that is likely due to either protein binding or liposome aggregation. As noted during the course of these studies, both DPPC and DSPC liposomes ag-

gregate rapidly when cooled to a temperature below the  $T_c$  of the acyl chain. In fact, in order to investigate the properties of pure PC systems, at least 0.5 mole% PEG<sub>2000</sub>-PE is required. Importantly, the circulation longevity of cholesterol-free DSPC:DSPE-PEG<sub>2000</sub> liposomes following *i.v.* administration was not influenced by the amount of PEG modified lipid (2–15 mole%), or the PEG molecular weight (750–5000). This is in contrast to previous studies investigating cholesterol-containing liposomes where PEG content and molecular weight are important considerations when optimizing the circulation lifetime of these liposomes [44,60].

In view of the unique observations obtained when using cholesterol-free liposomes, we postulate that the incorporation of PEG modified lipid is primarily responsible for minimizing liposome–liposome aggregation, although we cannot be certain that the surface grafted PEGs inhibit protein binding and this effect may be different when considering their behavior in cholesterol-free as compared to cholesterol-containing liposomes. Others have demonstrated that cholesterol is required to maintain stability of liposomes in the plasma compartment [7,13,51,61]. Many of these studies were completed with small unilamellar liposomes prepared using lipids that exhibited  $T_c$  below  $37^\circ\text{C}$ , and thus were likely in a fluid phase when injected into mammals. Bedu-Addo et al. and others have demonstrated that cholesterol-free liposomes exhibit a phase transition temperature [47], but this transition broadens and becomes difficult to measure when the cholesterol level increases [62]. When using liposomes prepared of defined acyl length PCs, heating them above the phase transition temperature and subsequent cooling them below the  $T_c$  causes membrane defects (grain boundaries) to form. The appearance of defects is clearly evident in the cryo-TEM shown in Fig. 6 and these membrane defects are believed to be the source of non-specific protein binding [61] which, in turn, may define whether the carrier is recognized by the cells of the MPS system. Addition of surface stabilizing compounds such as PEG may shield these defects from recognition by serum proteins, rendering them more stable than liposomes composed exclusively of saturated phospholipids. An inherent attribute of such a conclusion is that pure PC liposomes may display reduced protein binding attributes provided that the

membrane defects are shielded by PEGs. Our results suggest that this can be achieved for a broad range of PEG molecular weight species and surface grafting densities.

The entrapment of idarubicin into cholesterol-free DSPC:DSPE-PEG<sub>2000</sub> liposomes with an established pH gradient proved to be as effective with cholesterol-free liposomes when compared to cholesterol-containing formulations. As expected, however, the drug loading attributes of the cholesterol-free formulation were more dependent on the temperature used for loading and IDA could not be encapsulated at 65°C in cholesterol-free liposomes, a temperature higher than its phase transition temperature. Similarly, Unezaki et al. loaded thermo-sensitive (cholesterol-free) DSPC:DPPC:DSPE-PEG (1:9:0.61 molar ratio) liposomes with doxorubicin by the remote loading procedure at 60°C for 10 min and only achieved 65% encapsulation efficiency. Reduced loading may be a consequence of membrane destabilization at temperatures above the  $T_c$  of the bulk membrane component. Our studies demonstrated that >95% IDA was loaded into the PEG-PE stabilized DSPC liposomes at 37°C. The ability to load IDA into liposomes at a lower temperature than the phase transition temperature may be directly attributed to IDA's hydrophobicity [63]. Consistent with cholesterol-containing liposomes, drug loading for the cholesterol-free liposomes is dependent on liposome composition as well as the specific physico-chemical properties of the drug being used. Importantly, the cholesterol-free formulations may be particularly well suited for the more hydrophobic drugs. Woodle et al. hypothesized that by adding PEG to a membrane, one could eliminate the requirement of lipids with high phase transition temperature to allow greater control of leakage rates and other important bilayer properties [23]. Removing cholesterol from the membrane may facilitate even greater flexibility and control of drug leakage rates, when combined with the stabilization effects of PEGs.

Upon drug loading cryo-TEM images indicated that IDA was present in a precipitated form. This observation is consistent with other anthracyclines that have been encapsulated in liposomes by loading methods relying on the use of encapsulated citrate or ammonium sulfate [64]. It is interesting that Gallois

et al. have specifically studied IDA's interaction with phospholipid membranes concluding that IDA embeds within the bilayer forming a complex with phosphatidic acid and cholesterol [65]. Considering that neither cholesterol nor phosphatidic acid are present within our liposomes, the remote loading procedure allows IDA to be present at concentrations high enough for the anthracyclines to stack and self-associate [49]. Self-association may be more energetically favorable than interactions dependent on membrane partitioning, although the membrane partitioning behavior of IDA may play a direct role in enhancing the drug retention attributes observed here for DSPC:PEG-PE formulations. As shown clearly in Fig. 6, IDA was present in a precipitated form within cholesterol-containing liposomes, as well as cholesterol-free liposomes. This result suggests that enhanced retention within cholesterol-free liposomes was not solely a consequence of precipitate formation. Our studies demonstrated that membrane composition also governs drug release kinetics, and we continue to believe that the most important factor governing the release characteristics of a liposomally encapsulated drug is lipid composition. As modeled in Fig. 8, the release of entrapped idarubicin (present in both free and precipitated forms) from the aqueous core of a liposome to the external environment is dependent on the partitioning behavior of the drug. This, in turn, is dependent on pH, membrane surface charge and the chemical attributes of the lipid acyl chains. Although our initial rationale for employing cholesterol-free liposomes for retention was simple, our model suggests that release due to interaction of the drug with components of the liposome is complex. For example, the chemical reaction used to prepare PEG modified phospholipids results in the generation of an anionic lipid from a zwitterionic lipid. The presence of this charged lipid will influence drug release properties, as noted by others [66], and this is presumably due to enhanced partitioning of the encapsulated drug. Drug partitioning behavior will be dependent on a number of processes which are dictated, in part, by the equilibrium between protonated and unprotonated drug forms as they transfer from the precipitated complex trapped in the core of the liposome (see Fig. 6) through the bilayer interface and the bilayer itself. Although we have not

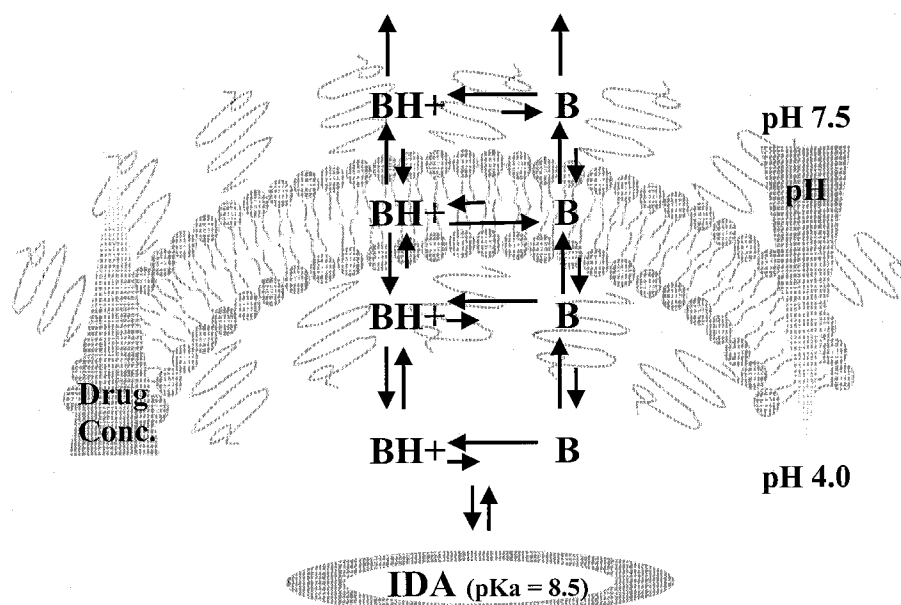


Fig. 8. Membrane partitioning of drugs encapsulated in liposomes through use of pH gradients and formation of a crystalline precipitate. IDA, protonated (BH<sup>+</sup>) and unprotonated (B) forms, are present in a dynamic equilibrium as they transfer from the precipitated complex trapped in the aqueous core of the liposome, through the bilayer interface and the bilayer itself. The release of IDA is dependent on the partitioning behavior of the drug, which is dependent on pH, membrane surface charge, and the chemical attributes of the lipid acyl chains. It is assumed that the rate limiting step in drug release is governed by permeation through the membrane rather than dissolution of the drug precipitate.

investigated the degree of partitioning of IDA within cholesterol-free and cholesterol-containing liposomes, we believe that membrane interactions are the most critical determinant of drug release.

In conclusion, we have demonstrated that cholesterol-free liposomes with surface grafted PEG may have unforeseen advantages over cholesterol-containing formulations. Inclusion of surface stabilizing components such as PEG eliminates the requirement of cholesterol within a membrane that exhibits very different drug release properties. In our case, we achieved enhanced retention of idarubicin, a hydrophobic agent readily released from conventional formulations. Future studies will focus on investigating drug release kinetics by altering loading parameters and PEG chemistry. In addition we will assess whether altering circulation longevity of IDA will impact the pharmacological properties of the drug in preclinical tumor models.

#### Acknowledgements

The authors wish to thank Dana Masin and Re-

becca Ng for providing expert technical support for the pharmacokinetic studies. The authors also acknowledge Prof. Katarina Edwards and Mr. Göran Karlsson for providing the facilities for the cryo-TEM investigation. This research was supported by the Canadian Institutes of Health Research (CIHR). N.D.S. is funded through a University Graduate Fellowship (UBC), the GREAT scholarship (Science Council of BC) and a University-Industry Partnered Fellowship sponsored by Canadian Institutes of Health Research (CIHR) and Celator Technologies, Inc.

#### References

- [1] P.S. Gill, J. Wernz, D.F. Scadden, P. Cohen, G.M. Mukwaya, J.H. von Roenn, M. Jacobs, S. Kempin, I. Silverberg, G. Gonzales, M.U. Rarick, A.M. Myers, F. Shepherd, C. Sawka, M.C. Pike, M.E. Ross, *J. Clin. Oncol.* 14 (1996) 2353–2364.
- [2] M. Newell, S. Milliken, D. Goldstein, C. Lewis, M. Boyle, G. Dolan, S. Ryan, D.A. Cooper, *Aust. New Zealand J. Med.* 28 (1998) 777–783.

- [3] G. Batist, G. Ramakrishnan, C.S. Rao, A. Chandrasekharan, J. Guthrie, T. Guthrie, P. Shah, A. Khojasteh, M.K. Nair, K. Hoelzer, K. Tkaczuk, Y.C. Park, L.W. Lee, *J. Clin. Oncol.* 19 (2001) 1444–1454.
- [4] R. Bittman, L. Blau, *Biochemistry* 11 (1972) 4831–4839.
- [5] D. Papahadjopoulos, K. Jacobson, S. Nir, T. Isac, *Biochim. Biophys. Acta* 311 (1973) 336–348.
- [6] R.A. Dornel, B. De Kruyff, *Biochim. Biophys. Acta* 457 (1976) 109–132.
- [7] C. Kirby, J. Clarke, G. Gregoriadis, *Biochem. J.* 186 (1980) 591–598.
- [8] J. Senior, G. Gregoriadis, *Life Sci.* 30 (1982) 2123–2136.
- [9] D. Papahadjopoulos, M. Cowden, H. Kimelberg, *Biochim. Biophys. Acta* 330 (1973) 8–26.
- [10] S.C. Semple, A. Chonn, P.R. Cullis, *Biochemistry* 35 (1996) 2521–2525.
- [11] G. Scherphof, F. Roerdink, M. Waite, J. Parks, *Biochim. Biophys. Acta* 542 (1978) 296–307.
- [12] G. Gregoriadis, C. Davis, *Biochem. Biophys. Res. Commun.* 89 (1979) 1287–1293.
- [13] J. Damen, J. Regts, G. Scherphof, *Biochim. Biophys. Acta* 665 (1981) 538–545.
- [14] H.M. Patel, N.S. Tuzel, B.E. Ryman, *Biochim. Biophys. Acta* 761 (1983) 142–151.
- [15] J.H. Senior, *Crit. Rev. Ther. Drug Carrier Syst.* 3 (1987) 123–193.
- [16] T.M. Allen, A. Chonn, *FEBS Lett.* 223 (1987) 42–46.
- [17] A. Gabizon, D. Papahadjopoulos, *Proc. Natl. Acad. Sci. USA* 85 (1988) 6949–6953.
- [18] A.L. Klibanov, K. Maruyama, V.P. Torchilin, L. Huang, *FEBS Lett.* 268 (1990) 235–237.
- [19] G. Blume, G. Cevc, *Biochim. Biophys. Acta* 1029 (1990) 91–97.
- [20] J. Senior, C. Delgado, D. Fisher, C. Tilcock, G. Gregoriadis, *Biochim. Biophys. Acta* 1062 (1991) 77–82.
- [21] T.M. Allen, C. Hansen, F. Martin, C. Redemann, A. Yan-Young, *Biochim. Biophys. Acta* 1066 (1991) 29–36.
- [22] T.M. Allen, C. Hansen, *Biochim. Biophys. Acta* 1068 (1991) 133–141.
- [23] M.C. Woodle, K.K. Matthey, M.S. Newman, J.E. Hidayat, L.R. Collins, C. Redemann, F.J. Martin, D. Papahadjopoulos, *Biochim. Biophys. Acta* 1105 (1992) 193–200.
- [24] S.K. Huang, K.D. Lee, K. Hong, D.S. Friend, D. Papahadjopoulos, *Cancer Res.* 52 (1992) 5135–5143.
- [25] N.Z. Wu, D. Da, T.L. Rudoll, D. Needham, A.R. Whorton, M.W. Dewhirst, *Cancer Res.* 53 (1993) 3765–3770.
- [26] A. Gabizon, R. Catane, B. Uziely, B. Kaufman, T. Safra, R. Cohen, F. Martin, A. Huang, Y. Barenholz, *Cancer Res.* 54 (1994) 987–992.
- [27] D. Papahadjopoulos, T.M. Allen, A. Gabizon, E. Mayhew, K. Matthey, S.K. Huang, K.D. Lee, M.C. Woodle, D.D. Lasic, C. Redemann et al., *Proc. Natl. Acad. Sci. USA* 88 (1991) 11460–11464.
- [28] A.A. Gabizon, *Cancer Res.* 52 (1992) 891–896.
- [29] N.L. Boman, D. Masin, L.D. Mayer, P.R. Cullis, M.B. Bally, *Cancer Res.* 54 (1994) 2830–2833.
- [30] H.J. Lim, D. Masin, T.D. Madden, M.B. Bally, *J. Pharmacol. Exp. Ther.* 281 (1997) 566–573.
- [31] N.L. Boman, L.D. Mayer, P.R. Cullis, *Biochim. Biophys. Acta* 1152 (1993) 253–258.
- [32] B.D. Ladbroke, R.M. Williams, D. Chapman, *Biochim. Biophys. Acta* 150 (1968) 333–340.
- [33] J.L. Lippert, W.L. Peticolas, *Proc. Natl. Acad. Sci. USA* 68 (1971) 1572–1576.
- [34] M.J. Hope, M.B. Bally, G. Webb, P.R. Cullis, *Biochim. Biophys. Acta* 812 (1985) 55–65.
- [35] J.F. Derksen, H.W. Morselt, G.L. Scherphof, *Biochim. Biophys. Acta* 931 (1987) 33–40.
- [36] M.B. Bally, L.D. Mayer, M.J. Hope, R. Nayar, in: G. Gregoriadis (Ed.), *Liposome Technology*, Vol. 3, 2nd edn., CRC Press, Boca Raton, FL, 1993, pp. 27–41.
- [37] L.D. Mayer, M.B. Bally, P.R. Cullis, *Biochim. Biophys. Acta* 857 (1986) 123–126.
- [38] M. Almgren, K. Edwards, J. Gustafsson, *Curr. Opin. Colloid Interface Sci.* 1 (1996) 270–278.
- [39] G. Adlaka-Hutcheon, M.B. Bally, C.R. Shew, T.D. Madden, *Nat. Biotechnol.* 17 (1999) 775–779.
- [40] W.M. Li, L. Xue, L.D. Mayer, M.B. Bally, *Biochim. Biophys. Acta* 1513 (2001) 193–206.
- [41] J. Damen, M. Waite, G. Scherphof, *FEBS Lett.* 105 (1979) 115–119.
- [42] K. Maruyama, T. Yuda, A. Okamoto, C. Ishikura, S. Kojima, M. Iwatsuru, *Chem. Pharm. Bull.* 39 (1991) 1620–1622.
- [43] K. Maruyama, T. Yuda, A. Okamoto, S. Kojima, A. Suginaka, M. Iwatsuru, *Biochim. Biophys. Acta* 1128 (1992) 44–49.
- [44] M.C. Woodle, M.S. Newman, J.A. Cohen, *J. Drug Targeting* 2 (1994) 397–403.
- [45] K. Edwards, M. Johnsson, G. Karlsson, M. Silvaner, *Biophys. J.* 73 (1997) 258–266.
- [46] A.K. Kenworthy, S.A. Simon, T.J. McIntosh, *Biophys. J.* 68 (1995) 1903–1920.
- [47] F.K. Bedu-Addo, P. Tang, Y. Xu, L. Huang, *Pharm. Res.* 13 (1996) 710–717.
- [48] A. Casazza, A. Di Marco, G. Bonadonna, V. Bonfante, C. Bertazzoli, O. Bellini, G. Pratesi, L. Sala, L. Ballerini, in: S. Crooke, S. Reich (Eds.), *Anthracyclines: Current Status and New Developments*, Academic Press, New York, 1980, pp. 403–430.
- [49] X. Li, D.J. Hirsh, D. Cabral-Lilly, A. Zirkel, S.M. Gruner, A.S. Janoff, W.R. Perkins, *Biochim. Biophys. Acta* 1415 (1998) 23–40.
- [50] M.B. Bally, R. Nayar, D. Masin, M.J. Hope, P.R. Cullis, L.D. Mayer, *Biochim. Biophys. Acta* 1023 (1990) 133–139.
- [51] C. Kirby, J. Clarke, G. Gregoriadis, *FEBS Lett.* 111 (1980) 324–328.
- [52] T.M. Allen, L.G. Cleland, *Biochim. Biophys. Acta* 597 (1980) 418–426.
- [53] M.B. Yatvin, J.N. Weinstein, W.H. Dennis, R. Blumenthal, *Science* 202 (1978) 1290–1293.
- [54] K. Maruyama, S. Umezaki, N. Takahashi, M. Iwatsuru, *Biochim. Biophys. Acta* 1149 (1993) 209–216.

- [55] S. Umezaki, K. Maruyama, N. Takahashi, M. Koyama, T. Yuda, A. Sugita, M. Iwatsuru, *Pharm. Res.* 11 (1994) 1180–1185.
- [56] A.K. Kenworthy, K. Hristova, D. Needham, T.J. McIntosh, *Biophys. J.* 68 (1995) 1921–1936.
- [57] G. Blume, G. Cevo, *Biochim. Biophys. Acta* 1146 (1993) 157–168.
- [58] H. Du, P. Chandaroy, S.W. Hui, *Biochim. Biophys. Acta* 1326 (1997) 236–248.
- [59] A.N. Nikolova, M.N. Jones, *Biochim. Biophys. Acta* 1304 (1996) 120–128.
- [60] A. Mori, A.L. Klibanov, V.P. Torchilin, L. Huang, *FEBS Lett.* 284 (1991) 263–266.
- [61] G. Scherphof, H. Morselt, J. Regts, J.C. Wilschut, *Biochim. Biophys. Acta* 556 (1979) 196–207.
- [62] B. De Kruyff, P.W. Van Dijck, R.A. Demel, A. Schuijff, F. Brants, L.L. Van Deenen, *Biochim. Biophys. Acta* 356 (1974) 1–7.
- [63] A.M. Casazza, *Cancer Treat. Rep.* 63 (1979) 835–844.
- [64] D.D. Lasic, P.M. Fredenk, M.C. Stuart, Y. Barenholz, T.J. McIntosh, *FEBS Lett.* 312 (1992) 255–258.
- [65] L. Gallois, M. Fiallo, A. Garnier-Suillerot, *Biochim. Biophys. Acta* 1370 (1998) 31–40.
- [66] M.S. Webb, D. Saxon, F.M. Wong, H.J. Lim, Z. Wang, M.B. Bally, L.S. Choi, P.R. Cullis, L.D. Mayer, *Biochim. Biophys. Acta* 1372 (1998) 272–282.

## CLINICAL DEVELOPMENT OF HISTONE DEACETYLASE INHIBITORS AS ANTICANCER AGENTS\*

---

Daryl C. Drummond,<sup>1</sup> Charles O. Noble,<sup>2,3</sup>  
Dmitri B. Kirpotin,<sup>1</sup> Zexiong Guo,<sup>2</sup> Gary K. Scott,<sup>4</sup>  
and Christopher C. Benz<sup>4</sup>

<sup>1</sup>Hermes Biosciences, Inc., South San Francisco, California 94080

<sup>2</sup>California Pacific Medical Center-Research Institute, San Francisco,  
California 94115

<sup>3</sup>University of California at San Francisco, San Francisco, California 94143

<sup>4</sup>Buck Institute for Age Research, Novato, California 94945

**Key Words** HDAC inhibitors, targeting chromatin structure and epigenetic mechanisms, transcription regulation, hydroxamic acids

■ **Abstract** Acetylation is a key posttranslational modification of many proteins responsible for regulating critical intracellular pathways. Although histones are the most thoroughly studied of acetylated protein substrates, histone acetyltransferases (HATs) and deacetylases (HDACs) are also responsible for modifying the activity of diverse types of nonhistone proteins, including transcription factors and signal transduction mediators. HDACs have emerged as uncredentialed molecular targets for the development of enzymatic inhibitors to treat human cancer, and six structurally distinct drug classes have been identified with in vivo bioavailability and intracellular capability to inhibit many of the known mammalian members representing the two general types of NAD<sup>+</sup>-independent yeast HDACs, Rpd3 (HDACs 1, 2, 3, 8) and Hda1 (HDACs 4, 5, 6, 7, 9a, 9b, 10). Initial clinical trials indicate that HDAC inhibitors from several different structural classes are very well tolerated and exhibit clinical activity against a variety of human malignancies; however, the molecular basis for their anticancer selectivity remains largely unknown. HDAC inhibitors have also shown preclinical promise when combined with other therapeutic agents, and innovative drug delivery strategies, including liposome encapsulation, may further enhance their clinical development and

\*Nonstandard abbreviations: AOE, 2-amino-8-oxo-9,10-epoxy-decanoic acid; ATRA, all-trans-retinoic acid; CBHA, m-carboxycinnamic acid bis-hydroxamide; CDK, cyclin-dependent kinase; DAC, 5-aza-2'-deoxycytidine; HAT, histone acetyltransferase; HDAC, histone deacetylase; HMT, histone methyltransferase; IMID-1, immunomodulatory thalidomide derivative 1; PB, phenyl butyrate; SAHA, suberoylanilide hydroxamic acid; SB, sodium butyrate; TRAIL, tumor necrosis factor-related apoptosis-inducing ligand; TSA, trichostatin A.

anticancer potential. An improved understanding of the mechanistic role of specific HDACs in human tumorigenesis, as well as the identification of more specific HDAC inhibitors, will likely accelerate the clinical development and broaden the future scope and utility of HDAC inhibitors for cancer treatment.

## INTRODUCTION

The packaging of DNA into the higher order and dynamic structure of chromatin provides a pivotal point of control for gene expression by regulating access of transcription factors to DNA. Chromatin is composed of multiple repeating units termed nucleosomes, which are comprised of 146 base pairs of DNA wrapped around a core of eight histone proteins composed of two copies each of H2A, H2B, H3, and H4. Posttranslational modifications play a prominent role in the regulation of gene expression and signal transduction pathways. Phosphorylation, methylation, acetylation, ubiquitination, and sumoylation are the known modifications thought to influence chromatin architecture and regulate gene transcription. The composition and consequences of these various histone modifications are often referred to as the histone code, orchestrating an intricate regulation of nucleosomal structure, DNA accessibility, and gene transcription (Figure 1). To date, acetylation is the most thoroughly studied of these modifications; and while the acetylation state of chromatin proteins is unquestionably very dynamic, it seems to depend on the net local balance between histone acetyltransferase (HAT) and histone deacetylase (HDAC) activities. Empirically observed is the fact that HDAC activity is invariably increased in cancer cells, resulting in altered gene transcription, impaired differentiation, increased cell survival, and dysregulated proliferation (1).

### Transcriptional Regulation and the Histone Code

Early models of how acetylation regulates transcription focused on the physical interactions of the basic histone proteins with negatively charged DNA. The addition of charge-neutralizing acetyl groups to lysine residues on histones disrupts interactions with DNA, resulting in decompaction of chromatin, greater access of the DNA to transcription factors, and the presence of a transcriptionally active genomic locus. However, there is considerable evidence that these models are oversimplified. In cell culture studies, less than 10% of transcriptionally active genes appear to be altered in response to treatment with HDAC inhibitors, with a near equal proportion of these being induced as repressed (2, 3). This suggests that regulation of gene expression by acetylation is more highly selective than would be expected by a simple and unregulated physical disruption of histone-DNA structure, and also likely involves chromatin-associated nonhistone proteins.

Nonetheless, the complex network of interdependent and site-specific histone modifications associated with restricted and sequence-specific DNA binding by transcription factors has resulted in a histone code hypothesis for gene-specific



transcriptional control (4, 5). The code is set by a variety of histone tail-derivatizing enzymes, including HATs for the acetylation of lysine residues (6), histone methyltransferases (HMTs) for methylation of histone lysine and arginine residues (7, 8), serine kinases for the phosphorylation of specific histone serine residues (9), ubiquitin ligase for the addition of the 76-amino-acid 9-kDa protein ubiquitin to specific lysine residues (10), and the sumoylation of lysine by the 11-kDa small ubiquitin-related modifier (SUMO) (11). In addition, the activities of modification destabilizing enzymes such as HDACs, methylases, phosphatases, and ubiquitin and ULP-related proteases help shape the status of the code. The complexity of transcriptional regulation by histone modifications is further enhanced by the interaction of HATs and HDACs with other proteins involved in chromatin modification, including methyl CpG-binding proteins and ATP-dependent chromatin-remodeling complexes, which can lead to replication propagated and more enduring epigenetic modifications of DNA, such as the gene silencing cytosine methylation of specific CpG dinucleotides (12–14).

The setting of the histone code involves establishing defined patterns of histone tail modifications, whereupon a particular modification in turn affects subsequent modifications. For example, histone deacetylation has been shown to activate lysine (K) methylation, resulting in relatively stable transcriptional silencing (15). In an eloquent experiment demonstrating sequential histone modifications, Kouzarides and colleagues showed that upon estrogen stimulation, H3 is acetylated initially at K18, then at K23, and finally methylated at R17 (16). A specific set of histone modifications was proposed to direct DNA methylation (17). The reading of the code can be accomplished through recognition of particular modifications or groups of modifications (18, 19). The bromodomain of proteins such as BRG1 and TAFII250 and the chromodomain of HP1 recognize acetylated lysines and methylated lysines, respectively (20–22). Certain combinations of modifications can also dictate the recruitment of various *cis*- or *trans*-acting regulatory proteins. The role of the particular modification in transcriptional signaling may also be influenced by the degree and stability of the modification. Lysine residues may be modified with one, two, or three methyl groups, and the degree of methylation determines if transcription of certain genes is activated or repressed (23, 24). The methylated lysines, and more so the methylated cytosines in DNA, are more stable modifications than the relatively dynamic modifications of histone tail acetylation and phosphorylation. Thus, with the lack of any known histone or DNA demethylases, methylation may be more important in epigenetic memory, whereas the acetylation status of histones may be more of a switch that can be rapidly reset and allow transcription to respond more rapidly to changes in the cell's environment.

The histone code is just beginning to be deciphered and thus its complexity and its role in carcinogenesis are far from understood. Although it is obvious that a wide variety of posttranslational protein modifications are responsible for regulating transcription of any given gene and as such can play important roles in human cancer cell behavior, the remainder of this review focuses specifically on the preclinical and clinical development of HDAC inhibitors as potential anticancer

agents. In this regard it is important to note that the activity of a wide variety of nonhistone transcription factors and co-regulators of transcription are known to be modified by acetylation, and both are structurally and functionally affected by HDAC inhibitors. Acetylation may enhance or inhibit the function of transcriptional activators as well as transcriptional repressors; therefore, enhancing their degree of acetylation by cell treatment with an HDAC inhibitor can either increase or repress the transcription of genes regulated by such nonhistone proteins (Table 1). TFIIIE (25), TFIIF (25), p53 (26), androgen receptor (27), estrogen receptor- $\alpha$  (28), and GATA-1 (29, 30) are promoter-binding and transcription-regulating proteins shown to be acetylated in response to HDAC inhibition. In addition, other DNA binding nonhistone proteins are functionally affected by acetylation. For example, HMG-17 is a nucleosomal binding protein responsible for unfolding the higher order structure of chromatin and thus exerts indirect control over gene transcription; and acetylation of HMG-17 has been shown to reduce its binding to chromatin (31).

### Classification of HDACs

There are three major groups or classes of mammalian HDACs based on their structural homologies to the three distinct yeast HDACs: Rpd3 (class I), Hda1 (class II), and Sir2/Hst (class III). Class III HDACs consist of the large family of sirtuins (SIRs) that are evolutionarily distinct, with a unique enzymatic mechanism dependent on the cofactor NAD<sup>+</sup>, and are virtually unaffected by all HDAC inhibitors currently under development (32, 33). This review focuses on the NAD<sup>+</sup>-independent class I and II HDACs (Figure 3), as they are evolutionarily similar, contain an active site zinc as a critical component of their enzymatic pocket, have been more thoroughly described in association with cancer, and are thought to be comparably inhibited by most currently available HDAC inhibitors. The Rpd3 homologous class I HDACs include HDAC1, HDAC2, HDAC3, and HDAC8. They are widely expressed in a variety of tissues and are primarily localized in the nucleus. The Hda1 homologous class II HDACs include HDAC4, HDAC5, HDAC6, HDAC7, HDAC9 (a and b isoforms), and HDAC10, and are structurally much larger in size. Class II HDACs can shuttle between the nucleus and cytoplasm (34–37), suggesting different functions and cellular substrates from Class I HDACs. HDAC6 in particular is predominantly localized in the cytoplasm (38). Class II HDACs also display a more limited tissue distribution (39–41). HDACs 4, 8, and 9 are expressed to a greater extent in tumor tissues than in normal tissues, with HDAC 4 demonstrating the greatest difference in this regard (39). Class II enzymes have also been shown to be specifically involved in differentiation (40). Finally, HDAC6 and HDAC10 are unique among class II HDACs in having two catalytic domains (37, 40). Although there is some evidence that certain HDAC inhibitors display different degrees of HDAC specificity, considerable research must still be performed to delineate differences in HDAC function, their roles in cancer, and their sensitivities to drugs. Some of these differentiating features are reviewed

TABLE 1 Nonhistone proteins whose acetylation may be increased by HDAC inhibitors

Protein	Intracellular function	Reference(s)
p53	Tumor suppressor	(26, 145, 146)
c-Myb	Protooncogene—regulates proliferation and differentiation	(147)
GATA-1	Differentiation of blood cells	(29, 30)
Estrogen receptor- $\alpha$	Stimulates growth of certain breast cancers	(28)
TFIIIE	General transcription factor	(25)
TFIIF	General transcription factor	(25)
Androgen receptor	Androgen-dependent transcription factor	(27)
hsp90	Chaperone—targets proteins for degradation by proteasome	(82)
$\alpha$ -tubulin	Microtubule component	(61, 148)
HMG-17	Unfolds higher order chromatin structure	(31)
HMG1	Essential architectural component for enhancosome assembly	(149)
TCF $\downarrow$	Transcriptional regulator	(150)
PCNA	DNA repair and replication, cell cycle control, chromatin remodeling	(151)
EKLF	Red cell-specific transcriptional activator	(152)
ACTR	Nuclear receptor coactivator, HAT	(153)
HNF-4	Transcriptional activation	(154)
Importin- $\alpha$	Nuclear import factor	(155)
NF- $\kappa$ B	Regulates antiapoptotic responses	(156)
ER81	Downstream effector of HER2/ene and Ras	(157)
SF-1	Transcription factor—expression of steroidogenic proteins	(158)
Ku70	Suppresses apoptosis	(159)
UBF	Structures DNA in ribosomal enhancosome	(160)
Sp3	Transcriptional activator or repressor	(161)
TAL1	Regulator of normal and leukemic hematopoiesis	(162)
YY1	Multifunction transcription factor	(163)
E2F1	Cell cycle activator—required for progression	(164)
MyoD	Stimulates cdk inhibitor p21	(165)

PCNA, proliferating cell nuclear antigen; SF-1, steroidogenic factor-1; UBF, architectural upstream binding factor.

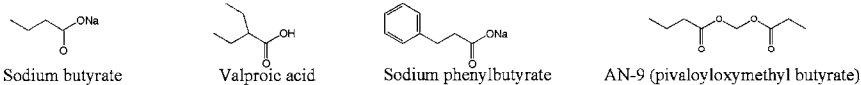
in detail elsewhere (39). Unraveling specific roles by these HDAC isozymes during human tumorigenesis will further incentivize development of more specific HDAC inhibitors (42), potentially enhancing their clinical activity as well as decreasing their nonspecific toxicities, while also optimizing potential interactions with other rationally designed and integrated therapeutic agents.

## STRUCTURAL CLASSES AND MECHANISTIC ACTIONS OF HDAC INHIBITORS

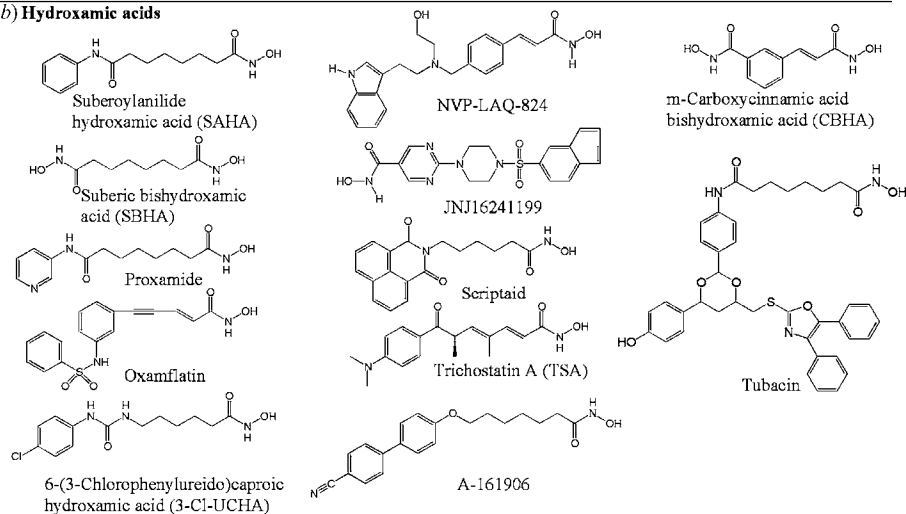
The six structurally distinct classes of HDAC inhibitors (Figure 2) act by binding to various portions of the catalytic domains within class I and II HDACs (Figure 3A). Although reviewed here briefly, a detailed examination of the medicinal chemistry and activity relationships for these structurally varied inhibitors is beyond the scope of this review, and the reader is directed to several excellent reviews on this subject (43–45). Hydroxamic acid-type chelators, including TSA, SAHA, and LAQ824, have three basic components (Figure 3B): (a) a hydroxamic acid moiety that chelates the active zinc in a bidentate manner, hydrogen bonds with residues composing the charge relay systems, and displaces the nucleophilic water molecule present in the active site; (b) a hydrophobic spacer that has a length optimal for spanning the length of the hydrophobic pocket and dimensions capable of navigating the narrowest segment of the cavity; and (c) a hydrophobic cap that blocks the entrance to the active site. Design and understanding of the enzymatic inhibitory mechanisms for various HDAC inhibitors was aided by solving the crystal structure of an HDAC homologue that shares significant homology with class I and class II HDACs, including all critical active site residues (46). The active site of class I and class II HDACs includes critical zinc and water molecules; two charge relay systems, where aspartate residues act to increase the basicity of histidine residues by polarizing the epsilon nitrogen; and an active site tyrosine residue that coordinates to the acetyl oxygen during the transition state (Figure 3C). The zinc ion acts by polarizing the acetyl carbonyl to make the carbonyl carbon a better electrophile for attack by the activated water molecule. Substitution of other divalent cations, or chelation of the zinc cation by a small-molecular-weight chelator, abolishes enzymatic activity. A hydrophobic pocket high in aromatic and glycine residues leads to the active site, with the narrowest point having a distance of 7.5 Å marked by two opposing phenylalanine residues. A depiction of the predicted transition state interaction between HDAC1 and the hydroxamic acid-type inhibitor LAQ824 is shown in Figure 3C. Hydroxamates with five or six carbon spacers were found to be the most active inhibitors (47), and replacement of the hydroxamic acid with a carboxylate was found to eliminate inhibitory activity (48).

Epoxyketone-based HDAC inhibitors, such as trapoxin B, HC-toxin, or 2-amino-8-oxo-9,10-epoxydecanoic acid (AOE), may act by chemically modifying an active site nucleophile with the epoxy group (49) and forming important

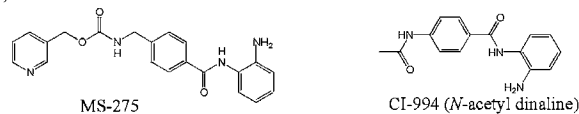
(a) Small molecular weight carboxylates



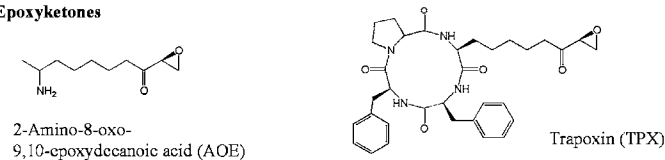
(b) Hydroxamic acids



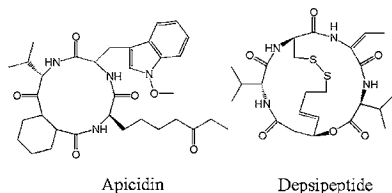
(c) Benzamides



(d) Epoxyketones



(e) Cyclic peptides



(f) Hybrid molecules

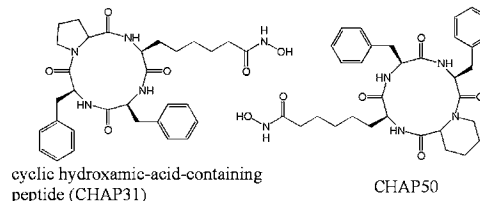


**Figure 2** Structural classes of HDAC inhibitors. Six basic classes of HDAC inhibitors are shown: (a) small-molecular-weight carboxylates, including sodium butyrate, valproic acid, and sodium phenylbutyrate; (b) hydroxamic acids, including CBHA, TSA, SAHA, and LAQ824; (c) benzamides, including MS-275 and CI-994; (d) epoxyketones, including AOE and trapoxin B; (e) cyclic peptides, including depsipeptide and apicidin; and (f) hybrid molecules, such as CHAP31 and CHAP50.

Ann. Rev. Pharmacol. Toxicol. 2005.45:495-528. Downloaded from www.annualreviews.org. Access provided by Repmins Desk, Inc. on 09/29/17. For personal use only.

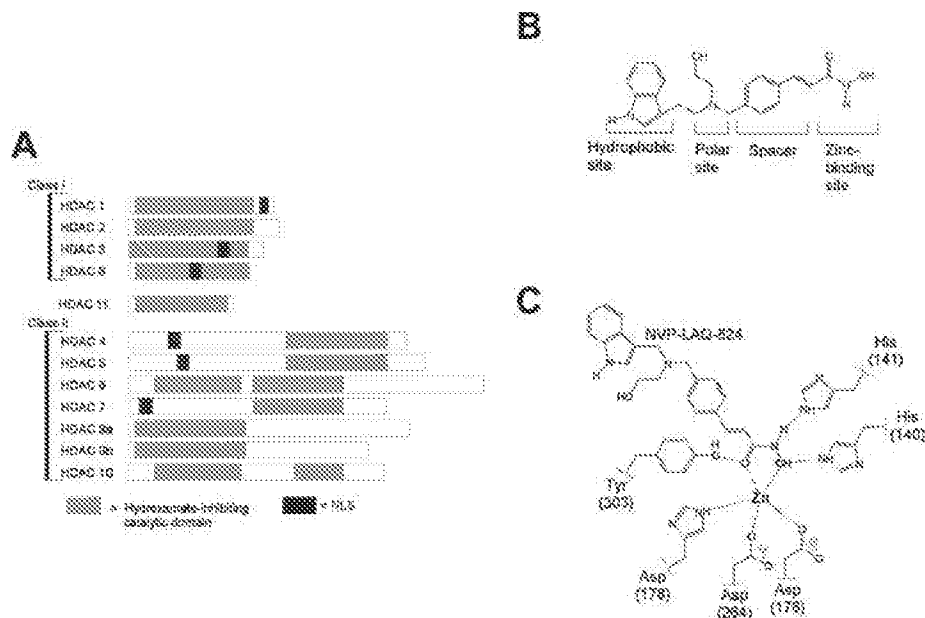


**Figure 3** Structural basis for hydroxamic acid inhibition of HDACs. (A) Structural homology of class I and II HDACs showing hydroxamate-inhibiting catalytic domains. (B) Functional components of hydroxamic acid-type HDAC inhibitors (LAQ824). Hydroxamic acid-based HDAC inhibitors are composed of four primary functional components: (a) a zinc-chelating hydroxamic acid, (b) a linker region, (c) a polar site, and (d) a hydrophobic cap that blocks the active site. (C) Predicted transition state inhibition of HDAC1 by LAQ824.

hydrogen bond contacts with the ketone. Elimination of the ketone, or reduction of the ketone to an alcohol, abolishes the activity of these molecules (50). Trapoxin B and HC-toxin also contain a five-carbon linker for transversing the cavity and a cyclic tetrapeptide capable of acting as a hydrophobic cap for the cavity. Trapoxin B is a hybrid molecule and can also be listed with the cyclic peptide HDAC inhibitors. The combination of cyclic peptide and epoxyketone resulted in nanomolar HDAC inhibitory activity.

The carboxylates or short-chain fatty acids, including sodium butyrate, valproic acid, and sodium phenylbutyrate, have much weaker HDAC inhibition constants ( $K_i$ s), commonly in the millimolar range. In spite of their weak activity, several of these agents have been studied clinically (51) owing in part to their clinical use for alternative medical indications. The most commonly studied members of this class are simple molecules with alkyl or phenylalkyl carboxylates. The carboxylate is thought to coordinate with the zinc ion in the active site, albeit more poorly than in the case of hydroxamates.

Cyclic peptide HDAC inhibitors have been discovered or developed that either contain an epoxyketone group (HC-toxin, trapoxin B) or are devoid of it (Apicidin,

Depsipeptide). In general, these inhibitors have nanomolar HDAC inhibitory activity and can have either irreversible (epoxyketone-based) or reversible mechanisms of action. The macrocyclic peptide portion of the inhibitor binds tightly to the rim or opening of the channel to the active site, whereas an aliphatic linker navigates the channel to the active site (44). Depsipeptide, also known as FK228, is a prodrug that requires intracellular reduction to liberate a sulfhydryl-containing aliphatic group that enters the active site and binds the active site zinc and water molecule (44, 52). Hybrid molecules, including CHAP31 and CHAP50, that possess both a cyclic peptide and an aliphatic hydroxamate have been prepared and shown to have a reversible mechanism of action and remarkable inhibitory activity when optimized in the range of 1–5 nanomolar (53, 54). The optimal linker in these studies was found to have five methylenes, similar to that described previously for other hydroxamates (47).

Inhibitors of the benzamide class, such as CI-994 (55) and MS-275 (56), are in general less active than members of the hydroxamate or cyclic peptide classes, with  $K_{i5}$  in the micromolar range (44, 56). The mechanism of HDAC inhibition for benzamides remains uncertain at present. In addition to the structural classes of HDAC inhibitors described thus far, a variety of inhibitors have been prepared that are not readily classified into one of the above mentioned five classes. Brosch and colleagues have recently described 3-(4-Aroyl-1-methyl-1H-2-pyrrolyl)-N-hydroxy-2-alkylamides containing a range of different metal chelating groups with  $IC_{50}$ s in the micromolar range (57, 58). Another series of Psammaplin derivatives containing novel metal chelating groups have demonstrated considerably greater inhibitory activity, with the most active of these compounds having nanomolar  $K_{i5}$  (59).

Little is presently known about the potential selectivity of various HDAC class I or II isoforms for structurally different inhibitors. HDAC6 and HDAC10 both possess two catalytic domains that appear to be differentially inhibited by drugs that preferentially bind near the entrance of the catalytic site (37, 54, 55). These class II HDAC isoforms appear relatively resistant to trapoxin when compared to class I HDACs. Depsipeptide, MS-275, and several of the hybrid CHAP derivatives also appear considerably more selective for HDAC1 over HDAC6 (54). TSA is generally considered a nonspecific HDAC inhibitor, as it has a similar  $K_i$  for all isoforms examined. Recently, Schrieber and colleagues described an HDAC6-specific inhibitor, tubacin (Figure 2), responsible for the deacetylation of tubulin, as well as another “histacin,” which appears to be a histone-selective deacetylase (60, 61). The continued development of isoform-specific inhibitors will undoubtedly remain a major emphasis of HDAC inhibitor development.

## ANTITUMOR MECHANISMS OF HDAC INHIBITORS

There is an everexpanding body of evidence supporting the involvement of, as well as structural alterations in, various HATs and HDACs with development of cancer (62, 63). Broadly speaking, this includes evidence for their genetic disruption

(e.g., translocation, amplification, mutation, overexpression) in a subset of hematological and epithelial malignancies, as well as the aberrant genomic recruitment of otherwise normal HDACs in conjunction with oncogenic transcription factors. Such observations have led to the conclusion that defects and/or imbalances in the genome's acetylation machinery accompany changes in local chromatin structure and oncogenic dysregulation of genes controlling cell cycle progression, differentiation, and apoptosis. Despite these observations and conclusions, there are as yet no specific HAT or HDAC measurements devised that can predict the sensitivity of any given tumor to any class of HDAC inhibitor.

It has also been generally accepted that more actively transcribed chromatin regions are associated with histone hyperacetylation and recruitment of HATs (although HDACs are also known to be recruited), and histone deacetylation associated with recruitment of HDACs often restores these genomically active regions to a more repressed and condensed chromatin state. Thus, an attractive paradigm for the antitumor action of HDAC inhibitors has been the induction of histone acetylation producing transcriptional activation of critical genes needed for tumor growth arrest (1, 43, 44, 64–67). Unquestionably, HDAC inhibitors produce a global increase in histone acetylation within hours of treatment of many different malignant and nonmalignant tissue types, including those showing little if any biological consequences upon treatment with HDAC inhibitors. Thus, while a global increase in the level of histone acetylation by itself cannot explain selective changes in gene expression or specific patterns of antitumor activity following HDAC inhibition, assaying for enhanced histone acetylation in readily sampled cells or tissues (e.g., peripheral white blood cells) is being routinely employed to demonstrate HDAC inhibitor bioavailability and activity. Greater attention is currently being given to the expanding list of nonhistone proteins acetylated in direct response to HDAC inhibition (Table 1), especially because many of these are tissue/development-specific (EKLF, GATA-1, ER $\alpha$ , MyoD), oncogenic (c-Myb), tumor-suppressing (p53), or even rather ubiquitous (TFIIIE, TFIIIF, TCF, HNF-4) transcription factors.

Virtually all HDAC inhibitors currently in clinical development show some degree of preclinical activity against malignant cells proliferating in culture and also tumors growing in animal models; this antitumor activity may be characterized as either inducing cytostasis (cell cycle arrest), differentiation, or apoptosis. However, the HDAC-dependent mechanisms accounting for the observed and rather selective modulation of gene expression, as well as specific patterns of antitumor activity, remain poorly understood. Several studies have now revealed that fewer than 10% of expressed genes in a given malignant cell population are affected by an antitumor dose of an HDAC inhibitor, with a near equal number of transcriptionally active genes being repressed as those being stimulated; structurally different HDAC inhibitors can similarly modulate expression of a relatively limited set of core genes (2, 3, 68). As shown in Table 2, among the commonly up- and down-modulated gene transcripts identified in these expression microarray studies, as well as in numerous single-gene expression studies (66–78), are



TABLE 2 Tumor-associated proteins whose transcriptional expression is altered in response to HDAC inhibitor treatment of cells

Regulated protein	Function (oncogenic or antioncogenic/tumor suppressing)	Reference(s)
<b>Downregulated by HDAC inhibitors (e.g., oncogenic)</b>		
HER2/neu	Growth factor receptor (EGFR class)	(81)
TGF- $\beta$	Regulates cell proliferation and differentiation through TGF- $\beta$ type II receptor	(166, 167)
Thioredoxin	Disulfide reductase, cytokine activity, can inhibit apoptosis	(168)
Telomerase	Prevents telomere erosion	(97)
RECK	Regulates matrix metalloproteinases	(86)
VEGF	Angiogenic factor	(87, 169)
bFGF	Angiogenic factor	(87)
Myb/c-MyBL2	Oncogenic transcription factor—regulation of transformation and differentiation	(68)
raf-1	Effector of Ras	(68)
cyclin A	Cell cycle regulator	(111)
cyclin B	Cell cycle regulator	(111)
DAF	Complement inhibitory protein	(170)
abl	Growth factor receptor, component of bcr/abl chimeric kinase	(68)
DEK	Putative role in regulating chromatin structure and postsplicing events	(68)
Proteasome	Degradation of misfolded or oxidized proteins	(68)
<b>Upregulated by HDAC inhibitors</b>		
Fas/Fas ligand	Proapoptotic	(76)
Bcl2	Proapoptotic	(78)
p53	Proapoptotic	(169)
Bak, Bax, Bim	Proapoptotic	(171)
c-myc	Inhibitor of differentiation	(100)
Caspase 3	Cysteine protease involved in apoptosis, proapoptotic	(125, 172)
Carboxypeptidase A3 (CPA3)	Carboxypeptidase, putative role in regulating differentiation	(173)
RECK	Negatively regulates matrix metalloproteinases	(86)
p21 <sup>WAF1/Cip1</sup>	Cell cycle regulation	(66, 70)
Gelsolin	Regulation of cell morphology	(70)

(Continued)

Annu. Rev. Pharmacol. Toxicol. 2005.45:495-528. Downloaded from www.annualreviews.org. Access provided by Reprints Desk, Inc. on 09/29/17. For personal use only.

TABLE 2 (Continued)

Regulated protein	Function (oncogenic or antioncogenic/tumor suppressing)	Reference(s)
ER $\alpha$	Estrogen-activated nuclear receptor regulates transcription of estrogen responsive genes	(174)
TSSC3	Regulates Fas-mediated apoptosis	(68)
IGFBP-3	Augments IGF actions, promotes apoptosis, and inhibits cell growth	(175)
TBP-2	Inhibits thiol-reducing activity of thioredoxin	(168)

Bak, Bcl2 antagonist killer; Bax, Bcl2-associated X protein; DAF, decay-accelerating factor; TBP-2, thioredoxin binding protein; TSSC3, tumor suppressing substrate transferable candidate.

those encoding known tumor-associated proteins that mediate proliferation and cell cycle progression, survival factors, growth factor receptors, kinases and signal transduction intermediates, DNA synthesis/repair enzymes, shuttling proteins, transcription factors, and proteases.

Some study has gone into the question of how HDAC inhibitors actually relieve transcriptional repression and reverse the differentiation arrest in malignancies such as acute leukemia, where differentiation arrest and the malignancy phenotype induced by such chimeric oncoproteins as PLZF-RAR $\alpha$ , PLZF-RAR $\alpha$ , or AML1/ETO can be reversed, at least in part, by HDAC inhibitors (69, 79). In other types of malignancies, HDAC inhibitors induce differentiation and/or apoptosis by activating transcription of CDKN1A through a p53-independent mechanism, producing increased levels of the cyclin-dependent kinase (CDK) inhibitor, p21<sup>WAF1/CIP1</sup> (66). Likewise, HDAC inhibitors have been observed to induce transcription of other tumor suppressor genes such as gelsolin and maspin (70, 71). When administered in combination with DNA demethylating agents such as 5-aza-2'-deoxycytidine, HDAC inhibition can fully restore transcriptional expression to various genes, including MLH1, TIMP3, CDKN2A, and CDK2NB, that have been epigenetically silenced by promoter methylation during the course of tumorigenesis (72, 73).

Apart from the upregulation of epigenetically silenced tumor suppressor proteins or induction of caspases and other proapoptotic proteins (26, 68, 74–78), there are emerging data showing HDAC-induced repression of critical transforming growth factor mechanisms, such as those involving oncogenic tyrosine kinases like bcr/abl and ErbB2 (80–82). We recently reported that HDAC inhibitors can selectively repress ErbB2 transcript levels by two distinct HDAC-dependent mechanisms: repression of new ErbB2 transcript synthesis and the accelerated decay of mature ErbB2 mRNA (81). The hydroxamic acid TSA was identified in a high-throughput cell-based chemical screen for its ability to repress ErbB2 promoter activity (81). Figure 4 (panel A) compares the potency of TSA against several

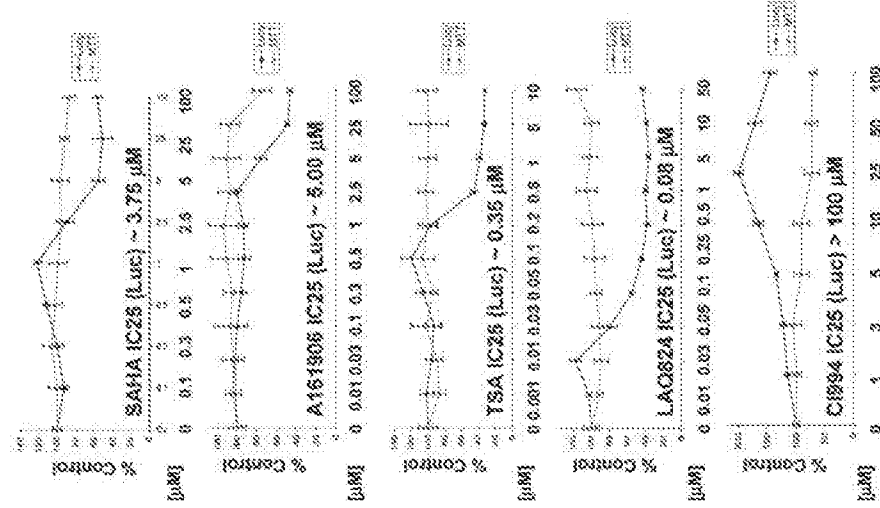
other HDAC inhibitors for their ability to inhibit ErbB2 promoter function. Of interest, the rank order of potency for the HDAC inhibitors shown in this screening assay (LAQ824 > TSA > A1616906 > SAHA >> CI994) is comparable to their relative antitumor activity against several ErbB2 overexpressing breast cancer cell lines. When evaluated further against SkBr3 and other ErbB2-dependent breast cancer cell lines (e.g., BT-474, MDA-453), HDAC inhibitors were shown to inhibit the synthesis and elongation of nascent ErbB2 transcripts as well as destabilize and accelerate the decay of mature cytoplasmic ErbB2 transcripts (Figure 4, panels B and C). Although ongoing preclinical studies are confirming that ErbB2-dependent cancers appear somewhat more sensitive to HDAC inhibitors than ErbB2-independent cancers, molecular studies are attempting to define the drug-sensitive HDAC-dependent nuclear and cytoplasmic mechanisms that differentially regulate ErbB2 transcription and ErbB2 transcript stability, respectively. The presence of multiple distinct HDAC-dependent mechanisms capable of controlling ErbB2 transcript levels suggests that even among ErbB2-dependent cancers, there will be differential sensitivity to structurally different classes of HDAC inhibitors. Other investigators have identified HDAC-dependent posttranslational mechanisms that can also downregulate the expression of oncoprotein kinases like ErbB2 and *bcr/abl* (80, 82). Acetylation of the chaperone protein, Hsp90, induced by HDAC inhibition, results in the enhanced proteasomal degradation of ErbB2 and *bcr/abl* kinases. These examples of multiple mechanisms by which HDAC inhibitors potentially downregulate critical oncogenic pathways also suggest new combinatorial strategies for possible clinical evaluation, including HDAC inhibitor treatment in conjunction with tyrosine kinase inhibitors (80, 82–84) or Hsp90 antagonists (85).

Apart from directly affecting transformed cells, HDAC inhibitors have also been shown to inhibit tumor angiogenesis, suggesting additional therapeutic mechanisms for the observed *in vivo* activity of these antitumor drugs (76, 86–88). Depsipeptide was shown to suppress the expression of pro-angiogenic factors, including vascular endothelial growth factor (VEGF) and basic fibroblast growth factor (bFGF) (87). VEGF and bFGF mRNA levels were significantly reduced in prostate tumor xenografts sensitive to this cyclic peptide HDAC inhibitor. The hydroxamic acid HDAC inhibitor TSA was shown to upregulate the RECK protein responsible in part for inhibiting tumor metastasis and angiogenesis through its action on matrix metalloproteases (86). The carboxylate and short-chain fatty acid HDAC inhibitor, valproic acid, was also shown to inhibit angiogenesis both *in vitro* and *in vivo* via a mechanism involving diminished expression of endothelial nitric oxide synthase (88). Additional miscellaneous or less well-studied tumor-associated mechanisms may prove to be important in determining the ultimate clinical utility of some HDAC inhibitors.

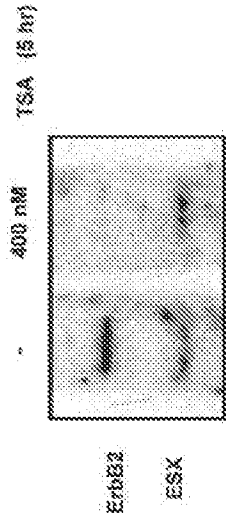
Last, various drug-resistance phenotypes have been shown to be modulated by HDAC inhibitors (89–95). Treatment of different multidrug-resistant cell lines with TSA or SAHA was shown to downregulate P-glycoprotein (93), helping

Ann. Rev. Pharmacol. Toxicol. 2005.45:495-528. Downloaded from www.annualreviews.org. Access provided by Reprints Desk, Inc. on 09/29/17. For personal use only.

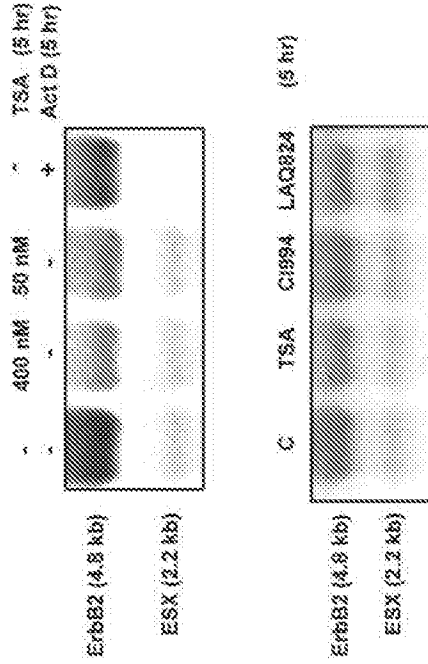
**A. ErbB2 promoter activity**



**B. Nascent ErbB2 transcript synthesis**



**C. Mature ErbB2 transcript levels**



reverse the multidrug-resistant phenotype. SAHA and oxamflatin were shown in separate studies to overcome multidrug resistance (89, 94), whereas in one study depsipeptide was shown to be a substrate for P-glycoprotein (94). In another study, depsipeptide was shown to inhibit cell growth in irinotecan-, etoposide-, and cisplatin-resistant cell lines in conjunction with its ability to inhibit telomerase expression and activity (90). Telomerase is responsible for adding telomeric repeats to the ends of chromosomes and is required for the relative immortality of cancer cells; other investigators have also shown an inhibitory effect of HDAC inhibitors on telomerase activity (96, 97). These diverse examples illustrate the immense need for further studies to understand the relative importance of the many potential *in vitro* and *in vivo* mechanisms by which HDAC inhibitors can produce antitumor responses.

**Figure 4** Transcriptional repression of ErbB2 induced by hydroxamic HDAC inhibitors is caused by a combination of both ErbB2 promoter repression and transcript destabilization. (A) Employing our previously described high-throughput screening assay (81), an ErbB2-independent subline of MCF-7 breast cancer cells (MCF/R06pGL-4) bearing a chromatin-integrated ErbB2 promoter-driven luciferase construct was used to compare the ErbB2 promoter repressing potency of four structurally different hydroxamic acid-type HDAC inhibitors (SAHA, A1616906, TSA, LAQ824) and a benzamide-type HDAC inhibitor (CI994). After 24 h culture exposure to the indicated drug doses, cell viability as measured by MTT assay (*squares*) shows little change, whereas specific repression of ErbB2 promoter activity is detected by luciferase expression (*diamonds*). The benzamide inhibitor (CI994) shows slight ErbB2 promoter stimulation with no evidence of promoter repression; in contrast, the hydroxamic acid inhibitors show ErbB2 promoter repression at different potencies as indicated by the 25% luciferase inhibitory concentration ( $\mu\text{M}$  IC25) values. (B) When ErbB2-dependent SkBr3 breast cancer cells in culture are treated for 5 h with an ErbB2 promoter-repressing dose of TSA, nascent ErbB2 transcript synthesis and elongation, as measured by nuclear run-off assays (81), appears completely inhibited, whereas nascent transcript synthesis of the Ets transcription factor ESX appears marginally increased. (C) Total RNA extracted and Northern blotted after 5-h treatment of cultured SkBr3 breast cancer cells shows treatment effects on mature long-lived ( $\sim 8$  h half-life) ErbB2 transcripts (4.8 kb) in comparison to short-lived ( $< 2$  h half-life) ESX transcripts (2.2 kb). Treatment for 5 h with an RNA polymerase inhibiting dose of Actinomycin D (10  $\mu\text{g}/\text{ml}$ ) demonstrates the expected absence of ESX transcripts and partial decline in total ErbB2 transcripts. In contrast, and after 5-h treatment with comparable doses of the HDAC inhibitors TSA, CI994, and LAQ824, ESX levels appear marginally increased, whereas ErbB2 transcript levels are reduced below levels caused by Act D treatment, demonstrating the independent ability of HDAC inhibitors to destabilize and accelerate the decay of mature ErbB2 transcripts.

## IN VIVO BIOLOGICAL AND CLINICAL CHARACTERISTICS OF HDAC INHIBITORS

### In Vivo Preclinical Antitumor Activity

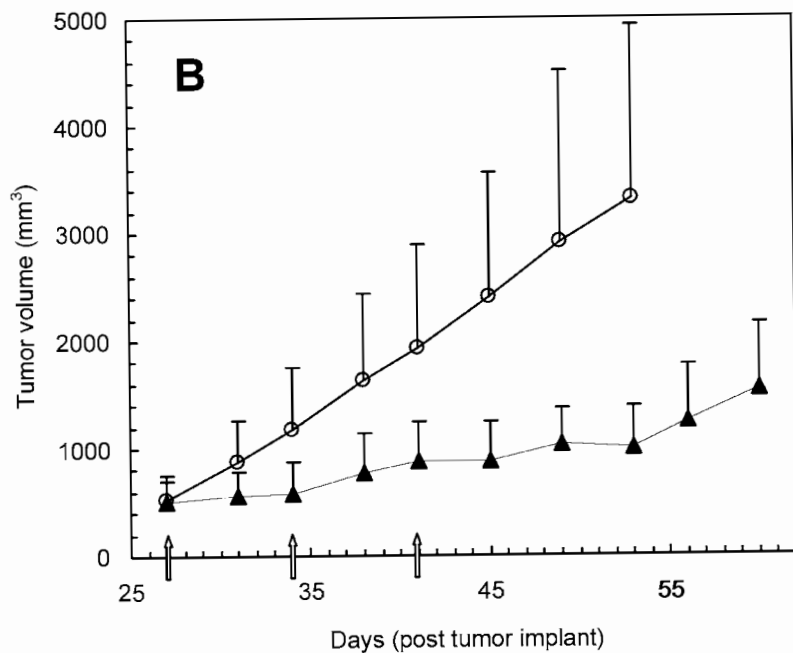
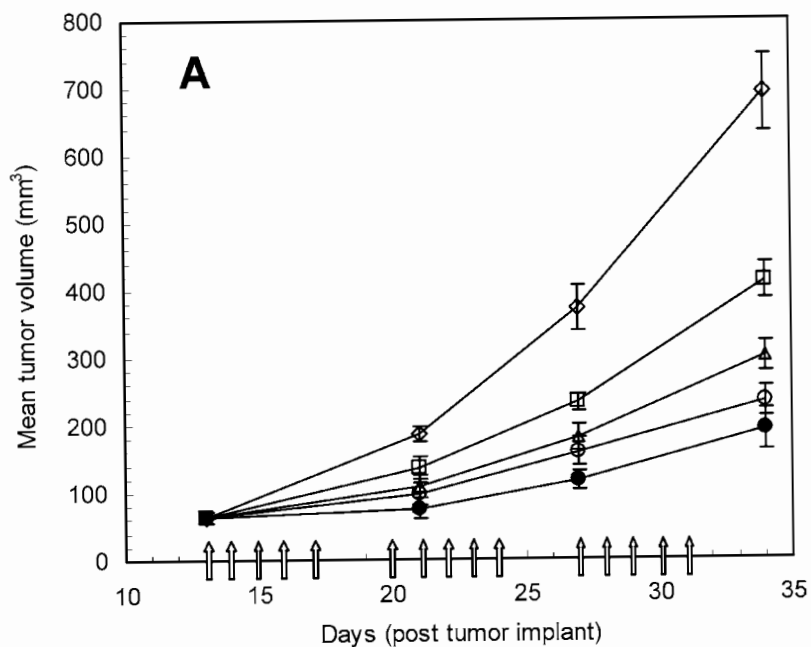
Numerous animal model studies have demonstrated significant antitumor efficacy for HDAC inhibitors from virtually every structural class (71, 87, 98–106). One of the newest clinical candidates, the hydroxamate JNJ1641199 (Figure 2), exhibited nanomolar HDAC inhibition and antitumor activity against lung, ovarian, and colon cancer xenograft models, along with excellent oral bioavailability (106). Another hydroxamate now in clinical trials, NVP-LAQ824 (Figure 2), shows potent antitumor activity against human colon (Figure 5A) and lung cancer xenograft models at submicromolar concentrations when administered parenterally every day and with a maximal tolerated dose (MTD) that exceeds 100 mg/kg (101). Likewise, TSA, SAHA, and pyridoxamide hydroxamates were previously shown to have in vivo antitumor activity with daily parenteral dosing associated with little systemic toxicity (98, 104, 105).

The cyclic peptide prodrug depsipeptide (FK228) demonstrates efficacy in leukemia and lymphoma models (100, 103), which can be further enhanced in combination with the cell-differentiating retinoid, ATRA (103). Depsipeptide was also recently shown to have clinical activity in treating T cell lymphoma in early Phase I/II trials (107).

Although most of the carboxylated short-chain fatty acid HDAC inhibitors have displayed limited potency in vivo owing to their lack of specificity and high drug-concentration requirements (51, 65), the prodrug AN-9 has shown good activity

**Figure 5** In vivo antitumor efficacy of hydroxamate-type HDAC inhibitor, LAQ824, is dependent on dose, schedule, and formulation. Insert arrows in both panels show treatment points. In vivo antitumor activity of LAQ824 was determined in (A) a human colon (HCT116) tumor xenograft model and (B) liposomal LAQ824 in an ErbB2-dependent human breast (BT474) tumor xenograft model. The drugs in both studies were administered intravenously. For the free LAQ824 study (A), treatments started when HCT116 tumors reached a mean size of 50 mm<sup>3</sup> and nude mice were injected 5 times per week for 3 weeks, for a total of 15 doses. The treatment groups were as follows: (*diamonds*) 10% DMSO/DSW (control), (*squares*) 10 mg/kg/dose LAQ824, (*triangles*) 25 mg/kg/dose LAQ824, (*open circles*) 50 mg/kg/dose LAQ824, and (*closed circles*) 100 mg/kg/dose LAQ824. For the liposomal LAQ824 study (B), BT474 breast tumor xenografts were allowed to grow to a size of approximately 250–300 mm<sup>3</sup>. Mice were then injected with either saline (*open circles*) or conventional liposomal LAQ824 (*closed triangles*) at a dose of 2.5 mg/kg weekly, for a total of 3 weeks, beginning on day 27. The data are expressed as mean tumor volume  $\pm$  standard error. (A) was adapted from Remiszewski et al. (101) with permission from the American Chemical Society.

Ann. Rev. Pharmacol. Toxicol. 2005.45:495-528. Downloaded from www.annualreviews.org. Access provided by Reprints Desk, Inc. on 09/29/17. For personal use only.



in several murine tumor and human tumor xenograft models (108), and has shown some encouraging results in early clinical trials (109).

The benzamide HDAC inhibitors, MS-275 (56, 71, 110, 111) and CI-994 (55), have also shown *in vivo* activity against various tumor models. MS-275 was shown to inhibit the growth of three different orthotopic pediatric tumor xenografts (110). In another study, MS-275 administered orally was shown to have potent antitumor activity against a series of seven different human tumors xenografts (71). Unfortunately, antitumor doses of MS-275 in mice were also myelosuppressive, causing decreases in red and white blood cells as well as platelets (111). A similar pattern of toxicity was observed with CI-994 (112); and thrombocytopenia was a major dose-limiting toxicity seen in Phase I and II clinical testing with CI-994 as well as with the cyclic peptide depsipeptide (113, 114).

### Clinical Toxicity and Antitumor Activity

Dose-limiting clinical toxicities and reported antitumor responses have been noted in Phase I and II clinical trials for the limited number of structurally varied HDAC inhibitors that have entered clinical testing to date. The carboxylate phenylbutyrate given by prolonged intravenous infusion has a dose-limiting toxicity (DLT) of somnolence and confusion, which has not been reported for the benzamide or hydroxamate HDAC inhibitors (115) or for the carboxylate prodrug AN-9 (109). The carboxylate valproic acid has been in clinical use for more than two decades as an anticonvulsant and thus has well-described pharmacologic properties and a well-tolerated side effect profile; clinical trials are in progress evaluating the antitumor potential of valproic acid as an HDAC inhibitor. Despite thrombocytopenia being a DLT for both CI-994 and depsipeptide, evidence for antitumor clinical activity upon oral daily dosing of CI-994 has been noted in patients with several epithelial types of advanced solid malignancies [including nonsmall cell lung cancer (NSCLC), renal cell carcinoma, and bladder cancer]. Likewise, two Phase I trials of depsipeptide have suggested that patients with T cell leukemia or lymphoma, as well as other occasional cases of refractory malignancies, may achieve clinical benefit from this HDAC inhibitor (113, 116). Curiously, depsipeptide is the only clinically tested HDAC inhibitor reported to date that is associated with a significant incidence of cardiac dysrhythmias and nonspecific EKG abnormalities (113). Among the hydroxamates, daily infusions of pyroxamide and LAQ824 are currently under Phase I clinical evaluation, whereas a trial of infusional SAHA was recently completed (115, 117). When given by 2-h infusions daily five times, SAHA had a MTD of 300 mg/m<sup>2</sup>/day. Among treated patients with advanced hematologic malignancies, myelosuppression (thrombocytopenia) was the DLT. In those with advanced solid tumors, myelosuppression was observed but was not a DLT; as well, nonspecific EKG changes without clinical signs or symptoms were common. Fatigue was commonly observed with SAHA treatment but was not dose-limiting and was similar to that previously reported for depsipeptide. Importantly, patients with renal cell carcinoma, head and neck squamous



carcinoma, papillary thyroid carcinoma, mesothelioma, B and T cell lymphomas, and Hodgkin's disease all showed some degree of clinical improvement (115).

### Pharmacokinetic Considerations

Although receiving less reported attention than studies elucidating the pharmacodynamics of various HDAC inhibitors, the pharmacokinetic characteristics and limitations of different HDAC inhibitors are of critical interest and will likely prove to be an important determinant of their ultimate clinical utility. Inhibition of intracellular HDAC activity commonly requires continuous systemic circulation and drug exposure to achieve maximal tumor cytostasis or apoptosis and clinical response. Rapid clearance, a high degree of protein binding, rapid metabolism, or rapid inactivation of reactive functional groups (i.e., epoxy groups) are factors that can adversely affect HDAC inhibitor bioavailability and antitumor activity. Although occasionally used in the clinic, prolonged or daily infusions of any drug are generally undesirable. The requirement of constant systemic exposure by parenteral administration to achieve an active antitumor drug concentration will most likely limit the clinical development of any HDAC inhibitor that is not orally bioavailable. For this reason, the clinical development of SAHA shifted from Phase I evaluation of daily intravenous infusions to a more recently designed oral formulation (115).

Novel drug delivery systems that allow for controlled drug release may help circumvent the clinical inconvenience of daily infusions as well as generally enhance the therapeutic index of HDAC inhibitors. We have recently evaluated the potential of liposomes for delivering the HDAC inhibitor LAQ824. When formulated properly, liposomes can entrap and concentrate amphipathic drugs (achieving >10,000 drug molecules per liposomal nanoparticle), releasing them slowly over time in the plasma or delivering them specifically to solid tumors where they deposit their drug in close proximity to the tumor, allowing for increased tumor accumulation and drug exposure (118). In a pilot study administering liposomal LAQ824 on a once-weekly schedule for three weeks, we observed significant growth arrest of rapidly growing human breast tumor xenografts (Figure 5B). As shown in other studies involving various tumor model systems, free LAQ824 requires daily injections of generally higher doses to slow tumor growth (Figure 5A). More recent studies with optimized formulations and targeted liposomal constructs have shown even greater efficacy (119).

### HDAC INHIBITORS IN COMBINATION WITH OTHER AGENTS

The greatest potential of HDAC inhibitors may lie in their ability to modulate the activity of other therapeutic agents. A variety of different drug combinations have demonstrated considerable promise in treating cancer. These are reviewed

more extensively in a separate review of the field (65), and are summarized in Table 3. The pretreatment or coadministration of HDAC inhibitors with a wide range of agents has repeatedly been shown to additively or synergistically enhance apoptosis of cancer cells in culture (68, 82, 85, 120–125) as well as antitumor efficacy in vivo (126–128). Notably, enhancements in activity have been observed when HDAC inhibitors are combined with a number of different commonly used chemotherapeutics (82, 120, 121). Nuclear receptor ligands (123, 127, 129, 130), Hsp90 antagonists (85), proteasome inhibitors (68, 84, 131), signal transduction inhibitors (80, 82, 124, 125, 132–136), and DNA demethylating agents (72, 73, 122, 128, 137) represent some of the more promising classes of agents. Demethylating agents such as 5-aza-2'-deoxycytidine (DAC) are particularly interesting owing to the interaction of DNA methylation with histone deacetylation in gene silencing of tumor suppressor genes, as mentioned above. Combinations of DAC with TSA or depsipeptide were shown to reactivate silenced tumor suppressor genes including *MLH1*, *TIMP3*, *CDKN2B*, *CDKN2A*, *ARH1*, gelsolin, and maspin (72, 73, 137), synergistically increasing the level of tumor cell apoptosis (122). Combinations of nuclear receptor ligands, such as all-*trans* retinoic acid (ATRA), or vitamin D analogs, such as 1,25-dihydroxyvitamin D, with HDAC inhibitors have been shown to increase differentiation and apoptosis in cancer cells (123, 127, 130) and also inhibit tumor growth in vivo (127, 130, 138). Small-molecule kinase inhibitors may also be rationally combined with HDAC inhibitors. Imatinib (Gleevec<sup>®</sup>) is a specific inhibitor of Bcr/Abl with impressive clinical activity in the treatment of chronic myeloid leukemia and selected other malignancies. Because LAQ824 has been shown to downregulate the expression of Bcr/Abl and also promote its degradation through acetylation of Hsp90 (80), combinations of imatinib with LAQ824 as well as other HDAC inhibitors, such as SAHA and apicidin, have been tested and shown to dramatically increase the apoptosis of Bcr/Abl positive leukemic cells (80, 83, 132, 133). A similar effect is seen when malignant cells known to be transformed by oncogenic tyrosine kinases (ErbB2/HER2, Src/Abl, PI3 kinase) are treated with HDAC inhibitors in combination with appropriate kinase inhibitors like Herceptin<sup>®</sup>, PD180970, or LY294002 (80, 82, 124).

As noted above, expression of the CDK inhibitor p21<sup>WAF1/CIP1</sup> is regulated by HDACs and plays a critical role in determining whether cells undergo differentiation or apoptosis in response to treatment with HDAC inhibitors (66, 70, 139). Flavopiridol is a CDK inhibitor that results in a disruption of p21<sup>WAF1/CIP1</sup> induction and induces apoptosis. Its combination with HDAC inhibitors (SAHA, depsipeptide, sodium butyrate) has been shown to result in a disruption of p21 induction and an additive or synergistic increase in tumor cell apoptosis (125, 135, 139, 140).

Proteasome inhibitors and Hsp90 antagonists represent two other groups of interesting agents that may be rationally combined with HDAC inhibitors. Hsp90 is a molecular chaperone that stabilizes and controls the intracellular trafficking of important client proteins, including ErbB2/HER2, Bcr/Abl, EGF, cyclin D1, c-Raf, and steroid receptors. The inhibition of Hsp90 with amsacrine antagonists, such as

TABLE 3 Therapeutic agents used in combination with HDAC inhibitors in preclinical and clinical studies

Combined therapeutic agent	HDAC inhibitor	Combined antitumor effects	Reference(s)
<b>Standard chemotherapy</b>			
Gemcitabine	CI-994	Phase II trial— increased toxicity	(176)
VP-16 (etoposide)	TSA, SAHA	Synergistic	(120)
cytarabine, etoposide, and topotecan	PB	Synergistic	(121)
Doxorubicin, melphalan, chloroambucil, cisplatin, carboplatin, fludarabine	PB	Additive	(121)
Taxotere, gemcitabine, epothilone B	LAQ824	Additive	(82)
Etoposide	TSA	Antagonistic	(177)
Fludarabine	MS-275	Synergistic	(178)
IMiD-1, dexamethasone	SAHA	Synergistic	(68)
<b>Demethylating agents</b>			
DAC	TSA, depsipeptide	Enhanced	(122)
	Depsipeptide	Synergistic	(73)
	PB	Synergistic	(128)
	PB	Enhanced	(179)
<b>Nuclear receptor ligands</b>			
ATRA	CBHA	Synergistic	(127)
1 $\alpha$ ,25-Dihydroxyvitamin D <sub>3</sub>	TSA	Synergistic	(123)
	SB		
<b>Signal transduction inhibitors</b>			
Imatinib mesylate (Gleevec)	Apicidin	Synergistic	(83)
	SAHA	Synergistic	(132)
Imatinib mesylate or PD180970	LAQ824	Synergistic	(80)
Herceptin	LAQ824	Synergistic	(82)
LY-29,4002	SAHA, SB, MS-275	Synergistic	(124)
Flavopiridol	SAHA	Synergistic	(125)
	SB	Synergistic	(135)
	Depsipeptide	Synergistic	(136, 140)
TRAIL	SB	Enhanced	(180)
	SB, SAHA	Synergistic	(181)
	LAQ824	Enhanced	(182)
<b>Hsp90 antagonists and proteasome inhibitors</b>			
17-AAG	SAHA	Synergistic	(85)
Bortezomib (PS-341)	SAHA	Synergistic	(68)
	SAHA, SB	Synergistic	(84)
	SB	Synergistic	(141)
MG132	SB	Synergistic	(131)

ATRA, all-*trans* retinoic acid; CBHA, *m*-carboxylsuccinamic acid bis-hydroxamide; DAC, 5-*aza*-2'-deoxyctidine; IMiD-1, immunomodulatory thalidomide derivative 1; TRAIL, tumor necrosis factor-related apoptosis-inducing ligand.

Ann. Rev. Pharmacol. Toxicol. 2005.45:495-528. Downloaded from www.annualreviews.org. Access provided by Reprints Desk, Inc. on 09/20/17. For personal use only.

17-AAG, results in proteasomal degradation of client proteins. Owing to the regulation of Hsp90 function by acetylation, the combination of HDAC inhibitors and Hsp90 antagonists is a reasonable therapeutic strategy. Experimentally, 17-AAG in combination with SAHA or sodium butyrate inhibited induction of p21<sup>WAF1/CIP1</sup>, inducing Bcl-2 cleavage, and synergistically enhanced tumor cell apoptosis (85). Proteasome inhibitors slow the degradation of many important and diverse cellular proteins, and their combination with HDAC inhibitors results in more complete inhibition of proteasome activity, which may synergistically enhance tumor cell apoptosis (68, 84, 131, 141).

There is additional evidence that HDAC inhibitors may improve the efficacy of radiation therapy (142). In this study, pretreatment with depsipeptide greatly increased radiation-induced apoptosis. In another study, the HDAC inhibitors phenylbutyrate, TSA, and valproic acid were able to reduce cutaneous radiation toxicity following radiotherapy (143). This poorly understood interaction whereby HDAC inhibitors potentially increase radiation-induced tumor cell death while decreasing normal host cell toxicity deserves further study, as it may lead to more novel clinical indications for HDAC inhibitors.

Although these provocative combination regimens based on cell culture studies have rational appeal, they must be explored more fully *in vivo* to assure that they do not also lead to enhanced host toxicity. One recent Phase II study of the combination of gemcitabine and CI-994 in patients with NSCLC demonstrated no improvement in efficacy over gemcitabine alone, primarily because of increased toxicity that limited dose intensity and reduced the net therapeutic index of the two-drug combination (176).

## CONCLUSIONS

The complexities of the histone code and the various other nuclear as well as cytoplasmic nonhistone proteins whose functions are modulated by acetylation underscore why HDAC inhibition was an empirically discovered, as well as novel, form of cancer therapy. The biology of the various HDAC isoforms and their relationship to tumorigenesis is just beginning to be elucidated and is largely driven by the perceived clinical potential of HDAC inhibitors. It remains to be seen if a more detailed understanding of the specific roles played by various HDAC isoforms during human tumorigenesis leads not only to development of isoform-specific inhibitors but also to more effective or less toxic antitumor therapeutics, as compared to the multiclass HDAC inhibitors that are currently undergoing clinical evaluation. Rationally designed combinations of HDAC inhibitors with various other types of approved or investigational anticancer agents are showing promise in tumor cell culture systems but must yet be proven in clinical trials. Of great interest to many cancer investigators is the potential ability to derepress the expression of epigenetically silenced tumor suppressor genes by administering HDAC inhibitors in combination with inhibitors of DNA methyltransferases. There is a

similar level of preclinical interest in combining inhibitors of oncogenic kinases with HDAC inhibitors to strategically downregulate critical oncogenic pathways at transcriptional and posttranslational levels. The potential ability of HDAC inhibitors to overcome various drug-resistance phenotypes is yet another preclinical strategy warranting clinical evaluation. Finally, little is presently published on the pharmacokinetics and biodistribution of various HDAC inhibitors now under clinical development. Owing to the preclinically determined need for constant drug exposure to achieve in vivo tumor mass reduction by net inhibitory effects on tumor cell proliferation and survival mechanisms, a more detailed study and comparison of the pharmacokinetic profiles for various HDAC inhibitors is needed. Present evidence suggests that more novel formulations and drug delivery strategies may be able to significantly enhance the therapeutic index of even the most potent and biologically active of currently available HDAC inhibitors. Although a clinical role for HDAC inhibitors as novel cancer therapeutics seems almost inevitable at present, their general clinical utility will likely depend greatly on the future development of molecular or cellular predictors of their antitumor activity.

#### ACKNOWLEDGMENTS

We are grateful to the following for supplying their respective HDAC inhibitors: Dr. Peter Atadja and Novartis Oncology for NVP-LAQ824, Dr. Alan Kraker and Pfizer Oncology for CI-994, Dr. Victoria Richon and Aton Pharma for SAHA, and Dr. Keith Glaser and Abbott for A-16,1906. We thank Crystal Berger and Cliff Amend at the Buck Institute for their excellent technical assistance. Daryl Drummond was supported in part by a New Investigator Award from the California Breast Cancer Research Program of the University of California, Grant Number 7KB-0066A. This work was supported in part by NIH grant R01-CA36773 (CCB) and a development project award from the National Cancer Institute Specialized Programs of Research Excellence (SPORE) in Breast Cancer (P50-CA 58207-01; CCB).

The *Annual Review of Pharmacology and Toxicology* is online at  
<http://pharmtox.annualreviews.org>

#### LITERATURE CITED

1. Cress WD, Seto E. 2000. Histone deacetylases, transcriptional control, and cancer. *J. Cell Physiol.* 184:1–16
2. Glaser KB, Staver MJ, Waring JF, Stender J, Ulrich RG, Davidsen SK. 2003. Gene expression profiling of multiple histone deacetylase (HDAC) inhibitors: defining a common gene set produced by HDAC inhibition in T24 and MDA carcinoma cell lines. *Mol. Cancer Ther.* 2:151–63
3. Van Lint C, Ernillani S, Verdin E. 1996. The expression of a small fraction of cellular genes is changed in response to histone hyperacetylation. *Gene Expr.* 5:245–53
4. Turner BM. 2002. Cellular memory and the histone code. *Cell* 111:285–91
5. Strahl BD, Allis CD. 2000. The language of covalent histone modifications. *Nature* 403:41–45

6. Sterner DE, Berger SL. 2000. Acetylation of histones and transcription-related factors. *Microbiol. Mol. Biol. Rev.* 64:435-59
7. Jenuwein T. 2001. Re-SET-ting heterochromatin by histone methyltransferases. *Trends Cell Biol.* 11:266-73
8. Lachner M, Jenuwein T. 2002. The many faces of histone lysine methylation. *Curr. Opin. Cell Biol.* 14:286-98
9. Cheung WL, Ajito K, Samejima K, Kloc M, Cheung P, et al. 2003. Apoptotic phosphorylation of histone H2B is mediated by mammalian sterile twenty kinase. *Cell* 113:507-17
10. Jason LJ, Moore SC, Lewis JD, Lindsey G, Ausio J. 2002. Histone ubiquitination: a tagging tail unfolds? *Bioessays* 24:166-74
11. Nathan D, Sterner DE, Berger SL. 2003. Histone modifications: now summoning sumoylation. *Proc. Natl. Acad. Sci. USA* 100:13118-20
12. Geiman TM, Robertson KD. 2002. Chromatin remodeling, histone modifications, and DNA methylation—how does it all fit together? *J. Cell Biochem.* 87:117-25
13. Nephew KP, Huang TH. 2003. Epigenetic gene silencing in cancer initiation and progression. *Cancer Lett.* 190:125-33
14. Claus R, Lubbert M. 2003. Epigenetic targets in hematopoietic malignancies. *Oncogene* 22:6489-96
15. Czermin B, Imhof A. 2003. The sounds of silence—histone deacetylation meets histone methylation. *Genetica* 117:159-64
16. Daujar S, Bauer UM, Shah V, Turner B, Berger S, Kouzarides T. 2002. Crosstalk between CARM1 methylation and CBP acetylation on histone H3. *Curr. Biol.* 12:2090-97
17. Jenuwein T, Allis CD. 2001. Translating the histone code. *Science* 293:1074-80
18. Beisel C, Imhof A, Greene J, Kremmer E, Sauer F. 2002. Histone methylation by the *Drosophila* epigenetic transcriptional regulator Ash1. *Nature* 419:857-62
19. Imhof A, Becker PB. 2001. Modifications of the histone N-terminal domains. Evidence for an "epigenetic code"? *Mol. Biotechnol.* 17:1-13
20. Jacobs SA, Taverna SD, Zhang Y, Briggs SD, Li J, et al. 2001. Specificity of the HP1 chromo domain for the methylated N-terminus of histone H3. *EMBO J.* 20:5232-41
21. Hassan AH, Prochasson P, Neely KE, Galasinski SC, Chandy M, et al. 2002. Function and selectivity of bromodomains in anchoring chromatin-modifying complexes to promoter nucleosomes. *Cell* 111:369-79
22. Agalioti T, Chen G, Thanos D. 2002. Deciphering the transcriptional histone acetylation code for a human gene. *Cell* 111:381-92
23. Santos-Rosa H, Schneider R, Banister AJ, Sherriff J, Bernstein BE, et al. 2002. Active genes are tri-methylated at K4 of histone H3. *Nature* 419:407-11
24. Zhang X, Yang Z, Khan SI, Horton JR, Tamaru H, et al. 2003. Structural basis for the product specificity of histone lysine methyltransferases. *Mol. Cell.* 12:177-85
25. Imhof A, Yang XJ, Ogryzko VV, Nakatani Y, Wolffe AP, Ge H. 1997. Acetylation of general transcription factors by histone acetyltransferases. *Curr. Biol.* 7:689-92
26. Juan LJ, Shia WJ, Chen MH, Yang WM, Seto E, et al. 2000. Histone deacetylases specifically down-regulate p53-dependent gene activation. *J. Biol. Chem.* 275:20436-43
27. Fu M, Rao M, Wang C, Sakamaki T, Wang J, et al. 2003. Acetylation of androgen receptor enhances coactivator binding and promotes prostate cancer cell growth. *Mol. Cell Biol.* 23:8563-75
28. Wang C, Fu M, Angelelli RH, Siconolfi-Baez L, Reutens AF, et al. 2001. Direct acetylation of the estrogen receptor alpha hinge region by p300 regulates transactivation and hormone sensitivity. *J. Biol. Chem.* 276:18375-83
29. Yamagata T, Mitani K, Oda H, Suzuki T, Honda H, et al. 2000. Acetylation of GATA-3 affects T-cell survival and

- homing to secondary lymphoid organs. *EMBO J.* 19:4676-87
30. Boyes J, Byfield P, Nakatani Y, Ogryzko V. 1998. Regulation of activity of the transcription factor GATA-1 by acetylation. *Nature* 396:594-98
  31. Herrera JE, Sakaguchi K, Bergel M, Trischmann L, Nakatani Y, Bustin M. 1999. Specific acetylation of chromosomal protein HMG-17 by PCAF alters its interaction with nucleosomes. *Mol. Cell Biol.* 19:3466-73
  32. Imai S, Armstrong CM, Kaeberlein M, Guarente L. 2000. Transcriptional silencing and longevity protein Sir2 is an NAD-dependent histone deacetylase. *Nature* 403:795-800
  33. Finnin MS, Donigian JR, Pavletich NP. 2001. Structure of the histone deacetylase SIRT2. *Nat. Struct. Biol.* 8:621-25
  34. Kao HY, Verdell A, Tsai CC, Simon C, Juguilon H, Khochbin S. 2001. Mechanism for nucleocytoplasmic shuttling of histone deacetylase 7. *J. Biol. Chem.* 276:47496-507
  35. Wang AH, Yang XJ. 2001. Histone deacetylase 4 possesses intrinsic nuclear import and export signals. *Mol. Cell Biol.* 21:5992-6005
  36. Gray SG, Ekstrom TJ. 2001. The human histone deacetylase family. *Exp. Cell Res.* 262:75-83
  37. Guardiola AR, Yao TP. 2002. Molecular cloning and characterization of a novel histone deacetylase HDAC10. *J. Biol. Chem.* 277:3350-56
  38. Verdell A, Curtet S, Brocard MP, Ronsseaux S, Lemerrier C, et al. 2000. Active maintenance of mHDA2/mHDAC6 histone-deacetylase in the cytoplasm. *Curr. Biol.* 10:747-49
  39. de Ruijter AJ, van Gennip AH, Caron HN, Kemp S, van Kuilenburg AB. 2003. Histone deacetylases (HDACs): characterization of the classical HDAC family. *Biochem. J.* 370:737-49
  40. Grozinger CM, Hassig CA, Schreiber SL. 1999. Three proteins define a class of human histone deacetylases related to yeast Hda1p. *Proc. Natl. Acad. Sci. USA* 96:4868-73
  41. Petrie K, Guidez F, Howell L, Healy L, Waxman S, et al. 2003. The histone deacetylase 9 gene encodes multiple protein isoforms. *J. Biol. Chem.* 278:16059-72
  42. Hu E, Dul E, Sung CM, Chen Z, Kirkpatrick R, et al. 2003. Identification of novel isoform-selective inhibitors within class I histone deacetylases. *J. Pharmacol. Exp. Ther.* 307:720-28
  43. Jung M. 2001. Inhibitors of histone deacetylase as new anticancer agents. *Curr. Med. Chem.* 8:1505-11
  44. Miller TA, Witter DJ, Belvedere S. 2003. Histone deacetylase inhibitors. *J. Med. Chem.* 46:5097-116
  45. Meinke PF, Liberato P. 2001. Histone deacetylase: a target for antiproliferative and antiprotozoal agents. *Curr. Med. Chem.* 8:211-35
  46. Finnin MS, Donigian JR, Cohen A, Richon VM, Rifkind RA, et al. 1999. Structures of a histone deacetylase homologue bound to the TSA and SAHA inhibitors. *Nature* 401:188-93
  47. Breslow R, Belvedere S, Gershell L. 2000. Development of cytodifferentiating agents for cancer chemotherapy. *Helv. Chim. Acta* 83:1685-92
  48. Woo SH, Frechette S, Abou Khalil E, Bouchain G, Vaisburg A, et al. 2002. Structurally simple trichostatin A-like straight chain hydroxamates as potent histone deacetylase inhibitors. *J. Med. Chem.* 45:2877-85
  49. Yoshida M, Horinouchi S, Beppu T. 1995. Trichostatin A and trapoxin: novel chemical probes for the role of histone acetylation in chromatin structure and function. *Bioessays* 17:423-30
  50. Shute RE, Dnnlap B, Rich DH. 1987. Analogues of the cytostatic and antimetogenic agents chlamydocin and HC-toxin: synthesis and biological activity of chloromethyl ketone and diazomethyl

- ketone functionalized cyclic tetrapeptides. *J. Med. Chem.* 30:71–78
51. Gore SD, Carducci MA. 2000. Modifying histones to tame cancer: clinical development of sodium phenylbutyrate and other histone deacetylase inhibitors. *Expert Opin. Invest. Drugs* 9:2923–34
  52. Furumai R, Matsuyama A, Kobashi N, Lee KH, Nishiyama M, et al. 2002. FK228 (depsipeptide) as a natural prodrug that inhibits class I histone deacetylases. *Cancer Res.* 62:4916–21
  53. Komatsu Y, Tomizaki KY, Tsukamoto M, Kato T, Nishino N, et al. 2001. Cyclic hydroxamic-acid-containing peptide 31, a potent synthetic histone deacetylase inhibitor with antitumor activity. *Cancer Res.* 61:4459–66
  54. Furumai R, Komatsu Y, Nishino N, Khochbin S, Yoshida M, Horinouchi S. 2001. Potent histone deacetylase inhibitors built from trichostatin A and cyclic tetrapeptide antibiotics including trapoxin. *Proc. Natl. Acad. Sci. USA* 98: 87–92
  55. el-Beltagi HM, Martens AC, Lelieveld P, Haroun EA, Hagenbeek A. 1993. Acetyldinoline: a new oral cytostatic drug with impressive differential activity against leukemic cells and normal stem cells—preclinical studies in a relevant rat model for human acute myelocytic leukemia. *Cancer Res.* 53:3008–14
  56. Suzuki T, Ando T, Tsuchiya K, Fukazawa N, Saito A, et al. 1999. Synthesis and histone deacetylase inhibitory activity of new benzamide derivatives. *J. Med. Chem.* 42: 3001–3
  57. Mai A, Massa S, Ragno R, Esposito M, Sbardella G, et al. 2002. Binding mode analysis of 3-(4-benzoyl-1-methyl-1H-2-pyrrolyl)-N-hydroxy-2-propenamide: a new synthetic histone deacetylase inhibitor inducing histone hyperacetylation, growth inhibition, and terminal cell differentiation. *J. Med. Chem.* 45:1778–84
  58. Ragno R, Mai A, Massa S, Cerbara I, Valente S, et al. 2004. 3-(4-Aroyl-1-methyl-1H-pyrrol-2-yl)-N-hydroxy-2-propenamides as a new class of synthetic histone deacetylase inhibitors. 3. Discovery of novel lead compounds through structure-based drug design and docking studies. *J. Med. Chem.* 47:1351–59
  59. Pina IC, Gautschi JT, Wang GY, Sanders ML, Schmitz FJ, et al. 2003. Psammoplins from the sponge *Pseudoceratina purpurea*: inhibition of both histone deacetylase and DNA methyltransferase. *J. Org. Chem.* 68:3866–73
  60. Haggarty SJ, Koeller KM, Wong JC, Butcher RA, Schreiber SL. 2003. Multidimensional chemical genetic analysis of diversity-oriented synthesis-derived deacetylase inhibitors using cell-based assays. *Chem. Biol.* 10:383–96
  61. Haggarty SJ, Koeller KM, Wong JC, Grozinger CM, Schreiber SL. 2003. Domain-selective small-molecule inhibitor of histone deacetylase 6 (HDAC6)-mediated tubulin deacetylation. *Proc. Natl. Acad. Sci. USA* 100:4389–94
  62. Pandolfi PP. 2001. Transcription therapy for cancer. *Oncogene* 20:3116–27
  63. Timmermann S, Lehmann H, Polesskaya A, Harel-Bellan A. 2001. Histone acetylation and disease. *Cell Mol. Life Sci.* 58: 728–36
  64. Marks P, Rifkind RA, Richon VM, Breslow R, Miller T, Kelly WK. 2001. Histone deacetylases and cancer: causes and therapies. *Nat. Rev. Cancer* 1:194–202
  65. Rosato RR, Grant S. 2004. Histone deacetylase inhibitors in clinical development. *Expert Opin. Invest. Drugs* 13: 21–38
  66. Richon VM, Sandhoff TW, Rifkind RA, Marks PA. 2000. Histone deacetylase inhibitor selectively induces p21WAF1 expression and gene-associated histone acetylation. *Proc. Natl. Acad. Sci. USA* 97:10014–19
  67. Vigushin DM, Coombes RC. 2002. Histone deacetylase inhibitors in cancer treatment. *Anticancer Drugs* 13:1–13



68. Mitsiades CS, Mitsiades NS, McMullan CJ, Poulaki V, Shringarpure R, et al. 2004. Transcriptional signature of histone deacetylase inhibition in multiple myeloma: biological and clinical implications. *Proc. Natl. Acad. Sci. USA* 101:540–45
69. Petti MC, Fazi F, Gentile M, Diverio D, De Fabritis P, et al. 2002. Complete remission through blast cell differentiation in PLZF/RARalpha-positive acute promyelocytic leukemia: in vitro and in vivo studies. *Blood* 100:1065–67
70. Han JW, Ahn SH, Park SH, Wang SY, Bae GU, et al. 2000. Apicidin, a histone deacetylase inhibitor, inhibits proliferation of tumor cells via induction of p21WAF1/Cip1 and gelsolin. *Cancer Res.* 60:6068–74
71. Saito A, Yamashita T, Mariko Y, Nosaka Y, Tsuchiya K, et al. 1999. A synthetic inhibitor of histone deacetylase, MS-27-275, with marked in vivo antitumor activity against human tumors. *Proc. Natl. Acad. Sci. USA* 96:4592–97
72. Cameron EE, Bachman KE, Myohanen S, Herman JG, Baylin SB. 1999. Synergy of demethylation and histone deacetylase inhibition in the re-expression of genes silenced in cancer. *Nat. Genet.* 21:103–7
73. Primeau M, Gagnon J, Mompalmer RL. 2003. Synergistic antineoplastic action of DNA methylation inhibitor 5-AZA-2'-deoxycytidine and histone deacetylase inhibitor depsipeptide on human breast carcinoma cells. *Int. J. Cancer* 103:177–84
74. Henderson C, Brancolini C. 2003. Apoptotic pathways activated by histone deacetylase inhibitors: implications for the drug-resistant phenotype. *Drug Resist. Update* 6:247–56
75. Johnstone RW, Licht JD. 2003. Histone deacetylase inhibitors in cancer therapy: is transcription the primary target? *Cancer Cell.* 4:13–18
76. Kwon SH, Ahn SH, Kim YK, Bae GU, Yoon JW, et al. 2002. Apicidin, a histone deacetylase inhibitor, induces apoptosis and Fas/Fas ligand expression in human acute promyelocytic leukemia cells. *J. Biol. Chem.* 277:2073–80
77. Cao XX, Mohiuddin I, Ece F, McConkey DJ, Smythe WR. 2001. Histone deacetylase inhibitor downregulation of bcl-xi gene expression leads to apoptotic cell death in mesothelioma. *Am. J. Respir. Cell Mol. Biol.* 25:562–68
78. Sawa H, Murakami H, Ohshima Y, Sugino T, Nakajyo T, et al. 2001. Histone deacetylase inhibitors such as sodium butyrate and trichostatin A induce apoptosis through an increase of the bcl-2-related protein Bad. *Brain Tumor. Pathol.* 18:109–14
79. Slack JL. 1999. The biology and treatment of acute promyelocytic leukemia. *Curr. Opin. Oncol.* 11:9–13
80. Nimmnanapalli R, Fuino L, Bali P, Gasparetto M, Glazak M, et al. 2003. Histone deacetylase inhibitor LAQ824 both lowers expression and promotes proteasomal degradation of Bcr-Abl and induces apoptosis of imatinib mesylate-sensitive or -refractory chronic myelogenous leukemia-blast crisis cells. *Cancer Res.* 63:5126–35
81. Scott GK, Marden C, Xu F, Kirk L, Benz CC. 2002. Transcriptional repression of ErbB2 by histone deacetylase inhibitors detected by a genomically integrated ErbB2 promoter-reporting cell screen. *Mol. Cancer Ther.* 1:385–92
82. Fuino L, Bali P, Wittmann S, Donapaty S, Guo F, et al. 2003. Histone deacetylase inhibitor LAQ824 down-regulates Her-2 and sensitizes human breast cancer cells to trastuzumab, taxotere, gemcitabine, and epothilone B. *Mol. Cancer Ther.* 2:971–84
83. Kim JS, Jennng HK, Cheong JW, Maeng H, Lee ST, et al. 2004. Apicidin potentiates the imatinib-induced apoptosis of Bcr-Abl-positive human leukaemia cells by enhancing the activation of mitochondria-dependent caspase cascades. *Br. J. Haematol.* 124:166–78

84. Yu C, Rahmani M, Conrad D, Subler M, Dent P, Grant S. 2003. The proteasome inhibitor bortezomib interacts synergistically with histone deacetylase inhibitors to induce apoptosis in Bcr/Abl+ cells sensitive and resistant to ST1571. *Blood* 102:3765-74
85. Rahmani M, Yu C, Dai Y, Reese E, Ahmed W, et al. 2003. Coadministration of the heat shock protein 90 antagonist 17-allylamino-17-demethoxygeldanamycin with suberoylanilide hydroxamic acid or sodium butyrate synergistically induces apoptosis in human leukemia cells. *Cancer Res.* 63:8420-27
86. Liu LT, Chang HC, Chiang LC, Hung WC. 2003. Histone deacetylase inhibitor up-regulates RECK to inhibit MMP-2 activation and cancer cell invasion. *Cancer Res.* 63:3069-72
87. Sasakawa Y, Naoe Y, Noto T, Inoue T, Sasakawa T, et al. 2003. Antitumor efficacy of FK228, a novel histone deacetylase inhibitor, depends on the effect on expression of angiogenesis factors. *Biochem. Pharmacol.* 66:897-906
88. Michaelis M, Michaelis UR, Fleming J, Suhan T, Cinatl J, et al. 2004. Valproic acid inhibits angiogenesis in vitro and in vivo. *Mol. Pharmacol.* 65:520-27
89. Ruefli AA, Bernhard D, Tainton KM, Kofler R, Smyth MJ, Johnstone RW. 2002. Suberoylanilide hydroxamic acid (SAHA) overcomes multidrug resistance and induces cell death in P-glycoprotein-expressing cells. *Int. J. Cancer* 99:292-98
90. Tsurutani J, Soda H, Oka M, Suenaga M, Doi S, et al. 2003. Antiproliferative effects of the histone deacetylase inhibitor FR901228 on small-cell lung cancer lines and drug-resistant sublines. *Int. J. Cancer* 104:238-42
91. Jing Y, Xia L, Waxman S. 2002. Targeted removal of PML-RARalpha protein is required prior to inhibition of histone deacetylase for overcoming all-trans retinoic acid differentiation resistance in acute promyelocytic leukemia. *Blood* 100:1008-13
92. Cote S, Zhou D, Bianchini A, Nervi C, Gallagher RE, Miller WH Jr. 2000. Altered ligand binding and transcriptional regulation by mutations in the PML/RARalpha ligand-binding domain arising in retinoic acid-resistant patients with acute promyelocytic leukemia. *Blood* 96:3200-8
93. Castro-Galache MD, Ferragut JA, Barbera VM, Martin-Orozco E, Gonzalez-Ros JM, et al. 2003. Susceptibility of multidrug resistance tumor cells to apoptosis induction by histone deacetylase inhibitors. *Int. J. Cancer* 104:579-86
94. Peart MJ, Tainton KM, Ruefli AA, Dear AE, Sedelies KA, et al. 2003. Novel mechanisms of apoptosis induced by histone deacetylase inhibitors. *Cancer Res.* 63:4460-71
95. Batova A, Shao LE, Diccianni MB, Yu AL, Tanaka T, et al. 2002. The histone deacetylase inhibitor AN-9 has selective toxicity to acute leukemia and drug-resistant primary leukemia and cancer cell lines. *Blood* 100:3319-24
96. Takakura M, Kyo S, Sowa Y, Wang Z, Yatabe N, et al. 2001. Telomerase activation by histone deacetylase inhibitor in normal cells. *Nucleic Acids Res.* 29:3006-11
97. Nakamura M, Saito H, Ebimura H, Wakabayashi K, Saito Y, et al. 2001. Reduction of telomerase activity in human liver cancer cells by a histone deacetylase inhibitor. *J. Cell Physiol.* 187:392-401
98. Vigushin DM, Ali S, Pace PE, Mirsaidi N, Ito K, et al. 2001. Trichostatin A is a histone deacetylase inhibitor with potent antitumor activity against breast cancer in vivo. *Clin. Cancer Res.* 7:971-76
99. Svechnikova I, Gray SG, Kundrotiene J, Ponthan F, Kogner P, Ekstrom TJ. 2003.

- Apoptosis and tumor remission in liver tumor xenografts by 4-phenylbutyrate. *Int. J. Oncol.* 22:579-88
100. Sasakawa Y, Naoe Y, Inoue T, Sasakawa T, Matsuo M, et al. 2003. Effects of FK228, a novel histone deacetylase inhibitor, on tumor growth and expression of p21 and c-myc genes in vivo. *Cancer Lett.* 195:161-88
  101. Remiszewski SW, Sambucetti LC, Bair KW, Bontempo J, Cesarz D, et al. 2003. N-hydroxy-3-phenyl-2-propenamides as novel inhibitors of human histone deacetylase with in vivo antitumor activity: discovery of (2E)-N-hydroxy-3-[4-[[[(2-hydroxyethyl)(2-(1H-indol-3-yl)ethyl)amino]methyl]phenyl]-2-propenamide (NVP-LAQ824). *J. Med. Chem.* 46:4609-24
  102. Kuefer R, Hofer MD, Aitug V, Zorn C, Genze F, et al. 2004. Sodium butyrate and tributyrin induce in vivo growth inhibition and apoptosis in human prostate cancer. *Br. J. Cancer* 90:535-41
  103. Kosugi H, Ito M, Yamamoto Y, Towatari M, Ueda R, et al. 2001. In vivo effects of a histone deacetylase inhibitor, FK228, on human acute promyelocytic leukemia in NOD/Shi-seid/seid mice. *Jpn. J. Cancer Res.* 92:529-36
  104. Butler LM, Webb Y, Agus DB, Higgins B, Tolentino TR, et al. 2001. Inhibition of transformed cell growth and induction of cellular differentiation by pyroxamide, an inhibitor of histone deacetylase. *Clin. Cancer Res.* 7:962-70
  105. Butler LM, Agus DB, Scher HI, Higgins B, Rose A, et al. 2000. Suberoylanilide hydroxamic acid, an inhibitor of histone deacetylase, suppresses the growth of prostate cancer cells in vitro and in vivo. *Cancer Res.* 60:5165-70
  106. Arts J, Van Emelen K, Angibaud P, Van Brandt S, Poncelet V, et al. 2003. *Small molecule inhibitors of histone deacetylases (HDACs): identification of JNJ16241199, a potent oral antitumoral agent.* Presented at AACR-NCI-EORTC Int. Conf. Mol. Targets Cancer Ther., Boston
  107. Piekarczyk RL, Robey R, Sandor V, Bakke S, Wilson WH, et al. 2001. Inhibitor of histone deacetylation, depsipeptide (FR901228), in the treatment of peripheral and cutaneous T-cell lymphoma: a case report. *Blood* 98:2865-68
  108. Siu LL, Von Hoff DD, Rephaeli A, Izbicka E, Cerna C, et al. 1998. Activity of pivaloyloxymethyl butyrate, a novel anticancer agent, on primary human tumor colony-forming units. *Invest. New Drugs* 16:113-19
  109. Patnaik A, Rowinsky EK, Villalona MA, Hammond LA, Britten CD, et al. 2002. A phase I study of pivaloyloxymethyl butyrate, a prodrug of the differentiating agent butyric acid, in patients with advanced solid malignancies. *Clin. Cancer Res.* 8:2142-48
  110. Jaboin J, Wild J, Hamidi H, Khanna C, Kim CJ, et al. 2002. MS-27-275, an inhibitor of histone deacetylase, has marked in vitro and in vivo antitumor activity against pediatric solid tumors. *Cancer Res.* 62:6108-15
  111. Fournel M, Trachy-Bourget MC, Yan PT, Kalita A, Bonfils C, et al. 2002. Sulfonamide anilides, a novel class of histone deacetylase inhibitors, are antiproliferative against human tumors. *Cancer Res.* 62:4325-30
  112. Volpe DA, LoRusso PM, Foster BJ, Parchment RE. 2004. In vitro and in vivo effects of acetylindoline on murine megakaryocytopoiesis. *Cancer Chemother. Pharmacol.* 54(1):89-94
  113. Sandor V, Bakke S, Robey RW, Kang MH, Blagosklonny MV, et al. 2002. Phase I trial of the histone deacetylase inhibitor, depsipeptide (FR901228, NSC 630176), in patients with refractory neoplasms. *Clin. Cancer Res.* 8:718-28
  114. Prakash S, Foster BJ, Meyer M, Wozniak A, Heilbrun LK, et al. 2001. Chronic oral administration of CI-994: a phase I study. *Invest. New Drugs* 19:1-11

115. Kelly WK, Richon VM, O'Connor O, Curley T, MacGregor-Curtelli B, et al. 2003. Phase I clinical trial of histone deacetylase inhibitor: suberoylanilide hydroxamic acid administered intravenously. *Clin. Cancer Res.* 9:3578-88
116. Piekartz RL, Robey R, Sandor V, Bakke S, Wilson WH, et al. 2001. Inhibitor of histone deacetylation, depsipeptide (FR901228), in the treatment of peripheral and cutaneous T-cell lymphoma: a case report. *Blood* 98:2865-68
117. Atadja P, Gao L, Kwon P, Troiani N, Walker H, et al. 2004. Selective growth inhibition of tumor cells by a novel histone deacetylase inhibitor, NVP-LAQ824. *Cancer Res.* 64:689-95
118. Drummond DC, Meyer OM, Hong E, Kirpotin DB, Papahadjopoulos D. 1999. Optimizing liposomes for delivery of chemotherapeutic agents to solid tumors. *Pharmacol. Rev.* 51:691-743
119. Benz C, Scott G, Berger C, Amend C, Guo Z, et al. 2003. Liposome encapsulation of histone deacetylase inhibitor enhances in vivo activity against ErbB2-positive breast cancers. *Clin. Cancer Res.* 9:6259s
120. Kim MS, Blake M, Baek JH, Kohlhagen G, Pommier Y, Carrier F. 2003. Inhibition of histone deacetylase increases cytotoxicity to anticancer drugs targeting DNA. *Cancer Res.* 63:7291-300
121. Witzig TE, Tirum M, Stenson M, Svingen PA, Kaufmann SH. 2000. Induction of apoptosis in malignant B cells by phenylbutyrate or phenylacetate in combination with chemotherapeutic agents. *Clin. Cancer Res.* 6:681-92
122. Zhu WG, Lakshmanan RR, Beal MD, Otterson GA. 2001. DNA methyltransferase inhibition enhances apoptosis induced by histone deacetylase inhibitors. *Cancer Res.* 61:1327-33
123. Rashid SF, Moore JS, Walker E, Driver PM, Engel J, et al. 2001. Synergistic growth inhibition of prostate cancer cells by 1 alpha,25 dihydroxyvitamin D(3) and its 19-nor-hexafluoride analogs in combination with either sodium butyrate or trichostatin A. *Oncogene* 20:1860-72
124. Rahmani M, Yu C, Reese E, Ahmed W, Hirsch K, et al. 2003. Inhibition of PI-3 kinase sensitizes human leukemic cells to histone deacetylase inhibitor-mediated apoptosis through p44/42 MAP kinase inactivation and abrogation of p21(CIP1/WAF1) induction rather than AKT inhibition. *Oncogene* 22:6231-42
125. Almenara J, Rosato R, Grant S. 2002. Synergistic induction of mitochondrial damage and apoptosis in human leukemia cells by flavopiridol and the histone deacetylase inhibitor suberoylanilide hydroxamic acid (SAHA). *Leukemia* 16:1331-43
126. Keen JC, Yan L, Mack KM, Pettit C, Smith D, et al. 2003. A novel histone deacetylase inhibitor, scriptaid, enhances expression of functional estrogen receptor alpha (ER) in ER negative human breast cancer cells in combination with 5-aza 2'-deoxycytidine. *Breast Cancer Res. Treat.* 81:177-86
127. Coffey DC, Kutko MC, Glick RD, Butler LM, Heller G, et al. 2001. The histone deacetylase inhibitor, CBHA, inhibits growth of human neuroblastoma xenografts in vivo, alone and synergistically with all-trans retinoic acid. *Cancer Res.* 61:3591-94
128. Belinsky SA, Klinge DM, Stidley CA, Issa JP, Herman JG, et al. 2003. Inhibition of DNA methylation and histone deacetylation prevents murine lung cancer. *Cancer Res.* 63:7089-93
129. Kosugi H, Towatari M, Hatano S, Kitamura K, Kiyoi H, et al. 1999. Histone deacetylase inhibitors are the potent inducer/enhancer of differentiation in acute myeloid leukemia: a new approach to anti-leukemia therapy. *Leukemia* 13:1316-24
130. Zhou DC, Kim SH, Ding W, Schultz C, Warrell RP Jr, Gallagher RE. 2002. Frequent mutations in the ligand-binding domain of PML-RARalpha after multiple relapses of acute promyelocytic leukemia:

- analysis for functional relationship to response to all-trans retinoic acid and histone deacetylase inhibitors in vitro and in vivo. *Blood* 99:1356-63
131. Giuliano M, Lauricella M, Calvaruso G, Carabillo M, Emanuele S, et al. 1999. The apoptotic effects and synergistic interaction of sodium butyrate and MG132 in human retinoblastoma Y79 cells. *Cancer Res.* 59:5586-95
  132. Yu C, Rahman M, Almenara J, Subler M, Krystal G, et al. 2003. Histone deacetylase inhibitors promote STI571-mediated apoptosis in STI571-sensitive and -resistant Bcr/Abl+ human myeloid leukemia cells. *Cancer Res.* 63:2118-26
  133. Nirmanapalli R, Fuino L, Stobaugh C, Richon V, Bhalla K. 2003. Cotreatment with the histone deacetylase inhibitor suberoylanilide hydroxamic acid (SAHA) enhances imatinib-induced apoptosis of Bcr-Abl-positive human acute leukemia cells. *Blood* 101:3236-39
  134. Rosato RR, Almenara JA, Yu C, Grant S. 2004. Evidence of a functional role for p21WAF1/CIP1 down-regulation in synergistic antileukemic interactions between the histone deacetylase inhibitor sodium butyrate and flavopiridol. *Mol. Pharmacol.* 65:571-81
  135. Rosato RR, Almenara JA, Cartee L, Betts V, Chellappan SP, Grant S. 2002. The cyclin-dependent kinase inhibitor flavopiridol disrupts sodium butyrate-induced p21WAF1/CIP1 expression and maturation while reciprocally potentiating apoptosis in human leukemia cells. *Mol. Cancer Ther.* 1:253-66
  136. Nguyen DM, Schrupp WD, Tsai WS, Chen A, Stewart JH, et al. 2003. Enhancement of depsipeptide-mediated apoptosis of lung or esophageal cancer cells by flavopiridol: activation of the mitochondria-dependent death-signaling pathway. *J. Thorac. Cardiovasc. Surg.* 125:1132-42
  137. Fujii S, Luo RZ, Yuan J, Kadota M, Oshimura M, et al. 2003. Reactivation of the silenced and imprinted alleles of ARHI is associated with increased histone H3 acetylation and decreased histone H3 lysine 9 methylation. *Hum. Mol. Genet.* 12:1791-800
  138. Pili R, Krszewski MP, Hager BW, Lantz J, Carducci MA. 2001. Combination of phenylbutyrate and 13-cis retinoic acid inhibits prostate tumor growth and angiogenesis. *Cancer Res.* 61:1477-85
  139. Rosato RR, Wang Z, Gopalkrishnan RV, Fisher PB, Grant S. 2001. Evidence of a functional role for the cyclin-dependent kinase-inhibitor p21WAF1/CIP1/MDA6 in promoting differentiation and preventing mitochondrial dysfunction and apoptosis induced by sodium butyrate in human myelomonocytic leukemia cells (U937). *Int. J. Oncol.* 19:181-91
  140. Nguyen DM, Schrupp WD, Chen GA, Tsai W, Nguyen P, et al. 2004. Abrogation of p21 expression by flavopiridol enhances depsipeptide-mediated apoptosis in malignant pleural mesothelioma cells. *Clin. Cancer Res.* 10:1813-25
  141. Denlinger CE, Keller MD, Mayo MW, Broad RM, Jones DR. 2004. Combined proteasome and histone deacetylase inhibition in non-small cell lung cancer. *J. Thorac. Cardiovasc. Surg.* 127:1078-86
  142. Zhang Y, Adachi M, Zhao X, Kawamura R, Imai K. 2004. Histone deacetylase inhibitors FK228, N-(2-aminophenyl)-4-[N-(pyridin-3-yl-methoxycarbonyl)amino-methyl]benzamide and m-carboxycinnamic acid bis-hydroxamide augment radiation-induced cell death in gastrointestinal adenocarcinoma cells. *Int. J. Cancer* 110:301-8
  143. Chung YL, Wang AJ, Yao LF. 2004. Anti-tumor histone deacetylase inhibitors suppress cutaneous radiation syndrome: implications for increasing therapeutic gain in cancer radiotherapy. *Mol. Cancer Ther.* 3:317-25
  144. Spotswood HT, Turner BM. 2002. An increasingly complex code. *J. Clin. Invest.* 110:577-82

145. Gu W, Roeder RG. 1997. Activation of p53 sequence-specific DNA binding by acetylation of the p53 C-terminal domain. *Cell* 90:595-606
146. Sakaguchi K, Herrera JE, Saito S, Miki T, Bustin M, et al. 1998. DNA damage activates p53 through a phosphorylation-acetylation cascade. *Genes Dev* 12:2831-41
147. Tomita A, Towatari M, Tsuzuki S, Hayakawa F, Kosugi H, et al. 2000. c-Myb acetylation at the carboxyl-terminal conserved domain by transcriptional co-activator p300. *Oncogene* 19:444-51
148. Hubbert C, Guardiola A, Shao R, Kawaguchi Y, Ito A, et al. 2002. HDAC6 is a microtubule-associated deacetylase. *Nature* 417:455-58
149. Munshi N, Merika M, Yie J, Seuger K, Chen G, Thanos D. 1998. Acetylation of HMG I(Y) by CBP turns off IFN beta expression by disrupting the enhanceosome. *Mol. Cell* 2:457-67
150. Waltzer L, Bienz M. 1998. Drosophila CBP represses the transcription factor TCF to antagonize Wingless signalling. *Nature* 395:521-25
151. Naryzhny SN, Lee H. 2004. The post-translational modifications of proliferating cell nuclear antigen (PCNA): acetylation, not phosphorylation, plays an important role in the regulation of its function. *J. Biol. Chem.* 279:20194-99
152. Zhang W, Bieker JJ. 1998. Acetylation and modulation of erythroid Kruppel-like factor (EKLF) activity by interaction with histone acetyltransferases. *Proc. Natl. Acad. Sci. USA* 95:9855-60
153. Chen H, Lin RJ, Xie W, Wilpitz D, Evans RM. 1999. Regulation of hormone-induced histone hyperacetylation and gene activation via acetylation of an acetylase. *Cell* 98:675-86
154. Soutoglou E, Ktrakili N, Talianidis I. 2000. Acetylation regulates transcription factor activity at multiple levels. *Mol. Cell* 5:745-51
155. Bannister AJ, Miska EA, Gorlich D, Kouzarides T. 2000. Acetylation of importin-alpha nuclear import factors by CBP/p300. *Curr. Biol.* 10:467-70
156. Chen LF, Greene WC. 2003. Regulation of distinct biological activities of the NF-kappaB transcription factor complex by acetylation. *J. Mol. Med.* 81:549-57
157. Goel A, Janknecht R. 2003. Acetylation-mediated transcriptional activation of the ETS protein ER81 by p300, P/CAF, and HER2/Neu. *Mol. Cell Biol.* 23:6243-54
158. Jacob AL, Lund J, Martinez P, Hedin L. 2001. Acetylation of steroidogenic factor 1 protein regulates its transcriptional activity and recruits the coactivator GCN5. *J. Biol. Chem.* 276:37659-64
159. Cohen HY, Lavu S, Bitterman KJ, Hekking B, Imahiyerobo TA, et al. 2004. Acetylation of the C terminus of Ku70 by CBP and PCAF controls Bax-mediated apoptosis. *Mol. Cell* 13:627-38
160. Pelletier G, Stefanovsky VY, Faubladier M, Hirschler-Laszkiewicz I, Savard J, et al. 2000. Competitive recruitment of CBP and Rb-HDAC regulates UBF acetylation and ribosomal transcription. *Mol. Cell* 6:1059-66
161. Ammanamanchi S, Freeman JW, Brattain MG. 2003. Acetylated sp3 is a transcriptional activator. *J. Biol. Chem.* 278:35775-80
162. Huang S, Qiu Y, Shi Y, Xu Z, Brandt SJ. 2000. P/CAF-mediated acetylation regulates the function of the basic helix-loop-helix transcription factor TAL1/SCL. *EMBO J.* 19:6792-803
163. Yao YL, Yang WM, Seto E. 2001. Regulation of transcription factor YY1 by acetylation and deacetylation. *Mol. Cell Biol.* 21:5979-91
164. Martinez-Balbas MA, Bauer UM, Nielsen SJ, Brehm A, Kouzarides T. 2000. Regulation of E2F1 activity by acetylation. *EMBO J.* 19:662-71
165. Sartorelli V, Puri PL, Hamanori Y, Ogrzyzko V, Chung G, et al. 1999.

- Acetylation of MyoD directed by PCAF is necessary for the execution of the muscle program. *Mol. Cell.* 4:725-34
166. Park SH, Lee SR, Kim BC, Cho EA, Patel SP, et al. 2002. Transcriptional regulation of the transforming growth factor beta type II receptor gene by histone acetyltransferase and deacetylase is mediated by NF-Y in human breast cancer cells. *J. Biol. Chem.* 277:5168-74
167. Lee BI, Park SH, Kim JW, Sansville EA, Kim HT, et al. 2001. MS-275, a histone deacetylase inhibitor, selectively induces transforming growth factor beta type II receptor expression in human breast cancer cells. *Cancer Res.* 61:931-34
168. Butler LM, Zhou X, Xu WS, Scher HI, Rifkind RA, et al. 2002. The histone deacetylase inhibitor SAHA arrests cancer cell growth, up-regulates thioredoxin-binding protein-2, and down-regulates thioredoxin. *Proc. Natl. Acad. Sci. USA* 99:11700-5
169. Kim MS, Kwon HI, Lee YM, Baek JH, Jang JE, et al. 2001. Histone deacetylases induce angiogenesis by negative regulation of tumor suppressor genes. *Nat. Med.* 7:437-43
170. Andoh A, Shimada M, Araki Y, Fujiyama Y, Bamba T. 2002. Sodium butyrate enhances complement-mediated cell injury via down-regulation of decay-accelerating factor expression in colonic cancer cells. *Cancer Immunol. Immunother.* 50:663-72
171. Zhang XD, Gillespie SK, Borrow JM, Hersey P. 2004. The histone deacetylase inhibitor suberic bishydroxamate regulates the expression of multiple apoptotic mediators and induces mitochondria-dependent apoptosis of melanoma cells. *Mol. Cancer Ther.* 3:425-35
172. Bernhard D, Skvortsov S, Tinhofer I, Hubl H, Greil R, et al. 2001. Inhibition of histone deacetylase activity enhances Fas receptor-mediated apoptosis in leukemic lymphoblasts. *Cell Death Differ.* 8:1014-21
173. Huang H, Reed CP, Zhang JS, Shridhar V, Wang L, Smith DL. 1999. Carboxypeptidase A3 (CPA3): a novel gene highly induced by histone deacetylase inhibitors during differentiation of prostate epithelial cancer cells. *Cancer Res.* 59:2981-88
174. Yang X, Ferguson AT, Nass SJ, Phillips DL, Butash KA, et al. 2000. Transcriptional activation of estrogen receptor alpha in human breast cancer cells by histone deacetylase inhibition. *Cancer Res.* 60:6890-94
175. Walker GE, Wilson EM, Powell D, Oh Y. 2001. Butyrate, a histone deacetylase inhibitor, activates the human IGF binding protein-3 promoter in breast cancer cells: molecular mechanism involves an Sp1/Sp3 multiprotein complex. *Endocrinology* 142:3317-27
176. Pawel JV, Shepherd F, Gatzmeier U, Natale RB, O'Brien ME, et al. 2002. Randomized phase 2 study of the oral histone deacetylase inhibitor CI-994 plus gemcitabine (Gem) vs placebo (PBO) plus GEM in second-line nonsmall cell lung cancer (NSCLC). *Am. Soc. Clin. Oncol. Annu. Meet.* A1239, Orlando, Florida
177. Johnson CA, Padget K, Austin CA, Turner BM. 2001. Deacetylase activity associates with topoisomerase II and is necessary for etoposide-induced apoptosis. *J. Biol. Chem.* 276:4539-42
178. Maggio SC, Rosato RR, Kramer LB, Dai Y, Rahmani M, et al. 2004. The histone deacetylase inhibitor MS-275 interacts synergistically with fludarabine to induce apoptosis in human leukemia cells. *Cancer Res.* 64:2590-600
179. Lemaire M, Momparler LF, Farinha NJ, Bernstein M, Momparler RL. 2004. Enhancement of antineoplastic action of 5-aza-2'-deoxycytidine by phenylbutyrate on L1210 leukemic cells. *Leuk. Lymphoma* 45:147-54
180. Hernandez A, Thomas R, Smith F, Sandberg J, Kim S, et al. 2001. Butyrate sensitizes human colon cancer cells to TRAIL-mediated apoptosis. *Surgery* 130:265-72

181. Rosato RR, Almenara JA, Dai Y, Grant S. 2003. Simultaneous activation of the intrinsic and extrinsic pathways by histone deacetylase (HDAC) inhibitors and tumor necrosis factor-related apoptosis-inducing ligand (TRAIL) synergistically induces mitochondrial damage and apoptosis in human leukemia cells. *Mol. Cancer Ther.* 2:1273-84
182. Guo F, Sigua C, Tao J, Bali P, George P, et al. 2004. Cotreatment with histone deacetylase inhibitor LAQ824 enhances Apo-2L/tumor necrosis factor-related apoptosis inducing ligand-induced death inducing signaling complex activity and apoptosis of human acute leukemia cells. *Cancer Res.* 64:2580-89



Ann. Rev. Pharmacol. Toxicol. 2005.45:495-528. Downloaded from www.annualreviews.org. Access provided by Reprints Desk, Inc. on 09/20/17. For personal use only.

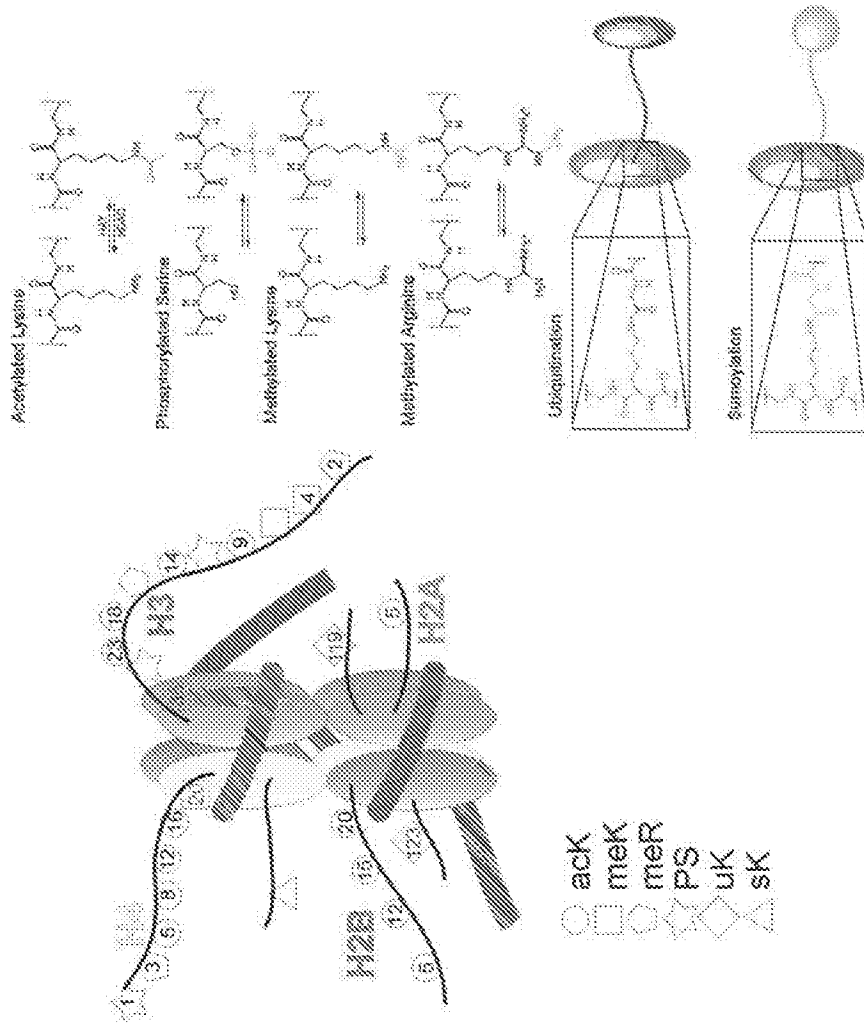


Figure 1 See legend on next page

**Figure 1** Histones can be modified in a variety of ways, primarily in the tails of core histones in a process that is referred to as the histone code. Acetylated lysine residues, methylated arginines, methylated lysines, phosphorylated serines, sumoylated lysines, and ubiquitinated lysine residues all contribute to the histone code. The relative positions for each modification on the various histone tails are depicted by symbols that are defined in the key. The actual chemical modification of the various amino acids in the histone tails is shown with the colored bonds indicating the modification and the amino acid residue shown in black. This figure was adapted from Turner (4) and Spotswood & Turner (144) with permission.

## CONTENTS

---

FRONTISPIECE— <i>Minor J. Coon</i>	xii
CYTOCHROME P450: NATURE'S MOST VERSATILE BIOLOGICAL CATALYST, <i>Minor J. Coon</i>	1
CYTOCHROME P450 ACTIVATION OF ARYLAMINES AND HETEROCYCLIC AMINES, <i>Donghak Kim and P. Peter Guengerich</i>	27
GLUTATHIONE TRANSFERASES, <i>John D. Hayes, Jack U. Flanagan, and Ian R. Jowsey</i>	51
PLEIOTROPIC EFFECTS OF STATINS, <i>James K. Liao and Ulrich Laufs</i>	89
FAT CELLS: AFFERENT AND EFFERENT MESSAGES DEFINE NEW APPROACHES TO TREAT OBESITY, <i>Max Lafontan</i>	119
FORMATION AND TOXICITY OF ANESTHETIC DEGRADATION PRODUCTS, <i>M.W. Anders</i>	147
THE ROLE OF METABOLIC ACTIVATION IN DRUG-INDUCED HEPATOTOXICITY, <i>B. Kevin Park, Neil R. Kitteringham, James L. Maggs, Munir Pirmohamed, and Dominic P. Williams</i>	177
NATURAL HEALTH PRODUCTS AND DRUG DISPOSITION, <i>Brian C. Foster, J. Thor Arnason, and Colin J. Briggs</i>	203
BIOMARKERS IN PSYCHOTROPIC DRUG DEVELOPMENT: INTEGRATION OF DATA ACROSS MULTIPLE DOMAINS, <i>Peter R. Bleck and William Z. Potter</i>	227
NEONICOTINOID INSECTICIDE TOXICOLOGY: MECHANISMS OF SELECTIVE ACTION, <i>Motohiro Tomizawa and John E. Casida</i>	247
GLYCERALDEHYDE-3-PHOSPHATE DEHYDROGENASE, APOPTOSIS, AND NEURODEGENERATIVE DISEASES, <i>De-Maw Chuang, Christopher Hough, and Vladimir V. Senatorov</i>	269
NON-MICHAELIS-MENTEN KINETICS IN CYTOCHROME P450-CATALYZED REACTIONS, <i>William M. Atkins</i>	291
EPOXIDE HYDROLASES: MECHANISMS, INHIBITOR DESIGNS, AND BIOLOGICAL ROLES, <i>Christophe Morisseau and Bruce D. Hammock</i>	311

NITROXYL (HNO): CHEMISTRY, BIOCHEMISTRY, AND PHARMACOLOGY, <i>Jon M. Fukuto, Christopher H. Switzer, Katrina M. Miranda, and David A. Wink</i>	335
TYROSINE KINASE INHIBITORS AND THE DAWN OF MOLECULAR CANCER THERAPEUTICS, <i>Raoul Tibes, Jonathan Trent, and Razelle Kurzrock</i>	357
ACTIONS OF ADENOSINE AT ITS RECEPTORS IN THE CNS: INSIGHTS FROM KNOCKOUTS AND DRUGS, <i>Bertil B. Fredholm, Jiang-Fan Chen, Susan A. Masino, and Jean-Marie Vaugeois</i>	385
REGULATION AND INHIBITION OF ARACHIDONIC ACID (OMEGA)-HYDROXYLASES AND 20-HETE FORMATION, <i>Deanna L. Kroetz and Fengyun Xu</i>	413
CYTOCHROME P450 UBIQUITINATION: BRANDING FOR THE PROTEOLYTIC SLAUGHTER? <i>Maria Almira Correia, Sheila Sadeghi, and Eduardo Mundo-Paredes</i>	439
PROTEASOME INHIBITION IN MULTIPLE MYELOMA: THERAPEUTIC IMPLICATION, <i>Dharminder Chauhan, Teru Hideshima, and Kenneth C. Anderson</i>	465
CLINICAL AND TOXICOLOGICAL RELEVANCE OF CYP2C9: DRUG-DRUG INTERACTIONS AND PHARMACOGENETICS, <i>Allan E. Rettie and Jeffrey P. Jones</i>	477
CLINICAL DEVELOPMENT OF HISTONE DEACETYLASE INHIBITORS, <i>Daryl C. Drummond, Charles O. Noble, Dmitri B. Kirpotin, Zexiong Guo, Gary K. Scott, and Christopher C. Benz</i>	495
THE MAGIC BULLETS AND TUBERCULOSIS DRUG TARGETS, <i>Ying Zhang</i>	529
MOLECULAR MECHANISMS OF RESISTANCE IN ANTIMALARIAL CHEMOTHERAPY: THE UNMET CHALLENGE, <i>Ravit Arav-Boger and Theresa A. Shapiro</i>	565
SIGNALING NETWORKS IN LIVING CELLS, <i>Michael A. White and Richard G.W. Anderson</i>	587
HEPATIC FIBROSIS: MOLECULAR MECHANISMS AND DRUG TARGETS, <i>Sophie Lotersztajn, Boris Julien, Fatima Teixeira-Clerc, Pascale Grenard, and Ariane Mallat</i>	605
ABERRANT DNA METHYLATION AS A CANCER-INDUCING MECHANISM, <i>Manel Esteller</i>	629
THE CARDIAC FIBROBLAST: THERAPEUTIC TARGET IN MYOCARDIAL REMODELING AND FAILURE, <i>R. Dale Brown, S. Kelley Ambler, M. Darren Mitchell, and Carlin S. Long</i>	657

EVALUATION OF DRUG-DRUG INTERACTION IN THE HEPATOBILIARY AND RENAL TRANSPORT OF DRUGS, <i>Yoshihisa Shitara, Hitoshi Sato, and Yuichi Sugiyama</i>	689
DUAL SPECIFICITY PROTEIN PHOSPHATASES: THERAPEUTIC TARGETS FOR CANCER AND ALZHEIMER'S DISEASE, <i>Alexander P. Ducruet, Andreas Vogt, Peter Wipf, and John S. Lazo</i>	725
INDEXES	
Subject Index	751
Cumulative Index of Contributing Authors, Volumes 41–45	773
Cumulative Index of Chapter Titles, Volumes 41–45	776
ERRATA	
An online log of corrections to <i>Annual Review of Pharmacology and Toxicology</i> chapters may be found at <a href="http://pharmtox.annualreviews.org/errata.shtml">http://pharmtox.annualreviews.org/errata.shtml</a>	



## Development of a highly stable and targetable nanoliposomal formulation of topotecan

Daryl C. Drummond<sup>a</sup>, Charles O. Noble<sup>a</sup>, Zexiong Guo<sup>b</sup>, Mark E. Hayes<sup>a</sup>, Ceirin Connolly-Ingram<sup>a</sup>, Bianca S. Gabriel<sup>a</sup>, Byron Hann<sup>c</sup>, Bin Liu<sup>c</sup>, John W. Park<sup>c</sup>, Keelung Hong<sup>a</sup>, Christopher C. Benz<sup>c,d</sup>, James D. Marks<sup>c</sup>, Dmitri B. Kirpotin<sup>a,\*</sup>

<sup>a</sup> Hermes Biosciences, Inc., 61 Airport Boulevard, Suite D, South San Francisco, CA 94080, United States

<sup>b</sup> First Affiliated Hospital of Jinan University, Guangzhou, 510630, PR China

<sup>c</sup> University of California at San Francisco, San Francisco, CA 94143, United States

<sup>d</sup> Buck Institute for Age Research, Novato, CA 94945, United States

### ARTICLE INFO

#### Article history:

Received 9 January 2009

Accepted 7 August 2009

Available online 15 August 2009

#### Keywords:

Liposomes

Topotecan

Erbb2

Antibody targeting

Nanoparticles

### ABSTRACT

Topotecan (TPT), a highly active anticancer camptothecin drug, would benefit from nanocarrier-mediated site-specific and intracellular delivery because of a labile lactone ring whose hydrolysis inactivates the drug, poor cellular uptake resulting from both lactone hydrolysis and a titratable phenol hydroxyl, and the schedule-dependency of its efficacy due to its mechanism of action. We have encapsulated topotecan in liposomes using transmembrane gradients of triethylammonium salts of polyphosphate (Pn) or sucroseoctasulfate (SOS). Circulation lifetimes were prolonged, and the rate of drug release *in vivo* depended on the drug load ( $T_{1/2} = 5.4$  h vs. 11.2 h for 124 and 260  $\mu$ g TPT/mol PL, respectively) and the nature of intraliposomal drug complexing agent used to stabilize the nanoliposome formulation ( $T_{1/2} = 11.2$  h vs. 27.3 h for Pn and SOS, respectively). Anti-EGFR and anti-HER2-immunoliposomal formulations dramatically increased uptake of topotecan compared to nontargeted nanoliposomal topotecan and poorly permeable free topotecan in receptor-overexpressing cancer cell lines, with a corresponding increase in cytotoxicity in multiple breast cancer cell lines and improved antitumor activity against HER2-overexpressing human breast cancer (BT474) xenografts. We conclude that stabilization of topotecan in nanoliposomes significantly improves the targetability and pharmacokinetic profile of topotecan, allowing for highly active formulations against solid tumors and immunotargeting to cancer-overexpressing cell surface receptors.

© 2009 Elsevier B.V. All rights reserved.

### 1. Introduction

Camptothecins are schedule-dependent topoisomerase I inhibitors that stabilize the typically transient Topo I-DNA cleavable complex, resulting in the accumulation of single-stranded breaks in DNA [1]. Liposome-formulations of camptothecins offer a variety of important advantages for improving the therapeutic activity of this important class of anti-cancer drugs. The slow and controlled release of camptothecins from a liposomal carrier provides for a sustained duration of exposure of the target cancer cells to bioavailable drug, thus increasing the probability the cell will be exposed to the therapeutic while in the drug-sensitive S-phase. Camptothecins are also chemically labile, demonstrating a reversible hydrolysis of the lactone ring to an inactive carboxylate at neutral pH [2,3]. Encapsulation in liposomes using electrochemical gradients can be used to stabilize the drug in the acidic interior of the carrier, where the equilibrium favors the active lactone

configuration [4–6]. Site-specific delivery to solid tumors due to the enhanced permeability and retention (EPR) effect can also result in a depot effect whereby drug is released slowly at the site of the tumor [7,8]. For these reasons, camptothecins have been an actively studied class of drugs in liposomal nanocarriers.

Liposomal formulations have been prepared of a wide range of camptothecins, including hydrophobic camptothecins such as the parent camptothecin [9], 9-nitrocamptothecin [10], DB-67 [11], and SN-38 [12], which are typically solubilized and carried in the lipid membrane. However, liposomal formulations of hydrophobic drugs are relatively unstable. Hydrophobic drugs rapidly redistribute out of the carrier upon entering the circulation, resulting in pharmacokinetics that are incrementally improved compared to the corresponding free drugs [13,14]. Highly stable formulations are required to take full advantage of the EPR effect in treating solid tumors, in maximizing the duration of exposure, and for molecular targeting using ligands to direct the liposome-encapsulated drug specifically to target cancer cells where the drug can then be released locally.

\* Corresponding author. Tel.: +1 650 873 2583x106; fax: +1 650 873 2501.

E-mail address: [dtkirpo@hermesbio.com](mailto:dtkirpo@hermesbio.com) (D.B. Kirpotin).

Weakly basic camptothecins such as topotecan [4,6,15], CKD-602 [16], lurtotecan [17], and irinotecan (CPT-11) [5,18] can be loaded into liposomes using gradient based-loading methods. However, simple pH-[17], ammonium sulfate [19], or divalent cation [6,18,20] gradients have not been as successful in stabilizing these camptothecin analogs as compared to liposome formulations of some anthracyclines [7,13,21], including doxorubicin and mitoxantrone. We have previously stabilized weakly basic drugs intraliposomally using the highly charged, non-

polymeric anionic polyol derivative, sucroseoctasulfate, in formulations referred to as nanoliposomes due to the nanosized drug complexes formed inside the liposomes [5,22]. These stable complexes reduce the pool of soluble drug available for diffusion from the nanocarrier *in vivo*. The result is considerable improvements in circulation lifetimes and *in vivo* drug retention [5,22–24], giving rise to highly active formulations of both ligand-targeted and nontargeted liposomal anti-cancer drugs [5,22–26].

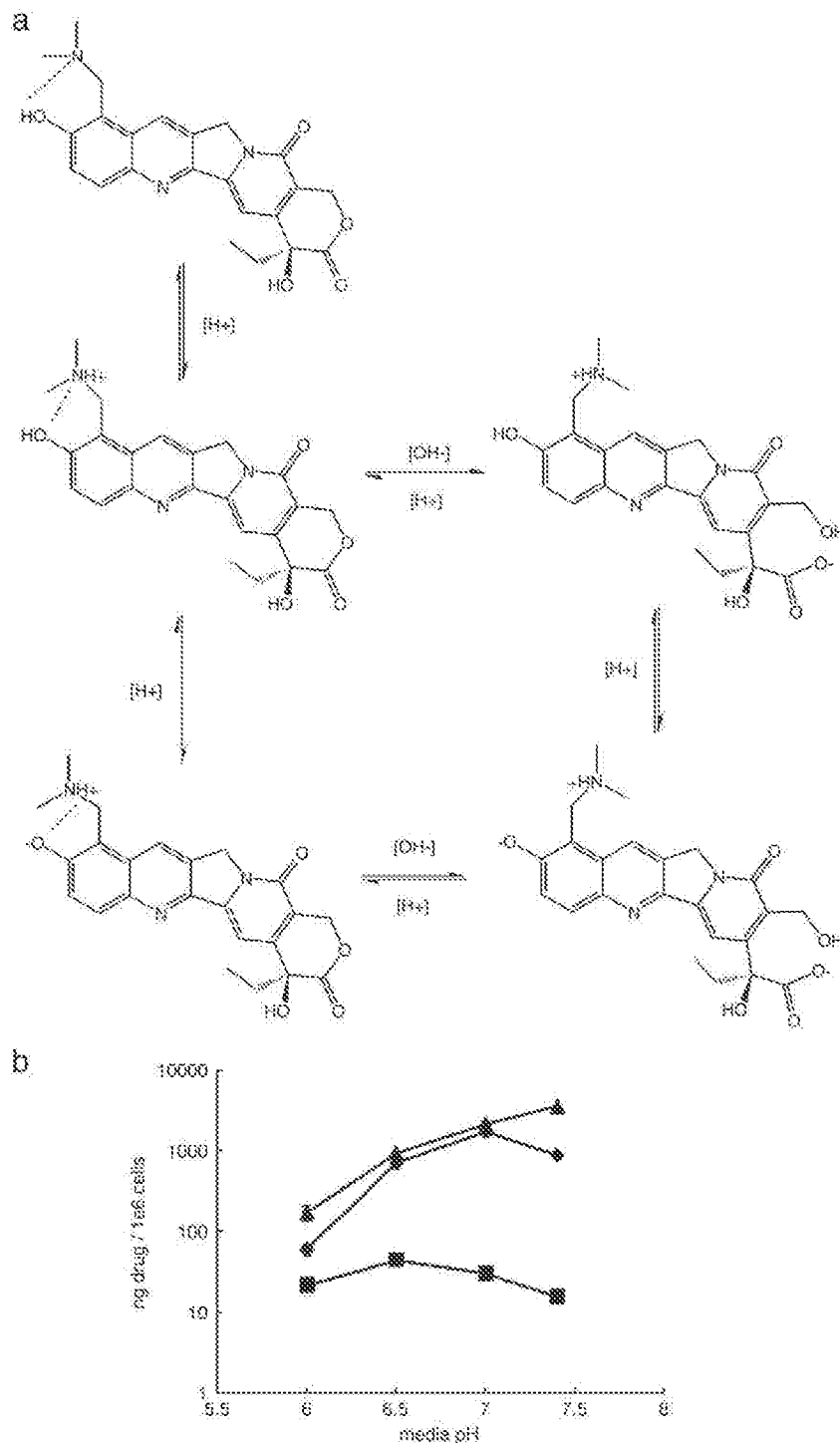


**Fig. 1.** (a) Ionization chemistry of topotecan in solution. Topotecan has three titratable functional groups in a physiologically relevant pH range. A basic dimethylaminomethyl group in the A-ring has a pKa of approximately 10.5. The phenolic hydroxyl group has a pKa between 6.5 and 7.0, considerably reduced compared to phenol due to stabilization through hydrogen bonding with the neighboring dimethylaminomethyl group. Additionally, the lactone in the E-ring is readily hydrolyzed at neutral pH to an inactive carboxylate ion. (b) Uptake of free TPT (■), CPT-11 (◆), and DOX (▲) in MDA-MB-231 cells exposed to each drug at a concentration of 10 µg/ml for 4 h at the indicated pH.

Topotecan is used clinically in the treatment of ovarian [27], small cell lung [28], and more recently, cervical cancer [29]. Its complex ionization chemistry [2,30] (Fig. 1A) results in relatively poor cellular uptake of topotecan relative to doxorubicin, or even another weakly basic camptothecin analog, CPT-11 (Fig. 1B). We have previously demonstrated its antitumor activity either as a single agent, or in combination with PEGylated liposomal doxorubicin in the treatment of malignant gliomas in rat xenografts when administered locally using convection-enhanced delivery [26]. Here we describe the formulation of these highly stable nanoliposome constructs of topotecan using polyanion-based intraliposomal capture and stabilization chemistries, and characterize their pharmacokinetics and *in vivo* formulation stability. We also demonstrate highly active antitumor activity in a prostate tumor xenograft model, as well as receptor-dependent activity of an anti-HER2 (F5) immunoliposomal topotecan in HER2-overexpressing breast cancer cells in culture and in a HER2-overexpressing breast tumor xenograft model in mice.

## 2. Materials and methods

### 2.1. Materials

1,2-Distearoyl-*sn*-glycero-3-phosphocholine (DSPC) and 1,2-distearoyl-*sn*-glycero-3-phosphoethanolamine-*N*-[methoxy(polyethylene glycol)-2000] (PEG-DSPE) were purchased from Avanti Polar Lipids (Alabaster, AL). Cholesterol was obtained from Calbiochem (La Jolla, CA). Sarcosine (sodium salt) was purchased from Toronto Research Chemicals, Inc. (North York, ON, Canada). Sodium polyphosphate ( $n = 13$ – $18$ ; "phosphate glass", also sold under the brand name "Calgon"), 1-(4,5-dimethylthiazol-2-yl)-3,5-diphenylformazan (MTT), morpholino-ethanesulfonic acid (MES) and *N*-(2-hydroxyethyl)piperazine-*N'*-(2-ethanesulfonic acid) free acid (HEPES) were purchased from Sigma-Aldrich (St. Louis, MO). Sepharose CL-4B and Sephadex G-75 size exclusion resins, Dowex 50W-8X-200 cation exchange resin, diethylamine and triethylamine were obtained from Sigma-Aldrich (St. Louis, MO). [ $^3$ H]-Cholesteryl hexadecyl ether was purchased from Perkin Elmer (Boston, MA) and topotecan hydrochloride was received as a kind gift of GlaxoSmithKline (King of Prussia, PA) or Taiwan Liposome Company (Taipei, Taiwan). Doxorubicin (Bedford Labs; Bedford, OH), Doxil (Alza Pharmaceuticals; Palo Alto, CA), and C225 (Cenuximab; Bristol-Myers Squibb, Princeton NJ) were obtained from the pharmacy. F5-PEG-DSPE conjugate was prepared from the purified anti-HER2 scFv F5, by conjugation to the maleimide-activated PEG termini of the PEG-DSPE lipid anchor through an engineered c-terminal cysteine as described previously [31].

### 2.2. Methods

#### 2.2.1. Preparation of liposomes

Solutions of diethylammonium and triethylammonium salts of sucrose octasulfate and poly(phosphate) ( $n = 13$ – $18$ ) were prepared by ion exchange chromatography from the corresponding commercially available sodium salts as previously described [5]. TEA<sub>8</sub>SOS and TEA-Pn were prepared and adjusted to a final concentration of 0.65 M SO<sub>4</sub> or 0.55 M PO<sub>4</sub>, respectively. The lipid matrix composition consisted of DSPC, Chol, and PEG-DSPE in a 3:2:0.015 molar ratio. The lipids were vacuum dried overnight, dissolved in absolute ethanol at 60–65 °C, and the ethanolic lipid solution was then dispersed rapidly in nine volumes of the preheated (60 °C) gradient-forming salt (either TEA<sub>8</sub>SOS and TEA-Pn) solution to a final concentration of 40–50 mM phospholipid (PL). The liposomes were formed by passage of the resulting suspension ten times through two stacked polycarbonate membranes with average pore size of either 0.08 or 0.1 μm (Whatman-Nuclepore; Florham Park, NJ), at 60–65 °C using a gas pressured extruder (Northern Lipids, Vancouver, BC). The extruded liposomes were kept at 60–65 °C for about 15 min, and quickly cooled down to 2–4 °C in an ice bath. Liposome size was determined by

photon correlation spectroscopy using a Coulter N4 Plus particle size analyzer (Beckman Coulter; Fullerton, CA) and reported as the volume-weighted average diameter ± standard deviation of the liposome size distribution.

Non-encapsulated triethylammonium salt was removed by size exclusion chromatography on Sepharose CL-4B (Pharmacia) equilibrated with a drug loading buffer consisting of 50 g/L Dextrose, 5 mM HEPES, pH 6.5 in water. The liposomes eluted near the void volume of the column and were assayed for phospholipid concentration using a phosphate assay of Bartlett [32] either directly, or after methanol-chloroform extraction using the Blich-Dyer extraction protocol [33] for samples containing poly(phosphate).

#### 2.2.2. Liposomal loading of topotecan

A stock aqueous solution of topotecan hydrochloride (TPT) at 10 or 20 mg/ml was prepared, and the pH was adjusted to 3.0 with 1 N HCl. The drug solution was filtered through 0.2 μm polyethersulfone (PES) filter using positive pressure, and immediately mixed with the aliquots of the liposome suspension in the loading buffer to achieve the necessary drug/lipid input ratio (100–600 g TPT/mol PL) to determine the effect of drug load on the efficiency of loading, or 350 g TPT/mol PL in other studies, unless specifically stated otherwise. The mixtures in glass containers were incubated at 60–65 °C with slow agitation for 30 min, and then quickly cooled in an ice-water bath (0–2 °C) for 5–15 min. Unencapsulated TPT, if any, was removed using size exclusion chromatography on Sephadex G-75 column (Amersham Pharmacia Biotech) eluted with HEPES buffered saline (pH 6.5). Nanoliposomal TPT (nLs-TPT) eluted from the column in the void volume fraction was assayed for liposome phospholipid and particle size as described above. Topotecan was quantified by HPLC using a Dionex system with a Phenomenex, Synergi Polar-RP column, 250 mm × 4.6 mm i.d., particle size of 4 μm, preceded by a Phenomenex, Synergi Polar-RP column, 4 mm × 3 mm i.d., guard cartridge. Prior to injection, the liposome samples were solubilized in methanol containing 1% acetic acid. A mobile phase consisting of 0.1% trifluoroacetic acid (A) and acetonitrile (B) employed in a linear gradient fashion ranging from 15% B to 48% B over 6 min followed by 7 min equilibration. TPT was detected by fluorescence (excitation 370 nm, emission 535 nm) with a retention time of 8.2 min.

#### 2.2.3. Preparation of anti-HER2 and anti-EGFR immunoliposomal formulations

Immunoliposomal TPT targeted to HER2-overexpressing cancer cells was prepared by co-incubation of nanoliposomal TPT with the highly internalizable anti-HER2 scFv F5 [34] conjugated through the engineered C-terminal cysteine to an amphiphilic anchor maleimido-PEG-DSPE, in a manner similar to described previously [31]. Specifically, F5-PEG-DSPE conjugate in the form of an aqueous micellar solution was added to the topotecan liposomes at a ratio of 15 μg of conjugated protein per μmol of liposomal phospholipid, or approximately 45 copies of F5 scFv per liposome. The mixture was incubated for 30 min at 60 °C, and chilled on ice. The reaction mixture was chromatographed on a Sepharose CL-4B gel filtration column to remove any residual micellar conjugate, unconjugated protein, and any traces of extraliposomal drug that may have been released during the incubation. The liposomes were eluted with HEPES-saline buffer pH 7.4, collected in the void volume of the column, sterile-filtered using 0.2 μm syringe filters, and stored at 4–6 °C. The amount of liposome-incorporated F5 is typically >90% of the added conjugate.

Immunoliposomes targeted to EGFR-expressing cells were prepared by the conjugation of proteolytically generated Fab' fragments of the anti-EGFR IgG C225 via maleimido-PEG-DSPE linker as follows. First, the linker (0.5 mol% of the liposome phospholipid) was added to the topotecan-loaded liposomes in physiological saline at pH 5.5 and incubated at 60 °C for 30 min to achieve the capture of the linker's hydrophobic domain into the liposome membrane. C225 Fab' were conjugated to the so prepared maleimido-PEG-DSPE bearing liposomes



at room temperature for 4 h following pH adjustment to 7.0, and nonreacted protein was removed using a Sepharose 4B size exclusion column equilibrated with HEPES-saline buffer pH 7.4. The subsequent purified fraction containing the immunoliposomal drug particle was analyzed for Fab', drug, and phospholipid content before evaluation in target-specific cellular uptake experiments. The C225-Hs-TPT used here incorporated  $28.7 \pm 1.6$  g Fab'/mol of liposomal phospholipid (46 Fab' per liposome particle). EGFR-targeted immunoliposomal doxorubicin was prepared from commercially available PEGylated liposomal doxorubicin (Doxil, Alza Corp.) in the same way as C225-immunoliposomal topotecan.

#### 2.2.4. Pharmacokinetics of nanoliposomal topotecan in rats and mice

For the blood pharmacokinetics (PK) study in rats, the liposomes (DSPC/cholesterol/PEG-DSPE molar ratio 3:2:0.015) were prepared and loaded with topotecan using TEA-Pn or TEA-sucroseoctasulfate (TEA<sub>8</sub>SOS) methods as described above. For lipid matrix quantification, the lipid matrix contained the nonexchangeable lipid label [<sup>3</sup>H]cholesterylhexadecylether ([<sup>3</sup>H]-CHE) at 0.5–1.5 mCi/mmol DSPC. The topotecan liposomes were administered i.v. to 4–6 week old female Sprague Dawley rats (body weight about 200 g) via indwelling central venous catheter at the dose of 5 mg/kg of body weight. Following the drug injection, the catheter was flushed with saline, and at selected times (up to 48 h post injection), used to draw the blood samples (0.2–0.3 ml) into heparinized syringes. The blood samples were transferred into 0.4 ml of cold phosphate buffered saline with 0.04% EDTA, blood cells were separated by centrifugation, and the supernatants (PBS-diluted plasma) were assayed for lipid by [<sup>3</sup>H]-CHE radioactivity counting (quenching corrected), and for topotecan by fluorometry (excitation 385 nm, emission 525 nm). The standard curve was obtained in the range of 10–2500 ng TPT/ml, and fit to second order polynomial (to account for self-quenching at higher drug concentration) after subtracting the plasma autofluorescence background. The assay results were corrected for plasma dilution, calculated from the weight of obtained blood sample and assuming hematocrit of 45%. Total blood dose of the drug and lipid was estimated from the blood volume calculated as 6% of the body weight.

#### 2.2.5. Cell uptake of immunoliposomal topotecan

HER2 positive (SKBR3, MDA-MB453, Calu-3, and HCC1569), EGFR positive (MDA-MB231, MDA-MB468), and control (MCF-7) cancer cell lines were obtained from ATTC (Manassas, VA) and grown in the supplier recommended complete growth media supplemented with 10% fetal calf serum, 50 µg/ml streptomycin sulfate and 50 U/ml penicillin G. Cells were incubated at 37 °C in a humidified incubator with 5% CO<sub>2</sub>, except for MDA-MB231 and MDA-MB468 which were grown in an atmosphere without additional CO<sub>2</sub>. A subline of the HER2 positive BT474 cell line (termed BT474 M2) was established by two rounds of selection for fast-growing subcutaneous tumors *in vivo* [35] and was grown in culture from explanted tumors in RPMI 1640 media supplemented with serum and antibiotic as above. Also used were a variety of the control line MCF-7 that were stably transfected with HER2 cDNA, referred to as MCF-7/HER2 (Clone 18) [36], grown in DMEM media with serum and antibiotics added as described above.

One day prior to the drug uptake studies, the cells were harvested by trypsinization (0.05% trypsin in versene-saline), counted and inoculated into 24-well cell culture plates at a density of 150,000 cells/well in 0.5 ml of the complete growth medium, and allowed to acclimate overnight. The medium was replaced with 1.0 ml of complete growth medium containing the indicated drug formulation at a concentration of 10 µg drug/ml. Triplicate wells were used for each condition. Control wells were incubated in the absence of drug and/or liposomes (to obtain background readings for drug assay). Immunoliposomes incubated with EGFR+ cell lines were C225 Fab'-targeted immunoliposomes and those incubated with HER2+ cell lines were P5 scFv targeted immunoliposomes. Immunoliposomal doxorubicin, nontargeted liposomal doxorubicin,

and free doxorubicin controls were also incubated with MDA-MB468 cells to study the effect of the specific anticancer drug on enhancement of cellular uptake. To measure the effect of pH on cell uptake of free drugs, free topotecan, doxorubicin, or CPT-11 were incubated in cell culture media equilibrated to pHs ranging from 6 to 7.4.

The cells were exposed to drug formulations at 37 °C for 4 h, after which time the cells were rinsed twice with 1 ml portions of PBS containing 1 mM EDTA. After PBS removal, 0.2 ml of 0.05% trypsin was added to the cells to allow them to detach. After detachment, 0.8 ml of PBS was added and the cell suspension transferred into a 1.5 ml centrifuge tube followed by centrifugation at 2000 rpm for 3 min to pellet cells. The supernatant was removed and the drug extracted by addition of 0.5 ml of 1% acetic acid in methanol by vortexing for 10 s. The samples were kept at –70 °C for 1 h followed by centrifugation at 10,000 rpm for 10 min and transfer of the supernatant to an HPLC vial for analysis. Topotecan, CPT-11, and doxorubicin were analyzed using the HPLC system described in "Preparation of anti-HER2 and anti-EGFR immunoliposomal formulations". Doxorubicin was eluted with a mobile phase consisting of 0.1% trifluoroacetic acid (A) and acetonitrile (B) with a gradient of 35% B–44% B over 12 min. Doxorubicin was detected by fluorescence (excitation 485 nm and emission 590 nm) with a retention time of 6.7 min. CPT-11 was eluted with a mobile phase consisting of 0.21 M triethylammonium acetate pH 5.5 (A) and acetonitrile (B) in an isocratic fashion over 12 min. CPT-11 was detected by fluorescence (excitation 370 nm and emission 420 nm) with a retention time of 6.0 min.

#### 2.2.6. Antitumor efficacy of nanoliposomal topotecan in DU145 prostate xenografts

NCR nu/nu athymic female mice (6 weeks old; Taconic Farms, Germantown, NY) were implanted with  $2 \times 10^6$  DU145 human prostate cancer cells subcutaneously in the upper back area as a 0.2-ml suspension in serum free media. Tumor growth was measured by caliper along the largest (length) and smallest (width) axes twice a week. Tumor volumes were calculated using the following formula: tumor volume = [(length) × (width) × 2]/2. At day 6 post tumor implantation (mean tumor volume, 150 mm<sup>3</sup>), animals were randomized into treatment groups of 10 animals per group and treated via i.v. (tail vein) injection as described in the text (5 mg/kg). Animals were dosed six times, on days 7, 12, 15, 20, 24, 27. Animals were weighed twice weekly. The animals whose tumors reached 20% of the body weight, or those with progressive weight loss reaching 20% or more were euthanized.

#### 2.2.7. Antitumor efficacy of liposomal and anti-HER2-immunoliposomal topotecan in BT-474 xenograft model

All animal studies were conducted in accordance with the IACUC approved protocol and NIH OLAW guidelines. HER2-overexpressing BT-474 human breast adenocarcinoma xenograft model was established as described in Park et al., 2002 [35]. The abundant presence of internalizing HER2 receptors on the selected sub-line was confirmed by flow cytometry using anti-HER2 (F5)-immunoliposomes with fluorescent marker. The cells established from explanted tumors were cultivated in RPMI-1640 medium supplemented with 10% fetal calf serum, 0.1 mg/ml streptomycin sulfate, and 100 U/ml Penicillin G in T150 flasks, and split 1:3 every week. At the final passage the cells were grown to confluency, harvested by trypsinization (0.05% trypsin in versene-saline), and resuspended in the growth medium without antibiotic at  $2 \times 10^8$  cells/ml. Six week old NCR nu/nu female mice (Taconic) received subcutaneous implantation of 60-day sustained release 17β-estradiol pellets (Innovative Research of America, Inc.). Two days later, the animals were inoculated subcutaneously in the right flank with 0.1 ml of the BT-474M2 cell suspension ( $2 \times 10^7$  cells). The tumor progression was monitored by palpation and caliper measurements of the tumors along the largest (length) and smallest

(width) axis twice a week. The tumor volume was calculated as (length)  $\times$  (width)<sup>2</sup> / 2.

At day 13 post-injections the animals having tumors in the range of 120–350 mm<sup>3</sup> were selected and randomized into 3 treatment and 1 control group of 12 animals each. The mice were treated with i.v. (tail vein) injections of topotecan formulations at the dose of 5 mg/kg body weight, or with equal volume of physiological saline twice weekly for total of three injections. General health of the animals was monitored daily. Tumor sizes and body weights were monitored twice weekly for up to day 53 post tumor inoculation. The animals whose tumors reached 20% of the body weight, or those with progressive weight loss reaching 20% or more were euthanized.

### 3. Results

#### 3.1. Effect of time, external pH, and drug load on loading efficiency for TPT in nanoliposomes

Two stabilized liposomal formulations of topotecan were prepared using drug loading methods which employ transmembrane gradients of diethyl or triethylammonium salts of the polyanionic polymer, linear polyphosphate ( $n=13-18$ ), or a non-polymeric polysulfated small molecule, sucroseoctasulfate. We chose one of the liposome prototype formulations, namely that made with DEA<sub>8</sub>SOS (0.65 M SO<sub>4</sub>) with an initial drug/lipid input ratio of 350 g/mol and measured the effect of loading time, loading buffer pH and drug-to-lipid ratio on entrapment efficiency (Fig. 2 (a–c) respectively). Loading at pH 6 was rapid, with approximately 85% of the applied topotecan (350 g TPT/mol PL) being loaded in the first 5 min, and quantitative loading observed after 15 min. The drug is stabilized intraliposomally through complexation of its titratable amine group with the highly charged multivalent anion of sucroseoctasulfate within the liposome. Mixing of TEA<sub>8</sub>SOS with topotecan in solution resulted in the formation of a gel, a physical state that likely aids the *in vivo* stability of the corresponding liposomal formulation.

The extraliposomal solution pH of the buffer had a dramatic effect on loading, with 100% efficiency achieved between pH 4.0 and 6.5, while a substantial reduction in drug entrapment efficiency ( $27.2 \pm 1.2\%$ ) was observed as the pH was increased above 6.5 (Fig. 2(b)). This may be as a consequence of the decreased amount of membrane-permeable electroneutral form of TPT present at pH 7 or above. However, loading was quantitative over a broad range of pH values from 4 to 6.5.

The liposomal drug capacity is indicated by the ratio of encapsulated drug to liposomal phospholipid (TPT/PL, g/mol). In order to discern the level of drug loading capacity that the liposomes may have, we performed a test by varying the input drug/lipid ratio and, after loading with subsequent drug purification, measured the output drug/lipid ratio. Efficient drug loading was measured over a wide range of drug-to-phospholipid ratios (100–550 g TPT/mol PL, Fig. 2(c)), demonstrating the technology offers control over producing topotecan liposomes of a desired payload with minimal loss of cytotoxic drug during preparation.

Using the sucroseoctasulfate formulation ( $[SO_4] = 0.65$  M), loading was quantitative up to a maximum of 525–550 g TPT/mol PL. At 550 g TPT/mol PL, this translates to 1.19 mol TPT/mol PL or assuming 80,000 phospholipid molecules/liposome for a 100 nm liposome, 95,460 TPT molecules/liposome. This is 4.5-fold greater than previously reported for doxorubicin [37], and nearly 10–20-fold greater than previously reported for liposomal formulations of other camptothecins; including SN-38 [12], lurtotecan [17], topotecan [6,38], and irinotecan [20]. We have recently completed stability studies with liposomal formulation of topotecan and shown them to be stable with respect to drug retention and particle size for a minimum of 2 years (data not shown). This data will be presented elsewhere.

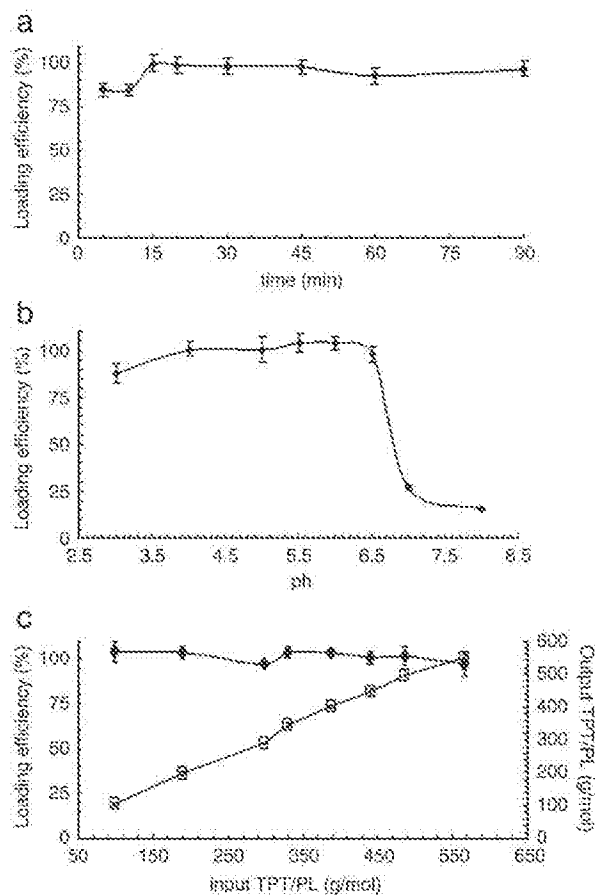


Fig. 2. The drug loading efficiency of DSPC/Chol/PEG-DSPE (3/2/0.15 mol/mol/mol) liposomes as a function of time (a), pH (b), and drug-to-lipid input ratio (c). Liposomal TPT was prepared at 350 g/mol PL with DEA<sub>8</sub>SOS (0.65 M DEA<sub>8</sub>SOS) for panels a and b. Loading was initiated by incubation at 60 °C and at the times indicated (a) or for 30 min (panels b and c). After removal of extraliposomal drug by gel permeation chromatography (PD10 columns) equilibrated with MBS, pH 7.25, the drug and lipid content of pre and post column samples were analyzed and % encapsulation calculated.

#### 3.2. *In vivo* pharmacokinetics and liposomal drug retention

The blood circulation properties of liposomal topotecan using both TEA-Pn and TEA<sub>8</sub>SOS with different drug payloads were studied in rats and are shown in Fig. 3. Despite their 90–100 nm size and very small concentration of PEGylated lipid (0.3 mol%), the liposomes showed good circulation longevity (plasma half-lives of the lipid matrix in the range of 12–20 h). The half life of TPT in the blood varied as a result of the specific formulation. nLS-TPT prepared using TEA-Pn and loaded at 150 g TPT/mol PL were cleared the fastest ( $t_{1/2} = 4.2$  h), while those loaded using TEA-Pn at 450 g TPT/mol PL were cleared at an intermediate rate ( $t_{1/2} = 6.0$  h). A second study in mice showed a similar result (see Supplementary Data). nLS-TPT prepared using TEA<sub>8</sub>SOS were cleared the slowest ( $t_{1/2} = 8.4$  h). The differences in drug clearance rates were primarily a result of the stability of encapsulation. Drug release rates characterized by half-release time ( $T_{1/2}$ ) were calculated using an exponential fit to the plot of drug/phospholipid ratio versus post injection time. The most stable formulation ( $T_{1/2} = 27.3$  h) was determined to be the liposomes loaded using the TEA<sub>8</sub>SOS gradient method, while those loaded using TEA-Pn displayed release rates that were dependent on the amount of topotecan loaded ( $T_{1/2} = 5.4$  h for the 150 g/mol and 11.2 h for the 450 g/mol formulations). Immunoliposomes were also prepared and shown to have nearly identical clearance rates for both the liposomal carrier and encapsulated topotecan, as well as topotecan release rates,

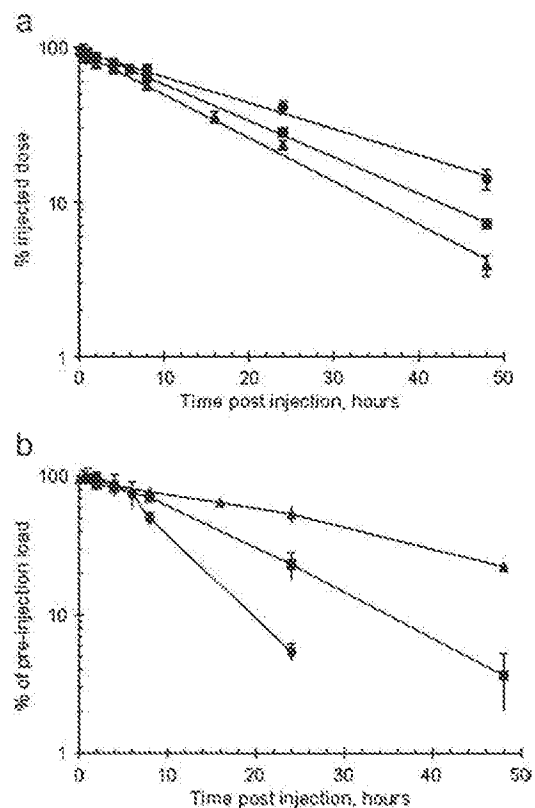


Fig. 3. (a) Blood pharmacokinetics of liposomal and immunoliposomal TPT after iv. administration in rats. The lipid formulation was DSPC/Chol/PEG-DSPE (3/2/0.015 mol/mol). The trapping agents used and the measured drug/lipid ratios were TEA-Pn, 124 mg/mmol ( $\blacklozenge$ ), TEA-Pn, 360 mg/mmol ( $\blacklozenge$ ), and TEA-SOS, 439 mg/mmol ( $\blacktriangle$ ) respectively. The injected dose was 5 mg TPT/kg animal weight (albino female rats, 9 weeks old, 200–220 g). (b) Plot shows the dynamics of the drug to lipid ratio in the blood of the iv. injected liposomes from above.

when compared to the nontargeted liposomal topotecan formulation (see Supplementary Data—Table S2).

### 3.3. In vitro cellular uptake

The ability of F5- or C225-targeted immunoliposomes to deliver topotecan (F5-ILs-TPT and C225-ILs-TPT) specifically into HER2- or EGFR-overexpressing cells, respectively, in cell culture was measured (Table 1). There was substantial cellular uptake of HER2- and EGFR-targeted liposomal topotecan in corresponding receptor-overexpressing cell lines. In the highest HER2-overexpressing breast cancer cell line, SKBR3, the uptake was equivalent to  $8.11 \times 10^9$  and  $7.34 \times 10^9$  TPT molecules/cell, respectively. Generally, the uptake for the immunoliposome formulation was 50–300 times higher than for non-targeted liposomal topotecan in the same line. In the EGFR-overexpressing MDA-MB468 breast cancer line, the uptake of EGFR-targeted nanoliposomal topotecan was  $1.92 \times 10^9$  TPT molecules/cell. Interestingly, uptake of free topotecan was also significantly lower than that of ILs-TPT in receptor-overexpressing cell lines (Table 1; 50–390-fold). This was different from the result seen with doxorubicin, where the uptake of free doxorubicin was actually higher than for EGFR-targeted immunoliposomal doxorubicin (Table 1).

The substantial improvement in cell uptake compared to free topotecan results in part from the exceptionally inefficient cell uptake of free topotecan under physiological conditions (Fig. 1B). At pH 7.4, the uptake of free topotecan was only 15.7 ng TPT/million cells after 4 h. This compared to 3546 ng/million cells for free doxorubicin and 888 ng/million cells for free CPT-11, or a 225- and 56.6-fold reduction in uptake, respectively. A pH-dependent uptake was observed for

Table 1  
Cellular drug uptake of liposomal topotecan at 4 h.

Cell line	Sample	Uptake (ng/1e5 cells)	T/TPT	T/Free
BT474 (HER2+)	Free TPT	25.4 ± 0.4		
	nLs-TPT	82.3 ± 16.1		
	F5-ILs-TPT	6203.4 ± 730.1	75.4 ± 8.95	244.4 ± 26.0
SKBR3 (HER2+)	Free TPT	14.4 ± 1.9		
	nLs-TPT	51.6 ± 4.3		
	F5-ILs-TPT	5020.0 ± 190.8	108.9 ± 9.8	390.3 ± 53.3
MCF-7/clon1E (HER2+)	Free TPT	36.9 ± 6.6		
	nLs-TPT	65.4 ± 5.0		
	F5-ILs-TPT	3952.1 ± 141.2	60.4 ± 5.1	107.1 ± 19.5
MCF-7 (HER2-)	Free TPT	93.7 ± 13.5		
	nLs-TPT	120.9 ± 12.6		
	F5-ILs-TPT	243.1 ± 29.3	2.8 ± 0.4	3.7 ± 0.6
HCC1569 (HER2+)	Free TPT	19.7 ± 3.4		
	nLs-TPT	36.0 ± 7.0		
	F5-ILs-TPT	978.0 ± 86.9	27.2 ± 5.8	49.6 ± 9.6
MDA-MB453 (HER2+)	Free TPT	11.5 ± 2.2		
	nLs-TPT	211.8 ± 12.2		
	F5-ILs-TPT	3435.9 ± 94.4	16.7 ± 1.0	298.8 ± 57.7
Calu-3 (HER2+)	Free TPT	15.1 ± 3.5		
	nLs-TPT	99.4 ± 4.5		
	F5-ILs-TPT	2991.1 ± 135.0	30.1 ± 1.9	198.1 ± 46.8
MDA-MB468 (EGFR+)	Free TPT	12.9 ± 0.3		
	nLs-TPT	22.2 ± 3.1		
	C225-ILs-TPT	3104 ± 41.6	139.8 ± 0.7	242.5 ± 6.5
	F5-ILs-TPT	48.4 ± 5.3	2.2 ± 0.2	3.8 ± 0.4
	Free DOX	2389 ± 178.3		
	nLs-DOX	39.5 ± 0.5		
MDA-231 (EGFR+)	C225-ILs-DOX	1768 ± 38.0	44.7 ± 3.1	0.74 ± 0.66
	Free CPT11	887.9 ± 81.4		
	nLs-CPT11	28.1 ± 7.9		
	C225-ILs-CPT11	2722.1 ± 176.1	96.9 ± 27.9	3.1 ± 0.3
	Free TPT	11.0 ± 0.4		
	nLs-TPT	3.7 ± 1.5		
BT474 (HER2+)	C225-ILs-TPT	436.7 ± 2.5	118 ± 4.8	39.7 ± 1.6

both camptothecins, with maximum uptake around pH 7 for CPT-11 and 6.5 for TPT. However, even at pH 6.5 the cellular uptake of TPT was considerably lower than for either doxorubicin or CPT-11. Indeed, in MDA-MB468 cells this low uptake of free TPT resulted in a 243-fold increase in uptake for the C225-ILs-TPT when compared to free TPT. By comparison, the camptothecin prodrug CPT-11, displayed only a 3.3-fold improvement in uptake for the targeted formulation. These results demonstrate that the specificity of drug delivery at the cellular level depends on both molecular targeting and the physicochemical properties of the specific drug being encapsulated. Consistent with these results were targeted cytotoxicity results that demonstrated significantly increased cytotoxicity for the F5-immunoliposomal topotecan when compared to both free topotecan and nontargeted nanoliposomal topotecan controls (see Supplementary Data).

### 3.4. Antitumor efficacy of nanoliposomal topotecan in a prostate (DU145) xenograft model and anti-HER2-immunoliposomal topotecan in a HER2-overexpressing BT-474 xenograft model

Antitumor efficacy of nLs-TPT loaded using the TEA<sub>5</sub>SOS gradient was evaluated in a rapidly growing DU145 prostate tumor xenograft model in nude mice (Fig. 4A). The mice were dosed biweekly at a dose of 5 mg/kg for a total of six doses. Nanoliposomal TPT demonstrated significant antitumor activity in this aggressive prostate tumor model, with statistically significant activity being observed after only two doses. After four doses, five of ten mice had no measurable tumor in the nLs-TPT arm with an average tumor volume of  $57 \pm 22 \text{ mm}^3$ , compared to  $1596 \pm 170$  for the saline control arm ( $p = 2.2 \times 10^{-7}$ ). After both four and five injections, the toxicity was tolerable. After four injections, the average weight loss was only 2.2%, with only one mouse demonstrating weight loss greater than 10% (at 12.2%). The

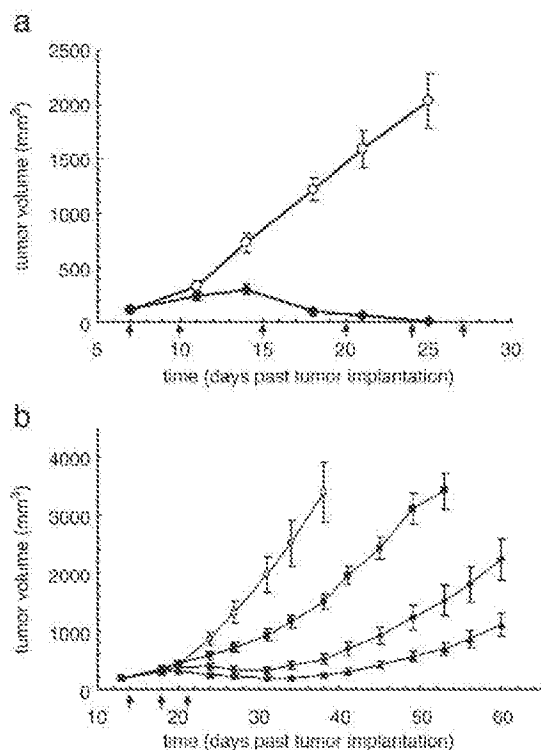


Fig. 4. Enhanced *in vivo* efficacy of liposomal topotecan against human prostate (DU-145; panel a) and breast (BT-474; panel b) cancer xenograft models. (a) DU145 tumors were treated with either saline (O) or nls-TPT (◆) at a dose of 5 mg/kg twice weekly once the tumors reached an average size of 150 mm<sup>3</sup>. (b) The prototype formulations using triethylammonium-polyphosphate gradient loading method was used in this study, and nls-TPT (◆), F5-LS-TPT (▲), saline control (O) and free TPT (■) were compared at a topotecan dose of 5 mg/kg/dose on days 14, 18, and 21 post tumor implantation. Error bars represent standard deviation of the mean.

results were similar after five injections with an average weight loss of 2.4% and only one mouse with a loss of greater than 10% (10.1%). However, following the sixth and final injection there was precipitous loss of weight with six of ten mice displaying weight loss of greater than 15% and requiring euthanasia. The four mice that survived rapidly recovered, and had reattained their pretreatment body weight by day 39. Future studies would limit the total number of doses to four to avoid the observed cumulative toxicity. However, it was apparent that substantial efficacy, including multiple complete regressions were observed in the nls-TPT arm prior to final dose and thus the onset of any significant toxicity.

Finally, we compared the antitumor efficacy of the free, non-targeted liposomal and HER2-targeted immunoliposomal topotecan in a xenograft tumor model of HER2-overexpressing human breast carcinoma in nude mice (Fig. 4B). Liposomal topotecan formulations loaded using the poly(phosphate) loading method were more active in tumor growth suppression than the free drug, and F5-targeted liposomal formulation was more active than the non-targeted one. The average tumor sizes at the end of the observation period were different among the treatment groups with high statistical significance (*p* values by non-paired 2-tailed Student's *t*-test:  $1.02 \times 10^{-8}$  for free v. immunoliposomal drug, 0.000101 for free v. liposomal drug, and 0.0014 for liposomal v. immunoliposomal drug). However, no complete regressions of tumors were detected. In the liposomal and immunoliposomal group, after initial regression, tumor regrowth occurred within 10 days of the last treatment. There was no tumor regression in the free drug group. Biweekly intravenous injections of 5 mg/kg nls-TPT beyond five doses proved intolerable and produced precipitous weight loss in more than half of the tumor bearing mice.

#### 4. Discussion

Weakly basic camptothecin analogs, such as topotecan or irinotecan, maintain an important role in cancer chemotherapy. Irinotecan is approved in the United States for the treatment of colorectal cancer, while topotecan has been approved for ovarian, small cell lung, and cervical cancers [27–29]. The constitutive expression of topoisomerase I provides both opportunities for the treatment of a broad range of malignancies, but also challenges in overcoming the severe hematological toxicities commonly associated with this class of drugs [39]. Site-specific delivery to solid tumors as a result of nonspecific accumulation of nanocarriers in solid tumors due to the EPR phenomenon [7,8], and potentially molecular targeting through the introduction of targeting ligands [40,41], promises to widen the therapeutic index for camptothecins. The schedule-dependency of camptothecins, requiring constant exposure to the drug to compensate for the S-phase specific mechanism of action and the reversible binding to Topo I [42,43], creates another opportunity for improving the activity through development of a controlled release formulation. Nanocarrier technologies that allow for carefully engineered drug release rates, so as to optimize exposure of cancer cells specifically to bioavailable drug, are now possible [13,44].

Topotecan contains several structural features that allow the drug to be efficiently loaded into liposomes or benefit from stable encapsulation and targeted drug delivery (Fig. 1). Unlike the more hydrophobic parent camptothecin compound, topotecan contains an *N,N*-dimethylaminoethyl functional group at the C-9 position ( $pK_a = 10.5$ ) [2] that confers water solubility and allows for active loading of the drug into the aqueous interior of liposomes using gradient based loading strategies. These gradient-based loading strategies have included ammonium gradients [19] and various divalent cation gradients [6,38,45], with various levels of effectiveness. Camptothecins also contain a hydrolytically sensitive lactone ring that undergoes a reversible pH-dependent conversion to an inactive carboxylate [2,3]. At  $pH \leq 4$ , topotecan is exclusively in the lactone form, and at  $pH \geq 7$  the carboxylate form predominates. Gradient-based loading strategies commonly result in an acidic interior where the drug can be stabilized in the active lactone configuration [5,6,15], thus allowing the stable delivery of the active form of topotecan directly to the tumor. Finally, topotecan contains a phenolic hydroxyl in the A-ring that has a  $pK_a$  of approximately 6.5–7.0 [2,30] (Fig. 1). This complex ionization chemistry ensures that topotecan is present in a charged form over a relatively broad pH range, which has implications for both drug loading and cellular uptake of the drug. At physiological pH (i.e.  $\geq 7$ ), the drug is a highly charged zwitterion in solution with a positively charged amine, as well as predominantly anionic phenolic hydroxylate anion in the A-ring and a carboxylate that arises from hydrolysis of the D-ring (Fig. 1). The result is inefficient loading into liposomes at pH greater than 7, despite a significant transmembrane electrochemical gradient (Fig. 2). However, between pH 4–6.5 the loading efficiency was greater than 95%, indicating that highly efficient loading is possible despite the complex ionization of topotecan.

The circulation lifetimes of various liposomal formulations of weakly basic camptothecin analogs (i.e. lurtotecan, irinotecan, and topotecan) have been significantly reduced compared to those of similar formulations of doxorubicin, primarily as a result of the poor retention of the drug while in the general circulation. In addition to passive encapsulation [4,46], ammonium sulfate [19,47], simple pH (citric acid) [45], and divalent cations [6,38,45] gradients have been employed to encapsulate topotecan. Indeed, topotecan loaded into liposomes using an ammonium sulfate gradient method resulted in less than 10% of the injected dose still in the circulation after 24 h [19]. Bally and colleagues compared liposomes loaded with citrate, ammonium sulfate,  $MnSO_4$ , and  $MnCl_2$  [45]. They demonstrated that while release *in vitro* was rapid for all four formulations, those

prepared using  $\text{SO}_4$  as the counterion were several fold more stable than nonsulfate formulations. In addition, the drug release rate decreased as the amount of topotecan loaded was increased by a factor of two. Even when liposomes employed sphingomyelin/cholesterol formulation to reduce drug leakage, the result was relatively rapid leakage with less than 10% of the loaded topotecan remaining in the liposome at 24 h [6], reflecting the difficulty in stabilizing topotecan against release in the circulation.

In this work, we demonstrate that triethylammonium salts of poly (phosphate) and sucroseoctasulfate can be used to stabilize liposomal topotecan *in vivo*, in a formulation that we refer to as nanoliposomes due to the nanosized drug complexes formed intraliposomally with the high charge density polyanions located inside the liposomes. Formulations prepared with TEA-Pi were relatively stable compared to the previously described ammonium sulfate or divalent cation-stabilized formulations (Fig. 3 and Supplementary Data). In rats, the half life ( $T_{1/2}$ ) of *in vivo* release increased from 5.4 to 12.2 hours as the drug-to-lipid ratio was increased from 150 to 450 g TPT/mol PL (Fig. 3). A similar trend was observed in mice, where four formulations that varied from 127 to 360 g TPT/mol PL were studied (Table S1). Here the amount of encapsulated topotecan at 24 h increased from  $6.7 \pm 2.5$  to  $32.3 \pm 9.8\%$  as the drug lipid ratio increased, suggesting that increasing concentrations of intraliposomal topotecan probably form more stable complexes that resist dissolution and subsequent transmembrane diffusion. Finally, substitution of the high charge density nonpolymeric small molecule polyol, sucroseoctasulfate, for a polyanionic polymer, polyphosphate, unexpectedly resulted in a dramatic improvement in both the circulation lifetimes ( $t_{1/2} = 8.4$  h) and especially in the *in vivo* drug release rate ( $T_{1/2} = 27.3$  h; Fig. 3), suggesting that sucroseoctasulfate is more effective at forming highly stable complexes with topotecan than is either sulfate or poly(phosphate).

The EPR phenomenon results in substantial increases in the tumor AUC for stable liposomal drugs, that can reach 100-fold or more when compared to the corresponding free drugs [7,23]. However, the introduction of a highly specific anti-HER2 targeting ligand into a stable liposomal formulation did not have a significant effect on the accumulation of the liposomes in HER2-overexpressing solid tumors [48]. Thus, the rate of delivery and accumulation of liposomal drugs in solid tumors is often limited by extravasation across the relatively permeable blood vessels that support these tumors, resulting in maximum accumulation between 24 and 48 h for highly stable formulations [7,13,48]. Drug release rates from the liposomal carrier are essential in determining the efficiency of delivery to solid tumors, and resulting antitumor efficacy [13]. Generally, even nontargeted liposomal drugs are more efficacious when the drug release rate is slow enough to allow the carrier to accumulate in the tumor, and subsequently release its drug, taking full advantage of the EPR effect. However, it is essential for ligand-targeted liposomes that the release rate is sufficiently slow to permit stable delivery to solid tumors, where the conjugated antibody fragments can then bind to their cell surface receptors and be internalized [13,40]. The highly stabilized nanoliposome formulations of topotecan described in this work met this criterion, and thus were further modified with anti-HER2 and anti-EGFR antibody fragments for immunotargeting.

Cell uptake studies showed efficient cellular uptake of the immunoliposomes, similar to that reported before for liposomes loaded with doxorubicin or encapsulated fluorophores [34,40,49]. However, notably different was the difference in efficiency relative to free drug. In cell culture, doxorubicin readily permeates the cell membrane, resulting in cellular concentrations of doxorubicin which are even superior to that observed with immunotargeted liposomal doxorubicin (Table 1) [49]. With topotecan, the ratio of uptake for ILs-TPT compared to free TPT in a range of cell lines targeted with either C225 Fab' to EGFR or P5 scFv to HER2/neu was between 28 and 390 fold (Table 1). This dramatic difference may be explained by the complex ionization chemistry of topotecan (Fig. 1), including the

rapid hydrolysis of the lactone ring in the cell growth medium in the presence of serum, generating the carboxylate form of the drug. The combination of the carboxylate and ionized phenolic hydroxyl at neutral pH likely results in a relatively low cellular permeability for free TPT. Others have also noted the relatively poor and pH-dependence of uptake for topotecan [50]. Thus, the ability of P5-conjugated immunoliposomes to deliver topotecan intracellularly is significantly more important than even for doxorubicin, and provides for a greater degree of specificity in delivery to receptor-over-expressing cancer cells due to the unique molecular structure of topotecan. Indeed, we have demonstrated a 3.4-fold improvement in uptake for a C225-targeted liposomal formulation of CPT-11 over unencapsulated CPT-11, the difference is considerably less than observed for topotecan. This suggests that while the lactone-to-carboxylate equilibrium common to both camptothecins has some role in the selectivity, that the high pKa amine immediately adjacent to an ionizable phenolic hydroxyl in topotecan results in significantly higher selectivity in uptake for the immunotargeted liposomal formulation.

An important consideration in the design of immunoliposomes for *in vivo* delivery of anticancer agents is whether conjugation of the antibody adversely effects the clearance of the liposomal carrier itself or the rate of drug leakage from the carrier [40]. We have optimized our conjugation strategy by employing fully human antibody fragments and by inserting only relatively small concentrations of antibody conjugate into the final liposomal topotecan construct. The results for anti-HER2 immunoliposomal topotecan are nearly identical topotecan and lipid concentrations in the blood at 1, 8, and 24 h, resulting in similar drug retention at the same time points (Supplementary Data).

Antitumor efficacy of both nontargeted and HER2-targeted nanoliposome formulations of topotecan was studied in prostate and breast tumor xenografts, respectively (Fig. 4). Nanoliposomal topotecan stabilized using sucroseoctasulfate was shown to have significant antitumor activity in a typically difficult to treat DU145 prostate tumor xenograft model (Fig. 4A). In this study, treatment every four days for a total of six doses resulted in substantial regressions and even complete cures in 5 of 10 mice for the nLs-TPT group. This group demonstrated statistically significant activity compared to the saline control group ( $p = 2.2 \times 10^{-7}$ ). Given the slow release of the drug, less frequent dosing should be possible while maintaining antitumor efficacy. A HER2-targeted immunoliposomal topotecan, stabilized using polyphosphate, showed targeted antitumor activity in a human breast (BT474) tumor xenograft model that was significantly improved compared to nontargeted nanoliposomal topotecan (Fig. 4B). These results demonstrate that with sufficient stabilization, liposomal formulations of topotecan are able to give rise to considerable antitumor activity. The activities and advantages of highly stabilized nanoliposomal formulations are likely to be accentuated clinically due to the considerably slower rate of tumor growth for most solid tumors in humans relative to rodents and due to the significantly longer circulation lifetimes of liposomal drugs in humans [13].

#### Appendix A. Supplementary data

Supplementary data associated with this article can be found, in the online version, at doi:10.1016/j.jconrel.2009.08.006.

#### References

- [1] M.J. Dennis, J.H. Beijnen, L.B. Grochow, L.J. van Warmerdam, An overview of the clinical pharmacology of topotecan, *Semin. Oncol.* 24 (1 Suppl 5) (1997) S5–12–S15–18.
- [2] J. Fassberg, V.J. Stella, A kinetic and mechanistic study of the hydrolysis of camptothecin and some analogues, *J. Pharm. Sci.* 81 (7) (1992) 676–684.

- [3] W.J. Underberg, R.M. Goossens, S.R. Smith, J.H. Beijnen, Equilibrium kinetics of the new experimental anti-tumour compound SK&F 104684-A in aqueous solution, *J. Pharm. Biomed. Anal.* 8 (3–12) (1999) 681–683.
- [4] T.G. Barris, Y. Guo, Stabilization of topotecan in low pH liposomes composed of distearoylphosphatidylcholine, *J. Pharm. Sci.* 83 (1994) 967–969.
- [5] D.C. Drummond, C.G. Noble, Z. Guo, K. Hong, J.W. Park, D.B. Kirpotin, Development of a highly active nanoliposomal irinotecan using a novel intraliposomal stabilization strategy, *Cancer Res.* 66 (6) (2006) 3271–3277.
- [6] P. Tardi, E. Choise, D. Masin, T. Redelmeier, M. Bally, T.D. Madden, Liposomal encapsulation of topotecan enhances anticancer efficacy in murine and human xenograft models, *Cancer Res.* 60 (13) (2000) 3389–3393.
- [7] D.C. Drummond, G. Meyer, K.L. Hong, D.B. Kirpotin, D. Papahadjopoulos, Optimizing liposomes for delivery of chemotherapeutic agents to solid tumors, *Pharm. Rev.* 51 (4) (1999) 691–743.
- [8] K. Greish, J. Fang, T. Inutsuka, A. Nagamitsu, H. Maeda, Macromolecular therapeutics: advantages and prospects with special emphasis on solid tumour targeting, *Clin. Pharmacokinet.* 42 (13) (2003) 1089–1105.
- [9] N.V. Koshkina, B.E. Gilbert, J.C. Waldrep, A. Seryshev, V. Knight, Distribution of camptothecin after delivery of a liposome aerosol or following intramuscular injection in mice, *Cancer Chemother. Pharmacol.* 44 (1999) 187–192.
- [10] V. Knight, N.V. Koshkina, J.C. Waldrep, B.C. Giovannella, B.E. Gilbert, Anticancer effect of 9-nitrocamptothecin liposome aerosol on human cancer xenografts in nude mice, *Cancer Chemother. Pharmacol.* 44 (1999) 177–186.
- [11] T.X. Xiang, B.D. Anderson, Stable supersaturated aqueous solutions of silatecan 7-*t*-butylidimethylsilyl-10-hydroxycamptothecin via chemical conversion in the presence of a chemically modified beta-cyclodextrin, *Pharm. Res.* 19 (8) (2002) 1215–1222.
- [12] J.A. Zhang, F. Xuan, M. Farfar, L. Ma, S. Ugwu, S. Ali, I. Alimad, Development and characterization of a novel liposome-based formulation of SN-38, *Int. J. Pharm.* 270 (1–2) (2004) 93–107.
- [13] D.C. Drummond, C.O. Noble, M.E. Hayes, J.W. Park, D.B. Kirpotin, Pharmacokinetics and in vivo drug release rates in liposomal nanocarrier development, *J. Pharm. Sci.* (2008).
- [14] A. Fahr, P. van Hoogevest, S. May, N. Bergstrand, S.L. Mø, Transfer of lipophilic drugs between liposomal membranes and biological interfaces: consequences for drug delivery, *Eur. J. Pharm. Sci.* 26 (3–4) (2005) 251–265.
- [15] E. Ramsay, J. Alnajim, M. Anantha, A. Taggar, A. Thomas, K. Edwards, G. Karlsson, M. Webb, M. Bally, Transition metal-mediated liposomal encapsulation of irinotecan (CPT-11) stabilizes the drug in the therapeutically active lactone conformation, *Pharm. Res.* 23 (12) (2006) 2799–2808.
- [16] W.C. Zamboni, S. Strychor, E. Joseph, D.R. Walsh, B.A. Zamboni, R.A. Parise, M.E. Tonda, N.Y. Yu, C. Engbers, J.L. Eisenman, Plasma, tumor, and tissue disposition of STEALTH liposomal CKD-602 (5-CKD602) and nonliposomal CKD-602 in mice bearing A375 human melanoma xenografts, *Clin. Cancer Res.* 13 (23) (2007) 7217–7223.
- [17] D.L. Emerson, R. Bendele, E. Brown, S. Chiang, J.P. Desjardins, L.C. Dibel, S.C. Gill, M. Hamilton, J.D. LeKay, L. Moon-McDermott, K. Moynihan, F.C. Richardson, S. Tomkinson, M.J. Luzzio, D. Baccanari, Antitumor efficacy, pharmacokinetics, and biodistribution of NX 211: a low-clearance liposomal formulation of irinotecan, *Clin. Cancer Res.* 6 (7) (2000) 2903–2912.
- [18] C.L. Messerer, E.C. Ramsay, D. Waterhouse, R. Ng, E.M. Simms, N. Harasym, P. Tardi, L.D. Mayer, M.B. Bally, Liposomal irinotecan: formulation development and therapeutic assessment in murine xenograft models of colorectal cancer, *Clin. Cancer Res.* 10 (19) (2004) 6638–6649.
- [19] J.J. Liu, R.L. Hong, W.F. Cheng, K. Hong, F.H. Chang, Y.L. Tseng, Simple and efficient liposomal encapsulation of topotecan by ammonium sulfate gradient: stability, pharmacokinetic and therapeutic evaluation, *Anti-Cancer Drugs* 13 (7) (2002) 709–717.
- [20] E.C. Ramsay, M. Anantha, J. Zastre, M. Meijs, J. Zunderhuis, D. Strutt, M.S. Webb, D. Waterhouse, M.B. Bally, Irinophore C: a liposome formulation of irinotecan with substantially improved therapeutic efficacy against a panel of human xenograft tumors, *Clin. Cancer Res.* 14 (4) (2008) 1208–1217.
- [21] A. Gabizon, H. Shmeeda, Y. Barenholz, Pharmacokinetics of pegylated liposomal Doxorubicin: review of animal and human studies, *Clin. Pharmacokinet.* 42 (5) (2003) 419–436.
- [22] D.C. Drummond, C. Marx, Z. Guo, G. Scott, C. Noble, D. Wang, M. Pallavicini, D.B. Kirpotin, C.C. Benz, Enhanced pharmacodynamic and antitumor properties of a histone deacetylase inhibitor encapsulated in liposomes or ErbB2-targeted immunoliposomes, *Clin. Cancer Res.* 11 (9) (2005) 3392–3401.
- [23] D.C. Drummond, C.G. Noble, Z. Guo, M.E. Hayes, J.W. Park, C.J. Ou, Y.L. Tseng, K. Hong, D.B. Kirpotin, Improved pharmacokinetics and efficacy of a highly stable nanoliposomal vinorelbine, *J. Pharmacol. Exp. Ther.* 328 (1) (2009) 321–330.
- [24] C.G. Noble, Z. Guo, M.E. Hayes, J.D. Marks, J.W. Park, C.C. Benz, D.B. Kirpotin, D.C. Drummond, Characterization of highly stable liposomal and immunoliposomal formulations of vincristine and vinblastine, *Cancer Chemother. Pharmacol.* (2009).
- [25] C.O. Noble, M.T. Krauze, D.C. Drummond, Y. Yamashita, R. Saito, M.S. Berger, D.B. Kirpotin, K.S. Bankiewicz, J.W. Park, Novel nanoliposomal CPT-11 infused by convection-enhanced delivery in intracranial tumors: pharmacology and efficacy, *Cancer Res.* 66 (5) (2006) 2801–2806.
- [26] R. Saito, M.T. Krauze, C.O. Noble, D.C. Drummond, D.B. Kirpotin, M.S. Berger, J.W. Park, K.S. Bankiewicz, Convection-enhanced delivery of Ls-TPT enables an effective, continuous, low-dose chemotherapy against malignant glioma xenograft model, *Neuro-oncology* 8 (3) (2006) 205–214.
- [27] S.L. Weithington, J.D. Wright, T.J. Herzog, Key role of topoisomerase I inhibitors in the treatment of recurrent and refractory epithelial ovarian carcinoma, *Expert. Rev. Anticancer Ther.* 8 (5) (2008) 819–831.
- [28] S.J. Nicum, M.E. O'Brien, Topotecan for the treatment of small-cell lung cancer, *Expert. Rev. Anticancer Ther.* 7 (6) (2007) 795–801.
- [29] M. Brave, R. Dagher, A. Farrell, S. Abraham, R. Samchanderi, J. Gokburu, B. Booth, X. Jiang, R. Sridhara, K. Justice, R. Pazdur, Topotecan in combination with cisplatin for the treatment of stage IVB, recurrent, or persistent cervical cancer, *Oncology (Williston Park)* 20(11) (2006) 1401–1404, 1410; discussion 1410–1411, 1415–1406.
- [30] A. Kearney, K. Patel, N. Palepu, Preformulation studies to aid in the development of a ready-to-use injectable solution of the antitumor agent, topotecan, *Int. J. Pharm.* 127 (1996) 229–237.
- [31] D.F. Nellis, D.L. Ekstrom, D.B. Kirpotin, J. Zhu, R. Andersson, T.L. Broadt, T.F. Ouellette, S.C. Perkins, J.M. Roach, D.C. Drummond, K. Hong, J.D. Marks, J.W. Park, S.L. Gardina, Preclinical manufacture of an anti-HER2 scFv-PEG-DSPC liposome-inserting conjugate. 1. Gram-scale production and purification, *Biotechnol. Prog.* 21 (1) (2005) 205–220.
- [32] C.R. Bartlett, Phosphorous assay in column chromatography, *J. Biol. Chem.* 234 (1959) 466–468.
- [33] E.C. Bligh, W.J. Dyer, A rapid method of total lipid extraction and purification, *Can. J. Biochem. Physiol.* 37 (1959) 911–917.
- [34] U.B. Nielsen, D.B. Kirpotin, E.M. Pickering, K. Hong, J.W. Park, M. Refaat, Shalaby, Y. Shao, C.C. Benz, J.D. Marks, Therapeutic efficacy of anti-ErbB2 immunoliposomes targeted by a phage antibody selected for cellular endocytosis, *Biochim. Biophys. Acta* 1591 (1–3) (2002) 109–118.
- [35] J.W. Park, K. Hong, D.B. Kirpotin, G. Colbern, R. Shalaby, J. Baseiga, Y. Shao, U.B. Nielsen, J.D. Marks, D. Moore, D. Papahadjopoulos, C.C. Benz, Anti-HER2 immunoliposomes: enhanced efficacy attributable to targeted delivery, *Clin. Cancer Res.* 8 (4) (2002) 1172–1181.
- [36] C.C. Benz, G.K. Scott, J.C. Sarup, R.M. Johnson, D. Tripathy, E. Coronado, H.M. Shepard, C.K. Osborne, Estrogen-dependent, tamoxifen-resistant tumorigenic growth of MCF-7 cells transfected with HER2/neu, *Breast Cancer Res. Treat.* 34 (2) (1992) 85–95.
- [37] P.K. Working, A.D. Dayan, Pharmacological-toxicological expert report – Caelyx (TM)–(StathIR) liposomal doxorubicin (HCl) – foreword, *Human Exp. Toxicol.* 15 (9) (1996) 751–785.
- [38] A.S. Taggar, J. Alnajim, M. Anantha, A. Thomas, M. Webb, E. Ramsay, M.B. Bally, Copper-topotecan complexation mediates drug accumulation into liposomes, *J. Control. Release* 114 (1) (2006) 78–88.
- [39] D.K. Armstrong, D. Spriggs, J. Levin, R. Foulin, S. Lane, Hematologic safety and tolerability of topotecan in recurrent ovarian cancer and small cell lung cancer: an integrated analysis, *Oncologist* 10 (9) (2005) 686–694.
- [40] C.O. Noble, D.B. Kirpotin, M.E. Hayes, C. Mamot, K. Hong, J.W. Park, C.C. Benz, J.D. Marks, D.C. Drummond, Development of ligand-targeted liposomes for cancer therapy, *Expert Opin. Ther. Targets* 8 (4) (2004) 335–353.
- [41] P. Sapra, T.M. Allen, Ligand-targeted liposomal anticancer drugs, *Prog. Lipid Res.* 42 (5) (2003) 439–462.
- [42] C.J.H. Gerrits, M.J.A. de Jonge, J.H.M. Schellens, G. Stoter, J. Verweij, Topoisomerase I inhibitors: the relevance of prolonged exposure for present clinical development, *Br. J. Cancer* 76 (1997) 952–962.
- [43] S. Guichard, A. Montazeri, E. Chatelet, I. Hennebelle, R. Bugat, P. Canal, Schedule-dependent activity of topotecan in OVCAR-3 ovarian carcinoma xenograft: pharmacokinetic and pharmacodynamic evaluation, *Clin. Cancer Res.* 7 (10) (2001) 3222–3228.
- [44] T.M. Allen, W.W. Cheng, J.I. Hare, K.M. Laginha, Pharmacokinetics and pharmacodynamics of lipidic nano-particles in cancer, *Anticancer Agents Med Chem* 6 (6) (2006) 513–523.
- [45] S.A. Abraham, K. Edwards, G. Karlsson, N. Hudon, L.D. Mayer, M.B. Bally, An evaluation of transmembrane ion gradient-mediated encapsulation of topotecan within liposomes, *J. Control. Release* 96 (3) (2004) 449–461.
- [46] D. Subramanian, M.T. Muller, Liposomal encapsulation increases the activity of the topoisomerase I inhibitor topotecan, *Oncol. Res.* 7 (1993) 461–469.
- [47] X. Li, W.L. Lu, G.W. Liang, G.R. Ruan, H.Y. Hong, C. Long, Y.T. Zhang, Y. Liu, J.C. Wang, X. Zhang, Q. Zhang, Effect of stealthy liposomal topotecan plus midodrine on the multidrug-resistant leukaemia cells in vitro and xenograft in mice, *Eur. J. Clin. Invest.* 36 (6) (2006) 409–418.
- [48] D.B. Kirpotin, D.C. Drummond, Y. Shao, M.R. Shalaby, K. Hong, U.B. Nielsen, J.D. Marks, C.C. Benz, J.W. Park, Antibody targeting of long-circulating lipidic nanoparticles does not increase tumor localization but does increase internalization in animal models, *Cancer Res.* 66 (13) (2006) 6732–6740.
- [49] C. Mamot, D.C. Drummond, U. Greiser, K. Hong, D.B. Kirpotin, J.D. Marks, J.W. Park, Epidermal growth factor receptor (EGFR)-targeted immunoliposomes mediate specific and efficient drug delivery to EGFR- and EGFRvIII-overexpressing tumor cells, *Cancer Res.* 63 (2003) 3154–3161.
- [50] A. Gabr, A. Kuin, M. Aalders, H. El-Gawly, L.A. Smets, Cellular pharmacokinetics and cytotoxicity of camptothecin and topotecan at normal and acidic pH, *Cancer Res.* 57 (21) (1997) 4811–4816.



## Improved Pharmacokinetics and Efficacy of a Highly Stable Nanoliposomal Vinorelbine

Daryl C. Drummond, Charles O. Noble, Zexiong Guo,<sup>1</sup> Mark E. Hayes, John W. Park, Ching-Ju Ou, Yun-Long Tseng, Keelung Hong, and Dmitri B. Kirpotin

Hermes Biosciences, Inc., South San Francisco, California (D.C.D., C.O.N., M.E.H., K.H., D.B.K.); Research Institute, California Pacific Medical Center, San Francisco, California (D.C.D., Z.G., M.E.H., D.B.K.); Department of Medicine, University of California at San Francisco, San Francisco, California (J.W.P.); and Taiwan Liposome Company, Taipei, Taiwan (C.-J.O., Y.-L.T., K.H.)

Received May 16, 2008; accepted October 22, 2008

### ABSTRACT

Effective liposomal formulations of vinorelbine (5' nor-anhydro-vinblastine; VRL) have been elusive due to vinorelbine's hydrophobic structure and resulting difficulty in stabilizing the drug inside the nanocarrier. Triethylammonium salts of several polyanionic trapping agents were used initially to prepare minimally pegylated nanoliposomal vinorelbine formulations with a wide range of drug release rates. Sulfate, poly(phosphate), and sucrose octasulfate were used to stabilize vinorelbine intraliposomally while in circulation, with varying degrees of effectiveness. The release rate of vinorelbine from the liposomal carrier was affected by both the chemical nature of the trapping agent and the resulting drug-to-lipid ratio, with liposomes prepared using sucrose octasulfate displaying the longest half-life in circulation (9.4 h) and in vivo retention in the nanoparticle ( $t_{1/2} = 27.2$  h). Efficacy was considerably improved in both a human colon carcinoma (HT-29) and a murine (C-26) colon carcinoma model

when vinorelbine was stably encapsulated in liposomes using triethylammonium sucrose octasulfate. Early difficulties in preparing highly pegylated formulations were later overcome by substituting a neutral distearoylglycerol anchor for the more commonly used anionic distearoylphosphatidylethanolamine anchor. The new pegylated nanoliposomal vinorelbine displayed high encapsulation efficiency and in vivo drug retention, and it was highly active against human breast and lung tumor xenografts. Acute toxicity of the drug in immunocompetent mice slightly decreased upon encapsulation in liposomes, with a maximum tolerated dose of 17.5 mg VRL/kg for free vinorelbine and 23.8 mg VRL/kg for nanoliposomal vinorelbine. Our results demonstrate that a highly active, stable, and long-circulating liposomal vinorelbine can be prepared and warrants further study in the treatment of cancer.

Nanoparticles such as small unilamellar liposomes have been shown to improve the pharmacokinetics and tumor localization of encapsulated drugs, modify the toxicities associated with a particular drug, and ultimately enhance antitumor efficacy compared with the nonencapsulated drug (Drummond et al., 2008). For the success of liposomal drug

delivery, the stable encapsulation of an amphipathic drug in the lumen (Mayer et al., 1985; Haran et al., 1993; Webb et al., 1995; Drummond et al., 2008) of liposomes with long-circulating properties (Allen et al., 2006; Drummond et al., 2008) is preferred, resulting in the ability of such liposomes to localize preferentially in solid tumors through the enhanced permeability and retention effect (Matsumura and Maeda, 1986; Drummond et al., 1999). A liposomal drug is in effect a prodrug, inactive until released from the confines of its carrier, rendering it bioavailable and capable of subsequently acting on its molecular target. Therefore, the ability of the carrier to deliver the active chemical agent to the site of disease, and to subsequently release the drug so as to achieve the desired therapeutic outcome, are equally important. Thus, the rates of drug release from the liposomal carrier in

This work was supported by California Breast Cancer Research Program of the University of California (Grant 7KB-0068); and by the National Cancer Institute Specialized Programs of Research Excellence in Breast Cancer (Grant P50-CA58207) and Brain Tumors (Grant P50-CA097257).

<sup>1</sup> Current affiliation: First Affiliated Hospital of Jinan University, Guangzhou, People's Republic of China.

Article, publication date, and citation information can be found at <http://jpet.aspetjournals.org>.

doi:10.1124/jpet.108.141200

**ABBREVIATIONS:** nLs-VRL, nanoliposomal vinorelbine; DSPC, 1,2-distearoyl-3-sn-phosphatidylcholine; PEG-DSG, methoxypolyethylene glycol-1,2-distearoylglycerol ether; PEG-DSPE, N-(methoxypoly(ethylene glycol)oxycarbonyl-1,2-distearoylphosphatidylethanolamine; PL, phospholipid; VRL, vinorelbine; CHE, cholesterylhexadecyl ether; HPLC, high-performance liquid chromatography; %ID, percentage of injected dose; MRT, mean residence time in the circulation; AUC<sub>∞</sub>, area under the concentration versus time curve in plasma based on the sum of exponential terms; MTD, maximal tolerated dose; CPT-11, 7-ethyl-10-hydroxycamptothecin; TEA, triethylammonium; SOS, sucrose octasulfate; TEA<sub>3</sub>SOS, triethylammonium sucrose octasulfate; Pn, poly(phosphate); pLs-VRL, pegylated liposomal vinorelbine; TEA-Pn, triethylammonium poly(phosphate).

vivo are critical for the optimal construction of a liposomal therapeutic.

Vinca alkaloids are potent anticancer agents that act by binding to tubulin and preventing tubulin assembly into microtubules, ultimately leading to mitotic inhibition and induction of apoptosis (Jordan et al., 1991). Vinorelbine (5'-nor-anhydro-vinblastine) is a clinically approved drug that is frequently used in the treatment of various cancers, including metastatic breast cancer (Weber et al., 1995) and non-small-cell lung cancer (Gridelli and De Vivo, 2002). Vinorelbine is better tolerated than many of the other vinca alkaloids, including reduced neurotoxicity (Mathé and Reizenstein, 1985) due to its reduced affinity for axonal microtubules (Binet et al., 1990). Liposome-based delivery may further improve the therapeutic index for vinorelbine through an improved pharmacokinetic profile and specific delivery to solid tumors, similar to that observed for liposomal doxorubicin. Although several liposomal formulations of vincristine have been described in the literature (Allen et al., 1995; Webb et al., 1995; Zhu et al., 1996; Embree et al., 1998), vinorelbine has been considerably more difficult to stabilize in liposomes (Semple et al., 2005; Zhigaltsev et al., 2005), resulting in a majority of the drug being released from the particle before reaching the tumor.

We have recently described a novel and highly effective intraliposomal stabilization strategy for improving the in vivo retention of difficult to formulate anticancer drugs (Drummond et al., 2005, 2006, 2008). We use the term "nanoliposomal drug" to describe a nanocarrier that includes a lipid scaffold encapsulating a nanoscale drug complex that improves drug retention in vivo. Here, we use this technology to prepare multiple nanoliposomal vinorelbine (nLs-VRL) formulations with a wide range of in vivo drug release rates. The development of a successful liposomal drug construct requires tailoring of the liposome formulation to the physicochemical properties of the drug to be encapsulated. Even different drugs within the same drug class often require distinctive formulations for optimal activity. Mitoxantrone, for example, is encapsulated too stably in liposomes typically used to entrap doxorubicin, and it requires a modification to the composition for optimal activity (Lim et al., 1997). Likewise, vincristine is stabilized much more easily in liposomes than vinorelbine (Semple et al., 2005; Zhigaltsev et al., 2005), despite both being vinca alkaloids. This work aimed to optimize the liposome formulation parameters for vinorelbine to produce a long-circulating, stable, and active liposomal vinorelbine.

Formulations of vincristine that included distearoylphosphatidylcholine (DSPC) were previously shown to be unstable, rapidly leaking their drug in the blood upon intravenous administration (Webb et al., 1995). Unexpectedly, the use of triethylammonium sucrose octasulfate gradients to prepare liposomal vinorelbine allowed for remarkable in vivo stability, even using a DSPC-based lipid membrane composition. The in vivo antitumor efficacy of liposomal vinorelbine was shown to be greatly improved upon liposome encapsulation using sucrose octasulfate as an intraliposomal trapping agent. The acute toxicity of this liposomal vinorelbine was also slightly improved compared with free vinorelbine.

## Materials and Methods

**Materials.** DSPC and poly(ethylene)glycol PEG<sub>2000</sub>-derivatized distearoylphosphatidylethanolamine (PEG-DSPE) were purchased from Avanti Polar Lipids (Alabaster, AL). Cholesterol was obtained from Calbiochem (La Jolla, CA). Vinorelbine tartrate (10 mg/ml; GlaxoSmithKline, Uxbridge, Middlesex, UK) was obtained from the pharmacy. Sucrose octasulfate (sodium salt) was purchased from Toronto Research Chemicals, Inc. (North York, ON, Canada). mPEG<sub>2000</sub>-distearoylglycerol (PEG-DSG) was purchased from NOF Corporation (White Plains, NY). Sepharose CL-4B and Sephadex G-75 size exclusion resins, Dowex 50W-8X-200 cation exchange resin, and triethylamine were all obtained from Sigma-Aldrich (St. Louis, MO). [<sup>3</sup>H]cholesterylhexadecyl ether (48.3 Ci/mmol) was purchased from PerkinElmer Life and Analytical Sciences (Boston, MA).

**Preparation of Liposomes.** Liposomes with entrapped polyvalent anionic salts were prepared as described previously (Drummond et al., 2006). In brief, triethylammonium salts of sucrose octasulfate and poly(phosphate) ( $n = 13-18$ ) were prepared by ion exchange chromatography from the corresponding commercially available sodium salts. Triethylammonium sulfate was prepared by titration of 250 mM sulfuric acid with concentrated triethylamine and diluted to a final concentration of 200 mM. Ammonium sulfate solution (0.25 M) was prepared by dissolving the commercial salt in water. The prototype lipid composition used in these studies was 3 mol parts of DSPC, 2 mol parts of cholesterol, and 0.015 mol parts of PEG-DSPE. For studies characterizing the effect of liposome PEGylation on the drug loading, PEG-DSPE was included in the lipid matrix at concentrations ranging from 0.5 to 10 mol% of the phospholipid (PL), or PEG-DSG was incorporated simply at 10 mol% of the PL. For in vivo stability studies, [<sup>3</sup>H]cholesterylhexadecyl ether was included at 0.5  $\mu$ Ci/ $\mu$ mol PL. Liposomes with the average size range of 8 to 95 nm or 100 to 115 nm were prepared by extrusion of lipid suspensions, hydrated in the polyvalent anionic salt solutions, through polycarbonate membranes (Nucleopore; Corning Life Sciences, Lowell, MA) with the pore size of 0.06 or 0.1  $\mu$ m, respectively. Particle size was determined by photon correlation spectroscopy using an N4 Plus particle size analyzer (Beckman Coulter, Fullerton, CA). The size is reported as volume weighted diameter  $\pm$  S.D. Unencapsulated multivalent anion salts were removed by gel filtration of on a Sepharose CL-4B column eluted with 5 mM HEPES-Na and 5% dextrose, pH 6.5.

**Loading of Vinorelbine.** Vinorelbine (VRL) in the form of stock solution of vinorelbine bitartrate (10 mg/ml USP) was added to the liposomes at a drug-to-phospholipid ratio of 350 g/mol, the pH was adjusted to 6.5 using 1 N NaOH, and the mixture was incubated at  $60 \pm 2^\circ\text{C}$  for 30 min. For characterizing the effect of the drug-to-PL ratio on drug loading, the amount of drug added was varied from 150 to 550 g VRL/mol PL. In all subsequent studies a VRL-to-PL ratio of 350 g VRL/mol PL was used. The mixture was then chilled on ice for 15 min, and unencapsulated drug was removed by Sephadex G-75 gel filtration chromatography, eluting with HBS-6.5 buffer (20 mM HEPES and 135 mM NaCl, pH 6.5). Aliquots of purified liposomes were then solubilized in a solution composed of methanol/0.1 M phosphoric acid [80:20 (vol:vol)] and analyzed for vinorelbine spectrophotometrically at 270 nm. Liposome phospholipid was quantified using the phosphate assay of Bartlett (1959) directly or after methanol-chloroform extraction for samples containing poly(phosphate) as the intraliposomal trapping agent.

**Pharmacokinetics of Liposomal VRL Formulations with Tunable Release Rates.** All studies involving animals were in accordance with institutionally approved animal research protocols. Liposomal VRL and lipid pharmacokinetics were studied in female Sprague-Dawley rats (190–210 g), with indwelling central venous catheters. Two rats per formulation were injected with a 0.2- to 0.3-ml bolus of [<sup>3</sup>H]CHE-labeled vinorelbine liposomes (5 mg of VRL per kg of the body weight). Blood samples (0.2–0.3 ml) were drawn at various times after injection and diluted with 0.3 ml of ice-cold



phosphate-buffered saline containing 0.04% EDTA, weighed, and the blood cells were separated by centrifugation. The supernatant fluids were collected and assayed for VRL by HPLC analysis as follows. The samples were spiked with vinblastine (internal standard), extracted with diethyl ether, and evaporated. The resulting residues were dissolved in the mobile phase consisting of aqueous 50 mM triethylammonium acetate, pH 5.5, and acetonitrile (58:42 by volume). The samples were loaded on a C-18 reverse phase silica column (250 × 4 mm i.d.; particle size, 5 μm; Supelco, Bellefonte, PA) preceded by a C-18 guard column. The column was eluted isocratically with the above-mentioned mobile phase at a flow rate of 1.0 ml/min. VRL was detected by absorbance at 270 nm. Typical retention times for VRL and vinblastine (internal standard) were 9.1 and 7.8 min, respectively, with a resolution of 2.1. Standards (0.25–25 μg/ml) were formed by addition of VRL (10 mg/ml USP stock solution) to blank rat plasma emulating the matrix of the samples. Recovery of VRL from plasma spikes ranged from 101 to 103% as determined by comparison with VRL extraction from phosphate-buffered saline. No interference was observed for either vinca alkaloid during the analysis of blank plasma. The average standard linearity ( $R^2$ ) was 0.9993 with a detection limit of 0.25 μg/ml. The batch-to-batch precision over the range of standards (indicated as relative S.D.) for VRL retention time and peak area was 3.5 and 4.2%, respectively.

The liposome lipid label was quantitated by scintillation radioactivity counting using conventional methods. The liposome preparations with known drug and [ $^3$ H]CHE-lipid concentration were used as standards. Radioactivity standards contain equal amount of diluted rat plasma to account for quenching. The amount of VRL and the liposome lipid in the blood was calculated assuming the blood volume in milliliters as 6.5% of the body weight in grams and the hematocrit of 40%. The total amount of the lipid and the drug in the blood was expressed as percentage of injected dose (%ID) and plotted against post-injection time. The release of drug from the liposomes was determined by monitoring changes in the drug-to-lipid ratio as a function of time. Because free vinorelbine is cleared rapidly from the blood once it escapes the carrier, the drug-to-lipid ratio in the blood is a direct indication of the amount of drug retained inside liposomes. In brief, the VRL and lipid concentrations were determined by HPLC and scintillation counting of [ $^3$ H]CHE, as described above. Because both DSPC (Silvius and Leventis, 1993) and [ $^3$ H]CHE (Pool et al., 1982) are nonexchangeable lipids, the concentration of liposomal phospholipid in the blood can be determined indirectly by measuring [ $^3$ H]CHE using standard scintillation counting and then comparing it directly to a standard curve of the [ $^3$ H]CHE where the liposomal phospholipid (DSPC) concentration has been determined by phosphate analysis (Bartlett, 1959). The VRL-to-PL ratio was then determined and expressed as grams of VRL per mole of PL at prescribed time points and then used to calculate the percentage of the preinjection VRL-to-PL ratio (percentage of original drug-to-PL ratio) by dividing the VRL-to-PL ratio determined at a specified time point by the VRL-to-PL ratio of the initially injected sample (time 0).

Because the plots generally showed good agreement with monoexponential kinetics (linearity in semilogarithmic scale), blood half-lives of the drug, the lipid, and of the drug release from the liposomes were calculated from the best fit of the data to monoexponential decay equation using the TREND option of the Excel computer program (Microsoft, Redmond, WA). Pharmacokinetic parameters, including the volume of distribution, clearance, the mean residence time in the circulation (MRT), and the area under the concentration versus time curve ( $AUC_{0-\infty}$ ), were all determined by noncompartmental pharmacokinetics data analysis using PK Solutions 2.0 software (Summit Research Services, Montrose, CO).

**Acute Toxicity of Liposomal VRL.** The acute toxicities of free VRL, nLs-VRL, and nondrug-loaded triethylammonium sucrose octasulfate-encapsulated liposomes were compared by determining the maximal tolerated dose (MTD) following single intravenous injection in regular (immunocompetent) mice (female Swiss-Webster mice). MTD determinations generally followed the protocol adopted by the

United States National Cancer Institute Developmental Therapeutics Program as described in our previous work (Drummond et al., 2006). A brief description of the steps follows. Step 1: A range-seeking step with the dose escalation factor of 1.8 is used until acute mortality or terminal morbidity (within >1 day after injection) is observed in any of the animals. The dose one step below the mortality/terminal morbidity dose is recorded. Step 2: A range-seeking step is used with the dose escalation factor of 1.15 until acute mortality or terminal morbidity (within >1 day after injection) is observed in any of the animals. The dose one step below the mortality/terminal morbidity dose is recorded at tentative MTD. Step 3: Validation step. A group of five animals is injected intravenously (tail vein) with free or liposomal VRL at tentative MTD determined at step 2. The animals are followed for 7 days; the animal body weight is recorded twice weekly and compared with the preinjection weight. General health of the animals is observed (alertness, grooming, feeding, excreta, skin, fur, and mucous membrane conditions, ambulation, breathing, posture). If during the observation period there is no mortality, progressive morbidity, or weight loss in excess of 15% of the preinjection body weight, the dose is considered to be validated as acute single injection MTD. If any of these effects occur, the experiment is repeated at the next lower dose by a factor 1.15. To obtain additional statistics for validation step, the body weight dynamics of surviving animals was followed for up to 11 days after injection. Liposomes containing triethylammonium sucrose octasulfate (TEA<sub>8</sub>SOS), prepared and purified as described above, but without the drug loading step, were used as a placebo (liposome-only) control. Free VRL (vinorelbine bitartrate USP, Navelbine; GlaxoSmithKline) was used directly from the vial and diluted with sterile 5% dextrose before injection.

**Antitumor Efficacy of Liposomal VRL.** The antitumor efficacy of nLs-VRL was studied in a syngeneic C-26 murine colon carcinoma tumor model, as well as in HT-29 (human colon carcinoma), BT-474 (human breast adenocarcinoma), and Calu-3 (human lung adenocarcinoma) xenograft models. All cells were acquired from American Type Culture Collection (Manassas, VA) and cultured according to American Type Culture Collection protocols. Cultured C-26 cells ( $2 \times 10^5$ ) were inoculated subcutaneously into the flank area of immunocompetent 6- to 8-week-old male BALB/c mice. At day 12 after inoculation, mice were randomly divided into six treatment groups of five animals per group. The tumor-bearing mice were injected through the tail-vein with free vinorelbine at 6, 8, or 12 mg/kg, and with nanoliposomal vinorelbine at 4 or 6 mg/kg every 3 days for a total of three injections. Cultured human carcinoma cells were similarly inoculated into homozygous nude mice (HT-29: BALB/c, female, 6 to 8 weeks old,  $1 \times 10^6$  cells; Calu-3: NCR *nu/nu*, male, 5 to 6 weeks old,  $1.5 \times 10^7$  cells; BT-474: NCR *nu/nu*, 5 to 6 weeks old, female,  $2 \times 10^7$  cells), except that in the BT-474 study, the animals were preimplanted with a 60-day sustained release 0.72-mg 17β-estradiol pellets (Innovative Research of America, Inc., Sarasota, FL). After the development of tumors, the animals were randomly assigned to treatment groups. Treatment by intravenous (tail vein) injection of free or liposomally formulated drug started at day 16 (HT-29: six animals/group, tumors 5–8 mm in diameter), day 25 (BT-474: eight animals/group, tumor volumes 144–369 mm<sup>3</sup>), or day 30 (Calu-3: nine animals/group, tumor volumes 70–150 mm<sup>3</sup>) according to the schedules and doses indicated under *Results*. Control groups received equal volumes of physiological saline. Tumor volumes (V) were determined twice weekly by caliper measurements of the long (L) and short (W) axis of the tumor and calculated using formula  $V = LW^2/2$  (Geran et al., 1972). Animal body weights were also determined twice weekly, and the general health of the animals was assessed daily to assess the extent of treatment-related toxicities. The average tumor sizes in control and treatment groups were plotted versus time and compared for statistical significance of the difference pairwise at various post-treatment days using Student's *t* test.

## Results

**Formulation of Vinorelbine in Minimally Pegylated Liposomes.** A novel intraliposomal stabilization process for stable and high-capacity liposomal entrapment of difficult to formulate basic amphipathic drugs such as vinorelbine has been developed. The method uses triethylammonium salts of polyanionic compounds such as polyphosphate or sucrose octasulfate as intraliposomal trapping agents to improve liposomal drug encapsulation stability in vivo. The polyanionic compounds are thought to form complexes with varying degrees of stability with vinorelbine, and possibly precipitate or gelate the drug inside the liposomes, thus enhancing its stability even further. Initial attempts to load vinorelbine using any gradient-based loading strategy, into liposomes stabilized with high concentrations of PEG-DSPE (10 mol% total phospholipid), resulted in exceptionally poor encapsulation efficiencies (<25%); thus, all early development efforts were carried out with liposomes containing only minimal concentrations of PEG-DSPE (0.5 mol%). Incubation of vinorelbine with the liposomes containing polyvalent anions and transmembrane gradient of triethylammonium ion resulted in the efficient loading of the drug. The amount of drug loaded per unit of lipid matrix, as well as the percentage of encapsulated drug, depended on the nature of polyvalent ion. At the drug/lipid ratio of 150 g/mol PL, the loading was quantitative (>95%) with all three anions [SO<sub>4</sub>, poly(phosphate) (Pn), and SOS]. At 350 g/mol PL, the loading efficiency of (TEA)<sub>2</sub>SO<sub>4</sub> liposomes decreased to 75%, whereas both polymeric (Pn) and nonpolymeric (SOS) multivalent anions provided nearly quantitative loading at 99.3 and 100.7%, respectively. Remarkably, loading in the liposomes with SOS remained practically quantitative for drug/lipid ratios of up to 450 g/mol PL (101.4%) and only slightly decreased (88%) at 550 g/mol PL. The drug/lipid ratio of 350 g/mol PL, accepted for further studies, corresponds to a molar ratio of approximately 1 drug per 3.08 phospholipids, which translates into approximately 30,000 VRL molecules per nanoliposomal particle. This degree of loading compares favorably (is approximately 2-fold higher) with other reported liposomal vinorelbine formulations (Semple et al., 2005; Zhigaltsev et al., 2005) and is more than four times higher than that used for liposomal vincristine (Webb et al., 1995; Embree et al., 1998).

**Pharmacokinetics of Liposomal Vinorelbine Formulated with Various Anions.** In rats, liposomal encapsulation dramatically reduced the clearance of VRL from the circulation and increased the MRT and AUC<sub>0-∞</sub> in the blood (Fig. 1; Table I). The extent of the improvement in the circulation longevity of the drug depended on the anion used to stabilize the drug inside the liposomes. Encapsulation in liposomes containing ammonium sulfate reduced the clearance of VRL from the circulation 220-fold. Encapsulation in the most stable liposome formulations using triethylammonium sucrose octasulfate resulted in an approximately 1500-fold reduction in clearance.

The in vivo stability of liposomal vinorelbine formulations was characterized by monitoring changes in the drug-to-lipid ratio over time as described under *Materials and Methods*. Liposomal vinorelbine formulated using ammonium sulfate was relatively unstable, with a  $t_{1/2}$  value for in vivo drug release of only 1.8 h. Although the pharmacokinetics of vinorelbine were improved upon encapsulation in ammonium

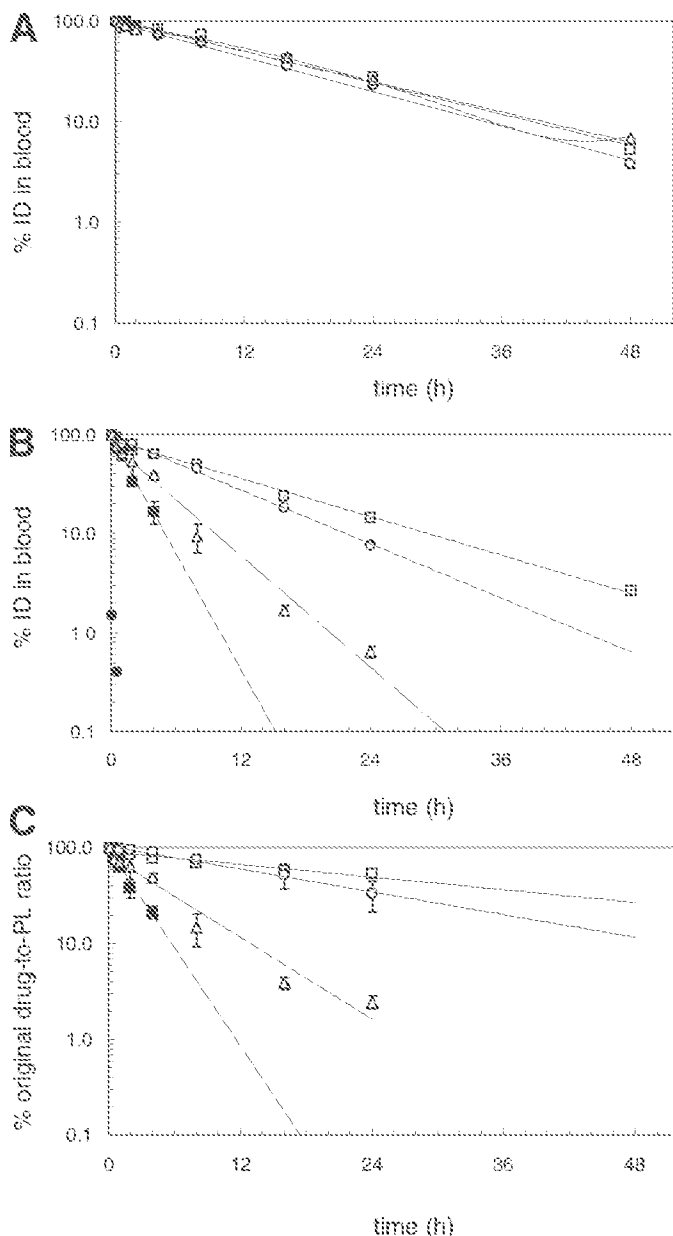


**Fig. 1.** Blood pharmacokinetics of the liposomal VRL after intravenous bolus administration in rats. The liposomes are loaded using pre-entrapped ammonium sulfate (●), TEA-Pn (○, △), or TEA<sub>2</sub>SOS (□). The liposomes were loaded at drug-to-phospholipid ratios of 220 μg VRL/μmol PL for the (NH<sub>4</sub>)<sub>2</sub>SO<sub>4</sub> formulation, 260 (△) or 350 (○) μg VRL/μmol PL for the poly(phosphate) formulation, and 350 μg VRL/μmol PL for the TEA<sub>2</sub>SOS formulation. Free VRL (●) was dissolved in 5% dextrose and injected. The pharmacokinetics of liposomal lipid (A) and VRL (B) were followed as a function of time using scintillation counting of [<sup>14</sup>C]cholesterylhexadecyl ether for determination of the lipid label and HPLC analysis for VRL quantitation in the plasma as described under *Materials and Methods*. Concentrations of both drug and lipid are given as %ID. C, dynamics of the drug-to-liposomal lipid ratio in the blood of a rat in vivo after intravenous bolus administration for each of the various liposomal vinorelbine formulations. Two rats were used for determination of the pharmacokinetics, and the average and cumulative errors of those measurements are plotted.

sulfate liposomes ( $t_{1/2}$  of 1.54 h versus 0.2 h), the rate of VRL release from the liposomes was considerably more rapid than the time required for maximal tumor localization of long-circulating liposomes (24–48 h). Liposomes loaded with VRL using TEA-Pn gradients were more stable than the (TEA)<sub>2</sub>SO<sub>4</sub> formulations and showed increased stability at

TABLE 1

Pharmacokinetic parameters for free and various liposomal vinorelbine formulations in rats

The data used to calculate the pharmacokinetic parameters for VRL when formulated either in the free form or liposomal form refer to the actual drug concentrations measured in the blood that were then used to calculate the %ID values found in the corresponding curves for Figs. 1B and 5A.

Formulation	$t_{1/2}$	AUC <sub>0-∞</sub>	CL	$V_d$	MRT	$t_{1/2}$ (VRL Release) <sup>a</sup>
	h	μg · h/ml	ml/h	ml		h
Free VRL	0.20	0.5	10,200	3607	0.3	
LS-VRL [(NH <sub>4</sub> ) <sub>2</sub> SO <sub>4</sub> ]	1.54	107.0	46.7	103.5	2.2	1.8
nLS-VRL [TEA-Pn-220]	3.25	253.2	19.7	92.6	4.7	4.2
nLS-VRL [TEA-Pn-350]	6.62	746.7	6.70	64.0	9.6	15.2
nLS-VRL [TEA-SOS]	9.43	879.3	5.69	77.4	13.6	27.2
pLS-VRL [TEA-SOS]	9.42	956.3	5.23	71.1	13.6	26.6

CL, clearance calculated from exponential terms;  $V_d$ , volume of distribution.<sup>a</sup>  $t_{1/2}$  value for VRL release refers to the half-life of VRL release from the liposomal carrier in the circulation upon intravenous administration.

higher drug-to-phospholipid ratios (Fig. 1C; Table 1). The liposomes loaded with VRL using TEA<sub>3</sub>SOS demonstrated the greatest stability, with a  $t_{1/2}$  value for drug leakage rate in circulation of 27.2 h.

**Acute Toxicity of Liposomal Vinorelbine.** The maximal tolerated dose of free VRL, nLS-VRL, and “empty” liposomes following a single intravenous dose was determined in normal Swiss-Webster mice. The MTD was 17.5 mg/kg for free VRL and 23.8 mg/kg for nanoliposomal VRL prepared with either 0.5% PEG-DSPE or 10% PEG-DSG. The relatively low toxicity of empty liposomes has been confirmed in numerous instances and is an attractive attribute for liposomes as drug delivery particles. However, in this study we perceived a need for confirming this low toxicity due to the nature of the trapping agent being used, i.e., sucrose octasulfate. Polyvalent anionic molecules, in particular, polymeric anions (heparin, suramin, dermatan sulfate, heparan sulfate, and dextran sulfate) are known to activate coagulation cascade enzymes and at high concentrations or suboptimal dosing, can even demonstrate considerable toxicity (Astrup et al., 1955; Flexner et al., 1991; Bitton et al., 1995). The MTD of empty liposomes formulated containing just TEA-SOS solution, was not achieved even at the highest administered dose of 583.2 μmol PL/kg. The dose of more than 600 μmol PL/kg was difficult to administer because of concentration and injection volume limitations. By comparison, the phospholipid dose at the MTD for nLS-VRL is 68 μmol PL/kg, and the dose typically used for *in vivo* efficacy studies (i.e., 5 mg VRL/kg) is 14.3 μmol PL/kg.

**Antitumor Efficacy of Liposomal VRL in Murine Models of Cancer.** Sparsely (0.5 mol% PEG-lipid) PEGylated liposomal vinorelbine (nLS-VRL) prepared using intraliposomal polyanionic stabilization was more effective than free drug against a variety of syngeneic or xenograft (human) tumors raised subcutaneously in mice. In a syngeneic murine colon carcinoma model (C-26), nLS-VRL prepared by the TEA<sub>3</sub>SOS method at 0.5 mol% PEG-DSPE and 350 g VRL/mol PL, and given in four intravenous injections spaced at 3 days in the dose of 4 mg VRL/kg/injection, was considerably more efficacious ( $P = 0.009$ ) in reducing the tumor growth than free drug given in the same schedule at 12 mg VRL/kg (Fig. 2A), indicating a minimal 3-fold improvement in the activity of nLS-VRL compared with free VRL. Due to the rapid growth rate of these tumors, it is possible that this improvement may prove to be even more substantial when nLS-VRL is tested in slower growing tumors, in which the rate of drug release relative to the rate of tumor growth is more substantial. The animal body weights in the course of

treatment showed little change (<10% decrease) consistent with the prior finding that the toxicity of liposomal vinorelbine was not in excess of that of free drug. Similar results were obtained with the same formulation in a human colon carcinoma xenograft model (HT-29) raised subcutaneously in homozygous nude mice. In the treatment regimen of four 5 mg VRL/kg *i.v.* doses of free or nLS-VRL, spaced at 3-day intervals, and initiated upon reaching an initial tumor diameter of 5 to 8 mm, nLS-VRL was considerably more efficacious in suppressing the growth of HT-29 tumors than free vinorelbine ( $P < 0.001$ ), causing tumors to regress, whereas in the free drug group the tumors always continued to grow (Fig. 2B). There was little change in the animals' body weight during the course of treatment, indicating again the treatment was well tolerated and that liposomalization did not increase drug toxicity.

**Effect of PEGylated Lipids on Loading of Vinorelbine in Liposomes.** Despite the early success developing a highly stable and long-circulating liposomal vinorelbine formulation that was only minimally pegylated, additional strategies were pursued to overcome the barriers in loading vinorelbine into highly pegylated liposomes similar in lipid compositions used in the commercial pegylated liposomal doxorubicin (Doxil; Alza/Johnson & Johnson, Palo Alto, CA). Previously, we had observed that liposomes loaded with vinorelbine using ammonium sulfate gradients displayed a reduced efficiency of loading when PEG-DSPE was incorporated at concentrations greater than 3 mol% of the phospholipid component (data not shown). Here, we investigated the effect of PEG-DSPE on loading of vinorelbine loaded in DSPC/cholesterol liposomes using the TEA<sub>3</sub>SOS gradient method described above. Loading was inhibited when the PEG-DSPE content was increased above 3 mol% (Fig. 3A). Loading in liposomes containing 10 mol% PEG-DSPE (a concentration similar to that used in the clinical preparation Doxil) was only 17.5% at this ratio. Substitution of the nonionic PEG-DSG for PEG-DSPE (Fig. 3B) resulted in quantitative loading at 10 mol% of the PEGylated lipid, suggesting the nonionic nature of PEG-DSG played a role in allowing for efficient VRL encapsulation using our drug loading and stabilization protocol. The pharmacokinetics of PEG-DSG-stabilized liposomes were similar to those of liposomal VRL containing only 0.5 mol% PEG-DSPE (Fig. 4A). Importantly, the inclusion of PEG-DSG in the formulation did not increase the rate of drug leakage from the liposomes (Fig. 4B; Table 1).

**Antitumor Efficacy of Pegylated Liposomal VRL in Human Breast and Lung Carcinoma Xenografts.** The antitumor efficacy of PEGylated liposomal vinorelbine (10

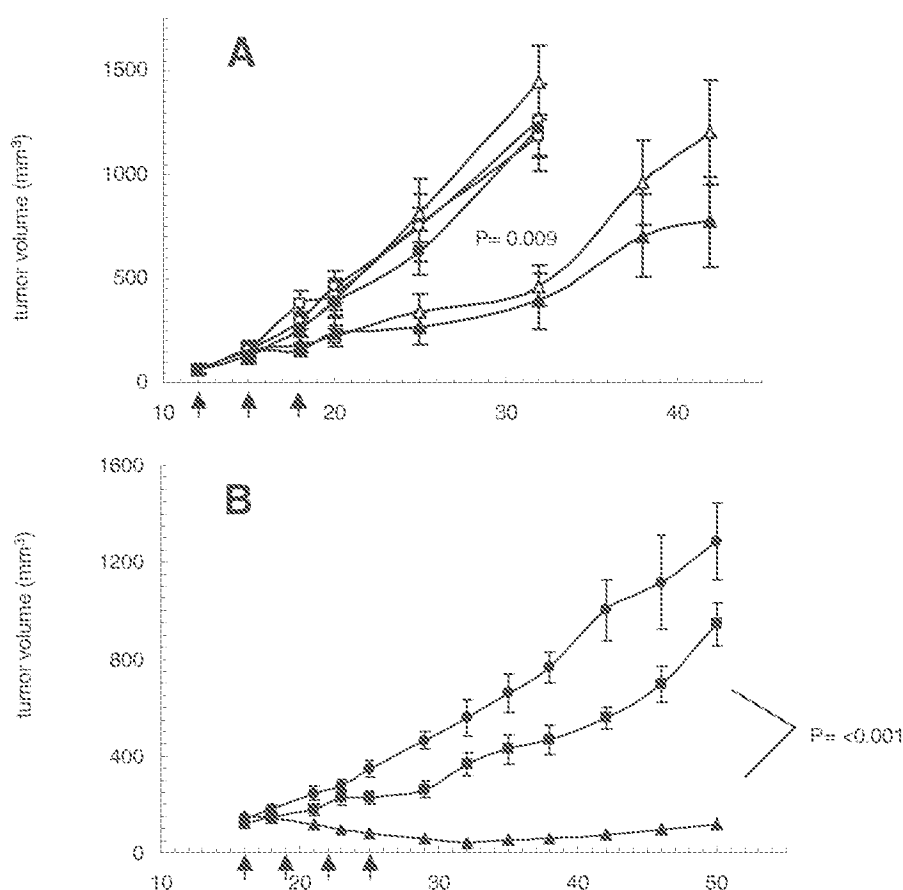


Fig. 2. Antitumor efficacy of free vinorelbine or liposomal vinorelbine in a syngeneic C-26 murine colon carcinoma model (A) and in HT-29 human colon cancer xenografts (B). A, male BALB/c mice inoculated subcutaneously with C-26 murine colon carcinoma cells were treated by intravenous administration with free VRL at 6 mg/kg (○), 8 mg/kg (□), or 12 mg/kg (■), or with nLs-VRL at 4 mg/kg (△) or 6 mg/kg (▲) every 3 days for a total of three injections (see arrows). Saline (●) designates the mice treated with drug- and liposome-free vehicle only. B, female BALB/c homozygous nude mice inoculated subcutaneously with HT-29 human colon carcinoma cells were treated with free VRL (○) or nLs-VRL (▲) at a dose of 5 mg VRL/kg through the tail vein every 3 days for a total of four injections (see arrows). Saline (●) designates the mice treated with drug- and liposome-free vehicle only. nLs-VRL was formulated using the TEA<sub>3</sub>SOS gradient method for the first two studies. *P* value of 0.009 refers to comparison of free VRL with nLs-VRL (4 mg/kg) at 32 days.

mol% PEG-DSG) was studied in a human breast carcinoma (BT-474) model, an estrogen-dependent ductal adenocarcinoma that overexpresses the C-ErbB2 (HER2) receptor (Fig. 5A). pLs-VRL loaded using sucrose octasulfate was noticeably more efficacious than free VRL in retarding tumor growth ( $P < 0.001$ ), resulting in tumor regressions and even one complete cure (one in seven). A final study looked at the efficacy of pLs-VRL in a human lung carcinoma xenograft (Calu-3) model (Fig. 5B). pLs-VRL demonstrated a statistically significant improvement over both free VRL ( $P = 0.027$ ) and saline controls ( $P = 0.006$ ). Similar to the previous two efficacy studies, the animal body weights in the course of treatment showed little change (<10% decrease) upon treatment with pLs-VRL in either of these two subsequent studies.

## Discussion

A significant effort has been made toward the development of liposomes with suitable sustained drug release rates, an important consideration for optimal drug delivery (Allen et al., 2006; Drummond et al., 2006). The requirements may vary considerably depending on the location of the therapeutic target and the mechanism of action of the drug to be delivered. For the treatment of solid tumors, highly stable liposome formulations are more desirable due to the need for stable encapsulation until the drug carriers can accumulate in the tumor due to the enhanced permeability and retention effect. Maximal accumulation in solid tumors usually occurs on the time scale of 24 to 48 h (Gabizon et al., 1997; Drummond et al., 1999). Conversely, the treatment of hematological cancers that reside in vascularly accessible locations may

benefit to a lesser extent on stability compared with the treatment of solid tumors. Allen and coworkers have recently observed efficacy with a liposomal vincristine that is superior to that of a significantly more stable liposomal doxorubicin formulation (Sapra et al., 2004). The mechanism of action may also play a role in determining the optimal drug release rate. Drugs that are schedule-dependent, such as vincristine or vinorelbine, will undoubtedly benefit from a different drug-release profile than schedule-independent drugs, including doxorubicin.

A variety of liposomal properties or formulation methods play important roles in determining the degree of stability and hence the rate of drug release from the liposomal carrier. A careful choice of liposomal lipids, including the inclusion of highly saturated phospholipids (Bally et al., 1990; Gabizon et al., 1993), the presence of cholesterol (Papahadjopoulos et al., 1972; Drummond et al., 1999), and appropriate mixtures of sphingomyelin and cholesterol (Kirby and Gregoriadis, 1983; Webb et al., 1995), all regulate the permeability of the liposomal membrane to encapsulated drugs. Drug retention is equally dependent on the physicochemical properties of the drug to be encapsulated and the use of transmembrane gradients to both load and stabilize liposomal formulations of weakly basic amphipathic drugs.

Transmembrane gradient-loading methods have been used to actively encapsulate amphipathic weak bases into liposomes at relatively high efficiencies. These include simple pH gradients (Mayer et al., 1985; Webb et al., 1995), ammonium gradients (Haran et al., 1993), and MnSO<sub>4</sub> gradients (Cheung et al., 1998). Although stable formulations of lipo-

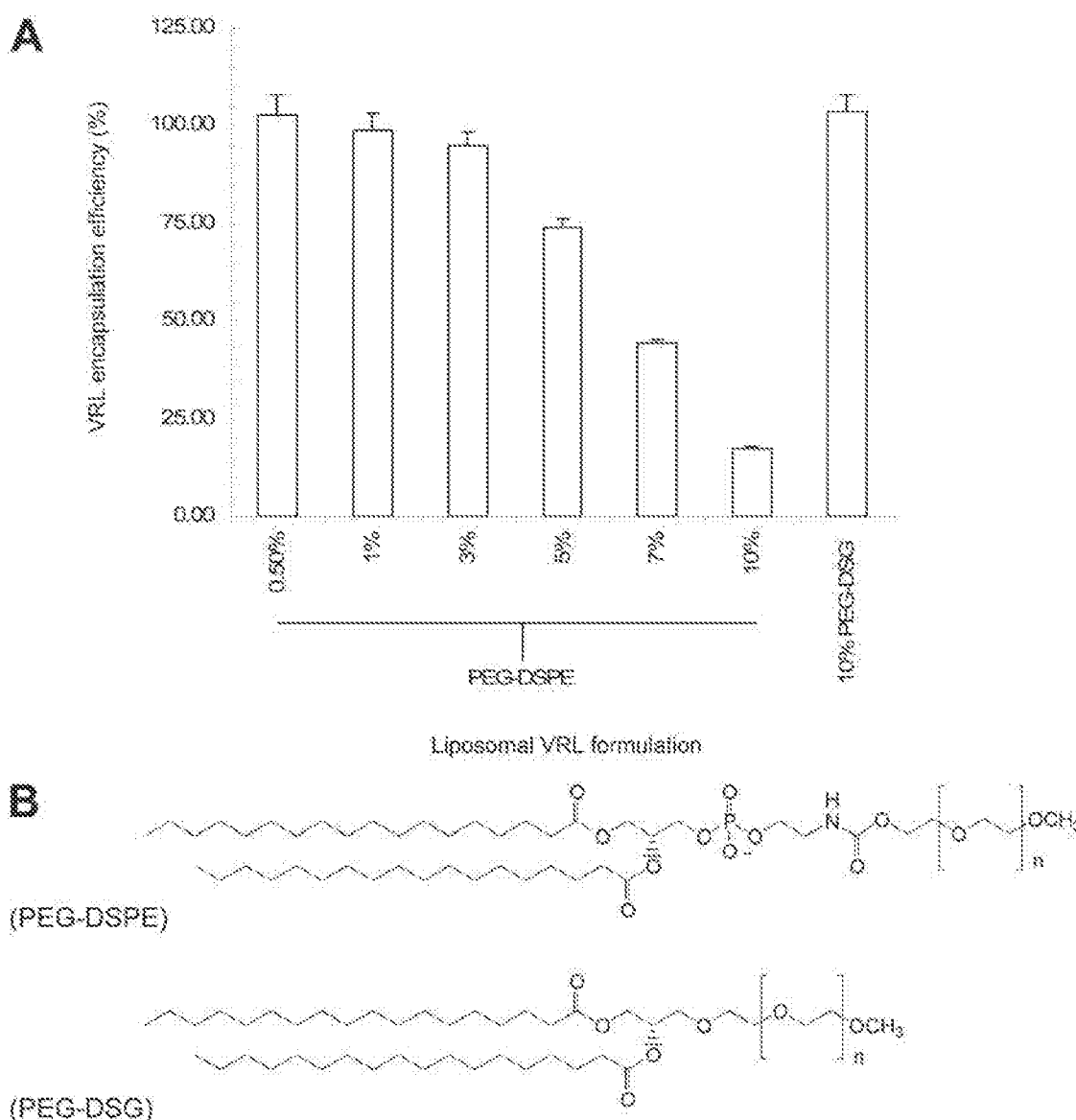


**Fig. 3.** Effect of inclusion of PEGylated lipids on VRL encapsulation in liposomes loaded using the TEA<sub>6</sub>SOS gradient-loading method. Liposomes containing TEA<sub>6</sub>SOS were incubated with VRL at pH 6.5 and 60°C for 30 min and then purified by gel filtration chromatography. The amount of drug loaded was determined relative to the theoretical drug entrapment to determine the loading efficiency (percentage). The liposomes tested had increasing concentrations of PEG-DSPE (0.5–10 mol%) or 10 mol% PEG-DSG present in the formulation (A). The chemical structures of PEG-DSPE and PEG-DSG are shown in B.

somal doxorubicin have been prepared using these methods, other drugs have proven more difficult to entrap with a similar degree of stability. A liposomal vincristine formulation has recently shown efficacy in a phase II clinical trials in lymphocytic leukemia (Thomas et al., 2006). This formulation resulted from the combination of a pH gradient remote-loading strategy for vincristine and the use of a formulation-stabilizing sphingomyelin and cholesterol lipid composition (Webb et al., 1995; Embree et al., 1998). Although the relatively stable encapsulation of vincristine in this case represents a significant advance in liposome technology, it is notable that the *in vivo* stability of the formulation remains significantly less than that observed for liposomal formulations of doxorubicin (Sapra et al., 2004). Vinorelbine and vinblastine present even greater challenges to stable encapsulation due to their more hydrophobic chemical structure (Semple et al., 2005; Zhigaltsev et al., 2005).

Ammonium gradients of citrate or dextran sulfate as counterions were successfully used to load vincristine into PEGylated phosphatidylcholine-based liposomes (Allen et al., 1995; Zhu et al., 1996). Liposomal vincristine formed using the polyanion suramin was nearly as stable as liposomal doxorubicin formulations prepared using ammonium sulfate gradients (Zhu et al., 1996). However, the increased stability did not readily translate into increased efficacy, with the more rapidly releasing ammonium citrate formulation demonstrating the greatest efficacy. This result illustrates the need to develop methods for regulating the drug-release rates of liposomal drug formulations to allow for stability in the circulation, but release of the active agent upon reaching the tumor.

We have recently described a method for stably encapsulating drugs with weakly basic amines that uses substituted ammonium salts of various polyanions (Drummond et al.,

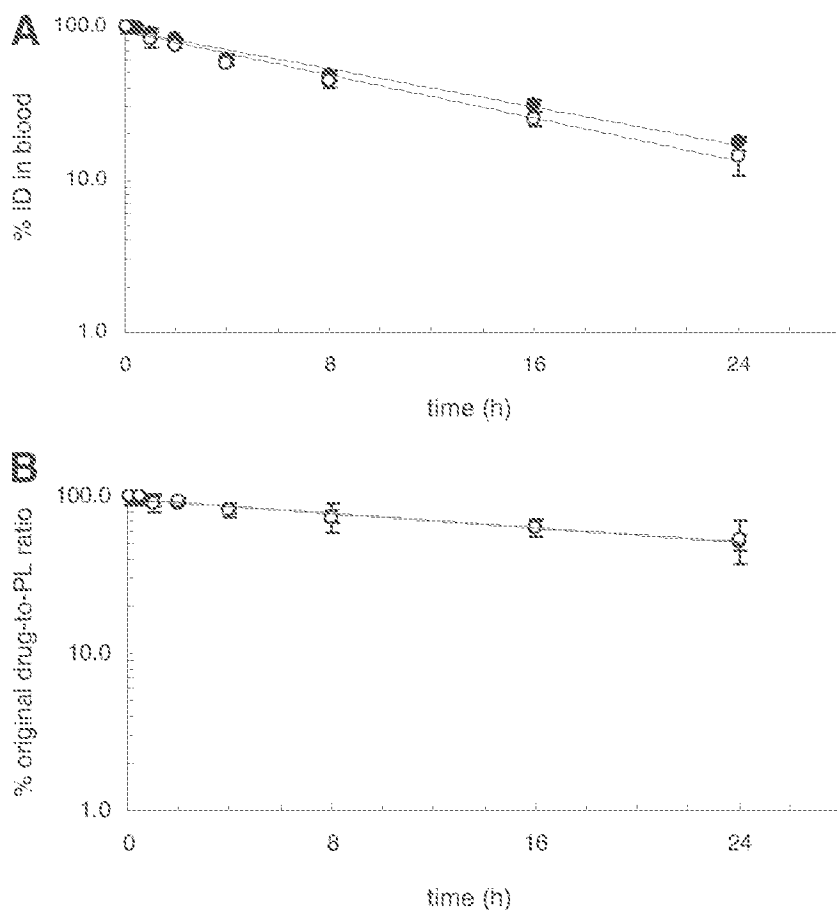


**Fig. 4.** Pharmacokinetics of vinorelbine and lipid matrix of minimally PEGylated (PEG-DSPE, 0.5 mol%; ○) and highly PEGylated (PEG-DSG, 10 mol%; ●) liposomes. The liposomes were loaded at a drug-to-phospholipid ratio of 350  $\mu\text{g}$  VRL/ $\mu\text{mol}$  PL using the TEA<sub>3</sub>SOS formulation method. The pharmacokinetics of VRL (A) were followed as a function of time using HPLC analysis for VRL quantitation in the plasma and the dynamics of the drug-to-liposomal lipid ratio in the blood of a rat (B) *in vivo* following intravenous bolus administration for each of the various liposomal vinorelbine formulations was also determined. Two rats were used for determination of the pharmacokinetics, and the average and cumulative errors of those measurements are plotted. Liposomal lipid concentrations in the blood were determined by scintillation counting of the nonexchangeable lipid marker [<sup>3</sup>H]cholesterylhexadecyl ether.

2005, 2006). For nanoliposomal vinorelbine formulations prepared using this technology, we show that the degree of *in vivo* stability can then be controlled by modifying the chemical nature of the polyanionic trapping agent used (i.e., SOS > poly-Pn > SO<sub>4</sub>) or by modifying the encapsulated drug-to-phospholipid ratio (350  $\mu\text{g}$  VRL/ $\mu\text{mol}$  PL > 220  $\mu\text{g}$  VRL/ $\mu\text{mol}$  PL). Using this strategy, we were able to effectively improve the *in vivo* drug-release rates over a wide range (Fig. 1C; Table 1). The most stable of these formulations used a polysulfated nonpolymeric sugar, sucrose octasulfate. Using liposomally entrapped triethylammonium salt of sucrose octasulfate allowed to load vinorelbine into liposomes at quite high drug-to-phospholipid ratios (>450  $\mu\text{g}$  VRL/ $\mu\text{mol}$  PL). The high degree of *in vivo* stability of these formulations suggests that the drug is retained long enough to remain within the liposomes following their accumulation in tumors. However, as demonstrated in multiple antitumor efficacy studies (Figs. 2 and 5), the rate of release is not so slow as to preclude its antitumor activity, and it is similar to that observed for remotely loaded doxorubicin liposomes (Sapra et al., 2004).

We hypothesize that increased stability of nLs-VRL prepared by the TEA-SOS method may be at least partially attributed to strong ionic interaction between sucrose octasulfate anion and the drug cation, resulting in stable complexation, potentially with gelation and/or precipitation of the complex within liposomes. In our experiments, mixing vinorelbine bitartrate at 1 to 5 mg/ml with the TEA<sub>3</sub>SOS solution at pH 5 to 7 resulted in gelation and development of turbidity, suggesting such complexation. Interestingly, re-

duction of intraliposomal solubility of vinorelbine by forming a salt with entrapped aromatic sulfonate, in particular, *p*-hydroxybenzene sulfonate, resulting in prolonged *in vivo* drug retention within sphingomyelin liposomes was reported recently (Zbigaltsev et al., 2006).

We hypothesized that stable encapsulation of vinorelbine in liposomes, and selective delivery to solid tumors, could increase its anticancer efficacy and potentially reduce its toxicity. We chose to use our most stable liposomal vinorelbine, loaded using a TEA<sub>3</sub>SOS gradient, due to the perceived requirement for stable encapsulation in treating solid tumors. Our results here demonstrated a slightly improved MTD (23.8 versus 17.5 mg VRL/kg) when vinorelbine was administered as a liposomal formulation compared with the free form of the drug. The drug-free liposomes were nontoxic at the highest achievable lipid dose. Although liposome encapsulation of schedule-independent drugs, such as doxorubicin, often result in a substantial decrease in the MTD when studied in animal models, schedule-dependent drugs have often displayed an increase in the MTD due to the sustained release of the drug from its carrier (Tardi et al., 2000; Drummond et al., 2005, 2008). However, the substantial increase in efficacy is enough to compensate and allow for an improvement in the therapeutic index for the liposomal drug. Thus, the minimal improvement in the MTD upon stable encapsulation of the schedule-dependent vinorelbine is not surprising.

Liposomal vinorelbine was also consistently and significantly more active than free vinorelbine in the treatment of colon and breast carcinoma models. A multidose study in a C-26 colon carcinoma model indicated liposomal vinorelbine

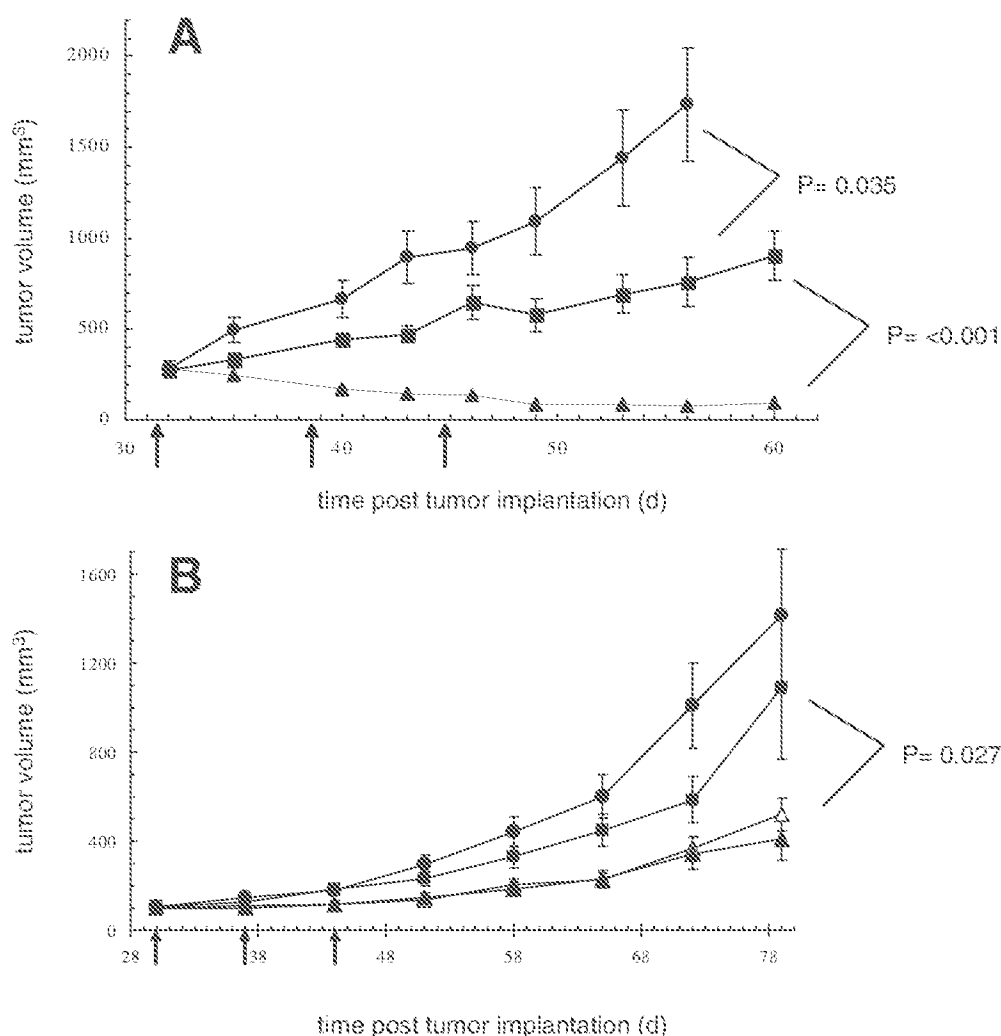


**Fig. 5.** Antitumor efficacy of PEGylated liposomal vinorelbine in (A) human breast (BT-474) tumor and (B) human lung (Calu-3) xenografts. A, female NCR *nu/nu* mice were subcutaneously implanted with 60-day sustained-release estrogen pellets and in 2 days were inoculated subcutaneously with a 0.1-ml suspension containing  $2 \times 10^7$  BT-474 cells. At day 25 after tumor cell inoculation, when the tumors reached approximately 200 mm<sup>3</sup> in size, the mice were randomized into three groups of eight animals per group and treated i.v. with saline (●), 5 mg/kg free VRL (⊙), or pLS-VRL with SOS as a counter-ion (▲), at a dose of 5 mg VRL/kg weekly for a total of three injections. The control group received an equal volume of normal saline. B, male NCR *nu/nu* mice were subcutaneously inoculated with  $1.5 \times 10^7$  Calu-3 cells and subsequently treated weekly (see arrows) with saline (●), 5 mg/kg free VRL (⊙), or 4 (▲) or 6 (▲) mg/kg VRL of pLS-VRL with SOS as a counter-ion when the tumors reached an average size of 105 mm<sup>3</sup>.

was a minimum of 3-fold more active than free vinorelbine in the treatment of this model (Fig. 2A). Together, the observed improved toxicity and antitumor efficacy suggest a significant widening of the therapeutic window by stable encapsulation of vinorelbine in liposomes.

Finally, a highly PEGylated liposome formulation of vinorelbine without the loss of loading efficiency or in vivo drug encapsulation stability was developed. Attempts to encapsulate VRL using an ammonium sulfate gradient indicated a significant inhibition of loading when PEG-DSPE was incorporated at greater than 3 mol% of the total phospholipid. We observed a similar inhibition when using a TEA<sub>0</sub>SOS gradient to load VRL (Fig. 3A). However, substitution of the nonionic PEG-distearoylglycerol (Fig. 3B) for PEG-DSPE resulted in quantitative loading, even at 10 mol% PEG-DSG. Interestingly, at the studied dose of 10 mg/kg, the pharmacokinetics of 10% PEG-DSG nLS-VRL in rats was nearly identical to that of minimally PEGylated (0.5 mol% PEG-DSPE) nLS-VRL. In addition, the rate of drug release from the liposome was not affected by inclusion of the PEGylated lipid. In previous studies, the use of the nonionic PEG-ceramide resulted in a significant improvement over PEG-DSPE; nevertheless, increased drug leakage was observed compared with non-PEGylated liposomes for several vincristine liposome formulations (Webb et al., 1998). Because the

inclusion of PEGylated lipids was shown to decrease dose dependence of the pharmacokinetic parameters of liposomally encapsulated drugs, thus improving or limiting the heterogeneity of the pharmacokinetics of liposomal drug formulations, the possibility of highly PEGylated VRL liposomes without the loss of formulation quality is valuable. This PEGylated nLS-VRL formulation prepared using the TEA<sub>0</sub>SOS gradient method was considerably more active than free VRL in a BT474 human breast tumor xenograft model, resulting not only in notable tumor growth suppression but also in a complete tumor regression in one of seven animals (Fig. 5).

We believe the development of this new highly stable and active nanoliposomal formulation of vinorelbine provides an opportunity to improve the therapeutic index of this drug, and improve the quality of life for patients being treated with it. Based on these considerations and the data presented here, the nLS-VRL formulation described in this work has entered clinical development.

#### References

- Allen TM, Cheng WW, Hare JL, and Laganis KM (2006) Pharmacokinetics and pharmacodynamics of lipidic nano-particles in cancer. *Anticancer Agents Med Chem* 6:513-523.
- Allen TM, Newman MS, Woodie MC, Mayhew E, and Uster PS (1995) Pharmacokinetics and anti-tumor activity of vincristine encapsulated in sterically stabilized liposomes. *Int J Cancer* 62:199-204.
- Astrup T, Flyger HH, and Gormsen J (1955) The anticoagulant activity and toxicity

- of dextran sulphate and a xylan polysulphuric acid. *Scand J Clin Lab Invest* 7:204-211.
- Bally MB, Nayar R, Masin D, Hope MJ, Cullis PR, and Mayer LD (1990) Liposomes with entrapped doxorubicin exhibit extended blood residence times. *Biochim Biophys Acta* 1023:133-139.
- Bartlett GR (1959) Phosphorous assay in column chromatography. *J Biol Chem* 234:466-468.
- Einet S, Chaineau E, Fellous A, Lataste H, Krihorian A, Couzinier JP, and Meisinger V (1990) Immunofluorescence study of the action of doxorubicin, vincristine and vinblastine on mitotic and axonal microtubules. *Int J Cancer* 46:262-266.
- Bilten KJ, Figg WD, Venzon DJ, Dalakas MC, Bowden C, Headlee D, Reed E, Myers CE, and Cooper MR (1995) Pharmacologic variables associated with the development of neurologic toxicity in patients treated with suramin. *J Clin Oncol* 13:2223-2229.
- Cheung BC, Sun TH, Leenhouts JM, and Cullis PR (1998) Loading of doxorubicin into liposomes by forming Mn<sup>2+</sup>-drug complexes. *Biochim Biophys Acta* 1414:205-216.
- Drummond DC, Marx C, Guo Z, Scott G, Noble C, Wang D, Pallavicini M, Kirpotin DE, and Benz CC (2005) Enhanced pharmacodynamic and antitumor properties of a histone deacetylase inhibitor encapsulated in liposomes or ErbB2-targeted immunoliposomes. *Clin Cancer Res* 11:3392-3401.
- Drummond DC, Meyer O, Hong K, Kirpotin DE, and Papahadjopoulos D (1999) Optimizing liposomes for delivery of chemotherapeutic agents to solid tumors. *Pharm Res* 51:691-743.
- Drummond DC, Noble CO, Guo Z, Hong K, Park JW, and Kirpotin DE (2006) Development of a highly active nanoliposomal irinotecan using a novel intraliposomal stabilization strategy. *Cancer Res* 66:3271-3277.
- Drummond DC, Noble CO, Hayes ME, Park JW, and Kirpotin DE (2008) Pharmacokinetics and in vivo drug release rates in liposomal nanocarrier development. *J Pharm Sci* 97:4696-4740.
- Embree L, Gelmon K, Tolcher A, Hudon N, Heggie J, DeRoos C, Logan P, Bally MB, and Mayer LD (1998) Pharmacokinetic behavior of vincristine sulfate following administration of vincristine sulfate liposome injection. *Cancer Chemother Pharmacol* 41:347-352.
- Flexner C, Barditch-Crovo PA, Kornhauser DM, Farzadegan H, Nerhood LJ, Chaisson RE, Bell KM, Lorentzen KJ, Hendrix CW, and Petty EG (1991) Pharmacokinetics, toxicity, and activity of intravenous dextran sulfate in human immunodeficiency virus infection. *Antimicrob Agents Chemother* 35:2544-2550.
- Gabizon A, Goren D, Horowitz AT, Tzemach D, Lissos A, and Siegal T (1997) Long-circulating liposomes for drug delivery in cancer therapy: a review of biodistribution studies in tumor-bearing animals. *Adv Drug Deliv Rev* 24:337-344.
- Gabizon AA, Barenholz Y, and Bialer M (1993) Prolongation of the circulation time of doxorubicin encapsulated in liposomes containing polyethylene glycol-derivatized phospholipid: pharmacokinetic studies in rodents and dogs. *Pharm Res* 10:703-708.
- Geran R, Greenberg N, MacDonald M, Schumacher A, and Abbott B (1972) Protocols for screening chemical agents and natural products against animal tumors and other biological systems. *Cancer Chemother Rep* 3:1-103.
- Gridelli C and De Vivo R (2002) Vinorelbine in the treatment of non-small cell lung cancer. *Curr Med Chem* 9:879-891.
- Harao G, Cohen R, Bar LK, and Barenholz Y (1993) Transmembrane ammonium sulfate gradients in liposomes produce efficient and stable entrapment of amphiphatic weak bases. *Biochim Biophys Acta* 1151:201-215.
- Jordan MA, Tarover D, and Wilson L (1991) Mechanism of inhibition of cell proliferation by vinca alkaloids. *Cancer Res* 51:2212-2222.
- Kirby C and Gregoriadis G (1982) The effect of lipid composition of small unilamellar liposomes containing melphalan and vincristine on drug clearance after injection into mice. *Biochem Pharmacol* 32:609-615.
- Lim HJ, Masin D, Madden TD, and Bally MB (1997) Influence of drug release characteristics on the therapeutic activity of liposomal mitoxantrone. *J Pharmacol Exp Ther* 281:566-573.
- Mathe G and Keizerstein P (1985) Phase I pharmacologic study of a new Vinca alkaloid: navelbine. *Cancer Lett* 27:285-293.
- Matsumura Y and Maeda H (1986) A new concept for macromolecular therapeutics in cancer chemotherapy: mechanism of tumorotropic accumulation of proteins and the antitumor agent SMANCS. *Cancer Res* 46:6387-6392.
- Mayer LD, Bally MB, Hope MJ, and Cullis PR (1985) Uptake of antineoplastic agents into large unilamellar vesicles in response to a membrane potential. *Biochim Biophys Acta* 816:294-302.
- Papahadjopoulos D, Nir S, and Oki S (1972) Permeability properties of phospholipid membranes: effect of cholesterol and temperature. *Biochim Biophys Acta* 266:561-583.
- Pool GL, French ME, Edwards RA, Huang L, and Lumb RH (1982) Use of radiolabeled hexadecyl cholesterol ether as a liposome marker. *Lipids* 17:448-452.
- Sapra P, Moose EH, Ma J, and Allen TM (2004) Improved therapeutic responses in a xenograft model of human B lymphoma (Namalwa) for liposomal vincristine versus liposomal doxorubicin targeted via anti-CD19 IgG2a or Fab' fragments. *Clin Cancer Res* 10:1100-1111.
- Semple SC, Leone R, Wang J, Leng EC, Klimuk SK, Essenhardt ML, Yuan ZN, Edwards K, Maurer N, Hope MJ, et al. (2005) Optimization and characterization of a sphingomyelin/cholesterol liposome formulation of vinorelbine with promising antitumor activity. *J Pharm Sci* 94:1024-1033.
- Silvius JB and Leventis R (1993) Spontaneous interlayer transfer of phospholipids: dependence on acyl chain composition. *Biochemistry* 32:13218-13225.
- Tardi P, Choie E, Masin D, Redebecker T, Bally M, and Madden TD (2000) Liposomal encapsulation of topotecan enhances anticancer efficacy in murine and human xenograft models. *Cancer Res* 60:3389-3393.
- Thomas DA, Sarris AH, Cortes J, Faderl S, O'Brien S, Giles FJ, Garcia-Manero G, Rodriguez MA, Cabanillas F, and Kantarjian H (2006) Phase II study of sphingosomal vincristine in patients with recurrent or refractory adult acute lymphocytic leukemia. *Cancer* 106:120-127.
- Webb MS, Harasym TO, Masin D, Bally MB, and Mayer LD (1995) Sphingomyelin-cholesterol liposomes significantly enhance the pharmacokinetic and therapeutic properties of vincristine in murine and human tumor models. *Br J Cancer* 72:896-904.
- Webb MS, Saxoa D, Wong FM, Lim HJ, Wang Z, Bally MB, Choi LS, Cullis PR, and Mayer LD (1998) Comparison of different hydrophobic anchors conjugated to polyethylene glycol: effects on the pharmacokinetics of liposomal vincristine. *Biochim Biophys Acta* 1372:272-282.
- Weber RL, Vogel C, Jones S, Harvey H, Hutchins L, Bigley J, and Huhnaker J (1995) Intravenous vinorelbine as first-line and second-line therapy in advanced breast cancer. *J Clin Oncol* 13:2722-2730.
- Zhigaltsev IV, Maurer N, Akhiong QF, Leone R, Leng E, Wang J, Semple SC, and Cullis PR (2005) Liposome-encapsulated vincristine, vinblastine and vinorelbine: a comparative study of drug loading and retention. *J Control Release* 104:103-111.
- Zhigaltsev IV, Maurer N, Edwards K, Karlsson G, and Cullis PR (2008) Formation of drug-arylsulfonate complexes inside liposomes: a novel approach to improve drug retention. *J Control Release* 110:378-386.
- Zhu G, Oto E, Vaage J, Quinn Y, Newman M, Engbers C, and Uster P (1996) The effect of vincristine-polyanion complexes in STEALTH liposomes on pharmacokinetics, toxicity and anti tumor activity. *Cancer Chemother Pharmacol* 39:138-142.

Address correspondence to: Dr. Daryl C. Drummond, Hermes Biosciences, Inc., 61 Airport Blvd., Suite D, South San Francisco, CA 94080. E-mail: drummond@hermesbio.com



## Liposome Targeting to Tumors using Vitamin and Growth Factor Receptors

DARYL C. DRUMMOND,\* KEELUNG HONG,\*  
JOHN W. PARK,† CHRISTOPHER C. BENZ,†  
AND DMITRI B. KIRPOTIN\*,†,‡, 1

\*Liposome Research Laboratory, California Pacific Medical Center Research Institute,  
San Francisco, California 94115; and

‡Department of Radiation Oncology and

†Department of Medicine, University of California at San Francisco,  
San Francisco, California 94143

- I. Introduction
- II. Targeting of Liposomes to Vitamin Receptors: The Case of Folic Acid
  - A. Folate Receptor as Internalizing Target on Malignant Cells
  - B. Folic Acid as a Targeting Ligand: Coupling to Liposomes
  - C. Interaction of Folate-Targeted Liposomes with FR-Overexpressing Cells
  - D. Delivery of Antineoplastic Drugs to Cancer Cells by Folate-Targeted Liposomes
  - E. Delivery of Genes and Antisense Oligonucleotides to Cells Using Folate Targeting
  - F. *In Vivo* Implications for Folate-Mediated Liposome Targeting
  - G. Other Vitamin Receptors as Targets for Ligandoliposomes
- III. Targeting Liposomes to Growth Factor Receptors
  - A. Growth Factor Receptors as Recognition Molecules of Malignant Cells
  - B. Design of HER2-Targeted Immunoliposomes
  - C. *In Vitro* Studies with Anti-HER2 Immunoliposomes
  - D. *In Vivo* Studies with Anti-HER2 Immunoliposomes
  - E. Targeted Delivery of Nucleic Acids to Cells through HER2 Receptors
  - F. Liposome Targeting Using Other Growth Factor Receptors
- IV. Conclusions and Future Perspectives
- References

---

Liposome-encapsulated anticancer drugs reveal their potential for increased therapeutic efficacy and decreased nonspecific toxicities due to their ability to enhance the delivery of chemotherapeutic agents to solid tumors. Advances in liposome technology have resulted in the development of ligand-targeted liposomes capable of selectively increasing the efficacy of carried agents against receptor-bearing tumor cells. Receptors for vitamins and growth factors have become attractive targets for ligand-directed liposomal therapies due to their high expression levels on various forms of cancer and

<sup>1</sup>To whom correspondence should be addressed.

their ability to internalize after binding to the liposomes conjugated to receptors' natural ligands (vitamins) or synthetic agonists (receptor-specific antibodies and synthetic peptides). This chapter summarizes various strategies and advances in targeting liposomes to vitamin and growth factor receptors *in vitro* and *in vivo* with special emphasis on two extensively studied liposome-targeting systems utilizing folate receptor and HER2/neu growth factor receptor.

© 2001 Academic Press.

---

## I. INTRODUCTION

Growth, nutrition, and differentiation are among the key functions of living cells that constitute our body. Energy-rich nutrients and structural building blocks, such as sugars, fats, and amino acids, are needed in abundance and enter cells from a lavish extracellular pool. To effectively metabolize the nutrients and build its own bulk, the cell needs vitamins and other enzyme cofactors that are not produced by the cell itself and must be absorbed from a relatively scant environment. Raw power of cellular growth provided by metabolism of nutrients is tamed by the process of cell growth control and differentiation based on intricate communication between the often remote groups of cells through hormones, chemical effectors, and growth factors. Cellular uptake of vitamins and response to hormones and effectors depends on receptor proteins that specifically interact with these substances and elicit proper physiological responses on the cellular level.

Growth and differentiation of the cells are the first functions to change dramatically when the cells become malignant. In malignant cells, the molecular machinery of hormone and growth factor receptors is changed to provide constant stimulation of unabridged cell growth and reduced ability for normal differentiation. Intensive biosynthesis of cellular components, in turn, requires increased supply of metabolic cofactors. Thus, normal and malignant cells often have profound differences in the abundance and function of vitamin and growth factor receptors. Because of these differences and because the receptors for water-soluble, hydrophilic molecules such as peptide hormones and vitamins are usually exposed at the cell surface, vitamin and growth factor receptors are promising "recognition tags" for targeted anticancer drug delivery.

In the malignant phenotype the expression levels of certain vitamin and growth factor receptors are often substantially elevated (Sporn and Roberts, 1985; Slamon *et al.*, 1987, 1989; Berchuck *et al.*, 1990; Weitman *et al.*, 1992; Ross *et al.*, 1994; Fan and Mendelsohn, 1998).

Antibodies, antibody fragments, and small molecule ligands with affinities to cell-surface receptors for vitamins and growth factors have been used to target a variety of toxins (Leamon and Low, 1992; Leamon *et al.*, 1993; Ramakrishnan *et al.*, 1996; Rosenblum *et al.*, 1999), radionuclides (Hartman *et al.*, 1994; Wilder *et al.*, 1996; Multani *et al.*, 1998; Iznaga-Escobar, 1998; Wilbur *et al.*, 1999), enzymes (Rodrigues *et al.*, 1995; Jinno *et al.*, 1996; Lu *et al.*, 1999) and small-molecule therapeutics (Sivam *et al.*, 1995; Uckun *et al.*, 1998; Tolcher *et al.*, 1999) specifically to receptor-overexpressing cancer cells. There are some limitations inherent to each of these approaches. Toxin conjugates, for example, are quite immunogenic and even at subtherapeutic doses still have nonspecific toxicity characteristic for the toxin domain. Frequent toxicity in this case is vascular leak syndrome (VLS), characterized by hypoalbuminemia, weight gain, hypotension, and peripheral and pulmonary edema resulting from extravasation of fluid and proteins from the vascular compartment (Vitetta *et al.*, 1991; Grossbard *et al.*, 1992, 1993; Sausville *et al.*, 1995; Stone *et al.*, 1996). Cancer cell-specific radionuclide-antibody conjugates have shown significant promise in the treatment of hematological cancers but are associated with significant hematological toxicities, are limited by the so-called binding-site barrier in solid tumors (Weinstein *et al.*, 1987), and may be limited to use in large clinical centers due to the need for complex dosimetry calculations and an on-site radiopharmacy (Multani and Grossbard, 1998; Iznaga-Escobar, 1998). All these types of targeted drug-delivery systems are limited by their rapid clearance from the circulation, low number of active drug delivered per targeting event (interaction of the targeted drug carrier with the target cell), and potential inactivation of the cytotoxic agent upon coupling to a targeting ligand or upon exposure to the biological media after administration into the body. These limitations, however, are not inherent to drug-delivery systems based on liposomes.

Liposomes were first described in 1960s when Bangham and co-workers discovered that lecithin swelling in aqueous buffers forms microscopic bodies composed of nested lipid bilayers enclosing aqueous interior (Bangham, 1963; Bangham *et al.*, 1965). During more than 3 decades since this discovery, liposomes have been the subject of numerous studies, books, and reviews. For details of current liposome technology we refer the reader to an excellent and comprehensive textbook by Lasic (1993) and to a recent book that offers state-of-the-art coverage of liposome drug delivery in general (Lasic and Papahadjopoulos, 1998).

Generally, liposomes are vesicular structures consisting of one or more enclosed lipid-bilayer membranes (lamellae) that encircle an

aqueous space containing the solute of interest, which in the context of this chapter is an anticancer active principle, whether it is a small-molecular-weight drug or a large macromolecule like DNA. Liposomes are generally produced when certain lipids, especially the natural lipid components of biomembranes, e.g., phosphatidylcholine, are allowed to swell in aqueous buffers and then are fragmented by mechanical shearing, ultrasonication, microfluidization, or extrusion through micro- or nanoporous membranes; alternatively, the lipids are solubilized in the presence of a dialyzable detergent which is then removed to allow the lipid molecules to associate in bilayers and form vesicles. Lipids in the membranes of liposomes are organized in two-dimensionally oriented (liquid crystalline) phases not unlike biological membranes; this property of liposomes prompted their use as a model of biomembranes in many biophysical and biochemical studies (Lasic, 1993).

The microcontainer nature of liposomes and their natural compatibility with living tissues makes them ideally suited as drug carriers. Water-soluble drugs can be loaded into liposomes simply by sequestering (entrapment) drug solution within liposomes during their formation. Moderately lipophilic drugs having the properties of weak acids or bases can be very effectively encapsulated by “active” or “remote” loading methods by creating a transmembrane gradient of pH and/or electrochemical potential that “drives” the drug into the liposome (Nichols and Deamer, 1976; Mayer *et al.*, 1985; Haran *et al.*, 1993). More lipophilic drugs with poor water solubility usually associate with the liposome bilayer.

Despite common structural features such as vesicular structure and bilayer organization of lipids, various types of liposomes differ with respect to size (from 30 nm to several micrometers), number of bilayers (unilamellar, oligolamellar, or multilamellar), lipid composition, surface charge, and presence or absence of so-called steric stabilization by the surface-attached sugar or hydrophilic polymers which may substantially improve the fate of drug-carrying liposomes in the body (Fig. 1). Common lipid components of liposome membranes, as mentioned above, are phospholipids, such as phosphatidylcholine, and sterols, such as cholesterol. Cholesterol is an important component of liposomal formulations because it reduces membrane permeability (Papahadjopoulos *et al.*, 1972; Mayhew *et al.*, 1979), and thus increases stability of encapsulated drug in the circulation, and because it limits the exchange of membrane components out of the liposomal membrane in blood plasma (Allen, 1981; Damen *et al.*, 1981). Anticancer drugs are commonly formulated into unilamellar liposomes 70–150 nm in size which allows them to permeate through the vasculature of tumors but

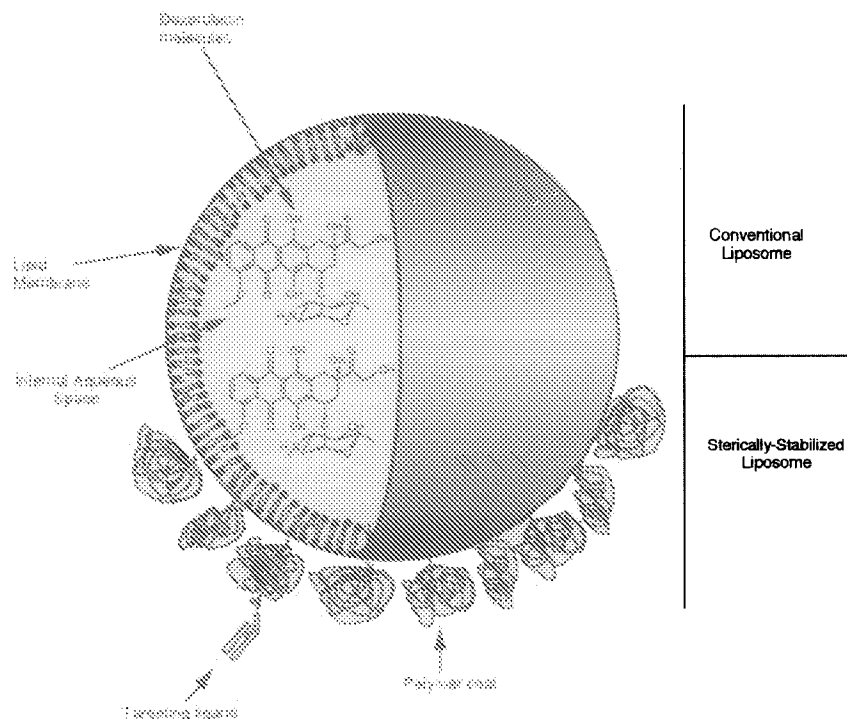


FIG. 1. Schematic representation of a drug-loaded liposome both with poly(ethylene glycol) coating (sterically stabilized liposome, SSL) or without coating ("conventional" liposome). The liposome has a lipid bilayer membrane that encapsulates internal aqueous space used to hold drug substances. Some amphiphilic drugs, such as doxorubicin, can be encapsulated at concentrations exceeding their aqueous solubility and form crystals in the liposome interior. Yet more hydrophobic drugs may be carried within the lipid bilayer. Further modification of the surface by covalently attaching targeting ligands such as small-molecule ligands (e.g., folic acid) or antibody fragments can result in liposomes that are specifically endocytosed by target cells that express a receptor for that ligand or an antigen for the antibody, i.e., folate receptor or growth factor receptor. Phospholipids, such as distearoylphosphatidylcholine (DSPC) and other phosphatidylcholines (lecithins), as well as cholesterol, are common components of systemically delivered liposome formulations, although other lipid compositions are possible.

not of normal tissues (Hobbs *et al.*, 1997). These liposomes are administered intravenously and should be able to persist in the circulation long enough to allow liposome extravasation into the tumor. Early liposomal formulations suffered from fast clearance from circulation by the cells of mononuclear phagocytic system. Significant advance in liposome technology was the discovery that coating of liposome surface with some oligosaccharides or polymers, especially poly(ethylene glycol)

(“sterically stabilized liposomes”) results in remarkably low blood-clearance rates (Gabizon and Papahadjopoulos, 1988; Klibanov *et al.*, 1990; Allen *et al.*, 1991; Papahadjopoulos *et al.*, 1991, Woodle and Lasic, 1992). This discovery, along with the development of highly efficient methods of “active” loading of drugs into liposomes (Cullis *et al.*, 1997) aided in the development of liposomal drugs all the way to clinic.

Clinical trials with liposomal drugs such as doxorubicin and vincristine have shown either similar or increased therapeutic efficacy when compared to the free drug, while significantly altering the toxicity profile and reducing many of the common nonspecific toxicities associated with the free drug (Muggia *et al.*, 1997; Ranson *et al.*, 1997; Gabizon, 1998; Northfelt *et al.*, 1998; Drummond *et al.*, 1999; Gelmon *et al.*, 1999; Shapiro *et al.*, 1999; Valero *et al.*, 1999). These benefits result from a variety of factors, the major one being the substitution of tumor tissue-specific biodistribution of the drug-loaded liposomes for a relatively nonspecific biodistribution of the drug itself (Hwang, 1987; Allen and Papahadjopoulos, 1993; Allen *et al.*, 1995a). Such alteration of the drug biodistribution is possible because of the drug persistence within the circulating liposomes, higher vascular permeability of tumor vessels for microparticles, and low clearance rate of liposomes from tumors which lack lymphatic drainage (for recent reviews see Gabizon *et al.*, 1997; Allen, 1998; Bally *et al.*, 1998; Martin, 1998; Drummond *et al.*, 1999; Gabizon and Barenholz, 1999). The net effect is an increased and selective extravasation of drug-loaded liposomes at the tumor site and an increased accumulation of liposomal drugs at the tumor. This “passive” targeting of liposomes to solid tumors not only increases the therapeutic index of liposome-loaded anticancer drugs, but also enables and benefits further “active,” ligand-directed targeting of drug-loaded liposomes to cancer cells.

Besides their propensity for extravasation into malignant rather than normal tissues, liposomes offer several other advantages as drug carriers for ligand-directed targeting (Rosenberg *et al.*, 1987; Lee and Low, 1994, 1995; Park *et al.*, 1995, 1997a, 1998a; Kirpotin *et al.*, 1997a, 1998). Liposomes can deliver much larger drug payloads per each targeting event. For example, one doxorubicin-loaded liposome internalized into cancer cells via a ligand-receptor interaction carries into the cell approximately  $2 \times 10^5$  molecules of the drug. Liposomes can protect the encapsulated drug from degradation by enzymes and neutralization by antibodies in the central compartment until the drug enters the target cell.

Ligand-directed targeting may increase the bioavailability of liposomal drug to target cells. For the drug to work, it must be released from

the carrier upon reaching the target tissue. Following extravasation, nontargeted liposomes are primarily found in the tumor interstitium surrounding the cancer cells. From relatively stable doxorubicin formulations, such as Doxil (Alza Corp.) the drug is released slowly in the area of close proximity to the tumor, where the free drug may then diffuse into the nearby cancer cells. Liposomes may also be modified for targeting to specific ligands on various target cells by either covalent or noncovalent conjugation of a targeting ligand to the liposome surface. If the liposome is targeted via conjugated ligands to internalizing receptors located preferentially on cancer cells, breakdown of the liposome and release of the drug occurs intracellularly, effectively increasing the amount of bioavailable drug (Machy *et al.*, 1982; Lee *et al.*, 1998; Drummond *et al.*, 1999). For this approach to be effective, the drug must be stable in the acidic environment of the endosomes and lysosomes and in the presence of degradative enzymes located in these intracellular organelles. Luckily, current anticancer drugs of choice for liposomal delivery, such as doxorubicin, daunorubicin, and vinca alkaloids, can escape the organelles of endocytic pathway intact; other drugs, however, such as cytosine arabinoside, may be degraded, resulting in significantly diminished activity (Huang *et al.*, 1983). In addition, liposome internalization may simply serve to limit the diffusion of the released drug away from the tumor, thus exposing more of the tumor to the cytostatic agent (Allen *et al.*, 1998). Active targeting of liposomes will also be important in treating hematological cancers where blood-borne malignant cells will be unable to benefit from the passive targeting approach used in treating solid tumors. Allen and co-workers have recently demonstrated encouraging results targeting liposomes to internalizing CD19 protein exposed on malignant B-cells *in vivo* (Lopes de Menezes *et al.*, 1998).

The above considerations indicate that the efficacy of ligand-directed liposome targeting is higher if after binding to the surface of the target cell the liposome becomes internalized by this cell. Because vitamin receptors often perform cellular transport function and growth factor-receptor complexes are often internalized by the cell as part of cellular response it is more likely that liposomes conjugated to ligands specific to these receptors will be also internalized and will satisfy this requirement. A number of studies where liposomes or lipid complexes were targeted to vitamin and growth factor receptors on cancer cells is given in Table I. Folate receptor is the only vitamin receptor with reported use in liposome targeting, although the use of other vitamin receptors such as that for pyridoxal phosphate or pyridoxine have been mentioned (Zalipsky *et al.*, 1998). Growth factor receptors reported in liposome

TABLE I  
LIGAND-LIPOSOMES TARGETED TO VITAMIN AND GROWTH FACTOR RECEPTORS

Receptor	Liposome composition	Substances delivered	Targeting ligand	Cell lines	Reference
FR	DSPC:Chol	Doxorubicin; marker	Folic acid	KB (human nasopharyngeal carcinoma), HeLa (human cervical carcinoma)	(Lee and Low, 1994, 1995); Wang and Low, (1998)
	HSPC:Chol:PEG-DSPE	Doxorubicin; marker	Folic acid	KB	Gabizon <i>et al.</i> (1999)
	Diplasmenyl(C <sub>16</sub> ) choline: dihydroChol	Ara-C; marker	Folic acid	KB	Rui <i>et al.</i> (1998)
	DSPC:Chol	Oligonucleotides	Folic acid	KB	Wang <i>et al.</i> (1995)
	Anionic liposome	plasmid DNA-polylysine complex	Folic acid	KB	Lee and Huang (1996)
HER-2/neu	PC:Chol; PC:Chol:PEG-DSPE (PC = POPC, HSPC, DSPC)	Doxorubicin; marker	Anti-HER2 Fab' Anti-HER2 scFv	SKBR-3, MCF-7, MCF7HER2; MBA-MD-453; BT-474 (human breast carcinomas); WI-38 (normal human lung)	Kirpotin <i>et al.</i> (1997a, 1997b, 1998, 2000); Park <i>et al.</i> (1996, 1997, 1998a, 1998b, 2000)
	HSPC:Chol:PEG-DSPE	Doxorubicin; marker	Anti-HER2 IgG	N-87 (human gastric carcinoma)	Goren <i>et al.</i> (1996)



EGFR	DOTAP:DOPE:PEG-DSPE	Phosphorothiate oligonucleotide	Anti-HER2 Fab'	SKBR-3	Meyer <i>et al.</i> (1998)
	DDAB:Chol;	Plasmid DNA	Anti-HER2 Fab'	SKBR-3	Park <i>et al.</i> (1997)
	DDAB:Chol:PEG-DSPE	[ <sup>3</sup> H]-inulin (marker)	Human EGF	Fibroblasts	Ishii <i>et al.</i> (1989)
	DPPC:Chol	<sup>125</sup> I-labeled antibody	Anti-human EGFR IgG (C225)	DU-145 (human prostate carcinoma)	Harding <i>et al.</i> (1997)
EGFR	DSPC:Chol:PEG-DSPE	Plasmid DNA	Human EGF	HEC-1A (adenocarcinoma)	Kikuchi <i>et al.</i> (1996)
	DC-Chol:DOPE			GCH-1 (human chorionic carcinoma)	
VEGFR	DSPC:Chol	Anti-VEGF nucleic acid aptamers	Anti-VEGF nucleic acid aptamers	HUVEC (human vascular endothelium)	Willis <i>et al.</i> (1998)
	EggPC:DPPE:Chol	FITC-dextran	Mouse NGF	PC12 (pheochromocytoma), HS294 (human melanoma)	Rosenberg <i>et al.</i> (1987)

targeting studies include the epidermal growth factor receptor, vascular endothelial growth factor receptor, and nerve growth factor receptor (Table I). A variety of different ligands have been used to target these receptors, including antibodies or antibody fragments, small molecules such as folic acid, small peptides/proteins such as the native growth factors, and nucleic acid aptamers. The two most well studied of these approaches are the folate-targeted liposomes using the small-molecule folic acid tethered to the end of a PEG-linked lipid anchor and the anti-HER2 Fab' or single-chain Fv-targeted liposomes (Table I). These two approaches make excellent case studies outlining general methodology in liposome targeting to internalizable cell surface epitopes using small effector molecules or an antibody and are discussed at length in the following sections in comparison to other modes of liposome targeting. It should be noted, however, that although the targeting of growth factor receptors has been primarily accomplished with antibodies or antibody fragments, and the targeting of vitamin receptors with their low-molecular-weight ligands, these approaches are not exclusive. For example, it is also possible and maybe even desirable in some instances to target growth factor receptors with their small-peptide ligands (for example, heregulin, EGF, NGF, and VEGF) or vitamin receptors with antibodies against appropriate receptors.

## II. TARGETING OF LIPOSOMES TO VITAMIN RECEPTORS: THE CASE OF FOLIC ACID

### A. FOLATE RECEPTOR AS INTERNALIZING TARGET ON MALIGNANT CELLS

The vitamin folic acid and its reduced derivatives can be taken up by cells using both a low-affinity ( $K_d \sim 1\text{--}5\ \mu\text{M}$ ) transmembrane protein responsible for the passive diffusion of reduced folates across the plasma membrane of cells and a high-affinity GPI-anchored protein ( $K_d \sim 0.01\text{--}1\ \text{nM}$ ) that accumulates folic acid in the cell following receptor-mediated endocytosis by a clathrin-independent pathway (Kane *et al.*, 1986, 1989; Kamen *et al.*, 1988). The former is referred to as the reduced folate carrier (RFC) and demonstrates a considerable preference for reduced folates, such as 5-methyltetrahydrofolate, methotrexate, and 5-formyltetrahydrofolate, compared to free folic acid (Henderson, 1990; Antony, 1992). The RFC is unable to bind or mediate the uptake of FA conjugates. The folate-binding protein (FBP), also referred to as the folate receptor (FR), is actually a class of receptors expressed in low levels on some normal epithelial cells (FR- $\alpha$  Zimmerman, 1990;

Holm *et al.*, 1991, 1992, 1993; Ross *et al.*, 1994; Patrick *et al.*, 1997), hematological cells (FR- $\beta$  and FR- $\gamma$ ; Shen *et al.*, 1994; Reddy *et al.*, 1999), and placenta (FR- $\beta$  Ratnam *et al.*, 1989). However, it is highly overexpressed in a number of different cancers (Mattes *et al.*, 1990; Boerman *et al.*, 1991; Weitman *et al.*, 1992, 1994; Garin-Chesa *et al.*, 1993; Ross *et al.*, 1994; Toffoli *et al.*, 1997). For the most part, FR- $\alpha$  is overexpressed in carcinomas such as ovarian carcinomas, while FR- $\beta$  is overexpressed in hematological cancers (Ross *et al.*, 1994). A wide variety of different therapeutic and diagnostic agents have been studied in folate-mediated targeting to malignant cells and tissues expressing FR (Leamon and Low, 1991; Leamon *et al.*, 1993; Lee and Low, 1995; Mathias *et al.*, 1996, 1998; Lu *et al.*, 1999). These studies were recently reviewed (Reddy and Low, 1998; Wang and Low, 1998). Folate and its various conjugates are taken up by cancer cells by receptor-mediated endocytosis (Antony *et al.*, 1985; Leamon and Low, 1991; Turek *et al.*, 1993; Lee and Low, 1994). The route of internalization for the FR is to some extent still controversial. It has been demonstrated that the FR becomes localized to non-clathrin-coated pits known as caveolae (Rothberg *et al.*, 1990; Turek *et al.*, 1993). Lending support to this mode of internalization, two specific inhibitors of caveolae assembly (nystatin) or internalization (phorbol-12-myristate) were shown to inhibit uptake of FA conjugates (Lee *et al.*, 1996), although neither drug inhibits clathrin-mediated endocytosis (Smart *et al.*, 1994). However, in other studies, folate receptors appear not to colocalize with caveolae (Mayor *et al.*, 1994; Wu *et al.*, 1997). Lending further support to the role of caveolae in folate uptake, FR chimeras targeted to clathrin-coated pits rather than caveolae were found to be unable to efficiently transport 5-methyltetrahydrofolate into the cytoplasm (Ritter *et al.*, 1995). Turek *et al.* (1993) showed that folic acid conjugates of BSA were taken up by caveolae and resided in multivesicular bodies at early time points (<60 min), but converged with the clathrin-mediated pathway used by transferrin conjugates at later times. However, clathrin-mediated endocytosis may be a relatively minor pathway for cells that overexpress very high numbers of the receptor (Rijnboutt *et al.*, 1996). A diagram indicating the various possible routes of uptake for both vitamin and growth factor receptors is given in Fig. 2. The final destination may be dependent on the multiplicity of the interaction between the targeted molecule and the receptor, where cross-linking of the receptors leads to uptake into caveolae (Mayor *et al.*, 1994). Due to the multiple copies of the folic acid conjugated to the liposome surface, liposomes may favor targeting to caveolae. Despite the large volume of work on the subject, a definitive answer as to the complete route of internalization following

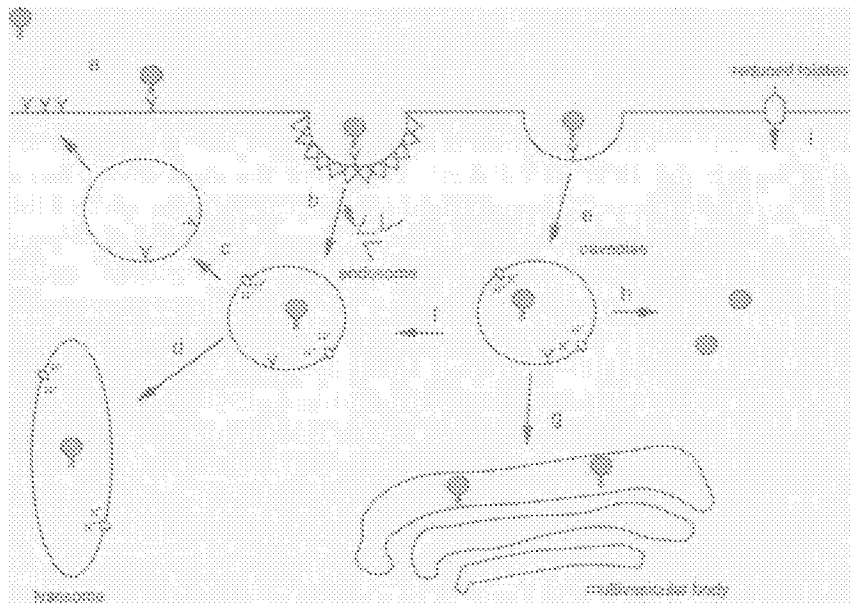


FIG. 2. Potential fates of ligand-targeted liposomes following binding to a target cell. Upon binding to cell-surface receptors, liposomes can either remain bound at the cell-surface, disassociate from the receptor, or accumulate in coated or noncoated invaginations. Following clathrin-mediated endocytosis (a), liposomes can be delivered to lysosomes (c) where they and their contents may be degraded by lysosomal peptidases and hydrolases. Receptors may be recycled back to the cell surface (b) or targeted for degradation in the lysosome (c). Some GPI-anchored receptors, such as the FR, can be taken up by caveolae-mediated endocytosis. Following internalization, the conjugated molecule can remain in caveolae, be transported to multivesicular bodies (g) or into the cytoplasm (h) and possibly reenter the lysosomal directed pathway (f). A substantial proportion of the folate-targeted molecules or liposomes appear to remain in a nondegradative compartment, allowing greater feasibility for delivering labile molecules *via* this route.

receptor binding is not known. An answer to this question may prove very important when selecting various molecules for encapsulation or complexation to lipid-based carriers.

Since FR- $\alpha$  is a GPI-anchored protein, phospholipase C treatment of FR- $\alpha$ -overexpressing cells results in a considerable loss of uptake of FA conjugates (Leamon and Low, 1992). In addition to the folate receptor, other receptors commonly found in caveolae include receptors for platelet-derived growth factor (PDGF receptor) (Liu *et al.*, 1996), bradykinin (de Weerd and Leeb-Lundberg, 1997), insulin (Goldberg *et al.*, 1987), and epidermal growth factor (EGFR; Mineo and Anderson, 1996). An extremely important advantage of targeting to this endocytic

pathway as compared to clathrin-mediated endocytic pathway is that the final destination of the targeted molecules in clathrin-mediated endocytosis is the lysosome, where degradative enzymes can degrade labile drugs, genes, or other biomolecules. The caveolae pathway appears to be rather nondestructive, as molecules are able to remain intact for up to days following binding to internalizing receptors (Leamon and Low, 1991; Wang *et al.*, 1995). This results in a significant enhancement of the activity for the delivered molecule (Leamon *et al.*, 1992; Rui *et al.*, 1998). In addition, similar to clathrin-coated vesicles, caveolae are also acidified to a relatively low pH (Lee *et al.*, 1996), allowing for the development of pH-sensitive liposomes for enhanced cytoplasmic delivery (Lee and Huang, 1996; Reddy and Low, 1998; Rui *et al.*, 1998).

#### B. FOLIC ACID AS A TARGETING LIGAND: COUPLING TO LIPOSOMES

Targeting of liposomes to folate receptors was demonstrated by using their natural ligand, folic acid, as a targeting moiety (Lee and Low, 1994). In order to act as liposome-targeting ligands folic acid molecules must be stably conjugated on the outer surface of the liposome in a way that does not impair receptor-binding properties of FA and allows unhindered interaction of the liposome-conjugated FA with FR. Ligands are attached to liposomes by conjugation to lipid molecules sufficiently hydrophobic to act as "membrane anchors" staying in the environment of hydrocarbon chains of the lipid bilayer rather than in the aqueous environment outside the liposome. Anchors with two closely positioned C<sub>16</sub>–C<sub>20</sub> alkyl or acyl chains, such as diacylglycerol derivatives, satisfy this requirement. Opposite to this hydrophobic domain, lipid anchor molecules usually have a chemically reactive group, such as primary amino, carboxy-, or thiol group, that can form a stable bond with the ligand (for review, see Park *et al.*, 1997c; Allen *et al.*, 1997). Distearoyl phosphatidylethanolamine and its N-derivatives are molecules of choice for many liposome–ligand conjugations. These lipid anchors are included in the liposome lipid composition before ligand conjugation or conjugated to ligands to form membranotropic conjugates that are later used to form ligandoliposomes. The molecule of folic acid has two carboxyl groups in its glutamate domain, of which the group in the  $\gamma$ -position can be modified without the loss of FR binding and has been used for making various FR-reactive conjugates, including liposomes. Folic acid has been coupled to preformed liposomes *via* a simple lipid anchor or to a lipid anchor with a PEG spacer having terminal primary amino group using water-soluble

carbodiimide EDAC (Lee and Low, 1994). In another approach, the conjugate was first synthesized and admixed into the lipids prior to the formation of the liposomes (Lee and Low, 1995). One of these coupling strategies is shown in Fig. 3. In this method, folate is first conjugated to diamino-polyethylene glycol using dicyclohexylcarbodiimide (DCC). In this reaction 70–80% of the conjugate contains the linker at the  $\gamma$ -carboxyl group; the remaining conjugate, however, contains the linker in the  $\alpha$ -position and is not reactive with FR. These two components can be separated by ion exchange chromatography due to the difference in pKs between the  $\alpha$ - and  $\gamma$ -carboxyl groups of the folate (pK 2.8 vs 4.5, respectively) (Fan *et al.*, 1991); however, the presence of the  $\alpha$ -derivative does not seem to have negative effect on the targeting properties of subsequently produced FA-conjugated liposomes. The monoderivatized PEG was isolated and reacted with the hydrophobic “anchor” *N*-succinyl-distearoylphosphatidylethanolamine using a similar conjugation step. If the presence of  $\alpha$ -conjugated folate is unacceptable, the conjugate can be constructed by stepwise addition of first, protected glutamic acid, and then, pteric acid to the activated lipid-PEG linker (Knepper *et al.*, 1990), but at a higher cost and with more effort. The liposome lipids and the conjugate were mixed in an organic solvent; following the evaporation of the solvent, they were hydrated together in an aqueous buffer and subjected to usual steps of dispersion and extrusion through nanoporous track-etched membranes to produce 100-nm unilamellar vesicles. This allowed for a more efficient coupling process, avoided the difficulty of developing rigorous and reproducible coupling methods using chemically activated hydrophobic linkers in aqueous solutions, and also eliminated the exposure of drug-loaded liposomes to potentially deleterious coupling reagents and conditions. Finally, one may envision even more elegant methods for the conjugation of folic acid and other water-soluble vitamins to preformed, drug-loaded liposomes based on the remarkable ability of hydrophobically modified poly(ethylene glycols) to merge spontaneously their hydrophobic domains into the liposome bilayers without liposome destruction or even permeabilization (Uster *et al.*, 1996). Indeed, the usefulness of this “insertion” method was recently demonstrated for preparation of peptide- and oligosaccharide-linked liposomes (Zalipsky *et al.*, 1998) as well as for even larger ligands such as antibodies (Ishida and Allen, 1999) and antibody fragments (Kirpotin *et al.*, 2000b). One advantage of using a small, naturally occurring molecule such as folic acid for ligand-mediated targeting, compared to a protein such as an antibody or antibody fragment, is the relatively higher shelf life of the conjugate. Proteins are often more sensitive to changes in environmental conditions

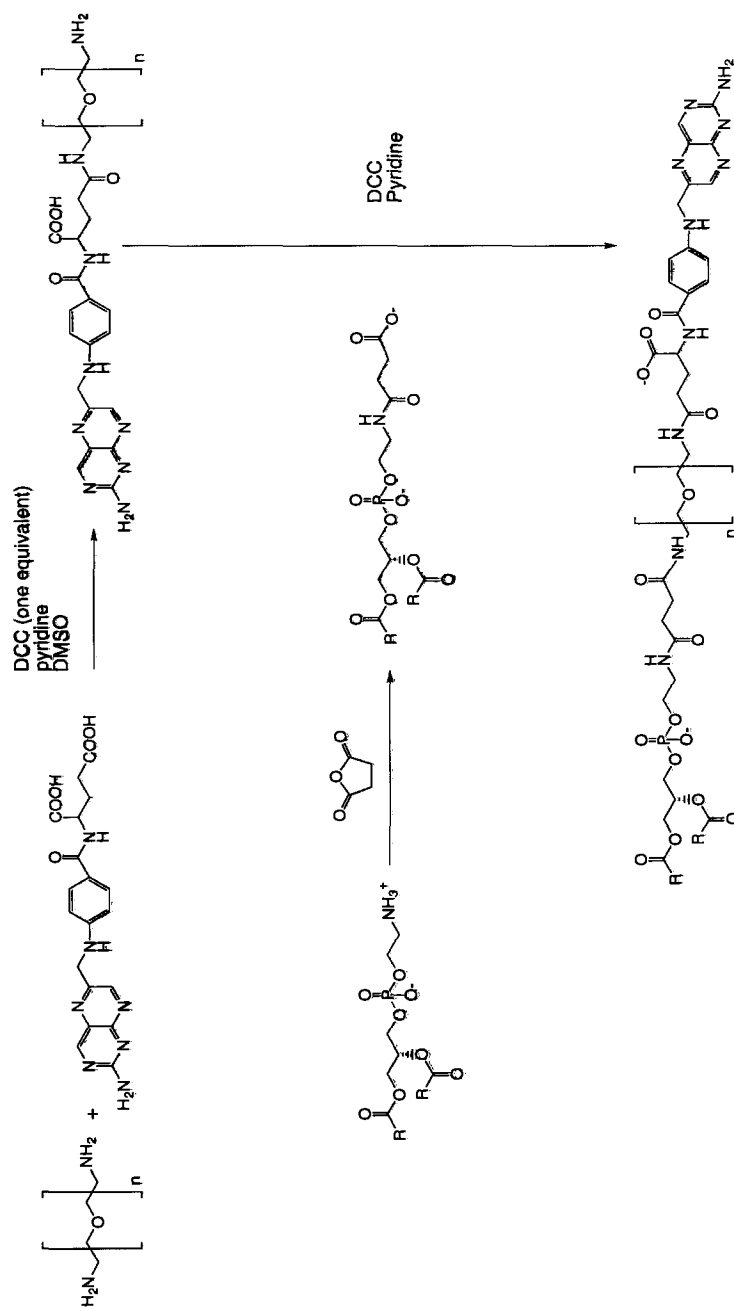


FIG. 3. Synthetic scheme for coupling of folic acid to a lipid anchor (1,2-distearoyl-3-*sn*-phosphatidylcholine; DSPE) via a poly(ethylene glycol) linker. Folic acid is first coupled to poly(ethylene glycol) bis-amine using dicyclohexylcarbodiimide as a coupling reagent. The monoderivatized folic acid-PEG conjugate is purified and subsequently coupled to *N*-succinyl-DSPE using a similar coupling reaction. *N*-succinyl-DSPE can be readily formed from DSPE and succinic anhydride in the presence of a weak organic base (Kung and Redemann, 1986).

and there may be significant stability concerns if they are stored for long periods at 4°C, conditions under which drug-loaded liposomes are normally stored.

### C. INTERACTION OF FOLATE-TARGETED LIPOSOMES WITH FR-OVEREXPRESSING CELLS

Folate-targeted liposomes were first prepared by conjugation of folic acid to a lipid anchor already present in liposome membranes (Lee and Low, 1994, 1995). The PEG spacer, linking FA to the lipid anchor, was determined to be essential in distancing the targeting ligand from the liposome surface to allow binding to the folate receptor on the surface of the cancer cells (Lee and Low, 1994). Little or no cell association was seen when any of several short spacers were used to conjugate folic acid to the surface of the liposome. However, we have noted that while the liposomes with short-spacer FA conjugates did not bind to FR-overexpressing cells, they were quite capable of binding the milk folate-binding protein, which is essentially an extracellular domain of the folate receptor shed from the cell membranes (Kirpotin and Kolhouse, 1993, unpublished observation). Apparently, certain length and flexibility of the liposome–ligand spacer was necessary to allow unhindered binding of the liposome-tethered folic acid to the cell surface receptor; the same may be true for other small-molecule ligands as well. Gabizon and co-workers (1999) showed that the length of the spacer was also important when using FA-PEG-DSPE conjugates on the liposomes containing also unmodified PEG-DSPE used to increase their circulation lifetimes. Cell association was markedly increased when folate was conjugated to liposomes using a PEG spacer greater in length than the PEG chain of the more abundant unmodified conjugate (Fig. 4). Thus, it appears important for the folic acid to be extended above the polymer coat of the liposome to reduce steric hindrance to its receptor and to benefit from the conformational flexibility of the polymer linker which may allow its better access to cell membrane receptors.

Lee and Low (1994) studied the kinetics of folate–liposome associations with the cells. When targeted to FA- $\alpha$ -overexpressing KB cells, FA-derivatized liposomes were seen only at the cell periphery at early times, but were seen throughout the cytoplasm as a punctate fluorescence pattern at later times (4 h). Both the kinetics of internalization and the total number of liposomes bound at saturation ( $2.5 \times 10^5$ ) were lower than for the much smaller albumin conjugates studied in an earlier work (Leamon and Low, 1991). The authors suggested the latter may be a result of the multivalent nature of FA display when present



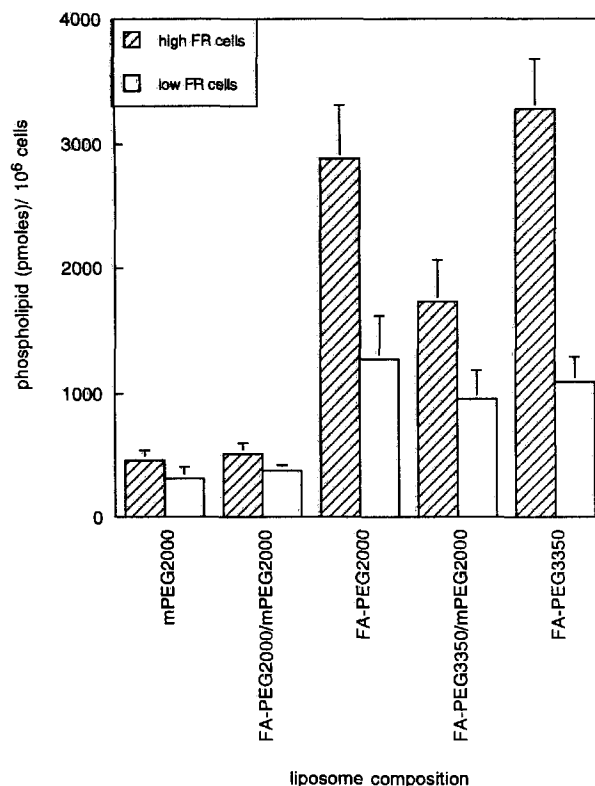


FIG. 4. Effect of PEG length on binding of FA-derivatized liposomes to KB cells. Liposome binding was determined by measuring the amount of cell associated [<sup>3</sup>H]Chol. Liposomes were incubated with KB cells having low (low FR) or high either low- or high (high FR)-folate receptor expression. High expression of folate was achieved by passaging the cells in folate-free medium (the only source of folate being endogenous folate in fetal calf serum, added to the medium at 10%). Liposomes contained folate-PEG-DSPE conjugates with PEG having molecular weights of either 2000 or 3350 (PEG2000 and PEG3350) and in either the presence or absence of PEG2000-DSPE at approximately 7% of total liposomal phospholipids. The cells were incubated with liposomes for 24 h at 37°C. From Gabizon *et al.* (1999), with permission from the American Chemical Society.

in the form of liposomes. The depressed rate of internalization may result from an increased steric hindrance to cell surface receptors due to the larger size of the liposome, compared to albumin. FA liposomes were also shown to be endocytosed by looking at the difference in acid-removable liposomes following incubations at both 4° and 37°C (Lee and Low, 1994). While FA liposomes incubated with KB cells at 4°C could be quantitatively removed from the cells by an acid wash, only

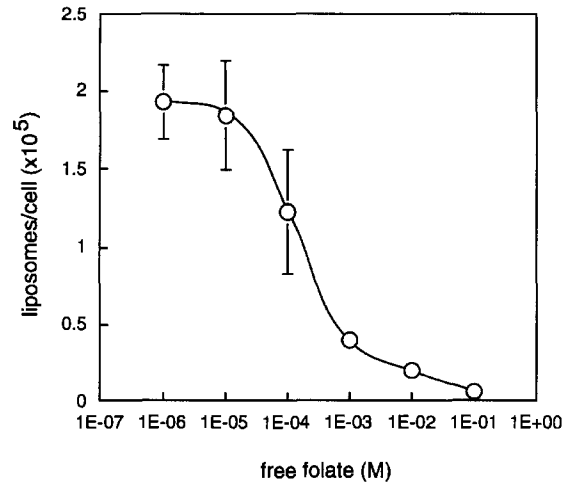


FIG. 5. Effect of folic acid on the uptake of folate-conjugated liposomes by KB cells. KB cells were incubated with calcein-loaded FA-derivatized liposomes for 4 h at 37°C in the presence of varying concentrations of free FA. The amount of cell-associated liposomes was determined from the calcein fluorescence in the detergent lysates of thoroughly rinsed cells. From Lee and Low(1994) with permission from ASBMB.

half of the liposomes could be removed following incubation at 37°C for 4 h. It is interesting that there are still a relatively high number of liposomes at the cell surface even at 4 h, a time where other receptors have been shown to be almost completely internalized to an intracellular localization. This may be a result of the different trafficking pathways involved in caveolae-mediated endocytosis compared to the more typically studied clathrin-mediated endocytosis, which terminates in the lysosome.

This association was shown to be specific for folate-mediated targeting by competitive inhibition studies with either free FA or antiserum against FR- $\alpha$  (Lee and Low, 1994). The inhibition of FA-derivatized liposome association with KB cells by free FA is shown in Fig. 5. Interestingly, a concentration approaching 1 mM free FA was required to inhibit FA-derivatized liposome uptake by KB cells (Fig. 5). This is in contrast to the relatively low  $K_d$  of free FA for the FR (0.01–1 nM; Kamen *et al.*, 1988) and the significantly lower concentrations of free FA (<200 nM) required to inhibit uptake of FA-deferoxamine conjugates (Wang *et al.*, 1996). The multivalent binding of liposome bound conjugates likely leads to this reduced inhibition and gives rise to a targetable therapeutic that may be useful *in vivo* when considering the

relatively low free FA concentrations in plasma (<20 nM; Antony *et al.*, 1985; Kamen *et al.*, 1988; Antony, 1992).

#### D. DELIVERY OF ANTINEOPLASTIC DRUGS TO CANCER CELLS BY FOLATE-TARGETED LIPOSOMES

Several studies have reported the cytotoxicity of drug-loaded FA-targeted liposomes to FR-overexpressing cancer cells (Lee and Low, 1995; Rui *et al.*, 1998). Folate-mediated targeting of doxorubicin-loaded liposomes was shown to increase the cytotoxicity of doxorubicin to FR-overexpressing KB cells when compared to both free doxorubicin (1.6-fold) and nontargeted liposomal doxorubicin (45-fold; Fig. 6). The extrapolation of these results to *in vivo* conditions gives rise to even more promising results due in part to the favorable pharmacokinetic properties of liposomal carriers (Hwang, 1987; Allen *et al.*, 1995a; Drummond *et al.*, 1999). For example, although there is only a 1.6-fold increase in cytotoxicity in cell culture studies, the area under the concentration versus time curve for tumors is approximately 8-fold greater for liposomal doxorubicin compared to free doxorubicin, meaning there is a greater exposure of the cancer cells to the drug *in vivo* when encapsulated in liposomes (Unezaki *et al.*, 1995; Gabizon *et al.*, 1997). This should accentuate the favorable results seen in cell-culture studies even further.

Ara-C has been effectively delivered to KB cells using FA targeting of pH-degradable liposomes composed of di-C<sub>16</sub>-plasmenylcholine (Rui *et al.*, 1998). The IC<sub>50</sub> of ara-C was increased approximately 6000-fold when delivered in folate-targeted pH-degradable liposomes (0.49 μM) compared to free ara-C (2.8 mM). These liposomes are programmed to decompose at a pH characteristic of endosomal compartments. While the authors suggest the heightened sensitivity to ara-C is due in large part to the pH-sensitive lipid composition, it is also possible that targeting to what has already been shown to be a relatively nondestructive endocytic pathway contributes substantially to the increased cytotoxicity. This approach may prove especially fruitful for delivering readily degradable drugs or macromolecules.

#### E. DELIVERY OF GENES AND ANTISENSE OLIGONUCLEOTIDES TO CELLS USING FOLATE TARGETING

Folic acid has also been used as a ligand to target genetic material and antisense oligonucleotides to FR-overexpressing cells (Gottschalk *et al.*, 1994; Wang *et al.*, 1995; Lee and Huang, 1996; Reddy and Low, 1998). Folic acid-derivatized polylysine conjugates were used to condense DNA

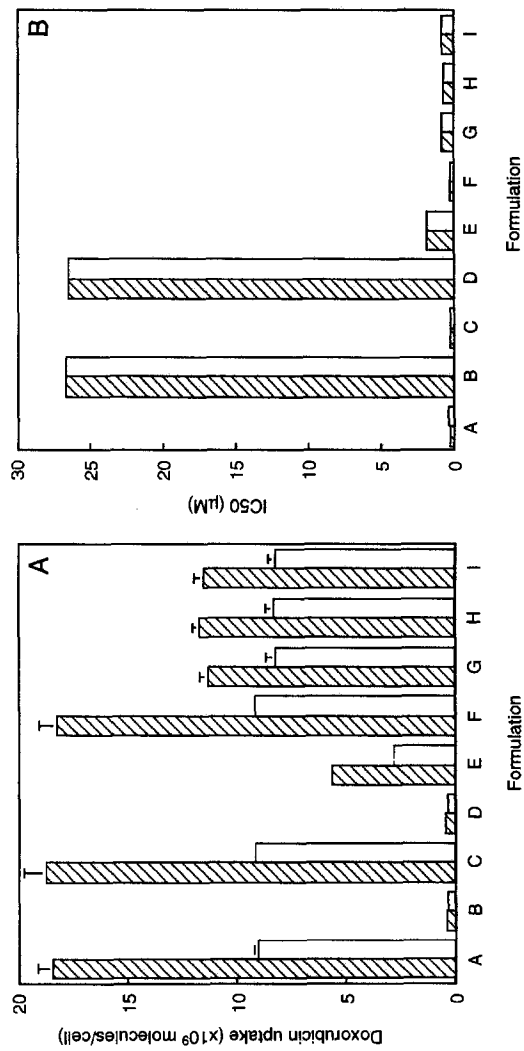


FIG. 6. Cellular uptake and cytotoxicity of folate-targeted and nontargeted formulations of doxorubicin. KB cells (cross-hatched bars) or HeLa cells (open bars) were incubated with doxorubicin formulation (100 µM DOX); folate-conjugated liposomal DOX without PEG coating (FA-L-DOX) (A); DOX in nontargeted, noncoated liposomes (L-DOX) (B); folate-conjugated PEG-coated liposomal DOX (FA-SSL-DOX) (C); nontargeted PEG-coated liposomal DOX (SSL-DOX) (D); FA-L-DOX + 1 mM folic acid (E); FA-L-DOX + 20 nM 5-methyltetrahydrofolate (F); free DOX (G); free DOX + "empty" folate-conjugated liposomes (H); free DOX + "empty" nontargeted liposomes (I). Cell-associated doxorubicin was determined by fluorescence spectroscopy, and cytotoxicity was determined using a tetrazolium (MTT) assay. IC<sub>50</sub> refers to the concentration of doxorubicin that results in 50% decrease in viability compared to sham-treated control. Adapted from Lee and Low (1995), with permission from Elsevier Science.

and antisense oligonucleotides and deliver them specifically to tumor cells (Gottschalk *et al.*, 1994; Citro *et al.*, 1992, 1994; Ginobbi *et al.*, 1997). Gene expression using these targeted complexes was shown to be dependent on the conjugated folate and was also markedly enhanced when coincubated with a replication-defective adenovirus, indicating the need for endosomal disruption for efficient release of DNA from intracellular organelles (Gottschalk *et al.*, 1994).

Lee and Huang (1996) developed a pH-sensitive lipid-DNA particle composed of polylysine-condensed DNA, DOPE, and the pH-sensitive lipid cholesteryl hemisuccinate (CHEMS). At low lipid-to-polylysine condensed DNA ratios the complexes were positively charged and gene expression was independent of folate targeting. However, at higher ratios, where the complexes obtained a net negative charge and a relatively small size (~74 nm), folate targeting resulted in a 20- to 30-fold increase in transfection efficiency when compared to cationic lipid-DNA complexes (DC-Chol:DOPE) and were significantly less cytotoxic. A similar approach complexed polylysine-condensed DNA with FA-targeted anionic liposomes containing the "caged" pH-sensitive lipid *N*-citraconyldioleoylphosphatidylethanolamine (*N*-cit-DOPE; Reddy and Low, 1998). This "caged" lipid was originally described by Drummond and Daleke (1995) and later shown to be useful in preparing pH-sensitive liposomes (Drummond and Daleke, 1997). The use of this "caged" *N*-cit-DOPE was shown to increase transfection efficiency by a factor of 4 to 5 when compared to the similar composition described by Lee and Huang (1996). Other folate-targeted cationic lipid based delivery vehicles may enhance transfection efficiencies even further, similar to the results seen with anti-HER2 targeted cationic lipid-DNA complexes (Section III,E). For lipid-based gene delivery vehicles, active targeting via receptors, such as the folate receptor.

Antisense oligonucleotides against the EGFR were delivered to KB cells via folate targeting to cultured KB cells (Wang *et al.*, 1995). The liposomes utilized in these experiments were composed of eggPC, cholesterol, and either with or without folate-PEG-DSPE. A fluorescein-labeled oligonucleotide was used to show a 16-fold increase in uptake over free oligonucleotides and a 9-fold increase over nontargeted liposomal oligonucleotide. Uptake could be inhibited by free folic acid (1 mM), demonstrating the specificity of internalization. However, delivery to the nucleus was relatively inefficient, likely due to the relatively stable lipid composition used in this particular formulation and thus inability to escape the confines of the endosomes or lysosomes. Finally, while folate-specific growth inhibition did occur, there was no significant difference in growth inhibition between the anti-EGFR oligonucleotide

and the scrambled sequence. These results suggest that folate targeting may be effective at delivering both oligonucleotides and plasmid DNA to receptor-overexpressing cells. However, the efficiency of delivery, both from the endosome and under *in vivo* conditions, needs to be increased and studied further.

#### F. *IN VIVO* IMPLICATIONS FOR FOLATE-MEDIATED LIPOSOME TARGETING

To date, folate targeting of liposomes has been almost exclusively studied in cell culture, with minimal work being completed *in vivo*. Mathias and co-workers (1996, 1998, 1999) have used folic acid to target small-molecule radiotracers for imaging folate receptor-overexpressing tumors *in vivo*. However, the pharmacokinetics of small-molecular-weight compounds such as these are undoubtedly different from those of sterically stabilized or even conventional liposomal carriers. For example, these relatively small-molecular-weight radioconjugates are found in high amounts in the kidney, an organ that would be relatively inaccessible to large liposomal carriers approximating 100 nm in size.

An important concern for use of a folate receptor targeting approach *in vivo* involves the toxicity to normal healthy tissues, specifically those of hematopoietic lineage. The  $\beta$ -isoform of the folate receptor (FR- $\beta$ ) is expressed in high levels on hematopoietic cells (Ross *et al.*, 1994; Shen *et al.*, 1994; Reddy *et al.*, 1999), and thus targeting of cytotoxic agents to this receptor may be expected to result in significant bone marrow toxicity. Fortunately, Reddy and co-workers (1999) were able to demonstrate that CD34+ hematopoietic cells do not bind FA-conjugated liposomes, although these cells overexpress FR- $\beta$ .

The final potential problem with targeting to cell-surface receptors using FA-conjugated liposomes is the binding-site barrier phenomenon observed for tumor-specific antibodies (Juweid *et al.*, 1992; Fujimori *et al.*, 1990): the binding of FA conjugates to FR- $\alpha$  at the site of liposome extravasation may limit its penetration of the tumor and thus accessibility to cancerous cells located any significant distance from the supporting vasculature. However, limited diffusion and the increased bioavailability of encapsulated drugs may be enough in itself to provide a significant improvement to nontargeted liposomes. An alternative approach may be to use antibody fragments against the folate receptor rather than use the ligand itself. The reduced avidity of the targeting ligand for the receptor may result in a more even tumor distribution of the carrier, similar to that seen with anti-HER2-targeted immunoliposomes (Section III,D). While speculation on the feasibility of targeting FRs *in vivo* suggests both significant promise and a degree of

uncertainty, the true test lies in the completion of efficacy studies in appropriate animal tumor models, such as in the treatment of ovarian cancers.

#### G. OTHER VITAMIN RECEPTORS AS TARGETS FOR LIGANDOLIPOSOMES

Few data are available on the targeting of liposomes to cells using receptors for vitamins other than folate. However, the successful development of folate targeting laid the methodological groundwork for the use of other vitamins as ligands for liposomal delivery. As the receptors of these vitamins become better understood with respect to routes of internalization and expression patterns on both normal and malignant cells, further development of other vitamin-targeted strategies will likely be attempted. At present, pyridoxine, pyridoxal phosphate, biotin, riboflavin, and nicotinamide have been reported as targeting ligands other than liposomes for therapeutic or diagnostic agents (Low *et al.*, 1997a,b; Holladay *et al.*, 1999). The developed conjugation strategies can be easily adapted for conjugation of these ligands to liposomes. Preparation of fully functional conjugates of cyanocobalamin (B<sub>12</sub>) with radioiodinated markers and spacer molecules was recently reported, and the chemistry appears amenable to liposome conjugation (Wilbur *et al.*, 1999; McEwan *et al.*, 1999).

Aside from specific targeting of their receptors, vitamins have been used in distinct roles in the development of liposome technology. Thus, biotin has been used as an adaptor molecule for conjugating targeting ligands to liposomes via a noncovalent biotin-streptavidin linkage (Rosenberg *et al.*, 1987; Harasym *et al.*, 1995; Wong *et al.*, 1997).  $\alpha$ -Tocopherol (vitamin E) has been used to prevent oxidative damage to liposomes during storage (Barenholz *et al.*, 1993). These functions of vitamins in liposome technology are out of the scope of this chapter. However, it is safe to say that the groundwork for the use of vitamins as liposome-targeting ligands in the clinic has been firmly set and awaits a promising future.

### III. TARGETING LIPOSOMES TO GROWTH FACTOR RECEPTORS

#### A. GROWTH FACTOR RECEPTORS AS RECOGNITION MOLECULES OF MALIGNANT CELLS

Like their effectors, hormone receptors present a family of structurally and functionally different proteins. Some hormone receptors, such as steroid receptors, are intracellular proteins that are inaccessible

for targeting. Steroid hormones may reach their receptors following diffusion across biological membranes. Receptors for other hormones, such as peptide hormones and growth factors that do not permeate the cell membrane, are plasma membrane proteins whose effector-binding domains are exposed on the cell surface. It is these accessible receptors that prove most valuable for cell-targeted delivery of drugs. The epidermal growth factor receptor (EGFR), fibroblast growth factor receptor (FGF receptor), and HER2/neu receptor have all been shown to be overexpressed in different malignancies (Sporn and Roberts, 1985; Slamon *et al.*, 1987, 1989; Mansson *et al.*, 1989; Beitz *et al.*, 1992; Khazaie *et al.*, 1993; Fox *et al.*, 1994; Scher *et al.*, 1995). In addition, angiogenic vascular endothelial cells supporting the tumor overexpress vascular endothelial growth factor (VEGF) receptors (Shibuya *et al.*, 1990; Tischer *et al.*, 1991; De Vries *et al.*, 1992). The expression levels of these various receptors have been associated with tumor proliferation or metastasis (Yu *et al.*, 1991, 1994; Niehans *et al.*, 1993). Often, high expression levels of these receptors are associated with an increased risk of recurrence or poor survival (Berchuck *et al.*, 1990; Borg *et al.*, 1990; Toi *et al.*, 1991; Chrysogelos and Dickson, 1994; Fix, 1994; Press *et al.*, 1997). These receptors are attractive targets due not only to their high expression levels on malignant cells but also because they have been shown to be endocytosed by receptor-bearing cells following binding of their appropriate ligand or an antibody agonist (Pastan and Willingham, 1981; Tagliabue *et al.*, 1991; Sorkin and Waters, 1993; French *et al.*, 1994; Hurwitz *et al.*, 1995; Kirpotin *et al.*, 1997a). Thus, similarly to vitamin receptors discussed above, targeting to one of these receptors potentially allows the therapeutic agent access to an internal localization in what can be called a "Trojan horse" approach.

The HER2/neu receptor recently became an extensively studied target for liposomes and lipid-based gene- and drug-delivery systems. This receptor is a glycosylated transmembrane protein of approximately 185 kDa that possesses tyrosine kinase activity. It is a member of the epidermal growth factor receptor (EGFR) family and is involved in many growth-signaling pathways within the cell, alone or in cooperation with other members of EGFR family. Several excellent reviews have described the basic biology and biochemistry of the HER2/neu receptor (Hynes and Stern, 1994; Hung and Lau, 1999). This protein has high levels of overexpression in different malignancies ( $10^5$ – $10^6$  receptors/cell), low level of expression in healthy tissues, and homogeneous and stable expression in primary tumors and sites of metastasis (Press *et al.*, 1990; Lewis *et al.*, 1993; Niehans *et al.*, 1993). These characteristics made this protein a prime molecular target for cancer



immunotherapy using a recombinant humanized monoclonal antibody (trastuzumab) and has recently made its way into the clinic (Baselga *et al.*, 1999; Pegram *et al.*, 1998; Shak, 1999). These properties are also likely responsible for the many encouraging preclinical results obtained with an anti-HER2-targeted immunoliposome carrying encapsulated doxorubicin (Section III,D).

#### B. DESIGN OF HER2-TARGETED IMMUNOLIPOSOMES

In contrast to the folate receptor targeting described above, where the natural ligand for FR was also the liposome-targeting ligand, targeting of liposomes to HER2 receptor exemplifies a different approach in which the targeting ligand is an antibody against extracellular portion of the receptor.

The history of antibody-targeted liposomes (immunoliposomes) encompasses two decades of research (Allen *et al.*, 1997). Although immunoliposomes or, in fact, any ligand-targeted liposomes have not yet made their way to the clinic, one can put forward a set of criteria for a successful practical design of immunoliposomes as cancer drug-delivery vehicles (Table II). As discussed in the preceding section, growth factor receptors and especially HER2/neu satisfy the criteria for target antigen selection quite well. Evidently, the targeting function of an immunoliposome requires only the presence of the antigen-binding domain, leaving a researcher with a choice of liposome-conjugated antibodies. A popular option of conjugating whole immunoglobulin molecules to liposomes appears suboptimal because of the poorly defined conjugation site, immunogenicity of xenogeneic IgG (Harding *et al.*, 1997), and enhanced blood clearance of immunoglobulin-conjugated liposomes mediated by mononuclear phagocyte Fc receptor (Aragnol and Leserman, 1986; Derksen *et al.*, 1988). The use of recombinant humanized anti-HER2 Fab' fragments proved to be a better solution. Cysteine residues at the hinge region provided a unique conjugation site by efficient thiol-maleimide chemistry (Martin *et al.*, 1981; Martin and Papahadjopoulos, 1982). Similarly to folate-conjugated liposomes, when steric stabilization of immunoliposomes is desirable in order to prolong their circulation lifetime for better distribution into a tumor, PEG coating hinders the binding of an antibody to cell surface receptors if the spacer between the antibody and the lipid anchor is too short. Attachment of Fab' fragments to the maleimide-activated terminal end of a liposome-linked PEG-lipid (PEG-DSPE) (Fig. 7) resulted in an unimpeded association of immunoliposomes with target cells while preserving long-circulating properties (Shahinian and Silvius, 1995; Zalipsky *et al.*,

## DESIGN CRITERIA FOR LIGAND-DIRECTED LIPOSOME TARGETING

Component	Considerations for optimum design
Target antigen	<p><i>Expression</i> Highly and homogeneously overexpressed in target tissue</p> <p><i>Function</i> Vital to tumor progression, so that down-modulation does not occur or is associated with therapeutic benefit</p> <p><i>Shedding of antigen</i> Limited, to avoid binding to soluble antigen and accelerated clearance</p>
Targeting ligand	<p><i>Affinity</i> High enough to ensure binding at low liposome concentrations Low enough to avoid "binding-site barrier" effect (Weinstein)</p> <p><i>Immunogenicity</i> Humanized MAb, to remove murine sequences. Use fragments without Fc portion (Fab', scFv) to avoid interaction with Fc receptor Small molecular weight ligands should not be immunogenic—may act as haptens</p> <p><i>Internalization</i> Efficient endocytosis by target cells is desirable</p> <p><i>Production</i> Easy and economical scale-up, e.g., by efficient bacterial expression system Stable during storage</p>
Ligand–liposome linkage	<p><i>Stability</i> Covalent attachment to hydrophobic anchor, stable in blood</p> <p><i>Attachment site</i> Away from the binding site to ensure correct orientation of antibody or ligand molecule. Well-defined, to ensure reproducibility and uniformity of coupling Avoids steric hindrance (e.g., from PEG) of ligand binding and internalization</p> <p><i>Chemical nature of the linker</i> Nontoxic, nonimmunogenic, and avoids opsonization Does not affect drug loading or membrane stability Excess linker may be quenched to avoid nonspecific coupling to biomolecules Good availability, economical manufacturing process</p>
Liposome	<p><i>Stability</i> Stable as intact construct <i>in vivo</i></p>

(continued)

TABLE II (continued)

Component	Considerations for optimum design
Drug	<i>Pharmacokinetics</i>
	Long circulating
	<i>Tumor penetration</i>
	Capable of extravasation in tumors
	Small diameter improves penetration into tumor tissue
	<i>Encapsulation</i>
	Efficient, high capacity (e.g., by remote loading)
	Encapsulated drug storage-stable and resists leakage
	<i>Bystander effect</i>
	Drug affects tumor cells not directly targeted (bystander cells)
<i>Interaction with target cells</i>	
Effective against target cell population	
Cytotoxicity enhanced by binding of ligand	

1996, 1998; Kirpotin *et al.*, 1998). An even better choice of liposome-targeting antibody may be single-chain Fv (scFv) fragments selected from phage-display libraries (Marks *et al.*, 1992; Schier and Marks, 1996). Single-chain Fvs are constructed from human immunoglobulin sequences and thus are likely to have little or no immunogenicity in humans. Phage-display selection and affinity maturation (Schier and Marks, 1996; Schier *et al.*, 1996) allow construction of scFvs with a broad range of specificities and binding characteristics. Single-chain Fvs are relatively small (26–29 kDa) recombinant proteins that can be produced in quantities in bacterial hosts, are easily purified, and can be engineered to contain a unique liposome conjugation site, for example, a C-terminal cysteine group, away from the antigen-binding site. Last but not least, a recently reported scFv selection technique based on phage internalization into live target cells (Becerril *et al.*, 1999) allows the creation of scFvs optimized not only for selective binding, but also for selective internalization by the target cells, which is a desirable component of liposome targeting (Nielsen *et al.*, 2000).

Anti-HER2 immunoliposomes targeted to HER2-overexpressing tumors were a subject of several recent studies (Goren *et al.*, 1996; Park *et al.*, 1995, 1997a, 1997b, 2000; Kirpotin *et al.*, 1997a, 1997b, 1998, 2000a). In these studies anti-HER2 immunoliposomes were constructed on the platform of sterically stabilized PEG-coated liposomes containing doxorubicin encapsulated by the ammonium ion gradient method. These liposomes are similar to liposomal doxorubicin, which has been recently introduced into the clinic under the trade name of Doxil (Alza Corp.) (Martin, 1998; Gabizon and Barenholz, 1999).

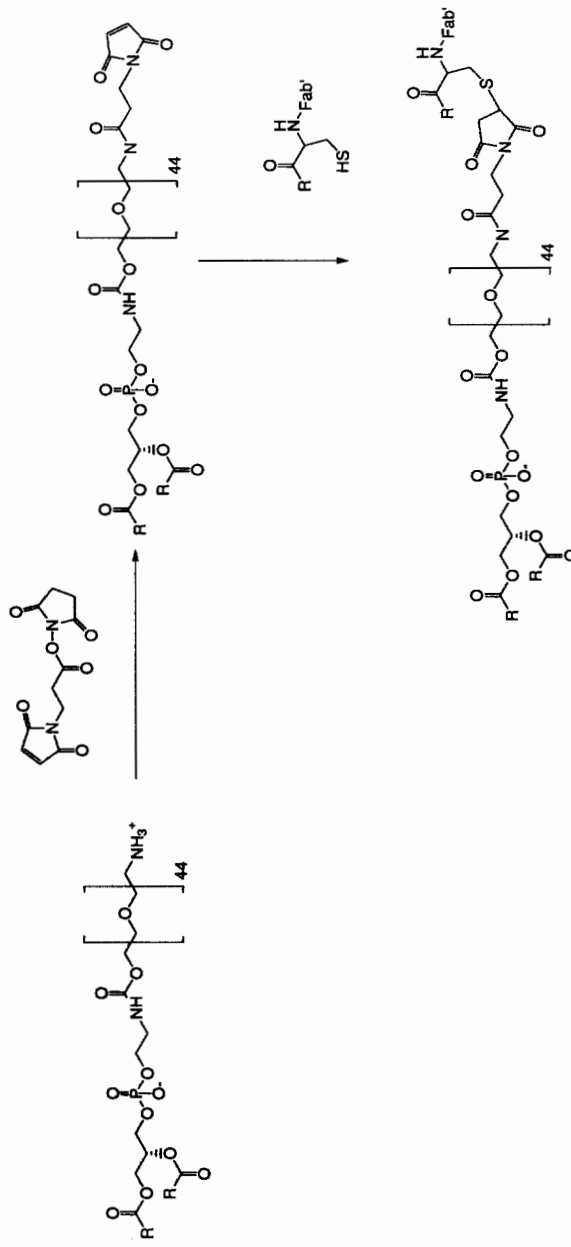


Fig. 7. Synthetic scheme for conjugation of Fab' fragments to liposomes. An amino-PEG-DSPE conjugate is derivatized with the bifunctional cross-linking reagent, N-(γ-maleimidopropionyloxy)succinimide. The obtained maleimide-terminated PEG-DSPE derivative can be incorporated into liposomes and subsequently derivatized with a Fab' or scFv fragment via reduced sulfhydryl group of peptide terminal cysteine, located away from the antigen-binding site specific for a cell-surface receptor. Alternatively, the fragments can be conjugated with maleimido-PEG-DSPE in solution and then captured into the liposome bilayer by co-incubation of the liposomes with the conjugate (Kirpotin *et al.*, 2000a).

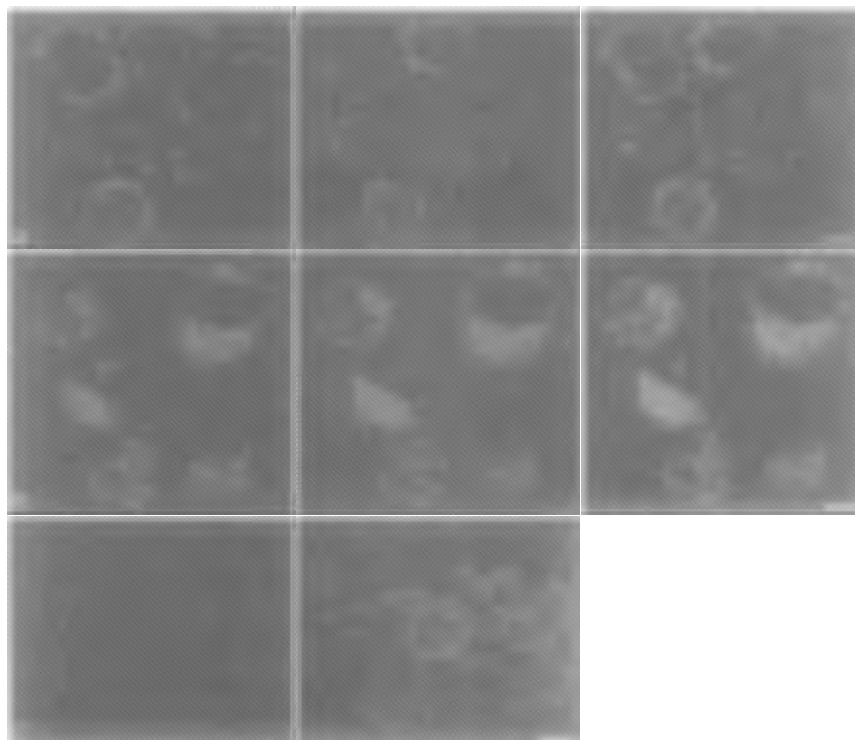


FIG. 8. Uptake of rhodamine-labeled antiHER2 immunoliposomes (left column) and fluorescein-labeled transferrin (middle column) by HER2-overexpressing SKBR3 cells (A,B) or by MCF-7 cells having low expression of HER2 (C). The cells were incubated with liposomes at 0.1 mM of liposome phospholipid and 37°C for 10 min (A) or 30 min (B and C). Liposome localization was visualized by confocal microscopy of intact cells. Superimposed images are shown in the right column. From Kirpotin *et al.* (1997) with permission from the American Chemical Society.

### C. *IN VITRO* STUDIES WITH ANTI-HER2 IMMUNOLIPOSOMES

Interaction of anti-HER2 sterically stabilized immunoliposomes with target cancer cells was first studied in the cultures of human breast carcinoma cells of either low (MCF-7;  $10^4$  receptors/cell) or high (SKBR-3;  $10^6$  receptors/cell) expression levels of the HER2 receptor. Confocal fluorescence microscopy showed colocalization of anti-HER2 targeted immunoliposomes and fluorescein-labeled transferrin (Fig. 8), indicating uptake by HER2-overexpressing cells of liposomes into the clathrin-mediated endocytic pathway (Park *et al.*, 1995; Kirpotin *et al.*, 1997a). MCF-7 cells expressing low levels of the HER2 receptor were able to

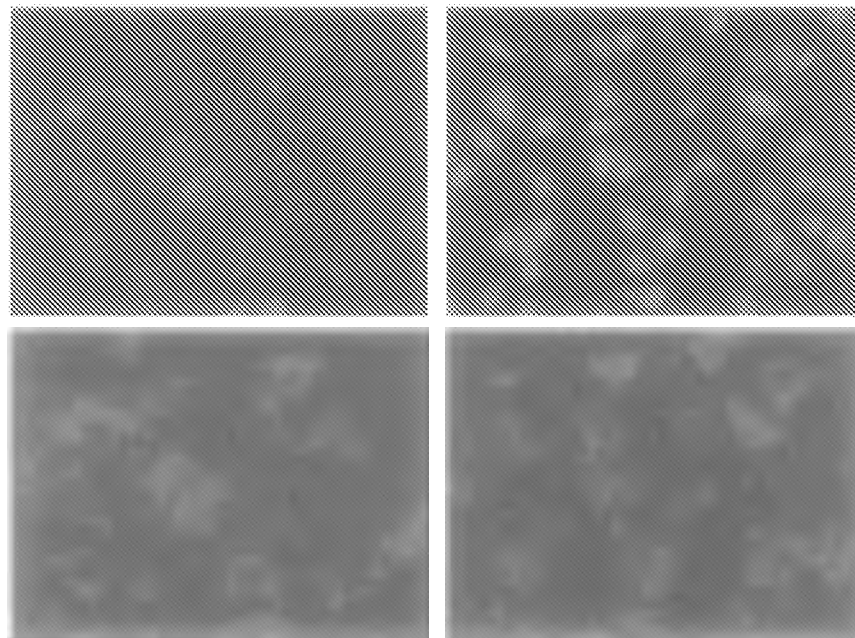


FIG. 9. Intracellular distribution of the components of PEG-DSPE-stabilized cationic liposome (DOTAP:DOPE:PEG-DSPE) complex with FITC-labeled phosphorothioate oligonucleotide (PS ODN) in HER2-overexpressing SKBR3 cells. (Top row) FITC-labeled PS ODN; (bottom row) rhodamine-labeled lipid. Only the complexes where a portion of PEG chains was conjugated to the anti-HER2 Fab' (left column) show nuclear delivery of the oligonucleotide. (Right column) Nontargeted complexes. From Meyer *et al.* (1998), with permission from ASBMB.

take up the transferrin conjugate but not the immunoliposomes. Similar results were obtained with anti-HER2-targeted liposomes containing cationic lipids and complexed with antisense oligonucleotides (Meyer *et al.*, 1998). In this case, not only were the targeted complexes endocytosed, but only those containing anti-HER2-conjugated Fab' were able to effectively deliver the oligonucleotide payload to the cell nuclei (Fig. 9). Both binding and endocytosis of anti-HER2-targeted immunoliposomes depended on the number of conjugated anti-HER2 Fab', which reached a plateau at approximately 30–40 Fab' per 100 nm liposome (Kirpotin *et al.*, 1997a). At 0.025 mM of liposome phospholipid in the cell growth medium, liposome uptake reached a maximum of 8,000–25,000 liposomes per cell after 3–4 h of incubation. Under these conditions, more than 80% of the liposomes were endocytosed. Uptake by low-HER2-expressing MCF-7 cells was undetectable.

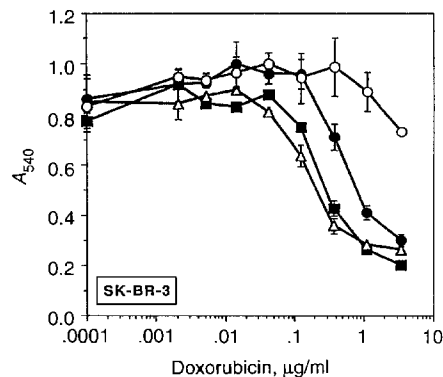


FIG. 10. *In vitro* cytotoxicity of the free or liposome-encapsulated doxorubicin in SKBR3 cells. The cells were treated with doxorubicin in anti-HER2 immunoliposomes without PEG coating ("conventional" immunoliposomes) (●), PEG-coated anti-HER2 immunoliposomes (○), PEG-coated immunoliposomes conjugated to an irrelevant Fab' (■), or free doxorubicin (□). From Park *et al.* (1995) with permission. © 1995 by the National Academy of Sciences.

Cytotoxicity experiments were performed with doxorubicin-loaded anti-HER2 immunoliposomes (Park *et al.*, 1995; Fig. 10). In these initial experiments, the antibody was conjugated directly to the liposome surface rather than to the distal end of a PEG spacer. These targeted immunoliposomes were shown to be as cytotoxic to HER2-overexpressing SKBR-3 cells as free doxorubicin ( $IC_{50} = 0.3 \mu\text{g/ml}$ ). Nontargeted liposomes or liposomes containing an irrelevant antibody were shown to be significantly less toxic than either anti-HER2 immunoliposomes or free doxorubicin. Liposomes containing the sterically hindering PEG-DSPE were shown to also reduce the cytotoxicity of the targeted formulation, presumably due to an interference of receptor binding by the conjugated polymer. Targeted immunoliposomes were also relatively nontoxic to HER2 negative lung fibroblast cells (WI-38). Binding of the immunoliposomes to the HER2 receptor does not ensure endocytosis. Liposomes conjugated to a HER2-specific antibody that did not induce internalization were only as cytotoxic as the nontargeted liposomal formulation (Goren *et al.*, 1996). This indicates how essential endocytosis is to increasing the effectiveness of doxorubicin delivery into target cells.

#### D. *IN VIVO* STUDIES WITH ANTI-HER2 IMMUNOLIPOSOMES

*In vivo* pharmacokinetic and antitumor efficacy studies in xenograft models have yielded very promising results using anti-HER2 immuno-

liposomes targeted by anti-HER2 Fab' and scFv (Park *et al.*, 1997a,b, 1998, 2000; Kirpotin *et al.*, 1997b, 1998, 2000). Pharmacokinetic studies in rats demonstrated minimal differences in circulation lifetimes between nontargeted sterically stabilized liposomes and anti-HER2 immunoliposomes even after repeated weekly injections of immunoliposomes ( $t_{1/2} \sim 16$  h). This is important because antibody conjugation has been previously shown to significantly reduce the circulation lifetimes of liposomes when attached directly to the liposome surface (Debs *et al.*, 1987) or to the termini of liposome-conjugated PEG chains (Mori *et al.*, 1991; Allen *et al.*, 1994, 1995b; Goren *et al.*, 1996; Zalipsky *et al.*, 1996), especially after repeated administration (Harding *et al.*, 1997). Evidently, the use of Fab' or scFv fragments for targeting eliminated unwanted interactions of extraneous IgG sequences with immune cells contributed to uncompromised pharmacokinetics of these immunoliposomes.

An interesting finding was that anti-HER2-targeted immunoliposomes did not accumulate in HER2-overexpressing human tumor xenografts to a greater extent than nontargeted sterically stabilized liposomes (Kirpotin *et al.*, 1997b, 2000). This was similar to the findings of Gabizon and co-workers, who developed a similar immunoliposome using a noninternalizable antibody for tumor targeting (Goren *et al.*, 1996). These results suggest that the rates of extravasation into the tumor and low rate of subsequent removal from the tumor control the accumulation of liposomes in the tumor and not active targeting. However, the distribution of liposomes within the tumor was more uniform compared to nontargeted SSL and was often found within the cancer cells themselves (Kirpotin *et al.*, 1997b, 2000), similar to that seen in HER2-overexpressing cells in culture (Kirpotin *et al.*, 1997a). Nontargeted sterically stabilized liposomes were most often found within tumor-resident macrophages. The greater penetration and more uniform distribution may be a result in part of the relatively low avidity of immune fragments compared to full antibodies. This may help partially overcome the binding site barrier resulting from tight antibody binding to receptors located at the surface of the tumor (Weinstein *et al.*, 1987; Fujimori *et al.*, 1990).

The favorable pharmacokinetics, tumor distribution, and endocytosis of anti-HER2 Fab' and scFv-immunoliposomes helped translate into higher antitumor efficacy of anti-HER2 liposomal doxorubicin in xenograft models of HER2-overexpressing human breast cancers in immunodeficient mice (Park *et al.*, 1997a, 2000). Injections of HER2-targeted or nontargeted liposomal doxorubicin or free doxorubicin were started when tumor volumes reached 200–1000 mm<sup>3</sup> and continued for total



of three weekly doses of 5 mg/kg. Antitumor efficacy was monitored by measuring the decrease in tumor size following start of treatment. Anti-HER2 immunoliposomes were shown to be more effective than saline control, free doxorubicin, or nontargeted SSL in reducing tumor size following this schedule of treatments (Table III). In addition a considerable number of tumors, up to 60%, completely regressed with no pathological evidence of tumor cells in the tumor inoculation site. Significant reduction in tumor size was achieved when the immunoliposome treatment was delayed until the tumor reached 1000 mm<sup>3</sup> in volume (Table III) (Park *et al.*, 2000). This is an unusual result for antitumor efficacy studies on xenografts, where treatment often starts at sizes equal to or less than 100 mm<sup>3</sup> due to the poor responsiveness of larger tumors to most chemotherapy. There were also no notable toxicities or weight loss in the nude mice treated with anti-HER2 immunoliposomes. Because the immunoglobulin with Fab portions identical to these liposome-conjugated Fab' suppresses the growth of HER2-overexpressing tumors (Baselga *et al.*, 1999) and, in fact, is now used in the clinic against HER2-overexpressing breast cancers (trastuzumab, Herceptin), control experiments were performed with "empty" anti-HER2 immunoliposomes and the combination of trastuzumab IgG with nontargeted liposomal doxorubicin. However, both these treatments were less effective than doxorubicin formulated into anti-HER2 immunoliposomes (Park *et al.*, 2000). Superior antitumor activity of doxorubicin delivered in HER2-targeted immunoliposomes against HER2-overexpressing xenografts appears to be the result of their specific internalization by malignant cells in the tumor (Kirpotin *et al.*, 1997b, 1998, 2000) and the overall *in vivo* performance of anti-HER2 immunoliposomes, as the targeted drug carrier was related to the fulfillment of the criteria for ligandoliposome design laid out in Table II).

#### E. TARGETED DELIVERY OF NUCLEIC ACIDS TO CELLS THROUGH HER2 RECEPTORS

Targeting gene delivery to malignant cells has also been shown to increase transfection efficiency using both viral (Goldman *et al.*, 1997; Boerger *et al.*, 1999; Gu *et al.*, 1999) and cationic lipid-based (Kao *et al.*, 1996; Kikuchi *et al.*, 1996; Park *et al.*, 1997b,c; de Lima *et al.*, 1999) gene-delivery approaches. Although cationic lipid-based gene delivery vehicles can be quite efficient *in vitro*, the need to modify the lipid compositions for increased stability *in vivo* also reduces their transfection competency. Modifying the complexes for specific targeting to growth factor receptors has been shown to help overcome some of this loss in

TABLE III  
 ANTITUMOR ACTIVITY OF VARIOUS DOXORUBICIN FORMULATIONS AGAINST BT-474  
 XENOGRAPTS IN NUDE MICE<sup>a,b</sup>

Treatment	Treatment started				Treatment outcome	
	At day	Tumor size, (mm <sup>3</sup> )	At day	Tumor size, (mm <sup>3</sup> )	<i>p</i>	Complete regressions/ total tumors
Study A						
Saline control	7	206 ± 25	43	4150 ± 2724		0/11
Ls-DOX	7	235 ± 38	43	425 ± 370		0/11
Anti-HER2 ILs-DOX (Fab')	7	232 ± 24	43	105 ± 132	0.013 (vs Ls-DOX)	5/10
Anti-HER2 ILs-DOX (scFv)	7	203 ± 32	43	50 ± 33	0.006 (vs Ls-DOX)	6/11
Study B						
DOX + Trastuzumab	25	999 ± 387	56	5100 ± 4035		0/10
Anti-HER2 ILs DOX	25	1031 ± 371	56	263 ± 175	0.006	0/10
Study C						
Saline control	16	370 ± 58	43	3800 ± 1270		0/10
Ls-DOX + Trastuzumab	16	353 ± 29	43	783 ± 344		0/10
Anti-HER2 ILs DOX	16	338 ± 29	43	295 ± 147	0.003	3/10

<sup>a</sup>Adapted from Park *et al.* (2000).

<sup>b</sup>Animals were treated according to the following protocols (tumor inoculation at day 0). *Study A*: 0.125 mg of doxorubicin encapsulated in nontargeted sterically stabilized liposomes (Ls-DOX) or in anti-HER2 immunoliposomes (anti-HER2 ILs-DOX) injected intravenously at days 7, 14, and 21. *Study B*: 0.05 mg of doxorubicin solution (DOX) (maximum tolerated dose) or 0.125 mg of anti-HER2 ILs-DOX injected intravenously at days 25, 32, and 39; DXR group also received 75 µg of anti-HER2 antibody (Trastuzumab) intraperitoneally at days 25, 28, 32, 35, 39, and 42. *Study C*: 0.1 mg of doxorubicin as SL-DOX or as anti-HER2 ILs-DOX injected intravenously at days 16, 22, and 29; Ls-DOX group also received 7.5 µg of Trastuzumab antibody intraperitoneally at days 16, 19, 22, 25, 29, and 32. Saline controls: animals received injections of excipient (HEPES- or phosphate-buffered physiological saline) instead of the drug injections. Tumor size data are mean ± standard deviation; *p*, probability of the null hypothesis for the difference of the mean tumor volumes between drug treatment groups at the indicated day (by the independent *t* test). The number of complete regressions is calculated at day 56.

efficiency (Park *et al.*, 1997b,c). Condensed and PEG-stabilized cationic lipid–DNA complexes were shown to have a 20-fold increase in reporter gene expression following addition of anti-HER2 Fab'-PEG-DSPE conjugates to the formulation (Kirpotin *et al.*, 1998). Receptor-specific targeting has also been shown to increase the amount of complexed agent reaching the nucleus. Thus, using cationic lipid complexes of antisense oligonucleotides, a significant increase in nuclear localization of fluorescein-labeled oligonucleotides was seen when anti-HER2 Fab'-PEG-DSPE conjugates were added to the composition (Meyer *et al.*, 1998).

The focus of this chapter has been on vitamin and growth factor receptors with respect to using them as targets for increasing binding and internalization of liposomes by malignant cells. However, liposomes and cationic lipid complexes can also be used to delivery therapeutic agents, such as antisense oligonucleotides or genes that code for inhibitory proteins or inhibit growth factor receptor expression by binding to nascent RNA (Wang *et al.*, 1995; Hung *et al.*, 1998; Muller *et al.*, 1998). For example, both cationic lipid–DNA complexes and adenoviral vectors have been used to deliver the E1A gene and the nontransforming simian virus 40 large-T-antigen mutant gene to tumors in both mice and humans (Yu *et al.*, 1995; Chang *et al.*, 1997; Hortobagyi *et al.*, 1998; Hung *et al.*, 1998). Both genes are thought to code for gene products that can repress HER-2/neu promoter function.

#### F. LIPOSOME TARGETING USING OTHER GROWTH FACTOR RECEPTORS

Liposome targeting to cells expressing NGFR, EGFR, and VEGFR has been reported. Harding *et al.* (1997) conjugated periodate-oxidized recombinant anti-EGFR immunoglobulin C225 to the liposomes coated with PEG, a portion of which was bearing terminal hydrazide groups. Increased *in vitro* uptake of anti-EGFR IgG-immunoliposomes by EGFR-expressing prostate cancer cells (DU-145) was demonstrated *in vitro*. IgG conjugation at approximately 13 IgG/molecules per liposome (100 nm) did not significantly reduce liposome circulation longevity; however, at higher IgG conjugation, the circulation half-life of the liposomes decreased threefold. Anti-EGFR IgG-immunoliposomes were highly immunogenic in rats, resulting in fast clearance upon repeated injections. No therapy studies or tumor-uptake data were presented. The targeting of both the NGF receptor and EGFR were accomplished also by using the hormone itself as a targeting ligand attached to the exterior of the liposome (Rosenberg *et al.*, 1987; Ishii *et al.*, 1987; Kikuchi *et al.*, 1996). In both studies, the growth factor-targeted liposomes were shown to be efficiently endocytosed by the target cells *in vitro*, either

fibroblasts (Ishii *et al.*, 1987) or PC12 pheochromocytoma cells (Rosenberg *et al.*, 1987). However, no *in vivo* therapeutic approaches were attempted in these studies, leaving a considerable amount of work to be done both *in vitro* and *in vivo*. FGF has been used to target toxins to FGFR-overexpressing cancer cells (Beitz *et al.*, 1992; Goldman *et al.*, 1997). Adenovirus was genetically engineered to express FGF sequences at the cell-seeking receptor sites of the capsid, thus redirecting viral tropism to FGF-overexpressing cells (Gu *et al.*, 1999). Because the size of adenovirus (90 nm) is in the size range of liposomes used for tumor drug delivery (70–120 nm), these data suggest that FGF would be a good targeting ligand also for liposomes. Cells expressing VEGF receptor were also targeted using an unusual ligand, nucleic acid aptamers (Willis *et al.*, 1998) developed by the process called SELEX (Ellington and Szostak, 1990). Although promising results were obtained in inhibiting cell proliferation in culture, the addition of the aptamers resulted in a dramatic decrease in circulation lifetimes when compared to nontargeted liposomes. A reduction in the number of aptamers attached to the liposome surface may increase circulation lifetimes for single injections. However, the potential immunogenicity of such a system may limit its usefulness if multiple injections are required. If these issues are resolved, aptamers may become a promising alternative for liposome targeting instead of more traditional peptide/protein ligands. These studies demonstrate potential of growth factor receptors in targeted liposome delivery, but also emphasize the importance of overall ligandoliposome design to realize the advantage of targeting in practice.

As it is the case with vitamin receptors (Section II,G), a largely unexplored area lies in using hormone receptors for liposome targeting. Peptide hormones and hormone-releasing factors, including plasma-stable peptide analogs and peptidomimetics, may be used as ligands to deliver liposomal drugs to endocrine tissues and hormone-responsive nonendocrine tissues such as breast and uterus. Thus, a recent study successfully used doxorubicin conjugate with luteinizing hormone-releasing hormone (LH-RH) to deliver the cytotoxic drug to a human prostate cancer xenograft (Koppán *et al.*, 1999). The experience of using these and other ligands reactive with hormone and growth factor receptors together with the principles of rational ligandoliposome design (Table II) will help to create a new generation of liposomal drug-delivery systems.

#### IV. CONCLUSIONS AND FUTURE PERSPECTIVES

Due to their unique place in providing for cellular growth and differentiation, and for their ability to internalize into the cell, vitamin

and growth factor receptors undergo changes in malignant cells that make these cellular markers good recognition tags for targeted oncological drug delivery using liposomes. To date, despite many promising *in vitro* studies in this area, little has been accomplished *in vivo*, possibly because the field of liposome pharmacology has not been advanced enough to provide for a practically feasible ligandoliposome. Now, with more liposome formulations entering the oncopharmaceutical market, the development of new advanced technologies for making targeting ligands (scFv, aptamers) and their conjugates to liposomes (PEG-DSPE anchors) will allow these compounds to enter the clinic. In this chapter the principles of ligandoliposome targeting were outlined; we also illustrated how these principles were implemented in two successful liposome targeting systems directed to folate receptor via its natural ligand, folic acid, and to HER2/neu growth factor receptor via an anti-HER2 antibody fragment. The successful methodologies developed in these exemplary cases are easy to extrapolate onto a vast variety of ligands and lipid-based drug-delivery constructs, bringing us closer to the time when ligand-directed liposome targeting becomes a routine method in drug delivery.

## ACKNOWLEDGMENTS

The authors are grateful to their late mentor and colleague Dr. Demetrios Papahadjopoulos, whose pioneering works and ideas shaped the field of liposome research and inspired many of the studies reported in this chapter, and to Drs. James D. Marks and Ulrik B. Nielsen (UCSF) for valuable discussions on single-chain antibodies. This work was supported in part by grants from the National Institutes of Health (CA 72452 and CA 58207-01) and the California Breast Cancer Research Program (2CB-0004 and 2CB-0250). Daryl Drummond is supported by a postdoctoral fellowship from the California Breast Cancer Research Program (4FB-0154).

## REFERENCES

- Allen, T. M. (1981). A study of phospholipid interactions between high-density lipoproteins and small unilamellar vesicles. *Biochim. Biophys. Acta* **640**, 385–397.
- Allen, T. M. (1998). Liposomal drug formulations: Rationale for development and what we can expect in the future. *Drugs* **56**, 747–756.
- Allen, T. M., and Papahadjopoulos, D. (1993) Sterically stabilized (“stealth”) liposomes: pharmacokinetic and therapeutic advantages. In “Liposome Technology: Interactions of Liposomes with the Biological Milieu” (G. Gregoriadis, Ed.), Vol. III, pp. 59–72. CRC Press, Boca Raton, FL.
- Allen, T. M., Hansen, C., Martin, F., Redemann, C., and Yau-Young, A. (1991). Liposomes containing synthetic lipid derivatives of poly(ethylene glycol) show prolonged circulation half-lives *in vivo*. *Biochim. Biophys. Acta* **1066**, 29–36.
- Allen, T. M., Agrawal, A. K., Ahmad, I., Hansen, C. B., and Zalipsky, S. (1994). Antibody-mediated targeting of long-circulating (Stealth<sup>®</sup>) liposomes. *J. Liposome Res.* **4**, 1–25.
- Allen, T. M., Hansen, C. B., and Lopes de Menezes, D. E. (1995a). Pharmacokinetics of long-circulating liposomes. *Adv. Drug Del. Rev.* **16**, 267–284.

- Allen, T. M., Brandeis, E., Hansen, C. B., Kao, G. Y., and Zalipsky, S. (1995b). A new strategy for attachment of antibodies to sterically stabilized liposomes resulting in efficient targeting to cancer cells. *Biochim. Biophys. Acta* **1237**, 99–108.
- Allen, T. M., Hansen, C. B., Kao, G. Y., Ma, J., Marjan, J. M. J., *et al.* (1997). Antibody-targeted liposomes: Prospects and problems. *Adv. Drug Del. Rev.* **24**, 243–
- Allen, T. M., Hansen, C. B., and Stuart, D. D. (1998). Targeted sterically stabilized liposomal drug delivery. In "Medical Applications of Liposomes" (D. D. Lasic and D. Papahadjopoulos, Eds.), pp. 545–565. Elsevier, New York.
- Antony, A. C. (1992). The biological chemistry of folate receptors. *Blood* **7**, 2807–2820.
- Antony, A. C., Kane, M. A., Portillo, R. M., Elwood, P. C., and Kolhouse, J. F. (1985). Studies of the role of a particular folate-binding protein in the uptake of 5-methyltetrahydrofolate by cultured human KB cells. *J. Biol. Chem.* **260**, 14911–14917.
- Aragno, D., and Leserman, L. D. (1986). Immune clearance of liposomes inhibited by an anti-Fc receptor antibody *in vivo*. *Proc. Natl. Acad. Sci. USA* **83**, 2699–2703.
- Bally, M. B., Lim, H., Cullis, P. R., and Mayer, L. D. (1998). Controlling the drug delivery attributes of lipid-based drug formulations. *J. Liposome Res.* **8**, 299–335.
- Bangham, A. D. (1963). Physical structure and behavior of lipids and lipid enzymes. *Adv. Lipid Res.* **1**, 65–104.
- Bangham, A. D., Standish, M. M., and Watkins, J. C. (1965). Diffusion of univalent ions across the lamellae of swollen phospholipids. *J. Mol. Biol.* **13**, 238–252.
- Baselga, J., Tripathy, D., Mendelsohn, J., Baughman, S., Benz, C. C., *et al.* (1999). Phase II study of weekly intravenous trastuzumab (Herceptin) in patients with HER2/neu-overexpressing metastatic breast cancer. *Semin. Oncol.* **26**, 78–83.
- Becerril, B., Poul, M.A., and Marks, J.D. (1999). Toward selection of internalizing antibodies from phage display libraries. *Biochem. Biophys. Res. Commun.* **255**, 386–393.
- Beitz, J. G., Davol, P., Clark, J. W., Kato, J., Medina, M., *et al.* (1992). Antitumor activity of basic fibroblast growth factor-saporin mitotoxin *in vitro* and *in vivo*. *Cancer Res.* **52**, 227–230.
- Berchuck, A., Kamel, A., Whitaker, R., Kerns, B., Olt, G., *et al.* (1990). Overexpression of HER-2/neu is associated with poor survival in advanced epithelial ovarian cancer. *Cancer Res.* **50**, 4087–4091.
- Boerger, A. L., Snitkovsky, S., and Young, J. A. (1999). Retroviral vectors preloaded with a viral receptor-ligand bridge protein are targeted to specific cell types. *Proc. Natl. Acad. Sci. USA* **96**, 9867–9872.
- Borg, Å., Tandon, A. K., Sigurdsson, H., Clark, G. M., Fernö, M., *et al.* (1990). HER-2/neu amplification predicts poor survival in node-positive breast cancer. *Cancer Res.* **50**, 4332–4337.
- Chang, J. Y., Xia, W., Shao, R., Sorgi, F., Hortobagyi, G. N., *et al.* (1997). The tumor suppression activity of E1A in HER-2/neu-overexpressing breast cancer. *Oncogene* **14**, 561–568.
- Chrysogelos, S. A., and Dickson, R. B. (1994). EGF receptor expression, regulation, and function in breast cancer. *Breast Cancer Res. Treatment* **29**, 29–40.
- Citro, G., Perrotti, D., Cucco, C., D'Agnano, I., Sacchi, A., *et al.* (1992). Inhibition of leukemia cell proliferation by receptor-mediated uptake of c-myc antisense oligodeoxynucleotides. *Proc. Natl. Acad. Sci. USA* **89**, 7031–7035.
- Citro, G., Szczylik, C., Ginobbi, P., Zupi, G., and Calabretta, B. (1994). Inhibition of leukaemia cell proliferation by folic acid-polylysine-mediated introduction of c-myc antisense oligodeoxynucleotides into HL-60 cells. *Br. J. Cancer* **69**, 463–467.

- Cullis, P. R., Hope, M. J., Bally, M. B., Madden, T. D., Mayer, L. D., and Fenske, D. B. (1997). Influence of pH gradients on the transbilayer transport of drugs, lipids, peptides and metal ions into large unilamellar vesicles. *Biochim. Biophys. Acta* **1331**, 187–211.
- Damen, J., Regts, J., and Scherphof, G. (1981). Transfer and exchange of phospholipid between small unilamellar liposomes and rat plasma high density lipoproteins: Dependence on cholesterol content and phospholipid composition. *Biochim. Biophys. Acta* **665**, 538–545.
- De Lima, M. C., Simoes, S., Pires, P., Gaspar, R., Slepishkin, V., and Düzgünes, N. (1999). Gene delivery mediated by cationic liposomes: From biophysical aspects to enhancement of transfection. *Mol. Membr. Biol.* **16**, 103–109.
- De Vries, C., Escobedo, J. A., Ueno, H., Houck, K., Ferrara, N., and Williams, L. T. (1992). The fms-like tyrosine kinase, a receptor for vascular endothelial growth factor. *Science* **255**, 989–991.
- De Weerd, W. F., and Leeb-Lundberg, L. M. (1997). Bradykinin sequesters B2 bradykinin receptors and the receptor-coupled Galpha subunits Galphaq and Galphai in caveolae in DDT1 MF-2 smooth muscle cells. *J. Biol. Chem.* **272**, 17858–17866.
- Debs, R. J., Heath, T. D., and Papahadjopoulos, D. (1987). Targeting of anti-Thy 1.1 monoclonal antibody conjugated liposomes in Thy 1.1 mice after intravenous administration. *Biochim. Biophys. Acta* **901**, 183–190.
- Derksen, J. T. P., Morselt, H. W. M., and Scherphof, G. L. (1988). Uptake and processing of immunoglobulin-coated liposomes by subpopulations of rat liver macrophages. *Biochim. Biophys. Acta* **971**, 127–136.
- Drummond, D. C., and Daleke, D. L. (1995). Synthesis and characterization of N-acylated, pH-sensitive ‘caged’ aminophospholipids. *Chem. Phys. Lipids* **75**, 27–41.
- Drummond, D. C., and Daleke, D. L. (1997). Development of pH-sensitive liposomes composed of a novel “caged” dioleoylphosphatidylethanolamine. *Biophys. J.* **72**, A13.
- Drummond, D. C., Meyer, O. M., Hong, K., Kirpotin, D., and Papahadjopoulos, D. (1999). Optimizing liposomes for delivery of chemotherapeutic agents to solid tumors. *Pharmacol. Rev.* **51**, 691–743.
- Ellington, A. D., and Szostak, J. W. (1990). *In vitro* selection of RNA molecules that bind specific ligands. *Nature*, **346**, 818–822.
- Fan, J., Vitols, K. S., and Huennekens, F. M. (1991). Biotin derivatives of methotrexate and folate. *J. Biol. Chem.* **266**, 14862–14865.
- Fan, Z., and Mendelsohn, J. (1998). Therapeutic application of anti-growth factor receptor antibodies. *Curr. Opinion Oncol.* **10**, 67–73.
- Fox, S. B., Smith, K., Hollyer, J., Greenall, M., Hastrich, D., and Harris, A. L. (1994). The epidermal growth factor receptor as a prognostic marker: Results of 370 patients and review of 3009 patients. *Breast Cancer Res. Treat.* **29**, 41–49.
- French, A. R., Sudlow, G. P., Wiley, H. S., and Lauffenburger, D. A. (1994). Postendocytic trafficking of epidermal growth factor-receptor complexes is mediated through saturable and specific endosomal interactions. *J. Biol. Chem.* **269**, 15749–15755.
- Fujimori, K., Covell, D. G., Fletcher, J. E., and Weinstein, J. N. (1990). A modeling analysis of monoclonal antibody percolation through tumors: A binding site barrier. *J. Nucl. Med.* **31**, 1191–1198.
- Gabizon, A. (1998). Clinical trials of liposomes as carriers of chemotherapeutic agents: synopsis and perspective. In “Medical Applications of Liposomes” (D. D. Lasic and D. Papahadjopoulos Eds.), pp. 625–634. Elsevier, New York.
- Gabizon, A., and Barenholz, Y. (1999). Liposomal anthracyclines: From basics to clinical approval of PEGylated liposomal doxorubicin. In “Liposomes: Rational Design” (A. S. Janoff Ed.), pp. 343–362. Marcel Dekker, New York.

- Gabizon, A., and Papahadjopoulos, D. (1988). Liposome formulations with prolonged circulation time in blood and enhanced uptake in tumors. *Proc. Natl. Acad. Sci. USA* **85**, 6949–6953.
- Gabizon, A., Goren, D., Horowitz, A. T., Tzemach, D., Lossos, A., and Siegal, T. (1997). Long-circulating liposomes for drug delivery in cancer therapy: A review of biodistribution studies in tumor-bearing animals. *Adv. Drug Delivery. Rev.* **24**, 337–344.
- Gabizon, A., Horowitz, A. T., Goren, D., Tzemach, D., Mandelbaum-Shavit, F., *et al.* (1999). Targeting folate receptor with folate linked to extremities of poly(ethylene glycol)-grafted liposomes: *in vitro* studies. *Bioconjugate Chem.* **10**, 289–298.
- Garin-Chesa, P., Campbell, I., Saigo, P. E., Lewis, J. L., Jr., Old, L. J., and Rettig, W. J. (1993). Trophoblast and ovarian cancer antigen LK26. Sensitivity and specificity in immunopathology and molecular identification as a folate-binding protein. *Am. J. Pathol.* **14**, 557–567.
- Gelmon, K. A., Tolcher, A., Diab, A. R., Bally, M. B., Embree, L., *et al.* (1999). Phase I study of liposomal vincristine. *J. Clin. Oncol.* **17**, 697–705.
- Ginobbi, P., Geiser, T. A., and Citro, G. (1997). Folic acid-polylysine carrier improves efficacy of c-myc antisense oligodeoxynucleotides on human melanoma (M14) cells. *Anticancer Res.* **17**, 29–36.
- Goldberg, R. I., Smith, R. M., and Jarett, L. (1987). Insulin and alpha 2-macroglobulin-methylamine undergo endocytosis by different mechanisms in rat adipocytes. I. Comparison of cell surface events. *J. Cell. Physiol.* **133**, 203–212.
- Goldman, C. K., Rogers, B. E., Douglas, J. T., Sosnowski, B. A., Ying, W., *et al.* (1997). Targeted gene delivery to Kaposi's sarcoma cells via the fibroblast growth factor receptor. *Cancer Res.* **57**, 1447–1451.
- Goren, D., Horowitz, A. T., Zalipsky, S., Woodle, M. C., Yarden, Y., and Gabizon, A. (1996). Targeting of stealth liposomes to erbB-2 (Her/2) receptor: *In vitro* and *in vivo* studies. *Br. J. Cancer* **74**, 1749–1756.
- Gottschalk, S., Cristiano, R. J., Smith, L. C., and Woo, S. L. (1994). Folate receptor mediated DNA delivery into tumor cells: Potosomal disruption results in enhanced gene expression. *Gene Ther.* **1**, 185–191.
- Grossbard, M. L., Freedman, A. S., Ritz, J., Coral, F., Goldmacher, V. S., *et al.* (1992). Serotherapy of B-cell neoplasms with anti-B4-blocked ricin: A phase I trial of daily bolus infusion. *Blood* **79**, 576–585.
- Grossbard, M. L., Lambert, J. M., Goldmacher, V. S., Spector, N. L., Kinsella, J., *et al.* (1993). Anti-B4-blocked ricin: A phase I trial of 7-day continuous infusion in patients with B-cell neoplasms. *J. Clin. Oncol.* **11**, 726–737.
- Gu, D. L., Gonzalez, A. M., Printz, M. A., Doukas, J., Ying, W., *et al.* (1999). Fibroblast growth factor 2 retargeted adenovirus has redirected cellular tropism: Evidence for reduced toxicity and enhanced antitumor activity in mice. *Cancer Res.* **59**, 2608–2614.
- Haran, G., Cohen, R., Bar, L. K., and Barenholz, Y. (1993). Transmembrane ammonium sulfate gradients in liposomes produce efficient and stable entrapment of amphiphathic weak bases. *Biochim. Biophys. Acta* **1151**, 201–215.
- Harasym, T. O., Tardi, P., Longman, S. A., Ansell, S. M., Bally, M. B., *et al.* (1995). Poly(ethylene glycol)-modified phospholipids prevent aggregation during covalent conjugation of proteins to liposomes. *Bioconjugate Chem.* **6**, 187–194.
- Harding, J. A., Engbers, C. M., Newman, M. S., Goldstein, N. I., and Zalipsky, S. (1997). Immunogenicity and pharmacokinetic attributes of poly(ethyleneglycol)-grafted immunoliposomes. *Biochim. Biophys. Acta* **1327**, 181–192.
- Henderson, G. B. (1990). Folate-binding proteins. *Ann. Rev. Nutr.* **10**, 319–335.



- Hobbs, S. K., Monsky, W. L., Yuan, F., Roberts, W. G., Griffith, L., Torchilin, V. P., and Jain, R. K. (1998). Regulation of transport pathways in tumor vessels: Role of tumor type and microenvironment. *Proc. Natl Acad. Sci. USA* **95**, 4607–4612.
- Holladay, S. R., Yang, Z.-F., Kennedy, M. D., Leamon, C. P., Lee, R. J., Jayamani, M., Mason, T., and Low, P. S. (1999). Riboflavin-mediated delivery of a macromolecule into cultured human cells. *Biochim. Biophys. Acta* **1426**, 195–204.
- Holm, J., Hansen, S. I., Hoier-Madsen, M., and Bostad, L. (1991). High-affinity folate binding in human choroid plexus: Characterization of radioligand binding, immunoreactivity, molecular heterogeneity and hydrophobic domain of the binding protein. *Biochem. J.* **280**, 267–271.
- Holm, J., Hansen, S. I., Hoier-Madsen, M., and Bostad, L. (1992). A high-affinity folate binding protein in proximal tubule cells of human kidney. *Kidney Int.* **41**, 50–55.
- Holm, J., Hansen, S. I., Sondergaard, K., and Hoier-Madsen, M. (1993). The high-affinity folate binding protein in normal and malignant mammary gland tissue. *Adv. Exp. Med. Biol.* **338**, 757–760.
- Hortobagyi, G. N., Hung, M. C., and Lopez-Berestein, G. (1998). A Phase I multicenter study of E1A gene therapy for patients with metastatic breast cancer and epithelial ovarian cancer that overexpresses HER-2/neu or epithelial ovarian cancer. *Hum. Gene Ther.* **9**, 1775–1798.
- Huang, A., Kennel, S. J., and Huang, L. (1983). Interactions of immunoliposomes with target cells. *J. Biol. Chem.* **258**, 14034–14040.
- Hung, M. C., and Lau, Y. K. (1999). Basic science of HER-2/neu: a review. *Semin. Oncol.* **26**, 51–59.
- Hung, M. C., Chang, J. Y. J., and Xing, X. M. (1998). Preclinical and clinical study of HER-2/neu-targeting cancer gene therapy. *Adv. Drug Deliv. Rev.* **30**, 219–227.
- Hurwitz, E., Stancovski, I., Sela, M., and Yarden, Y. (1995). Suppression and promotion of tumor growth by monoclonal antibodies to ErbB-2 differentially correlate with cellular uptake. *Proc. Natl. Acad. Sci. USA* **92**, 3353–3357.
- Hwang, K. J. (1987). Liposome pharmacokinetics. In "Liposomes: From Biophysics to therapeutics" (M. J. Ostro, Ed.), pp. 109–156. Marcel Dekker, New York.
- Hynes, N. E., and Stern, D. F. (1994). The biology of erbB-2/neu/HER-2 and its role in cancer. *Biochim. Biophys. Acta* **1198**, 165–184.
- Ishida, T., and Allen, T. M. (1999). Transfer of IgG-coupled PEG<sub>2000</sub>-DSPE from micelles into preformed doxorubicin-containing Stealth<sup>®</sup> liposomes (DXR-SL). *Proc. Int. Symp. Control. Rel. Bioact. Mater.* **26**, 785–786.
- Ishii, Y., Aramaki, Y., Hara, T., Tsuchiya, S., and Fuwa, T. (1989). Preparation of EGF-labeled liposomes and their uptake by hepatocytes. *Biochem. Biophys. Res. Commun.* **160**, 732–736.
- Jinno, H., Ueda, M., Ozawa, S., Kikuchi, K., Ikeda, T., *et al.* (1996). Epidermal growth factor receptor-dependent cytotoxic effect by an EGF-ribonuclease conjugate on human cancer cell lines—A trial for less immunogenic chimeric toxin. *Cancer Chemother. Pharmacol.* **38**, 303–308.
- Juweid, M., Neumann, R., Paik, C., Perez-Bacete, M. J., Sato, J., van Osdol, W., and Weinstein, J. N. (1992). Micropharmacology of monoclonal antibodies in solid tumors: Direct experimental evidence for a binding site barrier. *Cancer Res.* **52**, 5144–5153.
- Kamen, B. A., Wang, M.-T., Streckfuss, A. J., Peryea, X., and Anderson, R. G. W. (1988). Delivery of folates to the cytoplasm of MA104 cells is mediated by a surface membrane receptor that recycles. *J. Biol. Chem.* **263**, 13602–13609.
- Kane, M. A., Elwood, P. C., Portillo, R. M., Antony, A. C., and Kolhouse, J. F. (1986). The interrelationship of the soluble and membrane-associated folate-binding proteins in human KB cells. *J. Biol. Chem.* **261**, 15625–15631.

- Kane, M. A., and Waxman, S. (1989). Biology of disease: Role of folate binding proteins in folate metabolism. *Lab. Invest.* **60**, 737-746.
- Kao, G. Y., Chang, L.-J., and Allen, T. M. (1996). Use of targeted cationic liposomes in enhanced DNA delivery to cancer cells. *Cancer Gene Ther.* **3**, 250-256.
- Kikuchi, A., Sugaya, S., Ueda, H., Tanaka, K., Aramaki, Y., *et al.* (1996). Efficient gene transfer to EGF receptor overexpressing cancer cells by means of EGF-labeled cationic liposomes. *Biochem. Biophys. Res. Commun.* **227**, 666-671.
- Kirpotin, D., Park, J. W., Hong, K., Zalipsky, S., Li, W.-L., *et al.* (1997a). Sterically stabilized anti-HER2 immunoliposomes: Design and targeting to human breast cancer cells *in vitro*. *Biochemistry* **36**, 66-75.
- Kirpotin, D. B., Park, J. W., Hong, K., Shao, Y., Shalaby, R., *et al.* (1997b). Targeting of liposomes to solid tumors: The case of sterically stabilized anti-HER2 immunoliposomes. *J. Liposome Res.* **7**, 391-417.
- Kirpotin, D. B., Park, J. W., Hong, K., Shao, Y., Colbern, G., *et al.* (1998). Targeting of sterically stabilized liposomes to cancers overexpressing HER2/neu proto-oncogene. In "Medical Applications of Liposomes" (D. D. Lasic and D. Papahadjopoulos, Eds.), pp. 325-345. Elsevier, New York.
- Kirpotin, D. B., Hong, K., Park, J. W., Shalaby, R., Nielsen, U. B., Zheng, W., Shao, Y., Marks, J. D., Benz, C. C., and Papahadjopoulos, D. (2000a). Anti-HER2 immunoliposomes produced by spontaneous incorporation of an amphipathic poly(ethylene glycol)-antibody conjugate into the liposome membrane. *Proc. 91st Ann. Meet Am. Assoc. Cancer Res.* (submitted).
- Kirpotin, D. B., Hong, K., Park, J. W., Shao, Y., Shalaby, M. R., Colbern, G. C., Benz, C. C., and Papahadjopoulos, D. (2000b). Localization of anti-HER2 immunoliposomes in HER2- overexpressing breast cancer xenografts: Intracellular delivery via immunotargeting. *Nature Biotechnol.* (submitted).
- Klibanov, A. L., Maruyama, K., Torchilin, V. P., and Huang, L. (1990). Amphipathic polyethyleneglycols effectively prolong the circulation time of liposomes. *FEBS Lett.* **268**, 235-237.
- Knepper, T., Przybylski, M., Ahlers, M., and Ringsdorf, H. (1990). Methotrexate- and folate-lipid conjugates of defined chemical structures as antifolate analogs and transport probes. In "Chemistry and Biology of Pteridines 1989," pp. 1280-1283. W de Gruyter, Berlin.
- Koppan, M., Nagy, A., Schally, A. V., Plonowski, A., Halmos, G., Arencibia, J. M., and Groot, K. (1999). Targeted cytotoxic analog of luteinizing hormone-releasing hormone AN-207 inhibits the growth of PC-82 human prostate cancer in nude mice. *The Prostate* **38**, 151-158.
- Kung, V. T., and Redemann, C. T. (1986). Synthesis of carboxyacyl derivatives of phosphatidylethanolamine and use as an efficient method for conjugation of protein to liposomes. *Biochim. Biophys. Acta* **862**, 435-439.
- Lasic, D. (1993). "Liposomes: From Physics to Applications." Elsevier, Amsterdam.
- Lasic, D.D., and Papahadjopoulos, D. (Eds). (1998). "Medical Applications of Liposomes." Elsevier, Amsterdam.
- Leamon, C. P., and Low, P. S. (1991). Delivery of macromolecules into living cells: A method that exploits folate receptor endocytosis. *Proc. Natl. Acad. Sci. USA* **88**, 5572-5576.
- Leamon, C. P., and Low, P. S. (1992). Cytotoxicity of momordin-folate conjugates in cultured human cells. *J. Biol. Chem.* **267**, 24966-24971.
- Leamon, C. P., Pastan, I., and Low, P. S. (1993). Cytotoxicity of folate-Pseudomonas exotoxin conjugates toward tumor cells: Contribution of translocation domain. *J. Biol. Chem.* **268**, 24874-24884.

- Lee, R. J., and Huang, L. (1996). Folate-targeted, anionic liposome-entrapped polylysine-condensed DNA for tumor cell-specific gene transfer. *J. Biol. Chem.* **271**, 8481–8487.
- Lee, R. J., and Low, P. S. (1994). Delivery of liposomes into cultured KB cells via folate receptor-mediated endocytosis. *J. Biol. Chem.* **269**, 3198–3204.
- Lee, R. J., and Low, P. S. (1995). Folate-mediated tumor cell targeting of liposome-entrapped doxorubicin *in vitro*. *Biochim. Biophys. Acta* **1233**, 134–144.
- Lee, R. J., Wang, S., and Low, P. S. (1996). Measurement of endosome pH following folate receptor-mediated endocytosis. *Biochim. Biophys. Acta* **1312**, 237–242.
- Lee, R. J., Wang, S., Turk, M. J., and Low, P. S. (1998). The effects of pH and intraliposomal buffer strength on the rate of liposome content release and intracellular drug delivery. *Biosci. Rep.* **18**, 69–78.
- Lewis, G. D., Figari, I., Fendly, B., Wong, W. L., Carter, P., *et al.* (1993). Differential responses of human tumor cell lines to anti-p185<sup>HER2</sup> monoclonal antibodies. *Cancer Immunol. Immunother.* **37**, 255–263.
- Liu, Q., Kane, P. M., Newman, P. R., and Forgac, M. (1996). Site-directed mutagenesis of the yeast V-ATPase  $\beta$  subunit (Vma2p). *J. Biol. Chem.* **271**, 2018–2022.
- Lopes de Menezes, D. E., Pilarski, L. M., and Allen, T. M. (1998). *In vitro* and *in vivo* targeting of immunoliposomal doxorubicin to human B-cell lymphoma. *Cancer Res.* **58**, 3320–3330.
- Low, P. S., Horn, M. A., and Heinsteins, P. F. (1997a). Composition and method for tumor imaging. U.S. Patent US 5,688,488.
- Low, P. S., Horn, M. A., and Heinsteins, P. F. (1997b). Method for enhancing transmembrane transport of exogenous molecules. U.S. Patent US 5,635,382.
- Lu, J. Y., Lowe, D. A., Kennedy, M. D., and Low, P. S. (1999). Folate-targeted enzyme prodrug cancer therapy utilizing penicillin-V amidase and a doxorubicin prodrug. *J. Drug Target* **7**, 43–53.
- Machy, P., Barbet, J., and Leserman, L. D. (1982). Differential endocytosis of T and B lymphocyte surface molecules evaluated with antibody-bearing fluorescent liposomes containing methotrexate. *Immunology* **79**, 4148–4152.
- Mansson, P. E., Adams, P., Kan, M., and McKeehan, W. L. (1989). Heparin-binding growth factor gene expression and receptor characteristics in normal rat prostate and two transplantable rat prostate tumors. *Cancer Res.* **49**, 2485–2494.
- Marks, J. D., Hoogenboom, H. R., Griffiths, A. D., and Winter, G. (1992). Molecular evolution of proteins on filamentous phage: Mimicking the strategy of the immune system. *J. Biol. Chem.* **267**, 16007–16010.
- Martin, F. J. (1998). Clinical pharmacology and antitumor efficacy of DOXIL (pegylated liposomal doxorubicin). In "Medical Applications of Liposomes" (D. D. Lasic and D. Papahadjopoulos, Eds.), pp. 635–688. Elsevier, New York.
- Martin, F. J., and Papahadjopoulos, D. (1982). Irreversible coupling of immunoglobulin fragments to preformed vesicles: An improved method for liposome targeting. *J. Biol. Chem.* **257**, 286–288.
- Martin, F. J., Hubbell, W. L., and Papahadjopoulos, D. (1981). Immunospecific targeting of liposomes to cells: A novel and efficient method for covalent attachment of Fab' fragments via disulfide bonds. *Biochemistry* **20**, 4229–4238.
- Mathias, C. J., Wang, S., Lee, R. J., Waters, D. J., Low, P. S., and Green, M. A. (1996). Tumor-selective radiopharmaceutical targeting via receptor-mediated endocytosis of Gallium-67-deferoxamine-folate. *J. Nucl. Med.* **37**, 1003–1008.
- Mathias, C. J., Wang, S., Waters, D. J., Turek, J. J., Low, P. S., and Green, M. A. (1998). Indium-111-DTPA-folate as a potential folate-receptor-targeted radiopharmaceutical. *J. Nucl. Med.* **39**, 1579–1585.

- Mathias, C. J., Wang, S., Low, P. S., Waters, D. J., and Green, M. A. (1999). Receptor-mediated targeting of  $^{67}\text{Ga}$ -deferoxamine-folate to folate-receptor-positive human KB tumor xenografts. *Nucl. Med. Biol.* **26**, 23–25.
- Mayer, L. D., Bally, M. B., Hope, M. J., and Cullis, P. R. (1985). Uptake of antineoplastic agents into large unilamellar vesicles in response to a membrane potential. *Biochim. Biophys. Acta* **816**, 294–302.
- Mayhew, E., Rustum, Y. M., Szoka, F., and Papahadjopoulos, D. (1979). Role of cholesterol in enhancing the antitumor activity of cytosine arabinoside entrapped in liposomes. *Cancer Treatment Rep.* **63**, 1923–1928.
- Mayor, S., Rothberg, K. G., and Maxfield, F. R. (1994). Sequestration of GPI-anchored proteins in caveolae triggered by cross-linking. *Science* **264**, 1948–1951.
- McEwan, J. F., Veitch, H. S., and Russel-Jones, G. J. (1999). Synthesis and biological activity of ribose-5'-carbamate derivatives of vitamin B<sub>12</sub>. *Bioconjugate Chem.* **10**, 1131–1136.
- Meyer, O., Kirpotin, D., Hong, K., Sternberg, B., Park, J. W., *et al.* (1998). Cationic liposomes coated with polyethylene glycol as carriers of oligonucleotides. *J. Biol. Chem.* **273**, 15621–15627.
- Mineo, C., and Anderson, R. G. (1996). A vacuolar-type proton ATPase mediates acidification of plasmalemmal vesicles during potocytosis. *Exp. Cell Res.* **224**, 237–242.
- Mori, A., Klivanov, A. L., Torchilin, V. P., and Huang, L. (1991). Influence of the steric barrier activity of amphipathic poly(ethyleneglycol) and ganglioside GM1 on the circulation time of liposomes and on the target binding of immunoliposomes *in vivo*. *FEBS Lett.* **284**, 263–266.
- Muggia, F. M., Hainsworth, J. D., Jeffers, S., Miller, P., Groshen, S., *et al.* (1997). Phase II study of liposomal doxorubicin in refractory ovarian cancer: Antitumor activity and toxicity modification by liposomal encapsulation. *J. Clin. Oncol.* **15**, 987–993.
- Muller, M., Dietel, M., Turzynski, A., and Wiechen, K. (1998). Antisense phosphorothioate oligodeoxynucleotide down-regulation of the insulin-like growth factor I receptor in ovarian cancer cells. *Int. J. Cancer* **77**, 567–571.
- Multani, P. S., and Grossbard, M. L. (1998). Monoclonal antibody-based therapies for hematological malignancies. *J. Clin. Oncol.* **16**, 3691–3710.
- Nichols, J. W., and Deamer, D. W. (1976). Catecholamine uptake and concentration by liposomes maintaining pH gradients. *Biochim. Biophys. Acta* **455**, 269–271.
- Niehans, G. A., Singleton, T. P., Dykoski, D., and Kiang, D. T. (1993). Stability of HER-2/neu expression over time and at multiple metastatic sites. *J. Natl. Cancer Inst.* **85**, 1230–1235.
- Nielsen, U.B., Poul, M.A., Pickering, E. M., Kirpotin, D., Shalaby, R., Hong, K., Park, J. W., Papahadjopoulos, D., Benz, C. C., and Marks, J. D. (1999). Targeting of breast tumors with scFv antibodies selected for internalization from a phage display library. *Proc. Intern. Conf. Mol. Targets Cancer Therapeut. Clin. Cancer Res.* **5**(Suppl.). [Abstract 92]
- Northfelt, D. W., Dezube, B. J., Thommes, J. A., Miller, B. J., Fischl, M. A., *et al.* (1998). Pegylated-liposomal doxorubicin versus doxorubicin, bleomycin, and vincristine in the treatment of AIDS-related Kaposi's sarcoma: Results of a randomized phase III clinical trial. *J. Clin. Oncol.* **16**, 2445–2451.
- Papahadjopoulos, D., Allen, T. M., Gabizon, A., Mayhew, E., Matthey, K., *et al.* (1991). Sterically stabilized liposomes: Improvements in pharmacokinetics and antitumor therapeutic efficacy. *Proc. Natl. Acad. Sci. USA* **88**, 11460–11464.
- Papahadjopoulos, D., Nir, S., and Oki, S. (1972). Permeability properties of phospholipid

- membranes: effect of cholesterol and temperature. *Biochim. Biophys. Acta* **266**, 561–583.
- Park, J. W., Hong, K., Carter, P., Asgari, H., Guo, L. Y., *et al.* (1995). Development of anti-p185<sup>HER2</sup> immunoliposomes for cancer therapy. *Proc. Natl. Acad. Sci. USA* **92**, 1327–1331.
- Park, J. W., Hong, K., Kirpotin, D. B., Meyer, O., Papahadjopoulos, D., and Benz, C. C. (1997b). Anti-HER2 immunoliposomes for targeted therapy of human tumors. *Cancer Lett.* **118**, 153–160.
- Park, J. W., Hong, K., Kirpotin, D. B., Papahadjopoulos, D., and Benz, C. C. (1997a). Immunoliposomes for cancer treatment. *Adv. Pharmacol.* **40**, 399–435.
- Park, J. W., Hong, K., Kirpotin, D. B., Meyer, O., Papahadjopoulos, D., and Benz, C. C. (1997b). Anti-HER2 immunoliposomes for targeted therapy of human tumors. *Cancer Lett.* **118**, 153–160.
- Park, J., Hong, K., Zheng, W., Benz, C., and Papahadjopoulos, D. (1997c). Development of liposome- and anti-HER2 immunoliposome-plasmid complexes for efficient and selective gene delivery. *Proc Am Assoc Cancer Res* **38**, 342a.
- Park, J. W., Kirpotin, D., Hong, K., Colbern, G., Shalaby, R., *et al.* (1998a). Anti-HER2 immunoliposomes for targeted drug delivery. *Med. Chem. Res.* **8**, 383–391.
- Park, J. W., Kirpotin, D., Hong, K., Zheng, W., Shao, Y., *et al.* (1998b). Sterically stabilized immunoliposomes: Formulations for delivery of drugs and genes to tumor cells *in vivo*. In “Targeting of Drugs: Strategies for Stealth Therapeutic Systems” (G. Gregoriadis and F. McCormack, Eds.), Vol. 6, pp. 41–47. Plenum, New York.
- Park, J. W., Hong, K., Kirpotin, D. B., Colbern, G., Shalaby, R., Baselga, J., Shao, Y., Nielsen, U., Marks, J., Moore, D., Papahadjopoulos, D., and Benz, C. C. (2000). Anti-HER2 immunoliposomes: enhanced anticancer efficacy due to targeted delivery. *Nat. Biotechnol.* (submitted).
- Pastan, I. H., and Willingham, M. C. (1981). Receptor-mediated endocytosis of hormones in cultured cells. *Ann. Rev. Physiol.* **43**, 239–250.
- Patrick, T. A., Kranz, D. M., van Dyke, T. A., and Roy, E. J. (1997). Folate receptors as potential therapeutic targets in choroid plexus tumors of SV40 transgenic mice. *J. Neuro-Oncol.* **32**, 111–123.
- Pegram, M. D., Lipton, A., Hayes, D. F., Weber, B. L., Baselga, J. M., *et al.* (1998). Phase II study of receptor-enhanced chemosensitivity using recombinant humanized anti-p185<sup>HER2</sup>/neu monoclonal antibody plus cisplatin in patients with HER2/neu-overexpressing metastatic breast cancer refractory to chemotherapy treatment. *J. Clin. Oncol.* **16**, 2659–2671.
- Press, M. F., Cordon-Cardo, C., and Slamon, D. J. (1990). Expression of the HER-2/ neu proto-oncogene in normal human adult and fetal tissues. *Oncogene* **5**, 953–962.
- Press, M. F., Bernstein, L., Thomas, P. A., Meisner, L. F., Zhou, J.-Y., *et al.* (1997). HER-2/neu gene amplification characterized by fluorescence in situ hybridization: Poor prognosis in node-negative breast carcinomas. *J. Clin. Oncol.* **15**, 2894–2904.
- Ramakrishnan, S., Olson, T. A., Bautch, V. L., and Mohanraj, D. (1996). Vascular endothelial growth factor-toxin conjugate specifically inhibits KDR/flk-1-positive endothelial cell proliferation *in vitro* and angiogenesis *in vivo*. *Cancer Res.* **56**, 1324–1330.
- Ranson, M. R., Carmichael, J., O’Byrne, K., Stewart, S., Smith, D., and Howell, A. (1997). Treatment of advanced breast cancer with sterically stabilized liposomal doxorubicin: Results of a multicenter phase II trial. *J. Clin. Oncol.* **15**, 3185–3191.
- Ratnam, M., Marquardt, H., Duhring, J. L., and Freisheim, J. H. (1989). Homologous membrane folate binding proteins in human placenta: Cloning and sequence of a cDNA. *Biochemistry* **28**, 8249–8254.

- Reddy, J. A., Haneline, L. S., Srour, E. F., Antony, A. C., and Clapp, D. W. (1999). Expression and functional characterization of the beta-isoform of the  $\beta$ -isoform of the folate receptor on CD34+ cells. *Blood* **93**, 3940–3948.
- Reddy, J. A., and Low, P. S. (1998). Folate-mediated targeting of therapeutic and imaging agents. *CRC Crit. Rev. Therap. Drug Carrier Syst.* **15**, 587–627.
- Rijnbouts, S., Jansen, G., Posthuma, G., Hynes, J. B., Schornagel, J. H., and Strous, G. J. (1996). Endocytosis of GPI-linked membrane folate receptor- $\alpha$ . *J. Cell Biol.* **132**, 35–47.
- Rodrigues, M. L., Presta, L. G., Kotts, C. E., Wirth, C., Mordenti, J., *et al.* (1995). Development of a humanized disulfide-stabilized anti-p185HER2 Fv-b-lactamase fusion protein for activation of a cephalosporin doxorubicin prodrug. *Cancer Res.* **55**, 63–70.
- Rosenberg, M. B., Breakfield, X. O., and Hawrot, E. (1987). Targeting of liposomes to cells bearing nerve growth factor receptors mediated by biotinylated nerve growth factor. *J. Neurochem.* **48**, 865–875.
- Rosenblum, M. G., Shawyer, L. K., Marks, J. W., Brink, J., Cheung, L., and Langton-Webster, B. (1999). Recombinant immunotoxins directed against the c-erbB-2/HER2/neu oncogene product: *in vitro* cytotoxicity, pharmacokinetics, and *in vivo* efficacy studies in xenograft models. *Clin. Cancer Res.* **5**, 865–874.
- Ross, J. F., Chaudhuri, P. K., and Ratnam, M. (1994). Differential regulation of folate receptor isoforms in normal and malignant tissues *in vivo* and in established cell lines. *Cancer* **73**, 2432–2443.
- Rothberg, K. G., Ying, Y., Kolhouse, J. F., Kamen, B. A., and Anderson, R. G. (1990). The glycopospholipid linked folate receptor internalizes folate without entering the clathrin coated endocytic pathway. *J. Cell Biol.* **110**, 637–649.
- Rui, Y., Wang, S., Low, P. S., and Thompson, D. H. (1998). Dipalmitoylcholine-folate liposomes: An efficient vehicle for intracellular drug delivery. *J. Am. Chem. Soc.* **120**, 11213–11218.
- Sausville, E. A., Headlee, D., Stetler-Stevenson, M., Jaffe, E. S., Solomon, D., *et al.* (1995). Continuous infusion of the anti-CD22 immunotoxin IgG-RFB4-SMPT-dgA in patients with B-cell lymphoma: A phase I study. *Blood* **85**, 3457–3465.
- Scher, H. I., Sarkis, A., Reuter, V., Cohen, D., Netto, G., *et al.* (1995). Changing pattern of expression of the epidermal growth factor receptor and transforming growth factor alpha in the progression of prostatic neoplasms. *Clin. Cancer Res.* **1**, 545–550.
- Schier, R., and Marks, J. D. (1996). Efficient *in vitro* affinity maturation of phage antibodies using BIAcore guided selections. *Hum. Antibod. Hybridom.* **7**, 97–105.
- Schier, R., McCall, A., Adams, G. P., Marshall, K. W., Merritt H., Yim, M., Crawford, R. S., Weiner, L. M., Marks, C., and Marks, J. D. (1996). Isolation of picomolar affinity anti-c-erbB-2 single-chain Fv by molecular evolution of the complementary determining regions in the center of the antibody binding site. *J. Mol. Biol.* **263**, 551–567.
- Shak, S. (1999). Overview of the trastuzumab (Herceptin) anti-HER2 monoclonal antibody clinical program in HER2-overexpressing metastatic breast cancer. Herceptin Multinational Investigator Study Group. *Semin. Oncol.* **26**, 71–77.
- Shapiro, C. L., Ervin, T., Welles, L., Azarnia, N., Keating, J., Hayes, D. F. (1999). Phase II trial of high-dose liposome-encapsulated doxorubicin with granulocyte colony-stimulating factor in metastatic breast cancer. *J. Clin. Oncol.* **17**, 1435–1441.
- Shen, F., Ross, J. F., Wang, X., and Ratnam, M. (1994). Identification of a novel folate receptor, a truncated receptor, and receptor type beta in hematopoietic cells: cDNA cloning, expression, immunoreactivity, and tissue specificity. *Biochemistry* **33**, 1209–1215.

- Shibuya, M., Yamaguchi, S., Yamane, A., Ikeda, T., Tojo, A., *et al.* (1990). Nucleotide sequence and expression of a novel human receptor-type tyrosine kinase gene (ft) closely related to the *fms* family. *Oncogene* **5**, 519–524.
- Sivam, G. P., Martin, P. J., Reisfeld, R. A., and Mueller, B. M. (1995). Therapeutic efficacy of a doxorubicin immunoconjugate in a preclinical model of spontaneous metastatic human melanoma. *Cancer Res.* **55**, 2352–2356.
- Slamon, D. J., Clark, G. M., Wong, S. G., Levin, W. J., Ullrich, A., and McGuire, W. L. (1987). Human breast cancer: Correlation of relapse and survival with amplification of the *HER-2/neu* oncogene. *Science* **235**, 177–182.
- Slamon, D. J., Godolphin, W., Jones, L. A., Holt, J. A., Wong, S. G., *et al.* (1989). Studies of the *HER-2/neu* proto-oncogene in human breast and ovarian cancer. *Science* **244**, 707–712.
- Smart, E. J., Foster, D. C., Ying, Y. S., Kamen, B. A., and Anderson, R. G. W. (1994). Protein kinase C activators inhibit receptor-mediated potocytosis by preventing internalization of caveolae. *J. Cell Biol.* **124**, 307–313.
- Sorkin, A., and Waters, C. M. (1993). Endocytosis of growth factor receptors. *BioEssays* **15**, 375–381.
- Sporn, M. B., and Roberts, A. B. (1985). Autocrine growth factors and cancer. *Nature* **313**, 745–747.
- Stone, M. J., Sausville, E. A., Fay, J. W., Headlee, D., Collins, R. H., *et al.* (1996). A phase I study of bolus versus continuous infusion of the anti-CD19 immunotoxin, IgG-HD37-dgA, in patients with B-cell lymphoma. *Blood* **88**, 1188–1197.
- Tagliabue, E., Centis, F., Campiglio, M., Mastroianni, A., Martignone, S., *et al.* (1991). Selection of monoclonal antibodies which induce internalization and phosphorylation of p185HER2 and growth inhibition of cells with *HER2/neu* gene amplification. *Int. J. Cancer* **47**, 933–937.
- Tischer, E., Mitchell, R., Hartman, T., Silva, M., Gospodarowicz, D., *et al.* (1991). The human gene for vascular endothelial growth factor: Multiple protein forms are encoded through alternative exon splicing. *J. Biol. Chem.* **266**, 11947–11954.
- Toffoli, G., Cernigoi, C., Russo, A., Gallo, A., Bagnoli, M., and Boiocchi, M. (1997). Overexpression of folate binding protein in ovarian cancers. *Int. J. Cancer* **74**, 193–198.
- Toi, M., Osaki, A., Yamada, H., and Toge, T. (1991). Epidermal growth factor receptor expression as a prognostic indicator in breast cancer. *Eur. J. Cancer* **27**, 977–980.
- Tolcher, A. W., Sugarman, S., Gelmon, K. A., Cohen, R., Saleh, M., *et al.* (1999). Randomized phase II study of BR96-doxorubicin conjugate in patients with metastatic breast cancer. *J. Clin. Oncol.* **17**, 478–484.
- Turek, J. J., Leamon, C. P., and Low, P. S. (1993). Endocytosis of folate-protein conjugates: ultrastructural localization in KB cells. *J. Cell Sci.* **106**, 423–430.
- Uckun, F. M., Narla, R. K., Jun, X., Zeren, T., Venkatachalam, T., *et al.* (1998). Cytotoxic activity of epidermal growth factor-genistein against breast cancer cells. *Clin. Cancer Res.* **4**, 901–912.
- Unezaki, S., Mauryama, K., Ishida, O., Suginaka, A., Jun-ichi, H., and Iwatsuru, M. (1995). Enhanced tumor targeting and improved antitumor activity of doxorubicin by long-circulating liposomes containing amphipathic poly(ethylene glycol). *Int. J. Pharmaceut.* **126**, 41–48.
- Uster, P. C., Allen, T. M., Daniels, B. E., Mendez, C. J., Newman, M. S., and Zhu, G. Z. (1996). Insertion of poly(ethylene glycol) derivatized phospholipid into preformed liposomes results in prolonged *in vivo* circulation time. *FEBS Lett.* **386**, 243–246.
- Valero, V., Buzdar, A. U., Theriault, R. L., Azarnia, N., Fonseca, G. A., *et al.* (1999). Phase II trial of liposome-encapsulated doxorubicin, cyclophosphamide, and fluorouracil

- as first-line therapy in patients with metastatic breast cancer. *J. Clin. Oncol.* **17**, 1425–1434.
- Vitetta, E. S., Stone, M., Amlot, P., Fay, J., May, R., *et al.* (1991). Phase I immunotoxin trial in patients with B-cell lymphoma. *Cancer Res.* **51**, 4052–4058.
- Wang, S., and Low, P. S. (1998). Folate-mediated targeting of antineoplastic drugs, imaging agents, and nucleic acids to cancer cells. *J. Controlled Release* **53**, 39–48.
- Wang, S., Lee, R. J., Cauchon, G., Gorenstein, D. G., and Low, P. S. (1995). Delivery of antisense oligodeoxyribonucleotides against the human epidermal growth factor receptor into cultured KB cells with liposomes conjugated to folate via polyethylene glycol. *Proc. Natl. Acad. Sci. USA* **92**, 3318–3322.
- Wang, S., Lee, R. J., Mathias, C. J., Green, M. A., and Low, P. S. (1996). Synthesis, purification, and tumor cell uptake of <sup>67</sup>Ga-Deferoxamine-folate, a potential radiopharmaceutical for tumor imaging. *Bioconjugate Chem.* **7**, 56–62.
- Woodle, M.C., and Lasic, D. D. (1992). Sterically stabilized liposomes. *Biochim. Biophys. Acta* **1113**, 171–199.
- Weitman, S. D., Lark, R. H., Coney, L. R., Fort, D. W., Frasca, V., and Zurawski, V. R. (1992). Distribution of the folate receptor GP38 in normal and malignant cell lines and tissues. *Cancer Res.* **52**, 3396–3401.
- Wilbur, D. S., Pathare, P. M., Hamlin, D. K., Rothenberg, S. P., and Quadros, E. V. (1999). Radioiodination of cyanocobalamin conjugates containing hydrophilic linkers: Preparation of a radioiodinated cyanocobalamin monomer and two dimers, and assessment of their binding with transcobalamin II. *Bioconj. Chem.* **10**, 912–920.
- Willis, M. C., Collins, B., Zhang, T., Green, L. S., Sebesta, D. P., *et al.* (1998). Liposome-anchored vascular endothelial growth factor aptamers. *Bioconj. Chem.* **9**, 573–582.
- Wong, J. Y., Kuhl, T. L., Israelachvili, J. N., Mullah, N., and Zalipsky, S. (1997). Direct measurement of a tethered ligand-receptor interaction potential. *Science* **275**, 820–822.
- Yu, D., and Hung, M.-C. (1991). Expression of activated rat neu oncogene is sufficient to induce experimental metastasis in 3T3 cells. *Oncogene* **6**, 1991–1996.
- Yu, D., Matin, A., Xia, W., Sorgi, F., Huang, L., and Hung, M. C. (1995). Liposome-mediated *in vivo* E1A gene transfer suppressed dissemination of ovarian cancer cells that overexpress HER-2/neu. *Oncogene* **11**, 1383–1388.
- Yu, D., Wang, S.-S., Dulski, K. M., Tsai, C.-M., Nicolson, G. L., and Hung, M.-C. (1994). *C-erbB-2/neu* overexpression enhances metastatic potential of human lung cancer cells by induction of metastasis-associated properties. *Cancer Res.* **54**, 3260–3266.
- Zalipsky, S., Gittelman, J., Mullah, N., Qazen, M. M., and Harding, J. A. (1998). Biologically active ligand-bearing polymer-grafted liposomes. In “Targeting of Drugs: Strategies for Stealth Therapeutic Systems” (G. Gregoriadis and F. McCormack, Eds.), Vol. 6, pp. 131–138. Plenum, New York.
- Zalipsky, S., Hansen, C. B., Lopes de Menezes, D. E., and Allen, T. M. (1996). Long-circulating, polyethylene glycol-grafted immunoliposomes. *J. Controlled Release* **39**, 153–161.
- Zimmerman, J. (1990). Folic acid transport in organ-cultured mucosa of human intestine. Evidence for distinct carriers. *Gastroenterology* **99**, 964–972.



# Pharmacokinetics and *In Vivo* Drug Release Rates in Liposomal Nanocarrier Development

DARYL C. DRUMMOND,<sup>1</sup> CHARLES O. NOBLE,<sup>1</sup> MARK E. HAYES,<sup>1</sup> JOHN W. PARK,<sup>2</sup> DMITRI B. KIRPOTIN<sup>1</sup>

<sup>1</sup>Hermes Biosciences, Inc., South San Francisco, California 94080

<sup>2</sup>University of California at San Francisco, San Francisco, California 94143

Received 26 October 2007; accepted 22 January 2008

Published online 19 March 2008 in Wiley InterScience (www.interscience.wiley.com). DOI 10.1002/jps.21358

**ABSTRACT:** Liposomes represent a widely varied and malleable class of drug carriers generally characterized by the presence of one or more amphiphile bilayers enclosing an interior aqueous space. Thus, the pharmacological profile of a particular liposomal drug formulation is a function not only of the properties of the encapsulated drug, but to a significant extent of the pharmacokinetics, biodistribution, and drug release rates of the individual carrier. Various physicochemical properties of the liposomal carriers, the drug encapsulation and retention strategies utilized, and the properties of the drugs chosen for encapsulation, all play an important role in determining the effectiveness of a particular liposomal drug. These properties should be carefully tailored to the specific drug, and to the application for which the therapeutic is being designed. Liposomal carriers are also amenable to additional modifications, including the conjugation of targeting ligands or environment-sensitive triggers for increasing the bioavailability of the drug specifically at the site of disease. This review describes the rationale for selecting optimal strategies of liposomal drug formulations with respect to drug encapsulation, retention, and release, and how these strategies can be applied to maximize therapeutic benefit *in vivo*. © 2008 Wiley-Liss, Inc. and the American Pharmacists Association *J Pharm Sci* 97:4696–4740, 2008

**Keywords:** liposomes; nanocarriers; drug delivery; pharmacokinetics

Abbreviations used: %ID, percent of injected dose; ABC, accelerated blood clearance; CCL, coated cationic liposomal formulation; CED, convection-enhanced delivery; Chol, cholesterol; DB-67, 7-*t*-butyldimethylsilyl-10-hydroxycamptothecin; DHSM, dihydrosphingomyelin; DMPC, 1,2-dimyristoyl-3-*sn*-phosphatidylcholine; DOPC, 1,2-dioleoyl-3-*sn*-phosphatidylcholine; DOX, doxorubicin; DPPC, 1,2-dipalmitoyl-3-*sn*-phosphatidylcholine; DSPC, 1,2-distearoyl-3-*sn*-phosphatidylcholine; DSPG, 1,2-distearoyl-3-*sn*-phosphatidylglycerol; EPR, enhanced permeability and retention effect; HSPC, hydrogenated soy phosphatidylcholine; ILs, immunoliposomes; Ls, liposome; MPS, mononuclear phagocyte system; MTD, maximum tolerated dose; NDDP, *cis*-Bis-neodecanoate-*trans*-R,R-1,2-diaminocyclohexane platinum(II); NIPAM, poly(*N*-isopropylacrylamide); ODN, oligo-2'-deoxyribonucleotides; OSI-7904L, (S)-2-[5-[(1,2-dihydro-3-methyl-1-oxobenzo[f]quinazolin-9-yl)-methyl]amino-1-oxo-2-isoindolyn]-

glutaric acid; PEG, polyethylene glycol; PEG-DSG, methoxy-polyethylene glycol-1,2-distearoylglyceryl ether; PEG-DSPE, *N*-(polyethyleneglycol)distearoylphosphatidylethanolamine; PL, phospholipid; PLA<sub>2</sub>, phospholipase A<sub>2</sub>; PLD, pegylated liposomal doxorubicin; POPC, 1-palmitoyl, 2-oleoyl-3-*sn*-phosphatidylcholine; PPE, palmar-plantar erythrodysesthesia; SALP, stabilized antisense lipid particles; SM, sphingomyelin; SOS, sucroseoctasulfate; TEA, triethylammonium; TEA-SOS, triethylammonium sucroseoctasulfate; TPT, topotecan.

Correspondence to: Daryl C. Drummond (Telephone: 650-873-2583 ext. 109; Fax: 650-873-2501; E-mail: drummond@hermesbio.com)

*Journal of Pharmaceutical Sciences*, Vol. 97, 4696–4740 (2008)

© 2008 Wiley-Liss, Inc. and the American Pharmacists Association

## INTRODUCTION

Liposomes constitute a class of microparticulate or nanoparticulate drug carriers generally characterized by the presence of one or more amphiphile bilayers enclosing an interior aqueous space. Liposomes have been used to increase the therapeutic index of a wide range of antineoplastic agents.<sup>1</sup> This has primarily been accomplished by improving the pharmacokinetic profile or allowing for site-specific drug delivery to solid tumors. For example, pegylated liposomal doxorubicin (PLD; Doxil<sup>®</sup>, Alza/Johnson & Johnson, Mountain View, CA), a stable and long-circulating liposome formulation of doxorubicin, has become a widely used anticancer agent.<sup>1-3</sup> PLD has been approved for the treatment of Kaposi's sarcoma,<sup>4,5</sup> ovarian cancer,<sup>6,7</sup> and more recently multiple myeloma,<sup>8,9</sup> and has shown activity in other tumor types as well. The success of PLD has been difficult to replicate when attempting to encapsulate and deliver other classes of drugs, primarily as a result of suboptimal drug release rates, and thus the appropriate balance between long circulation lifetimes and bioavailability of alternative drugs (see Control of *In Vivo* Drug Release Rates Section).

A wide range of small molecule drugs of varying physicochemical properties have been studied in liposomal formulations. Some of these drugs are shown in Figure 1. Liposome formulations of various vinca alkaloids,<sup>10,11</sup> camptothecins,<sup>12-15</sup> taxanes,<sup>16,17</sup> platinum analogs,<sup>18,19</sup> or even certain anthracycline analogs<sup>20,21</sup> initially defied ready encapsulation and efficient delivery via liposomes, due to the drug retention in the resulting formulation being either unstable or overly stabilized. Fortunately, the properties that determine the clearance and drug retention of liposomes have continued to be elucidated, making it possible to engineer liposomal drugs using more advanced and rational strategies to develop therapeutics with activities that are optimal for both the encapsulated agent and its specific therapeutic application.

Drug carriers can serve multiple purposes. Certain hydrophobic drugs, such as paclitaxel, require high concentrations of toxic emulsifying agents to effectively solubilize the drug for parenteral administration. Nanocarriers can serve to simply solubilize the drug in a form that allows for elimination of the more toxic solubilizing agent, such as Cremophor<sup>®</sup>, but where the drug rapidly redistributes out of the particle once

in the circulation. Indeed, a nanoparticle albumin-bound paclitaxel formulation (ABI-007; Abraxane<sup>®</sup>; Abraxis Oncology, Bridgewater, NJ) was recently approved for the treatment of metastatic breast cancer. However, the pharmacokinetics of paclitaxel in ABI-007 are relatively similar to the Cremophor formulation<sup>22</sup> compared to the substantial differences commonly observed for highly stable liposomal drug formulations (Tab. 1), indicating that the drug may redistribute out of the albumin carrier once in the circulation. Despite the relatively small change in pharmacokinetic parameters, the resulting albumin formulation has demonstrated improvements in both antitumor efficacy and its toxicity profile, likely in part as a result of the elimination of Cremophor.<sup>23</sup>

Drugs retained in long circulating nanocarriers can also benefit from site-specific accumulation in the pathological sites such as tumors due to a discontinuous or otherwise more permeable microvasculature and a nonfunctioning lymphatics.<sup>24,25</sup> This phenomenon is also referred to as the enhanced permeability and retention (EPR) effect.<sup>1,26</sup> Liposomes of approximately 100 nm in size readily distribute into solid tumors, with an efficiency that depends partially on the anatomical location,<sup>25</sup> and a maximum accumulation occurring in the range of 24-48 h for long circulating liposomes in subcutaneous tumor models (Fig. 2).<sup>27</sup> Many normal tissues are supported by a continuous vasculature with relatively small gaps between neighboring endothelial cells.<sup>28,29</sup> The liver and spleen, two major organs of the mononuclear phagocyte system (MPS) are notable exceptions, as are also the other major sites of liposome clearance due to the presence of macrophages that efficiently phagocytose many nanosized particles such as liposomes.<sup>1,30</sup> The result of the EPR effect is an altered biodistribution for the nanocarrier-associated drug, with a notably higher concentration of the drug accumulating at the site of disease, and a lower concentration accumulating in healthy tissues at potential sites of toxicity.

Liposomes can also act as sustained release formulations of the active drug, providing consistent low level exposure of the targeted tissue to the drug. When optimally designed, this controlled release occurs to a large extent following the accumulation of the liposomal therapeutic in the tumor, or other site of disease. For drugs that are cell cycle dependent or whose molecular effects are particularly transient, and thus heavily dependent on the pharmacokinetics of a

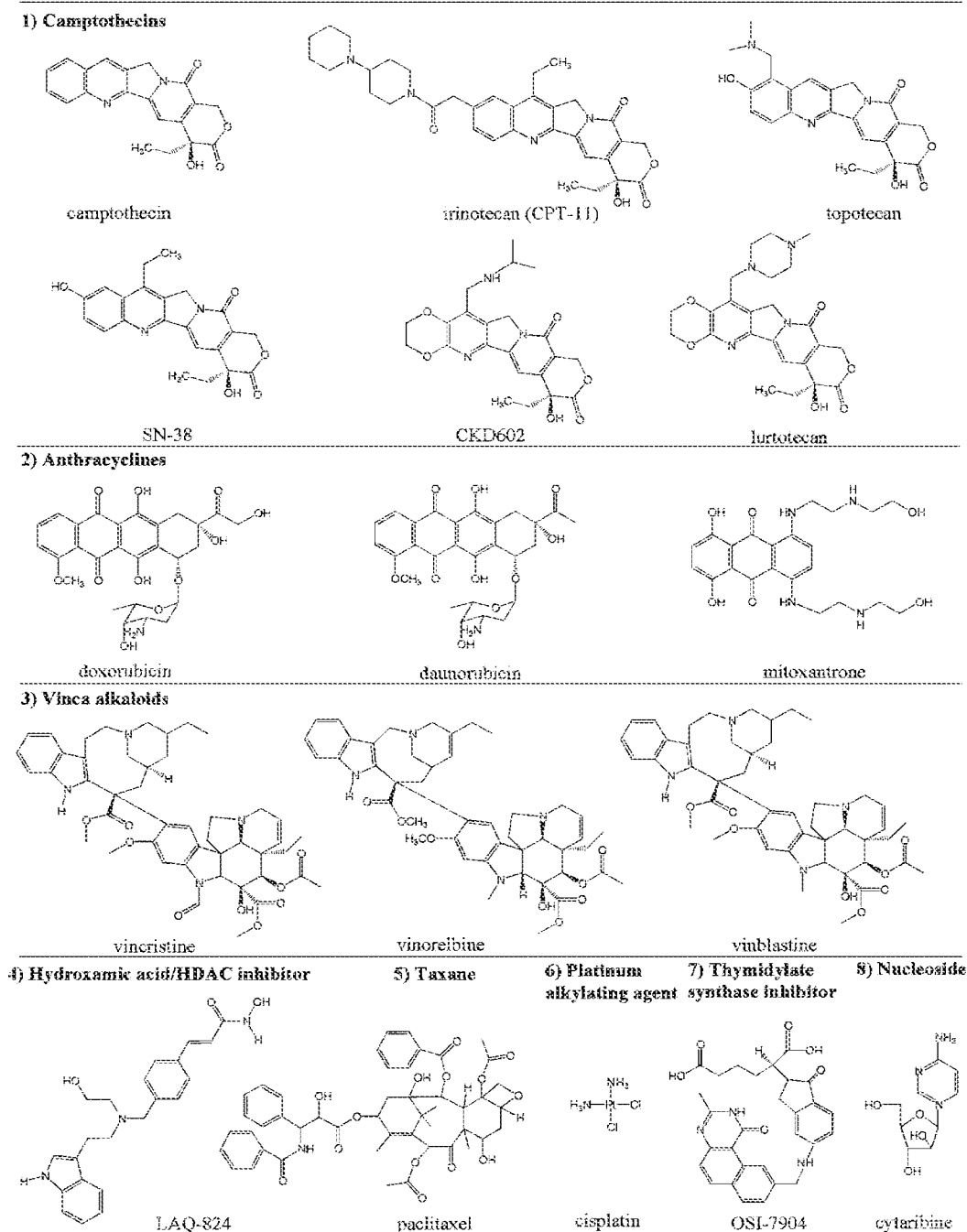


**Figure 1.** Structures of various anticancer drugs which have been incorporated in liposomal nanocarriers. The chemical structure of each directs the choice of optimal liposome loading method and also can influence stability of the resulting formulation.

specific agent, a sustained release of the drug in the plasma can improve antitumor activity and reduce the frequency of administration or need for long infusions.

Finally, liposomes or lipidic nanocarriers can be modified so that drug encapsulation is sensitive to

a specific stimulus, including changes in pH, light, oxidation, enzymatic degradation, heat, or radiation. These nanocarriers are thus engineered for triggered release of the encapsulated drug specifically at or near the site of disease being targeted for treatment. A drug whose mechanism of action

**Table 1.** Preclinical Pharmacokinetic Parameters of Various Chemotherapeutic Agents Administered as the Nanoparticle Formulation or Unencapsulated Small Molecule

	$t_{1/2}$ (h)	AUC <sub>∞</sub> (μg · h/mL)	CL (mL/h)	V <sub>d</sub> (mL)	MRT (h)
Paclitaxel	7.24	5.85	167 <sup>b</sup>	1750 <sup>b</sup>	nd
Abraxane	11.42	4.59	222 <sup>b</sup>	3666 <sup>b</sup>	nd
CPT-11	0.27	6.2	1609	616.4	0.4
nLs-CPT-11 (Pn)	6.8	1408	7.10	69.7	9.8
nLs-CPT-11 (SOS)	10.7	2134	4.69	72.3	15.4
Lurtotecan	0.832 <sup>c</sup>	0.069	254 <sup>c</sup>	nd	0.775
NX 211	2 <sup>c</sup>	127	0.177 <sup>c</sup>	nd	4.45
LAQ824	0.2	13.6	737.2	808	1.1
Ls-LAQ824	10.8	2198	4.5	70.7	15.5

AUC<sub>∞</sub>, area under the concentration versus time curve in plasma based on the sum of exponential terms; MRT, mean residence time; CL, clearance; V<sub>d</sub>, volume of distribution; Pn, polyphosphate-stabilized formulation; SOS, sucroseoctasulfate-stabilized formulation.

<sup>a</sup>Half-life calculated as  $t_{1/2\lambda z}$ .

<sup>b</sup>Assumes 0.2 kg rat weight (paper states 7–8 weeks).

<sup>c</sup>Assumes 22.5 g mouse weight (paper states 20–25 g).

benefits from a high peak concentration of bioavailable drug would be expected to benefit from triggered release, as would therapeutic agents that do not easily transverse lipid membranes and thus require a stimulus for increasing the efficiency of release of the specific agent from the carrier. Highly water soluble small molecular

weight drugs and nucleic-acid based therapeutics often fit into this latter category. These factors will be examined in detail in the Section titled Triggered Delivery of Encapsulated Therapeutics.

The following sections of this review discuss aspects of tailoring liposome formulations to specific applications and therapeutic agents. The pharmacokinetics and efficiency of drug delivery to sites of disease vary depending on a range of factors, including the specific liposome and drug employed. This is illustrated in Figure 2, where the pharmacokinetics of five different liposomal formulations of various camptothecins are shown. As can be seen, the pharmacokinetics vary widely even within the same class of drug, indicating that not all liposomal carriers are equivalent and that engineering is required to optimize the formulation and delivery of each therapeutic agent in a lipidic nanocarrier. The vast wealth of knowledge regarding the biophysical and pharmacological properties of liposomal delivery systems results in them being one of the most mature and well understood drug delivery systems. This knowledge base when advanced properly can aid in the more efficient and timely tailoring of liposomal delivery systems to specific therapeutic agents or applications, as well as provide a template for more rapidly moving forward newer classes of drug nanocarriers. In this review, we will also provide examples of liposome formulations that have been developed and studied preclinically or clinically, the factors that influence the effectiveness of their formulation, and how their pharmacokinetics and drug release rates affect their activities and toxicities.

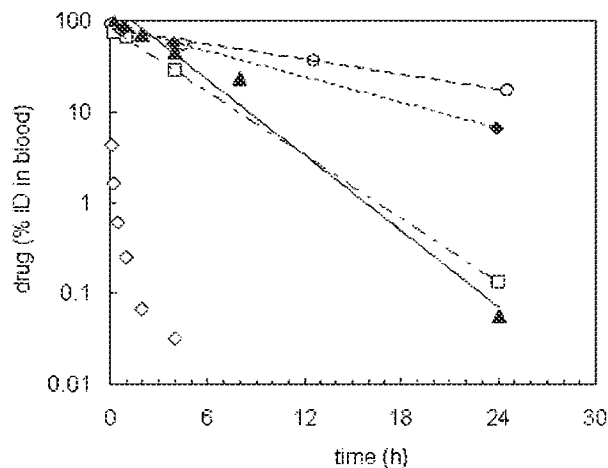


**Figure 2.** Blood pharmacokinetics of various camptothecin analogs administered as a liposomal formulation in mice. The data are reported as % injected dose (%ID) of the indicated camptothecin analog over time: 40 mg/kg liposomal CPT-11, three female Swiss Webster mice per time point (○); 50 mg/mL liposomal CPT-11, six SCID/Rag-2M mice per time point,<sup>141</sup> (◆); 1 mg/mL liposomal lurtotecan, four female Nu/Nu mice per time point,<sup>13</sup> (▲); 10 mg/kg liposomal topotecan, female BALB/c mice (□);<sup>15</sup> 10 mg/mL liposomal SN-33, three male CD2F1 mice per time point (◇).<sup>14</sup> This figure was adapted from Messerer et al.,<sup>141</sup> Emerson et al.,<sup>13</sup> and Pal et al.<sup>14</sup> with permission.

## FACTORS THAT INFLUENCE THE PHARMACOKINETICS OF LIPOSOMES

There are a wide range of factors that influence the pharmacokinetics and biodistribution of liposomal nanocarriers. The clearance of a liposome-associated drug from the blood is dependent on: (1) the rate of clearance of the liposomal carrier itself, (2) the rate of disassociation of the complexed, entrapped, or lipid membrane-solubilized drug from the carrier, and the (3) rate of clearance and metabolism of free drug upon its release. The pharmacokinetics of the actual liposomal carriers have been extensively reviewed over the years, and thus although the present Section will attempt to update and expand the current understanding on liposome pharmacokinetics, the readers are referred to several of these many excellent reviews for more in depth discussions of the individual effects outlined below.<sup>1,2,31-33</sup>

Following i.v. administration, nonpegylated liposomes display saturable nonlinear pharmacokinetics with relatively rapid clearance at low doses.<sup>32,33</sup> Although pegylated liposomes display log-linear pharmacokinetics over a wide range of doses,<sup>32</sup> the pharmacokinetics have also been shown to be more complicated at very low doses and upon repeated administration.<sup>30,34-38</sup> The physicochemical properties of the liposomal carrier, the dose, dosing schedule, the route of administration, the actual drug that is encapsulated, and the presence of targeting ligands or other "foreign" extraliposomal molecules can all affect the pharmacokinetics of the liposomal carrier. The role each of these factors play in determining the pharmacokinetics and delivery to the site of disease of liposomal therapeutics is described below.

### Lipid Composition and Charge

The effect of lipid composition on pharmacokinetics and clearance of liposomal carriers is complex and even to this date not fully explored. The choice of lipids can affect the clearance of a liposomal drug directly, by having an effect on the recognition and clearance of the liposomes themselves, or indirectly through modulation of the rate of drug release. This section will concentrate on the direct effects of the lipid composition on the clearance of the liposomal carrier. The indirect effects on drug retention will be explored in greater detail in Control of *In Vivo* Drug Release Rates Section.

The inclusion of cholesterol can act to stabilize liposomal phospholipid membranes to disruption by plasma proteins,<sup>39,40</sup> and results in decreased binding of plasma opsonins responsible for rapid clearance of liposomes from the circulation.<sup>41,42</sup> Cullis and coworkers<sup>43</sup> showed that cholesterol-free liposomes bound 3-4 times more protein than did cholesterol containing liposomes, and this correlated with a substantial increase in clearance from the blood of mice. Cholesterol-free liposomes have also been shown to aggregate rapidly in the absence of steric stabilization and it is observed that this size instability also leads to increased clearance<sup>44</sup> and decreased storage stability. However, even small concentrations of PEG-derivatized lipid were able to rescue the formulation, dramatically improving circulation lifetimes.<sup>44</sup> This is important because some drugs are known to be retained more efficiently in cholesterol-free liposomes.<sup>45,46</sup> The relationship between cholesterol and drug retention in liposomal carriers will be described in greater detail in the subsequent section.

The fluidity of the membrane can also effect the rate of clearance, with nonpegylated liposomes composed of unsaturated phospholipids and cholesterol displaying faster clearance rates than those containing saturated phospholipids.<sup>1,47,48</sup> In the absence of cholesterol, neutral phosphatidylcholine liposomes composed of highly saturated gel phase lipids were cleared more rapidly.<sup>43</sup> The rate of liposome clearance varied positively with both the concentration of plasma protein bound and the phase transition temperature of the phosphatidylcholine employed,<sup>43</sup> likely due to increased protein binding to exposed hydrophobic domains originating from packing defects in gel phase membranes. However, at concentrations of cholesterol greater than 30 mol%, the formation of a highly ordered crystalline state resulted in decreased protein binding for liposomes comprised of distearoylphosphatidylcholine (DSPC), and dramatically increased circulation lifetimes.<sup>43</sup> Substitution of sphingomyelin for the high phase transition DSPC increased circulation lifetimes in cholesterol containing liposomes,<sup>33,49</sup> likely due to the highly cohesive membranes<sup>50</sup> formed as a result of intermolecular hydrogen bonds between sphingomyelin and neighboring cholesterol,<sup>51,52</sup> or even other sphingomyelin<sup>53,54</sup> molecules, that reduced protein binding even further. Liposomes composed of hydrogenated sphingomyelin and cholesterol were recently shown to even further improve circulation lifetimes for both the liposomal carrier and the

encapsulated vincristine.<sup>55</sup> However, while non-pegylated (noncoated) liposomes appear to be extremely dependent on the lipid composition of the carrier, hydrophilic polymer-coated liposomes appear to be more flexible, allowing for a much greater range of lipid compositions beneath the polymer coat while still maintaining their long circulation lifetimes.<sup>1,48</sup>

Charged lipids can also affect liposome clearance, although the relationships can often be very complex.<sup>1</sup> In general the inclusion of high concentrations of either anionic or cationic lipids into liposomal membrane increases the clearance of liposomes from the circulation. High concentrations of anionic lipids increase accumulation in the liver and spleen.<sup>1,42,56</sup> In addition to the liver and spleen, increasing concentrations of cationic lipids enhance uptake by vascular endothelial cells primarily in the lung,<sup>57</sup> but also in angiogenic blood vessels supporting tumors,<sup>58,59</sup> and even at the blood brain barrier.<sup>60</sup> Poorly designed cationic lipid-nucleic acid complexes can be extremely polymorphic resulting in rapid aggregation in the presence of serum,<sup>61</sup> and subsequent accumulation in the small capillaries of the lung.<sup>62</sup> Care should be taken in constructing cationic lipidic nanocarriers, as other cationic nanoparticles have resulted in toxicity and disruption of the blood brain barrier.<sup>63</sup> However, even cationic liposomes or lipidic nanocarriers can be made stable and long circulating by reducing the content of cationic lipid and inclusion of PEG-lipid stabilizers.<sup>64,65</sup>

The correlation to charge for liposomes with a net negative charge is also dependent on the specific anionic lipid being utilized in the formulation, with small concentrations of anionic gangliosides, phosphatidylglycerol, phosphatidylinositol, and PEG-derivatized phosphatidylethanolamines either resulting in a small increase in clearance or a substantial reduction in clearance depending on the lipid and the precise lipid composition employed.<sup>1,47,56,66</sup> Other synthetic anionic acylated phosphatidylethanolamines have also been effective at improving circulation lifetimes.<sup>67,68</sup> However, the presence of phosphatidic acid, phosphatidylserine, and cardiolipin have generally been shown to dramatically increase the rate of clearance from the blood.<sup>1,42,56</sup> This discrepancy is in part due to the differences in protein/opsonin binding to membranes containing different anionic lipids. Liposomes comprised in part of the latter groups of anionic lipids have been shown to bind substantially higher concentrations of plasma proteins, while liposomes composed

of phosphatidylglycerol, phosphatidylinositol, and pegylated phosphatidylethanolamine show less protein binding.<sup>56,69</sup> The presence of phosphatidylserine on the surface of liposomes has even been shown to result in receptor-mediated clearance.<sup>70</sup> Thus, great care must be utilized when including charged lipid components into different liposomal therapeutics. As will be discussed in a later section, charged lipids also play a role in the stability of encapsulation or complexation of different therapeutic agents, and thus both circulation lifetimes and stability of association for the specific therapeutic will have to be considered and balanced in order to prepare the best formulation for a particular drug and application.

Pegylated liposomes represented a significant advance in liposome technology. Pegylated liposomes have been thoroughly reviewed.<sup>1,2,32</sup> In general, the inclusion of PEG-derivatized lipids was discovered to improve the circulation lifetimes of liposomes. The choice of lipid anchor and chemical linkages in preparing the specific PEG-conjugated lipid is important, as readily degradable linkages or lipid anchors of insufficient hydrophobicity can result in premature removal of the PEG-coat from the liposome surface and thus decrease the circulation lifetime of the carrier.<sup>71,72</sup> Even in the absence of steric stabilization by the grafted hydrophilic polymer layer, nonpegylated liposomes can be engineered to have reasonably long circulation lifetimes,<sup>1,33</sup> and may have other advantages, including increased rate of extravasation into solid tumors. However, PEGylation offers the advantage of utilizing a considerably greater variety of lipid compositions in the construction of the liposomes,<sup>1,44,48</sup> allowing for the use of unsaturated phospholipids, charged lipid components, or even the removal of cholesterol without significantly compromising circulation lifetimes. This is an important advantage considering that some of these components can play an important role in stabilizing the encapsulation of the therapeutic agent as well. There has also been noted in clinical studies that pegylated liposomal therapeutics<sup>73,74</sup> appear to display less heterogeneity in their pharmacokinetic parameters when compared to nonpegylated liposomal drugs.<sup>75-78</sup>

#### Dose, Schedule, and Route of Administration

Although as described above, the pharmacokinetics of pegylated liposomes do appear to be less

dependent on dose than their corresponding nonpegylated counterparts, the pharmacokinetics of pegylated liposomes are complicated by the "accelerated blood clearance" (ABC) phenomenon at very low lipid doses. The result is that microdoses of pegylated liposomes can result in substantially increased clearance of subsequent doses of liposomal drugs. The extent of the ABC phenomenon is dependent on both the time after the initial injection,<sup>36</sup> the presence of cytotoxic drug,<sup>34</sup> and the dose<sup>79</sup> of the initial injection. The effect appears to be mediated by specific IgM molecules against poly(ethylene)glycol.<sup>35,80</sup> Due to the schedule of drug administration in the clinic, the presence of the cytotoxic doxorubicin, and the higher lipid dose employed, the ABC phenomenon is not prominent in the case of pegylated liposomal doxorubicin.<sup>31</sup> However, it should be considered and tested for when using different drugs, especially when the drug's effective dose and stability of encapsulation dictates that relatively low lipid doses are to be used. In addition, although pegylated liposomal doxorubicin is frequently administered every 4 weeks to reduce the incidence of palmar-plantar erythrodysesthesia (PPE or "hand-foot" syndrome),<sup>81</sup> many other drugs do not display this particular toxicity and may be administered more frequently, thus increasing the possibility of the ABC phenomenon.

Nonpegylated liposome formulations are cleared from the circulation in a dose-dependent saturable manner.<sup>1,32,82</sup> Circulation lifetimes with these liposomes increase proportionately with increasing lipid dose. The decreased clearance by the mononuclear phagocyte system is thought to result from a combination of saturation of the metabolic pathways responsible for intracellular degradation of liposomal lipids<sup>83</sup> and due to depletion of serum opsonins at high lipid doses.<sup>34,85</sup> The results can be reasonably long circulating liposomes at moderate to high lipid doses.

As eluded to above, the schedule of administration can be very important, since too frequent administration can result, for example, in accumulation of the cytotoxic drugs at undesirable anatomical sites, such as skin.<sup>31,86</sup> However, repeated injections can also increase the accumulation of some liposomal drugs in solid tumors. Straubinger and coworkers<sup>87</sup> demonstrated this with brain neoplasms, where subsequent doses of liposomal doxorubicin accumulated more readily in intracranial brain tumors than the initial dose,

consistent with increased vascular permeability resulting from the initial doxorubicin dose.

Liposomal carriers have been administered using many different routes although by far the most common is intravenous. Liposomal anticancer drugs are given intravenously primarily because this route provides access to distant sites of metastasis, thus allowing the liposomal therapeutic to target both the primary tumor and various metastatic sites simultaneously. Delivery via certain routes, such as in intraperitoneal or subcutaneous administrations, may impair the efficiency of delivery to even the primary site.<sup>88,89</sup> The increased barrier to uptake from lymphatic capillaries at sizes above 18 nm<sup>90</sup> likely results in part in the poor systemic exposure when delivered subcutaneously. However, other routes of administration are warranted for specific applications. The most notable example is the multivesicular liposome formulation of cytarabine (DepoCyt<sup>TM</sup>), approved clinically for the treatment of malignant lymphomatous meningitis.<sup>91</sup> Although the large size (10–20  $\mu$ m) of this structure would preclude its administration via the i.v. route, when given intrathecally the elimination half-life of the drug is improved from 0.74 to 156 h in monkeys,<sup>92</sup> and releases cytotoxic concentrations of cytarabine that are maintained in the cerebrospinal fluid for a minimum of 2 weeks.<sup>91</sup>

The subcutaneous route of administration can be advantageous for targeting cells located in regional lymph nodes, such as dendritic cells, T- or B-lymphocytes, and macrophages. When administered subcutaneously, liposomes have been shown to pass through the lymphatic capillaries into the lymph nodes, prior to entering the general circulation.<sup>88,93</sup> Cullis and coworkers<sup>94</sup> have used this route to target antigen presenting cells concentrated in the lymph nodes with lipid nanoparticles of unmethylated CpG-containing oligonucleotides to induce an immune response.

Delivery of macromolecular carriers to the brain poses a significant challenge due in part to the blood brain barrier.<sup>95</sup> Although, brain tumors do possess a discontinuous vasculature similar to tumors localized in other areas of the body, the size of the pores is significantly smaller in the brain.<sup>25</sup> We and others have used convection-enhanced delivery (CED) to administer liposomes directly into the brain.<sup>96–99</sup> CED is a local delivery technique that uses a pressure-driven flow of therapeutic agents directly to the brain, enabling the delivery to a substantial volume of tissue, improving significantly the volume of distribution

relative to simple diffusion. Liposomes are particularly suitable for CED as the blood brain barrier is circumvented and the properties of the carrier particle direct the distribution of its contents within the brain tissue. The distribution of the liposome-encapsulated drug is determined by the infusion volume for formulations that are inert,<sup>98</sup> and thus do not interact either specifically or nonspecifically with the various cells in the brain.<sup>96,100</sup> We have recently demonstrated the improved pharmacokinetics and antitumor efficacy for liposomal CPT-11<sup>97</sup> (Fig. 3) and topotecan<sup>99</sup> using this methodology. The clearance of the CPT-11 from the brain was dose dependent and slow in rats, with a  $t_{1/2}$  of 19.7 days at the highest dose (Fig. 3) and although there was no observable toxicity at any dose, the efficacy in treating intracranial brain tumors was considerably improved compared to treatment with the free drug (median survival >100 days compared to 28.5 days for the free CPT-11 group and 19.5 days for the control). This route and method of delivery offers significant benefit over the more traditional intravenous delivery and will likely be even more important when treating diseases of the central nervous system where the vasculature is not compromised as it is with brain tumors. Importantly, the administration of a liposomal drug via CED can be guided by the simultaneous imaging of coadministered and similarly designed liposomal contrast agents.<sup>98,101</sup>

### Particle Size

The role of particle size in clearance of liposomes and other nanocarriers has been well studied. In general, increasing liposome size results in increased clearance from the blood, although the effect appears to be more dramatic for nonpegylated liposomes when compared to pegylated liposomes. The same may not follow for all nanoparticles, where very small particles (<4–8 nm)<sup>102,103</sup> may be cleared to some degree by glomerular filtration in the kidneys. But, due to the inherent instability (related to the high membrane curvature) and low entrapped volume of extremely small lipid vesicles (i.e., <40–50 nm), lipidic nanocarriers are not typically prepared at these small sizes. Small colloids may also extravasate from the liver microvasculature and accumulate in hepatocytes, although with relative inert pegylated liposomes the uptake in hepatocytes is negligible even down to 70 nm.<sup>104</sup> The magnitude of the liposome size

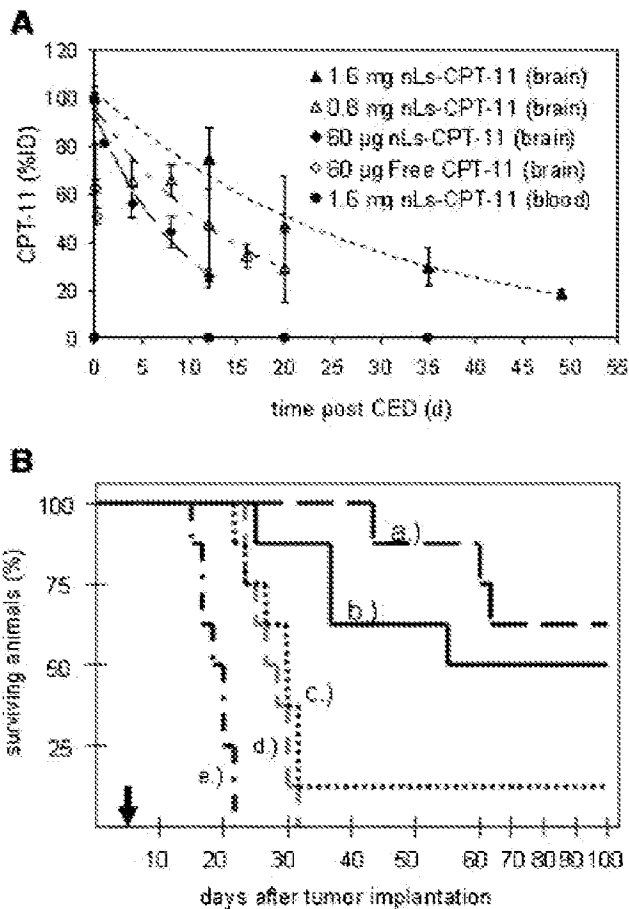


**Figure 3.** (A) Tissue pharmacokinetics of free CPT-11 and nanoliposomal CPT-11 in the normal adult rat brain and blood following single CED infusion of 20  $\mu$ L. All values are expressed as %ID versus time after CED. Drug concentrations were determined by HPLC assay for CPT-11  $\cdot$  HCl. CPT-11 concentrations in blood were all below the detection limit of 1 ng/mL ( $\sim$ 0.03 %ID). (B) Treatment of rats bearing orthotopic U87 tumors with a single CED infusion of free or nanoliposomal CPT-11. Five days after tumor implantation within the brain (arrow), rats were treated with: (a) nanoliposomal CPT-11 at 1.6 mg (80 mg/mL), (b) nanoliposomal CPT-11 at 0.8 mg (40 mg/mL), (c) nanoliposomal CPT-11 at 60  $\mu$ g (3 mg/mL), (d) free CPT-11 at 60  $\mu$ g (3 mg/mL), (e) liposomal DiIC<sub>18</sub>(3) without encapsulated drug (empty liposomes). Each group contained eight animals with the median survival and log rank test  $p$ -value versus control for each as follows: (a) >100 days,  $p = 4.93 \times 10^{-5}$ ; (b) 78 days,  $p = 1.70 \times 10^{-4}$ ; (c) 30 days,  $8.74 \times 10^{-4}$ ; (d) 28.5 days,  $p = 1.70 \times 10^{-5}$ ; (e) 19.5 days. This figure was adapted from Noble et al.<sup>97</sup> with permission.

effect on blood clearance is in part a function of the lipid composition employed. Pegylated liposomes are considerably less sensitive to the effects of size on blood clearance in the range of 80–250 nm,



than are corresponding nonpegylated liposome compositions.<sup>48,105</sup>

In addition, liposomes with smaller diameters are known to accumulate more readily into solid tumors partially as a result of their longer circulation lifetimes, but also due to their increased ability to extravasate across the tumor endothelium.<sup>51,106</sup> However, as we have previously suggested, the rate of clearance of the liposomes from the tumor has been a neglected pharmacokinetic parameter.<sup>1</sup> This rate of clearance may in fact be responsible for why liposomes of approximately 100–120 nm demonstrate optimum accumulation in many solid tumors, whereas even smaller liposomes (~60–80 nm) accumulate less efficiently despite their faster rate of extravasation and slower clearance from the circulation.<sup>106,107</sup>

### Encapsulated Drug

The efficiency by which a drug is retained within its carrier imparts the greatest effect on the resulting pharmacokinetics. However, a cytotoxic drug can also play a role in increasing the circulation lifetime of the liposomes themselves by in effect poisoning the macrophages of the mononuclear phagocyte system (MPS) in a process referred to as MPS blockade. For example, the delivery of doxorubicin via liposomes can result in a substantially increased circulation lifetime at higher lipid doses or upon frequent readministration compared to similarly designed liposomes without the loaded drug.<sup>108–110</sup> However, many drugs, including mitoxantrone,<sup>21</sup> may not show this effect, and there has been no systematic study evaluating the effects of the nature of the entrapped drug on the *in vivo* liposome clearance due to macrophage phagocytic activity.

Alternatively, different payloads may adversely affect the pharmacokinetics of a specific lipidic nanocarrier. For example, nucleic acid based therapeutics that contain cationic lipids can result in an immune response that dramatically increases the clearance of subsequently administered nanoparticles.<sup>111,112</sup> The addition of pegylated lipids also plays an important role on the magnitude of the immune response.<sup>112</sup> A more detailed analysis of the factors that influence the pharmacokinetics of nucleic acid based vectors is given in the final section on Specific Delivery Challenges for Nucleic Acids. However, these examples illustrate the importance of evaluating

the influence the encapsulated agents has on the pharmacokinetic properties of a particular lipidic nanocarrier, particularly in a multiple dosing format.

### Ligand-Conjugation

The conjugation of a targeting ligand to the surface of a nanocarrier can adversely affect its pharmacokinetics and biodistribution if not properly engineered, or if the epitope being targeted is not sufficiently specific for the diseased tissue or cell. Targeting ligands for liposomes or other nanocarriers can include a wide array of molecules. These include antibodies or antibody fragments, small molecule ligands such as folate, sugars, or even nucleic acids in the form of RNA aptamers.<sup>113,114</sup> Immunoliposomes constructed using antibodies or antibody fragments are among the most studied of these constructs. Usually, the antibody or a fragment is conjugated to a linker molecule that includes a hydrophobic moiety acting as an “anchor” within the lipid bilayer of the liposome, and an intermediate group that links the anchor to the antibody. Linkers containing aromatic groups have the potential to be immunogenic,<sup>115</sup> and should be avoided; they can easily be replaced with similar aliphatic linkers. If repeated administration of the immunoliposomal drug is planned, the targeting ligand itself should also not be immunogenic. Increased clearance of the carrier due to attachment of the targeting ligand should be minimized unless the antigen is readily accessible to the vascular compartment, and consequently increased clearance primarily results from target binding. The conjugation of anti-VEGF aptamer was shown to increase clearance of conjugated liposomes, although it was not evident whether the increase clearance was due to a recognition of the aptamer itself by opsonins or macrophages in the liver, or whether it was due to a cross reactivity with target antigen in the mouse.<sup>116</sup> Immunoliposomes prepared using full IgG molecules have been repeatedly shown to increase the rate of clearance compared to nontargeted liposomes,<sup>117–119</sup> resulting from recognition of the Fc portion of the antibody by Fc receptors on the surface of macrophages. However, the use of smaller fragments, such as Fab’s or scFvs, does not compromise circulation lifetimes.<sup>119–121</sup> The use of humanized or fully human antibodies is also desirable,<sup>113,120,121</sup> since repeated dosing of immunoliposomes containing

xenogenic protein sequences may result in immunogenicity.

## CONTROL OF *IN VIVO* DRUG RELEASE RATES

The rate of *in vivo* drug release is an extremely important parameter since it can influence the rate of clearance of the drug from the general circulation, the bioavailability and thus activity of the drug at its site of action, the targetability of the drug, and the observed toxicities.<sup>1,31</sup> Many groups have routinely attempted to demonstrate liposome stability using *in vitro* incubations in the presence of saline or plasma. Although these somewhat useful preliminary measures of formulation stability may serve to identify liposomal drug constructs with particularly poor drug retention, they nonetheless are inadequate predictors of the same formulation's stability *in vivo*. The *in vivo* encapsulated drug concentration can be determined either directly by measuring purified liposomal drug in plasma,<sup>11,78,122</sup> or indirectly by assuming that the clearance rate of the unencapsulated drug is sufficiently faster than the clearance rate of the liposome to allow for the rates of drug release to be calculated by simply following changes in the plasma drug-to-lipid ratios.<sup>12,123</sup> However, for hydrophobic drugs, or drugs that generally demonstrate significant protein or lipoprotein binding, these measurements can be considerably more difficult. Such protocols are imperative to accurately determining the stability of a particular liposomal construct in the circulation. For some drugs, the rate of *in vivo* drug release can be carefully controlled by manipulating physicochemical properties of the carrier or modifying the technology for entrapment or complexation of a therapeutic agent within the carrier.

### Gradient Loading Strategies

The drug encapsulation method is important in determining the *in vivo* stability of a particular liposomal drug construct. Drugs can be incorporated into liposomes using a variety of different strategies. Hydrophobic drugs can be simply solubilized in lipid membranes, albeit typically at low efficiencies (drug-to-lipid molar ratio of 1:20–1:100) and with poor stability in the circulation.<sup>124,125</sup> Drugs can also be encapsulated pas-

sively in the internal aqueous space by simply including them in the hydration media for the liposomal lipids.<sup>126,127</sup> Some therapeutic agents, including both small molecule drugs and nucleic acid based therapeutics, can be complexed with charged lipid components.<sup>128,129</sup> However, one of the most widely used and successful class of encapsulation methods employs transmembrane gradients and trapping agents to efficiently load, and subsequently stabilize, weakly basic amphipathic drugs in the liposomal lumen. These can include (1) simple pH gradients formed using citric acid solutions,<sup>130,131</sup> (2) ammonium ion gradients employing citrate<sup>132</sup> or sulfate<sup>133,134</sup> ammonium salts, (3) alkyl,<sup>135</sup> dialky, or trialkylammonium salts,<sup>12,136</sup> (4) gradients of transition metal concentration ( $\text{Cu}^{2+}$ ,  $\text{Mn}^{2+}$ ,  $\text{Zn}^{2+}$ ,  $\text{Mg}^{2+}$ ),<sup>137–139</sup> or even (5) transmembrane gradients of drug solubility.<sup>140</sup> The cation entrapped in the liposome interior plays a role in establishing a pH gradient across the membrane that helps drive the accumulation of weakly basic drugs into the liposome interior, or directly exchanges with the drug molecule. The counterion often plays an important role in stabilizing the formulation to premature leakage in the circulation or storage by forming stable complexes with the drugs upon encapsulation. A diagram depicting an example of the loading and subsequent stabilization process, where the gradient-forming cation is diethylammonium, and the complex-forming anion is sucrose octasulfate,<sup>12</sup> is shown in Figure 4.

A liposomal formulation of the camptothecin prodrug, irinotecan, displayed very different pharmacokinetics and *in vivo* drug release rates depending on the method used for encapsulation (Fig. 6C and D).<sup>12,141</sup> Using a manganese sulfate gradient loading, Bally and coworkers<sup>141</sup> prepared a liposome formulation with what would generally be considered an average but reasonable degree of stability for this difficult to stabilize class of agents ( $t_{1/2}$  of drug release of 8.3 h). However, when the same drug was complexed intraliposomally with the high charge density sulfated polyol, sucrose octasulfate, the *in vivo* drug release half-life improved to 56.8 h.<sup>12</sup> Irinotecan liposomes prepared using average molecular weight polyphosphate as the stabilizing anion displayed an intermediate degree of stability ( $t_{1/2}$  = 14 h).<sup>12</sup> The difference is important, because as noted previously, the maximum accumulation of liposomes in solid tumors is on the order of 24–48 h, and thus formulations that leak drug more rapidly than the half-life of

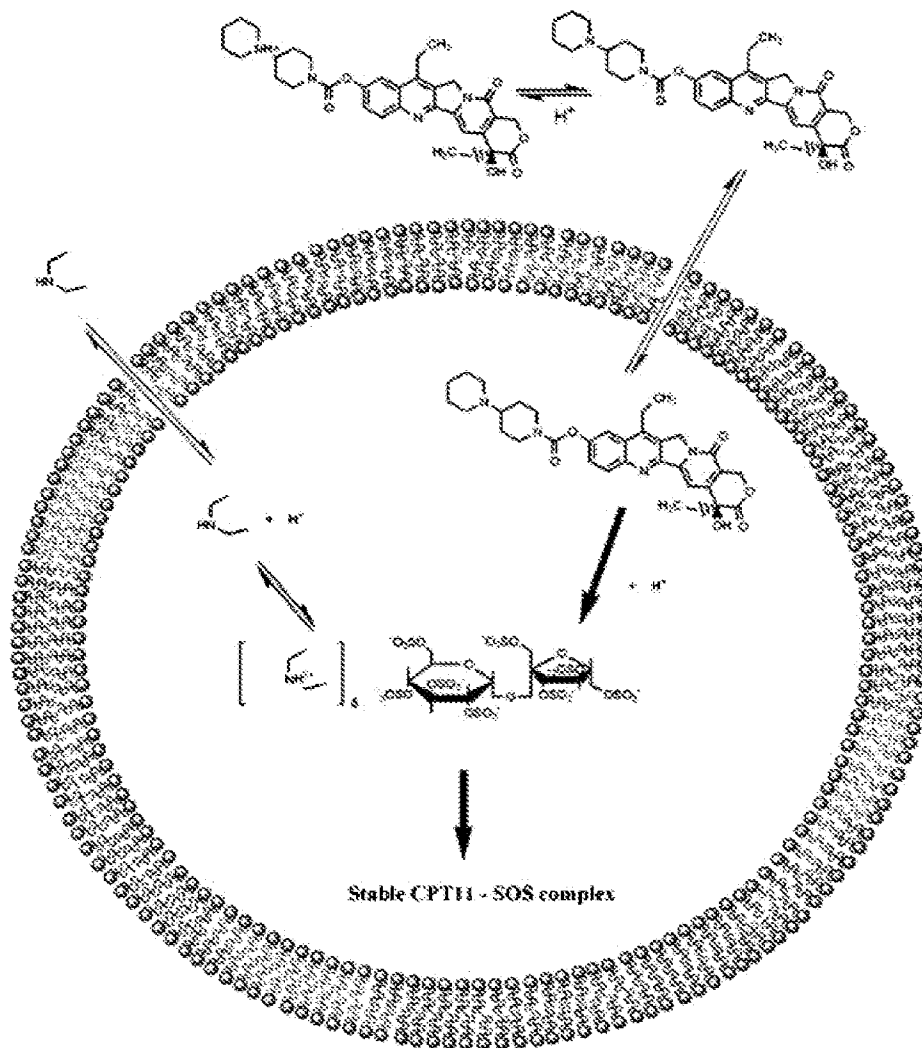


**Figure 4.** Schematic representing the liposomal loading and stabilization of CPT-11 with diethylammonium sucrose octasulfate contained within the liposome aqueous core. Diagram illustrates the chemical structure of CPT-11 in the cationic acid form and as the membrane-permeable neutral free base, in addition to the chemical structure of the DEA-SOS trapping agent.

accumulation in the tumor result in decreased antitumor activity and increased risk of systemic toxicities due to premature release in the blood.

The intraliposomal drug concentration also has an effect on the stability of liposomal drugs prepared using gradient loading methods. An early study where doxorubicin was loaded into eggPC/Chol liposomes using a simple pH gradient demonstrated that a lower drug-to-lipid ratio resulted in increased formulation stability *in vitro*.<sup>142</sup> This was thought to be due to the strength of the residual gradient in retaining the drug in the carrier. At higher drug-to-lipid ratios,

the pH-gradient across the membrane was exhausted thus resulting in increased leakage of the drug. Similarly, studies with pegylated liposomal doxorubicin showed that raising the concentration of gradient-forming salt, ammonium sulfate, used to load doxorubicin, from 155 to 250 mM, improved formulation stability.<sup>2,143</sup> Alternatively, studies using vincristine or irinotecan have shown that higher drug-to-lipid ratios result in increased stability,<sup>12,144</sup> possibly resulting from the intraliposomal drug concentrations exceeding the aqueous solubility of the drug. The formation of insoluble precipitates or gels has

been demonstrated for several drugs using cryo-electron microscopy (Fig. 5). When the intraliposomal drug concentration exceeds the threshold of the drug solubility, because of the high drug concentration, complexation with the intraliposomal stabilizing component, or both, the release of the drug from liposomes may acquire a desirable zero-order kinetics, due to the fact that the intraliposomal concentration of the releasable, that is, dissolved, drug is maintained constant via dissolution equilibrium with the intraliposomally precipitated portion of the drug.<sup>10</sup> However, depending on the potency of the drug to be encapsulated, it is wise to weigh the effect increasing drug-to-lipid ratio will have on the final dose of liposomes to be administered. As noted above, and especially for nonpegylated liposomes, many liposomes display dose-dependent pharmacokinetics; therefore higher drug-to-lipid ratios will result in decreasing lipid doses being administered and thus potentially faster clearance of the liposomal carrier itself. Even for pegylated liposomes, the combination of a high potency drug with a high drug-to-lipid ratio could result in a micro dose of liposomes being administered, and thus rapid clearance of the liposomal therapeutic, despite the presence of pegylation. Thus, although high drug-to-lipid formulations are useful for lower-to-moderate potency drugs, such as the prodrug CPT-11,<sup>12,97</sup> the release rates for higher potency drugs may be better modulated using alternative strategies, such as changes in the gradient or lipid composition being employed.

### Lipid Composition

A liposomally entrapped drug with a high degree of lipophilicity, once in the body, will tend to diffuse out of the liposome, crossing the liposome membrane along the gradient of its own concentration, the process to which the liposome membrane creates a kinetic barrier. Thus, the lipid composition of the liposome or lipidic nanocarrier can affect the rate at which a particular drug is released. The charge, phase transition, hydrogen-bonding capacity, membrane rigidifying potential, and presence of environmentally sensitive functional groups can all affect how efficiently a particular carrier retains each specific drug. Charged lipids, including the negatively charged cardiolipin or phosphatidylglycerol, have been used to complex

positively charged drugs<sup>135,145</sup> or even stabilize hydrophobic drugs such as paclitaxel or the highly active camptothecin, SN-38.<sup>17,146,147</sup> Small concentrations of charged lipids can provide sufficient electrostatic repulsion to prevent liposome aggregation upon addition of hydrophobic drugs to the membrane.<sup>148</sup> The observed improvements in stability over similarly designed neutral formulations do not necessarily result in liposomal drugs with long circulation lifetimes in the absence of other stabilization technologies. Additionally, a high content of charged lipid can adversely affect the liposome circulation, thus reducing or negating entirely the benefit resulting from the stabilization of the drug.<sup>149</sup> However, low concentrations of a negatively charged lipid have been shown to enhance the stability of a liposomal drug already encapsulated using a transmembrane electrochemical gradient.<sup>45,135</sup> Floxuridine retention increased dramatically upon inclusion of only 20 mol% of distearoylphosphatidylglycerol (DSPG) in DSPC liposomes<sup>45</sup> and in a separate study, the inclusion of either 15 or 55 mol% of DSPG in liposomes loaded with drug using a methylammonium gradient improved the retention of either vincristine or ciprofloxacin.<sup>135</sup> It was hypothesized that the inclusion of negatively charged lipids increased the membrane partition coefficient of weakly basic drugs improving their retention in liposomes maintaining a transmembrane pH-gradient. The presence of a negative charge at the membrane interface in other formulations has actually resulted in a decrease in formulation stability. In DSPC/Chol liposomes loaded with vincristine, the inclusion of the negatively charged PEG-DSPE in the membrane increased vincristine leakage in the circulation, while substitution with the neutral PEG-derivatized ceramide did not promote vincristine escape.<sup>72</sup> We have also observed an improved efficiency of loading for the more hydrophobic vinorelbine when prepared with high concentrations of the neutral PEG-derivatized distearoylglycerol (PEG-DSG), compared to PEG-DSPE (unpublished observations).

The cholesterol content of the liposome bilayer has also been shown to regulate drug retention. The presence of cholesterol helps prevent the destabilization of liposomal membranes by high-density lipoproteins in the blood,<sup>40,150</sup> and controls the permeability of membranes to small ions.<sup>151,152</sup> Various studies have demonstrated that the presence of cholesterol resulted in decreased leakage of ara-C from passively loaded

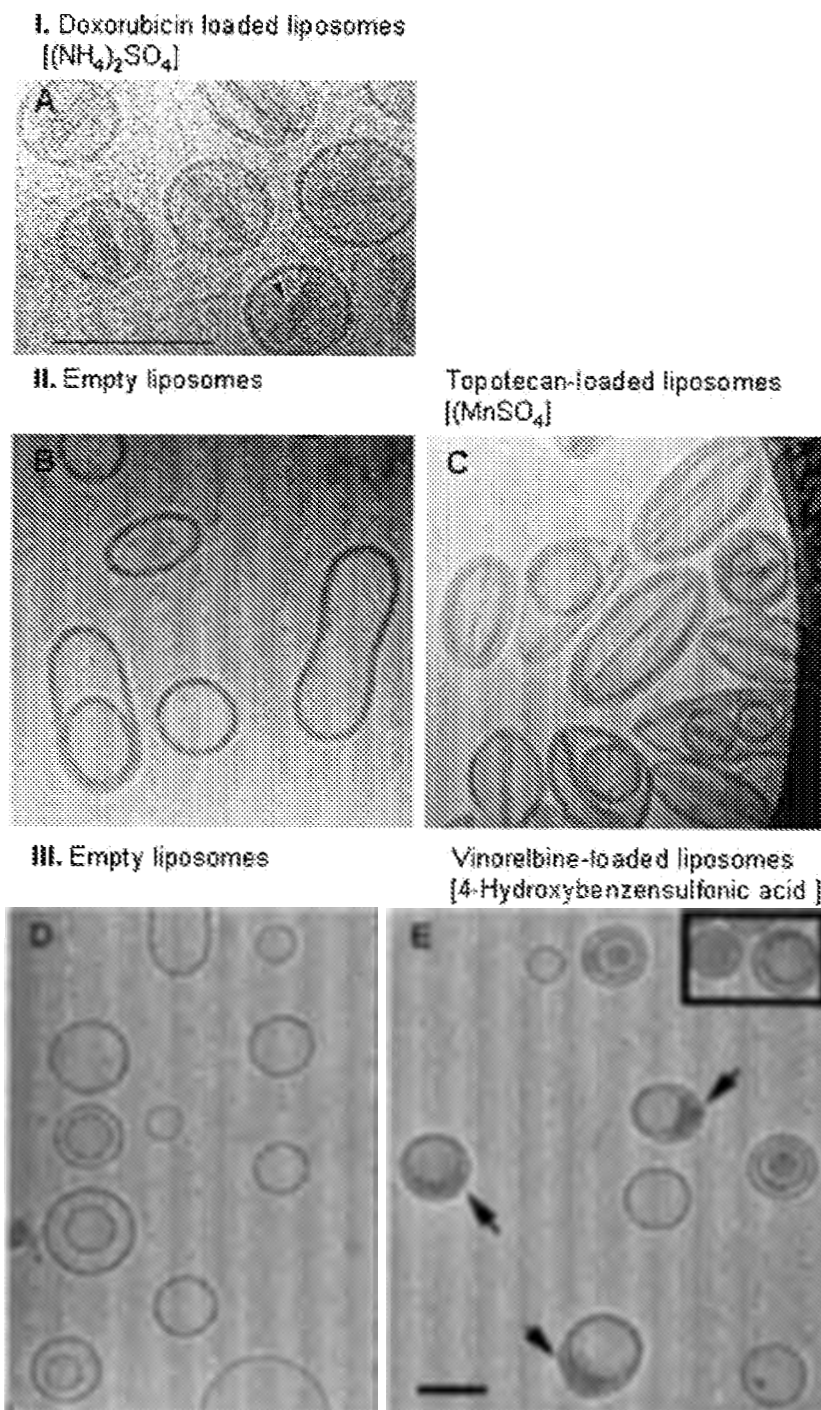


**Figure 5.** Electron micrographs of various liposomes containing crystallized drug after ion/pH-gradient loading. (NH<sub>4</sub>)<sub>2</sub>SO<sub>4</sub>-containing liposomes loaded with doxorubicin (A). MnSO<sub>4</sub> containing liposomes before (B) and after (C) loading with topotecan.<sup>137</sup> 4-Hydroxybenzensulfonic acid-containing liposomes before (D) and after (E) loading with vinorelbine.<sup>176</sup> This figure was adapted from Lasic et al.,<sup>296</sup> Abraham et al.,<sup>137</sup> and Zhigaltsev et al.<sup>176</sup> with permission.

liposomes,<sup>153</sup> and doxorubicin<sup>151</sup> or irinotecan<sup>45</sup> from gradient-loaded liposomes. The presence of cholesterol in liposomal membranes may influence or abolish this phase transition, and has a condensing effect on lipid membranes, forming highly cohesive lipid bilayers when present in lipid mixtures composed primarily of saturated phospholipids.<sup>59</sup> However, other studies have demonstrated an opposite affect, with increasing stability of encapsulation being observed for cholesterol free liposomes containing floxuridine<sup>45</sup> and idarubicin.<sup>46</sup>

The backbone and phase transition of the phospholipid component also influences drug retention. Phospholipids have a phase transition temperature at which they shift from a well-ordered gel phase to a fluid and disordered liquid crystalline state (Fig. 7). In general, liposomal

membranes are more permeable when the incubation temperature is above the phase transition for the particular lipids being employed. Thus, for short-chained or unsaturated phospholipids, physiological temperature (i.e., 37°C) is above the phase transition of many of these lipids and drug retention is severely compromised. On the other hand, highly saturated phospholipids such as DSPC or HSPC have a phase transition temperature (55–58°C) that is considerably greater than the temperature of the blood, therefore, the drug stability is more robust using liposomes comprised of these compositions. Doxorubicin was shown to be stably encapsulated in liposomes composed of DSPC/Chol, but released rapidly from liposomes composed of the highly unsaturated EggPC and cholesterol.<sup>108,154</sup> Doxorubicin-loaded pegylated liposomes composed of lipid compositions that

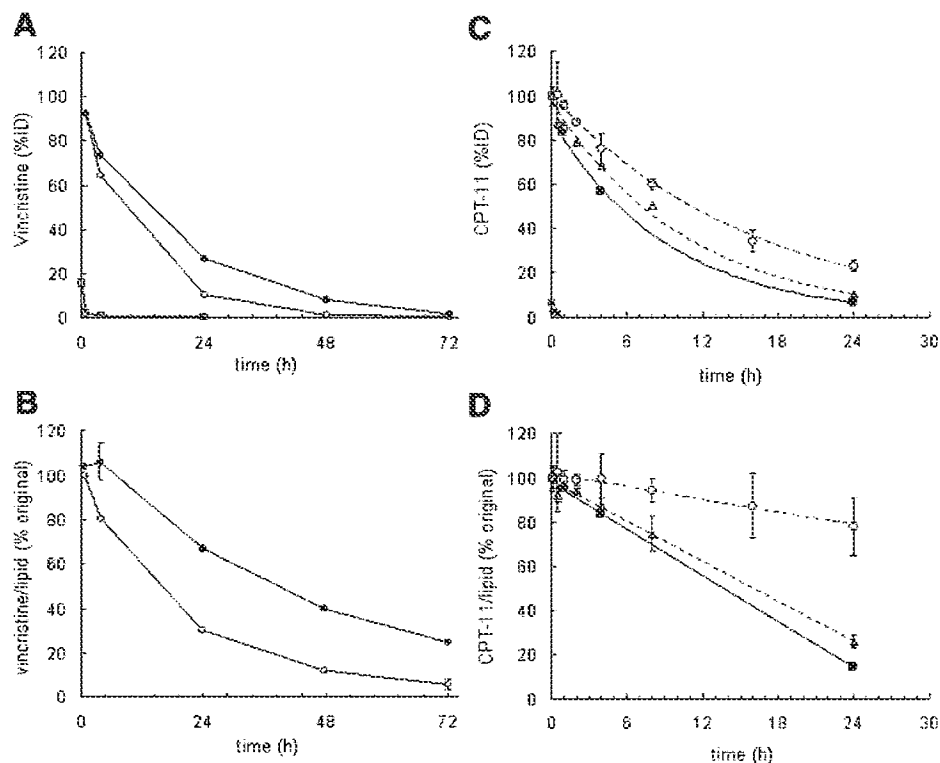


**Figure 6.** Effect of lipid composition on the pharmacokinetics liposomal vincristine and the effect of trapping agent on the pharmacokinetics of liposomal CPT-11. Liposomal vincristine composed of SM/Chol (●), DSPC/Chol (○), and free VCR (□) were evaluated. BDF1 mice were injected (i.v.) with each formulation at a drug dose of 2.0 mg/kg. The data is represented as % ID (A) and % original drug to lipid ratio (B). Free CPT-11 (25 mg/kg, ×) and liposomal CPT-11 formulated with triethylammonium sucrose octasulfate (10 mg/kg, ○), triethylammonium poly(phosphate) (10 mg/kg, ▲), and MnSO<sub>4</sub> (100 mg/kg, ■) were evaluated. Female Sprague-Dawley rats were used for all formulations except MnSO<sub>4</sub>, which were studied in SCID/Rag-2M mice. The data are represented as % ID (C) and % original drug to lipid ratio (D). This figure was adapted from Webb et al.,<sup>123</sup> and Drummond et al.<sup>12</sup> with permission.

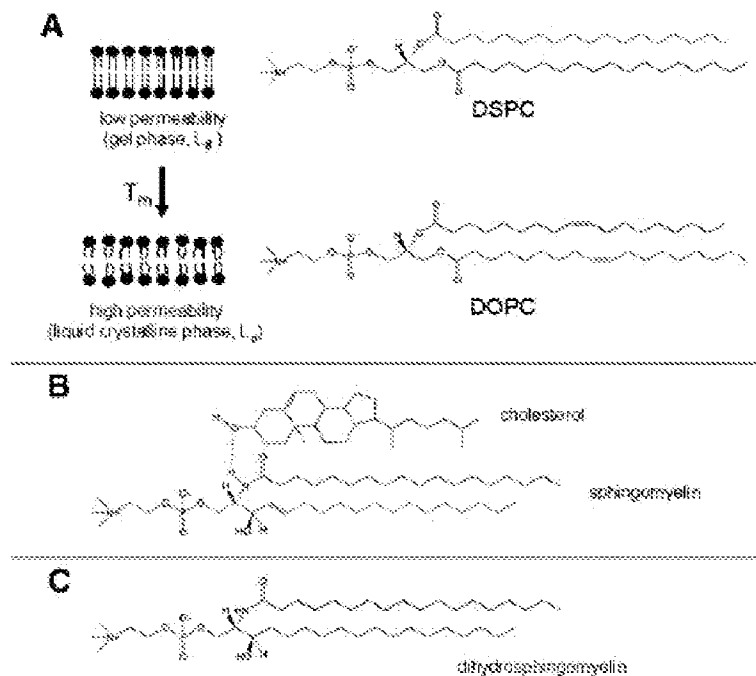


**Figure 7.** Effect of lipid structure on bilayer phase and permeability. (A) The structure of DSPC is shown illustrating complete saturation of the fatty acid chain. At 37°C a bilayer composed of DSPC will have a crystalline nature with low permeability contrasting DOPC which contains unsaturated bonds yielding a bilayer that is fluid-phase at 37°C and more permeable. (B) Illustration of the H-bonding that increases stability of bilayers composed of sphingomyelin and cholesterol. (C) Structure of dihydrosphingomyelin.

varied only in the specific phosphatidylcholine employed demonstrated clearance from the blood that correlated with the phase transition of the phosphatidylcholine (EggPC > DPPC > HSPC), reflecting the increased membrane permeability and thus leakage of doxorubicin for the EggPC and DPPC formulations.<sup>155</sup> Allen and coworkers<sup>156</sup> looked at a wider range of phosphatidylcholine species and were able to prepare pegylated liposomal doxorubicin formulations with an extensive range of drug release rates. For three of these formulations; liposomes prepared with DSPC, POPC, and DOPC resulted in a  $t_{1/2}$  in the plasma of 18.2, 11.9, and 2.1 h, respectively.

Sphingomyelin has also been shown to play a stabilizing role in membranes, particularly in the presence of cholesterol.<sup>52,157</sup> The result is tighter molecular packing of membrane lipids,<sup>50,158</sup> with a decrease in permeability to water and other solutes.<sup>159</sup> The high cohesiveness and reduced permeability of the membrane is thought to be due in part to strong hydrogen bonds between the amide nitrogen of sphingomyelin and the hydroxyl

group of cholesterol (Fig. 7B),<sup>51,52,158,160</sup> as well as neighboring sphingomyelin molecules.<sup>53,54,161</sup> In addition, due to the amide linkage in its backbone, sphingomyelin is also less sensitive to pH-dependent hydrolysis when compared to the relatively more sensitive ester linkages of most diacylphospholipids.<sup>123</sup> Importantly, formulations composed of sphingomyelin have been used to stabilize liposomes loaded with a wide range of drug molecules; including floxuridine,<sup>162</sup> vincristine (Fig. 6A and B),<sup>72,144,163</sup> vinblastine,<sup>10</sup> vinorelbine,<sup>10,164</sup> topotecan,<sup>15</sup> and ciprofloxacin.<sup>165</sup> One of these drugs, sphingosomal vincristine has undergone extensive clinical investigation for the treatment of lymphocytic leukemia.<sup>166</sup> Substitution of dihydrosphingomyelin (DHSM; Fig. 7C) for sphingomyelin has also been shown to improve the stability of encapsulation for vincristine even further.<sup>55</sup> The decreased molecular flexibility attributed to the *trans* double bond between C4 and C5 in sphingomyelin could reduce the participation of the hydroxyl group in intermolecular hydrogen bonds,<sup>54</sup> resulting in less efficient

molecular packing when compared to DHSM.<sup>167</sup> In addition, DHSM has been shown to have a higher affinity for cholesterol when compared to eggSM.<sup>168</sup> Thus, although its increased expense makes it less desirable than phosphatidylcholine in liposomal compositions, the ability of sphingomyelin or dihydrosphingomyelin to reduce the membrane permeability of certain drugs can play an important role in regulating the rate of drug release for certain difficult to stabilize small molecule drugs.

### Encapsulated Drug

The physicochemical properties of the therapeutic agent to be incorporated into the lipidic nanocarrier play an important role in determining its rate of release. We can generally break down drugs into five distinct classes: (1) water insoluble hydrophobic drugs, (2) amphipathic weak bases, (3) amphipathic weak acids, (4) highly water and membrane impermeable small molecular weight drugs, and (5) polyions such as nucleic acids. Some drugs can even be members of more than one class. Each class consists of its own formulation and delivery challenges.

The most commonly studied and easily engineered with regards to *in vivo* drug release rates are the amphipathic weak bases. These include many of the camptothecins, anthracyclines, and vinca alkaloids that are shown in Figure 1. Typically, these are loaded into liposomes using some form of a gradient based loading strategy that results in nearly quantitative encapsulation of the drug in the aqueous interior of liposomes. Although gradient-based loading strategies can vary greatly in their effectiveness, in general even poorly stabilizing gradients result in significant improvements in the pharmacokinetics of the encapsulated drug (see *Gradient-based loading strategies* below). However, even within a given class of drugs, the drug release rates can vary dramatically. For example, doxorubicin is stabilized easily using either simple pH-gradients<sup>130,131,169</sup> or ammonium sulfate gradients,<sup>133,134</sup> but is released slowly giving rise to an improved toxicity profile and antitumor efficacy. However, another member of this same class, mitoxantrone (Fig. 1), contains two weakly basic amines, compared to one for doxorubicin, and under similar encapsulation conditions produces formulations which are in fact too stable in the blood.<sup>21</sup> Because it is released more slowly

compared to doxorubicin, its activity is compromised and requires a modified lipid composition to promote release of the drug and improve efficacy.<sup>21,170</sup> Another member of this class, daunorubicin, is considerably more soluble in the presence of high concentrations of the citrate trapping agent,<sup>169</sup> and thus using the same pH gradients it is more difficult to stabilize by forming a precipitate. Epirubicin, being a simple enantiomer of doxorubicin, is similar with respect to solubility and formulation stability.<sup>135,169</sup> Similarly, although vincristine, vinorelbine, and vinblastine are all members of the vinca alkaloid class of anticancer drugs, they display very different release rates *in vitro* and *in vivo*.<sup>10,164</sup> Because vincristine is more hydrophilic than either vinorelbine or vinblastine,<sup>171</sup> it displays slower release rates and is more easily stabilized by simply changing the lipid composition of the carrier.<sup>10,123</sup> These examples help demonstrate that although many weakly basic amphipathic amines can be loaded efficiently into liposomes, the stability of encapsulation can very much depend on the overall structure of the specific drug.

Weakly acidic drugs, and drugs with more than one titratable functional group can pose different challenges. Although amphipathic weak acids can be in theory loaded using reverse pH gradients (i.e., pH lower on liposome exterior), including acetate gradients,<sup>172</sup> the high internal pH produced during gradient generation can introduce difficulties in chemical stability for either the drug being encapsulated or the resulting formulation. Due in part to this difficulty, these drugs are commonly loaded passively, where the encapsulation efficiency is at a maximum 30–35%.<sup>127,131</sup> The leakage of the thymidylate kinase inhibitor (OSI-7904L; OSI Pharmaceuticals, Melville, NY) from these liposomes is slow, resulting in prolonged circulation lifetimes relative to the unencapsulated drug.<sup>127</sup> Succinyl-derivatives of paclitaxel were loaded passively at low drug-to-lipid ratios (1:25, drug-to-lipid, mol:mol) where the still relatively hydrophobic prodrug was localized primarily in the liposome membrane.<sup>173</sup> The efficiency of loading was as high as 75% in negatively charged liposomes, but unfortunately the stability of these formulations in the blood was not reported.

Drugs that contain both weakly basic and weakly acidic groups pose a challenge, but can often be overcome depending on the  $pK_a$  and number of the various ionizable groups. A drug



that contains both a weakly basic amine and a phenolic hydroxyl group, with its relatively high  $pK_a$ , is still amenable to gradient based loading. However, if the  $pK_a$  of any amine is too high, requiring a relatively high external pH for loading, ionization of the phenolic group may occur, thus limiting membrane permeability. The camptothecin topotecan, contains both functional groups and is readily loadable at mildly acidic pH.<sup>15,99,137,139,174</sup> Ciprofloxacin has a conjugated carboxylic acid with a  $pK_a$  of 6.0.<sup>135</sup> The  $pK_a$  of ciprofloxacin is not as high as the phenolic hydroxyl of topotecan, but still high enough to allow for efficient loading using gradient loading methods. However, using a wide range of loading methods and lipid compositions, the stability of encapsulation for this zwitterionic drug has been relatively poor compared to other weakly basic amines,<sup>134,165,175,178</sup> likely resulting from its difficulty in forming stable intraliposomal complexes.<sup>177</sup> The presence of lower  $pK_a$  acids, including nonconjugated aliphatic carboxylic acids or phosphate groups, make it difficult to find a pH where both the acid and the amine would be neutralized, enabling the drug to readily penetrate the liposomal membrane and accumulate in the liposome interior.

Hydrophobic drugs represent a third class of drugs that have been formulated in liposomes. Paclitaxel,<sup>17,124,125,178,179</sup> 9-nitrocamptothecin,<sup>180-183</sup> SN-38,<sup>14,184</sup> docetaxel,<sup>185</sup> cis-Bis-neodecanoato-trans-R,R-1,2-diaminocyclohexane platinum(II) (NDDP),<sup>186-188</sup> and 7-*t*-butyldimethylsilyl-10-hydroxycamptothecin (DB-67)<sup>189</sup> are just a few of the hydrophobic drugs that have been solubilized in liposome membranes for delivery. Upon initial inspection, the choice of liposomes for delivery of hydrophobic drugs would appear to offer significant advantages to the pharmacology of this class of drugs by providing a low toxicity solubilizing agent for a class of drugs that has a significant limitation with regards to solubility. Drugs such as paclitaxel are often solubilized with emulsifying agents such as Cremophor-EL, which can add to the toxicity of the molecule itself when required at high concentrations.<sup>190,191</sup> The readily biodegradable phospholipid molecules would appear to offer a significant improvement over other emulsifying agents.

Liposome formulation of hydrophobic drugs does provide a method for increasing their solubility, however, the formulations are typically not stable against drug release upon entering the

circulation, thus offering at best small incremental advantages over other delivery strategies. Lipophilic drugs rapidly transfer between liposomal membranes and various biological interfaces, including cellular membranes and plasma proteins such as albumin and high density lipoproteins;<sup>192,193</sup> therefore, while these liposomes do often demonstrate some improvement in pharmacokinetic parameters when compared to other formulations, the drug clearance from the circulation is rapid compared to more stable liposome formulations. In Figure 2, we compare the hydrophobic drug, SN-38, solubilized in the lipid membranes of liposomes with four different sustained release formulations of camptothecins where the drugs are stably encapsulated in the liposome interior with varying efficiencies. As can be seen, the most stable sustained release formulations have extended pharmacokinetics with greater than 20% of the injected dose remaining in the circulation after 24 h. The formulation of SN-38 shows less than 0.1% of the injected dose still in the circulation after 6 h. Thus, although liposomes can certainly play a role in the delivery of hydrophobic drugs, their formulations are less likely to take advantage of the more significant promises of liposomal drug delivery related to long circulation lifetimes, selective accumulation in solid tumors, extended and sustained drug release, and molecular targeting. A notable exception is liposomes that are targeted to readily accessible targets, such as the endothelium. Cationic liposomes containing paclitaxel targeted to angiogenic blood vessels supporting solid tumor and have been shown to improve antitumor efficacy.<sup>58,194</sup> The net effect of these noted limitations is that although formulation in lipidic nanocarriers is capable of improving the pharmacodynamics of hydrophobic drugs, they are less likely to distinguish themselves from other delivery technologies in the manner possible with weakly basic amphipathic drugs. With these drugs, the pharmacokinetics and drug release rates can be readily modulated to fit the particular application, resulting in an efficiency of delivery that is superior to most other delivery technologies.

The final two classes of liposomal therapeutic agents are highly water soluble, including both small molecules and polyionic compounds, such as nucleic acid based therapeutics. Highly water soluble agents must overcome significant barriers related to efficient entrapment of the agent, the ability to make the agent bioavailable, and the

reduced potential for a bystander effect. Many highly water soluble small molecular weight drugs must be encapsulated passively because they are not amenable to gradient-based drug loading methods due to their minimal membrane permeability. However, nucleic acids, although highly water soluble, can be efficiently complexed with cationic lipids to form highly condensed lipidic nanoparticles.<sup>65,128,129,195</sup> Although liposome formulations of highly hydrophilic drugs are typically relatively stable with regards to encapsulation, the same properties that result in the high degree of stability also hinder release of the drug at the site of action. Some hydrophilic drugs, such as cytosine arabinoside or various thymidylate kinase inhibitors, can be taken up via

transporters in the membrane,<sup>196–199</sup> subsequent to release either intracellularly or extracellularly. Other drugs may require “triggered” release to improve their bioavailability. These examples illustrate the barriers and opportunities present for delivery of various classes of drugs, and emphasize the need to adapt a specific nanocarrier and delivery strategy to its encapsulated payload.

Fixed dose combination drug liposome formulations have been prepared by coencapsulating two or more drugs inside the same liposomes in an attempt to capture synergistic antitumor efficacy with minimal efficacy.<sup>45,200–202</sup> Ratiometric dosing results from maintaining an optimum fixed ratio of encapsulated drugs, resulting in synergistic improvements in cytotoxic activity over a long period of time. The challenge then becomes in being able to coordinate the drug release rates of two or more agents in order to maintain ratios that are synergistic with regards to activity. In Figure 8A and B, the rate of drug release is shown for liposomes prepared with coencapsulated vincristine and doxorubicin.<sup>200</sup> Under the gradient conditions used to load these drugs, doxorubicin is significantly more stable with regards to encapsulation when compared to vincristine. In a series of comprehensive and elegant studies, Bally and coworkers<sup>45</sup> were able to optimize formulations of floxuridine and irinotecan by modulating both the cholesterol

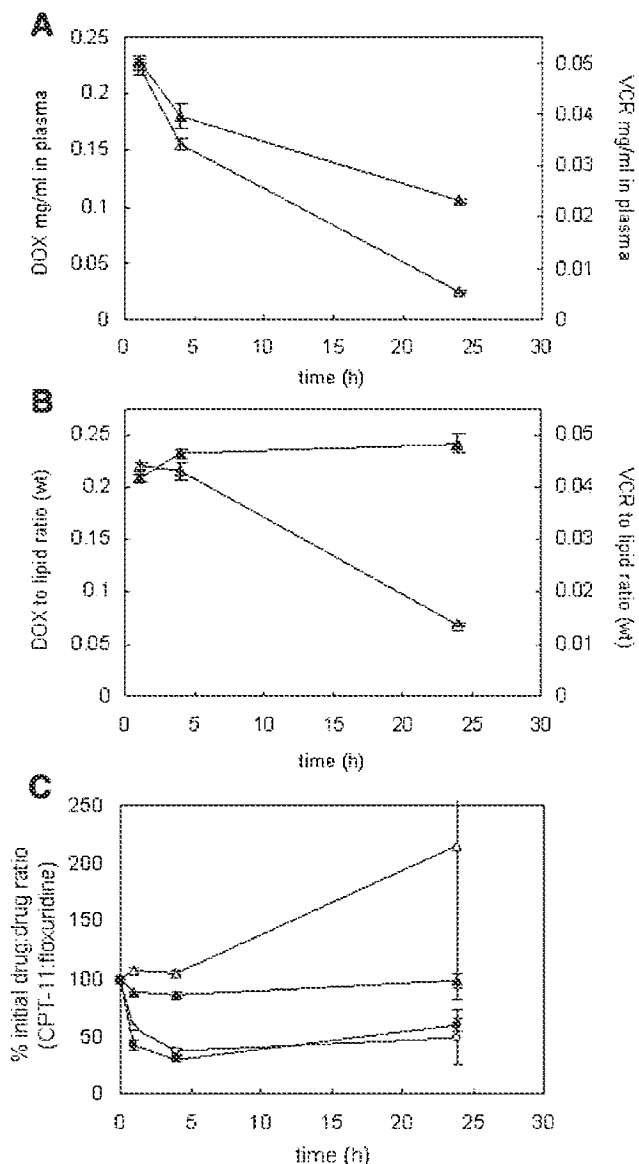


**Figure 8.** Pharmacokinetics of liposomes containing two separate chemotherapeutics. Plasma circulation and formulation stability of a liposomal drug administered as a single liposomal formulation containing both doxorubicin and vincristine. Female BALB/c mice were injected with coformulated liposomes at a dose of 10 mg/kg doxorubicin and 2.5 mg/kg vincristine. (A) Drug circulation in is indicated by the plasma concentration (mg/mL) of doxorubicin and vincristine. (B) Stability of the formulation is indicated as the drug-to-lipid ratio for doxorubicin and vincristine. Data points represent the mean  $\pm$  SD ( $n = 6$ ). (C) Liposomal drug retention of CPT-11 and floxuridine coformulated into particles of varying lipid composition are represented as the drug/drug ratio over time relative to the injected formulation. All formulations were injected (i.v.) into BALB/c mice ( $n = 3$ ) at a lipid dose of 370  $\mu$ mol/kg and a drug dose of 37  $\mu$ g CPT-11 and floxuridine/kg. The liposomes were composed of the following lipids: DSCP/Chol/DSPG (65:15:20 molar ratio),  $\Delta$ ; DSCP/Chol/DSPG (70:10:20 molar ratio),  $\blacktriangle$ ; DSCP/Chol/DSPG (75:5:20 molar ratio),  $\circ$ ; DSPC/DSPG (80:20 molar ratio),  $\bullet$ . This figure was adapted from Abraham et al.<sup>200</sup> and Tardi<sup>45</sup> with permission.

content and the drug-to-lipid ratios (Fig. 8C). The result is a ratio of irinotecan-to-floxuridine that remains relatively constant over the period of 24 h. However, as will be noted in subsequent sections, individual optimization of the activity or toxicity of a particular formulation is very dependent on the pharmacokinetics and drug release rates, often where more stable encapsulation results in improved efficacy. In these studies, although even higher retentions of irinotecan are indeed possible in liposomes, their attainment would have come at the expense of the ratiometric dose subsequent to injection for the combination. Thus, it remains difficult to maintain the optimal dose ratio and at the same time attain the optimum encapsulation stability for the individual drugs as a result of the inherent differences in stabilizing drugs of different structures in liposome formulations.

#### RELATIONSHIP OF PHARMACOKINETICS AND DRUG RELEASE RATES ON TOXICITY OF LIPOSOMAL DRUGS

The relationship relating pharmacokinetics, bioavailability, and toxicity is not as simple as is often suggested. The general dogma is that encapsulation and delivery of therapeutic agents in liposomes results in site-specific delivery of the therapeutic agent to the site of disease, reducing exposure to healthy tissues and increasing the exposure at the site of disease. The logical conclusion that is routinely drawn is that this combination of effects results in a decrease in toxicity for the liposomal formulation of the drug when compared to the unencapsulated drug delivered via the same route of administration. Although this can certainly be true for some drugs and specific toxicities, a more accurate observation for an optimized construct is that liposomal delivery can result in a shift in the toxicity profile and a widening of the therapeutic window. In addition, the specific liposomal formulation chosen and its pharmacokinetics and rate of drug release upon entering the circulation, can result in a dramatic difference in a specific toxicity and the overall toxicity profile observed.<sup>1,203</sup> Several examples will serve to illustrate these important points.

For many anthracyclines such as doxorubicin, cardiotoxicity is the therapy-limiting toxicity.<sup>204,205</sup> However, encapsulation in both pegylated and nonpegylated liposomal formulations of

doxorubicin has dramatically increased the cumulative dose of doxorubicin that can be administered, with greater than 2000 mg/m<sup>2</sup> being administered in some patients for PLD without identification of a maximum "safe dose" of the drug.<sup>206,207</sup> Encapsulation in liposomes is also allowing doxorubicin to be studied in combination with trastuzumab in HER2-overexpressing breast cancers<sup>208</sup> in a particularly active combination that is considered unacceptably toxic when doxorubicin is used in its free form.<sup>209</sup> This is thought to be due in part to the poor accumulation of liposomal or bioavailable doxorubicin in the heart tissue.<sup>143,210</sup> In addition, myelosuppression was reduced when doxorubicin was encapsulated stably in liposomes.<sup>143,211</sup> However, the effect on myelosuppression was dependent on drug release rate from the carrier, with the rapidly releasing eggPC/Chol formulations demonstrating similar levels and recovery from this toxicity as free doxorubicin, and the more stable DSPC/Chol formulation demonstrating substantially less myelosuppressive activity.<sup>211</sup> This translates clinically into where the dose-limiting toxicity for the rapid release eggPC/Chol formulation (Myocet or TLC-D99) remains myelosuppression,<sup>1,212</sup> while myelosuppression is generally considered mild with the slower release and longer circulating PLD.<sup>73,206</sup> Alopecia and vomiting were also generally reduced in the PLD treated patients. However, while the effects on many of the conventional toxicities typically associated with doxorubicin were reduced, different toxicities emerged. Mucositis and palmar-plantar erythrodysesthesia (PPE or hand-foot syndrome) were shown to be dose-limiting or common toxicities in patients treated with PLD.<sup>81,213</sup> The incidence of PPE is related to the dose intensity of PLD, and can be decreased to manageable levels using less frequent dosing (i.e., once every 4 weeks).<sup>81,213,214</sup> The appearance of PPE with PLD is thought to be related to both the slow rate of drug release from the carrier and the accumulation of PLD in skin,<sup>107,215</sup> especially over multiple injections at schedules that result in a further cumulative accumulation of doxorubicin in the skin.<sup>31,86</sup> Allen and coworkers<sup>156</sup> have also shown that the rate of release of doxorubicin from pegylated liposomes could affect the toxicity of the drug, despite the similar pharmacokinetics of the liposomal carrier itself. Here, liposomes with intermediate drug release rates were shown to have the greatest toxicity, a toxicity that was consistent with cardiotoxicity as supported by

gross pathological analysis. The totality of these observations suggest that the toxicity profile and severity of various toxicities that are typically associated with a particular drug can be affected by liposome encapsulation, and the particular pharmacokinetic and drug release properties of a particular formulation. In general, rapid release formulations display fewer changes in the toxicity profile than more stable longer circulating liposome formulations.

As noted above, the schedule of administration is also important in determining the degree of toxicity. Because highly stable and long circulating liposomes can result in bioavailable drug being exposed at sites of toxicity for days or weeks, there is both a delayed onset for many toxicities compared to what would be expected for the corresponding free drugs and a greater potential for accumulation of bioavailable drug at a particular site,<sup>31</sup> making schedule optimization imperative. Schedule-dependent drugs, whose activity and toxicity are dependent on the exposure to the therapeutic agent during a particular part of the cell cycle or upon continuous exposure to a particular agent can be dramatically affected by liposome encapsulation. Both camptothecins and histone deacetylase inhibitors are schedule dependent drugs. When they are released in a sustained release manner, the exposure of bioavailable drug to both healthy and tumor tissue is increased. The net effect can be a decrease in the MTD for the encapsulated drug when compared to the free drug.<sup>12,13,15,136,141,216</sup> The effect on camptothecins can be even more dramatic since liposome encapsulation also protects drugs from metabolism or chemical hydrolysis to inactive products. In the case of camptothecins, the lactone ring is hydrolyzed at neutral pH to an inactive carboxylate, and encapsulation in liposomes retains the drug in its active form, assuring that more active drug reaches the target site, but also potential sites of toxicity.<sup>12,15,138,141</sup> Accordingly, liposomal encapsulation of topotecan or the structurally related compound lurtotecan (Fig. 1) led to significantly increased toxicity.<sup>15,216</sup> However, in all cases the stable and specific delivery to the tumor, and subsequent sustained release of the drug results in an even greater improvement in the antitumor activity, resulting in a net increase in the therapeutic index for the drugs. Because the changes in the observed toxicities are rationally explained, manageable, and do not compromise the overall improvements in the therapeutic

index, the acknowledgment of these challenges and realities is instrumental for the liposome pharmacology field moving forward.

## EFFECT OF DRUG RELEASE RATES ON ANTITUMOR EFFICACY

Liposomes that displayed longer circulation lifetimes have typically displayed greater antitumor efficacy in various tumor models.<sup>1,2,31</sup> However, claims of superiority based on pharmacokinetics of the carrier alone must be carefully evaluated since often the differences between the formulations dictate both a change in the pharmacokinetics of the carrier as well as drug retention.<sup>217-219</sup> Although liposomes that display dramatic differences in pharmacokinetics generally show superior efficacy for the longer circulating constructs, liposomal drugs that display comparable pharmacokinetics and drug release rates can have similar antitumor activities.<sup>66,107,154,220,221</sup> Pegylated liposomal doxorubicins with marginal size variability were shown to have distinct pharmacokinetic parameters, but did not display significant differences in antitumor efficacy. However size disparity for either nonpegylated or pegylated liposomes that resulted in more significant differences in clearance rates, and thus accumulation in tumors, were shown to have significant effects on antitumor activity.<sup>107,220</sup> Likewise, when nonpegylated and pegylated liposomal doxorubicin formulations were administered at elevated doses, the variation in pharmacokinetics was reduced and the activities of the two formulations became similar.<sup>154,222</sup> Unfortunately it has become common to avoid modifications to the lipid composition or general liposome physicochemical properties because of their perceived effects on the circulation lifetime of the carrier itself, despite the comparably greater benefits that these alterations may provide to other aspects of the delivery process, such as *in vivo* drug release rates. Thus, it is important to consider the effects of formulation parameters on all aspects of the drug delivery process rather than just the pharmacokinetics of the carrier.

Although the correlation between circulation lifetime and antitumor activity is relatively strong, the correlation between antitumor activity and *in vivo* drug release rate is more complex. Allen and coworkers<sup>156</sup> have compared formulations of liposomal doxorubicin that varied from 14.9 to 118.4 h in their drug leakage half-lives. Increasing stability correlated with increasing

total and bioavailable drug in the tumor, and with increasing efficacy.<sup>81,156,223</sup> We have recently demonstrated this by comparing the antitumor activity of two liposomal irinotecan formulations against human colon carcinoma (HT-29) xenografts in nude mice (Fig. 9A).<sup>12</sup> The slow release liposomal formulation (release  $t_{1/2}$  = 56.8 h) using sucrose octasulfate (SOS) as an intraliposomal drug-stabilizing counterion was significantly more efficacious than the formulation with more moderate *in vivo* stability (release  $t_{1/2}$  = 14.0 h) that used polyphosphate instead of SOS. Liposomal formulations of vincristine stabilized using a sphingomyelin/cholesterol formulation were also shown to be more efficacious than a less stable formulation prepared using DSPC and cholesterol.<sup>123</sup>

We have shown a similar relationship for two anti-HER2 targeted formulations of vinorelbine (Fig. 9B). The formulation with the faster drug release rate (release  $t_{1/2}$  = 15.2 h) resulted in reduced efficacy in a HER2-overexpressing breast tumor (BT-474) xenograft model when compared to the more highly stable SOS-stabilized formulation (release  $t_{1/2}$  = 27.2 h). For ligand-targeted liposomes, the increased stability is considerably more important than for nontargeted liposomes, since the immunotargeted construct must remain intact in order to take advantage of the added benefit of molecular targeting. Targeted liposomal formulations of drugs with rapid release rates, such as hydrophobic drugs, can still show antitumor activity if targeted to antigens that are readily accessible to the vasculature, such as on leukemias, lymphomas, or micrometastases that are not limited by extravasation like in solid tumors.<sup>58,224,225</sup> However, even when targeting accessible targets, greater *in vivo* stability is often desirable. Anti-CD19 immunoliposomal doxorubicin formulations with drug release rates that varied from  $t_{1/2}$  of 1.9 to 315 h were compared in a B-cell lymphoma model and shown to have antitumor activity that correlated with the drug release rates.<sup>226</sup> Immunoliposomes with the fastest rate of doxorubicin release showed little efficacy, while the most stable formulations displayed the greatest activity.

However, the rate of drug release can be too slow, and in some instances results in poor activity despite their long circulating properties. Mitoxantrone formulated into DSPC/Chol liposomes was significantly more stable than a similar formulation prepared using DMPC/Chol (drug release rate <0.025 vs. 1.7  $\mu\text{g}$  MTX/ $\mu\text{g}$  lipid/h).

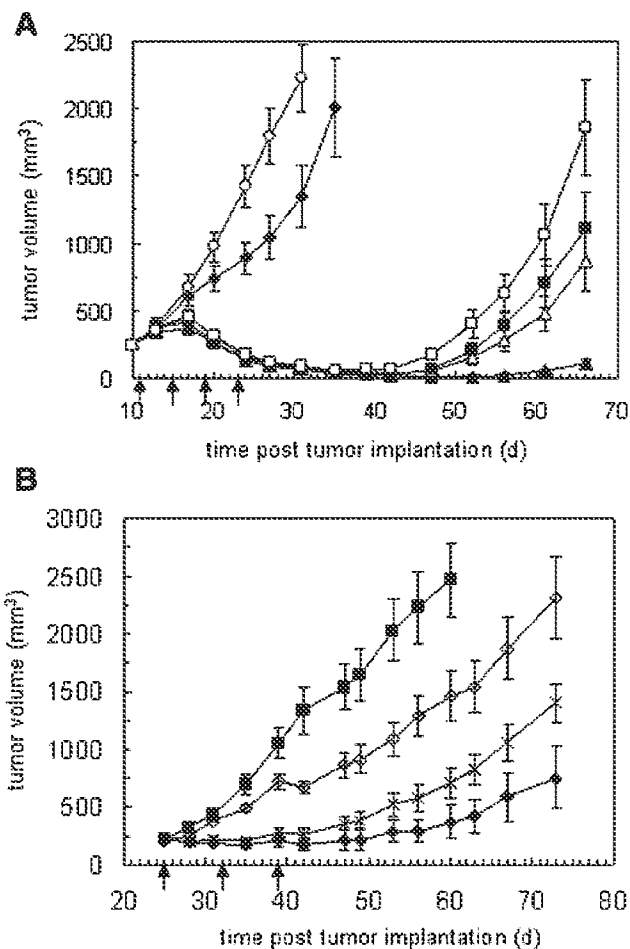


**Figure 9.** Antitumor efficacy of liposomal CPT-11 in an HT-29 model (A) and liposomal vinorelbine in a BT-474 model (B). (A) Liposomal CPT-11 treatment was initiated when the HT-29 xenografts reached an average size of 150–350 mm<sup>3</sup> and administered (*i.v.* bolus) on a 4-day interval on the days indicated by arrows. The following treatment groups were examined: (1) control (HEPES-buffered saline pH 6.5 ○); (2) free CPT-11, 50 mg/kg/dose (◆); (3) TEA-Pn liposomal CPT-11 at 25 mg/kg/dose (□); (4) TEA-Pn liposomal CPT-11 at 50 mg/kg/dose (■); (5) TEA-SOS liposomal CPT-11 at 25 mg/kg/dose (△); (6) TEA-SOS liposomal CPT-11 at 50 mg/kg/dose (▲). (B) Liposomal vinorelbine treatment was initiated when BT474 human breast xenografts reached an average size of 110–343 mm<sup>3</sup> and was administered once per week on days indicated by arrows. The following treatment groups were examined: (1) control (HEPES-buffered saline pH 6.5); (2) free vinorelbine at 5 mg/kg/dose (◇); (3) anti-HER2 TEA-Pn liposomal vinorelbine at 5 mg/kg/dose (×); (4) anti-HER2 TEA-SOS liposomal vinorelbine at 5 mg/kg/dose (◆). Error bars represent the standard error of the mean. This figure was adapted from Drummond et al.<sup>12</sup> with permission.

However, in both L1210 and P388 tumor models, the antitumor efficacy was increased significantly for the DMPC/Chol formulation.<sup>21</sup> In a second example, a pegylated liposomal formulation of cisplatin, was long circulating, and efficiently accumulated in tumors.<sup>227,228</sup> Cisplatin is a fairly hydrophilic drug with low membrane permeability; therefore it was encapsulated in the form of a concentrated solution into the liposome interior using a direct entrapment method.<sup>126</sup> Unfortunately, its release from liposomes was so slow that the drug was never made bioavailable at the site of the tumor,<sup>228</sup> and unencapsulated drug was either not measurable or exceptionally low in patient plasma samples.<sup>74,229</sup> The result was poor clinical responses in several different clinical trials.<sup>19,229</sup> Finally, vincristine liposome formulations with a half-time of release that varied from 6.1 to 117 h were tested for antitumor activity in a human mammary tumor model.<sup>144</sup> In this study, an increase in retention correlated with increasing antitumor activity at first, but was less effective in the highest stability formulation, truly exemplifying the spectrum of activity induced by drug release rate. An intermediate rate of release was optimal for antitumor activity with liposomal vincristine in this tumor model.

The above-cited elegant study by Johnston et al.<sup>144</sup> shows correlation of the drug release rate with antitumor activity in order to determine an optimum construct to move forward with in clinical development. However, the relationship between *in vivo* stability and antitumor efficacy in rodent tumor models may not translate perfectly across species for several reasons. First, circulation lifetimes for liposomal drugs can be considerably longer in humans when compared to rodents. For pegylated liposomal doxorubicin, a half life of 56–79 h was noted in humans,<sup>73,143</sup> compared to a half-life of 21–23 h in rodents.<sup>143</sup> Thus, for improved antitumor efficacy one would expect to require greater stabilities for optimum activity than would be required in a rodent model. In addition, tumors typically grow much slower in humans than in most animal models. Thus, an optimum rate of release may be significantly faster in mice, where the liposomal drug must both accumulate and be released in order to exert its activity before the tumors rapid growth overtakes the animal and makes it more difficult to treat. Finally, no one has systematically looked at the species-dependence of drug release rates *in vivo*. Differences in blood dilution factors and

the presence of disrupting plasma proteins may result in significant differences in drug leakage rates *in vivo*. Optimization in animal studies with regards to drug release should therefore only be considered a guide for further clinical drug development, with additional PK/PD modeling being required for extrapolating the optimum conditions to humans.<sup>230</sup>

## TRIGGERED DELIVERY OF ENCAPSULATED THERAPEUTICS

Triggered delivery of liposomal therapeutics can result from either a stimulus-induced increase in delivery of the liposomal carrier itself to the site of disease or as a result of increased drug release from the carrier. In some instances a particular trigger may be able to induce both increased localization of the liposomal carrier and increased drug release at the site of disease. Ideally, an encapsulated drug would be quantitatively retained in the carrier until the carrier lodges in the target site of the patient's body, and then released from the carrier at a desired rate. Site-specific increase of the drug release from the carrier is sometimes referred to as "triggered release," as it is deemed to be "triggered" by a factor inherently present at the target site, such as enhanced activity of a specific enzyme,<sup>231,232</sup> acidic pH,<sup>233,234</sup> or a high reducing potential.<sup>235,236</sup> The trigger can also be applied externally, such as localized heat,<sup>237–239</sup> light,<sup>240,241</sup> ultrasound,<sup>242</sup> or ionizing radiation. Thus, the triggered release of therapeutic agents offers the potential for increased site-specific bioavailability of the liposome associated drug. However, it is not clear to what extent the sophistication of some of the more multifaceted technologies, and the associated problems introduced from the added complexity, are justified by the specific application and the relative improvement in efficacy and toxicity that would result compared to simple sustained-release formulations.

The rate of *in vivo* drug release is most often considered in the blood since it is technically most straightforward to assay in this compartment, and readily contributes to the pharmacokinetics of the drug in the general circulation. However, the retention of drug is likely to be both different and important in various tissues, including both the site of disease and potential sites of toxicity, where interactions with cells and various tissue environments may play a significant role in determin-

ing how rapid a particular drug is released from its liposomal carrier. For example, tumor-residing, splenic, or liver macrophages can phagocytose liposomes, degrade the carriers, and release the drug,<sup>243-245</sup> thus substantially increasing the bioavailability of the drug in tissues compared to what is observed in the blood. For a stable liposomal drug formulation like pegylated liposomal doxorubicin, where one-half of the drug is released at more than 90 h,<sup>120,156</sup> the majority of doxorubicin release does not occur until after accumulation in the tumor. For more water soluble drugs, such as the thymidylate kinase inhibitor (S)-2-5-[(1,2-dihydro-3-methyl-1-oxo-benzo[*f*]quinazolin-9-yl)-methyl]amino-1-oxo-2-isindolyl]-glutaric acid (OSI-7904L; OSI Pharmaceuticals), where the rate of release is likely to be even slower, the mechanisms responsible for tumor-specific release are even more important. Although the drug release in the tumor environment is not well understood, there is evidence that the action of phospholipases, a slow dissipation of the gradients often used to load drugs, and metabolism by macrophages all may play a role in releasing the drug from the confines of the liposomes.<sup>1,231,245-247</sup>

A relatively small group of studies have been completed to actually look at both liposome-encapsulated and bioavailable free drug in tissues.<sup>31,223,228,248,249</sup> Allen and coworkers<sup>223</sup> first used doxorubicin accumulation in the nucleus as a measure of free doxorubicin exposure. They showed that the more stable liposome formulations composed of HSPC/Chol/PEG-DSPE demonstrated the highest concentrations of both total and bioavailable doxorubicin in the tumor, despite their slow rate of drug release in the plasma. Despite its liposome encapsulation, the AUC of bioavailable drug in the tumor was still 45-fold higher than in mice receiving free doxorubicin.<sup>223</sup> Zamboni et al.<sup>228</sup> developed a novel microdialysis probe to monitor released drug levels in solid tumors. They used this probe in combination with atomic absorption spectrometry to demonstrate the bioavailability of liposomally delivered cisplatin was very low. This is in agreement with the poor clinical activity,<sup>19,229</sup> and the low levels of free cisplatin in the plasma<sup>74,229</sup> observed with this drug, as described in the previous section. A triggered-release formulation of cisplatin thus may be beneficial to increase the amount of bioavailable drug in the tumor, while the release rates for other amphipathic drugs may be sufficient given normal cellular and physicochem-

ical mechanisms for drug release in the tumor. Biomacromolecular therapeutics such as proteins and nucleic acids pose a particularly daunting challenge due to their large size, high aqueous solubility, and *in vivo* lability. This class of agents would appear to be particularly well suited for formulation using "triggered" release nanocarriers.

In addition to triggered release of liposomal contents, a specific trigger can also induce increased accumulation of the liposomal carrier itself at the site of disease. Local hyperthermia has been shown to increase the accumulation of liposomal drugs in solid tumors,<sup>237,250-252</sup> as has radiation<sup>253,254</sup> and coadministration of a toxin-producing bacteria.<sup>255</sup> Molecular targeting with antibodies has resulted in increased accumulation in targets that are more vascularly accessible; including leukemias,<sup>256</sup> angiogenic blood vessels,<sup>257</sup> or small metastases.<sup>258</sup> The increased uptake in these tissues alone can provide for improved therapeutic efficacy, but when the stimulus results in both increased tumor localization and local release, then a further and more substantial improvement in efficacy results.

### Challenges with Triggered Systems

To create a triggered release liposome system, the liposome usually includes a responsive element that changes its structure upon external stimulus in such a way that the permeability of the liposome membrane is increased. The responsive element may be a lipid within the liposome bilayer, a polymer entrapped within the liposome, or a lipopolymer, anchoring a specific polymer chain to the liposome membrane (Fig. 11). Modifications of the lipid or polymer structure either directly perturb the membrane, or lead to the inability of the resulting lipid composition to form or maintain the bilayer phase. Due to changes in the lipid molecule geometry, the liposomes disintegrate, releasing their contents. The changes may be irreversible, or reversible, whereby the liposome seals itself following removal of the stimulus. While the concept of triggered release is attractive, the responsive element added to the liposome construct, or the changes required in the underlying physicochemical properties of the carrier, may adversely affect the clearance of the liposomes or the background rate of drug release. For example, some pH-sensitive liposome preparations are prepared with



substantial concentrations of anionic lipids or polymers that can increase their recognition by macrophages and thus clearance from the blood. Many of these formulations also require the use of unsaturated gel-phase phospholipid components to facilitate the fusion or collapse of the lipidic carrier once the trigger has occurred.<sup>233,234</sup> Unfortunately, the use of unsaturated lipids is often incompatible with stable drug encapsulation<sup>108,155,156</sup> for many drugs, inducing premature release of the drug in the circulation before the liposomes can reach their target. The attachment of fusogenic peptides to liposome surfaces has been shown to destabilize lipid membrane and enhance delivery of complexed nucleic acids to cells.<sup>259,260</sup> However, their conjugation to the surface raises serious questions about the immunogenicity of the modified nanocarriers, thus potentially compromising the pharmacokinetics of subsequently administered agent.

### Ligand Targeted Liposomes

Although ligand-targeted liposomes, such as immunoliposomes, were originally thought of as primarily a method for modifying the liposome's biodistribution and thus accumulation at the site of disease, it is clear now that the ligand's ability to induce endocytosis may have additional roles in improving activity, including delivering the lipidic nanocarrier to an intracellular location rich in degradative enzymes where disruption of the liposomal carrier is increased, thus improving the rate of drug release. Although not all ligand targeted liposomes use internalizing ligands, those that do may be considered as "triggered release" formulations. There are multiple examples demonstrating the importance of endocytosis of the liposomal drug for antitumor efficacy.<sup>120,121,261-263</sup> Indeed, due to the avidity effect of having multiple copies of a ligand displayed on the surface of a liposome, the observed activity is relatively independent of the intrinsic affinity of the individual ligand, as shown using anti-EGFR immunoliposome constructed with scFv antibodies against EGFR ranging in affinity from a  $K_D$  of 0.9 to 88 nM.<sup>264</sup> A similar result was shown with HER2 immunoliposomes, where despite displaying poorer binding, the F5 ( $K_D = 160$  nM) scFv-targeted construct actually showed the greatest effect due to its efficient internalisation.<sup>265</sup>

In Figure 10 we use the example of HER2-targeted immunoliposomes to demonstrate the

fact that although there is nearly identical localization of nontargeted and HER2-targeted immunoliposomes to solid tumors, there is a significant improvement in antitumor activity for the immunotargeted formulations. This demonstration that in solid tumors the rate of accumulation is limited by the extravasation of liposomes into the tumors,<sup>27</sup> as opposed to the targeting of specific epitopes, suggests that molecular targeting possibly acts to improve bioavailability of the encapsulated drug by directing intracellularly where it can be liberated by degradative enzymes and the typically harsh acidic environment of late endosomes and lysosomes.

### Thermosensitive Liposomes

Several strategies have been employed to prepare temperature-sensitive liposomes. These include the use of phospholipids components such as dipalmitoylphosphatidylcholine (DPPC) that have a phase transition slightly above 37°C, such that a small elevation of temperature to 43–45°C can result in a significant increase in membrane permeability.<sup>238,239</sup> A second strategy involves the attachment of thermosensitive polymers, such as poly(*N*-isopropylacrylamide) or NIPAM, that undergo their own phase transition near physiologically relevant temperatures, resulting in collapse of the polymer and destabilization of the liposomal membrane.<sup>266</sup> Finally, the use of mixtures of acyl chain-matched lysolipids with DPPC in liposomes results in a formulation that rapidly releases doxorubicin (Thermodox) when exposed to relative mild hyperthermia, 39–42°C.<sup>238,248</sup> The lower temperature requirement for this formulation as opposed to the DPPC/DSPC/Chol formulations is more clinically relevant. In addition, doxorubicin is released intravascularly, exposing the tumor vasculature to very high concentrations of the drug as the liposomes enter the locally heated tumor from the tumor periphery. This delivery strategy appears to be very promising for drugs such as doxorubicin, where the activity is dependent on the peak concentration of the drug. However, it is less clear how well schedule dependent drugs would benefit from this rapid burst of drug release. Indeed, these drugs may benefit more from a slower sustained release formulation. Thermodox is presently being studied in multiple clinical trials, using radiofrequency or microwave irradiation to carefully control local hyperthermia, and represents the triggered



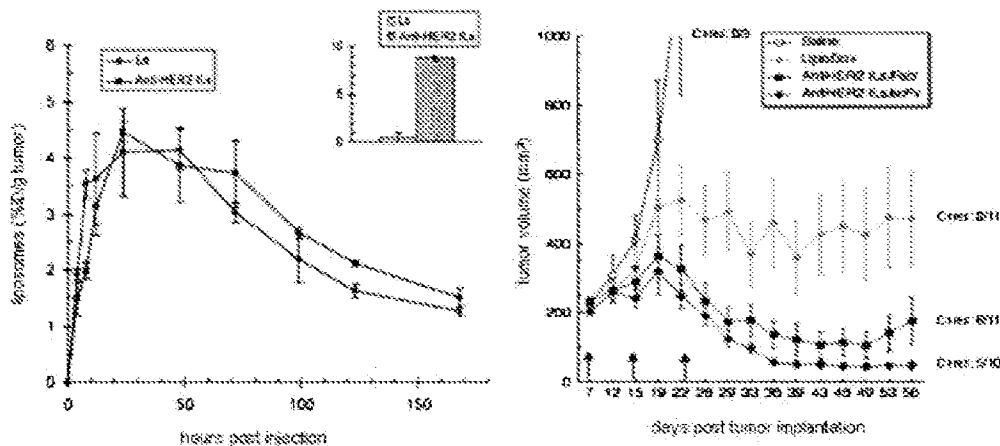


**Figure 10.** (A) Tumor pharmacokinetics of nontargeted liposomes and <sup>67</sup>Ga-labeled anti-HER2 immunoliposomes in subcutaneous BT-474 xenografts in nude mice. Data represent the mean  $\pm$  SD ( $n = 3$ ). Inset, *in vitro* uptake of nontargeted liposomes (solid column) and anti-HER2 immunoliposomes (cross-hatched column) in HER2 overexpressing SK-BR-3 cells. Uptake data represents nmol liposome phospholipid/ $10^6$  cells (mean  $\pm$  SD,  $n = 4$  experiments). (B) Efficacy of anti-HER2 immunoliposomal DOX in HER2 overexpressing subcutaneous BT-474/SF xenografts in mice. Immunoliposomes were targeted with the anti-HER2 ligand rhuMAb HER2-Fab' (■) or C6.5 scFv (◆). Control groups consisted of nontargeted liposomal DOX (●) and saline (○). Treatment groups were administered i.v. at a dose of 15 mg DOX/kg on the days indicated (arrows). All liposomes were pegylated (6 mol% of the total lipid). Both anti-HER2 immunoliposomes were significantly superior to liposomal DOX ( $p < 0.0001$  for both). Data represents mean tumor volume  $\pm$  SD. This Figure was adapted from Kirpotin et al.<sup>27</sup> and Park et al.<sup>121</sup> with permission.

approach currently furthest along with regards to clinical translation.

### pH-Sensitive Liposomes

This class of "triggered" liposomes is widely varied and includes acid-titratable polymers and lipids, acid-catalyzed hydrolysis of chemical bonds in novel lipid components of the liposome formulation, and fusogenic proteins or peptides (Fig. 11). pH-Titratable lipids are usually composed of a weakly acidic carboxyl functionality or a weakly basic amine, such as imidazole.<sup>233</sup> The initial concept was that the liposomes would become destabilized in the mildly acidic environment of solid tumors and become destabilized, releasing their contents.<sup>267</sup> However, the acidic regions of solid tumors are often only mildly acidic (pH 6.5–6.75), or are not readily accessible due to their distance from the supporting vasculature that provides the entrance point for the pool of available liposomal therapeutic.<sup>268</sup> Targeting

destabilization to the relatively acidic endosomes and lysosomes (pH 5.0–6.5) using internalizing ligands, has proven more successful,<sup>233,234</sup> but remains problematic for a variety of reasons. First, the inclusion of other stabilizing components such as PEG-lipids not only result in the desired increased circulation lifetimes, but also compromise the pH-sensitivity of the constructs.<sup>269</sup> pH-Sensitive liposomes prepared with acid sensitive lipids are also limited to a limited range of therapeutics that can be stably encapsulated in this type of carrier, typically those that are highly water soluble.

An alternative approach has been in the use of membrane destabilizing polyanions<sup>270</sup> or acid-cleavable lipids<sup>233,235</sup> that aid in the destabilization of the liposome membrane in response to mildly acidic pH. Methacrylic acid copolymers, succinylated poly(glycidol), and poly(ethylacrylic acid) are just a few of the pH-responsive polyanions that can be incorporated into liposome constructs (Fig. 11).<sup>270</sup> These polymers undergo conformational changes at acidic pH that result in

the polymer interacting strongly with the associated liposomal membrane, increasing its permeability to encapsulated molecules. Often the polymer is anchored in the membrane using a hydrophobic moiety conjugated either terminally or randomly within the structure of the polymer. The pH-sensitivity and efficiency of destabilization of the liposomes can be rationally modulated through changes to the polymer composition, density in the membrane, and underlying lipid composition. However, these factors add additional complexity to the molecule and must be balanced with their effects on encapsulation efficiency, *in vivo* drug encapsulation stability, and their effects on clearance of the particles from the circulation.

pH-Cleavable lipids include orthoester<sup>271</sup> or vinyl ether<sup>272,273</sup> linked PEG-lipid conjugates that may be useful in improving the intracellular delivery of nucleic acid based therapeutics, as endosomal escape has been shown in some studies to be hindered by the same PEG coat used to improve the circulation lifetimes *in vivo*. Modification of the substituents to the acid-sensitive bond can be used to vary the pH-selectivity and rate of cleavage over a wide range. The validation of these strategies *in vivo* is just recently beginning to be explored, but there is promise that their inclusion may help improve the delivery

of some of the more difficult classes of therapeutic agents, most notably nucleic acids.

### Other Triggered-Release Liposome Strategies

A range of alternative strategies for selectively destabilizing liposomes have also been employed with varying degrees of success. Thiolytically sensitive lipidic nanocarriers take advantage of the lower redox potential present intracellularly and the high concentration of free thiol groups in molecules such as glutathione to cleave disulfide linked lipids.<sup>235,236,274</sup> A high reducing potential has been shown to exist both in the cytoplasm and in intracellular compartments of the endocytic pathway.<sup>236,275</sup> The incorporation of certain redox-sensitive cationic lipids can dramatically improve transfection efficiency of nucleic acid-lipidic nanoparticles.<sup>276</sup> In an alternative strategy, disulfide linked cationic lipids can be used to control the assembly of nucleic acid carriers, allowing one to tailor the surface charge and general surface properties of the carrier following assembly of the particle.<sup>277</sup> The structures for several of these thiolytically sensitive lipids are shown in Figure 11.

Photosensitive liposomes have been developed to be responsive to the external application of light.<sup>240</sup> The mechanisms responsible for this

---

**Figure 11.** Chemical structures of various classes of environment or stimulus-sensitive lipids and polymers. Acid-cleavable lipids include (A) 1,2-di-*O*-(*Z*-1'-hexadecenyl)-*sn*-glycero-3-phosphocholine (DPPCs),<sup>278</sup> (B) *O*-(2*R*-1,2-di-*O*-(1'*Z*,9'*Z*-octadecadienyl)-glycerol)-*N*-(bis-2-aminoethyl)-carbamate (BCAT),<sup>273</sup> (C) *N*-citraconyl-dioleoylphosphatidylethanolamine (*N*-citraconyl-DOPE),<sup>297</sup> and (D) poly(ethyleneglycol)-diorthoester-distearoylglycerol (POD).<sup>298</sup> Reducible lipids include the cationic lipid (E) RPR 132775, an asymmetric disulfide lipid,<sup>276</sup> (F) thiocholesterol based cationic-lipid (TCL),<sup>277</sup> and (G) disulfide-linked poly(ethyleneglycol)-phospholipid (mPEG-DTP-DSPE).<sup>274</sup> pH-Titratable lipids represent a third class of triggerable lipids and include: H. 1-(3-(cholesteryloxycarbonylamino)propyl)imidazole (CHIM),<sup>299</sup> (I) cholesterylhemisuccinate (CHEMS),<sup>233,300</sup> and (J) 1,2-dioleoyl-*sn*-succinylglycerol (1,2-DOSG).<sup>301</sup> pH-Titratable polymers include (K) pH sensitive copolymer of *N*-isopropylacrylamide (NIPAM),<sup>302</sup> (L) poly(2-ethylacrylic acid) (PEAA),<sup>303</sup> and (M) hydrophobically modified succinylated poly(glycidol) (SucPG).<sup>304</sup> A fifth class of activateable lipids include photosensitive lipids such as (N) 1,2-bis(10-(2',4'-hexadienoxy)decanonyl)-*sn*-glycero-3-phosphocholine (bis-SorbPC),<sup>241</sup> and (O) 1,2-(4'-*n*-butylphenyl)azo-4'-( $\gamma$ -phenylbutyryl)-glycero-3-phosphocholine (Bis-Azo PC).<sup>305</sup> Enzyme-activated lipids include (P) cholesterol phosphate,<sup>306</sup> (Q) (*S*)-1-*O*-hexadecyl-3-hexadecanoyl-glycero-2-phosphocholine (1-*O*-DPPC'),<sup>231</sup> and the elastase-activated (R) *N*-acetyl alanyl alanyl 1,2-dioleoyl-*sn*-glycero-3-phosphatidylethanolamine (*N*-Ac-AA-DOPE).<sup>307</sup> The final class of triggerable lipids are composed of thermosensitive lipids and polymers; (S) 1,2-dipalmitoyl-*sn*-glycero-3-phosphatidylcholine (DPPC),<sup>239</sup> (T) thermosensitive copolymer of *N*-isopropylacrylamide (NIPAM),<sup>266</sup> and (U) lyso phosphatidylcholine (lyso-PC).<sup>238,248</sup>

sensitivity vary widely, and include (1) photo-induced isomerization to a form of the lipid that disrupts the packing of liposomal lipids in the membrane, (2) photo-induced polymerization of membrane lipids, resulting in lateral phase separation of the lipids, (3) photo-oxidation of plasmalogen vinyl ether linked lipids, and (4) photodeprotection of membrane destabilizing

lipids.<sup>240,241,278</sup> Activation of liposomes using light offers promise because parameters such as spatial control of irradiation, pulse duration and cycle, intensity and wavelength can all be modulated to optimize delivery. However, one of the limitations to date has been the minimal development of photo-activatable destabilization strategies that employ light at wavelengths capable of reasonable

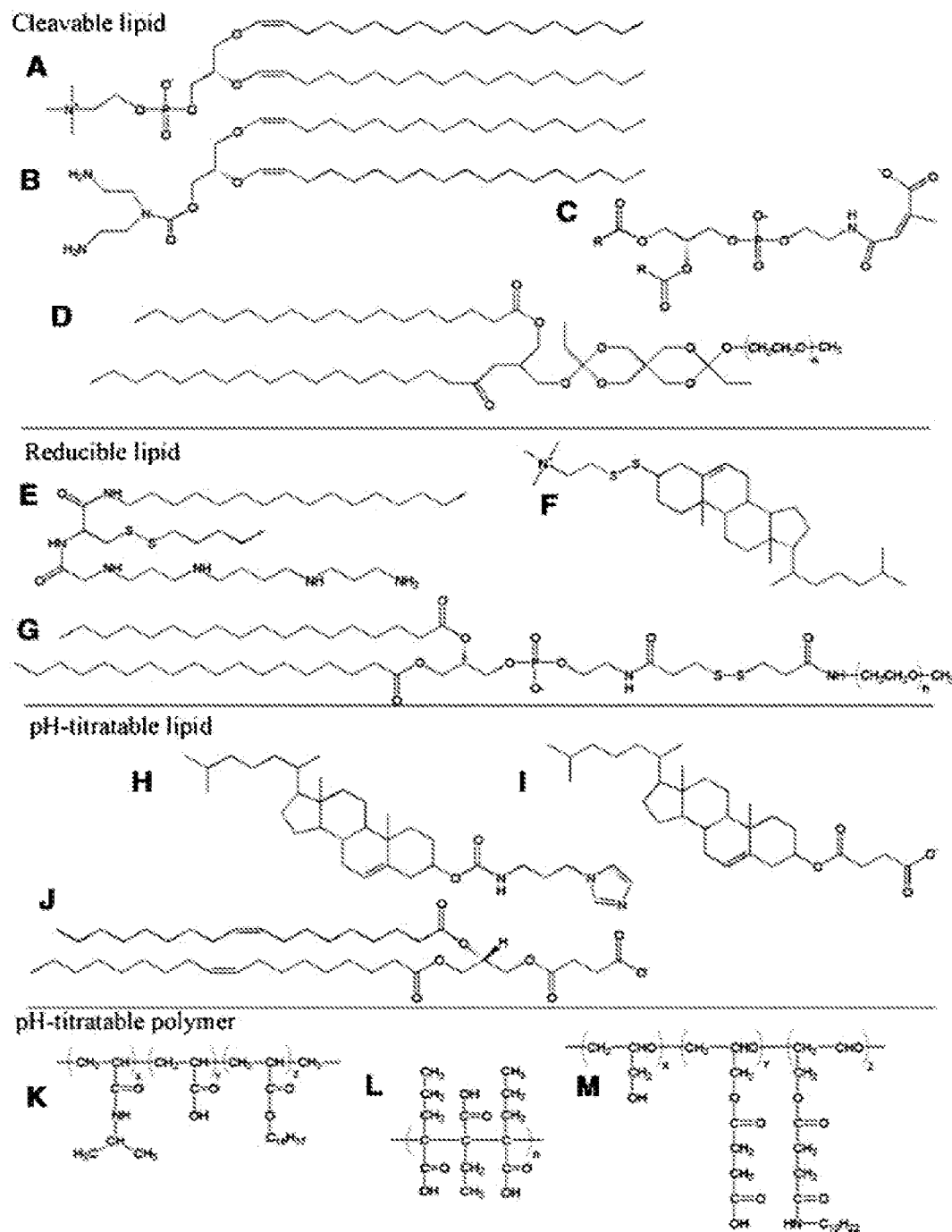


Figure 11.

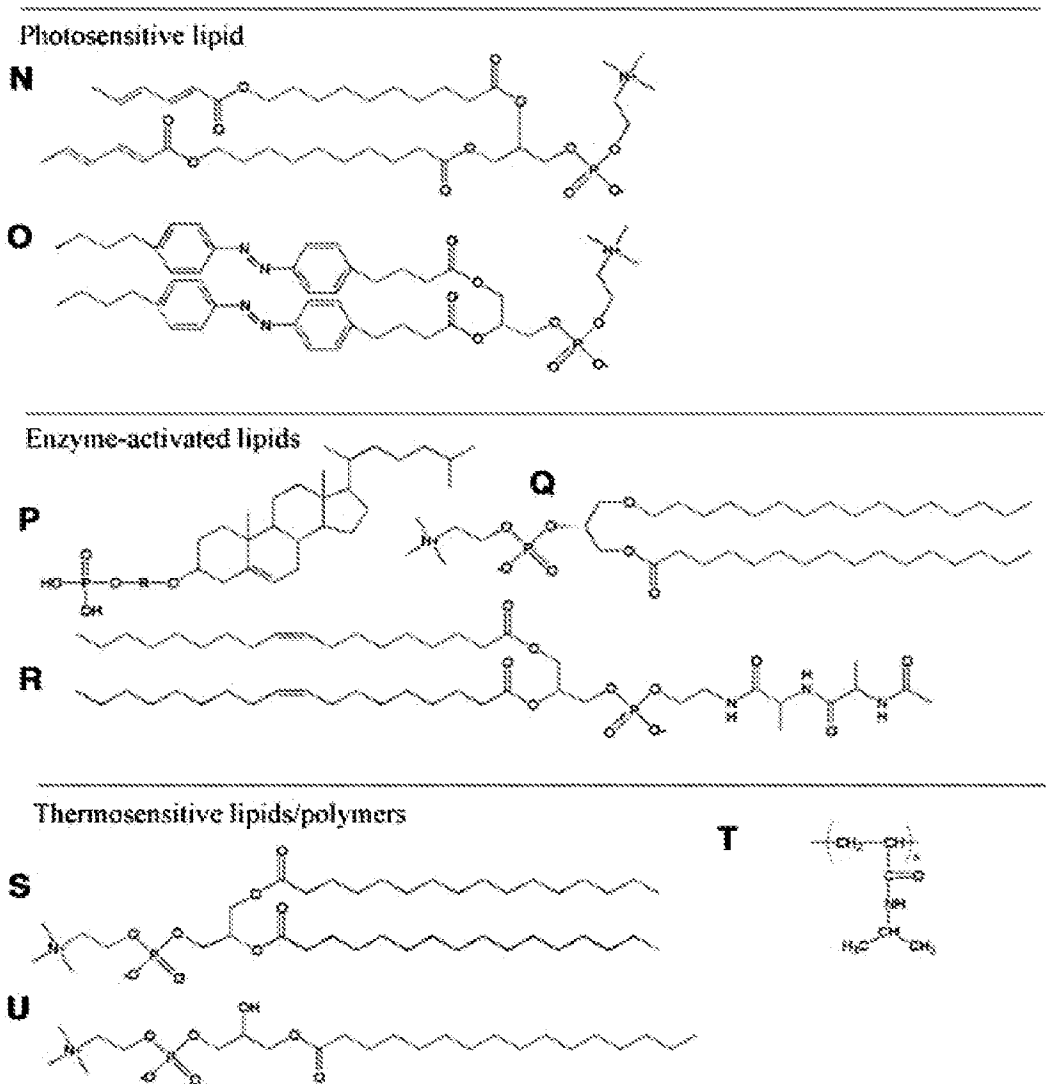


Figure 11. (Continued)

penetration in human tissue. Thompson and coworkers<sup>240,278</sup> have developed dipalmenylcholine liposomes containing water soluble photodynamic sensitizers capable of membrane destabilization and contents release at greater than 760 nm. Future development of these technologies that take into consideration the difficulties in penetration of the activating light source may offer the potential for controlled local delivery of encapsulated drug.

Enzyme-activated liposomes have been proposed to destabilize liposomal drugs locally at the site of disease where specific enzymes are often released extracellularly. Meers and coworkers developed elastase-responsive liposomes that could be activated extracellularly in the presence of elastase released by inflammatory

cells. Peptide-coupled (2–4 amino acids) unsaturated phosphatidylethanolamines were mixed with nonbilayer forming lipids such as DOPE to stabilize liposomal membranes under physiological conditions. Cleavage of these novel lipids with elastase or proteinase K resulted in fusion or contents release from the carriers. A more advanced approach in this area involves novel lipid molecules that are particularly sensitive to secretory phospholipase A<sub>2</sub> (PLA<sub>2</sub>), as a site specific trigger for delivery of encapsulated drugs in tumors and at sites of inflammation.<sup>231</sup> PLA<sub>2</sub> activity was shown to be increased in the presence of anionic pegylated lipids which is convenient due to the need for these lipids to improve delivery to sites of disease. However, the activity is diminished significantly in the presence of cholesterol,

potentially limiting the range of drugs that can be delivered using this approach. The lipid cleaved in this process is a masked anticancer ether lipid, or prodrug, and thus liberation of the active lipid itself imparts significant antitumor activity even in the absence of an encapsulated drug. Finally, the improved release of cisplatin from these liposomes was shown to result in improved antitumor efficacy when compared to free cisplatin or that delivered using a highly pegylated liposome formulation, SPI-077.<sup>231</sup> These results demonstrate there is significant promise in using extracellular enzymatic activities specific to a particular disease to locally activate certain liposomally delivered drugs, and may provide a mechanism for overcoming the relatively poor bioavailability limiting the effectiveness of more traditional formulations, such as was found with cisplatin.

Triggerable liposomes formulations certainly add an additional layer of complexity in their design when compared to more nonpegylated formulations, and it is important to ensure that this added complexity and expense ultimately give rise to a proportionate improvement in therapeutic activity or toxicity. Although they have been explored for the better part of three decades, triggerable formulations have only recently approached preclinical and clinical validation. In particular, highly water soluble drugs are likely to experience the most significant improvements in activity and represent the greatest unmet need with regards to lipid-based formulations.

### SPECIFIC DELIVERY CHALLENGES FOR NUCLEIC ACIDS

Nucleic acid based therapeutics are seen as a strategy for treating diseases at the level of genetic information transfer. The efficient delivery of these molecules to sites of their intended action remains a major obstacle, and of the available choices of delivery vehicles, nonviral lipid based carriers occupy a prominent place. The ability of a liposome to carry a functional nucleic acid into a cell was demonstrated in the early days of liposome pharmacology.<sup>279,280</sup> However, there is still a long path from these early studies to a workable carrier for nucleic acid pharmaceuticals. In addition to the numerous barriers that exist to delivering small molecule therapeutics by carriers such as liposomes, one also needs to consider the

challenges in releasing much larger polyanionic nucleic acids from the carrier, and their subsequent route to their intended site across many cellular and intracellular barriers.

One established technique for preparation of lipid based carriers for nucleic acids is based on the complexation of cationic liposomes, that is, liposomes containing significant amounts of cationically charged lipid species, with nucleic acids.<sup>281</sup> The rather heterogeneous complexes that form<sup>282</sup> are commonly referred to as lipoplexes. Many factors play an important role in the formation of these complexes and their subsequent behavior *in vivo* (e.g., lipid formulations, DNA-lipid ratios, mixing conditions, etc.). However, immediately after systemic administration many investigators have observed poor circulation times with fast clearance rates and the majority of the complexes often residing in the lungs, with subsequent clearance over time by the liver and spleen. For this reason lipoplexes may be quite suitable for gene delivery to lungs, and in addition it has been shown that lung tissue can be more susceptible to lipid-mediated transfection than for example the liver.<sup>283</sup> In contrast, more recently developed techniques for encapsulation of nucleic acids into lipid-based nanocarriers have given rise to more stable particles with longer circulation times, and therefore more suitable for accumulation in remote tumor sites.<sup>195,284</sup>

The immunostimulating effect of DNA in lipid carriers also a major consideration. Toxicities associated with the administration of nucleic acids formulated with cationic lipids include an inflammatory response characterized by increased production of the cytokines tumor necrosis factor alpha (TNF- $\alpha$ ), interferon- $\gamma$  (IFN $\gamma$ ), and interleukin-12 (IL-12), as well as hepatotoxicity, hematologic and serologic toxicities.<sup>285</sup> Their interaction with blood components can activate the complement system which can lead to opsonization of the complexes and rapid clearance by the MPS. Strategies for limiting the rates of clearance include reduction of cationic surface charge and modification of the surface properties with hydrophilic steric stabilizers such as polyethyleneglycol.<sup>286</sup> However, the same immunostimulating properties that contribute to accelerated clearance have also been shown to have a therapeutic effect in a number of instances.<sup>287,288</sup> In particular CpG sequences (known to be immunostimulating) are capable of activating macrophages, natural killer cells, T and B cells, dendritic cells and releasing a

plethora of cytokines, and when formulated into a lipid-DNA complex and injected systemically, shown to induce strong antitumor activities. Encapsulation of CpG containing ODN in stabilized antisense lipid particles (SALP) has showed enhanced immunogenicity compared to free ODN.<sup>288</sup> When used in GD2-targeted CCL, against neuroblastoma cells *in vivo*, the direct anti-sense (c-myc) action of loss of myb expression was enhanced by the indirect immunostimulating effect of the CpG motifs.<sup>289</sup>

Along with plasmid and antisense technologies, the recent advent of RNAi has led to tremendous interest in the development of new gene based therapies. Notably, it was recently shown that systemic delivery of a liposome formulation of apolipoproteinB siRNA can give greater than 90% silencing of the disease target in nonhuman primates.<sup>290</sup> Additionally, siRNA targeted against hepatitis B virus when encapsulated in a similar lipid formulation was shown to efficiently reduce HBV titer in mice.<sup>291</sup> Although a limited number of studies have offered some promise that effective delivery of siRNA can be achieved, the obstacles to the development of a robust and widely applicable siRNA delivery strategy remain substantial. Several of these obstacles are outlined below.

Recent technologies for complex preparation, has given rise to small, stable particles with improved pharmacokinetics and has been crucial to the recent successes.<sup>290,292,293</sup> The ability of the particles to circulate longer, interact with and/or accumulate with the target cells over longer periods of time is important. However, with respect to systemic therapeutic-nucleic acid delivery to solid tumors, the proposed EPR effect that liposomes benefit from may not be translate well for lipid-based gene carriers. Firstly, after accumulation in the tumor nucleic acid molecules are unlikely to "leak" out of the carrier in the same way that small molecule drugs may do from liposomes. Thus, the relatively important bystander effect that is common to many small molecules is unlikely to be directly applicable to the delivery of nucleic-acid based therapeutics. Secondly, even if they do manage to become free from the carrier, they have to cross the cell membrane, avoid degradation and get to the intended intracellular site. For siRNA and antisense oligonucleotides this involves transport to the cytoplasm, for plasmids it also encompasses transport to the nucleus for direct expression of the gene product. The cationic nature of most lipoplexes aids cell interaction, and can cause cell internalization by

cell fusion, endocytosis or interactions with extracellular glycosaminoglycans.<sup>294</sup> However, as noted in the previous sections, significant concentrations of cationic lipids can also have an adverse effect on the pharmacokinetics of the resulting nanoparticles, resulting in their rapid accumulation in the liver, or in lungs. The ability to successfully mask this cationic charge on the surface of the particle is key to the development of a successful nucleic acid delivery strategy.

However, the specific targeting of particles to cancer cells may seem a more appropriate strategy to improve specific-intracellular delivery. Targeting promotes increased delivery to the cells of interest with decreased nonspecific delivery to other cells. It was shown that while antibody targeting of liposomes does not increase the extent of tumor accumulation it can increase the amount of internalized drug in solid tumors.<sup>27</sup>

Recently, an alternative lipid based gene-delivery vehicle (Genospheres<sup>TM</sup>) was developed in our laboratory, which had the unusual property of being virtually inactive at delivering luciferase plasmids *in vitro*, unless targeted. Nucleic acids were mixed with cationic and neutral lipids in a liquid monophase comprised of ethanol and water to form a highly condensed and stable lipidic nanoparticle of approximately 100 nm in size. We subsequently used an anti-HER2 antibody-lipid conjugate, developed for intracellular delivery of liposomes, to induce cellular internalization of Genospheres in HER2 overexpressing cells<sup>128</sup> thereby giving rise to enhanced transfection selectivity in HER2-overexpressing cells.

Another approach to improving delivery of nucleic-acids from these lipidic vehicles is by utilizing the local cellular environment to "trigger" a change in the particle structure which can cause DNA release.<sup>129,233</sup> The objective is to be able to tune the triggerable response so that it occurs in the correct anatomical site, in such magnitude to elicit a dramatic response and that the presence of the triggerable lipid does not adversely affect the stability of the particle prior to receiving the stimulus. Appropriate stimuli, may include enzymatic cleavage, changes in local pH, temperature or redox potentials, and photosensitivity. For example, one of the main routes of cell entry for complexes is through an endocytic mechanism, and it is known that endosomal compartments are acidic and contain endogenous esterases and reducing agents. Therefore researchers have attempted to include environmentally responsive components into the complexes, to

utilize the change in local surroundings to release DNA more effectively. These components may include pH sensitive peptides and lipids, hydrolysable and redox-triggered sterically modified neutral lipid or hydrolysable cationic lipids. The introduction of environmentally sensitive moieties can occur in various ways. For examples of such and thorough discussions on these topics, the reader is referred.<sup>233,235,295</sup>

## SUMMARY

Significant advances have been made in recent years in controlling the pharmacokinetics and drug release profiles of weakly basic amphiphilic drugs in liposomal carriers. However, there still remains a fair degree of engineering to tailor a specific chemical entity to its carrier even within this class of drugs. Nonetheless, there are currently multiple examples of successfully formulated drugs from this class that are either already approved for use in oncology applications, or are in clinical development. The prolonged circulation lifetimes and sustained release of these drugs often results in improvements in antitumor efficacy, the overall therapeutic index, or the toxicity profile. Additional improvements in activity or cell-specific delivery for these formulations are being achieved through conjugation of targeting ligands against disease-specific epitopes overexpressed on the surface of cancer cells. The clinical validation of these second generation targeted lipidic nanotherapeutics is currently being investigated by several groups.

Other classes of drugs require more significant modifications to the carriers and delivery strategies to allow for site-specific drug delivery and activity. Formulations of hydrophobic drugs continue to suffer from poor encapsulation efficiencies and modest improvements to the pharmacokinetic profile compared to the more stable formulations of amphipathic drugs. The improvements noted are incremental in nature, and result in formidable competition from other delivery technologies; including albumin nanoparticles, simple emulsions, and polymer conjugates. Liposome formulations of hydrophilic drugs also continue to encounter significant obstacles related to encapsulation efficiency and bioavailability, and may require considerably more complex formulations such as various triggerable formulations, in order to efficiently deliver drug to the site of action. Nucleic acid based therapeutic strate-

gies, most notably siRNA, represent a tremendous opportunity for increasing the number of drugable targets for a particular disease. There is a substantial unmet need in the development of drug delivery systems for targeting and efficiently delivering nucleic acids to their site of action, which there is great hope that lipidic vectors can fill. Although there have certainly been advances in the stable and robust encapsulation of nucleic acids in lipid-based vectors, the field remains in its infancy and much work is still needed to validate these delivery systems *in vivo*, both preclinically and clinically.

Progress continues to be made on a wide range of fronts, and the engineering of lipidic nanocarriers is becoming more rationale as the physicochemical and pharmacological properties that control their disposition continue to be elucidated. The complexities of these various discoveries suggest the need for multidisciplinary teams of scientists that are able to more effectively optimize a liposomal therapeutic for a particular application. It should be clear that the "one size-fits all" mentality of many recent formulation efforts represents a gross oversimplification of the delivery challenges encountered for each new agent. Finally, other newer classes of nanotechnology would be served well to learn from the rich history and complexities encountered in the development of lipid-based vectors.

## ACKNOWLEDGMENTS

Much of the work reviewed within was supported by a variety of mechanisms, including a New Investigator Award (Daryl Drummond) from the California Breast Cancer Research Program of the University of California (Grant Number 7KB-0066), as well as grants from the National Cancer Institute Specialized Programs of Research Excellence (SPORE) in Breast Cancer (P50-CA58207) and Brain Tumors (P50-CA097257).

## REFERENCES

1. Drummond DC, Meyer O, Hong K, Kirpotin DB, Papahadjopoulos D. 1999. Optimizing liposomes for delivery of chemotherapeutic agents to solid tumors. *Pharmacol Rev* 51:691-743.
2. Gabizon A, Shmeeda H, Barenholz Y. 2003. Pharmacokinetics of pegylated liposomal Doxorubicin:

- Review of animal and human studies. *Clin Pharmacokinet* 42:419–436.
3. Allen TM, Martin FJ. 2004. Advantages of liposomal delivery systems for anthracyclines. *Semin Oncol* 31:5–15.
  4. Northfelt DW, Dezube BJ, Thommes JA, Miller BJ, Fischl MA, Friedman-Kien A, Kaplan LD, Mond CD, Mamelek RD, Henry DH. 1998. Pegylated-liposomal doxorubicin versus doxorubicin, bleomycin, and vincristine in the treatment of AIDS-related Kaposi's sarcoma: Results of a randomized phase III clinical trial. *J Clin Oncol* 16:2445–2451.
  5. Stewart S, Jablonowski H, Goebel FD, Arasteh K, Spittle M, Rios A, Aboulafia D, Galleshaw J, Dezube BJ. 1998. Randomized comparative trial of pegylated liposomal doxorubicin versus bleomycin and vincristine in the treatment of AIDS-related Kaposi's sarcoma. *J Clin Oncol* 16:683–691.
  6. Thigpen JT, Aghajanian CA, Alberts DS, Campos SM, Gordon AN, Markman M, McMeekin DS, Monk BJ, Rose PG. 2005. Role of pegylated liposomal doxorubicin in ovarian cancer. *Gynecol Oncol* 96:10–18.
  7. Muggia F, Hamilton A. 2001. Phase III data on Caelyx in ovarian cancer. *Eur J Cancer* 37:S15–S18.
  8. Manochakian R, Miller KC, Chanan-Khan AA. 2007. Bortezomib in combination with pegylated liposomal doxorubicin for the treatment of multiple myeloma. *Clin Lymphoma Myeloma* 7:266–271.
  9. Rifkin RM, Gregory SA, Mohrbacher A, Hussein MA. 2006. Pegylated liposomal doxorubicin, vincristine, and dexamethasone provide significant reduction in toxicity compared with doxorubicin, vincristine, and dexamethasone in patients with newly diagnosed multiple myeloma: A Phase III multicenter randomized trial. *Cancer* 106:848–858.
  10. Zhigaltsev IV, Maurer N, Akhong QF, Leone R, Leng E, Wang J, Semple SC, Cullis PR. 2005. Liposome-encapsulated vincristine, vinblastine and vinorelbine: A comparative study of drug loading and retention. *J Control Release* 104:103–111.
  11. Krishna R, Webb MS, St-Onge G, Mayer LD. 2001. Liposomal and nonliposomal drug pharmacokinetics after administration of liposome-encapsulated vincristine and their contribution to drug tissue distribution properties. *J Pharmacol Exp Ther* 298:1206–1212.
  12. Drummond DC, Noble CO, Guo Z, Hong K, Park JW, Kirpotin DB. 2006. Development of a highly active nanoliposomal irinotecan using a novel intraliposomal stabilization strategy. *Cancer Res* 66:3271–3277.
  13. Emerson DL, Bendele R, Brown E, Chiang S, Desjardins JP, Dihel LC, Gill SC, Hamilton M, LeRay JD, Moon-McDermott L, Moynihan K, Richardson FC, Tomkinson B, Luzzio MJ, Baccanari D. 2000. Antitumor efficacy, pharmacokinetics, and biodistribution of NX 211: A low-clearance liposomal formulation of lurtotecan. *Clin Cancer Res* 6:2903–2912.
  14. Pal A, Khan S, Wang YF, Kamath N, Sarkar AK, Ahmad A, Sheikh S, Ali S, Carbonaro D, Zhang A, Ahmad I. 2005. Preclinical safety, pharmacokinetics and antitumor efficacy profile of liposome-entrapped SN-38 formulation. *Anticancer Res* 25:331–341.
  15. Tardi P, Choice E, Masin D, Redelmeier T, Bally M, Madden TD. 2000. Liposomal encapsulation of topotecan enhances anticancer efficacy in murine and human xenograft models. *Cancer Res* 60:3389–3393.
  16. Sharma A, Mayhew E, Bolcsak L, Cavanaugh C, Harmon P. 1997. Activity of paclitaxel liposome formulations against human ovarian tumor xenografts. *Int J Cancer* 71:103–107.
  17. Guo W, Johnson JL, Khan S, Ahmad A, Ahmad I. 2005. Paclitaxel quantification in mouse plasma and tissues containing liposome-entrapped paclitaxel by liquid chromatography-tandem mass spectrometry: Application to a pharmacokinetics study. *Anal Biochem* 336:213–220.
  18. Lu C, Perez-Soler R, Piperdi B, Walsh GL, Swisher SG, Smythe WR, Shin HJ, Ro JY, Feng L, Truong M, Yalamanchili A, Lopez-Berestein G, Hong WK, Khokhar AR, Shin DM. 2005. Phase II study of a liposome-entrapped cisplatin analog (L-NDDP) administered intrapleurally and pathologic response rates in patients with malignant pleural mesothelioma. *J Clin Oncol* 23:3495–3501.
  19. Kim ES, Lu C, Khuri FR, Tonda M, Glisson BS, Liu D, Jung M, Hong WK, Herbst RS. 2001. A phase II study of STEALTH cisplatin (SPT-77) in patients with advanced non-small cell lung cancer. *Lung Cancer* 34:427–432.
  20. Forssen EA, Male-Brune R, Adler-Moore JP, Lee MJA, Schmidt PG, Krasieva TB, Shimizu S, Tromberg BJ. 1996. Fluorescence imaging studies for the disposition of daunorubicin liposomes (DaunoXome<sup>®</sup>) within tumor tissue. *Cancer Res* 56:2066–2075.
  21. Lim HJ, Masin D, Madden TD, Bally MB. 1997. Influence of drug release characteristics on the therapeutic activity of liposomal mitoxantrone. *J Pharmacol Exp Ther* 281:566–573.
  22. Sparreboom A, Scripture CD, Trieu V, Williams PJ, De T, Yang A, Beals B, Figg WD, Hawkins M, Desai N. 2005. Comparative preclinical and clinical pharmacokinetics of a cremophor-free, nanoparticle albumin-bound paclitaxel (ABI-007) and



- paclitaxel formulated in Cremophor (Taxol). *Clin Cancer Res* 11:4136–4143.
23. Gradishar WJ, Tjulandin S, Davidson N, Shaw H, Desai N, Bhar P, Hawkins M, O'Shaughnessy J. 2005. Phase III trial of nanoparticle albumin-bound paclitaxel compared with polyethylated castor oil-based paclitaxel in women with breast cancer. *J Clin Oncol* 23:7794–7803.
  24. Yuan F, Lwunig M, Huang SK, Berk DA, Papa-hadjopoulos D, Jain RK. 1994. Microvascular permeability and interstitial penetration of sterically stabilized (stealth) liposomes in a human tumor xenograft. *Cancer Res* 54:3352–3356.
  25. Hobbs SK, Monsky WL, Yuan F, Roberts WG, Griffith L, Torchilin VP, Jain RK. 1998. Regulation of transport pathways in tumor vessels: Role of tumor type and microenvironment. *Proc Natl Acad Sci USA* 95:4607–4612.
  26. Matsumura Y, Maeda H. 1986. A new concept for macromolecular therapeutics in cancer chemotherapy: Mechanism of tumoritropic accumulation of proteins and the antitumor agent SMANCS. *Cancer Res* 46:6387–6392.
  27. Kirpotin DB, Drummond DC, Shao Y, Shalaby MR, Hong K, Nielsen UB, Marks JD, Benz CC, Park JW. 2006. Antibody targeting of long-circulating lipidic nanoparticles does not increase tumor localization but does increase internalization in animal models. *Cancer Res* 66:6732–6740.
  28. Lum H, Malik AB. 1994. Regulation of vascular endothelial barrier function. *Am J Physiol* 267:L223–L241.
  29. Michel CC, Curry FE. 1999. Microvascular permeability. *Physiol Rev* 79:703–761.
  30. Moghimi SM, Szebeni J. 2003. Stealth liposomes and long circulating nanoparticles: Critical issues in pharmacokinetics, opsonization and protein-binding properties. *Prog Lipid Res* 42:463–478.
  31. Allen TM, Cheng WW, Hare JJ, Laginha KM. 2006. Pharmacokinetics and pharmacodynamics of lipidic nano-particles in cancer. *Anticancer Agents Med Chem* 6:513–523.
  32. Allen TM, Hansen CB, Lopes de Menezes DE. 1995. Pharmacokinetics of long-circulating liposomes. *Adv Drug Deliv Rev* 16:267–284.
  33. Hwang KJ. 1987. Liposome pharmacokinetics. In: Ostro MJ, editor. *Liposomes: From biophysics to therapeutics*. 1st edition. New York: Marcel Dekker, Inc. pp 109–156.
  34. Ishida T, Atobe K, Wang X, Kiwada H. 2006. Accelerated blood clearance of PEGylated liposomes upon repeated injections: Effect of doxorubicin-encapsulation and high-dose first injection. *J Control Release* 115:251–258.
  35. Ishida T, Ichihara M, Wang X, Yamamoto K, Kimura J, Majima E, Kiwada H. 2006. Injection of PEGylated liposomes in rats elicits PEG-specific IgM, which is responsible for rapid elimination of a second dose of PEGylated liposomes. *J Control Release* 112:15–25.
  36. Ishida T, Maeda R, Ichihara M, Irimura K, Kiwada H. 2003. Accelerated clearance of PEGylated liposomes in rats after repeated injections. *J Control Release* 88:35–42.
  37. Laverman P, Brouwers AH, Dams ETM, Oyen WJG, Storm G, Van Rooijen N, Corstens FHM, Boerman OC. 2000. Preclinical and clinical evidence for disappearance of long-circulating characteristics of polyethylene glycol liposomes at low lipid dose. *J Pharmacol Exp Therap* 293:996–1001.
  38. Zhou R, Mazurchuk R, Straubinger RM. 2002. Antivasculature effects of doxorubicin-containing liposomes in an intracranial rat brain tumor model. *Cancer Res* 62:2561–2566.
  39. Chobanian JV, Tall AR, Brecher PI. 1979. Interaction between unilamellar egg yolk lecithin vesicles and human high density lipoprotein. *Biochemistry* 18:180–187.
  40. Damen J, Regts J, Scherphof G. 1981. Transfer and exchange of phospholipid between small unilamellar liposomes and rat plasma high density lipoproteins: Dependence on cholesterol content and phospholipid composition. *Biochim Biophys Acta* 665:538–545.
  41. Senior J, Gregoriadis G. 1982. Stability of small unilamellar liposomes in serum and clearance from the circulation: The effect of the phospholipid and cholesterol components. *Life Sci* 30:2123–2136.
  42. Senior JH. 1987. Fate and behaviour of liposomes in vivo: A review of controlling factors. *CRC Crit Rev Therap Drug Carrier System* 3:123–193.
  43. Semple SC, Chonn A, Cullis PR. 1996. Influence of cholesterol on the association of plasma proteins with liposomes. *Biochemistry* 35:2521–2525.
  44. Dos Santos N, Allen C, Doppen AM, Anantha M, Cox KA, Gallagher RC, Karlsson G, Edwards K, Kenner G, Samuels L, Webb MS, Bally MB. 2007. Influence of poly(ethylene glycol) grafting density and polymer length on liposomes: Relating plasma circulation lifetimes to protein binding. *Biochim Biophys Acta* 1768:1367–1377.
  45. Tardi PG, Gallagher RC, Johnstone S, Harasym N, Webb M, Bally MB, Mayer LD. 2007. Coencapsulation of irinotecan and floxuridine into low cholesterol-containing liposomes that coordinate drug release in vivo. *Biochim Biophys Acta* 1768:678–687.
  46. Dos Santos N, Mayer LD, Abraham SA, Gallagher RC, Cox KA, Tardi PG, Bally MB. 2002. Improved retention of idarubicin after intravenous injection obtained for cholesterol-free liposomes. *Biochim Biophys Acta* 1561:188–201.
  47. Gabizon A, Price DC, Huberty J, Bresalier RS, Papahadjopoulos D. 1990. Effect of liposome composition and other factors on the targeting of lipo-

- comes to experimental tumors: Biodistribution and imaging studies. *Cancer Res* 50:6371–6378.
48. Woodle MC, Matthey KK, Newman MS, Hidayat JE, Collins LR, Redemann C, Martin FJ, Papa-hadjopoulos D. 1992. Versatility in lipid compositions showing prolonged circulation with sterically stabilized liposomes. *Biochim Biophys Acta* 1105:193–200.
  49. Allen TM, Hansen C, Martin F, Redemann C, Yau-Young A. 1991. Liposomes containing synthetic lipid derivatives of poly(ethylene glycol) show prolonged circulation half-lives in vivo. *Biochim Biophys Acta* 1066:29–36.
  50. Needham D, Nunn RS. 1990. Elastic deformation and failure of lipid bilayer membranes containing cholesterol. *Biophys J* 58:997–1009.
  51. Sankaram MB, Thompson TE. 1990. Interaction of cholesterol with various glycerophospholipids and sphingomyelin. *Biochemistry* 29:10670–10675.
  52. Veiga MP, Arrondo JL, Goni FM, Alonso A, Marsh D. 2001. Interaction of cholesterol with sphingomyelin in mixed membranes containing phosphatidylcholine, studied by spin-label ESR and IR spectroscopies. A possible stabilization of gel-phase sphingolipid domains by cholesterol. *Biochemistry* 40:2614–2622.
  53. Niemela P, Hyvonen MT, Vattulainen I. 2004. Structure and dynamics of sphingomyelin bilayer: Insight gained through systematic comparison to phosphatidylcholine. *Biophys J* 87:2976–2989.
  54. Talbott CM, Vorobyov I, Borchman D, Taylor KG, DuPre DB, Yappert MC. 2000. Conformational studies of sphingolipids by NMR spectroscopy. II. Sphingomyelin. *Biochim Biophys Acta* 1467:326–337.
  55. Johnston MJ, Semple SC, Klimuk SK, Ansell S, Maurer N, Cullis PR. 2007. Characterization of the drug retention and pharmacokinetic properties of liposomal nanoparticles containing dihydro-sphingomyelin. *Biochim Biophys Acta* 1768:1121–1127.
  56. Chonn A, Semple SC, Cullis P. 1992. Association of blood proteins with large unilamellar liposomes in vivo: Relation to circulation lifetimes. *J Biol Chem* 267:18759–18765.
  57. Yeeprae W, Kawakami S, Suzuki S, Yamashita F, Hashida M. 2006. Physicochemical and pharmacokinetic characteristics of cationic liposomes. *Pharmazie* 61:102–105.
  58. Schmitt-Sody M, Strieth S, Krasnici S, Sauer B, Schulze B, Teifel M, Michaelis U, Naujoks K, Dellian M. 2003. Neovascular targeting therapy: Paclitaxel encapsulated in cationic liposomes improves antitumoral efficacy. *Clin Cancer Res* 9:2335–2341.
  59. Campbell RB, Fukumura D, Brown EB, Mazzola LM, Izumi Y, Jain RK, Torchilin VP, Munn LL. 2002. Cationic charge determines the distribution of liposomes between the vascular and extravascular compartments of tumors. *Cancer Res* 62:6831–6836.
  60. Blau S, Jubeh TT, Haupt SM, Rubinstein A. 2000. Drug targeting by surface cationization. *Crit Rev Ther Drug Carrier Syst* 17:425–465.
  61. Li S, Tseng WC, Stolz DB, Wu SP, Watkins SC, Huang L. 1999. Dynamic changes in the characteristics of cationic lipidic vectors after exposure to mouse serum: Implications for intravenous lipofection. *Gene Ther* 6:585–594.
  62. McLean JW, Fox EA, Baluk P, Bolton PB, Haskell A, Pearlman R, Thurston G, Umemoto EY, McDonald DM. 1997. Organ-specific endothelial cell uptake of cationic liposome-DNA complexes in mice. *Am Physiol Soc* 273:H387–H404.
  63. Lockman PR, Koziara JM, Mumper RJ, Allen DD. 2004. Nanoparticle surface charges alter blood-brain barrier integrity and permeability. *J Drug Target* 12:635–641.
  64. Ambegia E, Ansell S, Cullis P, Heyes J, Palmer L, MacLachlan I. 2005. Stabilized plasmid-lipid particles containing PEG-diacylglycerols exhibit extended circulation lifetimes and tumor selective gene expression. *Biochim Biophys Acta* 1669:155–163.
  65. Monck MA, Mori A, Lee D, Tam P, Wheeler JJ, Cullis PR, Scherrer P. 2000. Stabilized plasmid-lipid particles: Pharmacokinetics and plasmid delivery to distal tumors following intravenous injection. *J Drug Target* 7:439–452.
  66. Gabizon A, Chemla M, Tzemach D, Horowitz AT, Goren D. 1996. Liposome longevity and stability in circulation: Effects on the in vivo delivery to tumors and therapeutic efficacy of encapsulated anthracyclines. *J Drug Target* 3:391–398.
  67. Ahl PL, Bhatia SK, Meers F, Roberts P, Stevens R, Dause R, Perkins WR, Janoff AS. 1997. Enhancement of the in vivo circulation lifetime of L-alpha-distearoylphosphatidylcholine liposomes: Importance of liposomal aggregation versus complement opsonization. *Biochim Biophys Acta* 1329:370–382.
  68. Park YS, Maruyama K, Huang L. 1992. Some negatively charged phospholipid derivatives prolong the liposome circulation in vivo. *Biochim Biophys Acta* 1108:257–260.
  69. Chonn A, Semple SC, Cullis PR. 1991. Separation of large unilamellar liposomes from blood components by a spin column procedure: Towards identifying plasma proteins which mediate liposome clearance in vivo. *Biochim Biophys Acta* 1070:215–222.
  70. Kamps JA, Scherphof GL. 1998. Receptor versus non-receptor mediated clearance of liposomes. *Adv Drug Deliv Rev* 32:81–97.
  71. Parr MJ, Ansell SM, Choi LS, Cullis PR. 1994. Factors influencing the retention and chemical stability of poly(ethylene glycol)-lipid conjugates

- incorporated into large unilamellar vesicles. *Biochim Biophys Acta* 1195:21–30.
72. Webb MS, Saxon D, Wong FM, Lim HJ, Wang Z, Bally MB, Choi LS, Cullis PR, Mayer LD. 1998. Comparison of different hydrophobic anchors conjugated to poly(ethylene glycol): Effects on the pharmacokinetics of liposomal vincristine. *Biochim Biophys Acta* 1372:272–282.
  73. Lyass O, Uziely B, Ben-Yosef R, Tzemach D, Heshing NI, Lotem M, Brufman G, Gabizon A. 2000. Correlation of toxicity with pharmacokinetics of pegylated liposomal doxorubicin (Doxil) in metastatic breast carcinoma. *Cancer* 89:1037–1047.
  74. Meerum Terwogt JM, Groenewegen G, Pluim D, Maliepaard M, Tibben MM, Huisman A, ten Bokkel Huinink WW, Schot M, Welbank H, Voest EE, Beijnen JH, Schellens JM. 2002. Phase I and pharmacokinetic study of SPI-77, a liposomal encapsulated dosage form of cisplatin. *Cancer Chemother Pharmacol* 49:201–210.
  75. Bedikian A, Vardeleon A, Smith T, Campbell S, Namdari R. 2006. Pharmacokinetics and urinary excretion of vincristine sulfate liposomes injection in metastatic melanoma patients. *J Clin Pharmacol* 46:727–737.
  76. Dark GG, Calvert AH, Grimshaw R, Poole C, Swenerton K, Kaye S, Coleman R, Jayson G, Le T, Ellard S, Trudeau M, Vasey P, Hamilton M, Cameron T, Barrett E, Walsh W, McIntosh L, Eisenhauer EA. 2005. Randomized trial of two intravenous schedules of the topoisomerase I inhibitor liposomal lurtotecan in women with relapsed epithelial ovarian cancer: A trial of the national cancer institute of Canada clinical trials group. *J Clin Oncol* 23:1859–1866.
  77. Kehrer DF, Bos AM, Verweij J, Groen HJ, Loos WJ, Sparreboom A, de Jonge MJ, Hamilton M, Cameron T, de Vries EG. 2002. Phase I and pharmacologic study of liposomal lurtotecan, NX 211: Urinary excretion predicts hematologic toxicity. *J Clin Oncol* 20:1222–1231.
  78. Mross K, Niemann B, Massing U, Drevs J, Unger C, Bhamra R, Swenson CE. 2004. Pharmacokinetics of liposomal doxorubicin (TLC-D99; Myocet) in patients with solid tumors: An open-label, single-dose study. *Cancer Chemother Pharmacol* 54:514–524.
  79. Ishida T, Harada M, Wang XY, Ichihara M, Irimura K, Kiwada H. 2005. Accelerated blood clearance of PEGylated liposomes following preceding liposome injection: Effects of lipid dose and PEG surface-density and chain length of the first-dose liposomes. *J Control Release* 105:305–317.
  80. Wang X, Ishida T, Kiwada H. 2007. Anti-PEG IgM elicited by injection of liposomes is involved in the enhanced blood clearance of a subsequent dose of PEGylated liposomes. *J Control Release* 119:236–244.
  81. Lorusso D, Di Stefano A, Carone V, Fagotti A, Pisconti S, Scambia G. 2007. Pegylated liposomal doxorubicin-related palmar-plantar erythrodysesthesia ('hand-foot' syndrome). *Ann Oncol* 18:1159–1164.
  82. Allen TM, Hansen C. 1991. Pharmacokinetics of stealth versus conventional liposomes: Effect of dose. *Biochim Biophys Acta* 1068:133–141.
  83. Allen TM, Smuckler EA. 1985. Liver pathology accompanying chronic liposome administration in mouse. *Res Comm Chem Path Pharmacol* 50:281–290.
  84. Oja CD, Semple SC, Chonn A, Cullis PR. 1996. Influence of dose on liposome clearance: Critical role of blood proteins. *Biochim Biophys Acta* 1281:31–37.
  85. Semple SC, Chonn A, Cullis PR. 1998. Interactions of liposomes and lipid-based carrier systems with blood proteins: Relation to clearance behaviour in vivo. *Adv Drug Deliv Rev* 32:3–17.
  86. Charrois GJ, Allen TM. 2003. Multiple injections of pegylated liposomal Doxorubicin: Pharmacokinetics and therapeutic activity. *J Pharmacol Exp Ther* 306:1058–1067.
  87. Arnold RD, Mager DE, Slack JE, Straubinger RM. 2005. Effect of repetitive administration of Doxorubicin-containing liposomes on plasma pharmacokinetics and drug biodistribution in a rat brain tumor model. *Clin Cancer Res* 11:8856–8865.
  88. Allen TM, Hansen CB, Guo LSS. 1993. Subcutaneous administration of liposomes: A comparison with the intravenous and intraperitoneal routes of injection. *Biochim Biophys Acta* 1150:9–16.
  89. Cabanes A, Tzemach D, Goren D, Horowitz AT, Gabizon A. 1998. Comparative study of the antitumor activity of free doxorubicin and polyethylene glycol-coated liposomal doxorubicin in a mouse lymphoma model. *Clin Cancer Res* 4:499–505.
  90. Swartz MA, Berk DA, Jain RK. 1996. Transport in lymphatic capillaries. I. Macroscopic measurements using residence time distribution theory. *Am J Physiol* 270:H324–H329.
  91. Angst MS, Drover DE. 2006. Pharmacology of drugs formulated with DepoFoam: A sustained release drug delivery system for parenteral administration using multivesicular liposome technology. *Clin Pharmacokinet* 45:1153–1176.
  92. Mantripragada S. 2002. A lipid based depot (DepoFoam technology) for sustained release drug delivery. *Prog Lipid Res* 41:392–406.
  93. Oussoren C, Storm G. 2001. Liposomes to target the lymphatics by subcutaneous administration. *Adv Drug Deliv Rev* 50:143–156.
  94. Wilson KD, Raney SG, Sekirov L, Chikh G, Dejong SD, Cullis PR, Tam YK. 2007. Effects of intravenous and subcutaneous administration on the

- pharmacokinetics, biodistribution, cellular uptake and immunostimulatory activity of CpG ODN encapsulated in liposomal nanoparticles. *Int Immunopharmacol* 7:1064–1075.
95. Huynh GH, Deen DF, Szoka FC, Jr. 2006. Barriers to carrier mediated drug and gene delivery to brain tumors. *J Control Release* 110:236–259.
  96. MacKay JA, Deen DF, Szoka FC, Jr. 2005. Distribution in brain of liposomes after convection enhanced delivery; modulation by particle charge, particle diameter, and presence of steric coating. *Brain Res* 1035:139–153.
  97. Noble CO, Krauze MT, Drummond DC, Yamashita Y, Saito R, Berger MS, Kirpotin DB, Bankiewicz KS, Park JW. 2006. Novel nanoliposomal CPT-11 infused by convection-enhanced delivery in intracranial tumors: Pharmacology and efficacy. *Cancer Res* 66:2801–2806.
  98. Saito R, Krauze MT, Bringas JR, Noble C, McKnight TR, Jackson P, Wendland MF, Mamot C, Drummond DC, Kirpotin DB, Hong K, Berger MS, Park JW, Bankiewicz KS. 2005. Gadolinium-loaded liposomes allow for real-time magnetic resonance imaging of convection-enhanced delivery in the primate brain. *Exp Neurol* 196:381–389.
  99. Saito R, Krauze MT, Noble CO, Drummond DC, Kirpotin DB, Berger MS, Park JW, Bankiewicz KS. 2006. Convection-enhanced delivery of Ls-TPT enables an effective, continuous, low-dose chemotherapy against malignant glioma xenograft model. *Neuro-Oncology* 8:205–214.
  100. Saito R, Krauze MT, Noble CO, Tamas M, Drummond DC, Kirpotin DB, Berger MS, Park JW, Bankiewicz KS. 2006. Tissue affinity of the infusate affects the distribution volume during convection-enhanced delivery into rodent brains: Implications for local drug delivery. *J Neurosci Methods* 154:225–232.
  101. Saito R, Bringas JR, McKnight TR, Wendland MF, Mamot C, Drummond DC, Kirpotin DB, Park JW, Berger MS, Bankiewicz KS. 2004. Distribution of liposomes into brain and rat brain tumor models by convection-enhanced delivery monitored with magnetic resonance imaging. *Cancer Res* 64:2572–2579.
  102. Lund U, Rippe A, Venturoli D, Tenstad O, Grubb A, Rippe B. 2003. Glomerular filtration rate dependence of sieving of albumin and some neutral proteins in rat kidneys. *Am J Physiol Renal Physiol* 284:F1226–F1234.
  103. Ohlson M, Sorensson J, Haraldsson B. 2000. Glomerular size and charge selectivity in the rat as revealed by FITC-ficoll and albumin. *Am J Physiol Renal Physiol* 279:F84–F91.
  104. Litzinger DC, Buiting AMJ, van Rooijen N, Huang L. 1994. Effect of liposome size on the circulation time and intraorgan distribution of amphipathic poly(ethylene glycol)-containing liposomes. *Biochim Biophys Acta* 1190:99–107.
  105. Allen TM, Hansen C, Rutledge J. 1989. Liposomes with prolonged circulation times: Factors affecting uptake by reticuloendothelial and other tissues. *Biochim Biophys Acta* 981:27–35.
  106. Nagayasu A, Uchiyama K, Kiwada H. 1999. The size of liposomes: A factor which affects their targeting efficiency to tumors and therapeutic activity of liposomal antitumor drugs. *Adv Drug Deliv Rev* 40:75–87.
  107. Charrois GJ, Allen TM. 2003. Rate of biodistribution of STEALTH liposomes to tumor and skin: Influence of liposome diameter and implications for toxicity and therapeutic activity. *Biochim Biophys Acta* 1609:102–108.
  108. Bally MB, Nayar R, Masin D, Hope MJ, Cullis PR, Mayer L. 1990. Liposomes with entrapped doxorubicin exhibit extended blood residence times. *Biochim Biophys Acta* 1023:133–139.
  109. Lim HJ, Parr MJ, Masin D, McIntosh NL, Madden TD, Zhang G, Johnstone S, Bally MB. 2000. Kupffer cells do not play a role in governing the efficacy of liposomal mitoxantrone used to treat a tumor model designed to assess drug delivery to liver. *Clin Cancer Res* 6:4449–4460.
  110. Parr MJ, Bally MB, Cullis PR. 1993. The presence of GM1 in liposomes with entrapped doxorubicin does not prevent RES blockade. *Biochim Biophys Acta* 1168:249–252.
  111. Judge A, McClintock K, Phelps JR, MacLachlan I. 2006. Hypersensitivity and loss of disease site targeting caused by antibody responses to PEGylated liposomes. *Mol Ther* 13:328–337.
  112. Semple SC, Harasym TO, Clow KA, Ansell SM, Klimuk SK, Hope MJ. 2005. Immunogenicity and rapid blood clearance of liposomes containing polyethylene glycol-lipid conjugates and nucleic Acid. *J Pharmacol Exp Ther* 312:1020–1026.
  113. Noble CO, Kirpotin DB, Hayes ME, Mamot C, Hong K, Park JW, Benz CC, Marks JD, Drummond DC. 2004. Development of ligand-targeted liposomes for cancer therapy. *Expert Opin Ther Targets* 8:335–353.
  114. Sapra P, Allen TM. 2003. Ligand-targeted liposomal anticancer drugs. *Prog Lipid Res* 42:439–462.
  115. Peeters JM, Hazendonk TG, Beuvery EC, Tesser GI. 1989. Comparison of four bifunctional reagents for coupling peptides to proteins and the effect of the three moieties on the immunogenicity of the conjugates. *J Immunol Methods* 120:133–143.
  116. Willis MC, Collins B, Zhang T, Green LS, Sebesta DP, Bell C, Kellogg E, Gill SC, Magallanez A, Knauer S, Bendele RA, Gill PS, Janic N. 1998. Liposome-anchored vascular endothelial growth factor aptamers. *Bioconjug Chem* 9:573–582.

117. Aragnol D, Leserman LD. 1986. Immune clearance of liposomes inhibited by an anti-Fc receptor antibody in vivo. *Proc Natl Acad Sci USA* 83:2699–2703.
118. Harding JA, Engbers CM, Newman MS, Goldstein NI, Zalipsky S. 1997. Immunogenicity and pharmacokinetic attributes of poly(ethyleneglycol)-grafted immunoliposomes. *Biochim Biophys Acta* 1327:181–192.
119. Sapro P, Moase EH, Ma J, Allen TM. 2004. Improved therapeutic responses in a xenograft model of human B lymphoma (Namalwa) for liposomal vincristine versus liposomal doxorubicin targeted via anti-CD19 IgG2a or Fab' fragments. *Clin Cancer Res* 10:1100–1111.
120. Mamot C, Drummond DC, Noble CO, Kallab V, Guo Z, Hong K, Kirpotin DB, Park JW. 2005. Epidermal growth factor receptor-targeted immunoliposomes significantly enhance the efficacy of multiple anticancer drugs in vivo. *Cancer Res* 65:11631–11638.
121. Park JW, Hong K, Kirpotin DB, Colbern G, Shalaby R, Baselga J, Shao Y, Nielsen UB, Marks JD, Moore D, Papahadjopoulos D, Benz CC. 2002. Anti-HER2 immunoliposomes: Enhanced efficacy attributable to targeted delivery. *Clin Cancer Res* 8:1172–1181.
122. Mayer LD, St-Onge G. 1995. Determination of free and liposome-associated doxorubicin and vincristine levels in plasma under equilibrium conditions employing ultrafiltration techniques. *Anal Biochem* 232:149–157.
123. Webb MS, Harasym TO, Masin D, Bally MB, Mayer LD. 1995. Sphingomyelin-cholesterol liposomes significantly enhance the pharmacokinetic and therapeutic properties of vincristine in murine and human tumour models. *Br J Cancer* 72:896–904.
124. Sharma A, Sharma US, Straubinger RM. 1996. Paclitaxel-liposomes for intracavitary therapy of intraperitoneal P388 leukemia. *Cancer Lett* 107:265–272.
125. Zhang JA, Anyarambhatla G, Ma L, Ugwu S, Xuan T, Sardone T, Ahmad I. 2005. Development and characterization of a novel Cremophor EL free liposome-based paclitaxel (LEP-ETU) formulation. *Eur J Pharm Biopharm* 59:177–187.
126. Peleg-Shulman T, Gibson D, Cohen R, Abra R, Barenholz Y. 2001. Characterization of sterically stabilized cisplatin liposomes by nuclear magnetic resonance. *Biochim Biophys Acta* 1510:278–291.
127. Desjardins J, Emerson DL, Colagiovanni DB, Abbott E, Brown EN, Drolet DW. 2004. Pharmacokinetics, safety, and efficacy of a liposome encapsulated thymidylate synthase inhibitor, OSI-7904L [(S)-2-[5-[(1,2-dihydro-3-methyl-1-oxobenzof[quinazolin-9-yl)methyl]amino-1-oxo-2-isoin-dolynl]-glutaric acid] in mice. *J Pharmacol Exp Ther* 309:894–902.
128. Hayes ME, Drummond DC, Kirpotin DB, Zheng WW, Noble CO, Park JW, Marks JD, Benz CC, Hong K. 2006. Genospheres: Self-assembling nucleic acid-lipid nanoparticles suitable for targeted gene delivery. *Gene Ther* 13:646–651.
129. Li W, Szoka FC, Jr. 2007. Lipid-based nanoparticles for nucleic acid delivery. *Pharm Res* 24:438–449.
130. Cullis PR, Hope MJ, Bally MB, Madden TD, Mayer LD, Fenske DB. 1997. Influence of pH gradients on the transbilayer transport of drugs, lipids, peptides and metal ions into large unilamellar vesicles. *Biochim Biophys Acta* 1331:187–211.
131. Mayer LD, Bally MB, Hope MJ, Cullis PR. 1985. Uptake of antineoplastic agents into large unilamellar vesicles in response to a membrane potential. *Biochim Biophys Acta* 816:294–302.
132. Allen TM, Newman MS, Woodle MC, Mayhew E, Uster PS. 1995. Pharmacokinetics and antitumor activity of vincristine encapsulated in sterically stabilized liposomes. *Int J Cancer* 62:199–204.
133. Haran G, Cohen R, Bar LK, Barenholz Y. 1993. Transmembrane ammonium sulfate gradients in liposomes produce efficient and stable entrapment of amphiphathic weak bases. *Biochim Biophys Acta* 1151:201–215.
134. Lasic DD, Ceb B, Stuart MC, Guo L, Frederik PM, Barenholz Y. 1995. Transmembrane gradient driven phase transitions within vesicles: Lessons for drug delivery. *Biochim Biophys Acta* 1239:145–156.
135. Maurer-Spurej E, Wong KF, Maurer N, Fenske DB, Cullis PR. 1999. Factors influencing uptake and retention of amino-containing drugs in large unilamellar vesicles exhibiting transmembrane pH gradients. *Biochim Biophys Acta* 1416:1–10.
136. Drummond DC, Marx C, Guo Z, Scott G, Noble C, Wang D, Pallavicini M, Kirpotin DB, Benz CC. 2005. Enhanced pharmacodynamic and antitumor properties of a histone deacetylase inhibitor encapsulated in liposomes or ErbB2-targeted immunoliposomes. *Clin Cancer Res* 11:3392–3401.
137. Abraham SA, Edwards K, Karlsson G, Hudon N, Mayer LD, Bally MB. 2004. An evaluation of transmembrane ion gradient-mediated encapsulation of topotecan within liposomes. *J Control Release* 96:449–461.
138. Ramsay E, Alnajim J, Anantha M, Taggar A, Thomas A, Edwards K, Karlsson G, Webb M, Bally M. 2006. Transition metal-mediated liposomal encapsulation of irinotecan (CPT-11) stabilizes the drug in the therapeutically active lactone conformation. *Pharm Res* 23:2799–2808.

139. Taggar AS, Alnajim J, Anantha M, Thomas A, Webb M, Ramsay E, Bally MB. 2006. Copper-topotecan complexation mediates drug accumulation into liposomes. *J Control Release* 114:78–88.
140. Kirpotin DB. 2000. Compound-loaded liposomes and methods for their preparation, U.S. Patent 6,110,491, August 29.
141. Messerer CL, Ramsay EC, Waterhouse D, Ng R, Simms EM, Harasym N, Tardi P, Mayer LD, Bally MB. 2004. Liposomal irinotecan: Formulation development and therapeutic assessment in murine xenograft models of colorectal cancer. *Clin Cancer Res* 10:6638–6649.
142. Mayer LD, Tai LCL, Bally MB, Mitlenes GN, Ginsberg RS, Cullis PR. 1990. Characterization of liposomal systems containing doxorubicin entrapped in response to pH gradients. *Biochim Biophys Acta* 1025:143–151.
143. Working PK, Dayan AD. 1996. Pharmacological-toxicological expert report—Caelyx(TM)—(Stealth(R) liposomal doxorubicin HCl)—Foreword. *Human Exp Toxicol* 15:751–785.
144. Johnston MJ, Semple SC, Klimuk SK, Edwards K, Eisenhardt ML, Leng EC, Karlsson G, Yanko D, Cullis PR. 2006. Therapeutically optimized rates of drug release can be achieved by varying the drug-to-lipid ratio in liposomal vincristine formulations. *Biochim Biophys Acta* 1758:55–64.
145. Gabizon AAM, Barenholz M. 1986. Comparative long-term study of the toxicities of free and liposome-associated doxorubicin in mice after intravenous administration. *J Natl Cancer Inst* 77:459–469.
146. Khan S, Ahmad A, Guo W, Wang YF, Abu-Qare A, Ahmad I. 2005. A simple and sensitive LC/MS/MS assay for 7-ethyl-10-hydroxycamptothecin (SN-38) in mouse plasma and tissues: Application to pharmacokinetic study of liposome entrapped SN-38 (LE-SN38). *J Pharm Biomed Anal* 37:135–142.
147. Zhang JA, Xuan T, Parmar M, Ma L, Ugwu S, Ali S, Ahmad I. 2004. Development and characterization of a novel liposome-based formulation of SN-38. *Int J Pharm* 270:93–107.
148. Sharma A, Straubinger RM. 1994. Novel taxol formulations: Preparation and characterization of taxel-containing liposomes. *Pharm Res* 11:889–896.
149. Gabizon A, Shiota R, Papahadjopoulos D. 1989. Pharmacokinetics and tissue distribution of doxorubicin encapsulated in stable liposomes with long circulation times. *J Natl Cancer Inst* 81:1484–1488.
150. Allen TM. 1981. A study of phospholipid interactions between high-density lipoproteins and small unilamellar vesicles. *Biochim Biophys Acta* 640:385–397.
151. Papahadjopoulos D, Cowden M, Kimelberg H. 1973. Role of cholesterol in membranes. Effects on phospholipid-protein interactions, membrane permeability and enzymatic activity. *Biochim Biophys Acta* 330:8–26.
152. Papahadjopoulos D, Nir S, Oki S. 1972. Permeability properties of phospholipid membranes: Effect of cholesterol and temperature. *Biochim Biophys Acta* 266:561–583.
153. Mayhew E, Rustum YM, Szoka F, Papahadjopoulos D. 1979. Role of cholesterol in enhancing the antitumor activity of cytosine arabinoside entrapped in liposomes. *Cancer Treat Rep* 63:1923–1928.
154. Mayer LD, Cullis PR, Bally MB. 1998. Designing therapeutically optimized liposomal anticancer delivery systems: Lessons from conventional liposomes. In: Papahadjopoulos La, editor. *Medical applications of liposomes*. 1st edition. New York: Elsevier Science B.V.
155. Gabizon AA, Barenholz Y, Bialer M. 1993. Prolongation of the circulation time of doxorubicin encapsulated in liposomes containing polyethylene glycol-derivatized phospholipid: Pharmacokinetic studies in rodents and dogs. *Pharm Res* 10:703–708.
156. Charrois GJ, Allen TM. 2004. Drug release rate influences the pharmacokinetics, biodistribution, therapeutic activity, and toxicity of pegylated liposomal doxorubicin formulations in murine breast cancer. *Biochim Biophys Acta* 1663:167–177.
157. Cullis PR, Hope MJ. 1980. The bilayer stabilizing role of sphingomyelin in the presence of cholesterol: A 31P NMR study. *Biochim Biophys Acta* 597:533–542.
158. Li XM, Momsen MM, Smaby JM, Brockman HL, Brown RE. 2001. Cholesterol decreases the interfacial elasticity and detergent solubility of sphingomyelins. *Biochemistry* 40:5954–5963.
159. Lande MB, Donovan JM, Zeidel ML. 1995. The relationship between membrane fluidity and permeabilities to water, solutes, ammonia, and protons. *J Gen Physiol* 106:67–84.
160. Bittman R, Kasireddy CR, Mattjus P, Slotte JP. 1994. Interaction of cholesterol with sphingomyelin in monolayers and vesicles. *Biochemistry* 33:11776–11781.
161. Mombelli E, Morris R, Taylor W, Fraternali F. 2003. Hydrogen-bonding propensities of sphingomyelin in solution and in a bilayer assembly: A molecular dynamics study. *Biophys J* 84:1507–1517.
162. Simmons SF, Kramer FA. 1977. Liposomal entrapment of floxuridine. *J Pharm Sci* 66:984–986.
163. Kirby C, Gregoriadis G. 1983. The effect of lipid composition of small unilamellar liposomes containing melphalan and vincristine on drug clear-

- ance after injection into mice. *Biochem Pharmacol* 32:609–615.
164. Semple SC, Leone R, Wang J, Leng EC, Klimuk SK, Eisenhardt ML, Yuan ZN, Edwards K, Maurer N, Hope MJ, Cullis PR, Ahkong QF. 2005. Optimization and characterization of a sphingomyelin/cholesterol liposome formulation of vincorelbine with promising antitumor activity. *J Pharm Sci* 94:1024–1038.
  165. Fenske DB, Wong KF, Maurer E, Maurer N, Leenhouts JM, Boman N, Amankwa L, Cullis PR. 1998. Ionophore-mediated uptake of ciprofloxacin and vincristine into large unilamellar vesicles exhibiting transmembrane ion gradients. *Biochim Biophys Acta* 1414:188–204.
  166. Thomas DA, Sarris AH, Cortes J, Faderl S, O'Brien S, Giles FJ, Garcia-Manero G, Rodriguez MA, Cabanillas F, Kantarjian H. 2006. Phase II study of sphingosine vincristine in patients with recurrent or refractory adult acute lymphocytic leukemia. *Cancer* 106:120–127.
  167. Kuikka M, Ramstedt B, Ohvo-Rekila H, Tuuf J, Slotte JP. 2001. Membrane properties of D-erythro-N-acyl sphingomyelins and their corresponding dihydro species. *Biophys J* 80:2327–2337.
  168. Li LK, So L, Spector A. 1985. Membrane cholesterol and phospholipid in consecutive concentric sections of human lenses. *J Lipid Res* 26:600–609.
  169. Madden TD, Harrigan PR, Tai LCL, Bally MB, Mayer LD, Redelmeier TE, Loughrey HC, Tilcock CPS, Reinish LW, Cullis PR. 1990. The accumulation of drugs within large unilamellar vesicles exhibiting a proton gradient: A survey. *Chem Phys Lipids* 53:37–46.
  170. Adlakh-Hutcheon G, Bally MB, Shew CR, Madden TD. 1999. Controlled destabilization of a liposomal drug delivery system enhances mitoxantrone antitumor activity. *Nat Biotech* 17:775–779.
  171. Lobert S, Fahy J, Hill BT, Duflos A, Etievant C, Correia JJ. 2000. Vinca alkaloid-induced tubulin spiral formation correlates with cytotoxicity in the leukemic L1210 cell line. *Biochemistry* 39:12053–12062.
  172. Clere S, Barenholz Y. 1995. Loading of amphipathic weak acids into liposomes in response to transmembrane calcium acetate gradients. *Biochim Biophys Acta* 1240:257–265.
  173. Ceruti M, Crosasso P, Brusa P, Arpicco S, Dosio F, Cattel L. 2000. Preparation, characterization, cytotoxicity and pharmacokinetics of liposomes containing water-soluble prodrugs of paclitaxel. *J Control Release* 63:141–153.
  174. Liu JJ, Hong RL, Cheng WF, Hong K, Chang FH, Tseng YL. 2002. Simple and efficient liposomal encapsulation of topotecan by ammonium sulfate gradient: Stability, pharmacokinetic and therapeutic evaluation. *Anti-Cancer Drugs* 13:709–717.
  175. Webb MS, Boman NL, Wiseman DJ, Saxen D, Sutton K, Wong KF, Logan P, Hope MJ. 1998. Antibacterial efficacy against an in vivo *Salmonella typhimurium* infection model and pharmacokinetics of a liposomal ciprofloxacin formulation. *Antimicrob Agents Chemother* 42:45–52.
  176. Zhigaltsev IV, Maurer N, Edwards K, Karlsson G, Cullis PR. 2006. Formation of drug-arylsulfonate complexes inside liposomes: A novel approach to improve drug retention. *J Control Release* 110:378–386.
  177. Maurer N, Wong KF, Hope MJ, Cullis PR. 1998. Anomalous solubility behavior of the antibiotic ciprofloxacin encapsulated in liposomes: A <sup>1</sup>H-NMR study. *Biochim Biophys Acta* 1374:9–20.
  178. Campbell RB, Balasubramanian SV, Straubinger RM. 2001. Influence of cationic lipids on the stability and membrane properties of paclitaxel-containing liposomes. *J Pharm Sci* 90:1091–1105.
  179. Fetterly GJ, Straubinger RM. 2003. Pharmacokinetics of paclitaxel-containing liposomes in rats. *AAPS PharmSci* 5:E32.
  180. Gilbert BE, Seryshev A, Knight V, Brayton C. 2002. 9-nitrocamptothecin liposome aerosol: Lack of subacute toxicity in dogs. *Inhal Toxicol* 14:185–197.
  181. Verschraegen CF, Gilbert BE, Huaranga AJ, Newman R, Harris N, Leyva FJ, Keus L, Campbell K, Nelson-Taylor T, Knight V. 2000. Feasibility, phase I, and pharmacological study of aerosolized liposomal 9-nitro-20(S)-camptothecin in patients with advanced malignancies in the lungs. *Ann NY Acad Sci* 922:352–354.
  182. Verschraegen CF, Gilbert BE, Loyer E, Huaranga A, Walsh G, Newman RA, Knight V. 2004. Clinical evaluation of the delivery and safety of aerosolized liposomal 9-nitro-20(s)-camptothecin in patients with advanced pulmonary malignancies. *Clin Cancer Res* 10:2319–2326.
  183. Zhang LJ, Xing B, Wu J, Xu B, Fang XL. 2008. Biodistribution in mice and severity of damage in rat lungs following pulmonary delivery of 9-nitrocamptothecin liposomes. *Pulm Pharmacol Ther* 21:239–246.
  184. Sadzuka Y, Takabe H, Sonobe T. 2005. Liposomalization of SN-38 as active metabolite of CPT-11. *J Control Release* 108:453–459.
  185. Immordino ML, Brusa P, Arpicco S, Stella B, Dosio F, Cattel L. 2003. Preparation, characterization, cytotoxicity and pharmacokinetics of liposomes containing docetaxel. *J Control Release* 91:417–429.
  186. Mori A, Wu S-P, Han I, Khokhar AR, Perez-Soler R, Huang L. 1996. In vivo antitumor activity of cis-bis-neodecanoato-trans-R,R-1,2-diaminocyclohexane platinum(II) formulated in long-circulating liposomes. *Cancer Chemother Pharmacol* 37:435–444.



187. Perez-Soler R, Shin DM, Siddik ZH, Murphy WK, Huber M, Lee SJ, Khokhar AR, Hong WK. 1997. Phase I clinical and pharmacological study of liposome-entrapped NDDP administered intrapleurally in patients with malignant pleural effusions. *Clin Cancer Res* 3:373-379.
188. Dragovich T, Mendelson D, Kurtin S, Richardson K, Von Hoff D, Hoos A. 2006. A Phase 2 trial of the liposomal DACH platinum L-NDDP in patients with therapy-refractory advanced colorectal cancer. *Cancer Chemother Pharmacol* 58:759-764.
189. Bom D, Curran DP, Zhang J, Zimmer SG, Bevins R, Kruszewski S, Howe JN, Bingcang A, Latus LJ, Burke TG. 2001. The highly lipophilic DNA topoisomerase I inhibitor DB-67 displays elevated lactone levels in human blood and potent anticancer activity. *J Control Release* 74:325-333.
190. Gelderblom H, Verweij J, Nooter K, Sparreboom A. 2001. Cremophor EL: The drawbacks and advantages of vehicle selection for drug formulation. *Eur J Cancer* 37:1590-1598.
191. Szebeni J, Muggia FM, Alving CR. 1998. Complement activation by Cremophor EL as a possible contributor to hypersensitivity to paclitaxel: An in vitro study. *J Natl Cancer Inst* 90:300-306.
192. Fahr A, van Hoogevest P, Kuntsche J, Leigh ML. 2006. Lipophilic drug transfer between liposomal and biological membranes: What does it mean for parenteral and oral drug delivery? *J Liposome Res* 16:281-301.
193. Fahr A, van Hoogevest P, May S, Bergstrand N, S Leigh ML. 2005. Transfer of lipophilic drugs between liposomal membranes and biological interfaces: Consequences for drug delivery. *Eur J Pharm Sci* 26:251-265.
194. Strieth S, Eichhorn ME, Sauer B, Schulze B, Teifel M, Michaelis U, Dellian M. 2004. Neovascular targeting chemotherapy: Encapsulation of paclitaxel in cationic liposomes impairs functional tumor microvasculature. *Int J Cancer* 110:117-124.
195. Stuart DD, Allen TM. 2000. A new liposomal formulation for antisense oligodeoxynucleotides with small size, high incorporation efficiency and good stability. *Biochim Biophys Acta* 1463:219-229.
196. Assaraf YG. 2006. The role of multidrug resistance efflux transporters in antifolate resistance and folate homeostasis. *Drug Resist Updat* 9:227-246.
197. Borst P, Evers R, Koel M, Wijnholds J. 2000. A family of drug transporters: The multidrug resistance-associated proteins. *J Natl Cancer Inst* 92:1295-1302.
198. Matherly LH, Hou Z, Deng Y. 2007. Human reduced folate carrier: Translation of basic biology to cancer etiology and therapy. *Cancer Metastasis Rev* 26:111-128.
199. Zhang J, Visser F, King KM, Baldwin SA, Young JD, Cass CE. 2007. The role of nucleoside transporters in cancer chemotherapy with nucleoside drugs. *Cancer Metastasis Rev* 26:85-110.
200. Abraham SA, McKenzie C, Masin D, Ng R, Harasym TO, Mayer LD, Bally MB. 2004. In vitro and in vivo characterization of doxorubicin and vincristine coencapsulated within liposomes through use of transition metal ion complexation and pH gradient loading. *Clin Cancer Res* 10:728-738.
201. Mayer LD, Harasym TO, Tardi PG, Harasym NL, Shew CR, Johnstone SA, Ramsay EC, Bally MB, Janoff AS. 2006. Ratiometric dosing of anticancer drug combinations: Controlling drug ratios after systemic administration regulates therapeutic activity in tumor-bearing mice. *Mol Cancer Ther* 5:1854-1863.
202. Ramsay EC, Dos Santos N, Dragowska WH, Laskin JJ, Bally MB. 2005. The formulation of lipid-based nanotechnologies for the delivery of fixed dose anticancer drug combinations. *Curr Drug Deliv* 2:341-351.
203. Waterhouse DN, Tardi PG, Mayer LD, Bally MB. 2001. A comparison of liposomal formulations of doxorubicin with drug administered in free form: Changing toxicity profiles. *Drug Saf* 24:903-920.
204. Jones RL, Swanton C, Ewer MS. 2006. Anthracycline cardiotoxicity. *Expert Opin Drug Saf* 5:791-809.
205. Minotti G, Menna P, Salvatorelli E, Cairo G, Gianni L. 2004. Anthracyclines: Molecular advances and pharmacologic developments in antitumor activity and cardiotoxicity. *Pharmacol Rev* 56:185-229.
206. Andreopoulou E, Gaiotti D, Kim E, Downey A, Mirchandani D, Hamilton A, Jacobs A, Curtin J, Muggia F. 2007. Pegylated liposomal doxorubicin HCL (PLD; Caelyx/Doxil): Experience with long-term maintenance in responding patients with recurrent epithelial ovarian cancer. *Ann Oncol* 18:716-721.
207. Ewer MS, Martin FJ, Henderson C, Shapiro CL, Benjamin RS, Gabizon AA. 2004. Cardiac safety of liposomal anthracyclines. *Semin Oncol* 31:161-181.
208. Chia S, Clemons M, Martin LA, Rodgers A, Gelmon K, Pond GR, Panasci L. 2006. Pegylated liposomal doxorubicin and trastuzumab in HER-2 overexpressing metastatic breast cancer: A multicenter phase II trial. *J Clin Oncol* 24:2773-2778.
209. Slamon DJ, Leyland-Jones B, Shak S, Fuchs H, Paton V, Bajamonde A, Fleming T, Eiermann W, Wolter J, Pegram M, Baselga J, Norton L. 2001. Use of chemotherapy plus a monoclonal antibody against HER2 for metastatic breast cancer that overexpresses H ER2. *N Engl J Med* 344:783-792.
210. Working PK, Newman MS, Huang SK, Mayhew E, Vaage J, Lasic DD. 1994. Pharmacokinetics, bio-distribution, and therapeutic efficacy of doxorubi-



- cin encapsulated in Stealth® liposomes (Doxil®). *J Liposome Res* 4:667–687.
211. Bally MB, Nayar R, Masin D, Cullis PR, Mayer LD. 1990. Studies on the myelosuppressive activity of doxorubicin entrapped in liposomes. *Cancer Chemother Pharmacol* 27:13–19.
  212. Casper ES, Schwartz GK, Sugarman A, Leung D, Brennan MF. 1997. Phase I trial of dose-intense liposome-encapsulated doxorubicin in patients with advanced sarcoma. *J Clin Oncol* 15:2111–2117.
  213. Al-Batran SE, Meerpohl HG, von Minckwitz G, Atmaca A, Klesberg U, Harbeck N, Lerbs W, Hecker D, Sehouli J, Knuth A, Jager E. 2006. Reduced incidence of severe palmar-plantar erythrodysesthesia and mucositis in a prospective multicenter phase II trial with pegylated liposomal doxorubicin at 40 mg/m<sup>2</sup> every 4 weeks in previously treated patients with metastatic breast cancer. *Oncology* 70:141–146.
  214. Amantea M, Newman MS, Sullivan TM, Forrest A, Working PK. 1999. Relationship of dose intensity to the induction of palmar-plantar erythrodysesthesia by pegylated doxorubicin in dogs. *Hum Exp Toxicol* 18:17–26.
  215. Gabizon A, Goren D, Horowitz AT, Tzemach D, Lossos A, Siegal T. 1997. Long-circulating liposomes for drug delivery in cancer therapy: A review of biodistribution studies in tumor-bearing animals. *Adv Drug Deliv Rev* 24:337–344.
  216. Colbern GT, Dykes DJ, Engbers C, Musterer R, Hiller A, Pegg E, Saville R, Weng S, Luzzio M, Uster P, Amantea M, Working PK. 1998. Encapsulation of the topoisomerase I inhibitor GL147211C in pegylated (STEALTH) liposomes: Pharmacokinetics and antitumor activity in HT29 colon tumor xenografts. *Clin Cancer Res* 4:3077–3082.
  217. Mayhew EG, Lasic D, Babbar S, Martin FJ. 1992. Pharmacokinetics and antitumor activity of epirubicin encapsulated in long-circulating liposomes incorporating a polyethylene glycol-derivatized phospholipid. *Int J Cancer* 51:302–309.
  218. Sakakibara T, Chen FA, Kida H, Kunieda K, Cuenca RE, Martin FJ, Bankert RB. 1996. Doxorubicin encapsulated in sterically stabilized liposomes is superior to free drug or drug-containing conventional liposomes at suppressing growth and metastases of human lung tumor xenografts. *Cancer Res* 56:3743–3746.
  219. Williams SS, Alosco TR, Mayhew E, Lasic DD, Martin FJ, Bankert RB. 1993. Arrest of human lung tumor xenograft growth in severe combined immunodeficient mice using doxorubicin encapsulated in sterically stabilized liposomes. *Cancer Res* 53:3964–3967.
  220. Mayer LD, Tai LCL, Ko DSC, Masin D, Ginsberg RS, Cullis PR, Bally MB. 1989. Influence of vesicle size, lipid composition, and drug-to-lipid ratio on the biological activity of liposomal doxorubicin in mice. *Cancer Res* 49:5922–5930.
  221. Parker SE, Ducharme S, Norman J, Wheeler CJ. 1997. Tissue distribution of the cytofectin component of a plasmid-DNA/cationic lipid complex following intravenous administration in mice. *Hum Gene Ther* 8:393–401.
  222. Parr MJ, Masin D, Cullis PR, Bally MB. 1997. Accumulation of liposomal lipid and encapsulated doxorubicin in murine lewis lung carcinoma: The lack of beneficial effects of coating liposomes with poly(ethylene glycol). *J Pharmacol Exp Therapeut* 280:1319–1327.
  223. Laginha KM, Verwoert S, Charrois GJ, Allen TM. 2005. Determination of doxorubicin levels in whole tumor and tumor nuclei in murine breast cancer tumors. *Clin Cancer Res* 11:6944–6949.
  224. Mori A, Kennel SJ, Waalkes MvB, Scherphof GL, Huang L. 1995. Characterization of organ-specific immunoliposomes for delivery of 3',5'-O-dipalmityl-5-fluoro-2'-deoxyuridine in a mouse lung-metastasis model. *Cancer Chemother Pharmacol* 35:447–456.
  225. Pattillo CB, Sari-Sarraf F, Nallamothu R, Moore BM, Wood GC, Kiani MF. 2005. Targeting of the antivascular drug combretastatin to irradiated tumors results in tumor growth delay. *Pharm Res* 22:1117–1120.
  226. Allen TM, Mumbengegwi DR, Charrois GJ. 2005. Anti-CD19-targeted liposomal doxorubicin improves the therapeutic efficacy in murine B-cell lymphoma and ameliorates the toxicity of liposomes with varying drug release rates. *Clin Cancer Res* 11:3567–3573.
  227. Newman MS, Colbern GT, Working PK, Engbers C, Amantea M. 1999. Comparative pharmacokinetics, tissue distribution, and therapeutic effectiveness of cisplatin encapsulated in long-circulating, pegylated liposomes (SPI-077) in tumor-bearing mice. *Cancer Chemother Pharmacol* 43:1–7.
  228. Zamboni WC, Gervais AC, Egorin MJ, Schellens JH, Zuhowski EG, Pluim D, Joseph E, Hamburger DR, Working PK, Colbern G, Tonda ME, Potter DM, Eiseman JL. 2004. Systemic and tumor disposition of platinum after administration of cisplatin or STEALTH liposomal-cisplatin formulations (SPI-077 and SPI-077 B103) in a preclinical tumor model of melanoma. *Cancer Chemother Pharmacol* 53:329–336.
  229. White SC, Lorigan P, Margison GP, Margison JM, Martin F, Thatcher N, Anderson H, Ranson M. 2006. Phase II study of SPI-77 (sterically stabilized liposomal cisplatin) in advanced non-small-cell lung cancer. *Br J Cancer* 95:822–828.
  230. Harashima H, Tsuchihashi M, Iida S, Doi H, Kiwada H. 1999. Pharmacokinetic/pharmacody-

- namic modeling of antitumor agents encapsulated into liposomes. *Adv Drug Deliv Rev* 40:39–61.
231. Andresen TL, Jensen SS, Jorgensen K. 2005. Advanced strategies in liposomal cancer therapy: Problems and prospects of active and tumor specific drug release. *Prog Lipid Res* 44:68–97.
  232. Meers P. 2001. Enzyme-activated targeting of liposomes. *Adv Drug Deliv Rev* 53:265–272.
  233. Drummond DC, Zignani M, Leroux J. 2000. Current status of pH-sensitive liposomes in drug delivery. *Prog Lipid Res* 39:409–460.
  234. Torchilin VP. 2006. Recent approaches to intracellular delivery of drugs and DNA and organelle targeting. *Annu Rev Biomed Eng* 8:343–375.
  235. Guo X, Szoka FC, Jr. 2003. Chemical approaches to triggerable lipid vesicles for drug and gene delivery. *Acc Chem Res* 36:335–341.
  236. Saito G, Swanson JA, Lee KD. 2003. Drug delivery strategy utilizing conjugation via reversible disulfide linkages: Role and site of cellular reducing activities. *Adv Drug Deliv Rev* 55:199–215.
  237. Kong G, Anyarambhatla G, Petros WP, Braun RD, Colvin OM, Needham D, Dewhirst MW. 2000. Efficacy of liposomes and hyperthermia in a human tumor xenograft model: Importance of triggered drug release. *Cancer Res* 60:6950–6957.
  238. Needham D, Dewhirst MW. 2001. The development and testing of a new temperature sensitive drug delivery system for the treatment of solid tumors. *Adv Drug Deliv Rev* 53:285–305.
  239. Gaber MH, Wu NZ, Hong K, Huang SK, Dewhirst MW, Papahadjopoulos D. 1996. Thermosensitive liposomes: Extravasation and release of contents in tumor microvascular networks. *Int J Radiat Oncol Biol Phys* 36:1177–1187.
  240. Shum P, Kim JM, Thompson DH. 2001. Phototriggering of liposomal drug delivery systems. *Adv Drug Deliv Rev* 53:273–284.
  241. Spratt T, Bondurant B, O'Brien DF. 2003. Rapid release of liposomal contents upon photoinitiated destabilization with UV exposure. *Biochim Biophys Acta* 1611:35–43.
  242. Schroeder A, Avnir Y, Weisman S, Najajreh Y, Gabizon A, Talmon Y, Kost J, Barenholz Y. 2007. Controlling liposomal drug release with low frequency ultrasound: Mechanism and feasibility. *Langmuir* 23:4019–4025.
  243. Derksen JTP, Morselt HWM, Scherphof GL. 1988. Uptake and processing of immunoglobulin-coated liposomes by subpopulations of rat liver macrophages. *Biochim Biophys Acta* 971:127–136.
  244. Dijkstra J, van Galen WJM, Hulstaert CE, Kalicharan D, Roerdink FH, Scherphof GL. 1984. Interaction of liposomes with Kupffer cells in vitro. *Exp Cell Res* 150:161–176.
  245. Storm G, Steerenberg PA, Emmen F, Waalkes MvB, Crommelin DJA. 1988. Release of doxorubicin from peritoneal macrophages exposed in vivo to doxorubicin-containing liposomes. *Biochim Biophys Acta* 965:136–145.
  246. Gabizon AA. 1995. Liposome circulation time and tumor targeting: Implications for cancer chemotherapy. *Adv Drug Deliv Rev* 16:285–294.
  247. Lasic DD. 1993. *Liposomes: From physics to applications*. editors. New York: Elsevier. p 580.
  248. Ponce AM, Viglianti BL, Yu D, Yarmolenko PS, Michelich CR, Woo J, Bally MB, Dewhirst MW. 2007. Magnetic resonance imaging of temperature-sensitive liposome release: Drug dose painting and antitumor effects. *J Natl Cancer Inst* 99:53–63.
  249. Viglianti BL, Abraham SA, Michelich CR, Yarmolenko PS, MacFall JR, Bally MB, Dewhirst MW. 2004. In vivo monitoring of tissue pharmacokinetics of liposome/drug using MRI: Illustration of targeted delivery. *Magn Reson Med* 51:1153–1162.
  250. Huang SK, Stauffer PR, Hong K, Guo JWH, Phillips TL, Huang A, Papahadjopoulos D. 1994. Liposomes and hyperthermia in mice: Increased tumor uptake and therapeutic efficacy of doxorubicin in sterically stabilized liposomes. *Cancer Res* 54:2186–2191.
  251. Shan S, Flowers C, Peltz CD, Sweet H, Maurer N, Kwon EJ, Krol A, Yuan F, Dewhirst MW. 2006. Preferential extravasation and accumulation of liposomal vincristine in tumor comparing to normal tissue enhances antitumor activity. *Cancer Chemother Pharmacol* 58:245–255.
  252. van Bree C, Krooshoop JJ, Rietbroek RC, Kipp JB, Bakker PJ. 1996. Hyperthermia enhances tumor uptake and antitumor efficacy of thermostable liposomal daunorubicin in a rat solid tumor. *Cancer Res* 56:563–568.
  253. Davies Cde L, Lundström LM, Frengen J, Eikenes L, Bruland SØS, Kaalhus O, Hjelstuen MH, Brekken C. 2004. Radiation improves the distribution and uptake of liposomal doxorubicin (caelyx) in human osteosarcoma xenografts. *Cancer Res* 64:547–553.
  254. Sonveaux P, Dessy C, Brouet A, Jordan BF, Gregoire V, Gallez B, Balligand JL, Feron O. 2002. Modulation of the tumor vasculature functionality by ionizing radiation accounts for tumor radiosensitization and promotes gene delivery. *FASEB J* 16:1979–1981.
  255. Cheong I, Huang X, Bettgowda C, Diaz LA, Jr, Kinzler KW, Zhou S, Vogelstein B. 2006. A bacterial protein enhances the release and efficacy of liposomal cancer drugs. *Science* 314:1308–1311.
  256. Longman SA, Cullis PR, Choi L, de Jong G, Bally MB. 1995. A two-step targeting approach for delivery of doxorubicin-loaded liposomes to tumor cells in vivo. *Cancer Chemother Pharmacol* 36:91–101.

257. Pastorino F, Brignole C, Marimpietri D, Cilli M, Gambini C, Ribatti D, Longhi R, Allen TM, Corti A, Ponzoni M. 2003. Vascular damage and anti-angiogenic effects of tumor vessel-targeted liposomal chemotherapy. *Cancer Res* 63:7400–7409.
258. Emanuel N, Kedar E, Bolotin EM, Smorodinsky N I, Barenholz Y. 1996. Targeted delivery of doxorubicin via sterically stabilized immunoliposomes: Pharmacokinetics and biodistribution in tumor-bearing mice. *Pharm Res* 13:861–868.
259. Legendre J-Y, Szoka FC, Jr. 1993. Cyclic amphipathic peptide-DNA complexes mediate high-efficiency transfection of adherent mammalian cells. *Proc Natl Acad Sci USA* 90:893–897.
260. Parente RA, Nir S, Szoka FC, Jr. 1988. pH-dependent fusion of phosphatidylcholine small vesicles: Induction by a synthetic amphipathic peptide. *J Biol Chem* 263:4724–4730.
261. Lopes de Menezes DE, Pilarski LM, Allen TM. 1998. In vitro and in vivo targeting of immunoliposomal doxorubicin to human B-cell lymphoma. *Cancer Res* 58:3320–3330.
262. Sapra P, Allen TM. 2002. Internalizing antibodies are necessary for improved therapeutic efficacy of antibody-targeted liposomal drugs. *Cancer Res* 62:7190–7194.
263. Sugano M, Egilmez NK, Yokota SJ, Chen FA, Harding J, Huang SK, Bankert RB. 2000. Antibody targeting of doxorubicin-loaded liposomes suppresses the growth and metastatic spread of established human lung tumor xenografts in severe combined immunodeficient mice. *Cancer Res* 60:6942–6949.
264. Zhou Y, Drummond DC, Zou H, Hayes ME, Adams GP, Kirpotin DB, Marks JD. 2007. Impact of single-chain Fv antibody fragment affinity on nanoparticle targeting of epidermal growth factor receptor-expressing tumor cells. *J Mol Biol* 371:934–947.
265. Nielsen UB, Kirpotin DB, Pickering EM, Hong K, Park JW, Refaat Shalaby M, Shao Y, Benz CC, Marks JD. 2002. Therapeutic efficacy of anti-ErbB2 immunoliposomes targeted by a phage antibody selected for cellular endocytosis. *Biochim Biophys Acta* 1591:109–118.
266. Kono K. 2001. Thermosensitive polymer-modified liposomes. *Adv Drug Deliv Rev* 53:307–319.
267. Yatvin MB, Kruetz W, Horwitz BA, Shinitzky M. 1980. pH-Sensitive liposomes: Possible clinical implications. *Science* 210:1253–1255.
268. Martin GR, Jain RK. 1994. Noninvasive measurement of interstitial pH profiles in normal and neoplastic tissue using fluorescence ratio imaging microscopy. *Cancer Res* 54:5670–5674.
269. Slepishkin VA, Simoes S, Dazin P, Newman MS, Guo LS, Pedroso de Lima MC, Duzgunes N. 1997. Sterically stabilized pH-sensitive liposomes. Intracellular delivery of aqueous contents and prolonged circulation in vivo. *J Biol Chem* 272:2382–2388.
270. Yessine MA, Leroux JC. 2004. Membrane-destabilizing polyanions: Interaction with lipid bilayers and endosomal escape of biomacromolecules. *Adv Drug Deliv Rev* 56:999–1021.
271. Li W, Huang Z, MacKay JA, Grube S, Szoka FC, Jr. 2005. Low-pH-sensitive poly(ethylene glycol) (PEG)-stabilized plasmid nanolipoparticles: Effects of PEG chain length, lipid composition and assembly conditions on gene delivery. *J Gene Med* 7:67–79.
272. Shin J, Shum P, Thompson DH. 2003. Acid-triggered release via dePEGylation of DOPE liposomes containing acid-labile vinyl ether PEG-lipids. *J Control Release* 91:187–200.
273. van den Bossche J, Shin J, Shum P, Thompson DH. 2006. Design, synthesis and application of vinyl ether compounds for gene and drug delivery. *J Control Release* 116:e:1–3.
274. Kirpotin D, Hong K, Mullah N, Papahadjopoulos D, Zalipsky S. 1996. Liposomes with detachable polymer coating: Destabilization and fusion of dioleoylphosphatidylethanolamine vesicles triggered by cleavage of surface-grafted poly(ethylene glycol). *FEBS Lett* 388:115–118.
275. Yang J, Chen H, Vlahov IR, Cheng JX, Low PS. 2006. Evaluation of disulfide reduction during receptor-mediated endocytosis by using FRET imaging. *Proc Natl Acad Sci USA* 103:13672–13677.
276. Wetzer B, Byk G, Frederic M, Airiau M, Blanche F, Pitard B, Scherman D. 2001. Reducible cationic lipids for gene transfer. *Biochem J* 356:747–756.
277. Huang Z, Li W, Mackay JA, Szoka FC, Jr. 2005. Thiocholesterol-based lipids for ordered assembly of bioresponsive gene carriers. *Mol Ther* 11:409–417.
278. Gerasimov OV, Boomer JA, Qualls MM, Thompson DH. 1999. Cytosolic drug delivery using pH- and light-sensitive liposomes. *Adv Drug Deliv Rev* 38:317–338.
279. Fraley R, Subramani S, Berg P, Papahadjopoulos D. 1980. Introduction of liposome-encapsulated SV40 DNA into cells. *J Biol Chem* 255:10431–10435.
280. Wilson T, Papahadjopoulos D, Taber R. 1979. The introduction of poliovirus RNA into cells via lipid vesicles (liposomes). *Cell* 17:77–84.
281. Felgner PL, Gadek TR, Holm M, Roman R, Chan HW, Wenz M, Northrop JP, Ringold GM, Danielson M. 1987. Lipofectin: A highly efficient, lipid-mediated DNA-transfection procedure. *Proc Natl Acad Sci USA* 84:7413–7417.
282. Sternberg B, Hong K, Zheng W, Papahadjopoulos D. 1998. Ultrastructural characterization of cationic liposome-DNA complexes showing enhanced

- stability in serum and high transfection activity in vivo. *Biochim Biophys Acta* 1375:23–35.
283. Liu Y, Mounkes LC, Liggitt HD, Brown CS, Solodin I, Heath TD, Debs RJ. 1997. Factors influencing the efficiency of cationic liposome-mediated intravenous gene delivery. *Nat Biotech* 15:167–173.
  284. Monck MA, Mori A, Lee D, Tam P, Wheeler JJ, Cullis PR. 2000. Stabilized plasmid-lipid particles: Pharmacokinetics and plasmid delivery to distal tumors following intravenous injection. *J Drug Tar* 7:439–452.
  285. Zhang J-S, Liu F, Huang L. 2005. Implications of pharmacokinetic behavior of lipoplex for its inflammatory toxicity. *Adv Drug Deliv Rev* 57: 689–698.
  286. Plank C, Mechetner E, Szoka FC, Jr, Wagner E. 1996. Activation of the complement system by synthetic DNA complexes: A potential barrier for intravenous gene delivery. *Hum Gene Ther* 7:1437–1446.
  287. Dow SW, Fradkin LG, Liggitt DH, Willson AP, Heath TD, Potter TA. 1999. Lipid-DNA complexes induce potent activation of innate immune responses and antitumor activity when administered intravenously. *J Immunol* 163:1552–1561.
  288. Mui B, Raney SG, Semple SC, Hope MJ. 2001. Immune stimulation by a CpG-containing oligodeoxynucleotide is enhanced when encapsulated and delivered in lipid particles. *J Pharmacol Exp Ther* 298:1185–1192.
  289. Brignole C, Pastorino F, Marimpietri D, Pagnan G, Pistorio A, Allen TM, Pistoia V, Ponzoni M. 2004. Immune cell-mediated antitumor activities of GD2-targeted liposomal c-myc antisense oligonucleotides containing CpG motifs. *J Natl Cancer Inst* 96:1171–1180.
  290. Zimmermann TS, Lee AC, Akinc A, Bramlage B, Bumcrot D, Fedoruk MN, Harborth J, Heyes JA, Jeffs LB, John M, Judge AD, Lam K, McClintock K, Nechev LV, Palmer LR, Racie T, Rohl I, Seiffert S, Shaumugam S, Sood V, Soutschek J, Toudjarska I, Wheat AJ, Yaworski E, Zedalis W, Koteliansky V, Manoharan M, Vornlocher HF, MacLachlan I. 2006. RNAi-mediated gene silencing in non-human primates. *Nature* 4:111–114.
  291. Morrissey DV, Lockridge JA, Shaw L, Blanchard K, Jensen K, Breen W, Hartsough K, Machemer L, Radka S, Jadhav V, Vaish N, Zinnen S, Vargeese C, Bowman K, Shaffer CS, Jeffs LB, Judge A, MacLachlan I, Polisky B. 2005. Potent and persistent in vivo anti-HBV activity of chemically modified siRNAs. *Nat Biotechnol* 23:1002–1007.
  292. Pastorino F, Brignole C, Marimpietri D, Pagnan G, Morando A, Ribatti D, Semple SC, Gambini C, Allen TM, Ponzoni M. 2003. Targeted liposomal c-myc antisense oligonucleotides induce apoptosis and inhibit tumor growth and metastases in human melanoma models. *Clin Cancer Res* 9: 4595–4605.
  293. Xu L, Huang CC, Huang W, Tang WH, Rait A, Yin YZ, Cruz I, Xiang LM, Pirolo KF, Chang EH. 2002. Systemic tumor-targeted gene delivery by anti-transferrin receptor scFv-immunoliposomes. *Mol Cancer Therapeut* 1:337–346.
  294. Ruponen M, Ronkko S, Honkakoski P, Pelkonen J, Tammi M, Urtti A. 2001. Extracellular glycosaminoglycans modify cellular trafficking of lipoplexes and polyplexes. *J Biol Chem* 276:33875–33880.
  295. Martin B, Sainlos M, Aissaoui A, Oudrhiri N, Hauchecorne M, Vigneron JP, Lehn JM, Lehn P. 2005. The design of cationic lipids for gene delivery. *Curr Pharm Des* 11:375–394.
  296. Lasic DD, Frederick PM, Stuart MCA, Barenholz Y, McIntosh TJ. 1992. Gelation of liposome interior: A novel method for drug encapsulation. *FEBS Lett* 312:255–258.
  297. Drummond DC, Daleke DL. 1995. Synthesis and characterization of N-acylated, pH-sensitive 'caged' aminophospholipids. *Chem Phys Lipids* 75:27–41.
  298. Choi JS, MacKay JA, Szoka FC, Jr. 2003. Low-pH-sensitive PEG-stabilized plasmid-lipid nanoparticles: Preparation and characterization. *Bioconjug Chem* 14:420–429.
  299. Budker V, Gurevich V, Hagstrom JE, Bortzov F, Wolff JA. 1996. pH-sensitive, cationic liposomes: A new synthetic virus-like vector. *Nat Biotechnol* 14: 760–764.
  300. Chu C-J, Dijkstra J, Lai M-Z, Hong K, Szoka FC. 1990. Efficiency of cytoplasmic delivery by pH sensitive liposomes to cells in culture. *Pharm Res* 7:824–834.
  301. Collins D, Litzinger DC, Huang L. 1990. Structural and functional comparisons of pH-sensitive liposomes composed of phosphatidylethanolamine and three different diacylsuccinylglycerols. *Biochim Biophys Acta* 1025:234–242.
  302. Zignani M, Drummond DC, Meyer O, Hong K, Leroux JC. 2000. In vitro characterization of a novel polymeric-based pH-sensitive liposome system. *Biochim Biophys Acta* 1463:383–394.
  303. Chen T, McIntosh D, He Y, Kim J, Tirrell DA, Scherrer P, Fenske DB, Sandhu AP, Cullis PR. 2004. Alkylated derivatives of poly(ethylacrylic acid) can be inserted into preformed liposomes and trigger pH-dependent intracellular delivery of liposomal contents. *Mol Membr Biol* 21:385–393.
  304. Kono K, Torikoshi Y, Mitsutomi M, Itoh T, Emi N, Yanagie H, Takagishi T. 2001. Novel gene delivery systems: Complexes of fusigenic polymer-modified liposomes and lipoplexes. *Gene Ther* 8: 5–12.

305. Bisby RH, Mead C, Morgan CG. 2000. Active uptake of drugs into photosensitive liposomes and rapid release on UV photolysis. *Photochem Photobiol* 72:57-61.
306. Davis SC, Szoka FC. 1998. Cholesterol phosphate derivatives: Synthesis and incorporation into a phosphatase and calcium-sensitive triggered release liposome. *Bioconjug Chem* 9:783-792.
307. Pak CC, Erukulla RK, Ahi PL, Janoff AS, Meers P. 1999. Elastase activated liposomal delivery to nucleated cells. *Biochim Biophys Acta* 1419:111-126.

---

## Intraliposomal Trapping Agents for Improving In Vivo Liposomal Drug Formulation Stability

Daryl C. Drummond<sup>1</sup>, Mark E. Hayes, Charles O. Noble IV, and Dmitri B. Kirpotin

*Hermes Biosciences, Inc., South San Francisco, California, U.S.A.*

**John W. Park**

*University of California at San Francisco Comprehensive Cancer Center, San Francisco, California, U.S.A.*

**Zexiong Guo**

*First Affiliated Hospital of Jinan University, Guangzhou, P.R. China*

### INTRODUCTION

Controlling the rate of drug release from liposomal carriers is essential for optimum drug delivery (1,2). Liposome formulations that are too unstable release their drug while still in the general circulation, thus reducing the benefits of site-specific drug delivery resulting from the enhanced permeability

---

<sup>1</sup>Daryl C. Drummond is supported in part by a New Investigator Award from the California Breast Cancer Research Program of the University of California, Grant Number 7KB-0066.

and retention effect and allowing for many of the systemic toxicities associated with the unencapsulated agent. Formulations that are too stable risk not making the drugs bioavailable, and thus able to act on their molecular targets. Furthermore, delivery strategies that rely on molecular targeting of solid tumors, including immunoliposomes, require that the liposomal drug formulation arrive at the cancer cell intact to take full advantage of the benefits of targeting (3,4).

A wide range of drug-entrapment strategies based on various ion gradients have been hailed for their ability to quantitatively load certain weakly basic or weakly acidic drugs into the liposomal lumen (5–12). Of equal importance is the ability of these remote-loading strategies to stabilize the drug, so that upon administration the drug is retained inside the liposome until reaching its site of action. Although several drugs in the anthracycline class of anticancer agents have been stabilized with relative ease, this stability has been replicated less successfully when alternative classes of drugs have been entrapped. For example, vincristine (VCR) (13–16) and various camptothecin (17–19) liposome formulations are substantially more unstable than doxorubicin formulations (14) prepared using similar lipid compositions and drug-loading methodologies.

This chapter discusses the use of intraliposomal trapping agents to maximize the retention of weakly basic amphipathic drugs while in the circulation. We have employed gradients of substituted ammonium salts of poly(anionic) polymers and polyols to encapsulate and retain drugs more stably inside liposomes. To date, we have used these strategies to encapsulate and stabilize a number of both standard and novel anticancer chemotherapeutic agents inside liposomes (Fig. 1). The polyanionic trapping agents form stable intraliposomal complexes with the weakly basic drug, possibly forming precipitates or gels inside the liposome. A diagram depicting the stabilization process is shown in Figure 2A. Here, the novel histone deacetylase inhibitor, LAQ824 (Novartis Pharmaceuticals; East Hanover, New Jersey, U.S.A.), is shown in a complex with a sulfated polyol, sucrose octasulfate. The disruption of the complex and the subsequent transmembrane diffusion of the drug govern the apparent *in vivo* stability of the liposomal formulation. Chemical structures for some of the anionic trapping agents employed for liposomal drug stabilization are shown in Figure 2B. The large majority of formulations that have employed remote-loading strategies have used either citrate or sulfate as the counterion for protons,  $Mn^{2+}$ , or ammonium (6,8,16,19,20). Our experience has been that liposomal drug formulations prepared using these anions as trapping agents often result in poor *in vivo* stability for a number of well-established and novel anticancer agents. This chapter describes our efforts to improve the *in vivo* stability of these liposomal drugs using polyanionic trapping agents, including polyphosphate, sucrose octasulfate, and inositol hexaphosphate.

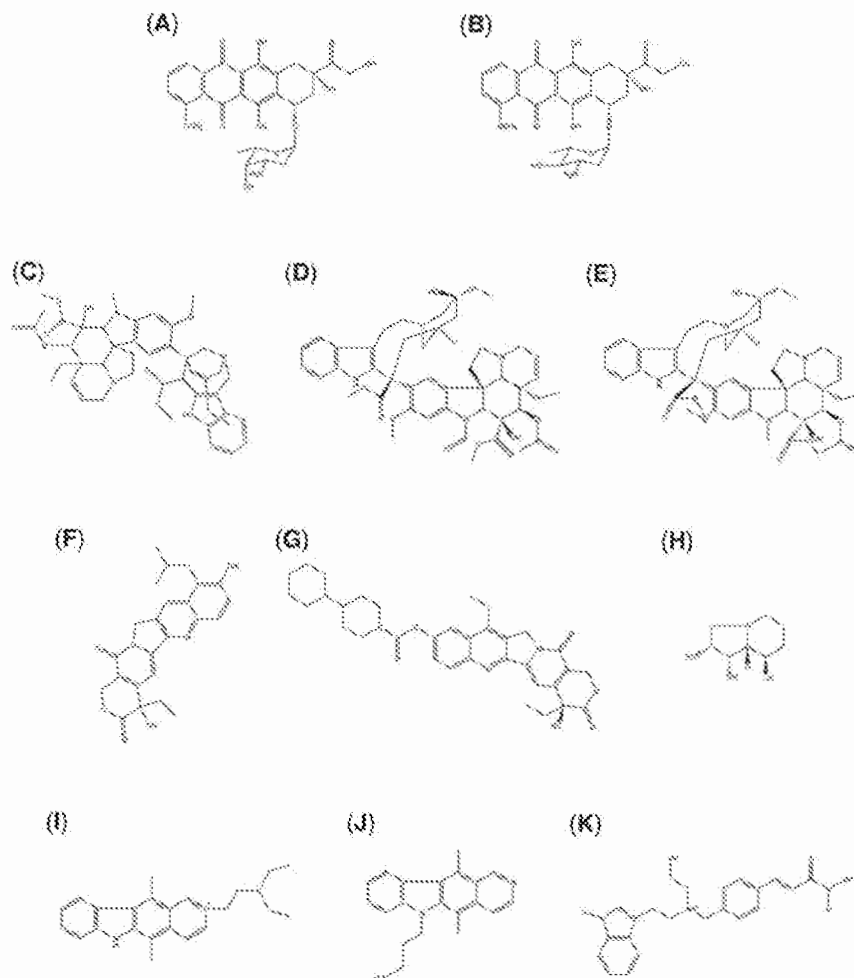


**Figure 1** Chemical structures of some amphipathic weak bases that have been loaded and stabilized in liposomes using trialkylammonium salts of polyanionic trapping agents in our lab. (A) Doxorubicin, (B) epirubicin, (C) vinorelbine, (D) vincristine, (E) vinblastine, (F) topotecan, (G) irinotecan, (H) swainsonine, (I) 2-diethylaminoethyl-ellipticinium, (J) 6-(3-aminopropyl)ellipticine, and (K) LAQ824.

## METHODS

### Preparation of Trapping Solutions and Liposomes

Many of the salts employed in the preparation of remote-loading gradients are commercially available and thus involve nothing more than dissolving



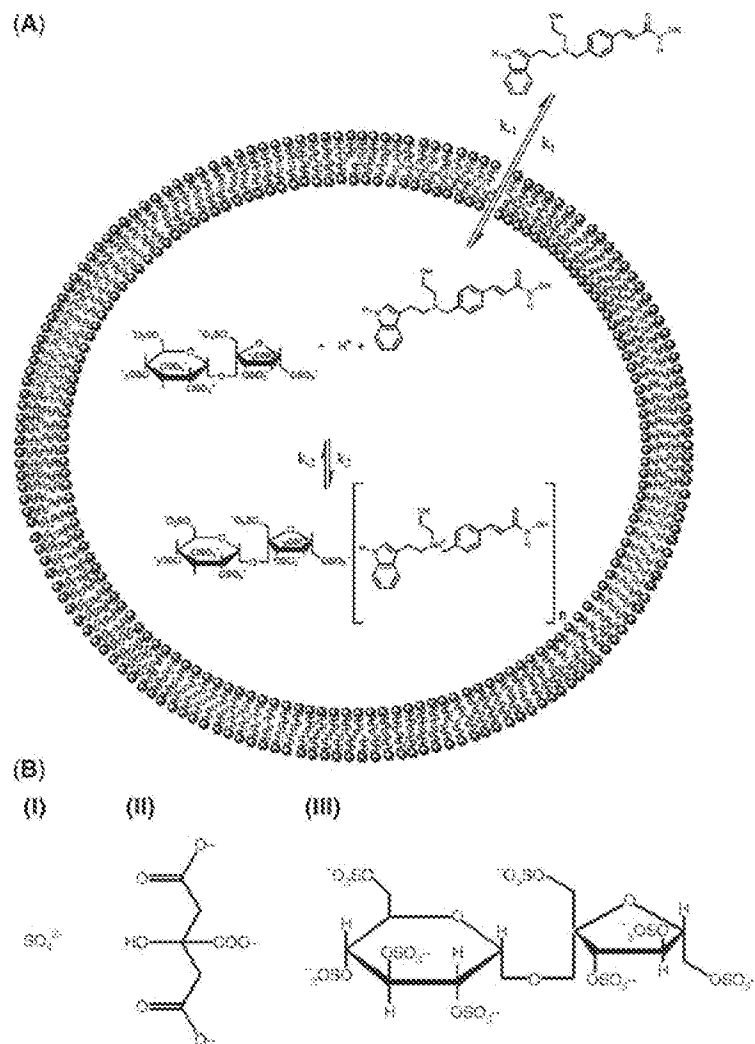


**Figure 2** (Continued on facing page) Intraliposomal drug stabilization using polyanionic trapping agents. (A) Depiction of intraliposomal stabilization of LAQ824 using the polyanionic polyol, sucrose octasulfate. Upon sequestration in the liposomal lumen, the drug forms a stable complex with sucrose octasulfate, possibly forming a gel or precipitate. The rates of dissolution of the precipitate, disruption of the complex, and transmembrane diffusion of the drug all contribute to the in vivo stability of the liposomal drug formulation. (B) Chemical structures of poly(anionic) trapping agents: (I) sulfate, (II) citrate, (III) sucrose octasulfate, (IV) poly(phosphate), (V) suramin, and (VI) dextran sulfate.

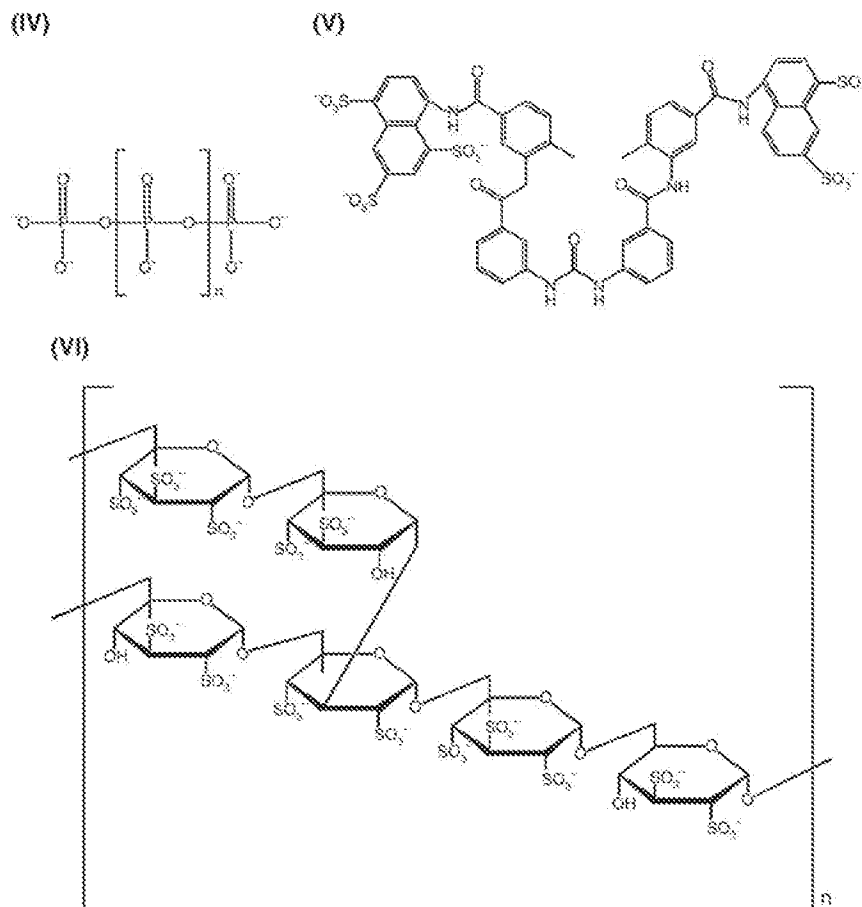


Figure 2 (Continued from previous page)

the salt in water to the desired concentration and, in some instances, adjusting the pH into a range acceptable for the chemical and physical stability of the liposome formulation (pH 4–8, but preferably 5–7). Manganese sulfate, ammonium sulfate, ammonium citrate, and citric acid are a few of the salts that are readily available, and perhaps noncoincidentally represent the large majority used in remote-loading strategies. Other polyanionic trapping agents require exchange of the counter ion for one more suitable for drug loading. We prefer the use of substituted ammonium salts, including triethylamine, diethylamine, 2-diethylaminoethanol, and 4-(2-hydroxyethyl)-morpholine for this purpose. However, we should emphasize that it is also possible to load weakly basic amphipathic drugs into liposomes using other cationic species, including

Downloaded by [Reprints Desk] at 12:30 09 October 2017

ammonium and even sodium (21). Other pharmaceutically acceptable substituted ammonium salts are described in *Handbook of Pharmaceutical Salts* (22).

If the trapping agent is available in the acid form, then simple titration with the chosen amine gives rise to the desired salt. However, many polyanionic compounds are not stable in this form and only available as salts with other cations;  $\text{Na}^+$ ,  $\text{K}^+$ ,  $\text{Ca}^{2+}$ , or  $\text{Mg}^{2+}$ . Ion-exchange chromatography can be used to prepare the most suitable salt. Typically, an appropriate cation-exchange resin (e.g., Dowex 50Wx8-200, Dow Chemical Co.) is washed with 1N solutions of NaOH and HCl, and subsequently equilibrated with higher concentrations of HCl to maintain the resin in the hydrogen form. A concentrated solution of the polyanionic compound is then added to the column and eluted with water, using a conductivity meter to detect elution of the acidic form of the polyanion. The polyanion is then immediately titrated with the substituted amine of choice to give the desired salt. An electrode specific for the initial cationic species (e.g.,  $\text{Na}^+$  electrode) can be used to measure the efficiency of exchange. The salt is then diluted to a concentration, preferably chosen to maximize the drug load, while preventing unusually high osmotic imbalances that might result in the liposomes bursting during drug loading or in the presence of plasma (23,24).

Liposomes can be prepared using a wide range of methods that have been thoroughly reviewed in a previous edition of this series (Vol I, 2nd ed.) and elsewhere (25); therefore, it will not be described in great detail here. Our preference for liposome formation involves dissolving the lipids in ethanol at an elevated temperature followed by rapid mixing with an aqueous solution of the trapping agent (typically corresponding to 0.5–0.75 M substituted ammonium salt) equilibrated at the same temperature, followed by sizing of the liposomes using high-pressure extrusion (Vol I, Chapter 4 of this series). The liposomes are typically characterized with regard to particle size to ensure the liposome size is acceptable for the desired application before proceeding with the generation of the gradient.

### Gradient Generation and Drug Loading

The gradient for the polyanionic trapping agent is generated by removal of the extraliposomal salt using gel filtration chromatography, dialysis, ion-exchange chromatography, or a combination of these approaches. Typically, gel filtration chromatography is utilized for bench-scale preparations, whereas dialysis is preferred for large-scale production. Ion-exchange chromatography is particularly useful for removing trace amounts of polyanionic trapping agents that may precipitate drugs outside the liposomes prior to their loading. The external solution is then exchanged for one that contains both an isotonicity agent (sucrose, dextrose, saline) and an appropriate buffer. The concentration of the isotonicity agent used is selected to minimize the potential for osmotic shock resulting in liposome lysis during drug

loading at elevated temperatures. The specific agent employed is chosen to allow for drug solubilization. For example, although doxorubicin is soluble and can be loaded in saline solutions, many other drugs are salted out when saline is present, thus requiring the use of a nonionic isotonicity agent, such as sucrose or dextrose. The buffer is chosen to support the pH optimum for drug loading. A study of drug loading at different pHs can be used to determine this optimum. Although many drugs are loaded under a pH wide range, some drugs have multiple titratable groups or are affected by neighboring substituents such that only a narrow pH range can be used to obtain loading, while avoiding the extremes of pH that may result in chemical degradation of either the drug or liposomal lipid components.

Drug loading is initiated by adding the drug at the desired drug-to-lipid ratio and raising the temperature to above the phase transition of the phospholipid (PL) component. Some loading may proceed below the phase transition, but it is generally less efficient than that observed at higher temperatures. Upon addition of the drug, the pH of the extraliposomal solution may require further adjustment. Many drugs are available as acidic salts and, depending on the amount of drug added, their addition may adversely affect the pH of the solution, so that it falls out of the optimum required for loading. The samples are then incubated for a determined amount of time, in our hands typically 30 minutes at 60°C. Others have shown loading to be complete in as short as 10 to 15 minutes for phosphatidylcholine-containing formulations (12,26). Finally, the loading reaction is quenched rapidly by lowering the temperature rapidly below the phase transition. For research-scale preparations, this simply involves incubation on ice for 15 to 20 minutes.

### Assessing Drug Entrapment and Retention

#### Assessing Drug Entrapment

To assess drug entrapment or drug retention, the drug-to-lipid ratio is determined and compared to an initial ratio, either a preloading ratio in the case of drug-entrapment determinations or a preincubation ratio in the case of drug-retention assays. For research-scale liposome preparations, the drug-loaded liposomes are commonly purified to remove unencapsulated drug following drug loading. Purification can be accomplished by gel filtration chromatography, dialysis, or ion-exchange chromatography. For large-scale-manufactured liposomes, it is often not necessary or even desirable to purify the final product, as a result of the high efficiency of drug encapsulation observed with many agents prepared using remote-loading strategies. However, in such cases, quality control often involves taking a sample of the batch, purifying it, and determining the efficiency of encapsulation by comparing the drug-to-lipid ratio of the purified liposomes to those prior to drug-loading. The drug can be analyzed by a variety of methods,

depending on the chemical nature of the drug itself, including high-performance liquid chromatography, fluorimetry, or simply UV/Vis spectrophotometry. The lipid is commonly determined by phosphate analysis (27), but can also be determined using a radioactively labeled and nonexchangeable lipid marker, such as [<sup>3</sup>H]cholesterylhexadecylether. Two parameters are important in characterizing drug encapsulation in liposomes. The first is the drug load, expressed commonly as grams of drug/gram or mol of lipid, and the second is entrapment efficiency, expressed as the percentage of drug encapsulated as a function of the initial preload ratio [Eq. (1)]:

$$\text{Entrapment efficiency (\%)} = 100 \times \frac{[\text{drug/lipid}]_p}{[\text{drug/lipid}]_i} \quad (1)$$

where  $[\text{drug/lipid}]_p$  refers to the determined drug-to-lipid ratio following purification of the loaded liposomes and  $[\text{drug/lipid}]_i$  refers to the drug-to-lipid ratio of the initial preparation prior to loading or purification.

The drug load can provide some information about the amount of drug that can be loaded into each liposome. This amount may be limited by the size of the liposome, the chemical nature of the trapping agent, the physicochemical properties of the drug, or the magnitude of the gradient prepared. The second parameter gives an indication of how efficient the drug-encapsulation process was under a specific set of conditions (temperature, pH, input drug-to-lipid ratio, liposome size, and lipid composition).

#### Drug Retention

The characterization of drug retention is important for determining the stability of the liposomal drug formulation during storage and while in the general circulation. In order to effectively characterize any liposome drug-trapping method, it is important to determine the stability using conditions that mimic both situations. For stability during storage, the liposomal drug should be concentrated to a concentration suitable for injection and stored in the presence of the excipient (i.e., isotonicity and buffering agents) to be used during storage. Because the excipients may influence the gradients used to retain the drug in liposomes, it is important to mimic the conditions to be used in the final product as precisely as possible. Stability studies are best performed under the conditions employed during storage, typically 4°C to 6°C for most gradient-loaded liposomal drugs. Accelerated stability studies at elevated temperatures have also been performed, but with the important qualification that the elevated temperature may affect drug formulation stability in an indirect fashion by altering the physical state of the liposomal membrane. Although discrete phase transitions are often reported for lipid membranes, there are sometimes pretransitions, phase transitions that are obscured by the presence of cholesterol (chol), or transitions that are less well understood (28), which may indeed affect the membrane permeability of the

drug or ions used to create the gradients essential for their entrapment. Thus, without careful modeling, it may be difficult to predict what would in fact occur at the actual temperature used during storage. Drug retention during storage can be determined by removing an aliquot or a vial of liposomal drug at prescribed times and then measuring the drug and PL components following purification as described above. The amount of drug that remains entrapped is then compared to the amount of drug associated with the liposome at time = 0 to determine the drug retention.

Drug retention in the blood is a considerably more complicated undertaking. Multiple formulations prepared using different drug-trapping agents can be initially screened by simple incubation in the presence of human plasma to get a general idea of the effect of plasma proteins on formulation stability. Incubation in the presence of saline or other isotonic buffers does not provide a sufficient reservoir of drug-binding sites for the liposome-associated drugs and thus may result in a false sense of security with regard to the stability of the formulation. Unfortunately, it is often common practice to initially describe the stability of a liposomal drug by its degree of drug retention in one of these simple media. Our preference is to screen formulation methods initially using a microdialysis assay where small wells containing liposomes are separated from a significantly larger reservoir of human plasma by a filter with pore sizes of 30 nm. The large dilution factor provides a more stringent test of the liposome's stability than a simple 1:2 to 1:5 dilution with plasma. At prescribed times, an aliquot of the sample is then removed and purified by gel filtration chromatography. The lipid is then measured by either scintillation counting of [<sup>3</sup>H]CHE or phosphate analysis of PLs. The drug is determined by fluorimetry or HPLC and the drug-to-lipid ratio of the purified liposome is calculated and compared to the initial liposome preparation to determine the amount of drug leakage. A representative study is shown in Figure 3A for multiple liposome formulations of liposomal 4-(3-aminopropyl)ellipticine. Purification is not absolutely required if using [<sup>3</sup>H]CHE, but is necessary to remove phosphate-containing species in the plasma if a simple phosphate assay is used.

Although these assays allow for rapid screening of multiple formulation methods to remove rapidly leaking formulations from further consideration, they are not necessarily an accurate predictor of the liposomal drug's stability in vivo. The most rigorous test of liposomal drug retention is to measure the change in drug-to-lipid ratio in vivo using small rodent models (13,16). Small molecular weight free drugs are commonly cleared at a considerably faster rate than same drugs encapsulated in liposomes. Thus, a reduction in the drug-to-lipid ratio is an excellent indicator of the degree of drug leakage from the liposome in vivo. If further screening is required, then single or dual time point (e.g., 8 and 24 hours) studies in mice have allowed us to reduce further the liposomal drug formulations being considered. A complete pharmacokinetic study in rats, measuring both lipid ([<sup>3</sup>H]CHE) and drug, concentrations will give a complete data set, including information about

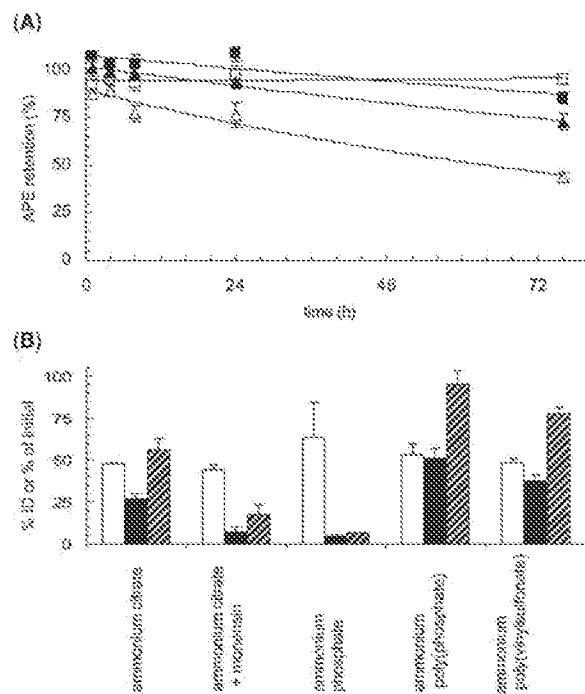


**Figure 3** In vitro (A) and in vivo (B) stability of APE encapsulation in liposomes prepared using a wide range of intraliposomal trapping agents. All formulations were composed of 1,2-distearoyl-3-*sn*-phosphatidylcholine: cholesterol: *N*-(polyethylene glycol)distearoylphosphatidylethanolamine (DSPC:Cho:PEG-DSPE) (3:2:0.015, mol:mol:mol). Cholesterylhexadecylether ( $[^3\text{H}]\text{CHE}$ ) was added at a ratio of 0.5  $\mu\text{Ci}/\mu\text{mol}$  PL for the in vivo study. All liposomes were loaded at a APE-to-PL ratio of 100 g/mol. All formulations had an identical triethylammonium or ammonium concentration of 0.55 M. (A) Liposomes were prepared using the following trapping agents; poly(phosphate) (■), linear triphosphate (□), trimetaphosphate (△), and sulfate (▲). Liposome samples were incubated with human plasma in a microdialysis assay at prescribed time points, purified by gel filtration chromatography, and analyzed for both drug (fluorimetry) and lipid (liposomal  $\text{PO}_4$ ). The APE-to-PL ratio was then calculated and compared to the initial ratio, prior to incubation, to determine the amount of APE retained in the liposomes. (B) Liposomal APE was prepared using ammonium salts of various polyanionic trapping agents and administered intravenous to Swiss-Webster mice. At 24 hours, the mice were sacrificed and the blood collected and analyzed for both APE and lipid ( $[^3\text{H}]\text{CHE}$ ) scintillation counting. The %ID in the blood at 24 hours for liposomal lipid and APE are depicted by the white and black bars, respectively. The corresponding APE-to-PL ratio (normalized to the ratio of the administered liposomes) is shown using the hatched bars. *Abbreviations:* %ID, percentage injected dose; APE, 6-(3-aminopropyl)jellipticine; PL, phospholipid.

the pharmacokinetics of the liposome carrier itself, its encapsulated drug, and the rate of drug leakage from the formulation.

## FACTORS INFLUENCING IN VIVO DRUG RETENTION

### Anion or Polyanion Used as Trapping Agent

Our experience and that of others is that the use of pH,  $Mn^{2+}$ , or ammonium gradients to load various anticancer drugs can result in quantitative loading of a wide range of drugs (6,8,9,12,13,19,26,29). However, with the exception of anthracycline class of drugs, many drugs from other classes leak rapidly from liposomes in the blood. Our experience has been that the anionic counterion plays an important role as a trapping agent, forming a stable complex with the drug inside the liposome and limiting its transmembrane diffusion once in the circulation. However, different counterions display varying levels of effectiveness in their ability to stabilize the drug. An example of this is shown in Figure 3. Initially an *in vitro* microdialysis assay was performed as described above, incubating liposome formulations loaded with 6-(3-aminopropyl)ellipticine (APE), but prepared using triethylammonium (TEA) salts of various anions, with human plasma at 37°C and then measuring the amount of drug retained over time (Figure 3A). As can be observed, sulfate was a relatively poor trapping agent for this particular drug, with greater than 25% of the drug having leaked by 24 hours and 50% by 72 hours. Liposomes formed with trimetaphosphate, a cyclical phosphate derivative, also leaked but less readily than the sulfate. Liposomes formed using tripolyphosphate or polyphosphate ( $n=13-18$ ) were considerably more stable in this assay. It should be noted that when the liposomes prepared using the sulfate salt were examined *in vivo*, the drug leaked even more rapidly (data not shown).

A study in mice considering the concentrations of drug and lipid in the blood at 24 hours, as well as the relative drug-to-lipid ratios, is shown in Figure 3B. It was observed that phosphate was the poorest stabilizer of APE in liposomes, followed by citrate, poly(vinylsulfonate), and poly(phosphate). When poly(phosphate) was used as the stabilizing anion, the amount of drug retained in the liposomes was greater than 95% at 24 hours. We have recently developed liposomal formulations of the histone deacetylase inhibitor LAQ824 (29), vinorelbine (VNB) (30), and irinotecan (31) in a complex with sucrose octasulfate that demonstrate remarkable *in vivo* stability. These results demonstrate that the chemical nature of the trapping agent employed in drug loading can dramatically affect the *in vivo* stability of the subsequent liposome preparation.

Some questions have also been raised about the activity of liposomal agents prepared using polyanions because highly stable liposomes loaded with



either VCR or a weakly basic camptothecin derivative, and encapsulated using dextran sulfate or suramin, displayed either decreased activity (11) or increased toxicity (32). We have encapsulated a wide range of agents and observed considerable activity both in vitro (Fig. 4) and in vivo (29). Targeted liposomal therapeutics are particularly dependent on formulation stability, as they must reach their target intact in order to optimally take advantage of the molecular targeting. A liposomal ellipticine analog (APE) was shown to have considerable HER2-specific cytotoxic activity in HER2-overexpressing breast cancer cells (Fig. 4), demonstrating that the drug could be made bioavailable in a relevant time period. Our preference has been for the use of the high charge density polyols, most notably sucrose octasulfate. The use of these agents has resulted in a number of highly stable and active liposome formulations of anticancer drugs (29–31). In addition, sucrose octasulfate is

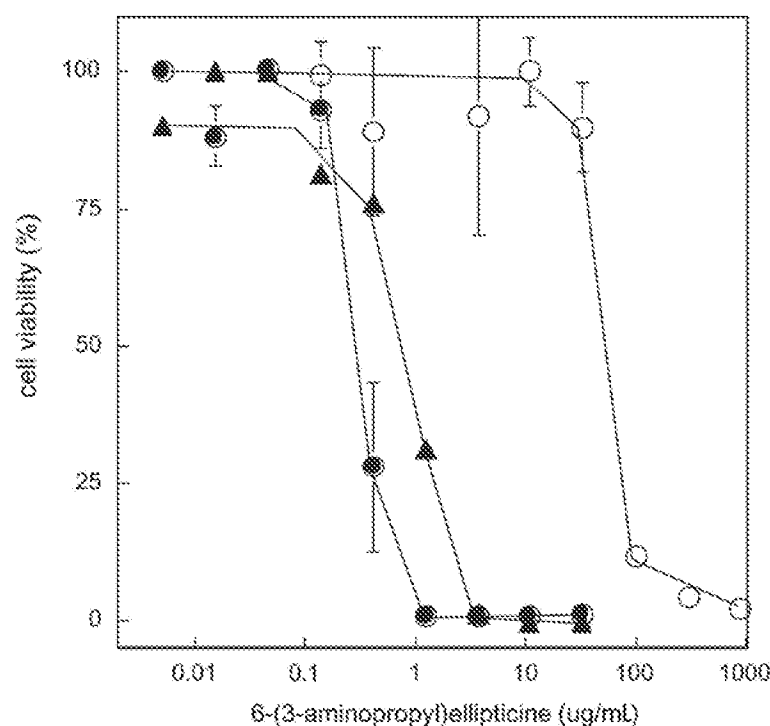


**Figure 4** Cytotoxicity of HER2-directed liposomal APE in HER2-overexpressing BT474 human breast carcinoma cells. Cells were plated at a density of 5000 cells/well and incubated for four hours with varying concentrations of unencapsulated (●), liposomal (○), or antiHER2 (F5)-immunoliposomal (▲). Cells were assayed for viability using a standard tetrazolium-based assay three days later. *Abbreviation:* APE, 6-(3-aminopropyl)ellipticine.

readily manufactured in a defined form that is more difficult to control with polymers. It is also free of serious systemic toxicities and does not display the anticoagulant activity (33) associated with many other polyanionic polymers.

### Precipitation or Gelation of Drug

Doxorubicin loaded into liposomes using ammonium sulfate gradients was shown to form intraliposomal crystals that were thought to stabilize the drug inside the liposome (7). Similar structures were later observed with liposomes loaded with doxorubicin using the pH gradient method with citrate as the counterion (34). It is possible that intraliposomal gelation or precipitation plays an important role in stabilizing the drug inside the liposomes, and that various counterions precipitate or gelate the drug more efficiently. Indeed, we have observed using microscopy that APE forms precipitates with either poly(phosphate) or poly(vinylsulfonate), but not with sulfate or citrate (unpublished observation). In contrast, doxorubicin forms precipitates with both citrate and sulfate under the same conditions. Although precipitation or gelation may play a role in the stabilization process, it does not ensure *in vivo* drug retention similar to that seen with doxorubicin-citrate or doxorubicin-sulfate formulations. Bally et al. have recently demonstrated that topotecan similarly forms what appears to be intraliposomal precipitates (Fig. 5) (19). However, these liposomes release topotecan at a considerably faster rate than observed for similar doxorubicin formulations, suggesting that the precipitation is not solely sufficient for *in vivo* stability.

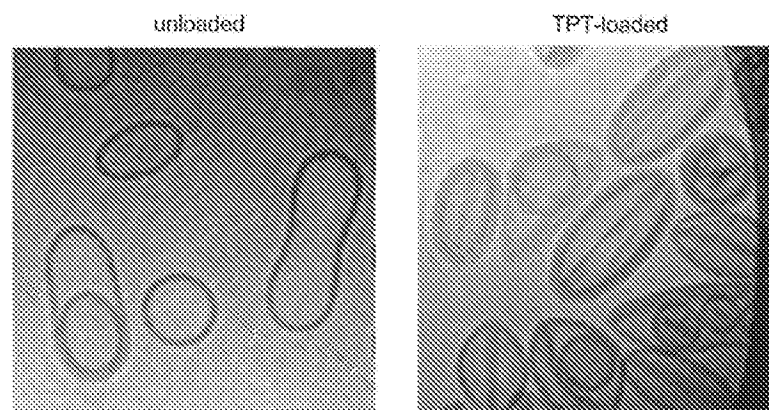


**Figure 5** An electron micrograph of unloaded liposomes or liposomal topotecan stabilized in a  $\text{SO}_4$  complex following loading using  $\text{MnSO}_4$  gradients in the presence of the ionophore A23187 at a ratio of topotecan-to-lipid of 0.2 (wt:wt). *Source:* From Ref. 35.

### Drug-to-Lipid Ratio

The concentration of drug loaded into the liposome can effect the stability of the final formulation. An early study demonstrated that using drug-to-lipid ratios that were too high resulted in less stable formulations, possibly resulting from dissipation of the pH-gradient used for drug loading (15,16,36). However, more recent studies (19), including those of our own, have shown that liposomes with higher drug loads have markedly increased stability. The higher intraliposomal drug concentrations could drive the formation of stable intraliposomal precipitates as the drug surpasses the aqueous solubility of drug inside the liposome. Thus, there may exist a balance between the formation of stable precipitates and gels inside the liposomes and the dissipation of a pH gradient that may help keep the drug in a less membrane permeable charged form inside the liposome. We have observed that the use of polyanionic trapping agents, such as sucrose octasulfate, allow for liposome drug loading at remarkably high drug-to-lipid ratios. An example of this is shown in Figure 6. Here the vinca alkaloid, VNB, is shown to load quantitatively up to a drug-to-PL ratio of 450 g VNB/mol PL. The high drug loads result in part from the increased concentrations of anionic groups that can be loaded into liposomes when present as a polyanion, without causing a destabilizing osmotic imbalance.

### Lipid Composition, Size, and Osmolarity

The lipid composition of the liposome membrane plays an important role in controlling the rate of drug release. The phase transition temperature of the liposomal lipids in part determines the rate of drug leakage, with liposomes containing lipids of shorter lengths or unsaturations displaying increased rates of drug leakage (37–40). In these studies, doxorubicin leaked from liposomes composed of unsaturated phosphatidylcholines significantly faster than liposomes prepared from hydrogenated phosphatidylcholines or distearoylphosphatidylcholine. The presence of chol also helps reduce the permeability of PLs vesicles to small molecular weight drugs or ions (41–43). Finally, the inclusion of sphingomyelin into liposome formulations containing chol has also been shown to reduce membrane permeability to drugs or small molecular weight ions (13,44). This possibly results from an increased membrane cohesiveness due to intermolecular hydrogen bonding between neighboring chol hydroxyl groups and sphingomyelin amide nitrogens (45,46). However, sphingomyelin is presently a costly lipid to use as a major component of a liposomal therapeutic. Fortunately, it appears that drug retention can be in large part controlled through modulation of intraliposomal drug complexes as described above, although further improvements in the drug-release profile upon inclusion of sphingomyelin are possible.

The size of the liposome determines the entrapped volume (47) and thus limits the amount of drug that can be entrapped in a single liposome.

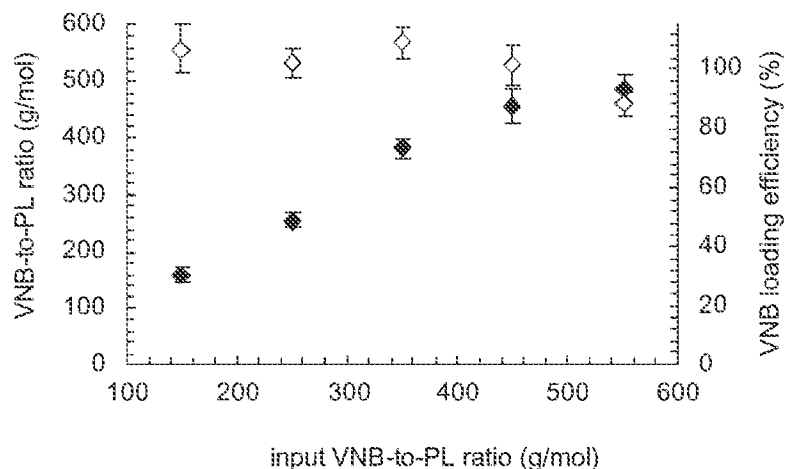


**Figure 6** Determination of the loading capacity for VNB in liposomes prepared using gradients of TEA sucroseoctasulfate (0.65 M TEA). Liposomal loading efficiency as a function of input vinorelbine (VNB)-to-phospholipid (PL) ratio. 1,2-distearoyl-3-*sn*-phosphatidylcholine/cholesterol/*N*-(polyethylene glycol)distearoylphosphatidylethanolamine (DSPC/cho/PEG-DSPE) 3:2:0.015, mol:mol:mol liposomes were loaded with VNB, with the initial amount of VNB added to the liposomes varying from 150 to 550  $\mu\text{g}$  VNB/ $\mu\text{mol}$  PL. Following incubation for 30 minutes at 60°C, the loading mixture was quenched on ice and unencapsulated drug was removed by gel filtration chromatography using a Sephadex G-75 column eluted with Hepes-buffered saline (pH 6.5). The resulting VNB-to-PL ratio, following loading, was determined by quantitating both VNB and PL in the resulting purified liposomal VNB formulation, and the loading efficiency by comparing this ratio to the input ratio. *Abbreviations:* VNB, vinorelbine; PL, phospholipid; TEA, triethylammonium.

However, a high radius of curvature at very small liposome sizes (i.e., ~50–70 nm) may also result in membrane defects that increase the permeability of drugs or gradient-forming ions, thus also adversely affecting liposomal drug retention. We have observed with both topotecan and VNB, loaded under specific conditions (drug load and specific trapping agents), that decreasing vesicle size below 80 nm resulted in an increased rate of drug release from the carrier.

Osmotic imbalances are also important to control when designing liposomal drug formulations. In the presence of plasma or high temperatures, significant osmotic imbalances can result in liposome lysis and release of the internal contents (23,24,48). As described above, it is possible to reduce these imbalances and thus encapsulate higher concentrations of anionic sites for drug-binding with the use of high-density polyanionic compounds for trapping drugs inside liposomes.

## COLLOIDAL AND CHEMICAL STABILITY CONSIDERATIONS

The chemical and colloidal stability of liposomal drug formulations prepared using remote-loading gradients is an important concern for maintaining highly stable and active liposomal therapeutics. A detailed discussion of the colloidal stability of lipid vesicles is beyond the scope of this chapter and the reader is referred to several excellent reviews on the subject (49,50). However, in general, aggregation can be minimized by inclusion of anionic lipids or polymer-coated surfaces. Because aggregated vesicles may have a greater propensity for increased drug leakage, it is important to minimize the level of aggregation during both storage and while in circulation. The concentration of liposomes in the vial, as well as the chosen excipient, may also help determine the degree of colloidal stability for the final liposome preparation.

Because the gradients prepared can result in extremes of pH under some circumstances, it is important to characterize the stability of both the encapsulated agent during storage and the liposomal lipids. Fortunately, many drugs demonstrate increased stability at low pH and thus are not adversely affected by entrapment using these methods. However, some drugs such as VCR can be inactivated at low pH. VCR is deformylated at low pH, resulting in an inactive byproduct (Fig. 7A). When liposomes are prepared that result in a relatively low internal pH, the inactive by-product appears over time during storage (Fig. 7B). Fortunately, this reaction can be controlled to some extent by modulating the trapping agent used. For example, citrate has a reasonable buffering capacity; therefore, under certain conditions, it can keep the pH in a range where this inactivation is minimized. The use of sulfate as a trapping agent is more problematic due to its poor buffering ability; therefore, it is more difficult to control the resulting deformylation. Although typically less sensitive to extremes in pH, lipids also have sensitive bonds, most notably the sn-2 ester bond of PLs. If not carefully controlled, the resulting lysolipids and fatty acids can destabilize liposome membranes, resulting in increased drug leakage. Mayer et al. have shown that the substitution of sphingomyelin for phosphatidylcholine can help alleviate this problem, as the amide bonds present in sphingomyelin are considerably less sensitive to acid (13). The use of reverse pH gradients (5) where the interior is alkalized is more of a concern as more chemical entities are sensitive to alkaline inactivation when compared to acidic inactivation.

## CONCLUSIONS

This chapter reviews the methodology and characterization of novel intraliposomal drug stabilization strategies. In order to achieve highly stable

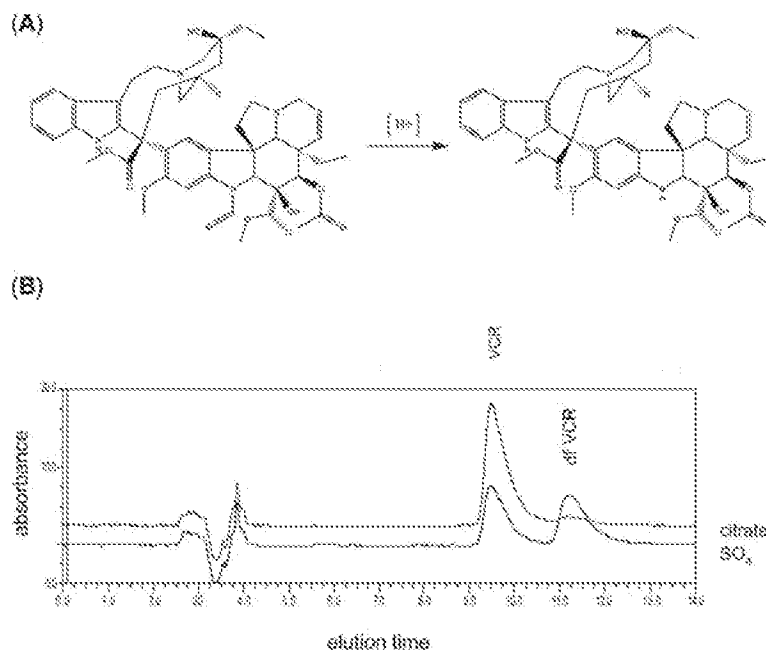


**Figure 7** The stability of liposomal VCR in liposomes prepared using different triethylammonium ion gradients. VCR can be deformed under acidic conditions, similar to those found in the intraliposomal lumen of remote-loaded liposomes. (A) The deformed product is inactive compared to the parent drug. (B) HPLC chromatograms show peaks for both VCR ( $t_r = 9.5$  minutes) and deformed VCR ( $t_r = 11.1$  minutes) for liposomes prepared with either sulfate or citrate as the intraliposomal trapping agent and stored for three months at  $4^\circ\text{C}$  to  $6^\circ\text{C}$ . *Abbreviation:* VCR, vincristine.

liposomal drug formulations where the drug is retained in the liposome while in the general circulation, drugs were complexed with polyanionic trapping agents, and preferably polyanionic polyols, inside the liposomes. The resulting formulations were considerably more stable than liposomes prepared using traditional remote-loading strategies that employ citrate or sulfate. We have also demonstrated that these formulations are highly active, and thus able to release the drug at a rate reasonable enough to achieve cytotoxicity of targeted formulations *in vitro* and efficacy *in vivo*. Finally, the stabilization strategies must be optimized depending on the agent to be entrapped to provide for chemical stability of both the lipid and drug components. We believe these improvements in liposome technology will help the field move beyond its initial success with delivery of anthracyclines to a wider range of drugs.

## REFERENCES

1. Drummond DC, Meyer O, Hong K, et al. Optimizing liposomes for delivery of chemotherapeutic agents to solid tumors. *Pharmacol Rev* 1999; 51(4):691.
2. Allen TM, Cullis PR. Drug delivery systems: entering the mainstream. *Science*. 2004; 303(5665):1818.
3. Sapra P, Allen TM. Ligand-targeted liposomal anticancer drugs. *Prog Lipid Res* 2003; 42(5):439.
4. Noble CO, Kirpotin DB, Hayes ME, et al. Development of ligand-targeted liposomes for cancer therapy. *Expert Opin Ther Targets* 2004; 8(4):335.
5. Clerc S, Barenholz Y. Loading of amphiphathic weak acids into liposomes in response to transmembrane calcium acetate gradients. *Biochim Biophys Acta* 1995; 1240:257.
6. Haran G, Cohen R, Bar LK, et al. Transmembrane ammonium sulfate gradients in liposomes produce efficient and stable entrapment of amphiphathic weak bases. *Biochim Biophys Acta* 1993; 1151:201.
7. Lasic DD, Ceh B, Stuart MCA, et al. Transmembrane gradient driven phase transitions within vesicles: lessons for drug delivery. *Biochim Biophys Acta* 1995; 1239:145.
8. Fenske DB, Wong KP, Maurer E, et al. Ionophore-mediated uptake of ciprofloxacin and vincristine into large unilamellar vesicles exhibiting transmembrane ion gradients. *Biochimica Biophysica Acta* 1998; 1414(1-2):188.
9. Cullis PR, Hope MJ, Bally MB, et al. Influence of pH gradients on the transbilayer transport of drugs, lipids, peptides and metal ions into large unilamellar vesicles. *Biochim Biophys Acta* 1997; 1331:187.
10. Abraham SA, McKenzie C, Masin D, et al. In vitro and in vivo characterization of doxorubicin and vincristine coencapsulated within liposomes through use of transition metal ion complexation and pH gradient loading. *Clin Cancer Res* 2004; 10:728.
11. Zhu G, Oto E, Vaage J, et al. The effect of vincristine-polyanion complexes in STEALTH liposomes on pharmacokinetics, toxicity and anti tumor activity. *Cancer Chemother Pharmacol* 1996; 39:138.
12. Madden TD, Harrigan PR, Tai LCL, et al. The accumulation of drugs within large unilamellar vesicles exhibiting a proton gradient: a survey. *Chem Phys Lipids* 1990; 53:37.
13. Webb MS, Harasym TO, Masin D, et al. Sphingomyelin-cholesterol liposomes significantly enhance the pharmacokinetic and therapeutic properties of vincristine in murine and human tumour models. *Br J Cancer* 1995; 72:896.
14. Sapra P, Moase EH, Ma J, et al. Improved therapeutic responses in a xenograft model of human B lymphoma (Namalwa) for liposomal vincristine versus liposomal doxorubicin targeted via anti-CD19 IgG2a or Fab fragments. *Clin Cancer Res* 2004; 10:1100.
15. Mayer LD, Nayar R, Thies RL, et al. Identification of vesicle properties that enhance the antitumor activity of liposomal vincristine against murine L1210 leukemia. *Cancer Chemother Pharmacol* 1993; 33:17.
16. Boman NL, Mayer LD, Cullis PR. Optimization of the retention properties of vincristine in liposomal systems. *Biochim Biophys Acta* 1993; 1152(2):253.

17. Messerer CL, Ramsay EC, Waterhouse D, et al. Liposomal irinotecan: formulation development and therapeutic assessment in murine xenograft models of colorectal cancer. *Clin Cancer Res* 2004; 10(19):6638.
18. Liu JJ, Hong RL, Cheng WF, et al. Simple and efficient liposomal encapsulation of topotecan by ammonium sulfate gradient: stability, pharmacokinetic and therapeutic evaluation. *Anti-Cancer Drugs* 2002; 13(7):709.
19. Abraham SA, Edwards K, Karlsson G, et al. An evaluation of transmembrane ion gradient-mediated encapsulation of topotecan within liposomes. *J Control Release* 2004; 96(3):449.
20. Allen TM, Newman MS, Woodle MC, et al. Pharmacokinetics and anti-tumor activity of vincristine encapsulated in sterically stabilized liposomes. *Int J Cancer* 1995; 62:199.
21. Kirpotin DB. Compound-loaded liposomes and methods for their preparation. United States Patent, 6,110,491, 2000.
22. Stahl PH, Wermuth CG, eds. *Handbook of Pharmaceutical Salts*. Weinheim: Wiley-VCH, 2002.
23. Mui BLS, Cullis PR, Evans EA, et al. Osmotic properties of large unilamellar vesicles prepared by extrusion. *Biophys J* 1993; 64:443.
24. Mui BLS, Cullis PR, Pritchard PH, et al. Influence of plasma on the osmotic sensitivity of large unilamellar vesicles prepared by extrusion. *J Biol Chem* 1994; 269:7364.
25. Woodle MC, Papahadjopoulos D. Liposome preparation and size characterization. *Meth Enzymol* 1989; 171:193.
26. Harrigan PR, Wong KF, Redelmeier TE, et al. Accumulation of doxorubicin and other lipophilic amines into large unilamellar vesicles in response to transmembrane pH gradients. *Biochim Biophys Acta* 1993; 1149(2):329.
27. Bartlett GR. Phosphorous assay in column chromatography. *J Biol Chem* 1959; 234:466.
28. Tristram-Nagle S, Nagle JF. Lipid bilayers: thermodynamics, structure, fluctuations, and interactions. *Chem Phys Lipids* 2004; 127(1):3.
29. Drummond DC, Marx C, Guo Z, et al. Enhanced pharmacodynamic and anti-tumor properties of a histone deacetylase inhibitor encapsulated in liposomes or ErbB2-targeted immunoliposomes. *Clin Cancer Res* 2005; 11:3392-3401.
30. Mamot C, Drummond DC, Noble CO, et al. Epidermal growth factor receptor-targeted immunoliposomes significantly enhance the efficacy of multiple anticancer drugs in vivo. *Cancer Res* 2005; 65:1631-1638.
31. Drummond DC, Noble CO, Guo Z, Hong K, Park JW, Kirpotin DB. Development of a highly active nanoliposome irinotecan using a novel intraliposomal stabilization strategy. *Cancer Res* 2006; 66:3271-1638.
32. Colbern GT, Dykes DJ, Engbers C, et al. Encapsulation of the topoisomerase I inhibitor GL147211C in pegylated (STEALTH) liposomes: pharmacokinetics and antitumor activity in HT29 colon tumor xenografts. *Clin Cancer Res* 1998; 4:3077.
33. Fisher RS. Sucralfate: a review of drug tolerance and safety. *J Clin Gastroenterol* 1981; 3(Suppl 2):181.
34. Li X, Hirsh DJ, Cabral-Lilly D, et al. Doxorubicin physical state in solution and inside liposomes loaded via a pH gradient. *Biochim Biophys Acta* 1998; 1415(1):23.



35. Abraham SA, Edwards K, Karlsson G, Hudon N, Mayer LD, Bally MB. An evaluation of transmembrane gradient-mediated encapsulation of topotecan within liposomes. *J Control Release* 2004; 96:449–461.
36. Mayer LD, Tai LCL, Bally MB, et al. Characterization of liposomal systems containing doxorubicin entrapped in response to pH gradients. *Biochim Biophys Acta* 1990; 1025:143.
37. Gabizon AA, Barenholz Y, Bialer M. Prolongation of the circulation time of doxorubicin encapsulated in liposomes containing polyethylene glycol-derivatized phospholipid: pharmacokinetic studies in rodents and dogs. *Pharm Res* 1993; 10(5):703.
38. Charrois GJ, Allen TM. Drug release rate influences the pharmacokinetics, biodistribution, therapeutic activity, and toxicity of pegylated liposomal doxorubicin formulations in murine breast cancer. *Biochim Biophys Acta* 2004; 1663(1–2):167.
39. Bally MB, Nayar R, Masin D, et al. Liposomes with entrapped doxorubicin exhibit extended blood residence times. *Biochim Biophys Acta* 1990; 1023(1):133.
40. Mayer LD, Cullis PR, Bally MB. Designing therapeutically optimized liposomal anticancer delivery systems: lessons from conventional liposomes. In: Papahadjopoulos L, ed. *Medical Applications of Liposomes*. New York: Elsevier Science, 1998.
41. Papahadjopoulos D, Nir S, Oki S. Permeability properties of phospholipid membranes: effect of cholesterol and temperature. *Biochim Biophys Acta* 1972; 266(3):561.
42. Papahadjopoulos D, Jacobson K, Nir S, et al. Phase transitions in phospholipid vesicles. Fluorescence polarization and permeability measurements concerning the effect of temperature and cholesterol. *Biochim Biophys Acta* 1973; 311:330.
43. Mayhew E, Rustum YM, Szoka F, et al. Role of cholesterol in enhancing the antitumor activity of cytosine arabinoside entrapped in liposomes. *Cancer Treat Rep* 1979; 63:1923.
44. Kirby C, Gregoriadis G. The effect of lipid composition of small unilamellar liposomes containing melphalan and vincristine on drug clearance after injection into mice. *Biochem Pharmacol* 1983; 32(4):609.
45. Smaby JM, Momsen M, Kulkarni VS, et al. Cholesterol-induced interfacial area condensations of galactosylceramides and sphingomyelins with identical acyl chains. *Biochemistry* 1996; 35:5696.
46. Schmidt CF, Barenholz Y, Thompson TE. A nuclear magnetic resonance study of sphingomyelin in bilayer systems. *Biochemistry* 1977; 16:2649.
47. Perkins WR, Minchey SR, Ahl PL, et al. The determination of liposome captured volume. *Chem Phys Lipids* 1993; 64:197.
48. Allen TM, Mehra T, Hansen C, et al. Stealth liposomes: an improved sustained release system for 1- $\beta$ -D-arabinofuranosyleytosine. *Cancer Res* 1992; 52:2431.
49. Lasic DD, Papahadjopoulos D. Liposomes and biopolymers in drug and gene delivery. *Curr Opin Solid State Mater Sci* 1996; 1:392.
50. Heurtault B, Saurinier P, Pech B, et al. Physico-chemical stability of colloidal lipid particles. *Biomaterials* 2003; 24(23):4283.

# 9

---

## Liposomal Drug Delivery Systems for Cancer Therapy

---

*Daryl C. Drummond, PhD,  
Dmitri Kirpotin, PhD, Christopher C. Benz, MD,  
John W. Park, MD, and Keelung Hong, PhD*

### CONTENTS

INTRODUCTION  
FORMULATION ISSUES  
ANIMAL PHARMACOLOGY  
CLINICAL RESULTS  
ACTIVE TARGETING OF LIPOSOMES  
CONCLUSIONS  
ACKNOWLEDGMENTS  
REFERENCES

---

### 1. INTRODUCTION

Liposomes are currently one of the most well-studied drug delivery systems used in the treatment of cancer. They are being employed in the treatment of a wide variety of human malignancies (1–4). Their large size relative to the gaps in the vasculature of healthy tissues inhibits their uptake by these tissues, thus avoiding certain nonspecific toxicities. However, the “leaky” microvasculature supporting solid tumors allows for the uptake of these large (~ 100 nm) drug carriers (5–8) and their subsequent interaction with cancer cells (9), or release of the encapsulated drug specifically near the tumor, where it can diffuse into the tumor in its free form (10,11). Liposomes have many other potential advantages over the corresponding free drugs, including favorable pharmacokinetic properties, where encapsulation of a usually rapidly cleared drug results in a considerable increase in the circulation lifetime for the drug (12–14). In addition, encapsulation or complexation of a normally labile therapeutic agent, such as DNA, antisense oligonucleotides, or the lactone ring of camptothecins, can protect the agent from premature degradation by enzymes in the plasma or from simple hydrolysis. The result of liposome formulation can thus be a substantial increase in antitumor efficacy when compared to the free drug or standard chemotherapy regimens (15–17).

From: *Drug Delivery Systems in Cancer Therapy*  
Edited by: D. M. Brown © Humana Press Inc., Totowa, NJ

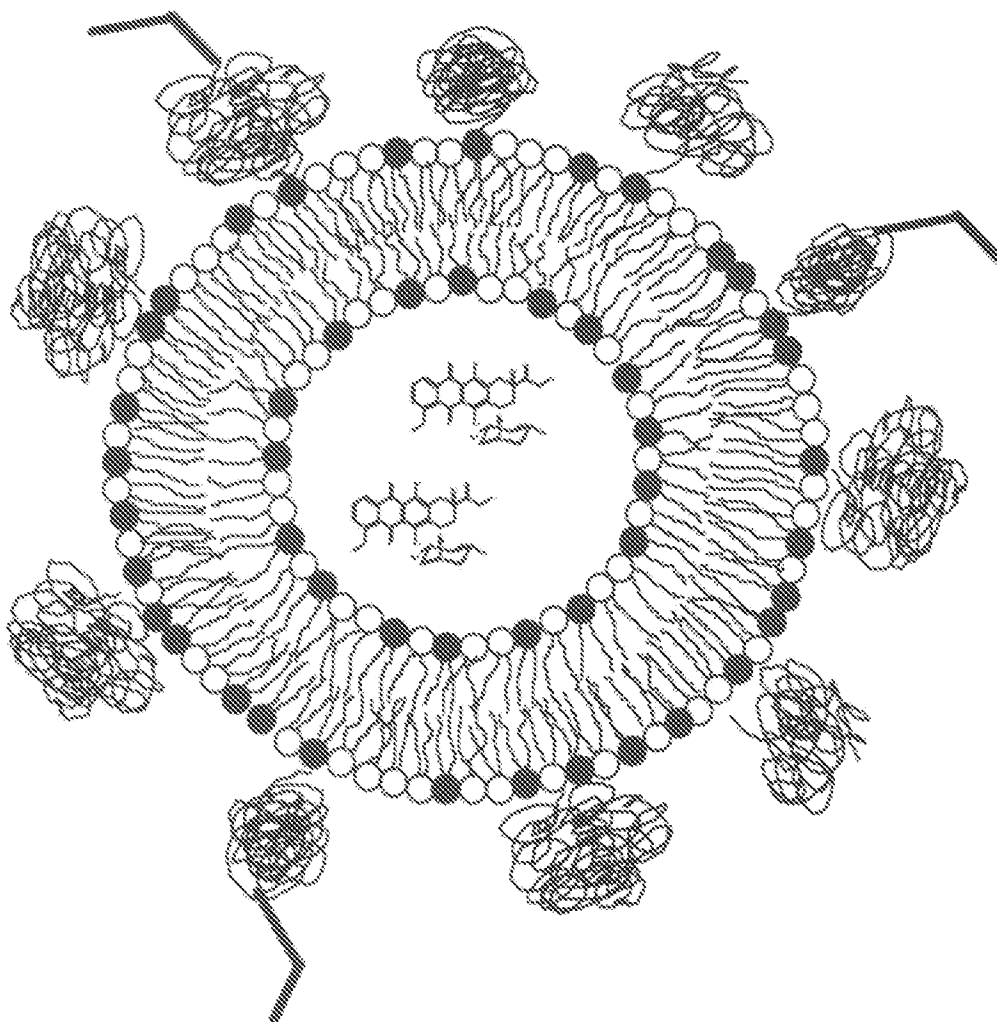


**Fig. 1.** Diagram of a sterically stabilized liposome containing the antineoplastic drug, doxorubicin. Liposomes are composed of a lipid membrane that encloses an internal aqueous space. This aqueous space can be used to entrap drugs following passive loading of the agent by its inclusion in the hydration media or remote-loading using ion- or pH-gradients. The lipids used to compose the liposomal membrane can be both phospholipids, such as phosphatidylcholine, and neutral lipids, such as cholesterol. In addition sterically stabilized liposomes contain a lipid-anchored PEG-coating that reduces its uptake by macrophages. Finally, targeting ligands, such as single-chain antibody fragments, can be attached to the terminal ends of PEG and used to actively direct the liposomal carriers to tumor-specific antigens.

A diagram of a liposome is given in Fig. 1. Liposomes are composed of a lipid bilayer that may contain both phospholipids, such as phosphatidylcholine, and neutral lipids, such as cholesterol. The lipid bilayer encloses an internal aqueous space that can be utilized to carry antineoplastic drugs, imaging agents, proteins, and even genes. The surface of the liposome can be modified with hydrophilic polymers, such as polyethylene glycol (PEG), to reduce interactions with reticuloendothelial cells responsible for their elimination from the systemic circulation (13,18–21). The pharmacological properties of liposomes can be widely varied by modifying the lipid composition of the liposome, the therapeutic agent to be encapsulated, the method of drug encapsulation, the surface

**Table 1**  
**Important Considerations in the Design of Liposome-Formulated Therapeutics**

<i>Component</i>	<i>Considerations for optimum design</i>
<i>Liposome</i>	<p><i>Stability</i></p> <ul style="list-style-type: none"> <li>Stable as intact construct in vivo</li> <li>Lipid components chemically stable during storage</li> </ul> <p><i>Pharmacokinetics</i></p> <ul style="list-style-type: none"> <li>Long circulating (small diameter, steric stabilization, charge optimization)</li> </ul> <p><i>Tumor penetration</i></p> <ul style="list-style-type: none"> <li>Capable of extravasation in solid tumors</li> <li>Small diameter improves penetration into tumor tissue</li> </ul>
<i>Drug</i>	<p><i>Encapsulation</i></p> <ul style="list-style-type: none"> <li>Efficient, high capacity (remote loading or passive entrapment)</li> <li>Encapsulated drug resists leakage during storage and minimizes leakage in systemic circulation</li> </ul> <p><i>Bystander Effect</i></p> <ul style="list-style-type: none"> <li>Agent affects tumor cells not directly targeted (bystander cells)</li> </ul> <p><i>Interaction with Tumor Cells</i></p> <ul style="list-style-type: none"> <li>Effective against target cell population</li> <li>If internalized, therapeutic agent capable of escaping internal organelles and/or stable to degradative environment in lysosomes</li> </ul>

charge density, the presence or absence of steric stabilization, the size of the carrier, the presence of a targeting ligand on the liposome surface, the dose to be administered, and the route of administration. Thus, it is essential that the cancer researcher understand how these various properties affect the pharmacokinetics, biodistribution, and the bioavailability of the entrapped therapeutic agent to maximize the therapeutic index. Several additional reviews discuss in detail how these different characteristics act to modify the pharmacological properties of liposomes and liposomal drugs (3,12,13,22–26).

## 2. FORMULATION ISSUES

### *2.1. Effects of Liposome Physical Properties on Pharmacokinetics and Tissue Distribution*

There are many formulation issues to consider when designing a liposomal or lipid-based carrier system for a particular therapeutic agent. The various properties of the carrier have to be considered when taking into account the interactions of liposomes with the biological milieu. Many of the optimal properties for design of a liposome-based therapeutic are given in Table 1. For example, relatively small unilamellar liposomes (70–150 nm) are often desirable when treating solid tumors because they are taken up less readily by reticuloendothelial system (RES) macrophages (12,26,27) and able to extravasate more readily into solid tumors (5,28). However, large multilamellar vesicles have been used when the drug was administered at a peripheral site and effectively acted as a slow release depot for the drug from that site (29), or where the drug was targeted to the RES, as is the case for some infectious diseases (30). Surface charge is another important and often misunderstood property of liposomal carriers that affects their disposition in vivo (3,26,31,32). Although certain anionic phospholipid

components have been shown to increase liposome clearance *in vivo* (26,33), other sterically shielded anionic lipids have been shown to substantially increase circulation half-lives of liposomal carriers (19,31,34,35). In addition, surface charge density and the presence of gel phase phospholipid components may also play a role in the magnitude of the charge effect on liposome clearance (3,32,36).

Along with surface charge and size, other physical characteristics of the carrier such as membrane fluidity play a role in liposome and drug circulation lifetimes. In the absence of steric stabilization, liposomes that contain fluid-phase lipid components, such as unsaturated phospholipids, are cleared more rapidly from the circulation than liposomes containing gel-phase phospholipids (26,37). This is presumably due to the increased potential for binding of serum opsonins to liposomes that, in turn, bind macrophages and result in more rapid uptake of the carrier by macrophages (38–40). The presence of cholesterol in the formulation also prevents disintegration of the carrier by lipoproteins in the blood and, thus, is thought to be essential in maintaining a stable liposome formulation *in vivo* (41,42). Steric stabilization of liposomal carriers, by addition of polymer-coated lipid conjugates, is thought to both reduce the binding of serum opsonins to the liposome surface and reduce interactions of bound opsonins with receptors on the surface of RES macrophages, thus reducing clearance (43–47). Depending on the nature of the ligand attached, ligands such as antibodies, used for specific targeting of receptor-overexpressing cancer cells, can also alter the pharmacokinetics of liposomes (Subheading 5.). The importance of understanding the interactions of these relative physical properties, and their effect on liposome disposition *in vivo*, cannot be emphasized enough.

## 2.2. Formulation Stability

There are other formulation issues, such as *in vivo* formulation stability, degree of drug entrapment, and ability to make the agent bioavailable at the site of action, that determine the degree of success of a delivery-specific approach to treating cancer. In order to carry a cytotoxic agent specifically to solid tumors while avoiding healthy tissues, the drug must be stably encapsulated in the liposome interior when in the general circulation. Drugs vary in their ability to be stably entrapped depending on the physicochemical properties of the drug, the method of drug entrapment, and the lipid composition of the carrier (3,23,48). In general, amphipathic drugs such as doxorubicin and vincristine are the most ideal for delivery via liposomes. These drugs can be entrapped inside liposomes at concentrations exceeding their aqueous solubility by using remote-loading techniques involving pH or ion gradients across the membrane surface (49–54). Using one of these methods, the degree of entrapment can approach 100% for certain drugs. The presence of cholesterol and high-phase transition phospholipids, such as sphingomyelin (SM) and highly saturated phospholipids, enhance the stability of these formulations (55,56). Hydrophobic drugs, such as paclitaxel, are carried in the lipid bilayer rather than the aqueous interior (57–59). However, they usually require a large excess of lipid to completely solubilize the drug and prevent their recrystallization. In addition, this class of drugs/therapeutic agents is often rapidly redistributed to extraliposomal sites including plasma lipoproteins (57,60,61). A third class of compounds, the highly hydrophilic class, are able to be stably entrapped in liposomes by passive entrapment, although at low yields (< 33%) relative to active loading. However, release of the drug from the liposome may be slow and require an external trigger such as pH (62–65) or temperature (66–68) to release the drug from the carrier.

### 2.3. Release of Therapeutic Agents from Liposomal Carriers

Another important, yet often neglected parameter in designing liposomal carriers is the rate of release of drug from the liposome. In order to be effective in treating a particular malignancy, liposomes must be able to make their drug bioavailable, preferably at the site of the tumor. Upon release, the drug can subsequently diffuse into the target cell by passive diffusion or be taken up by membrane transporters, such as nucleoside transporters (69,70) or the reduced folate carrier (71,72). The majority of drugs studied thus far have been amphipathic in nature and thus able to passively diffuse from the liposomal carrier with a rate that depends on the lipid composition of the carrier, the mode of drug entrapment, the osmolarity of the entrapped species, and the effects of local stimuli (3,50,68,73–76). These liposomal drugs can either be released rapidly ( $t_{1/2}$  = minutes to hours), where an important fraction of the drug is released from the carrier while in the circulation, or slowly ( $t_{1/2}$  = hours to days), where the liposome accumulates in the tumor at a rate more rapid than the rate for drug release. More complicated liposome systems are also being developed that rely on programmed loss of a protective PEG coating (77–79), temperature-mediated (67,68) or pH-mediated (62,64) membrane destabilization, or specific enzymatic destabilization of liposomes (80). Continued optimization of drug leakage rates is needed to more fully take advantage of the increased tumor accumulation of drug afforded by liposome encapsulation.

## 3. ANIMAL PHARMACOLOGY

### 3.1. Pharmacokinetics and Biodistribution of Liposomal Drugs

The half-life of sterically-stabilized liposomal doxorubicin (SSL-DOX) in the systemic circulation ( $t_{1/2}$ ) is approx 22–24 h in rats (81,82), and 45 h in humans (15). For SSL-DOX, the  $t_{1/2}$  is relatively independent of dose (15), while for conventional formulations without the steric PEG coat, the  $T_{1/2}$  increases rapidly with increasing dose. This increase in circulation lifetimes with increasing dose is thought to be because of either saturation of RES macrophages with liposomal lipid (12,26,27) or drug-induced toxicity of RES macrophages (55,83), with either mechanism resulting in reduced clearance. Drug-induced toxicity has been observed with SSL-DOX as well, but only at relatively high doses (2). The rate of clearance for SSL-DOX in rats is approx 60-fold lower than free doxorubicin in rats (82). This translates into a similar increase in the area under the curve (AUC) for concentration versus time for SSL-DOX when compared to free doxorubicin. The significant increases in plasma AUCs and reductions in clearance following liposome encapsulation were also observed in humans (15,84,85), although the relative difference was considerably less for conventional formulations (84,85) than for a sterically stabilized formulation (15). As mentioned earlier, these effects are likely due to the ability of the steric PEG coat to reduce recognition of liposomes by RES macrophages. Fig. 2A shows the effect of liposome encapsulation on clearance of vincristine (VCR) from the circulation of SCID mice bearing A431 tumors (73). This figure emphasizes the importance of formulation stability on liposome clearance. When 1,2-distearoyl-3-*sn*-phosphatidylcholine (DSPC) is replaced with sphingomyelin, the liposome is able to more readily retain vincristine when in the circulation, and this translates into reduced drug clearance. For doxorubicin, DSPC/Chol liposomes are sufficient to hold the drug while in the circulation and, thus, the importance of tailoring the liposomal carrier to the drug to be encapsulated is demonstrated (Subheading 2.2.). The increased circulation

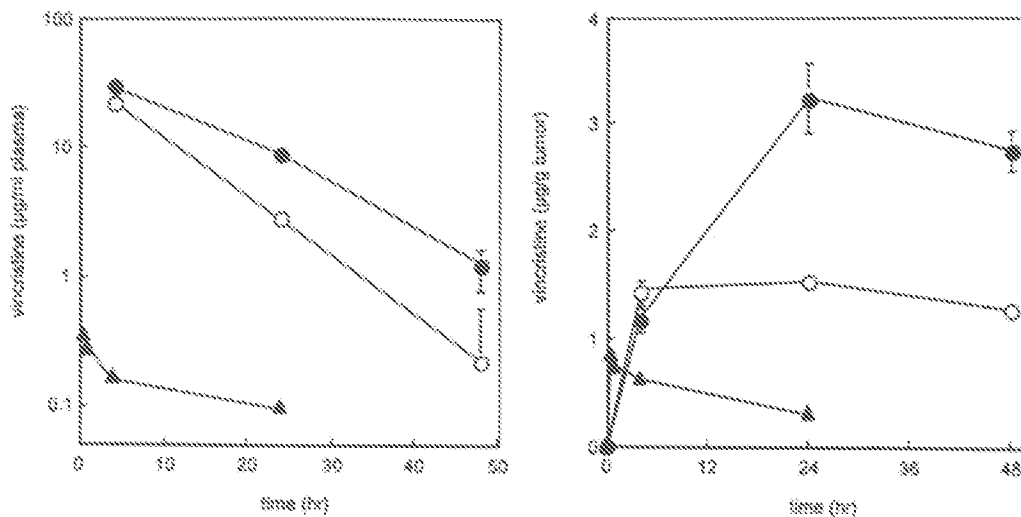


**Fig. 2.** Pharmacokinetics of free and liposome-encapsulated vincristine. Plasma (A) and tumor (B) levels of vincristine were determined after administration of free vincristine (▲), or vincristine entrapped in DSPC/Chol (○) or SM/Chol (●) liposomes. The tumor model used was that of a squamous cell carcinoma (A431 tumors) in SCID mice. The dose of vincristine was 2 mg/kg for all samples and the lipid dose for the liposome formulations was 20 mg/kg. (This figure was taken from Webb et al. *Br J Cancer* 1995; 72:896–904, with permission.)

lifetime of liposomal drugs also helps translate into increased tumor accumulation of drug (36,86–88). As can be seen in Fig. 2B, the more stable SM/Chol liposomal vincristine formulation shows considerably greater levels of vincristine accumulation in the tumor.

The biodistribution of liposomal and free drugs are determined by a variety of factors, including circulation lifetimes, the presence of phagocytic cells, and the vascular barrier of the particular tissue. Most free drugs redistribute rapidly to tissues due to their small size and membrane-permeable amphipathic nature, and they are often rapidly excreted by the kidneys. The result is a large volume of distribution for the free drug. Stable liposomal formulations, on the other hand, have a relatively small volume of distribution that is not much greater than the volume of the central compartment (15,82,85). This is because of the inability of liposomes to pass through the vasculature and accumulate in these tissues as a result of their prohibitively large size (~100 nm). Liposomes distribute primarily to the liver and spleen owing to the high number of phagocytic macrophages in these tissues that are responsible for their elimination (33,89,90). The presence of a steric coat reduces the rate of liposome accumulation in these organs, although the spleen and liver remain the major sites for their disposition in vivo (21,43,89). The ability to avoid uptake by these two major tissues allows for a greater probability of their accumulation in other target tissues, such as sites of inflammation (91–93) or various malignancies (15,19,36,87–89).

Accumulation of liposomal drugs in solid tumors occurs as a result of extravasation through a discontinuous microvasculature supporting the tumor and the absence of functioning lymphatics (6–8,94–97). The average size of the discontinuities varies greatly depending on the tumor microenvironment but, in general, are much greater (100–780 nm) than the size of the most commonly employed liposomes (~100 nm) (5,7). Factors that control the rate of accumulation of liposomal drugs in tumors are not

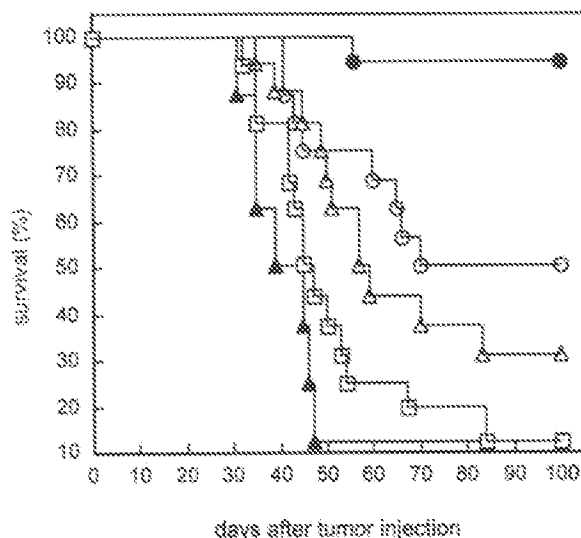


**Fig. 3.** Antitumor efficacy of free DOX (●) and SSL-DOX (○ ●), either alone (●, ○) or in combination with liposomal IL-2 (●), in the treatment of M109 pulmonary metastases. Control animals treated with saline (□) or liposomal IL-2 alone (▲) are also shown. BALB/c mice were inoculated intravenously (iv) with M109 tumor cells ( $10^6$  cells) and DOX or SSL-DOX was administered on Day 7 after tumor inoculation at a dose of 8 mg/kg and IL-2 at a dose of 50,000 Cetus U/dose on Days 10, 13, and 16. (This figure was modified from Cabanes et al. *Clin Cancer Res* 1999; 5:687–693, with permission.)

fully understood at this time. Factors such as the size of the liposome relative to the gaps in the microvasculature, the stability of the formulation, the tumor microenvironment, and the presence of a PEG coat are likely involved in determining how rapidly liposomes extravasate across the tumor vasculature (3,5,7,36,98–100). In general, the accumulation of free drug in tumor is relatively fast, reaching maximal levels within 1 hour. However, liposomal accumulation is much slower, with maximal accumulation in tumors varying from 8–48 h, depending on the formulation (11,36,88,98,101–103). Total drug levels in the tumor can peak much earlier if the formulation at least partially leaks its contents while in the circulation, as is the case for rapid-release systems such as phosphatidylcholine derived from egg (eggPC:Chol) liposomes (100,103), although the overall tumor AUC is considerably lower than for long-circulating slow-release formulations. The ability to manipulate vascular permeability, pharmacokinetic parameters, and the biodistribution of liposomal drugs for increased specificity of delivery to malignant tissues is extremely important in the design of more efficacious and less toxic liposomal drug delivery systems.

### 3.2. Antitumor Efficacy of Liposomal Drugs

Both sterically stabilized liposomal (SSL-) and conventional liposomal (CL-) drugs have been examined for antitumor efficacy in a wide variety of different tumor models (9,19,20,59,81,87,98,101,104–107). Liposomal anthracycline formulations have been by far the most widely studied, although in recent years other liposomal drugs and combinations of drugs have been increasingly developed (59,73,105,106,108). Many of these studies demonstrated a considerable survival advantage or reduction in tumor



size following treatment with liposomal therapeutics when compared to free drug controls. When conventional and sterically stabilized formulations were compared directly at clinically relevant doses, the sterically stabilized formulations showed superior efficacy in most instances (36,89,103,109). In a few studies, where exceedingly high and nonrelevant doses were used (83,98) or where the tumor was localized to either the liver or spleen (the major depots for liposomes in vivo) (110), conventional formulations were shown to have similar efficacy to SSL formulations. Combinations of liposomal drugs with other therapeutic agents, such as interleukin 2 (IL-2) have been shown to increase therapeutic efficacy even further (Fig. 3) (106). The use of drug combinations employing liposomal drugs will help increase the effectiveness of anticancer treatments by allowing drugs with different modes of action and drug resistance to be administered with a reduction in many of their dose-limiting toxicities. These studies give rise to significant hope that liposomal drugs will provide considerable improvements in therapeutic efficacy in addition to their well-documented reductions in many common toxicities (Subheading 4.2.).

#### 4. CLINICAL RESULTS

There are presently many liposomal agents for the treatment of cancer that are already approved, awaiting approval by the appropriate drug regulatory agencies, in clinical trials, or in development by an everincreasing number of liposome or lipid-based formulation companies. A list of these products and their current status of development is given in Table 2. The most developed of liposome-formulated products are those containing anthracyclines. Anthracyclines are good candidates for liposome encapsulation due to their broad activity against a wide variety of human malignancies (111,112) and the physicochemical properties that facilitate their stable entrapment inside liposomes (3,23,48). However, other drugs such as vincristine (4,113) and lurtotecan (114,115) are beginning to show considerable promise in early clinical studies.

##### 4.1. Efficacy of Liposomal Drugs

Encapsulation of a therapeutic agent inside liposomes can result in a reduction in the grade of certain important toxicities, an increase in efficacy due to preferential accumulation in tumors or active targeting, a better quality of life owing to the mode of delivery or shift in toxicities, or a combination of these outcomes. Until recently, AIDS-related Kaposi's sarcoma had been the most commonly treated neoplasm in clinical trials using liposomal agents (16,17,85,86,116–119). Single agent therapy using standard chemotherapy was ineffective in treating Kaposi's sarcoma and combination regimens including doxorubicin (DOX), bleomycin, and VCR (ABV regimens), or simply bleomycin and VCR (BV regimens), have been used in the clinical setting. However, both SSL-DOX and CL-daunorubicin have shown significant activity against Kaposi's sarcoma in various clinical trials (16,17,85,86,116–119). Response rates varied considerably depending on the trial design and patient characteristics, but these approached 70–75% as a single agent in some trials (116,118,120,121) and was more effective than either free doxorubicin or the standard chemotherapy regimens (16,17).

SSL-DOX was also effective in the treatment of breast (122) and ovarian cancers (123,124). In addition, there were fewer problems with patient compliance because of the moderate degree of most toxicities (Subheading 4.2.; 125). SSL-DOX was shown to accumulate in bone metastases from patients with breast carcinomas (126). Rapid-

Table 2  
Liposome- or Lipid-Based Therapeutics for the Treatment of Cancer

<i>Company</i>	<i>Product</i>	<i>Progress</i>
Alza Corporation (Palo Alto, CA)	Doxil: sterically stabilized (Stealth®) liposome formulation of doxorubicin	Approved for the treatment of ovarian cancer and Kaposi's sarcoma
Elan Pharmaceuticals (Dublin, Ireland)	Myocet: eggPC/Chol liposome formulation of doxorubicin TLC ELL-12: liposomal ether lipid	Approved in Europe
Gilead Sciences (Foster City, CA)	DaunoXome: DSPC/Chol liposome formulation of daunorubicin NX 211: Liposomal lurtotecan	Approved for the treatment of Kaposi's sarcoma Phase I: solid tumors, hematological malignancies
Inex Pharmaceuticals (Vancouver, BC, Canada)	Onco TCS: SM/Chol formulation of vincristine INXC-6295: liposomal mitoxantrone INCX-3001: liposomal camptothecins	Phase III: relapsed lymphoma Phase II: small cell lung cancer and first line lymphoma In development In development
Hermes Biosciences, Inc. (San Francisco, CA)	Anti-HER2 directed immunoliposome containing doxorubicin	Scale-up for phase I clinical trials (HER2 breast cancers)
Endovasc Ltd., Inc. (Montgomery, TX)	Liprostin TM: liposomal PGE1 formulation	In development
DepoTech (San Diego, CA)/Skye Pharma PLC (London, UK)	DepoCyt: a sustained-release multivesicular lipid-based formulation of cytosine arabinoside	Approved in US for lymphomatous meningitis
Biomira Inc. (Edmonton, AB, Canada)	Theratope®: MUC1-specific vaccine	Phase III: metastatic breast cancer
Valentis, Inc. (Burlingame, CA)	Cationic lipid-DNA complexes of IL-12 gene Cationic lipid-DNA complexes of IL-2 gene	Phase I/II: head and neck tumors Phase IIa: malignant melanoma (w/superantigen) Phase IIb: head and neck (w/chemotherapy)
Aronex Pharmaceuticals, Inc. (The Woodlands, TX)	Platar (Aroplatin™): liposomal form of <i>cis</i> -Bis-neodecanoato-trans-R,R-1,2-diaminocyclohexane platinum(II) Atragen: liposomal form of all- <i>trans</i> retinoic acid	Phase II: mesothelioma (lung cancer) Phase II: renal cell carcinoma Phase II: Promyelocytic leukemia Phase II: Prostate cancer Phase I/II: Renal cell carcinoma Phase I/II: Bladder cancer

(Continued)

Table 2  
(Continued)

<i>Company</i>	<i>Product</i>	<i>Progress</i>
	Annamycin: lipid-based anthra-cycline formulation (not recognized by MDR transporter)	Phase II: breast cancer
NeoPharm, Inc. (Bannockburn, IL) / Pharmacia (Peapack, NJ)	LEP: liposome-encapsulated paclitaxel LED: liposome-encapsulated doxorubicin	Phase II: various neoplasms  Phase II: prostate and breast cancer

release CL-DOX had similar efficacy against metastatic breast cancer but was administered at almost twice the dose (75 mg/m<sup>2</sup>) as that used for SSL-DOX (127). Elevation to even greater doses (135 mg/m<sup>2</sup> every 3 wk) was not associated with any additional clinical benefit (128). In another study, CL-DOX was combined with cyclophosphamide and 5-fluorouracil to achieve a response rate of 73%, and a median duration of response of approx 11 mo in the treatment of metastatic breast cancer (129). Other combinations are also being enthusiastically explored. A Phase I study combining SSL-DOX with vinorelbine for the treatment of metastatic breast cancer has been completed with relatively few toxicities observed (130). SSL-DOX is also currently being combined with paclitaxel (131,132) or cyclophosphamide (133) for the treatment of metastatic breast cancer in different clinical trials. Combinations of CL-DOX with docetaxel or Herceptin® in clinical trials are also planned. Although both CL-DOX and SSL-DOX have been shown to be effective in treating ovarian and metastatic breast cancer when used as single agents, combinations with drugs having nonoverlapping modes of action or drug resistance may give rise to greater response rates and milder toxicities when compared to standard chemotherapy regimens.

Liposomal doxorubicin (L-DOX) and L-Daunorubicin are being studied in clinical trials in a number of other cancers as well. SSL-DOX was found to be ineffective for the treatment of soft tissue sarcomas (134) or advanced hepatocellular carcinoma (135), despite the mild toxicity profile. Both of these studies were completed with patients who had advanced disease and a poor prognosis. CL-daunorubicin was also ineffective against hepatocellular carcinomas using doses of 100 mg/m<sup>2</sup> every 3 wk (136). CL-daunorubicin is being studied for the treatment of tumors of the central nervous system (137,138), with some effectiveness being noted in early trial results. SSL-DOX is being studied in combination with conventionally fractionated radiotherapy for the treatment of both head-and-neck cancer and non-small cell lung cancer (139). This approach was shown to be feasible, although further study was suggested to determine the exact role of such a combination in the treatment of these cancers.

One of the most promising nonanthracycline liposome formulations is CL-vincristine. Liposomes in this formulation are composed of SM and Chol, and are loaded with vincristine using a pH-gradient method (4,73). Phase I trials have been completed and have shown the liposomal formulation to be considerably less neurotoxic than the free drug (4). In addition, preliminary Phase II trial results for the treatment of non-Hodgkin's lymphomas (NHL) have shown CL-vincristine to be effective against transformed or aggressive NHL, but relatively ineffective in treating indolent NHL (113).

Some preclinical studies have been completed with a SSL-vinorelbine as well, but clinical studies with these or similar formulations have not yet been performed (108,140). A number of other liposomal drugs are also in clinical trials and continue to show promise in the treatment of cancer (Table 2). The full potential of liposomes in increasing the efficacy of antineoplastic agents has yet to be fully realized and further improvements in carrier design and treatment approach should lead to even greater advances in the future.

#### 4.2. Toxicity Profiles of Liposomal Drugs

Liposome encapsulation results in a substantial shift in the toxicity profile of antineoplastic agents. For example, many of the common toxicities associated with free doxorubicin are considerably milder upon encapsulation of the drug inside liposomes (82,90,122,141). These include cardiotoxicity, alopecia, nausea, vomiting, and local tissue necrosis at the site of injection due to extravasation of the drug. Cardiotoxicity is the therapy-limiting toxicity of many anthracyclines (111,142), whereas myelosuppression is often the dose-limiting toxicity (111,143,144) of the free drug. The reduced ability of liposomal drugs to pass through the healthy endothelium into healthy tissues, such as cardiac muscle (145), reduces considerably these toxicities (90,117,141,146,147). Myelosuppression remains the dose-limiting toxicity for the two CL-anthracycline formulations in the clinical setting (84,117,146,148), although at reduced levels when compared to free drug; this toxicity can be partially controlled through the addition of colony-stimulating factors (146). The severity of many of the common toxicities are dependent on the rate of leakage from the liposomal carrier (90,149,150). Liposomes that leak their contents more readily while in the circulation, for example, fast-release systems such as eggPC:Chol, usually have higher degrees of these toxicities. Liposome encapsulation of vincristine was shown to reduce the severity of neurotoxicity observed with the free drug (4) and the association of antitumor ether lipids with liposomes reduces the incidence of hemolytic anemia seen with other formulations of these lipids (151,152).

However, depending on the mode of liposome encapsulation, certain other toxicities may be amplified. For example, with CL formulations, there is a greater risk of acquiring opportunistic infections (153) owing to localization of the drug in RES macrophages and the resulting macrophage toxicity (154–156). This problem is accentuated in immune deficient patients, such as AIDS patients with Kaposi's sarcoma. In patients treated with SSL-DOX, palmar-plantar erythrodysesthesia syndrome, or hand and foot syndrome (H-F syndrome), they become dose limiting (122,157,158). This painful desquamation of the skin on the hands and feet can be overcome by modifying the dose intensity (122,159). In addition, mucositis is also slightly elevated in patients receiving SSL-DOX (15,125,158). However, similar to H-F syndrome, this toxicity can be controlled by simple dose reduction. It is interesting to note that both of these toxicities are also seen in patients treated with prolonged infusions of certain chemotherapeutic drugs, such as doxorubicin (125,160,161). Thus, the increase in these toxicities may result from either increased accumulation of long-circulating SSL in skin or because of the slow release of free doxorubicin from the liposomal carrier over an extended duration of time while in the circulation. Thus, although many of the commonly observed toxicities for free anthracyclines are reduced upon liposome encapsulation, the presence of alternative toxicities prevents dose intensification to achieve greater efficacy.

## 5. ACTIVE TARGETING OF LIPOSOMES

Thus far, we have been concerned primarily with liposomes that are passively targeted to solid tumors owing to their favorable pharmacokinetic parameters and the enhanced permeability of the tumor microvasculature. However, an additional increase in anti-cancer cytotoxicity or antitumor efficacy has been observed in cancers treated with ligand-directed liposomes to tumor-specific antigens located on the surface of cancer cells (9,24,162–167). An important criteria for their enhanced effectiveness is internalization of the bound liposome; this allows the liposomal drug access to the interior of the cancer cell, limits diffusion of the active agent away from the site of action, and results in the degradation of the carrier and, thus, release of the active agent from the confines of its carrier (3,162). Vitamin and growth factor receptors are some of the more attractive targets because of their elevated levels of expression on neoplastic tissues and their ability to be internalized following binding to certain epitopes (24,25,168–170). These types of targets have been the most commonly exploited in our laboratories.

There are many additional barriers to be overcome when actively targeting liposomes *in vivo*. Some preferable characteristics of ligand-targeted liposomal therapeutics and their targeted receptors are given in Table 3. These should be considered in addition to the properties of the carrier described in Table 1 for nontargeted liposomal therapeutics. For example, if liposomal drug formulations were unable to retain their drug while in the circulation, then little clinical benefit would result from active targeting owing to loss of the active agent before reaching the target site. Ligands can be covalently bound to liposomes using a variety of different chemical linkages (171–178). To ensure binding to cell surface receptors, ligands have been placed at the ends of PEG spacers to place them at a significant distance from the liposome surface and thus prevent steric hinderance of binding due to other moieties (44,177), such as the PEG-DSPE used to increase circulation lifetimes *in vivo*. A very important characteristic of the targeting ligand is that it should be relatively nonimmunogenic. The attachment of antibodies to the surface of liposomes, either directly (179), or via a PEG spacer (180–184), has been shown to result in increased clearance and greater accumulation in RES organs. This effect is even more pronounced after repeated administration (180). Fab' fragments can be attached to liposomes in an orientation-specific manner (177,185,186), and are less immunogenic due to their lack of an Fc region which can cause recognition by the Fc receptor on macrophages (187,188). In addition, "humanized" antibody fragments have been conjugated to liposomes in an attempt to further reduce the immunogenicity (9,25,165,177,189). Repeated administration of these liposomes resulted in no observed differences in pharmacokinetic parameters (190). Another important characteristic is the nature of the hydrophobic anchor. As was mentioned above, PEG is often used as a spacer to prevent steric hinderance of the attached ligand to its receptor. However, this spacer can also result in the conjugate being more hydrophilic and thus more readily extracted from the liposome while in the circulation. The conjugate should have a minimum of a distearoylglycero-based lipid anchor to prevent its extraction (191). These characteristics of the liposomal carrier control the disposition *in vivo* and will ultimately help determine its effectiveness as a drug delivery vehicle. Thus, while valuable, the addition of targeting ligands to the liposome formulation results in a considerable increase in the complexity of drug delivery with a significant number of new *in vivo* barriers to overcome.

**Table 3**  
**Desirable Ligand-Targeted Liposomal Therapeutics**

<i>Component</i>	<i>Considerations for optimum design</i>
<i>Target antigen</i>	<p><i>Expression:</i> Highly and homogeneously overexpressed in target tissue</p> <p><i>Function:</i> Vital to tumor progression, so that down-modulation does not occur or is associated with therapeutic benefit</p> <p><i>Shedding of antigen:</i> Limited, to avoid binding to soluble antigen and accelerated clearance</p>
<i>Targeting ligand</i>	<p><i>Affinity:</i> High enough to ensure binding at low liposome concentrations Low enough to avoid "binding-site barrier" effect (Weinstein)</p> <p><i>Immunogenicity:</i> Humanized MAb, to remove murine sequences. Use fragments without Fc portion (Fab', scFv) to avoid interaction with Fc receptor Small molecular weight ligands should not be immunogenic; may act as haptens</p> <p><i>Internalization:</i> Efficient endocytosis by target cells is desirable for increasing drug release from the carrier Drug should be stable following internalization or able to efficiently escape the endosomal and lysosomal compartments (e.g., pH-sensitive liposomes)</p> <p><i>Production:</i> Easy and economical scale-up, e.g., by efficient bacterial expression system Stable during storage</p>
<i>Membrane anchor</i>	<p><i>Stability:</i> Covalent attachment to hydrophobic anchor, stable in blood Protein ligands are stable during storage</p> <p><i>Attachment site</i> Away from the binding site, to ensure correct orientation of antibody or ligand molecule. Well-defined, to ensure reproducibility and uniformity of coupling Avoids steric hindrance (e.g., from PEG) of ligand binding and internalization Potential for being inserted into preformed and drug-loaded liposomes</p> <p><i>Chemical nature of the linker</i> Non-toxic, non-immunogenic, and avoids opsonization Does not affect drug loading or membrane stability Excess linker may be quenched to avoid non-specific coupling to bio molecules Good availability, economical manufacturing process</p>

The antigen being targeted should be located on the cell surface, be overexpressed on tumors and minimally expressed on healthy tissues having access to the vasculature, preferably be endocytosed following liposome binding, be vital to tumor progression so that the targeted antigen is not completely downmodulated, and have limited shedding. The accessibility of the targeted receptor is also a serious consideration. Targets that are readily accessible, such as those having direct exposure to the vasculature are in theory more attractive for active targeting. Small metastases, hematological cancers, and endothelial cells are examples of this class of targets and have been targeted using ligand-directed liposomes (163,164,182,192–194). However, when considering targets such as small metastases or hematological cancers, the heterogeneity of expression becomes very important. The failure of a certain subset of tumor cells or metastases to express the desired receptor may result in a population of resistant tumors.

Solid tumors are thought to be relatively more difficult to treat because of the poor penetration of liposomes into the tumor mass (95) and owing to the binding site barrier (195–197) whereby targeted liposomes are localized to target receptors on the surface of the tumor mass. However, by using small molecular weight and low-affinity ligands to target receptors on the tumor surface liposomes are able to partially bypass the binding site barrier and distribute more uniformly within the tumor (Kirpotin et al., unpublished observations) (3,24). The enhanced activity in solid tumors may be because of an enhanced bioavailability of the drug following degradation in the lysosomes of cancer cells and the reduced diffusion of released drug from the tumor. Solid tumors will likely suffer less from receptor heterogeneity because neighboring nonoverexpressing cancer cells may be killed by drug released from adjacent or dying cells: the bystander effect. One important consideration when targeting internalizing receptors is the stability of the drug to be encapsulated. Because endocytosis often results in accumulation of liposomes in the degradative and acidic environment of late endosomes and lysosomes, a therapeutic agent labile under these conditions may be ineffective (198). It should be noted that, unlike targeting more accessible antigens, liposomes targeted to receptors on solid tumors do not accumulate in these tumors to an extent greater than for similar nontargeted formulations (102,189). This suggests that accumulation of targeted liposomes in solid tumors is limited not by specific binding to cell surface receptors, but by the rate of extravasation across the tumor microvasculature and the degree of trapping in these tumors owing to the lack of a functioning lymphatics. It also suggests that the observed increases in efficacy are caused by differences in the bioavailability and distribution of the drug in the tumor following extravasation. These results with solid tumors are encouraging and suggest that, using optimized liposome constructs, other solid tumors may be effectively targeted in the future.

## 6. CONCLUSIONS

Great progress has been and is continuing to be made in the development of liposomal drugs for treating human malignancies. Greater optimization of physical properties controlling both pharmacokinetic parameters of liposomal drugs and drug release rates from liposomal carriers are still needed and could yield even greater increases in the therapeutic index of these drugs. Combinations of liposomal drugs or conventional free drugs with liposomal drugs need to be explored further in the clinical setting, and many of these studies are currently underway with the anthracycline formulations Doxil® or Evacet™. Tremendous opportunities also remain in increasing the specificity of deliv-

ery by ligand-directed targeting of liposomes to tumor-specific antigens located on tumor cell surfaces. The mechanisms affecting their delivery in vivo have yet to be fully explored and continued study in this area is needed. Finally, advances in the development of delivery systems for therapeutic genes and antisense oligonucleotides using cationic lipid-based formulations are beginning to offer promise for the development of complimentary therapies. The considerable achievements in the liposome field over the past several decades, and the excitement of the yet unknown, provide significant promise and opportunity that drug delivery systems such as liposomes will provide unprecedented increases in the therapeutic index of anticancer drugs and give rise to great improvements in the overall quality of life for cancer patients.

### ACKNOWLEDGMENTS

This work was supported in part by grants from the NIH (1R01CA72452 & 1R01CA71653-01) and the California Breast Cancer Research Program (2CB-0004). The work of Daryl C. Drummond is supported by a postdoctoral fellowship from the Breast Cancer Research Program of the University of California, Grant Number 4FB-0154.

### REFERENCES

1. Gabizon AA. Clinical trials of liposomes as carriers of chemotherapeutic agents: synopsis and perspective, in *Medical Applications of Liposomes* (Lasic DD, Papahadjopoulos D, eds). Elsevier Science B.V., New York, 1998, pp 625–634.
2. Martin FJ. Clinical pharmacology and antitumor efficacy of DOXIL (pegylated liposomal doxorubicin), in *Medical Applications of Liposomes* (Lasic DD, Papahadjopoulos D, eds). Elsevier Science B.V., New York, 1998, pp 635–688.
3. Drummond DC, Meyer OM, Hong K, Kirpotin DB, Papahadjopoulos D. Optimizing liposomes for delivery of chemotherapeutic agents to solid tumors. *Pharmacol Rev* 1999; 51:691–743.
4. Gelmon KA, Tolcher A, Diab AR, et al. Phase I study of liposomal vincristine. *J Clin Oncol* 1999; 17:697–705.
5. Hobbs SK, Monsky WL, Yuan F, et al. Regulation of transport pathways in tumor vessels: role of tumor type and microenvironment. *Proc Natl Acad Sci USA* 1998; 95:4607–4612.
6. Huang SK, Martin FJ, Jay G, Vogel J, Papahadjopoulos D, Friend DS. Extravasation and transcytosis of liposomes in Kaposi's sarcoma-like dermal lesions of transgenic mice bearing the HIV Tat gene. *Am J Path* 1993; 143:10–14.
7. Yuan F, Lwunig M, Huang SK, Berk DA, Papahadjopoulos D, Jain RK. Microvascular permeability and interstitial penetration of sterically stabilized (stealth) liposomes in a human tumor xenograft. *Cancer Res* 1994; 54:3352–3356.
8. Yuan F, Dellian M, Fukumura D, et al. Vascular permeability in a human tumor xenograft: molecular size dependence and cutoff size. *Cancer Res* 1995; 55:3752–3756.
9. Park JW, Hong K, Kirpotin DB, Meyer O, Papahadjopoulos D, Benz CC. Anti-HER2 immunoliposomes for targeted therapy of human tumors. *Cancer Lett* 1997; 118:153–160.
10. Horowitz AR, Barenholz Y, Gabizon AA. In vitro cytotoxicity of liposome-encapsulated doxorubicin: dependence on liposome composition and drug release. *Biochim Biophys Acta* 1992; 1109:203–209.
11. Vaage J, Donovan D, Working P, Uster P. Cellular distribution of DOXIL<sup>®</sup> within selected tissues, assessed by confocal laser scanning microscopy, in *Medical Applications of Liposomes* (Lasic D, Papahadjopoulos D, ed). Elsevier Science B.V., New York, 1998, pp 275–282.
12. Hwang KJ, Liposome pharmacokinetics, in *Liposomes: from biophysics to therapeutics* (Ostro MJ, ed). Marcel Dekker, New York, 1987, pp 109–156.
13. Allen TM, Hansen CB, Lopes de Menezes DE. Pharmacokinetics of long-circulating liposomes. *Adv Drug Del Rev* 1995; 16:267–284.
14. Allen TM, Stuart DD. Liposome pharmacokinetics. Classical, sterically-stabilized, cationic liposomes and immunoliposomes, in *Liposomes: Rational Design* (Janoff AS, ed). Marcel Dekker, New York, 1999, pp 63–87.



15. Gabizon A, Catane R, Uziely B, Kaufman B, Safra T. Prolonged circulation time and enhanced accumulation in malignant exudates of doxorubicin encapsulated in polyethylene-glycol coated liposomes. *Cancer Res* 1994; 54:987–992.
16. Northfelt DW, Dezube BJ, Thommes JA, et al. Pegylated-liposomal doxorubicin versus doxorubicin, bleomycin, and vincristine in the treatment of AIDS-related Kaposi's sarcoma: results of a randomized phase III clinical trial. *J Clin Oncol* 1998; 16:2445–2551.
17. Stewart S, Jablonowski H, Goebel FD, et al. Randomized comparative trial of pegylated liposomal doxorubicin versus bleomycin and vincristine in the treatment of AIDS-related Kaposi's sarcoma. *J Clin Oncol* 1998; 16:683–691.
18. Klibanov AL, Maruyama K, Torchilin VP, Huang L. Amphipathic polyethyleneglycols effectively prolong the circulation time of liposomes. *FEBS Lett* 1990; 268:235–237.
19. Papahadjopoulos D, Allen TM, Gabizon A, et al. Sterically stabilized liposomes: improvements in pharmacokinetics and antitumor therapeutic efficacy. *Proc Natl Acad Sci USA* 1991; 88:11,460–11,464.
20. Allen TM, Newman MS, Woodle MC, Mayhew E, Uster PS. Pharmacokinetics and anti-tumor activity of vincristine encapsulated in sterically stabilized liposomes. *Int J Cancer* 1995; 62:199–204.
21. Woodle MC. Controlling liposome blood clearance by surface-grafted polymers. *Adv Drug Del Rev* 1998; 32:139–152.
22. Bally MB, Lim H, Cullis PR, Mayer LD. Controlling the drug delivery attributes of lipid-based drug formulations. *J Liposome Res* 1998; 8:299–335.
23. Barenholz Y. Design of liposome-based drug carriers: from basic research to application as approved drugs, in *Medical Applications of Liposomes* (Lasic DD, Papahadjopoulos D, eds). Elsevier Science B.V., New York, 1998, pp 545–565.
24. Kirpotin DB, Park JW, Hong K, et al. Targeting of liposomes to solid tumors: the case of sterically stabilized anti-HER2 immunoliposomes. *J Liposome Res* 1997; 7:391–417.
25. Park JW, Hong K, Kirpotin DB, Papahadjopoulos D, Benz CC. Immunoliposomes for cancer treatment. *Adv Pharmacol* 1997; 40:399–435.
26. Senior JH. Fate and behaviour of liposomes in vivo: a review of controlling factors. *CRC Crit Rev Therap Drug Carrier System* 1987; 3:123–193.
27. Abra RM, Hunt CA. Liposome disposition in vivo. III. Dose and vesicle-size effects. *Biochim Biophys Acta* 1981; 666:493–503.
28. Ishida O, Maruyama K, Sasaki K, Iwatsuru M. Size-dependent extravasation and interstitial localization of polyethyleneglycol liposomes in solid tumor-bearing mice. *Int J Pharmaceut* 1999; 190:49–56.
29. Senior JH. Medical applications of multivesicular lipid-based particles: DepoFoam™ encapsulated drugs, in *Medical Applications of Liposomes* (Lasic DD, Papahadjopoulos D, eds). Elsevier Science B.V., New York, 1998, pp 733–750.
30. Johnson EM, Ojwang JO, Szekely A, Wallace TL, Warnock DW. Comparison of in vitro antifungal activities of free and liposome-encapsulated nystatin with those of four amphotericin B formulations. *Antimicrob Agents Chemother* 1998; 42:1412–1416.
31. Woodle MC, Matthey KK, Newman MS, et al. Versatility in lipid compositions showing prolonged circulation with sterically stabilized liposomes. *Biochim Biophys Acta* 1992; 1105:193–200.
32. Ahl PL, Bhatia SK, Meers P, et al. Enhancement of the in vivo circulation lifetime of L-alpha-distearoylphosphatidylcholine liposomes: importance of liposomal aggregation versus complement opsonization. *Biochim Biophys Acta* 1997; 1329:370–382.
33. Senior J, Crawley JCW, Gregoriadis G. Tissue distribution of liposomes exhibiting long half-lives in the circulation after intravenous injection. *Biochim Biophys Acta* 1985; 839:1–8.
34. Gabizon A, Papahadjopoulos D. Liposome formulations with prolonged circulation time in blood and enhanced uptake in tumors. *Proc Natl Acad Sci USA* 1988; 85:6949–6953.
35. Allen TM, Hansen C, Martin F, Redemann C, Yau-Young A. Liposomes containing synthetic lipid derivatives of poly(ethylene glycol) show prolonged circulation half-lives in vivo. *Biochim Biophys Acta* 1991; 1066:29–36.
36. Gabizon A, Chemla M, Tzemach D, Horowitz AT, Goren D. Liposome longevity and stability in circulation: effects on the in vivo delivery to tumors and therapeutic efficacy of encapsulated anthracyclines. *J Drug Target* 1996; 3:391–398.
37. Gregoriadis G, Senior J. The phospholipid component of small unilamellar liposomes controls the rate of clearance of entrapped solutes from the circulation. *FEBS Lett* 1980; 119:43–46.
38. Patel HM. Serum opsonins and liposomes: their interaction and opsonophagocytosis. *CRC Crit Rev Therap Drug Carrier System* 1992; 9:39–90.

39. Semple SC, Chonn A. Liposome-blood protein interactions in relation to liposome clearance. *J Liposome Res* 1996; 6:33–60.
40. Moghimi SM, Patel HM. Serum opsonins and phagocytosis of saturated and unsaturated phospholipid liposomes. *Biochim Biophys Acta* 1989; 984:384–387.
41. Allen TM. A study of phospholipid interactions between high-density lipoproteins and small unilamellar vesicles. *Biochim Biophys Acta* 1981; 640:385–397.
42. Damen J, Regts J, Scherphof G. Transfer and exchange of phospholipid between small unilamellar liposomes and rat plasma high density lipoproteins: dependence on cholesterol content and phospholipid composition. *Biochim Biophys Acta* 1981; 665:538–545.
43. Allen TM. The use of glycolipids and hydrophilic polymers in avoiding rapid uptake of liposomes by the mononuclear phagocyte system. *Adv Drug Del Rev* 1994; 13:285–309.
44. Klibanov AL, Maruyama K, Beckerleg AM, Torchilin VP, Huang L. Activity of amphipathic poly(ethylene glycol) 5000 to prolong the circulation time of liposomes depends on the liposome size and is unfavorable for immunoliposomes binding to target. *Biochim Biophys Acta* 1991; 1062:142–148.
45. Lasic DD, Martin FJ, Gabizon A, Huang SK, Papahadjopoulos D. Sterically stabilized liposomes: a hypothesis on the molecular origin of the extended circulation times. *Biochim Biophys Acta* 1991; 1070:187–192.
46. Needham DKH, McIntosh TJ, Dewhirst M, Lasic DD. Polymer-grafted liposome: physical basis for the “stealth” property. *J Liposome Res* 1992; 2:411–430.
47. Needham D, Zhelev DV, McIntosh TJ. Surface chemistry of the sterically stabilized PEG-liposome, in *Liposomes: Rational Design* (Janoff AS, ed). Marcel Dekker, New York, 1999, pp 13–62.
48. Barenholz Y, Cohen R. Rational design of amphiphile-based drug carriers and sterically stabilized carriers. *J Liposome Res* 1995; 5:905–932.
49. Lasic DD, Ceh B, Stuart MCA, Guo L, Frederik PM, Barenholz Y. Transmembrane gradient driven phase transitions within vesicles: lessons for drug delivery. *Biochim Biophys Acta* 1995; 1239:145–156.
50. Haran G, Cohen R, Bar LK, Barenholz Y. Transmembrane ammonium sulfate gradients in liposomes produce efficient and stable entrapment of amphiphathic weak bases. *Biochim Biophys Acta* 1993; 1151:201–215.
51. Fenske DB, Wong KF, Maurer E, et al. Ionophore-mediated uptake of ciprofloxacin and vincristine into large unilamellar vesicles exhibiting transmembrane ion gradients. *Biochim Biophys Acta* 1998; 1414:188–204.
52. Cullis PR, Hope MJ, Bally MB, Madden TD, Mayer LD, Fenske DB. Influence of pH gradients on the transbilayer transport of drugs, lipids, peptides and metal ions into large unilamellar vesicles. *Biochim Biophys Acta* 1997; 1331:187–211.
53. Madden TD, Harrigan PR, Tai LCL, et al. The accumulation of drugs within large unilamellar vesicles exhibiting a proton gradient: a survey. *Chem Phys Lipids* 1990; 53:37–46.
54. Mayer LD, Bally MB, Hope MJ, Cullis PR. Uptake of antineoplastic agents into large unilamellar vesicles in response to a membrane potential. *Biochim Biophys Acta* 1985; 816:294–302.
55. Bally MB, Nayar R, Masin D, Hope MJ, Cullis PR, Mayer L. Liposomes with entrapped doxorubicin exhibit extended blood residence times. *Biochim Biophys Acta* 1990; 1023:133–139.
56. Gabizon AA, Barenholz Y, Bialer M. Prolongation of the circulation time of doxorubicin encapsulated in liposomes containing polyethylene glycol-derivatized phospholipid: pharmacokinetic studies in rodents and dogs. *Pharm Res* 1993; 10:703–708.
57. Allison BA, Pritchard PH, Richter AM, Levy JG. The plasma distribution of benzoporphyrin derivative and the effects of plasma lipoproteins on its biodistribution. *Photochem Photobiol* 1990; 52:501–507.
58. Sharma A, Sharma US, Straubinger RM. Paclitaxel-liposomes for intracavitary therapy of intraperitoneal P388 leukemia. *Cancer Lett* 1996; 107:265–272.
59. Sharma A, Mayhew E, Bolcsak L, Cavanaugh C, Harmon P. Activity of paclitaxel liposome formulations against human ovarian tumor xenografts. *Int J Cancer* 1997; 71:103–107.
60. Reddi E. Role of delivery vehicles for photosensitizers in the photodynamic therapy of tumors. *J Photochem Photobiol B: Biol* 1997; 37:189–95.
61. Ramaswamy M, Wallace TL, Cossum PA, Wasan KM. Species differences in the proportion of plasma lipoprotein lipid carried by high-density lipoproteins influence the distribution of free and liposomal nystatin in human, dog, and rat plasma. *Antimicrob Agents Chemother* 1999; 43:1424–1428.

62. Zignani M, Drummond DC, Meyer O, Hong K, Leroux JC. In vitro characterization of a novel polymeric-based pH-sensitive liposome system. *Biochim Biophys Acta* 2000; 1463:383–394.
63. Düzgünes N, Straubinger RM, Baldwin PA, Papahadjopoulos D. pH-Sensitive Liposomes: Introduction of foreign substances into cells, in *Membrane Fusion* (Wilschut J, Hoekstra D, eds). Marcel Dekker, New York, 1991, pp 713–730.
64. Litzinger DC, Huang L. Phosphatidylethanolamine liposomes: drug delivery, gene transfer, and immunodiagnostic applications. *Biochim Biophys Acta* 1992; 1113:201–227.
65. Torchilin VP, Zhou F, Huang L. pH-Sensitive liposomes. *J Liposome Res* 1993; 3:201–255.
66. Huang SK, Stauffer PR, Hong K, et al. Liposomes and hyperthermia in mice: increased tumor uptake and therapeutic efficacy of doxorubicin in sterically stabilized liposomes. *Cancer Res* 1994; 54:2186–2191.
67. Gaber MH, Wu NZ, Hong K, Huang SK, Dewhirst MW, Papahadjopoulos D. Thermosensitive liposomes: extravasation and release of contents in tumor microvascular networks. *Int J Radiat Oncol Biol Phys* 1996; 36:1177–1187.
68. Gaber MH, Hong K, Huang SK, Papahadjopoulos D. Thermosensitive sterically stabilized liposomes: formulation and in vitro studies on the mechanism of doxorubicin release by bovine serum and human plasma. *Pharm Res* 1995; 12:1407–1416.
69. Wiley JS, Jones SP, Sawyer WH, Paterson ARP. Cytosine arabinoside influx and nucleoside transport sites in acute leukemia. *J Clin Invest* 1982; 69:479–489.
70. Plageman PGW, Marz R, Wohlhueter RM. Transport and metabolism of deoxycytidine and 1- $\beta$ -D-arabinofuranosyl-cytosine into cultured Novikoff rap hepatoma cells, relationship to phosphorylation, and regulation of triphosphate synthesis. *Cancer Res* 1978; 38:978–989.
71. Westerhof GR, Rijnbouts S, Schornagel JH, Pinedo HM, Peters GJ, Jansen G. Functional activity of the reduced folate carrier in KB, MA104, and IGROV-I cells expressing folate binding protein. *Cancer Res* 1995; 55:3795–3802.
72. Westerhof GR, Jansen G, van Emmerik N, et al. Membrane transport of natural folates and antifolate compounds in murine L1210 Leukemia cells: role of carrier- and receptor-mediated transport systems *Cancer Res* 1991; 51:5507–5513.
73. Webb MS, Harasym TO, Masin D, Bally MB, Mayer LD. Sphingomyelin-cholesterol liposomes significantly enhance the pharmacokinetic and therapeutic properties of vincristine in murine and human tumour models. *Br J Cancer* 1995; 72:896–904.
74. Li X, Cabral-Lilly D, Janoff AS, Perkins WR. Complexation of internalized doxorubicin into fiber bundles affects its release rate from liposomes. *J Liposome Res* 2000; 10:15–27.
75. Maurer-Spurej E, Wong KF, Maurer N, Fenske DB, Cullis PR. Factors influencing uptake and retention of amino-containing drugs in large unilamellar vesicles exhibiting transmembrane pH gradients. *Biochim Biophys Acta* 1999; 1416:1–10.
76. Mui BL-S, Cullis PR, Pritchard PH, Madden TD. Influence of plasma on the osmotic sensitivity of large unilamellar vesicles prepared by extrusion. *J Biol Chem* 1994; 269:7364–7370.
77. Adlakha-Hutcheon G, Bally MB, Shew CR, Madden TD. Controlled destabilization of a liposomal drug delivery system enhances mitoxantrone antitumor activity. *Nature Biotech* 1999; 17:775–779.
78. Kirpotin D, Hong K, Mullah N, Papahadjopoulos D, Zalipsky S. Liposomes with detachable polymer coating: destabilization and fusion of dioleoylphosphatidylethanolamine vesicles triggered by cleavage of surface-grafted poly(ethylene glycol). *FEBS Lett* 1996; 388:115–118.
79. Zalipsky S, Qazen M, Walker JA, 2nd, Mullah N, Quinn YP, Huang SK. New detachable poly(ethylene glycol) conjugates: cysteine-cleavable lipopolymers regenerating natural phospholipid, diacyl phosphatidylethanolamine. *Bioconj Chem* 1999; 10:703–707.
80. Pak CC, Erukulla RK, Ahl PL, Janoff AS, Meers P. Elastase activated liposomal delivery to nucleated cells. *Biochim Biophys Acta* 1999; 1419:111–126.
81. Mayhew EG, Lasic D, Babbar S, Martin FJ. Pharmacokinetics and antitumor activity of epirubicin encapsulated in long-circulating liposomes incorporating a polyethylene glycol-derivatized phospholipid. *Int J Cancer* 1992; 51:302–309.
82. Working PK, Dayan AD. Pharmacological-toxicological expert report – Caelyx™. (Stealth® liposomal doxorubicin HCl) – Foreword. *Hum Exp Toxicol* 1996; 15:751–785.
83. Parr MJ, Masin D, Cullis PR, Bally MB. Accumulation of liposomal lipid and encapsulated doxorubicin in murine lewis lung carcinoma: the lack of beneficial effects of coating liposomes with poly(ethylene glycol). *J Pharmacol Exp Therapeut* 1997; 280:1319–1327.
84. Cowens JW, Creaven PJ, Greco WR, et al. Initial clinical (phase I) trial of TLC D-99 (doxorubicin encapsulated in liposomes). *Cancer Res* 1993; 53:2796–2802.

85. Gill PS, Espina BM, Muggia F, Cabriaes S, Tulpule A, Esplin JA, Phase I/II clinical and pharmacokinetic evaluation of liposomal daunorubicin. *J Clin Oncol* 1995; 13:996–1003.
86. Northfelt DW, Martin FJ, Working P, et al. Doxorubicin encapsulated in liposomes containing surface-bound polyethylene glycol: pharmacokinetics, tumor localization, and safety in patients with AIDS-related Kaposi's Sarcoma. *J Clin Pharmacol* 1996; 36:55–63.
87. Gabizon A, Goren D, Horowitz AT, Tzemach D, Lossos A, Siegal T. Long-circulating liposomes for drug delivery in cancer therapy: A review of biodistribution studies in tumor-bearing animals. *Adv Drug Del Rev* 1997; 24:337–344.
88. Forssen EA, Coulter DM, Proffitt RT. Selective in vivo localization of daunorubicin small unilamellar vesicles in solid tumors. *Cancer Res* 1992; 52:3255–3261.
89. Huang SK, Mayhew E, Gilani S, Lasic DD, Martin FJ, Papahadjopoulos D. Pharmacokinetics and therapeutics of sterically stabilized liposomes in mice bearing C-26 colon carcinoma. *Cancer Res* 1992; 52:6774–6781.
90. Mayer LD, Tai LCL, Ko DSC, et al. Influence of vesicle size, lipid composition, and drug-to-lipid ratio on the biological activity of liposomal doxorubicin in mice. *Cancer Res* 1989; 49:5922–5930.
91. Laverman P, Boerman OC, Oyen, WJG, Dams ETM, Storm G, Corstens FHM. Liposomes for scintigraphic detection of infection and inflammation. *Adv Drug Del Rev* 1999; 37:225–235.
92. Bakker-Woudenberg IAJM, Lokerse AF, Kate MTt, Storm G. Enhanced localization of liposomes with prolonged blood circulation time in infected lung tissue. *Biochim Biophys Acta* 1992; 1138:318–326.
93. Oyen WJG, Boerman OC, Storm G, et al. Detecting infection and inflammation with technetium-99m-labeled Stealth® liposomes. *J Nucl Med* 1996; 37:1392–1397.
94. Jain RK. Delivery of molecular medicine to solid tumors. *Science* 1996; 271:1079–1080.
95. Huang SK, Lee K-D, Hong K, Friend DS, Papahadjopoulos D. Microscopic localization of sterically stabilized liposomes in colon carcinoma-bearing mice. *Cancer Res* 1992; 52:5135–5143.
96. Matsumura Y, Maeda H. A new concept for macromolecular therapeutics in cancer chemotherapy: mechanism of tumorotropic accumulation of proteins and the antitumor agent. SMANCS *Cancer Res* 1986; 46:6387–6392.
97. Maeda H, Matsumura Y. Tumorotropic and lymphotropic principles of macromolecular drugs. *CRC Crit Rev Therap Drug Carrier Syst* 1989; 6:193–210.
98. Mayer LD, Dougherty G, Harasym TO, Bally MB. The role of tumor-associated macrophages in the delivery of liposomal doxorubicin to solid murine fibrosarcoma tumors. *J Pharmacol Exp Therapeut* 1997; 280:1406–1414.
99. Mayer LD, Cullis PR, Bally MB. Designing therapeutically optimized liposomal anticancer delivery systems: lessons from conventional liposomes, in *Medical Applications of Liposomes* (Papahadjopoulos LA, ed). Elsevier Science B.V., New York, 1998.
100. Harasym TO, Cullis PR, Bally MB. Intratumor distribution of doxorubicin following i.v. administration of drug encapsulated in egg phosphatidylcholine/cholesterol liposomes. *Cancer Chemother Pharmacol* 1997; 40:309–317.
101. Siegal T, Horowitz A, Gabizon A. Doxorubicin encapsulated in sterically stabilized liposomes for the treatment of a brain tumor model: biodistribution and therapeutic efficacy. *J Neurosurg* 1995; 83:1029–1037.
102. Goren D, Horowitz AT, Zalipsky S, Woodle MC, Yarden Y, Gabizon A. Targeting of stealth liposomes to erbB-2 (Her/2) receptor: In vitro and in vivo studies. *Br J Cancer* 1996; 74:1749–1756.
103. Krishna R, St-Louis M, Mayer LD. Increased intracellular drug accumulation and complete chemosensitization achieved in multidrug-resistant solid tumors by co-administering valspodar (PSC 833) with sterically stabilized liposomal doxorubicin. *Int J Cancer* 2000; 85:131–141.
104. Allen TM, Mehra T, Hansen C, Chin YC. Stealth liposomes: an improved sustained release system for 1-β-D-arabinofuranosylcytosine. *Cancer Res* 1992; 52:2431–2439.
105. Colbern GT, Dykes DJ, Engbers C, et al. Encapsulation of the topoisomerase I inhibitor GL147211C in pegylated (STEALTH) liposomes: pharmacokinetics and antitumor activity in HT29 colon tumor xenografts. *Clin Cancer Res* 1998; 4:3077–3082.
106. Cabanes A, Even-Chen S, Zimberoff J, Barenholz Y, Kedar E, Gabizon A. Enhancement of antitumor activity of polyethylene glycol-coated liposomal doxorubicin with soluble and liposomal interleukin 2. *Clin Cancer Res* 1999; 5:687–693.
107. Newman MS, Colbern GT, Working PK, Engbers C, Amantea M. Comparative pharmacokinetics, tissue distribution, and therapeutic effectiveness of cisplatin encapsulated in long-circulating, pegylated liposomes (SPI-077) in tumor-bearing mice. *Cancer Chemother Pharmacol* 1999; 43:1–7.

108. Colbern G, Vaage J, Donovan D, Uster P, Working P. Tumor uptake and therapeutic effects of drugs encapsulated in long-circulating pegylated STEALTH® liposomes. *J Liposome Res* 2000; 10:81–92.
109. Unezaki S, Mauryama K, Ishida O, Suginaka A, Jun-ichi H, Iwatsuru M. Enhanced tumor targeting and improved antitumor activity of doxorubicin by long-circulating liposomes containing amphipathic poly(ethylene glycol). *Int J Pharmaceut* 1995; 126:41–48.
110. Chang CW, Barber L, Ouyang C, Masin D, Bally MB, Madden TD. Plasma clearance, biodistribution and therapeutic properties of mitoxantrone encapsulated in conventional and sterically stabilized liposomes after intravenous administration in BDF1 mice. *Br J Cancer* 1997; 75:169–177.
111. Doroshaw JH, Anthracyclines and anthracenediones, in *Cancer chemotherapy and biotherapy: principles and practice* (Chabner BA, Longo DL, eds). Lippincott-Raven, Philadelphia, 1996, pp 409–433.
112. Young RC, Ozols RF, Myers CE. The anthracycline antineoplastic drugs. *N Engl J Med* 1981; 305:139–153.
113. Sarris AH, Hagemester F, Romaguera J, et al. Liposomal vincristine in relapsed non-Hodgkin's lymphomas: early results of an ongoing phase II trial. *Ann Oncol* 2000; 11:69–72.
114. Kruszewski S, Chavan AS, Gryczynski I, Lakowicz JR, Burke TG. Comparison of the human blood chemistry of free versus liposomal forms of the clinically-relevant topoisomerase I inhibitor lurtotecan (GI147221). *Am Assoc Cancer Res* 2000; 41:A2056.
115. Gelmon KA, Eisenhauer E, Renyo L, et al. Phase I study of NX211 (liposomal lurtotecan) given as an intravenous infusion on days 1 2 & 3 every 3 weeks in patients with solid tumors- and NCIC Clinical Trials Group study. *Am Assoc Cancer Res* 2000; 41:A3879.
116. Amantea MA, Forrest A, Northfelt DW, Mamelok R. Population pharmacokinetics and pharmacodynamics of pegylated-liposomal doxorubicin in patients with AIDS-related Kaposi's sarcoma. *Clin Pharmacol Therap* 1997; 61:301–311.
117. Gill PS, Wernz J, Scadden DT, et al. Randomized phase III trial of liposomal daunorubicin versus doxorubicin, bleomycin, and vincristine in AIDS-related Kaposi's sarcoma. *J Clin Oncol* 1996; 14:2353–2364.
118. Girard PM, Bouchaud O, Goetschel A, Mukwaya G, Eestermans G, Ross M. Phase II study of liposomal encapsulated daunorubicin in the treatment of AIDS-associated mucocutaneous Kaposi's sarcoma. *Aids* 1996; 10:753–757.
119. Presant CA, Scolaro M, Kennedy P, et al. Liposomal daunorubicin treatment of HIV-associated Kaposi's sarcoma. *Lancet* 1993; 341:1242–1243.
120. Tulpule A, Yung RC, Wernz J, et al. Phase II trial of liposomal daunorubicin in the treatment of AIDS-related pulmonary Kaposi's sarcoma. *J Clin Oncol* 1998; 16:3369–3374.
121. Harrison M, Tomlinson D, Stewart S. Liposomal-entrapped doxorubicin: an active agent in AIDS-related Kaposi's sarcoma. *J Clin Oncol* 1995; 13:914–920.
122. Ranson MR, Carmichael J, O'Byrne K, Stewart S, Smith D, Howell A. Treatment of advanced breast cancer with sterically stabilized liposomal doxorubicin: results of a multicenter phase II trial. *J Clin Oncol* 1997; 15:3185–3191.
123. Muggia FM. Clinical efficacy and prospects for use of pegylated liposomal doxorubicin in the treatment of ovarian and breast cancers. *Drugs* 1997; 54:22–29.
124. Muggia FM, Hainsworth JD, Jeffers S, et al. Phase II study of liposomal doxorubicin in refractory ovarian cancer: antitumor activity and toxicity modification by liposomal encapsulation. *J Clin Oncol* 1997; 15:987–993.
125. Alberts DS, Garcia DJ. Safety aspects of pegylated liposomal doxorubicin in patients with cancer. *Drugs* 1997; 54 Suppl. 4:30–35.
126. Symon Z, Peysen A, Tzemach D, et al. Selective delivery of doxorubicin to patients with breast carcinoma metastases by stealth liposomes. *Cancer* 1999; 86:72–78.
127. Harris L, Winer E, Batist G, Rovira D, Navaria R, Lee L. Phase III study of TLC D-99 (liposome encapsulated doxorubicin) vs. free doxorubicin (DOX) in patients with metastatic breast carcinoma (MBC). *Proc Am Soc Clin Oncol* 1998; 17:124a.
128. Shapiro CL, Ervin T, Welles L, Azarnia N, Keating J, Hayes DF. Phase II trial of high-dose liposome-encapsulated doxorubicin with granulocyte colony-stimulating factor in metastatic breast cancer. *J Clin Oncol* 1999; 17:1435–1441.
129. Valero V, Buzdar AU, Theriault RL, et al. Phase II trial of liposome-encapsulated doxorubicin cyclophosphamide, and fluorouracil as first-line therapy in patients with metastatic breast cancer. *J Clin Oncol* 1999; 17:1425–1434.
130. Burstein HJ, Ramirez MJ, Petros WP, et al. Phase I study of Doxil and vinorelbine in metastatic breast cancer. *Ann Oncol* 1999; 10:1113–1116.

131. Woll PJ, Carmichael J, Chan S, Howell A, Ranson M, Miles D, Welbank H. Phase II study results on safety and tolerability of caelyx® (Doxil®) in combination with paclitaxel in the treatment of metastatic breast cancer. *Proc Am Soc Clin Oncol* 1999; 18:A442.
132. Modiano M, Taylor C, Sharpington R, Ng M, Martinez A. Phase I study of Doxil® (pegylated liposomal doxorubicin) plus escalating doses of taxol® in the treatment of patients with advanced breast or gynecologic malignancies. *Proc Am Soc Clin Oncol* 1999; 18:A848.
133. Silverman P, Overmoyer B, Holder L, Tripathy D, Marrs N, Sharpington T. Doxil® and intravenous cyclophosphamide as first-line therapy for patients with metastatic breast cancer (MBC): interim results of an ongoing pilot trial. *Proc Am Soc Clin Oncol* 1999; 18:A435.
134. Garcia AA, Kempf RA, Rogers M, Muggia FM. A phase II study of Doxil (liposomal doxorubicin): lack of activity in poor prognosis soft tissue sarcomas. *Ann Oncol* 1998; 9:1131–1133.
135. Halm U, Etzrodt G, Schiefke I, et al. A phase II study of pegylated liposomal doxorubicin for treatment of advanced hepatocellular carcinoma. *Ann Oncol* 2000; 11:113–114.
136. Yeo W, Chan KK, Mukwaya G, et al. Phase II studies with DaunoXome in patients with nonresectable hepatocellular carcinoma: clinical and pharmacokinetic outcomes. *Cancer Chemother Pharmacol* 1999; 44:124–130.
137. Boiardi A, Pozzi A, Salmaggi A, Eoli M, Zucchetti M, Silvani A. Safety and potential effectiveness of daunorubicin-containing liposomes in patients with advanced recurrent malignant CNS tumors. *Cancer Chemother Pharmacol* 1999; 43:178–179.
138. Zucchetti M, Boiardi A, Silvani A, Parisi I, Piccolrovazzi S, D'Incalci M. Distribution of daunorubicin and daunorubicinol in human glioma tumors after administration of liposomal daunorubicin. *Cancer Chemother Pharmacol* 1999; 44:173–176.
139. Koukourakis MI, Koukouraki S, Giatromanolaki A, et al. Liposomal doxorubicin and conventionally fractionated radiotherapy in the treatment of locally advanced non-small-cell lung cancer and head and neck cancer. *J Clin Oncol* 1999; 17:3512–3521.
140. Kirpotin DB, Park JW, Demetzos K, et al. Stealth® liposomal vinorelbine: synthesis stability and antitumor activity against human breast and lung cancer xenografts. *Proc Am Assoc Cancer Res* 1999a; 40:417.
141. Working PK, Newman MS, Sullivan T, Yarrington J. Reduction of the cardiotoxicity of doxorubicin in rabbits and dogs by encapsulation in long-circulating, pegylated liposomes. *J Pharmacol Exp Therap* 1999; 289:1128–1133.
142. Von Hoff DD, Layard MW, Basa P, et al. Risk factors for doxorubicin-induced congestive heart failure. *Ann Intern Medicine* 1979; 91:710–717.
143. Legha SS, Hortobagyi GN, Benjamin RS. Anthracyclines, in *Cancer Chemotherapy by Infusion* (Lokich JJ, ed). 1 Ed. Precept Press, Inc. Chicago, 1987, pp 130–144.
144. Speth PAJ, van Hoesel QGCM, Haanen C. Clinical pharmacokinetics of doxorubicin. *Clin Pharmacokin* 1988; 15:15–31.
145. Working PK, Newman MS, Huang SK, Mayhew E, Vaage J, Lasic DD. Pharmacokinetics, biodistribution, and therapeutic efficacy of doxorubicin encapsulated in Stealth® liposomes (Doxil®). *J Liposome Res* 1994; 4:667–687.
146. Casper ES, Schwartz GK, Sugarman A, Leung D, Brennan MF. Phase I trial of dose-intense liposome-encapsulated doxorubicin in patients with advanced sarcoma. *J Clin Oncol* 1997; 15:2111–2117.
147. Kanter PM, Bullard GA, Ginsberg RA, et al. Comparison of the cardiotoxic effects of liposomal doxorubicin (TLC D-99) versus free doxorubicin in beagle dogs In vivo. 1993; 7:17–26.
148. Conley BA, Egorin MJ, Whitacre MY, Carter DC, Zuhowski EG. Phase I and pharmacokinetic trial of liposome-encapsulated doxorubicin. *Cancer Chemother Pharmacol* 1993; 33:107–112.
149. Bally MB, Nayar R, Masin D, Cullis PR, Mayer LD. Studies on the myelosuppressive activity of doxorubicin entrapped in liposomes. *Cancer Chemother Pharmacol* 1990; 27:13–19.
150. Oussoren C, Eling WMC, Crommelin DJA, Storm G, Zuidema J. The influence of the route of administration and liposome composition on the potential of liposomes to protect tissue against local toxicity of two antitumor drugs. *Biochim Biophys Acta* 1998; 1369:159–172.
151. Perkins WR, Dause RB, Li X, et al. Combination of antitumor ether lipid with lipids of complementary molecular shapes reduces its hemolytic activity. *Biochim Biophys Acta* 1997; 1327:61–68.
152. Ahmad I, Filep JJ, Franklin JC, et al. Enhanced therapeutic effects of liposome-associated 1-*O*-Octadecyl-2-*O*-methyl-sn-glycero-3-phosphocholine. *Cancer Res* 1997; 57:1915–1921.
153. White RM. Liposomal daunorubicin is not recommended in patients with less than advanced HIV-related Kaposi's sarcoma. *Aids* 1997; 11:1412–1413.
154. Allen TM, Murray L, MacKeigan S, Shah M. Chronic liposome administration in mice: effects on reticuloendothelial function and tissue distribution. *J Pharmacol Exp Therap* 1984; 229:267–275.

155. Daemen T, Hofstede G, Kate MTT, Bakker-Woudenberg IAJM, Scherphof G. Liposomal doxorubicin-induced toxicity: depletion and impairment of phagocytic activity of liver macrophages. *Int J Cancer* 1995; 61:716–721.
156. Daemen T, Regts J, Meesters M, Ten Kate MT, Bakker-Woudenberg IAJM, Scherphof GL. Toxicity of doxorubicin entrapped within long-circulating liposomes. *J Controlled Release* 1997; 44:1–9.
157. Gabizon A, Isacson R, Libson E, et al. Clinical studies of liposome-encapsulated doxorubicin. *Acta Oncol* 1994; 33:779–786.
158. Uziely B, Jeffers S, Isacson R, et al. Liposomal doxorubicin: antitumor activity and unique toxicities during two complementary phase I studies. *J Clin Oncol* 1995; 13:1777–1785.
159. Amantea M, Newman MS, Sullivan TM, Forrest A, Working PK. Relationship of dose intensity to the induction of palmar-plantar erythrodysesthesia by pegylated doxorubicin in dogs. *Hum Exp Toxicol* 1999; 18:17–26.
160. Lokich JJ, Moore C. Chemotherapy-associated palmar-plantar erythrodysesthesia syndrome. *Ann Intern Med* 1984; 101:798–800.
161. Vogelzang NJ, Ratain MJ. Cancer chemotherapy and skin changes. *Ann Intern Med* 1985; 103:303–304.
162. Allen TM, Hansen CB, Stuart DD. Targeted sterically stabilized liposomal drug delivery, in *Medical Applications of Liposomes* (Lasic DD, Papahadjopoulos D, eds). Elsevier Science B.V., New York, 1998, pp 545–565.
163. Ahmad I, Longenecker M, Samuel J, Allen TM. Antibody-targeted delivery of doxorubicin entrapped in sterically stabilized liposomes can eradicate lung cancer in mice. *Cancer Res* 1993; 53:1484–1488.
164. Lopes de Menezes DE, Pilarski LM, Allen TM. In vitro and in vivo targeting of immunoliposomal doxorubicin to human B-cell lymphoma. *Cancer Res* 1998; 58:3320–3330.
165. Park JW, Hong K, Carter P, et al. Development of anti-p185<sup>HER2</sup> immunoliposomes for cancer therapy. *Proc Natl Acad Sci USA* 1995; 92:1327–1331.
166. Tseng Y-L, Hong R-L, Tao M-H, Chang F-H. Sterically stabilized anti-idiotype immunoliposomes improve the therapeutic efficacy of doxorubicin in a murine B-cell lymphoma model. *Int J Cancer* 1999; 80:723–730.
167. Lee RJ, Low PS. Folate-mediated tumor cell targeting of liposome-entrapped doxorubicin in vitro. *Biochim Biophys Acta* 1995; 1233:134–144.
168. Wang S, Low PS. Folate-mediated targeting of antineoplastic drugs, imaging agents, and nucleic acids to cancer cells. *J Control Rel* 1998; 53:39–48.
169. Lee RJ, Low PS. Folate-targeted liposome for drug delivery. *J Liposome Res* 1997; 7:455–466.
170. Drummond DC, Hong K, Park JW, Benz CC, Kirpotin DB. (2000) *Liposome Targeting to Tumors Using Vitamin and Growth Factor Receptors*. Vitamins and Hormones. Edited by Litwack G., in press.
171. Hansen CB, Kao GY, Moase EH, Zalipsky S, Allen TM. Attachment of antibodies to sterically stabilized liposomes: evaluation comparison and optimization of coupling procedures. *Biochimica et Biophysica Acta* 1995; 1239:133–144.
172. Zalipsky S, Gittelman J, Mullah N, Qazen MM, Harding JA. Biologically active ligand-bearing polymer-grafted liposomes, in *Targeting of drugs 6: strategies for stealth therapeutic systems* (Gregoriadis, G., McCormack B. eds). Plenum, New York, 1998, pp 131–138.
173. Zalipsky S, Mullah N, Harding JA, Gittelman J, Guo L, DeFrees SA. Poly(ethylene glycol)-grafted liposomes with oligopeptide or oligosaccharide ligands appended to the termini of the polymer chains. *Bioconj Chem* 1997; 8:111–118.
174. Zalipsky S, Puntambekar B, Boulikas P, Engbers CM, Woodle MC. Peptide attachment to extremities of liposomal surface grafted PEG chains: preparation of the long-circulating form of laminin pentapeptide, YIGSR. *Bioconj Chem* 1995; 6:705–708.
175. Zalipsky S. Functionalized poly(ethylene glycol) for preparation of biologically relevant conjugates. *Bioconj Chem* 1995; 6:150–165.
176. Zalipsky S. Synthesis of an end-group functionalized polyethylene glycol-lipid conjugate for preparation of polymer-grafted liposomes. *Bioconj Chem* 1993; 4:296–299.
177. Kirpotin D, Park JW, Hong K, et al. Sterically stabilized anti-HER2 immunoliposomes: design and targeting to human breast cancer cells in vitro. *Biochemistry* 1997; 36:66–75.
178. Lee RJ, Low PS. Delivery of liposomes into cultured KB cells via folate receptor-mediated endocytosis. *J Biol Chem* 1994; 269:3198–3204.
179. Debs RJ, Heath TD, Papahadjopoulos D. Targeting of anti-Thy 1.1 monoclonal antibody conjugated liposomes in Thy 1.1 mice after intravenous administration. *Biochim Biophys Acta* 1987; 901:183–190.

180. Harding JA, Engbers CM, Newman MS, Goldstein NI, Zalipsky S. Immunogenicity and pharmacokinetic attributes of poly(ethyleneglycol)-grafted immunoliposomes. *Biochim Biophys Acta* 1997; 1327:181–192.
181. Allen TM, Agrawal AK, Ahmad I, Hansen CB, Zalipsky S. Antibody-mediated targeting of long-circulating (Stealth®) liposomes. *J Liposome Res* 1994; 4:1–25.
182. Allen TM, Ahmad I, Lopes de Menezes DE, Moase EH. Immunoliposome-mediated targeting of anti-cancer drugs in vivo. *Biochem Soc Trans* 1995; 23:1073–1079.
183. Mori A, Klibanov AL, Torchilin VP, Huang L. Influence of the steric barrier activity of amphipathic poly(ethyleneglycol) and ganglioside GM1 on the circulation time of liposomes and on the target binding of immunoliposomes in vivo. *FEBS Lett* 1991; 284:263–266.
184. Zalipsky S, Hansen CB, de Menezes DEL, Allen TM. Long-circulating, polyethylene glycol-grafted immunoliposomes. *J Controlled Release* 1996; 39:153–161.
185. Martin FJ, Hubbell WL, Papahadjopoulos D. Immunospecific targeting of liposomes to cells: a novel and efficient method for covalent attachment of Fab' fragments via disulfide bonds. *Biochemistry* 1981; 20:4229–4238.
186. Martin FJ, Papahadjopoulos D. Irreversible coupling of immunoglobulin fragments to preformed vesicles. An improved method for liposome targeting. *J Biol Chem* 1982; 257:286–288.
187. Derksen JTP, Morselt HWM, Scherphof GL. Uptake and processing of immunoglobulin-coated liposomes by subpopulations of rat liver macrophages. *Biochim Biophys Acta* 1988; 971:127–136.
188. Aragnol D, Leserman LD. Immune clearance of liposomes inhibited by an anti-Fc receptor antibody in vivo. *Proc Natl Acad Sci USA* 1986; 83:2699–2703.
189. Kirpotin DB, Park JW, Hong K, et al. Targeting of sterically stabilized liposomes to cancers overexpressing HER2/neu proto-oncogene, in *Medical Applications of Liposomes* (Lasic DD, Papahadjopoulos D, eds). Elsevier Science B.V., New York, 1998, pp 325–345.
190. Park JW, Hong K, Kirpotin DB, et al. Anti-HER2 immunoliposomes: enhanced efficacy attributable to targeted delivery. *Clin Cancer Res* 2002; 8:1172–1181.
191. Parr MJ, Ansell SM, Choi LS, Cullis PR. Factors influencing the retention and chemical stability of poly(ethylene glycol)-lipid conjugates incorporated into large unilamellar vesicles. *Biochim Biophys Acta* 1994; 1195:21–30.
192. Scherphof GL, Kamps JAAM, Koning GA. In vivo targeting of surface-modified liposomes to metastatically growing carcinoma cells and sinusoidal endothelial cells in the rat liver. *J Liposome Res* 1997; 7:419–432.
193. Mori A, Kennel SJ, Waalkes MvB, Scherphof GL, Huang L. Characterization of organ-specific immunoliposomes for delivery of 3',5'-O-dipalmitoyl-5-fluoro-2'-deoxyuridine in a mouse lung-metastasis model. *Cancer Chemother Pharmacol* 1995; 35:447–456.
194. Oku N, Tokudome Y, Koike C, et al. Liposomal Arg-Gly-Asp analogs effectively inhibit metastatic B16 melanoma colonization in murine lungs. *Life Sci* 1996; 58:2263–2270.
195. Fujimori K, Covell DG, Fletcher JE, Weinstein JN. A modeling analysis of monoclonal antibody percolation through tumors: a binding site barrier. *J Nucl Med* 1990; 31:1191–1198.
196. Weinstein JN, Eger RR, Covell DG, et al. The pharmacology of monoclonal antibodies. *Ann NY Acad Sci* 1987; 507:199–210.
197. Jain RK. Delivery of novel therapeutic agents in tumors: physiological barriers and strategies. *J Natl Cancer Inst* 1989; 81:570–576.
198. Huang A, Kennel SJ, Huang L. Interactions of immunoliposomes with target cells. *J Biol Chem* 1983; 258:14,034–14,040.



## Efficacy of Prophylactic Anti-diarrhoeal Treatment in Patients Receiving Campto for Advanced Colorectal Cancer

J. DUFFOUR<sup>1</sup>, S. GOURGOU<sup>1</sup>, J.F. SEITZ<sup>2</sup>, P. SENESSE<sup>1</sup>, O. BOUTET<sup>3</sup>, D. CASTERA<sup>4</sup>, A. KRAMAR<sup>1</sup> and M. YCHOU<sup>1</sup>

<sup>1</sup>CRLC Val d'Aurelle, Paul Lamarque, Montpellier; <sup>2</sup>Hopital La Timone, 264 rue St-Pierre, Marseille; <sup>3</sup>Centre Hospitalier, avenue Alphonse Daudet, Bagnols sur Ceze; <sup>4</sup>Clinique Saint Pierre, rue Jean Gallia, Perpignan, France

**Abstract.** This study assessed the efficacy of combined prophylactic and curative anti-diarrhoeal medication in advanced colorectal patients treated by irinotecan. Thirty-four pre-treated eligible patients were evaluated. There were 44% women, the median age was 65 and 38% of the patients had a 0 performance status. The patients received sucralfate (4g/d) and nifuroxazide (600mg/d) prophylactic treatment on days 0-7. In the case of severe diarrhoea, preventive treatment was replaced by loperamide (12mg/d) and diosmectite (9g/d). Grade 3 delayed diarrhoea occurred in 18% of patients (90%CI: [9.5-28.9]) and 4.6% of cycles. No grade 4 delayed diarrhoea was observed. Twenty-nine patients (85%) received the preventive treatment at cycle 1, while 14% (90%CI: [6.2-25.7]) experienced grade 3 delayed diarrhoea in 3.7% of cycles for a median 4.5 days. The objective response rate was 8% (90%CI [1.4-23.1]) among the 25 assessable patients. Preventive combined treatment is effective in reducing the incidence of severe delayed diarrhoea, and it should be proposed to patients treated with mono-therapy Campto(r) and evaluated in poly-chemotherapy protocols.

Colorectal cancer is one of the most common cancers in the USA and Europe (1). Before the start of our study, treatment with 5FU modulated by folinic acid was the most widely used first-line treatment for patients with metastatic colorectal cancer, allowing a response rate (RR) of about 20% and a median survival of 11 months (2), according to various regimens. Nevertheless, new anticancer drugs were still needed to improve the prognosis of patients who had failed to respond to this first-line 5FU-based chemotherapy.

Irinotecan hydrochloride trihydrate (Campto®) is a potent topoisomerase I inhibitor, that blocks the DNA replication step of the enzyme, leading ultimately to cell death (3, 4) and

demonstrates notable anti-tumour activity, mainly against various solid tumours including colorectal cancer (5-12). Previous monotherapy trials (13-17) have shown the efficacy of irinotecan in patients with advanced colorectal cancer as have combination trials with either fluorouracil and calcium folinate (18), or oxaliplatin, or raltitrexed. The major limiting toxicities associated with irinotecan were mainly diarrhoea and neutropenia. Delayed diarrhoea was a significant side-effect with grade 3-4 occurring in 22% to 41% of patients and 12% of cycles. This diarrhoea, observed usually after the third day, is unpredictable, often correlated with neutropenia and can lead to toxic death from dehydration if an anti-diarrhoeal protocol is not quickly applied (hospitalisation in 6% of the cycles for i.v. rehydration). If this side-effect is taken care of early on, the incidence can be reduced to 25%. This disorder is probably caused by a secretory mechanism with an exsudative (19, 20).

Although several therapeutic measures (21, 22) have been described, high-dose loperamide is considered the standard treatment in Europe and the United States (23) but can induce secondary complications (constipation, subobstruction, microbial pullulation in the intestine lumen with increased risk of sepsis); so this curative treatment must be given promptly, after the first loose stool, for a maximum of 48 consecutive hours.

Preventive treatment by racecadotril (Tiorfan®), a selective inhibitor of enkephalinase, with a specific antisecretory mechanism, has been tested (24). However, it had no effect on delayed diarrhoea and its prophylactic use cannot be recommended.

The present study was designed to evaluate the effect of a 7-day prophylactic treatment with both sucralfate (Ulcara®) (an anti-ulcerous) and nifuroxazide (Erecefuryl®) (antiseptic) on the incidence of campto®-induced delayed diarrhoea (particularly grade 3-4 diarrhoea) and secondarily, to assess the efficacy of combined anti-diarrhoeal curative medication with both loperamide (Imodium®) and diosmectite (Smecta®) on the duration of the delayed diarrhoea (Smecta®, which protects colonic mucosa, is used to decrease the doses of loperamide). The rationale to test this preventive treatment was based on some preclinical studies in mice

*Correspondence to:* Dr Marc Ychou, CRLC Val d'Aurelle, Paul Lamarque, Parc Euromedecine, 34 298 Montpellier cedex 5, France. Tel: (33)4 67 61 31 36, Fax: (33)4 67 61 30 22, e-mail: mychou@valdorel.fr

*Key Words:* Irinotecan, prophylactic treatment, delayed diarrhoea.

showing jejunal villous atrophy after exposure to Campto® and on the role of microbial pullulation.

### Patients and Methods

**Patients.** The patients had to meet the following criteria: histologically-proven metastatic adenocarcinoma of the colon or rectum; documented tumour progression under 5FU-based chemotherapy; more than one bidimensionally measurable target lesion or non-measurable disease; WHO performance status of 2 or less; age 18-75 years; life expectancy  $\geq$  3 months; not less than one previous palliative treatment; a wash out period of at least 4 weeks from the last course of chemotherapy; and written informed consent. Laboratory data requirements for each patient before study entry were as follows: absolute neutrophil count  $\geq$   $2.0 \times 10^3/\text{mm}^3$ , platelet count  $\geq$   $100 \times 10^3/\text{mm}^3$ , haemoglobin level  $\geq$  10 g/dL, serum creatinine level  $\leq$  135  $\mu\text{mol/L}$ , prothrombin time  $\geq$  50%, total bilirubin level  $\leq$  1.5 x IUNL (institutional upper normal limit) and transaminases  $\leq$  2.5 x IUNL.

Patients were excluded for the following reasons: past chronic enteropathy or extensive bowel resection; unresolved diarrhoea or severe uncontrolled infection before inclusion; major organ failure; childbearing potential; history of other cancer (with the exception of excised cervical or basal/squamous skin cell carcinoma); severe diarrhoea during previous treatment (5FU).

**Study design and chemotherapy regimen.** All patients were treated with CPT-11 (Campto®) 350  $\text{mg}/\text{m}^2$  by intravenous infusion for 30 minutes every 3 weeks, with provision for dose reduction or delay in the case of severe toxicity or progression. The patients could be fully evaluated for preventive or curative treatment efficacy after having received at least one cycle. Delayed diarrhoea was defined as any episode of increased frequency of stools occurring after the first 24 hours following irinotecan infusion.

In order to prevent delayed diarrhoea, all patients received preventive treatment from day 0 to day 7 by sucralfate (Ulcars®) (4 g/d) in combination with nifuroxazide (Erecefuryl® 200) (600 mg/d). In spite of this prophylactic medication, if delayed diarrhoea did occur, curative treatment by both loperamide (Imodium®) (12 mg/d) and diosmectite (Smecta®) (9 g/d) was to be administered over 48 hours in place of the former treatment; if diarrhoea lasted for more than 48 hours, and/or was considered serious, then the patients were to be hospitalised and treated supportively as required.

The primary endpoint of this multicenter study was the reduction in the incidence of grade 3-4 Campto®-induced delayed diarrhoea. The secondary endpoints included reduction of the duration of grade 3-4 diarrhoea and confirmation of tumour efficacy (response rate assessment). The efficacy of prophylactic treatment was based on the reduction in the incidence of Campto®-induced delayed diarrhoea and the decrease in the number of patients and/or cycles requiring curative treatment. This data was validated by a self-reported questionnaire filled out every day by the patient. The assessment of curative treatment was based on the duration of early diarrhoea as well as the number of cycles with diarrhoea leading to hospitalisation.

Preventive anti-emetic treatment was given routinely. If a cholinergic syndrome occurred, it was to be treated with atropine 0.25 mg subcutaneously which could be used as a precautionary measure for subsequent cycles.

Tumour responses were determined according to WHO criteria. Changes in performance status, weight and pain were also measured. Toxicity was assessed at each cycle (except haematology weekly) and graded according to WHO (except diarrhoea which was graded according to NCI).

**Statistical considerations.** The incidence of grade 3-4 Campto®-induced delayed diarrhoea is presented as a percentage with a 90% confidence interval (90%CI) obtained from the binomial distribution. If the upper

one-sided 90% confidence interval is less than 25% then this would reflect a significant level of decrease due to prophylactic treatment. It was planned to enter 50 patients into this multicentre study. For this sample size, we would need to observe less than 9 patients with severe delayed diarrhoea for the result to be considered statistically significant and clinically meaningful.

### Results

**Patients characteristics.** A total of 37 patients were included in this study, between May 1997 and May 1999, from five centres in France, two-thirds of which were from one centre. Recruitment was interrupted due to a marked decrease in the accrual rate from small centres. Three patients were considered ineligible: one had incomplete baseline data; one patient had abnormal initial transaminase ALAT levels  $>$  2.5 IUNL and one patient had stopped previous chemotherapy only 2 weeks prior to inclusion as compared to the required minimum 4-week washout period. Thirty-four patients were retained for analysis and are referred to as the intention to treat (ITT) population. Among these patients, 29 received, from the first cycle, at least one cycle of anti-diarrhoeal preventive treatment and were considered assessable for the incidence of delayed diarrhoea (85%). This patient population is referred to as the per-protocol population (PP). Among the 29 patients assessable for diarrhoea, 25 received at least 3 cycles of Campto(r) and were considered assessable for efficacy.

Baseline demographic and pre-treatment characteristics for the ITT population are presented in Table I. One half (17 patients) were symptomatic at study entry, while three were locally recurrent. Among the 5 patients who received a previous adjuvant regimen, the median delay between the last cycle and inclusion was 7 months (range: 5.5-27.9). Median follow-up was 12 months.

**Campto® drug exposure.** A total of 139 cycles of Campto® were administered in the ITT population; 14 patients (41%) received 6 cycles. Twenty patients discontinued treatment before 6 cycles; 5 patients after cycle 1 and 15 after 3 cycles: 8 due to disease progression, 6 for toxicity; 2 patients refused further treatment, 3 patients moved out of the area and were lost to follow-up and 1 patient with stable disease interrupted treatment due to fatigue. No interruption due to severe diarrhoea occurred. The dose of Campto® was reduced during treatment in 3 patients (9%) due to toxicity (2 patients experienced grade 3 delayed diarrhoea and one early grade 3 diarrhoea). Six cycles (5.7%) were delayed from 4 to 7 days and four cycles (3.8%) for more than 7 days; the most common reason being toxicity (early and delayed grade 2 diarrhoea in one patient, grade 3 nausea-vomiting in two patients, and grade 2-3 neutropenia in 2 patients). The median dose-intensity was: 116  $\text{mg}/\text{m}^2/\text{week}$  (range: 84.7-120.0). The median relative dose intensity was 1.0 (range: 0.7-1.0) with only 6% of patients having a relative dose intensity of less than 80%.

*Delayed diarrhoea.* Prophylactic treatment for diarrhoea was administered at least once in 29 PP patients from the first cycle (85%), as recommended by the protocol (Table II). In this population, a total of 120 cycles were given, for which preventive treatment was given for 83 cycles (69%). Curative medication was given at least once in 18 patients (62%) and 40 cycles (33%). Compliance to prophylactic and curative treatments are shown in Table II.

The overall incidence of delayed diarrhoea, whatever the grade, in the ITT population was 65% representing 34% of cycles. No grade 4 delayed diarrhoea was observed. The incidence of grade 3 delayed diarrhoea occurred in 18% of patients (90%CI: [9.5-28.9]) and 4.6% of cycles. Cycles in which preventive treatment was given resulted in the manifestation of grade 3 delayed diarrhoea in 3.3% of cycles, as compared to 10% in cycles without preventive treatment, but the difference was not significant ( $p = 0.16$ ). However, at the first cycle the incidence of grade 3 delayed diarrhoea was 40% for the 5 patients who did not receive preventive treatment as compared to 7% for the 29 PP patients who received the prophylactic treatment ( $p = 0.09$ ).

In the PP population, only four patients experienced a grade 3 diarrhoea in 3.7% cycles: two patients at the first cycle and two at the third (Table II). Beyond the third cycle, no severe delayed diarrhoea was observed and the incidence of grade 1-2 delayed diarrhoea decreased across cycles. Of the four patients with severe delayed diarrhoea, three had had previous digestive illnesses. The estimated rate of grade 3 delayed diarrhoea in the PP population was thus 14% (90%CI: [6.2-25.7]).

Regarding the efficacy of curative treatment, the median duration of diarrhoea was 4.5 days (range 1 to 21). Among the six patients with grade 3 delayed diarrhoea, 2 discontinued the treatment with Campto® after the first cycle because of several grade 3 toxicities (nausea/vomiting and/or mucositis). One patient only received preventive treatment at the first cycle; diarrhoea then occurred at the third cycle and he withdrew from the trial after 4 cycles because of progression. Two patients were prophylactically treated from the second cycle after onset of grade 3 diarrhoea at cycle 1. Another patient, in spite of preventive and curative medication at each of the 6 cycles, experienced grade 2 diarrhoea across all cycles and developed an episode of grade 3 diarrhoea at the third cycle. The dose levels of anti-diarrhoeal treatment were decreased at this cycle for this patient.

No patient withdrew from the study due to severe diarrhoea and only one patient (3%) required an 11-day hospitalisation at the first cycle, related to both grade 3 diarrhoea and grade 4 neutropenia.

*Other toxicities.* Severe toxic effects are shown in Table III. Other gastro-intestinal toxicities, involving a cholinergic syndrome observed within the first 24 hours after Campto® infusion, occurred in 13 ITT patients (38%) and 18 out of 131 evaluated cycles (14%). Grade 3 early diarrhoea was observed

for 4 ITT patients (12%) for 4 cycles (3%). No grade 4 was observed. Asthenia was one of the most frequent side-effects observed in the 34 ITT patients; nevertheless, among the 21 patients affected (62%), only two experienced a serious status (grade 3). Alopecia occurred in 30 patients (88%) with 20 grade 3 (59%); three of the four patients without alopecia only received one cycle of Campto®. Mucositis occurred in 7 patients (20%) and two patients experienced a grade 3. Grade 1-2 fever was observed for 35% of patients.

There were no deaths attributed to Campto® toxicity; 5 patients discontinued treatment with Campto due to toxicity: 4 from the first cycle (grade 3 mucositis; grade 2 nausea/vomiting associated with grade 2 delayed diarrhoea and grade 2 fever; grade 4 neutropenia associated with grade 3 delayed diarrhoea and grade 3 nausea/vomiting and febrile neutropenia associated with grade 2 delayed diarrhoea; grade 3 asthenia necessitating hospitalisation) and one at the third cycle (deterioration in performance status). The median neutrophil nadir in the three populations was  $2196 \text{ mm}^3$ , ranging from 126 to 13,000.

*Efficacy.* In the 34 ITT patient population, 2 achieved a partial response, 11 had stable disease, 14 had progressive disease and 7 were not evaluated. This was due to 5 withdrawals at the first cycle and one at the third cycle due to toxicity, while for one patient the response data were not available. The two patients with a partial response had had one and three prior chemotherapy regimens, respectively. Responses according to the number of previous palliative chemotherapy regimens are provided in Table IV. The objective response rate in the 25 evaluable patients was 8% (90% CI: [1.4-23.1]) with 36% of patients with stable disease. The median survival was 10.9 months for the 34 ITT patients (range: 1.8-26.0) and 13.2 months for the 25 evaluable patients (range: 2.7-22.0).

## Discussion

Delayed diarrhoea is recognised as the major limiting toxicity of Campto® at a dose of  $350 \text{ mg/m}^2$  given every 3 weeks. The results of this study showed that, for compliant patients who received prophylactic medication at the first cycle combining sucralfate (Ulcars®) and nifuroxazide (Forcefuryl®), the overall incidence of delayed diarrhoea concerned 62% of patients and 36% of cycles as compared to 88% and 60%, respectively in the Van Custem study (17). The efficacy of this prophylactic medication is even more significant in reducing grade 3-4 delayed diarrhoea in these patients since the incidence of grade 3-4 delayed diarrhoea in the PP population was 14% (90%CI: 6.2-25.7%), which is significantly less than the usual 25%. This compares with an incidence of 18% (90%CI: 9.5-28.9%) in the overall population, since some patients were not treated with the anti-diarrhoeal preventive combination.

Moreover, the absence of grade 4 delayed diarrhoea and

the low rate of related hospitalisation confirmed that delayed diarrhoea can be significantly reduced with preventive treatment. The rate of this serious adverse event, for compliant patients, was lower in our study as compared to previous studies: 39% of patients and 12% of cycles (13), 32% of patients and 8% of cycles (19), 26% of patients and 7% of cycles (17), and even less than the 22% of patients reported by Rougier (15) and Gunningham (16).

However, most of the toxic events than delayed diarrhoea, including asthenia (62%), alopecia (88%), and mucositis (20%), whatever the grade, were consistent with that reported by previous studies (17, 16, 24). Therefore, considering the higher overall toxicity of the drug in this study, compared with that of various trials, and a good relative dose intensity of Campto®, the safety profile could be overestimated. The significantly lower incidence of delayed diarrhoea could be attributable to the use of prophylactic treatment. Moreover, the median duration of delayed diarrhoea of 4.5 days is comparable with the 5 days reported by Rougier (13) and 3 days reported by Van Custem (17).

Patient compliance with preventive medication was good during the first two cycles (85%), but then slowly decreased across cycles. This was due to the progressive overall decrease in the appearance of delayed diarrhoea and consequently so as to avoid problems linked to constipation. In the study with Tiorfan reported by Ychou (24), delayed diarrhoea was observed in 85% of patients and 55% of cycles, including 41% of patients and 18% of cycles with grade 3-4. Our findings confirmed a more effective anti-diarrhoea activity with sucralfate 4 g/day and nifuroxazide 600 mg/day as a prophylactic treatment in the prevention of delayed diarrhoea. Also, 1% of cycles and 3% of patients required diarrhoea-related hospitalisation in our study as compared to the usual 4 to 6% of the cycles and 4 to 16% of patients (24, 17, 13).

Concerning the patients who developed severe delayed diarrhoea, it was not possible to evaluate whether preventive treatment in conjunction with curative treatment could have a secondary effect in decreasing the incidence and/or the severity of late diarrhoea during subsequent cycles, due to the small sample of patients with grade 3 late diarrhoea in our study (6 patients in ITT population and 4 patients PP1). Only a randomised study could answer this question.

The population of our study was older than in most studies of this kind, with a poorer clinical status at study entry: PS < 1 in only 38% of patients and 50% with tumour-related symptoms; 59% of patients were pre-treated by at least two previous lines of palliative chemotherapy. The poor response rate of 8% in patients evaluable for response, which was not the primary objective of this study, can be explained in part by the large proportion of patients with several previous chemotherapy regimens, even though one patient responded after 3 prior treatments, and partly by the poor performance status of the patients in our study. As far as early diarrhoea in the population evaluable for toxicity is concerned, 38% of

patients and 10% of cycles is close to those results reported by Saliba (43% and 10%) (19) and Rougier (51% and 17%) (13).

In conclusion, preventive treatment by a combination of Ulcar® and Ercefuryl® allows the decrease of both the incidence and severity of delayed diarrhoea (particularly grade 3-4 diarrhoea) induced by Campto® in monotherapy. This prophylactic treatment could be systematically proposed to patients in this setting, but it remains to be validated with combined chemotherapies using Campto®.

## References

- Cunningham D and Findlay M: The chemotherapy of colon cancer can no longer be ignored. *Eur J Cancer* 15: 2077-9, 1993.
- Piedbois P: Modulation of fluorouracil by leucovorin in patients with advanced colorectal cancer: evidence in terms of response rate. *Advanced Colorectal Cancer Meta-Analysis Project J Clin Oncol* 10: 896-905, 1992.
- Creemers GJ, Lund B and Verweij J: Topoisomerase I inhibitors: topotecan and irinotecan. *Cancer Treat Rev* 20: 73-96, 1994.
- Chen AY and Liu LF: DNA topoisomerases: essential enzymes and lethal targets. *Annu Rev Pharmacol Toxicol* 34: 191-218, 1994.
- Suminaga M: Phase I study of CPT11, a derivation of camptothecin. 16th Congress of Chemotherapy, Jerusalem-Israel 1989, (abstr 51).
- Abigerres D, Chabot GG, Armand JP, Herait P, Gouyette A and Gandia D: Phase I and pharmacologic studies of the camptothecin analog irinotecan administered every 3 weeks in cancer patients. *J Clin Oncol* 13: 210-21, 1995.
- Rowinsky EK, Grochow LB, Ettinger DS, Sartorius SE, Lubejko BG, Chen TL, Rock MK and Donchower RC: Phase I and pharmacological study of the novel topoisomerase I inhibitor 7-ethyl-10-(4-(1-piperidino)-1-piperidino)carbonyloxycamptothecin (CPT-11) administered as a ninety-minute infusion every 3 weeks. *Cancer Res* 54: 427-36, 1994.
- Negoro S, Fukuoka M, Masuda N, Takada M, Kusonoki Y, Matsui K, Takifuji N, Kudoh S, Niitani H and Taguchi T: Phase I study of weekly intravenous infusions of CPT-11, a new derivative of camptothecin, in the treatment of advanced non-small cell lung cancer. *J Natl Cancer Inst* 83: 1164-8, 1991.
- de Forni M, Bugat R, Chabot GG, Culine S, Extra JM, Gonyette A, Madelaine I, Marty ME and Mathieu-Boue A: Phase I and pharmacokinetic study of the camptokinetic study of the camptothecin derivative irinotecan, administered on a weekly schedule in cancer patients. *Cancer Res* 54: 4347-54, 1994.
- Rothenberg ML: Irinotecan (CPT11) as a second-line therapy for patients with 5-FU-refractory colorectal cancer (ENG). *Proc Am Soc Clin Oncol* 13: 1994.
- Catimel G, Chabot GG, Guastalla JP, Dumortier A, Cote C, Engel C, Gonyette A, Mathieu-Boue A, Mahjoubi M and Clavel M: Phase I and pharmacokinetic study of irinotecan (CPT-11) administered daily for three consecutive days every three weeks in patients with advanced solid tumors. *Ann Oncol* 6: 133-40, 1995.
- Ohe Y, Sasaki Y, Shinkai T, Eguchi K, Tamura T, Kojima A, Kunikane H, Okamoto H, Karato A, Ohnatsu H *et al*: Phase I study and pharmacokinetics of CPT-11 with 5-day continuous infusion. *J Natl Cancer Inst* 84: 972-4, 1992.
- Rougier P, Bugat R, Douillard JY, Culine S, Suc E, Brunet P, Becouarn Y, Ychou M, Marty M, Extra JM, Bonneterre J, Adenis A, Seitz JF, Ganem G, Namer M, Controy T, Negrier S, Merrouche Y, Burki F, Mousseau M, Herait P and Mahjoubi M: Phase II study of irinotecan in the treatment of advanced colorectal cancer in chemotherapy-naïve patients and patients pretreated with fluorouracil-based chemotherapy. *J Clin Oncol* 15: 251-60, 1997.
- Ychou M, Kramar A, Raoul JL, Desseigne F, Hua A, Vernillet L and

- Merrouche Y: Final results of a phase II study using CPT-11 high dose (500mg/m<sup>2</sup>) as first line chemotherapy in patients with metastatic colorectal cancer (MCRC). Proc Am Soc Clin Oncol 19: 249a, 2000.
- 15 Rougier P, Van Cutsem E, Bujetta E, Niederle N, Possinger K, Labianca R, Navarro M, Morant R, Bleiberg H, Wils J, Awad L, Heraït P and Jacques C: Randomised trial of irinotecan *versus* fluorouracil by continuous infusion after fluorouracil failure in patients with metastatic colorectal cancer. Lancet 352: 1407-12, 1998.
- 16 Cunningham D, Pyrhonen S, James RD, Punt CJ, Hickish TF, Heikkilä R, Johannesen TB, Starkhammar H, Topham CA, Awad L, Jacques C and Heraït P: Randomised trial of irinotecan plus supportive care *versus* supportive care alone after fluorouracil failure for patients with metastatic colorectal cancer. Lancet 352: 1413-8, 1998.
- 17 Van Cutsem E, Cunningham D, Ten Bokkel Huinink WW, Punt CJ, Alexopoulos CG, Dirix L, Symann M, Blijham GH, Cholet P, Fillet G, Van Groenigen C, Vannetzel JM, Levi F, Panagos G, Unger C, Wils J, Cote C, Blanc C, Heraït P and Bleiberg H: Clinical activity and benefit of irinotecan (CPT-11) in patients with colorectal cancer truly resistant to 5-fluorouracil (5-FU). Eur J Cancer 35: 54-9, 1999.
- 18 Douillard JY, Cunningham D, Roth AD, Navarro M, James RD, Karasek P, Jandik P, Iveson T, Carmichael J, Alakl M, Gruia G, Awad L and Rougier P: Irinotecan combined with fluorouracil compared with fluorouracil alone as first-line treatment for metastatic colorectal cancer: a multicentre randomised trial. Lancet 355: 1041-7, 2000.
- 19 Saliba F, Hagipantelli R, Misset JJ, Bastian G, Vassal G, Bonnay M, Heraït P, Cote C, Mahjoubi M, Mignard D and Cvitkovic E: Pathophysiology and therapy of irinotecan-induced delayed-onset diarrhea in patients with advanced colorectal cancer: a prospective assessment. J Clin Oncol 16: 2745-51, 1998.
- 20 Hagipantelli R, SI and Misset JL: Pathophysiology and therapy of Irinotecan (CPT-11) induced delayed onset diarrhea (DD): a prospective assessment. Proc Am Soc Clin Oncol 14: 464, 1995.
- 21 Lestingi TM, Ve, Gray W *et al*: A phase I trial of CPT-11 in solid tumors with G-CSF and antidiarrheal support. Proc Am Soc Clin Oncol 14: 1480, 1995.
- 22 Lenfers BH, Loeffler TM, Droege CM and Hausamen TU: Substantial activity of budesonide in patients with irinotecan (CPT-11) and 5-fluorouracil induced diarrhea and failure of loperamide treatment. Ann Oncol 10: 1251-3, 1999.
- 23 Abigeres D, Armand JP, Chabot GG, Da Costa L, Fadel E, Cote C, Heraït P and Gandia D: Irinotecan (CPT-11) high-dose escalation using intensive high-dose loperamide to control diarrhea. J Natl Cancer Inst 86: 446-9, 1994.
- 24 Ychou M, Douillard JY, Rougier P, Adenis A, Mousseau M, Dufour P, Wendling JJ, Burki F, Mignard D and Marty M: Randomized comparison of prophylactic antidiarrheal treatment *versus* no prophylactic antidiarrheal treatment in patients receiving CPT-11 (irinotecan) for advanced 5-FU-resistant colorectal cancer: an open-label multicenter phase II study. Am J Clin Oncol 23: 143-8, 2000.

Received March 4, 2002

Accepted July 3, 2002

# Nanoliposomal Irinotecan and Metronomic Temozolomide for Patients With Recurrent Glioblastoma

## *BrUOG329, A Phase I Brown University Oncology Research Group Trial*

Heinrich Elinzana, MD, Steven Toms, MD, Jordan Robison, BA, Alex Mohler, MD, Arieana Carcieri, PA, Deus Ciela, MD, Jennifer Donnelly, RN, Dylan Disano, BS, John Vatketich, BS, John Baekey, MA, Ashlee Sturtevant, MA, Kelsey MacKinnon, BS, Roxanne Wood, BA, and Howard Safran, MD

**Background:** Liposomal formulations may improve the solubility and bioavailability of drugs potentially increasing their ability to cross the blood-brain barrier. We performed a phase I study to determine the maximum tolerated dose and preliminary efficacy of pegylated nanoliposomal irinotecan (nal-IRI)+metronomic temozolomide (TMZ) in patients with recurrent glioblastoma.

**Patients and Methods:** Patients with glioblastoma who progressed after at least 1 line of therapy were eligible. All patients received TMZ 50 mg/m<sup>2</sup>/d until disease progression. Three dose levels of nal-IRI were planned, 50, 70, and 80 mg/m<sup>2</sup>, intravenously every 2 weeks. Patients were accrued in a 3+3 design. The study included a preliminary assessment after the first 13 evaluable patients. The trial would be terminated early if 0 or 1 responses were observed in these patients.

**Results:** Twelve patients were treated over 2 dose levels (nal-IRI 50 and 70 mg/m<sup>2</sup>). At dose level 2, nal-IRI 70 mg/m<sup>2</sup>, 2 of 3 patients developed dose-limiting toxicities including 1 patient who developed grade 4 neutropenia and grade 3 diarrhea and anorexia and 1 patient with grade 3 diarrhea, hypokalemia fatigue, and anorexia. Accrual to dose level 1 was expanded to 9 patients. The Drug Safety Monitoring Board (DSMB) reviewed the data of the initial 12 patients—there were 0/12 responses (0%) and the median progression-free survival was 2 months and accrual was halted.

**Conclusions:** The maximum tolerated dose of nal-IRI was 50 mg/m<sup>2</sup> every 2 weeks with TMZ 50 mg/m<sup>2</sup>/d. The dose-limiting toxicities were diarrhea and neutropenia. No activity was seen at interim analysis and the study was terminated.

**Key Words:** glioblastoma, nanoliposomal irinotecan, phase I

(*Am J Clin Oncol* 2020;00:000–000)

The standard initial treatment for glioblastoma is maximal safe resection followed by concurrent radiation and temozolomide (TMZ) then additional adjuvant TMZ. In a phase III study, there was an increase in median survival (14.6 vs 12.1 mo,  $P < 0.0001$ ) with the addition of TMZ to radiation as

compared with radiation alone.<sup>1</sup> Furthermore, there was an improvement in 2-year survival with TMZ and radiation as compared with radiation alone, 26.5% versus 10.4%, respectively.<sup>1</sup> A phase III study also showed that survival was further increased with the addition of tumor treating fields to TMZ and radiation.<sup>2</sup>

Unfortunately, virtually all patients relapse initial adjuvant treatment. Rechallenge with dose-dense TMZ schedules such as continuous dose (metronomic) schedules is an option.<sup>3</sup> Continuous therapy with metronomic regimens may inhibit tumor angiogenesis through the suppression of tumor endothelium regeneration and O<sup>6</sup>-methylguanine methyltransferase (MGMT) depletion of the tumor endothelium.<sup>4,5</sup> Woo et al<sup>6</sup> administered TMZ daily at 50 mg/m<sup>2</sup>/d in 30 patients with recurrent glioblastoma. The median progression-free survival (PFS) was 2 months (range, 0.5 to 16 mo). The median overall survival from the start of therapy to death was 6 months (95% confidence interval: 5.1-6.9).

More effective agents are clearly needed in glioblastoma. The addition of bevacizumab to continuous low-dose TMZ was not superior to TMZ alone in terms of PFS or overall survival.<sup>7</sup> Irinotecan may have modest activity in glioblastoma. In a study by Friedman et al,<sup>8,9</sup> 9 of 60 patients (16%) with progressive or recurrent glioblastoma had a partial response to irinotecan. The blood-brain barrier markedly reduces drug absorption preventing irinotecan the opportunity to reach its target in the brain.<sup>9</sup> Nanoliposomal irinotecan is a nanoliposomal encapsulation of irinotecan. A nanoliposome, or submicron bilayer lipid vesicle, is a new technology for the encapsulation and delivery of bioactive agents.<sup>10</sup> Nanoliposomes improve the solubility and bioavailability of irinotecan markedly increasing the ability of irinotecan to cross the blood-brain barrier with favorable pharmacokinetic and biodistribution properties in preclinical animal models.<sup>10</sup> For example, Noble et al<sup>11</sup> evaluated a nanoliposomal irinotecan (nal-IRI) as an intravenous treatment in an intracranial U87MG brain tumor model in mice, and irinotecan and SN-38 levels were analyzed in malignant and normal tissues. Tissue analysis demonstrated favorable properties for nal-IRI, including a 10.9-fold increase in tumor area under the curve for nal-IRI compared with free irinotecan and 35-fold selectivity for tumor versus normal tissue exposure.<sup>11</sup>

Multiple in vitro and clinical studies support the rationale for combining a topoisomerase I inhibitor such as irinotecan and an alkylating agent such as TMZ.<sup>12–14</sup> The principle mechanism of action of a topoisomerase I inhibitor is mainly S phase-specific inhibition of DNA replication. In contrast, an

From the Brown University Oncology Research Group, Providence, RI. Supported by Ipsen.

The authors declare no conflicts of interest.

Reprints: Howard Safran, MD, Department of Medicine, The Rhode Island Hospital, 593 Eddy Street, Providence, RI 02906. E-mail: hsafran@lifespan.org.

Copyright © 2020 Wolters Kluwer Health, Inc. All rights reserved.

ISSN: 0277-3732/20/000-000

DOI: 10.1097/COC.0000000000000780

alkylating agent directly damages DNA. The combination of a topoisomerase inhibitor with an alkylating agent is a rational, established strategy for increasing tumor-cell killing.<sup>12-14</sup> We, therefore, performed a phase I study to determine the maximum tolerated dose (MTD) of the combination of nal-IRI in combination with TMZ and assessed the preliminary clinical efficacy of the combination.

## PATIENTS AND METHODS

### Study Design

This was a phase I investigator-initiated study coordinated by the Brown University Oncology Research Group. The study was supported in part by Ipsen.

### Patients

Eligibility criteria required patients to have pathologically confirmed glioblastoma, the progressive disease after at least 1 line of therapy, and have received TMZ and radiation. Patients were required to be 18 years and older, have a Karnofsky Performance Score  $\geq 60$ , be on a stable corticosteroid dose for at least 7 days before starting treatment, able to tolerate contrast-enhanced magnetic resonance images (MRIs), and have the assessable disease at baseline by brain MRI. Laboratory requirements included absolute neutrophil count (ANC)  $\geq 1500/\text{mm}^3$ , platelets  $\geq 100,000/\text{mm}^3$ , hemoglobin  $\geq 9.0$  g/dL, total bilirubin  $\leq 1 \times$  upper limit of normal (ULN), albumin levels  $\geq 3.0$  g/dL, aspartate aminotransferase, alanine aminotransferase  $\leq 2.5 \times$  ULN, and serum creatinine  $\leq 1.5 \times$  ULN. Written informed consent was required. Patients were excluded if they had a coexisting medical condition that could interfere with their participation or compliance with the study. Use of CYP3A4 enzyme-inducing anticonvulsants and strong CYP3A4 inducers were not allowed. The study was approved by the institutional review board and registered clinicaltrials.gov NCT03119064.

### Treatment

One treatment cycle was 14 days. Patients received TMZ, 50 mg/m<sup>2</sup>/d, until disease progression. Three dose levels of nal-IRI were planned: 50, 70, and 80 mg/m<sup>2</sup> intravenously over 90 minutes every 2 weeks. Patients received dexamethasone and a 5-HT<sub>3</sub> antagonist before nal-IRI. Atropine could be prescribed prophylactically for patients who had experienced acute cholinergic symptoms in previous cycles. Premedication before TMZ was not required and could be administered as per institutional standard of care.

A new course of treatment could not begin until the neutrophil count was  $\geq 1500/\mu\text{L}$ , platelet count  $\geq 75,000/\mu\text{L}$  and recovery from other clinically significant, nonhematologic toxicities to  $\leq$  grade 2. If the patient did not meet these criteria by the next scheduled cycle, treatment was delayed until these requirements were met. Patients who required a treatment delay of  $> 4$  weeks due to toxicity were removed from protocol treatment.

Dose-limiting toxicities (DLTs) were defined as the following toxicities occurring during the first 2 cycles of therapies: grade 4 neutropenia (ANC  $< 500/\mu\text{L}$ ) for  $> 7$  days, ANC  $< 1000/\mu\text{L}$  with fever or infection, platelets  $< 25,000/\mu\text{L}$ , platelets  $< 50,000/\mu\text{L}$  requiring transfusion, grade 3 or 4 treatment-related nonhematologic toxicities excluding alopecia. Grade 3 nausea, vomiting, or diarrhea were only be considered DLTs if they occurred despite maximal medical support. Grade 3 or 4 electrolyte abnormalities were not considered DLTs if the electrolyte disorder could be corrected to grade 2 or less within 72 hours. Delay of treatment for  $> 2$  weeks due to toxicity was also considered a DLT.

### Dose Modifications

Patients could resume treatment following a DLT, with a dose level reduction in both drugs, once they recovered from treatment-related nonhematologic toxicities to  $\leq$  grade 2 and their platelet count was  $\geq 100,000/\text{mm}^3$  and their absolute neutrophil count was  $1500/\text{mm}^3$ . Patients experiencing a DLT could have a 1 dose level reduction of nal-IRI (dose level -1 of nal-IRI was 43 mg/m<sup>2</sup> every 2 wk) and dose level -1 of TMZ was 25 mg/m<sup>2</sup>/d. Patients experiencing a second DLT were removed from protocol treatment.

### Evaluation of Tumor Response and Toxicity

The response was assessed by the Macdonald criteria.<sup>15</sup> Toxicities were graded using The National Cancer Institute's Common Toxicity Criteria (CTCAE), version 4.0.

### Statistics

Three patients were to be accrued to level 1. If no DLTs were observed following completion of 4 weeks of treatment (2 cycles) then accrual to dose level 2 could proceed. If a DLT was observed in 1 of the first 3 patients in a dose level, then accrual for that level was expanded to 6 patients. Accrual continued in this way until the MTD was determined. Two or more instances of DLT in a cohort of 6 patients resulted in the preceding dose level being defined as the MTD. The secondary objective was to assess the preliminary response rate and PFS of nal-IRI with continuous low-dose TMZ in patients with recurrent glioblastoma.

The activity was defined as a complete or partial response as defined by the via Macdonald criteria.<sup>15</sup> The trial was to differentiate between a 10% level of activity and a 30% level of activity. Specifically, the hypothesis tested was:  $H_0: P \leq 0.1$  versus  $H_1: P \geq 0.3$ .

A Simon 2-stage design was utilized. The first 13 evaluable patients treated at the MTD would be assessed for response. The trial would be terminated early if 0 or 1 responses were observed in these patients, and it would be concluded that the true response rate was unlikely to be  $> 10\%$ . If at least 2 responses were observed, accrual could continue until a total of 25 evaluable patients were enrolled in the study. The characteristics of this study design were as follows: The probability of erroneously concluding that the treatment was active ( $P \geq 0.3$ ) when it was actually not effective ( $P \leq 0.1$ ) would be  $< 0.098$ , that is,  $\alpha = 0.098$ . Time to progression was determined by the Kaplan-Meier method from the time of study enrollment.

## RESULTS

Twelve patients were enrolled between June 26, 2018, and November 15, 2019. Patient characteristics are shown in Table 1. Six patients were initially enrolled to dose level 1, nal-IRI 50 mg/m<sup>2</sup>, and TMZ 50 mg/m<sup>2</sup> daily. Of the 6 patients, 1 had grade 3 elevation of hepatic transaminases, 1 patient had grade 2 nausea and vomiting, and 2 had grade 2 electrolyte abnormalities. Three patients were then entered on dose level 2, nal-IRI 70 mg/m<sup>2</sup> and TMZ, 50 mg/m<sup>2</sup> daily.

The first patient on dose level 2 developed grade 3 diarrhea, hypokalemia, anorexia fatigue, and nausea. Subsequently, the third patient at this dose level developed grade 4 neutropenia and grade 3 diarrhea, anorexia, and dehydration. Therefore, dose level 2 exceeded the total tumor dose. Three additional patients were treated at dose level 1 without DLTs. All toxicities are shown in Table 2.

### Response and PFS

All patients were assessable for response. There were no partial responses. Of the 12 patients, 10 had progressive disease at 2 months and 2 had progressive disease at 3 months. Figure 1

**TABLE 1.** Patient Demographic and Clinical Characteristics

Characteristics	All Patients (N = 12), n (%)
Age (y)	
Median	58
Range	39-70
Sex	
Male	10 (83)
Female	2 (17)
KPS	
100	1 (8)
90	5 (42)
80	1 (8)
70	4 (36)
60	1 (8)
IDH1	
Wild-type	12 (100)
Mutated	0 (0)
MGMT	
Methylated	7 (58)
Unmethylated	5 (42)
No prior treatments	
1	8 (67)
2	1 (8)
3	1 (8)
4	2 (17)
Prior bevacizumab	
Yes	2 (17)
No	10 (83)

IDH1 indicates isocitrate dehydrogenase 1; KPS, Karnofsky Performance Score; MGMT, O<sup>6</sup>-methylguanine methyltransferase.

shows PFS. The median PFS was 2 months. The Brown University Oncology Research Group Drug Safety Monitoring Board (DSMB) reviewed the data from the initial 12 patients and the study was terminated.

### DISCUSSION

The MTD for nal-IRI was 50 mg/m<sup>2</sup> every 2 weeks with continuous daily dosing of TMZ, 50 mg/m<sup>2</sup>/d. The DLTs were diarrhea in 2 of 3 patients and 1 of these patients also had grade 4 neutropenia and grade 3 anorexia and dehydration. We were not able to administer the Food and Drug Administration–approved dose of 70 mg/m<sup>2</sup> every 2 weeks as was utilized in the NAPOLI-1 trial of nal-IRI with 5-fluorouracil and leucovorin in recurrent

**TABLE 2.** Treatment-emergent Adverse Events, Grades 2 to 4

Adverse Event	n (%)		
	Grade 2	Grade 3	Grade 4
Neutropenia	0 (0)	0 (4)	1 (8)
Thrombosis	0 (0)	1 (8)	0 (0)
ALT/AST	1 (8)	1 (8)	0 (0)
Hypokalemia	1 (8)	1 (8)	0 (0)
Hypophosphatemia	1 (0)	0 (0)	0 (0)
Hypokalemia	0 (0)	1 (4)	0 (0)
Nausea	1 (8)	1 (8)	0 (0)
Fatigue	1 (8)	1 (8)	0 (0)
Diarrhea	0 (0)	2 (16)	0 (0)
Anorexia	0 (0)	2 (16)	0 (0)
Dehydration	0 (0)	1 (8)	0 (0)
Gastritis	1 (8)	0 (0)	0 (0)
Urticaria	1 (8)	0 (0)	0 (0)

ALT indicates alanine aminotransferase; AST, aspartate aminotransferase

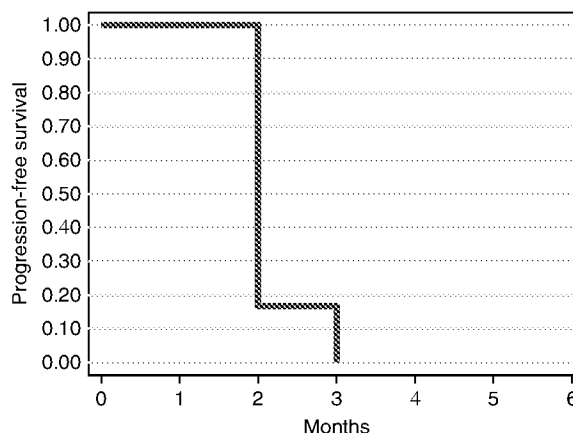


**FIGURE 1.** Progression-free survival of all patients.

pancreatic cancer.<sup>16</sup> In the NAPOLI-1 trial, nal-IRI was withheld or delayed for adverse reactions in 62% of patients receiving nal-IRI, 5-fluorouracil, and leucovorin; the most frequent adverse reactions requiring interruption or delays were neutropenia, diarrhea, fatigue, vomiting, and thrombocytopenia.<sup>16</sup>

There was no activity of nal-IRI+TMZ in this phase 1 trial in glioblastoma with no responses in 12 patients. The Brown University Oncology Research Group DSMB terminated the study when the threshold for activity (> 2 responses in the first 13 patients) was not achieved. Ten of 12 patients had disease progression at the initial 2-month restaging MRI and the other 2 patients had progressive disease by 3 months.

The complete lack of activity, including a 0% response rate and a 2-month PFS, was disappointing. All patients had previously received concurrent TMZ and radiation therapy followed by adjuvant TMZ and had experienced disease progression. We had hypothesized that the combination of nal-IRI with TMZ would have efficacy even in patients who had progressed on prior TMZ. Single-agent irinotecan and metronomic TMZ have each reported somewhat better results than observed with the combination.<sup>3-8</sup> While the MGMT unmethylated patients who had already progressed on a TMZ containing regimen were unlikely to respond to metronomic TMZ, ~42% of the patients on this trial had methylated MGMT.

Toxicities prevented administration of full dose nal-IRI in this trial, however, dose reductions of nal-IRI did not significantly affect the outcome in pancreatic cancer.<sup>17</sup> In retrospect, more in vitro testing with better animal models could have been performed on this combination before the initiation of the clinical study. The ability of nal-IRI to cross the blood-brain barrier was uncertain and the synergy of the combination had not been tested in vitro and in animal models of gliomas. Moreover, phase 0 studies which look to assess pharmacokinetics and target drug delivery may help in future study designs. Glioblastoma remains a highly lethal and refractory disease. Further research is needed to develop more effective treatments based on the pathobiology of this cancer.

### REFERENCES

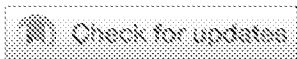
1. Stupp R, Mason WP, Van den Bent MJ, et al. Radiotherapy plus concomitant and adjuvant TMZ for glioblastoma. *N Engl J Med.* 2005;352:987–996.
2. Taphoorn MJB, Dirven L, Kanner A, et al. Influence of treatment with tumor-treating fields on health-related quality of life of patients with newly diagnosed glioblastoma a secondary analysis of a randomized clinical trial. *JAMA Oncol.* 2018;4:495–504.



3. Franceschi E, Omuro AM, Lassman AB, et al. Salvage TMZ for prior TMZ responders. *N Engl J Med*. 2005;104:2473–2476.
4. Wick W, Platten M, Weller M. New (alternative) TMZ regimens for the treatment of glioma. *Neuro-Oncology*. 2008;11:69–79.
5. Ko KK, Lee ES, Joe YA, et al. Metronomic treatment of TMZ increases anti-angiogenicity accompanied by down-regulated O6-methylguanine-DNA methyltransferase expression in endothelial cells. *Exp Ther Med*. 2011;2:343–348.
6. Woo JY, Yang SH, Lee YS, et al. Continuous low-dose TMZ chemotherapy and microvessel density in recurrent glioblastoma. *J Korean Neurosurg Soc*. 2015;58:426–431.
7. Verhoeff JJ, Lavini C, van Linde ME, et al. Bevacizumab and dose-intense TMZ in recurrent high-grade glioma. *Ann Oncol*. 2010;21:1723–1727.
8. Friedman HS, Prados MD, Wen PY, et al. Bevacizumab alone and in combination with irinotecan in recurrent glioblastoma. *J Clin Oncol*. 2009;27:4733–4740.
9. Nau R, Sörgel F, Eiffert H. Penetration of drugs through the blood-cerebrospinal fluid/blood-brain barrier for treatment of central nervous system infections. *Clin Microbiol Rev*. 2010;23:858–883.
10. Spring BQ, Bryan Sears R, Zheng LZ, et al. A photoactivable multi-inhibitor nanoliposome for tumour control and simultaneous inhibition of treatment escape pathways. *Nat Nanotechnol*. 2016;11:378–387.
11. Noble CO, Krauze MT, Drummond DC, et al. Pharmacokinetics, tumor accumulation and antitumor activity of nanoliposomal irinotecan following systemic treatment of intracranial tumors. *Nanomedicine (Lond)*. 2014;9:2099–2108.
12. Kushner BH, Kramer K, Modak S, et al. Irinotecan plus TMZ for relapsed or refractory neuroblastoma. *J Clin Oncol*. 2006;24:5271–5276.
13. Casey DA, Wexler LH, Merchant MS, et al. Irinotecan and TMZ for Ewing sarcoma: The Memorial Sloan-Kettering experience. *Pediatr Blood Cancer*. 2009;53:1029–1034.
14. Blanchette P, Lo A, Ng P, et al. Irinotecan and TMZ in adults with recurrent sarcoma. *J Solid Tumors*. 2015;5:105–110.
15. Macdonald DR, Cascino TL, Schold SC, et al. Response criteria for phase II studies of supratentorial malignant glioma. *J Clin Oncol*. 1990;8:1277–1280.
16. Rehman SS, Lim K, Wang-Gillam A. Nanoliposomal irinotecan plus fluorouracil and folinic acid: a new treatment option in metastatic pancreatic cancer. *Expert Rev Anticancer Ther*. 2016;16:485–492.
17. Wang-Gillam A, Hubner R, Mirakhor B, et al. Dose modifications of liposomal irinotecan (nal-IRI)+5-fluorouracil/leucovorin (5-FU/LV) in NAPOLI-1: impact on efficacy. *J Clin Oncol*. 2018;36:388.

CENTRAL NERVOUS SYSTEM TUMORS

## Nanoliposomal irinotecan and metronomic temozolomide for patients with recurrent glioblastoma: BrUOG329, a phase IB/IIA Brown University Oncology Research Group (BrUOG) trial.



[Heinrich Elinzano](#), [Jessica B. McMahon](#), [Alex B. Mohler](#), [Jordan B. Robison](#), [Ariana B. Carciari](#), [Steven A. Toms](#), [Deus B. Cielo](#), [Wendy B. Turchetti](#), [John Vaskevich](#), [Roxanne Wood](#), [Amy Webber](#), [Howard Safran](#)

Rhode Island Hospital, Providence, RI; Rhode Island Hospital-The Warren Alpert Medical School of Brown University, Providence, RI; Brown University Oncology Research Group, Providence, RI

[Show Less](#)

[Abstract Disclosures](#)

### Abstract

e14548

**Background:** Nanoliposomal irinotecan (nal-IRI) is a novel formulation of irinotecan, encapsulating drug molecules within long-circulating liposome-based nanoparticles with resulting favorable pharmacokinetic and biodistribution properties. Nanoliposomes improve the solubility and bioavailability of drugs and potentially increase their ability to cross the blood brain barrier. We performed a phase I study to determine the maximum tolerated dose (MTD) and preliminary efficacy of nal-IRI in combination with metronomic temozolomide (TMZ) in patients with recurrent glioblastoma. **Methods:** Patients with recurrent glioblastoma who had progressed after at least 1 line of therapy with a KPS of > 60 were eligible. All patients received TMZ 50 mg/m<sup>2</sup> PO daily with nal-IRI IV every 2 weeks until disease progression. Three dose levels of nal-IRI were planned, 50 mg/m<sup>2</sup>, 70 mg/m<sup>2</sup> and 80 mg/m<sup>2</sup>. Dose limiting toxicities (DLTs) were defined as those occurring during the first 2 cycles (28 days) of treatment. Patients were accrued in a 3+3 design. Accrual at the MTD level was to be expanded to 25 patients, unless the study was terminated early if 0-1 responses were observed in the first 13 evaluable patients. **Results:** Twelve patients were treated over 2 dose levels (nal-IRI 50-70 mg/m<sup>2</sup>). At dose level 2, nal-IRI 70mg/m<sup>2</sup>, 2 of 3 patients developed DLTs, including one patient who developed grade 4 neutropenia, grade 2 diarrhea and grade 3 anorexia and one patient with grade 3 diarrhea, grade 3 hypokalemia and grade 3

anorexia. Accrual at nal-IRI 50 mg/m<sup>2</sup>, defined as the MTD, was expanded to 9 patients. Treatment-related toxicities at this dose level included grade 3 ALT (N = 1). As there were no responses seen in the initial 12 patients (0/12, 0%), the BrUOG Data Safety Monitoring Board terminated the study. **Conclusions:** The MTD of nal-IRI was 50 mg/m<sup>2</sup> every 2 weeks with TMZ 50mg/m<sup>2</sup>/day. DLTs were grade 3 diarrhea and anorexia. No antitumor activity was seen in the first 12 patients and the study was terminated. Clinical trial information: NCT03119064.

© 2020 American Society of Clinical Oncology

**Research Sponsor:**

Ipsen